Agronomy Research

Established in 2003 by the Faculty of Agronomy, Estonian Agricultural University

Aims and Scope:

Agronomy Research is a peer-reviewed international Journal intended for publication of broad-spectrum original articles, reviews and short communications on actual problems of modern biosystems engineering incl. crop and animal science, genetics, economics, farm- and production engineering, environmental aspects, agro-ecology, renewable energy and bioenergy etc. in the temperate regions of the world.

Copyright:

***Agronomy Research* online:**

Agronomy Research is available online at: http://agronomy.emu.ee/

Acknowledgement to Referees:

The Editors of *Agronomy Research* would like to thank the many scientists who gave so generously of their time and expertise to referee papers submitted to the Journal.

Abstracted and indexed:

SCOPUS, EBSCO, CABI Full Paper and Thompson Scientific database: (Zoological Records, Biological Abstracts and Biosis Previews, AGRIS, ISPI, CAB Abstracts, AGRICOLA (NAL; USA), VINITI, INIST-PASCAL.)

Subscription information:

Institute of Technology, EULS
St. Kreutzwaldi 56, 51014 Tartu, ESTONIA
E-mail: timo.kikas@emu.ee

Journal Policies:

Estonian University of Life Sciences, Estonian Research Institute of Agriculture, Latvia University of Life Sciences and Technologies, Aleksandras Stulginskis University, Lithuanian Research Centre for Agriculture and Forestry and Editors of *Agronomy Research* assume no responsibility for views, statements and opinions expressed by contributors. Any reference to a pesticide, fertiliser, cultivar or other commercial or proprietary product does not constitute a recommendation or an endorsement of its use by the author(s), their institution or any person connected with preparation, publication or distribution of this Journal.

ISSN 1406-894X

CONTENTS

Agronomy Research **16**(4), 1569–1579, 2018
https://doi.org/10.15159/AR.18.166

Assessment of *Calotropis* natural dye extracts on the efficiency of dye-sensitized solar cells

A.H. Alami[1,2,*], K. Aokal[2], D. Zhang[1,2], M. Tawalbeh[1], A. Alhammadi[1] and A. Taieb[1]

[1]University of Sharjah, Sustainable and Renewable Energy Engineering Department, AE2727272 Sharjah, United Arab Emirates
[2]University of Sharjah, Centre for Advanced Materials Research, AE27272 Sharjah, United Arab Emirates
[*]Correspondence: aalalami@sharjah.ac.ae

Abstract. This work presents the construction and testing of solar cells sensitized with natural dyes extracted from plants indigenous to the desert. *Calotropis* plants are self-sufficient as they grow in very harsh environments, and yet are not consumed by humans or livestock due to their irritating agents to the skin and eyes. The energy generators of these plants are the leaves, which are crushed and processed to produce the dye solution. Also, the *Calotropis* leaves are covered in a white powder that is thought to aid in mitigating the heat by scattering incident radiation. This powder material is examined and added to the dye as it proved advantageous for the overall cell efficiency, which reached 0.214% compared with 0.108% for cells with no powder. The produced cells are also compared with ones sensitized by spinach, another common natural sensitizer for dye-sensitized solar cells, and the performance proved to be significantly better. The fact that *Calotropis* is a non-food plant is an added advantage to utilizing it as a dye source, along with its intrinsic heat resistance that allows it to survive the harsh desert conditions all year round.

Key words: *Calotropis*, dye-sensitized solar cells, natural dyes.

INTRODUCTION

Photovoltaic (PV) solar energy systems are growing rapidly worldwide with an average annual rate of 6.8% and about 50 GW of new instillations every year (BNEF, 2015; Breyer et al., 2017). It is also estimated that this growth will continue and would reach around 206 GW in 2040 (REN21, 2016) and the speculated cumulative PV instillations by 2050 would be around 4,512 GW (Smith & Bogust, 2018). In specific, it is speculated by the United States Department of Energy that the electricity production through solar energy systems may count for 27% of the total electricity produced in the U.S by 2050 (Liu et al., 2018).

Geographic location and climatological conditions play a vital role in determining the performance and efficiency of any PV system (Makrides et al., 2010). Solar irradiance and temperature are the most important meteorological parameters that influence the performance of PV systems (Wang et al., 2017). Hence, the PV system's power output fluctuates throughout the day and from season to season based on the variation of the temperature and irradiance spectrum (Kaltiya et al., 2014; Phinikarides et al., 2015).

The United Arab Emirates (UAE), lies between 22°30′ and 26°10′ north latitude and between 51° and 56°25′ east longitude which provides a basis of good solar energy exposure. This high solar exposure suggests that PV technology has a great potential as alternative power source in the future of UAE. Combining that with the region's sub-tropical and arid climate, it has been regarded as a potential to establish several PV power plants (Said et al., 2018).

Nowadays, there are three main generations of solar cell technologies. The first generation is the most commonly used. It includes monocrystalline and polycrystalline silicon cells produced from wafers that differ by crystallization levels, where each wafer can supply 2–3 watt power. The highest recorded lab efficiency achieved for this technology was around 25% (Wu et al., 2015; Polman et al., 2016). However, silicon solar cells are rigid, they have a harmful impact on the environment, their production requires a considerable amount of energy, and therefore a high production cost (Sherwani et al., 2010; Wu et al., 2015). The second generation solar cells are usually termed thin films due to their relatively thin semiconducting layer, which can be up to a few micrometres thick. This technology is based on amorphous silicon, copper indium gallium diselenide (CIGS) and cadmium telluride (CdTe). The cost of the second generation solar cells is relatively low, though, their efficiency is lower when compared to the first generation with a lab efficiency close to 18.4% (Hosenuzzaman et al., 2015; Ghosh, 2017). However, gabs frequently generated especially when manufacturing large cells due to the lack of uniformity. This leads to module efficiencies lower than the lab efficiency mentioned earlier. For instance, the best module efficiency for copper indium gallium diselenide (CIGS) and cadmium telluride (CdTe) are 13.4% and 10.7%, respectively (Sharma et al., 2017).

Third generation solar cells are the ones that use non-silicon based components and they categorized to four main types: nano crystal based, polymer based, concentrated, and dye-sensitized solar cells (Choubey et al., 2012). Third generation solar cells are not restrained by the Shockley Quieisser limit (Shockley & Queisser, 1961) and they offer the possibility of facile large-scale production with reliance on materials that are readily available and potentially inexpensive. Nevertheless, their performance and stability are restricted when compared to first and second generation technologies. This has prompted extensive studies in the technology. The efficiency for the third generation varies depending on the base of the solar cell. For instance, the dye sensitized solar cell efficiency is around 10% while the organic and nanotech solar cell is about 3–8% (Sharma et al., 2015).

Dye-sensitized solar cells are one of the most common third generation technologies with their active materials solely comprised of the dye material and an electrolyte. DSSCs are photonic devices that convert light into electricity. Their structures comprise of a porous semiconducting thin film with adsorbed dye molecules. Inspired by photosynthesis- the natural process that plants use to convert sunlight into energy, they have received considerable attention since O'Regan and Gratzel reported an -initially- outstanding high conversion efficiency of nearly 10% (O'Regan & Gratzel, 1991) using nanocrystalline mesoporous TiO_2 films. These films can be prepared using simple techniques such as: spin coating, dip coating, and screen printing.

Since UAE is a desert area, it experiences extremely hot temperatures most of the year. Despite that this harsh climate, there are more than 678 types of terrestrial plant species acclimatized to this climate. The main types of these terrestrial are ferns, flowering plants, ryophytes and mosses (Raghwa et al., 2014). One of the abundant plants in UAE is the *Calotropis* and it is the subject of this study. *Calotropis*, also known as Sodom's apple milkweed, is one of the most popular and spread flowering plant in UAE, which can easily grow in very poor soils. It belongs to Apocynaceae family, about 2.5–6 meter-tall and has white and purple waxy flowers grouped as clusters (Rahimi, 2015). Plants develop normally adaption mechanisms to survive the light fluctuations in its environment. They may adapt either by controlling the light absorption capacity or by controlling the amount of light energy being captured (Jones & Rotenberg, 2011). They optimize light absorption by adjusting the leaf orientation aiding the plants to cope with the excess amount of solar radiation especially at midday. Under extreme lighting conditions, the plants accumulate excess excitation energy that will inevitably lead to photoinhibition and further reduction in the photosynthetic efficiency. Desert plants, in particular, enter a stage where they go into energy storage mode, and all energy harvested from solar radiation goes into providing sustenance to the embryos. These embryos will dry up at a certain point and be transported in air to plant themselves away from the mother plant. Another mechanism with which plants resist excess solar absorption is by changing the deep green colour of the leaves into a pale shade of yellow that absorbs light mostly in the UV region, instead of the former case of mid-visible wavelengths.

Due to the natural origins, it is well known and expected that the extracted natural dyes contain more than one pigments. The mixed composition of the natural dyes generally does not hinder the operation of DSSCs; on the contrary, the blended dyes usually exhibit extended absorption range well beyond that of a single pigment which is beneficial for improving cell efficiency (Chang & Lo, 2010).

Spinach is a well-studied chlorophyll-based natural sensitizer containing mostly chlorophyll-a and chlorophyll-b [Journal of Alloys and Compounds 495 (2010) 606–610]. By comparing the UV-Vis absorption spectrum of dye solutions extracted from Calotropis against spinach (as shown below), it can be observed that similar to spinach, the natural dyes from Calotropis contains mostly chlorophyll-a and chlorophyll-b, as indicated by the absorbance peaks at ~ 470 nm and ~ 660 nm. As future work, the detailed composition and purity of the pigments may be determined by spectro-photometry of chlorophylls to which separate chlorophyll content could be assessed in accordance to the absorbance of the pigment extract at its characteristic wavelength. The equations, first populated by Arnon, follow a certain trend for extraction and aim to provide absorbance coefficients for resolving the two chlorophylls in the mixture depending on the chosen solvent (Ritchie, 2006).

This work investigates using a natural sensitizer extracted from Calotropis, a plant indigenous to the deserts of Sharjah, United Arab Emirates, for natural dye-sensitized solar cell applications. The plant in question is a non-food item, as compared with other natural green sensitizers such as spinach. The latter will be used to sensitize another set of cells for benchmarking purposes, as it is one of the popular natural sensitizers. Since the leaves of the plant also feature a powder material on its surfaces, the effect of adding this powder to the sensitizing dye will also be examined. A detailed account on cell components selection and construction will be given, as well as an electrochemical cell impedance analysis, and cell performance parameters. The proposed dye material comes from a plant that is abundant, adaptive to harsh environmental conditions and also inconsumable as source of sustenance for people and livestock makes it a very attractive natural sensitizer both ecologically and economically. This being said, the obtained results are not expected to surpass synthetic sensitizers, such as ruthenium-based dyes in terms of performance (power output and efficiency), the natural dye extract proposed here are far more economical and are readily available.

MATERIALS AND METHODS

Photo-electrode and counter-electrode preparation

The photo-electrode was used as-received from Solaronix (http://shop.solaronix.com/solar-cell-kits/test-cell-kits/test-cell-spare-parts.html). It is composed of glass substrates of 20 × 20 × 2 mm with a coating of TCO22-7 FTO. The 6 × 6 mm active area of titania coating consists of an active layer of Titanium nanoxide covered by a reflective layer of Titanium nanoxide, both of which were prepared by screen-printing. The electrodes were fired up to around 400 °C for 30 minutes and left to cool to around 60 °C before being immersed in the dye solution. The counter electrode substrate, also used as-received from Solaronix, comprises of the same dimensions of the photo-electrode and FTO coating. The 20 × 20 mm active area was prepared by screen-printing for a homogenous surface using the Platisol T/SP precursor.

Dye Extraction

The leaves were first rinsed thoroughly with water and left to dry in air. 4.23 g of the leaves with an average surface area of 1 cm^2 were placed in 25 mL of ethanol and degassed for 10 minutes. The leaves were then sonicated for 20 minutes, after which the leaves were filtered out and the remaining solution was filtered through a PTFE syringe filter of 0.45 μm pores. Each electrode (now at 60 °C) was submerged in 7 mL of the solution. The dye was covered and stored in a dark environment overnight for dye adsorption.

Powder Composition

XRF (X-ray fluorescence) from Horiba, XGT 7200 operating with a Rh target, a tube voltage of 50 kV and tube current of 1mA is used to determine the elemental composition of the dye materials.

Optical Characterization

Optical characterizations were carried out via Maya 2000-Pro high-resolution spectrometers (OceanOptics). The dedicated spectrometer measured a wavelength range from 400 nm to 800 nm with a resolution of 0.2 nm. For reflectance measurement, we used a ISP-REF integrating sphere with a WS-1 reflectance standard for reflectance calibration from OceanOptics. The transmissivity of the stained titania electrodes was measured an HL-2000 tungsten halogen light source and was converted into absorbance by Eq. 1 (SHU, 2018).

$$A(a.u) = 2 - \log(\%T) \quad (1)$$

The integrating sphere (OceanOptics ISP-REF, with a sample aperture of 0.4 inch) has a built-in tungsten halogen light source (Ocean Optics LS-1-LL) and is capable of measuring specular and diffuse reflectance. The reflectance standard is used to store baseline absorptance (0%) spectra to facilitate comparison between the various compositions.

Solar Cell Assembly

After the staining process, the photoelectrode was rinsed by ethanol to remove any excess dye residues and was allowed to dry in air. The powder from the bottom of the Calotropis leaf was carefully tapped onto the active area of the stained substrate with an amount equivalent to an area of 0.5 cm^2 on the leaf is added to the solution.

Subsequently, a Meltonix 1170-60 sealing film gasket was placed around electrode active area and the space was filled with an iodide/tri-iodide based electrolyte (Iodolyte AN-50 from Solaronix). The DSSC was then assembled by placing the photoelectrode and counterelectrode in place with binder clips.

Cell performance testing and temperature response study/impedance testing

The current-voltage (*I*-*V*) measurements of DSSCs were carried out with a Keithley 2400 SourceMeter under an ABET SunLite solar simulator at AM1.5G and 1,000 W m^{-2} irradiance at room temperature (25 °C).

Impedance spectra were obtained using an impedance analyzer potentiostat (VSP-300) under illumination with the sun simulator. An AC signal of 14.2 mV was applied to the cell under 1-Sun conditions. The frequency range was varied between 100 kHz and 0.1 Hz with a fixed applied bias voltage of the open circuit potential of the DSSC with a potential resolution of 20 μV. The spectra were fitted using the Z-Fit analysis software from Bio-logic.

RESULTS AND DISCUSSION

Powder composition

The XRF analysis of the powder material found covering the *Calotropis* leaves has revealed that it is composed mainly of calcium (~60%), chlorine (~16%) and iron (~8%) and the rest are traces of various elements that registered on both top and bottom leaf surfaces. The optical effect of this material manifest in terms of heat input mitigation, as a radiation scattering mechanism that is coupled with the leaf reflectivity. In this work, the powder will also be added to the extracted dye to capitalize on the ionic species that appear to exist in its composition. The full XRF analysis of the *Calotropis* leaves is shown in Table 1. Fig. 1 (a) and (b) also show the leaves with and without powder, respectively.

Table 1. Summary of XRF analysis of *Calotropis* leaves

Element	Mg	Si	P	S	Cl	K	Ca	Ti	Cr	Mn	Fe	Ni	Zn	Sr
Mass %	4.15	8.33	0.77	5.70	7.58	0.96	59.42	0.83	0.15	0.71	10.36	0.28	0.25	0.51

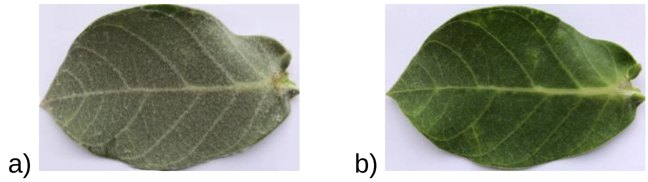

Figure 1. Calotropis leaves a) with powder and b) without powder.

Optical properties

The effect of the presence of the powder material on the leaves (before crushing) and on the dye extract (after crushing) is investigated. The reflectivity of the leaves is measured from both sides (top and bottom) for the as-is leaves (with powder) and for cleaned leaves (without powder). For the latter case, both sides showed similar reflectivity trends over the test spectrum (400–800 nm) with the top side exhibiting less reflective losses especially in the visible region, as shown in Fig. 2 (a).

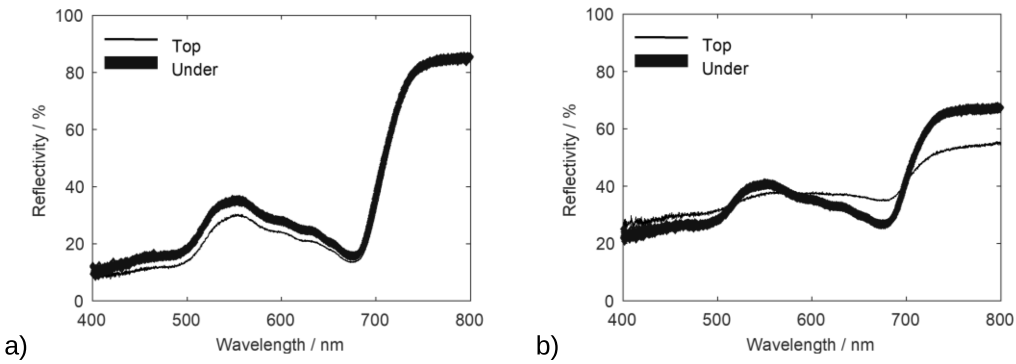

Figure 2. Reflectivity measurement for leaves (a) cleaned from powder and (b) with powder layer intact.

The as-is leaves shows a big decrease of reflectivity in close to the infrared region, with the top side exhibiting a less pronounced knee around the 680 nm mark compared with the bottom side as seen Fig. 2 (b). The reflectivity of the bottom side in the infrared region for the with-powder case is also around 44% more than the top side. These trends indicate that the enhanced reflectivity of the bottom surface of the leaves work to direct any stray rays to the top surface of adjacent leaves by reflecting off their bottom surface. This is especially true for a small portion of the visible region (between ~ 520–270 nm) and also for the NIR portion between 700–800 nm.

The powder itself as a solid-state material, however, exhibits different reflectivity depending on the side from which it has been collected as seen in Fig. 3.

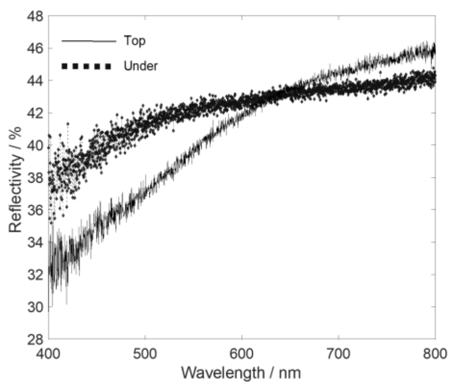

Figure 3. Reflectivity of the powder material.

The bottom powder is more reflective between 400–600 nm, while its counterpart from the top takes over after 650 nm, allowing more absorbance of the low energy incidence on the topside, mainly to mitigate heat generation within the plant.

Following the dye extraction from *Calotropis* leaves, another optical assessment was conducted by applying the dye on a photoelectrode (FTO with TiO_2 deposit). Fig. 4 shows its absorbance results compared with a bare TiO_2 reference, and another electrode soaked with the chlorophyll II pigment source (spinach), which is a common natural sensitizer used in literature (Chang et al., 2010). The bandgaps are also calculated and shown in inset.

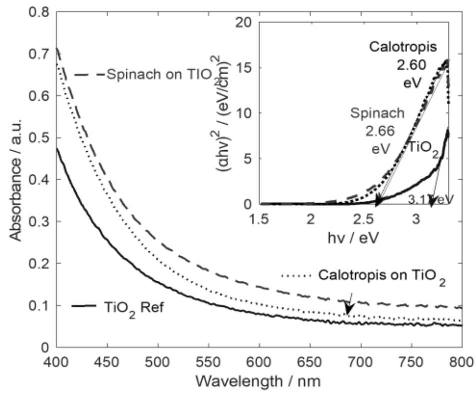

Figure 4. Spectral absorbance of *Calotropis* dye compared with a bare titania photoelectrode and another soaked in spinach (chlorophyll II). The bandgaps are calculated via T_{auc} formula.

The absorbance curves show the expected higher spectral absorbance at the violet-blue region for both spinach and the *Calotropis* dyes, with the former leveling off at the edge of the visible region as the latter continues its decline towards the infrared regime. As will be explained later, this has a noticeable effect in enhancing cell performance with less heat-generating radiation being absorbed into the photoelectrode.

Impedance test

To test for applicability of the dye to be used in DSSCs, further details into the workings of the cell are discussed with the aid of impedance spectra.

The impedance test results and its frequency response are shown in Figs 5 and 6. It is evident from Fig. 5 that the overall shape of the EIS spectra is characteristic of DSCs obtained at open circuit potential (Gamry, 2018). There is a bulge at high frequencies followed by a wide semicircle at intermediate frequencies and ending with a tail at low frequencies. This indicates that the cell construction is good for the current test conditions.

The arc observed at high frequencies (shown inset of Fig. 5), is attributed to the charge transfer processes at the counter-electrode/electrolyte interface. It is not very pronounced which indicates that the electrode is still active and could be enhanced/pre-treated for better cell performance.

At intermediate frequencies, the wide peak seen is attributed to the electron diffusion in the TiO_2 film and the electron transfer at the TiO_2/electrolyte interface. It is evident that the diameter of the semicircle in the intermediate frequency region was large proving the capability of the effective suppression of the back reaction of the injected electrons with tri-iodide species in the electrolyte, this leads to a relatively high value of photovoltage.

At low frequencies, the tail of the peak corresponds to a slow diffusion process of I_3^- in the electrolyte. With time and at relatively high illumination, the electrolyte loses its viscosity making it harder to transport ions through the electrolyte and this peak would disappear. This peak usually becomes more pronounced for fully degraded cells because of the increase in tri-iodide species in the electrolyte that is seen to accelerate the recapture of electrons in the conduction band, which in turn reduces availability within the oxide layer. For the case at hand, the concentration of the tri-iodide species is of a relatively low concentration compared to iodide species and is seen as an advantage to reduce charge recombination and its adverse effect on cell performance.

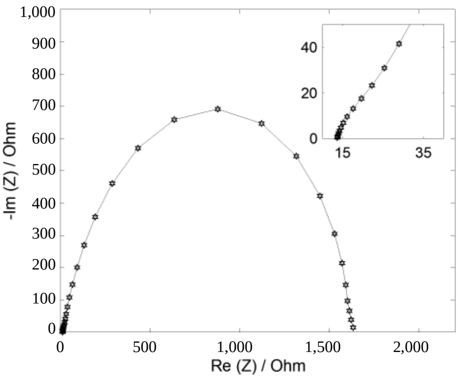

Figure 5. Nyquist plot of tested cell.

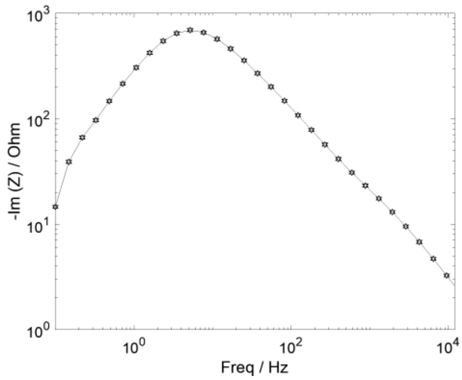

Figure 6. Frequency response of the tested cell.

The Bode plot of the assembled cell is shown in Fig. 6 for the frequency response of the cell. The more the main peak shifts to the right, the higher the rate of transfer at TiO_2/dye/electrolyte interface. It can be observed that the cell is not performing at optimal conditions, which means that better efficiencies can be obtained from the cell with more appropriate ambient test conditions (e.g. irradiance, temperature, electrolyte concentration).

Cell testing

DSSCs using dyes extracted from the leaves of *Calotropis* (with and without the powder on the leaves of *Calotropis* added onto the stained photoelectrode) were assembled and tested at room temperature under simulated 1-sun AM1.5G irradiance. As a reference, a DSSC using dye extracted from spinach was also tested, which is a proven robust natural dye in DSSC studies (Syafinar et alıo, 2015). The current density-voltage (J-V) characteristic curves are plotted in Fig. 7 along with the experimental error bars, while the corresponding photovoltaic parameters of these DSSCs are summarized in Table 2.

From the results, both solar cells using dye extracted from *Calotropis* (with and without adding powder) showed better performance compared to the spinach cell, suggesting that the dye from *Calotropis* can be served as an excellent natural light sensitizer. Furthermore, it is evident that the addition of the powder from the *Calotropis* leaves led to an overall performance enhancement in *Calotropis*-based DSSCs. Notably, the open circuit voltage (V_{OC}) was improved from 0.410 to 0.573 V and fill factor (FF) was increased from 47.6% to 63.2%. This considerable improvement in FF is due to the addition of the powder material and the more efficient charge transfer process it introduces between the dye and the redox couple, as indicated in literature (Al-Alwani et al., 2015). These findings are also consistent with our findings from the impedance tests described above. In addition, the short-circuit current density (J_{SC}) increased slightly from 0.555 to 0.592 mA cm^{-2} which may correspond to the changes in cell optical reflectivity as measured in Fig. 3. Consequently, the power conversion efficiency (PCE) of DSSCs using *Calotropis* dye was significantly enhanced from 0.108% to 0.214%.

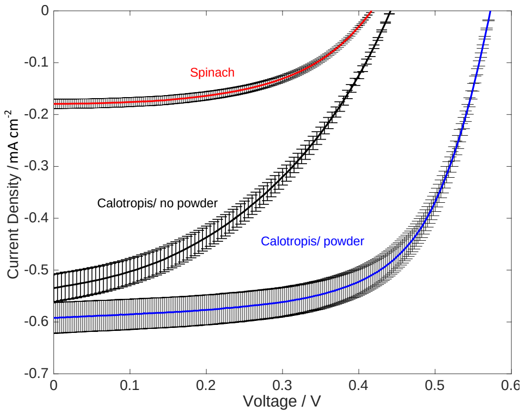

Figure 7. Current density-voltage (*J*-*V*) characteristics of DSSCs using dyes from *Calotropis* and spinach, shown with experimental error bars.

Table 2. Summary of photovoltaic parameters for DSSCs

Parameter	Spinach	Calotropis (no powder)	Calotropis (with powder)
J_{sc}, mA cm^{-2}	0.18	0.55	0.59
V_{oc}, V	0.41	0.41	0.57
FF, %	52.70	47.60	63.20
PCE, %	0.04	0.11	0.21

CONCLUSIONS

This work assessed the performance enhancement of solar cells sensitized via a natural dye extracted from a non-food plant (*Calotropis*) that is both native to and abundant in the desert regions of the United Arab Emirates. The dye used in a number of dye-sensitized solar cells has shown good enhancement of power output and efficiency (~67% more power and ~87% more power) compared with a common natural sensitizer (spinach). The *Calotropis* leaves are also covered with a powder that is thought to help mitigate heat generated within the leaf due to incident radiation in the harsh desert climate. This presence of this powder on the leaf prompted using it with the extracted dye (leaves are used without cleaning off the powder), as its composition shows a significant number of ionic species that would enhance the catalytic activity of the cell. This is proven when another set of cells were constructed with powder added to *Calotropis* dye extracts showed a further significant enhancement on the power, fill factor and efficiency. The latter reached 0.214%, a 50% enhancement over its non-powder counterpart. The future work will include better dye.

REFERENCES

Al-Alwani, M.A.M, Mohamad, A.B, Kadhum, A.A.H. & Ludin, N.A. 2015. Effect of solvents on the extraction of natural pigments and absorption onto TiO2 for dye-sensitized solar cell applications. Spectrochimica Acta Part A: *Molecular and Biomolecular Spectroscopy* **138**, 130–137.

Bhattacharya, S. Chakrabarti, H. & Reehal, V. Lakshminarayanan (eds). *Advances in optical science and engineering*. Springer proceedings in physics, vol. **194**. Springer, Singapore.

Bloomberg new energy finance. New energy outlook 2015. BNEF: London, 2015; June 23.

Breyer, C., Bogdanov, D., Gulagi, A., Aghahosseini, A., Barbosa, L.S.N.S., Koskinen, O., Barasa, M., Caldera, U. Afanasyeva, S., Child, M., Farfan, J. & Vainikka, P. 2017. On the role of solar photovoltaics in global energy transition scenarios. Prog. Photovolt: *Res. Appl*. **25**, 727–745.

Chang, H. & Lo, Y. 2010. Pomegranate leaves and mulberry fruit as natural sensitizers for dye-sensitized solar cells. *Solar Energy* **84**(10), 1833–1837.

Chang, H., Wu, H., Chen, T., Huang, K., Jwo, C. & Lo, Y. 2010. Dye-sensitized solar cell using natural dyes extracted from spinach and ipomoea. *Journal of Alloys and Compounds* **495**(2), 606–610.

Choubey, P.C., Oudhia, A. & Dewangan, R. 2012. *A review: solar cell current scenario and future trends*. Recent Research in Science and Technology 4. pp. 99–101.

Gamry.com. 2018. *Dye Solar Cells - DSC - Impedance Measurements, application note*. [online] Available at: https://www.gamry.com/application-notes/physechem/dye-solar-cells-impedance-measurements/ [Accessed 9 Feb. 2018].

Ghosh, K. 2017. Status and Technology of Present Day Solar Cells. *Springer Proceedings in Physics*, pp.19–28.

Hosenuzzaman, M., Rahim, N.A., Selvaraj, J., Hasanuzzaman, M., Malek, A.B.M.A. & Nahar, A. 2015. Global prospects, progress, policies, and environmental impact of solar photovoltaic power generation. *Renewable and Sustainable Energy Reviews* **41**, 284–297.

Jones, H.G. & Rotenberg, E. 2011. *Energy, Radiation and Temperature Regulation in Plants*. In: eLS. John Wiley & Sons, Ltd: Chichester.

Kaltiya, J.M.S., Abubakar, M.S. & Itodo, I.N. 2014. Prediction of global solar radiation using Angstrom-Page equation model for Makurdi Benue State, Nigeria. *American Journal of Engineering Research* **3**, 145–150.

Liu, Y., You, S., Tan, J., Zhang, Y. & Liu, Y. 2018. Frequency response assessment and enhancement of the U.S. power grids towards extra-high photovoltaic generation penetrations – an industry perspective. *IEEE Transactions on Power Systems* **PP**(99), 1–1.

Makrides, G., Zinsser, B., Norton, M., Georghiou, G.E., Schubert, M. & Werner, J.H. 2010. Potential of photovoltaic systems in countries with high solar irradiation. *Renewable and Sustainable Energy Reviews* **14**(2010), 754–762.

O'Regan, B. & Gratzel, M. 1991. A low-cost, high-efficiency solar cell based on dye-sensitized colloidal TiO2 films. *Nature* **353**, 737–740.

Phinikarides, A., Makrides, G., Zinsser, B., Schubert, M. & Georghiou, G.E. 2015. Analysis of photovoltaic system performance time series: Seasonality and performance loss. *Renew. Energy* **77**, 51–63.

Polman, A., Knight, M., Garnett, E.C., Ehrler, B. & Sinke, W.C.2016. Photovoltaic materials: Present efficiencies and future challenges. *Science* **352**, 307–315.

Raghwa, G. 2014. *Life in the plant kingdom*. Developed Environment Agency – Abu Dhabi (EAD) and the Energy and Resources Institute (TERI), United Arab Emirates, ISBN 978-9948-20-720-7.

Rahimi, M. 2015. Pharmacognostical Aspects and Pharmacological activities of Calotropis procera. *Bull. Env. Pharmacol. Life Sci.* **4**. pp. 156–162.

Renewable energy policy network for the 21st century. Renewables 2016 – global status report, Paris. 2016. www.ren21.net/wp-content/uploads/ 2016/06/GSR_2016_Full_Report_REN21.pdf.

Ritchie, R. 2006. Consistant sets of spectrophotometric chlorophyll equations for acetone, methanol and ethanol solvents. *Photosyn Res*. **89**(1), 27–41.

Said, Z., Alshehhi, Abdulla, A. & Mehmood, A. 2018. Predictions of UAE's renewable energy mix in 2030. *Renewable Energy* **118**, 779–789.

Sharma, S., Jain, K.K. & Sharma, A. 2015. Solar cells: In research and applications—a review. *Materials Sciences and Applications* **6**, pp 1145–1155.

Sharma, S., Siwach, B., Ghoshal, S.K. & Mohan, D. 2017. Dye sensitized solar cells: From genesis to recent drifts. *Renewable and Sustainable Energy Reviews* **70**, 529–537.

Sheffield Hallam University. 2018. *Beer's Law*. Sheffield: Sheffield Hallam University.

Sherwani, A.F., Usmani, J.A. & Varun. 2010. Life cycle assessment of solar PV based electricity generation systems: A review. *Renewable and Sustainable Energy Reviews* **14**, 540–544.

Shockley, W. & Queisser, H.J. 1961. Detailed balance limit of efficiency of p-n junction solar cells. *Journal of Applied Physics* **32**, 510–519.

Smith, Y. & Bogust, P. 2018. Review of Solar Silicon Recycling. *Energy Technology* **2018**, 463–470.

Syafinar, R., Gomesh, N., Irwanto, M., Fareq, M. & Irwan, Y. 2015. Chlorophyll Pigments as Nature Based Dye for Dye-Sensitized Solar Cell (DSSC). *Energy Procedia* **79**, 896–902.

Wang, H., Munoz-Garcia, M.A., Moreda, G.P. & Alonso-Garcia, M.C. 2017. Seasonal performance comparison of three grid connected photovoltaic systems based on different technologies operating under the same conditions. *Solar Energy* **144**, 798–807.

Wu, J., Lan, Z., Lin, J., Huang, M., Huang, Y., Fan, L. & Luo, G.2015. Electrolytes in Dye-Sensitized Solar Cells. *Chemical Reviews* **115**, 2136−2173.

Agronomy Research **16**(4), 1580–1589, 2018
https://doi.org/10.15159/AR.18.178

The impact of weather conditions on microclimate in storage facilities

J. Bradna*, J. Šimon, D. Hájek and D. Vejchar

Research institute of Agricultural Engineering, p. r. i., Drnovská 507, CZ16101 Prague 6 - Ruzyně, Czech Republic
*Correspondence: jiri.bradna@vuzt.cz

Abstract. The key to maintaining good qualitative parameters of stored grain on farms is to achieve and maintain suitable storage temperatures relative to the outside temperature. In the framework of this research, the main focus was on typical representatives of grain storage facilities used in the Czech agriculture. In the post-harvest period after the crops were stored in the chosen storage facilities, the temperature of the material was monitored at 15-minute intervals using an external temperature probe as well as the temperature and dew point of the outdoor air. A simple linear regression model was used for data analysis. The correlated temperature dependence of the stored grain varies considerably in the monitored storage facilities. The storage halls were characterized by a low dependence (r = 0.2208) of the temperature of the material on the outside air temperature in the first 4 months following the harvest when the grains were being stabilized by active aeration. In addition to the grain and the air temperature, the second focus was monitoring the dew point, i.e. assessing the risk of water vapour condensation on the surface in the upper layer of the stored grain, which is very undesirable for maintaining the quality of the stored grain. The results show that the monitored storage hall can be characterized by the ability to maintain the required climate due to outdoor climatic conditions. In general, this ability mainly depends on the type and design of the storage facility, the aeration system and also the storage capacity. Mainly during spring the dew point and water vapour condensation can often happen within the grain, therefore the need to focus on appropriate measures such as reduced aeration or increased grain mixing, and thus avoiding the formation of critical spots.

Key words: grain storage, temperature variation, aeration, postharvest treatment.

INTRODUCTION

The supply of grain for food processing is seasonal due to the local weather conditions and possibilities of agriculture production, whereas the food industries require a continuous supply of raw materials (Laszlo & Adrian, 2009). This rises problems with logistic system and mainly with sophisticated storage areas. Achieving the necessary postharvest quality of stored grain is often the main problem in agricultural storage facilities. The qualitative indicators of produce are controlled and maintained during storage by adjustment of the physical environment. Lowering the temperature and water activity in stored grains is one task of climate control inside a storage facility so that the biological activity of the potential biological agents is minimised (Jia et al., 2001). Contamination or destruction of stored grains can be caused by insects, mites and fungi and their biological products. An important step for quality assurance is also the postharvest treatment (precise cleaning, sorting) and optimized transport routes in postharvest lines to prevent grain damage during this period (Skalický et al., 2008; Fourar-Belaifa et al., 2011).

Stored grains are living organisms which will react to their microclimatic conditions. Deterioration of stored grain may result from improper combinations of physical, chemical and biological variables (Cetiner et al., 2017). Heat, moisture and carbon-dioxide which are produced by respiration of undried grains and they promote the activities of decomposing organisms. The rate of reproduction and growth of these organisms is mostly dependent on temperature and moisture content of the grains (Capouchová et al., 2009). The grain forms an ecological system in which the grain and other organisms interact while being influenced by the ambient conditions (Polišenská et al., 2010). The knowledge of grain behaviour during storage, safety guidelines for storage, facility management and quality control procedures can be used to minimise quality loss in stored grain (Kibar, 2015). Low temperatures are important for maintaining the quality of the grains and ideal storage conditions in silos (Kibar, 2016).

Modern methods of storing grains are in silos (grain towers), storage halls or in small units (storage palette boxes, big bags etc.) which serve for seeding purposes or end producers. Among these, metal silos are the most preferred and built due to long-term protection effect on the stored grains. Furthermore, metal silos can take different shapes (mostly cylindrical or rectangular) and volumes from tens to thousands of tons (Skalický et al., 2008).

In comparison with storage halls, metal silos experience more moisture condensation resulting from temperature fluctuations within the silo and hot spots due to elevated temperatures in some parts often without the possibility to increase the aeration enough (Hammami et al., 2017). Storage halls can have bigger potential storage volume and possibility of better aeration because of smaller height of stored layer and variability in design of installed aeration ducts. Mathematical models can be developed for prediction of temperatures and moisture content at specific locations in the stored grains (Laszlo & Adrian, 2009; Casada, 2000; Jia et al., 2001). These models can be used to optimize the locations of sensors for detecting increased temperatures in stored grains.

Temperature distribution in the material is affected by multiple factors. Firstly, they are weather conditions such as ambient air temperature, air convection, solar radiation, location of the warehouse with respect to prevailing local wind direction. Second set are the structure, design and size of the warehouse. Convective heat transfer is not the only active heat transfer mechanism in a storage hall or silo. It should be noted that the unaccounted effect of ambient temperature and relative humidity on the bottom layer of the silo is equally of great significance (Yang et al., 2002).

In this article, the ability of a storage hall to maintain the required climate inside a as depending on outdoor climatic conditions was evaluated. To address these problems this storage facility had been equipped with an installation of sufficient aeration system with floor aeration ducts. Therefore, the objective of this research was to evaluate temperature changes inside the storage area and their dependence on climate conditions with statistical methods.

MATERIALS AND METHODS

A long-term storage experiment on a farm in the Central Bohemian Region monitored the impact of outdoor conditions on the microclimate within the storage environment and the consumption of electrical energy for aeration. The main stored products in this particular warehouse are wheat and malting barley. In the monitored period (2016–2017 season) 1,800 t of barley malt were stored in both halves of the storage hall i.e. 3600 t in total. The building length is 59 m and width is 19 m. There was used semi-circular aeration ducts with dimensions height 35 cm and width 65 cm, length of one section 90 cm, together 20 sections. Each aeration duct was connected to one medium pressure radial vent that provide 20–30 $m^3 h^{-1}$ of air per tonne of stored grain and the required pressure of 1,500 Pa.

To measure the temperature of air between the grains, penetration probes with Pt1000 temperature sensors were installed in the material layer reaching to depth of 2.1 meters and placed 4 meters from the walls. The data was collected by a 4-channel Comet R3120 datalogger for long-term recording. A Comet S3631 datalogger was placed in the middle of the monitored part of the warehouse above the layer to record ambient air temperature and relative humidity, and one additional penetration probe to measure again the temperature at 2.1 m depth. The penetration temperature probes were placed so that they were not directly above any of the aeration ducts. Another Comet S3120 data logger was placed on the northern side of the storage building to measure the temperature and relative humidity of the outdoor environment in the immediate vicinity of the storage hall. Temperature variations within the storage hall over 12 month period in 2 storage seasons have been measured and evaluated.

We also measured the electric power consumption for aeration using a dual channel logger Comet S7021 with pulse and binary input to define how aeration influence inside temperature. The recording interval of all data loggers was set to 15 minutes. Arithmetic average of temperatures from the five measuring points was used to describe the temperature between grains at any given time. The dependencies between selected parameters were evaluated using linear regression,

$$y = a + bx\ (R^2), \qquad (1)$$

where y – dependent variable (daily temperature difference in grain, daily temperature in grain); a – y-intercept; b – slope of the line; x – independent variable (daily electric power consumption, daily outdoor temperature), R^2 – determination coefficient.

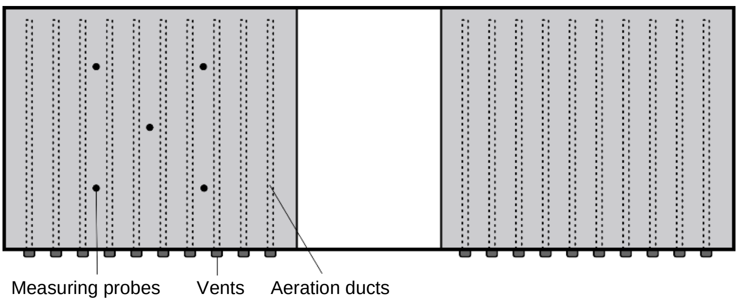

Figure 1. The measurement points in the storage hall viewed from above.

Fig. 1 shows the location of the probes inside the warehouse. The whole measurement took place in one half of the warehouse. About 1,800 t of malting barley was stored in the monitored portion.

The measured quantities: t_m – the air temperature inside the stored grain (measured at a depth of 2.1 m); t_{dpi} – dew point temperature in ambient air inside the warehouse; φ_i – relative ambient air humidity in the warehouse; t_e – outside air temperature; t_{dpe} – dew point temperature outside; φ_e – relative humidity outside; E – electric power consumption for aeration.

Technical data of used thermo-hygrometers Comet R3120, S3120, S3631: temperature measuring range -30 to 70 °C: accuracy 0.4 °C, accuracy of humidity measurement 2.5% RH, resolution of reading 0.1 °C, 0.1 RH.

RESULTS AND DISCUSSION

The monthly summaries of the monitored parameters of the indoor environment of the storage hall are shown in Tables 1–3.

Table 1. Monthly minimum values of the observed parameters of microclimatic conditions

Month/Year	t_m °C	t_{dpi} °C	φ_i %	t_e °C	t_{dpe} °C	φ_e %
7/2016	18.9	7.4	27.5	9.8	7.1	15.6
8/2016	15.8	3.6	20.2	6.8	4.8	24.7
9/2016	18.8	2.6	20	5.8	3.4	23.5
10/2016	19.5	0.2	29.1	1.8	0.7	27.8
11/2016	18.1	-8.8	34.6	-5	-9.2	34.4
12/2016	15.5	-11.1	33.5	-8.4	-11.1	41
1/2017	12.8	-17.7	44.5	-14.1	-18	53.4
2/2017	11.5	-10.1	25.3	-8	-10.4	32.3
8/2017	15.5	5.8	22.3	9.6	5.7	32.9
9/2017	16.5	3.3	33.5	6.6	3.6	44.1
10/2017	17.3	-2.8	34.1	0.5	-2.1	48.8
11/2017	16.7	-4.5	52.6	0	-3.8	63.7

Table 2. Monthly average values of the observed microclimatic conditions

Month/Year	t_m °C	t_{dpi} °C	φ_i %	t_e °C	t_{dpe} °C	φ_e %
7/2016	21.17	14.33	64.67	20.11	13.85	50.65
8/2016	20.9	12.29	59.92	18.9	12.2	49.21
9/2016	20.63	10.88	59.44	17.61	11.16	50
10/2016	20.5	5.61	80.58	8.02	6.01	67.07
11/2016	19.01	0.91	80.58	3.22	0.42	80.81
12/2016	16.75	-2.12	81.81	-0.01	-2.42	84.2
1/2017	14.4	-7.84	75.76	-5.23	-8.3	79.27
2/2017	12.03	-2.15	73.54	1.67	-2.64	74.45
8/2017	19.27	12.8	59.16	20.66	13.31	64.29
9/2017	17.82	8.88	74.75	12.88	9.23	79.5
10/2017	17.58	7.32	78.19	10.54	7.78	83.67
11/2017	17.09	1.88	83.27	4.29	2.42	87.96

Table 3. Monthly maximum values of the observed microclimatic conditions

Month/Year	t_m °C	t_{dpi} °C	φ_i %	t_e °C	t_{dpe} °C	φ_e %
7/2016	24.5	19.7	95.2	32.2	19	74.2
8/2016	30.9	23.7	95.4	30	19	75.5
9/2016	23	16.5	96.3	30.1	17.6	75.7
10/2016	21.3	12.1	97.7	23.2	12.2	78.8
11/2016	19.6	8.8	97.9	13.1	8.5	97.3
12/2016	18.2	6.7	94.7	9.8	6.6	96.5
1/2017	15.7	0.2	92.4	2.8	0	93.6
2/2017	12.9	6.7	96.2	12	6.7	95
8/2017	22	18.7	96.2	34	21.4	96.4
9/2017	19.3	15	98	21.9	15.6	99.1
10/2017	17.8	14.5	97.8	20.9	14.1	100
11/2017	17.4	7.2	97.3	12.4	7.9	100

Monthly temperature summaries inside the stored malting barley and outside temperatures are shown in Figs 2–3.

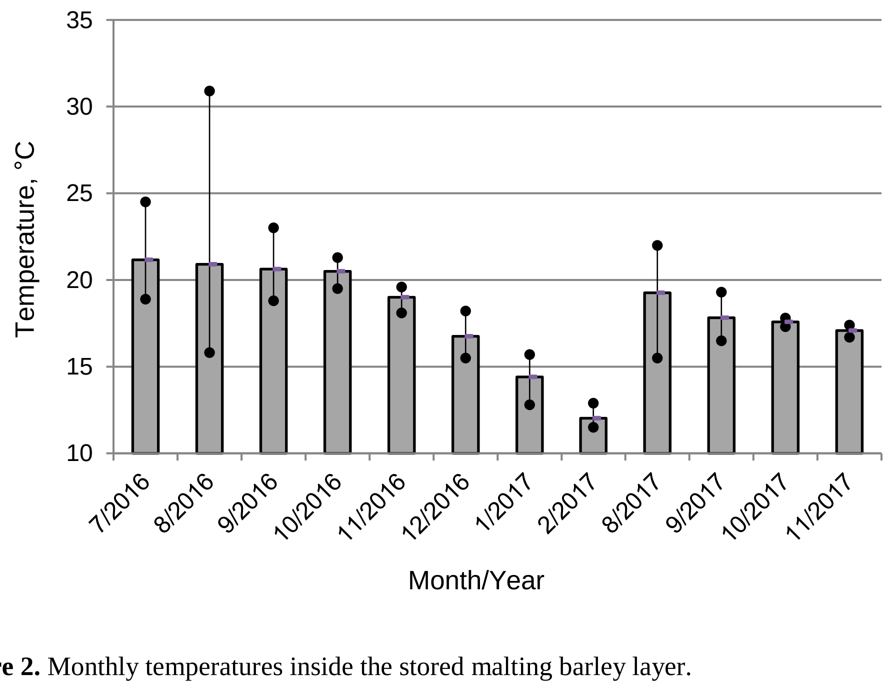

Figure 2. Monthly temperatures inside the stored malting barley layer.

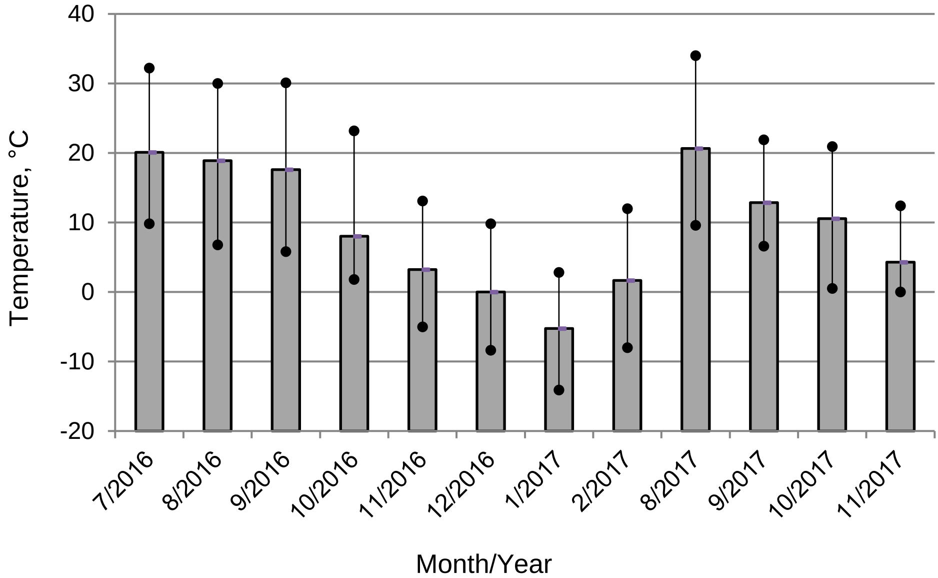

Figure 3. Monthly outside temperatures in the location of the observed storage facility.

The graph of average daily temperatures and the consumption of electrical energy for aeration during a period of storage is shown in Fig. 4.

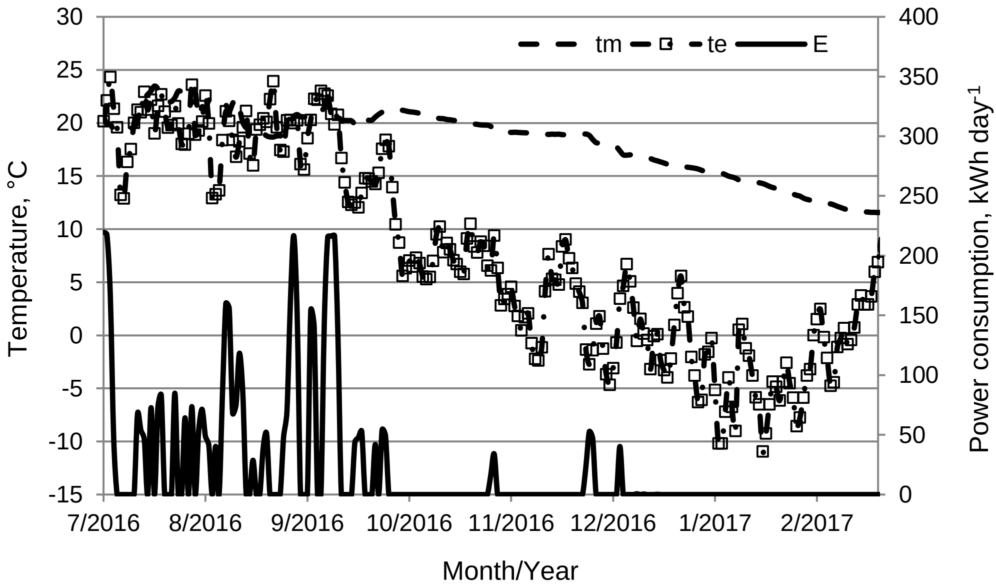

Figure 4. Daily average temperatures and electric power consumption for aeration.

Daily temperature difference and daily electric power consumption for aeration are shown in Fig. 5.

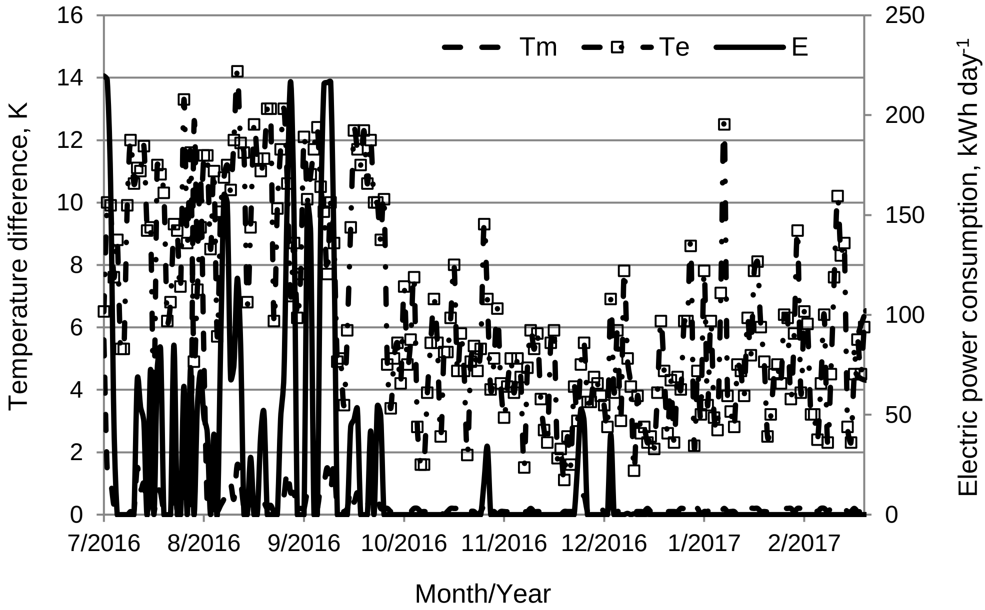

Figure 5. Daily temperature difference and daily electric power consumption for aeration.

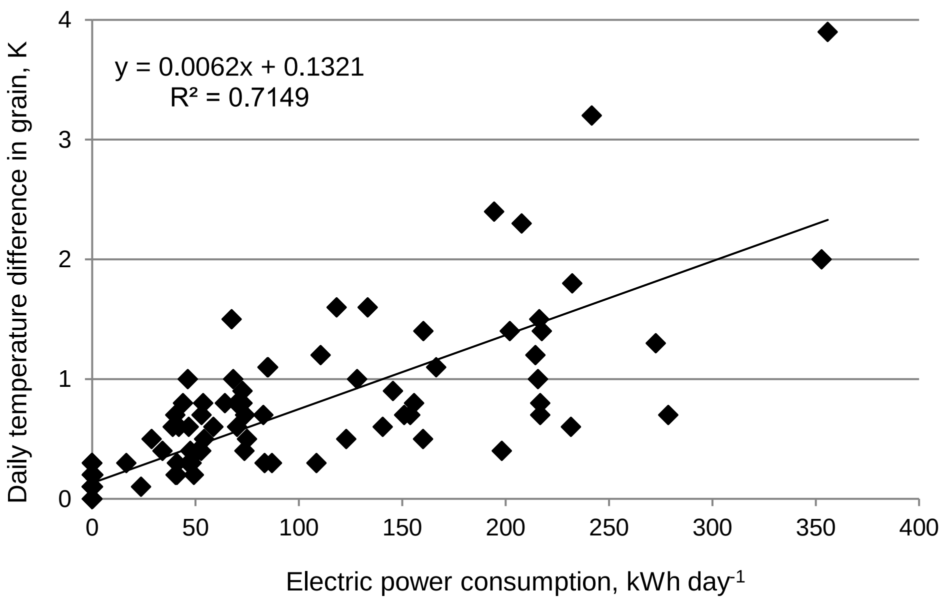

Figure 6. The effect of daily electric power consumption of aeration on daily temperature difference in the malting barley layer.

The daily fluctuations in the temperature inside the stored material in dependence on the consumed energy for aeration are shown in Fig. 6. The linear regression model shows a very strong dependence (r = 0.8455) of daily temperature fluctuations on the consumption of electricity for aeration. Dependence of the average daily temperature inside the grain on outside temperature is shown in Fig. 7. The monitored storage space shows good ability to maintain the required climate in unfavourable outdoor climatic conditions compared, for example, to tower silos due to the capacity and insulation capabilities. Fig. 7 shows a simple linear regression model of the temperature dependence of the stored material inside the store at the outside temperature. This dependence is determined by the thermal insulation properties of the perimeter shell of the warehouse, the use of aeration technology as well as the storage capacity. The correlation coefficient 0.6898 shows strong dependence in the long-term data from entire storage season. During the first 4 months after harvest when grain stabilization by active aeration are used, this dependence is only very weak (r = 0.2208).

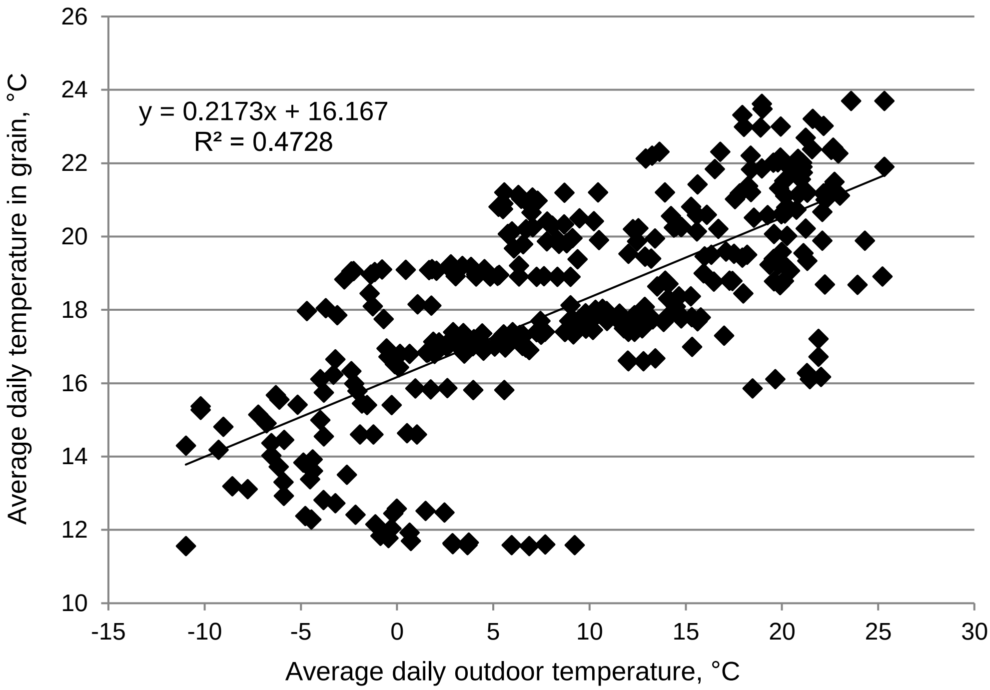

Figure 7. The effect of average daily outdoor temperature on average daily temperature in the malting barley layer.

Generally, in storage halls thanks to storing more grain and to characteristics of storage halls, the trends will be as shown in Figs 2 and 3, Tables 1–3, where the temperature fluctuations within the stored material (air between grains) are not significant and the temperature only copies the general trend from outside temperature, respectively the indoor environment of the warehouse. The temperature inside the material reacts less sensitively to the temperature fluctuations of the external environment due to the good insulation properties of the hall warehouse.

It is also important to note that the temperature difference between the one measured in material layer and inside ambient temperature should be less than 5 °C, as is shown in Fig. 4 at the beginning two months of storage season. Alabadan (2006) reported that the ambient temperatures during the dry season were higher than the wet season. Lawrence et al. (2013) found that the grain surface temperature within a silo was higher than the ambient by 5 °C, which is in agreement with the results herein. Similarly, Lawrence & Maier (2012) reported a difference of 4 °C between different configurations of a silo for maize storage.

Fig. 4 and Fig. 5 indicate that the temperature inside the barley were still higher when the ambient temperature began to decrease in September. The high temperature can cause the stored grains to spoil. The higher temperatures above the grain surface might have been influenced by solar radiation between the roofing and surface layer. To avoid this problem it is necessary to use the installed aeration system in autumn months to let the excess heat escape (Laszlo & Adrian, 2009). Zhang et al. (2016) also show similar results in temperature variation in small grain steel silos installed in a storage hall.

CONCLUSIONS

The key to preserving good qualitative parameters in stored malting barley is to achieve and maintain a suitable storage temperature without major temperature fluctuations. The most favourable grain storage temperatures are generally set at 5–10 °C. The temperature 25 °C should not be exceeded over a long period of time, therefore it is essential to aerate the storage of the commodity immediately after the harvest. The results of the monitoring show a very strong dependence of temperature changes during the day in the barley on the consumption of electricity for aeration. Moreover, the long-term dependence of the average daily average temperature inside the barley on the average daily outside temperature has been demonstrated, but this dependence is significantly lower than in conventional tower silos due to the thermal insulation properties of the perimeter shell, the aeration system used and the capacity of the stored material. Moreover, the results show that this dependence is very weak during the first four months after the harvest, when the stored material is being stabilized by active aeration.

Temperature variations within the storage hall over 12 month period in 2 storage seasons have been measured and evaluated. Temperature variations at 2.1 m depth inside the layer of barley grain increased from July through the end of September in comparison with the measured outdoor temperature and in comparison with the rest of the season. This may probably be associated with heat of respiration of the grains together with the accumulated heat gain during the day and long hours of solar radiation. The variation occurring from July to the start of dry season (October) might be responsible for the slight temperature build up in September. This may imply that the storage hall will need aeration to decrease excessive heat build-up that may lead to deterioration of stored grains quality and possible presence of insects, fungi and their products.

ACKNOWLEDGEMENTS. This research was supported by the Ministry of Agriculture of the Czech Republic, project NAZV QJ1510204 and by an institutional project of the Ministry of Agriculture of the Czech Republic (RO0617).

REFERENCES

Alabadan, B.A. 2006. Temperature changes in bulk stored maize. *AU J. T.* **9**(3), 187–192.

Capouchová I, Papoušková L, Hajšlová J, Prokinová E, Kostelanská M, Škeříková A, Dvořáček V, Pazderů K, Faměra O. 2009. Risk of Fusarium infection occurence for wheat baking quality. *Úroda* **12**, 521–526 (in Czech).

Casada, M.E. 2000. Adapting a grain storage model in a 2-D generilised coordinate system. *ASAE Annual International Meeting*, pp. 1–14.

Cetiner, B., Acar, O., Kahraman, K., Sanal, T. & Koksel, H. 2017. An investigation on the effect of heat-moisture treatment on baking quality of wheat by using response surface methodology. *Journal of Cereal Science* **74**, 103–111.

Fourar-Belaifa, R., Fleurat-Lessard, F. & Bouznad, Z. 2011. A systemic approach to qualitative changes in the stored-wheat ecosystem: Prediction of deterioration risks in unsafe storage conditions in relation to relative humidity level, infestation by Sitophilus oryzae (L.), and wheat variety. *Journal of Stored Products Research* **47**(1), 48–61.

Hammami, F., Ben Mabrouk, S. & Mami, A. 2017. Numerical investigation of low relative humidity aeration impact on the moisture content of stored wheat. *International Journal of Modeling, Simulation, and Scientific Computing* **8**(2), 1740002.

Jia, C., Suna, D.W. & Caob, C. 2001. Computer simulation of temperature changes in a wheat storage bin. *Journal of Stored Products Research* **37**, 165–177.

Kibar, H. 2015. Influence of storage conditions on the quality properties of wheat varieties. *Journal of Stored Products Research* **62**, 8–15.

Kibar, H. 2016. Determining the functional characteristics of wheat and corn grains depending on storage time and temperature. *Journal of Food Processing and Preservation* **40**(4), 749–759.

Laszlo, R. & Adrian, T. 2009. Simulation of changes in a wheat storage bin regarding temperature. Analele Universităţii Din Oradea, Fascicula: Protecţia Mediului **14**(1), pp. 239–244.

Lawrence, J., Maier, D.E. & Stroshine, R.L. 2013. Three-dimensional transient heat, mass, momentum, and species transfer in the stored grain ecosystem: Part II. Model validation. *Transaction of the American Society of Agricultural and Biological Engineering* **56**(1), 181–201.

Lawrence, J. & Maier, D.E. 2012. Prediction of temperature distributions in peaked, levelled and inverted cone grain mass configurations during aeration of corn. *Applied Engineering in Agriculture, American Society of Agricultural and Biological Engineers* **28**(5), 685–692.

Polišenská, I, Pfohl-Leszkowicz, A, Hadjeba, K, Dohnal, V, Jirsa, O, Denešová, O, Ježková, A, & Macharačková, P. 2010. Occurence of ochratoxin A and citrinin in Czech cereals and comparison of two HPLC methods for ochratoxin A detection. *Food Additives and Contaminants* **27**(11), 1545–1557.

Skalický, J., Kroupa, P., Bradna, J. & Pastorková, L. 2008. *Ošetřování a skladování zrnin ve věžových a halových skladech*. [*Grain treatment and storage in tower silos and indoor storehouses*]. 1. vyd. Praha: Výzkumný ústav zemědělské techniky, 80 pp. ISBN 978-80-86884-38-7

Yang, W., Jia, C.C., Siebenmorgen, T.J., Howell, T.A. & Cnossen, A.G. 2002. Intra-kernel moisture responses of rice to drying and tempering treatments by finite-element simulation. *Transaction of the American Society of Agricultural and Biological Engineering* **45**(4), 1037–1044.

Zhang, L., Chen, X., Liu, H., Peng, W., Zhang, Z. & Ren, G. 2016. Experiment and simulation research of storage for small grain steel silo. *International Journal Agricultural and Biological Engineering* **9**(3), 170–178.

Agronomy Research **16**(4), 1590–1606, 2018
https://doi.org/10.15159/AR.18.173

Mathematical model of cleaning potatoes on surface of spiral separator

V. Bulgakov[1], S. Nikolaenko[1], M. Arak[2], I. Holovach[1], Z. Ruzhylo[1] and J. Olt[2,*]

[1]National University of Life and Environmental Sciences of Ukraine, Heroyiv Oborony street 15, UA03041Kyiv, Ukraine
[2]Estonian University of Life Sciences, Institute of Technology, Kreutzwaldi 56, EE51006 Tartu, Estonia
[*]Correspondence: jyri.olt@emu.ee

Abstract. Cleaning potato tubers from soil impurities and plant debris after digging them out of soil is a topical problem in the work process of potato production. Therefore, the engineering of new designs of potato heap separators necessitates the further studying of them and the optimisation of their kinematic and design parameters, which must not only ensure the high quality of cleaning, but also rule out the possibility of damaging the tubers. The aim of this study is to determine the design and kinematic parameters of the improved design of the spiral potato separator, which will ensure the high quality of cleaning and rule out the possibility of damaging the tubers, on the basis of the development of the new theory of potato tuber's motion on the surface of the separator. An analytical study has been carried out resulting in the construction of the equivalent schematic model of the interaction between the potato tuber and separator, the tuber being approximated by a material point on the surface formed by the two cantilevered spirals, which are the separator's tools. The separator's spirals are driven to rotate and at the same time they can perform oscillations in the vertical and axial plane under the action of the varying load generated by the continuous feeding of the potato heap for separation. In the model, the forces acting on the potato tuber's body are applied to it, the coordinate axes that have been selected and appropriately oriented are shown. A system of equations has been set up for the constructed equivalent schematic model, comprising three differential equations of the potato tuber body's motion on the surface of the trough formed by the two cantilevered spirals. The determined kinematic and design parameters will allow to raise the quality of cleaning potato tubers from soil impurities and plant debris.

Key words: potato, tuber, separation, impact interaction, impact impulse, rational parameters.

INTRODUCTION

Improving the quality of the cleaning of potatoes from soil impurities and plant debris directly after their digging out from the soil allows considerably improving the main indicators of the potato harvesting work process. In order to determine the optimum design and kinematic parameters of the engineered design, it is necessary to investigate analytically the process of interaction between the potato tuber and the helical cleaning surface of the separator, i.e. to construct the analytical mathematical model of the said process. The subsequent numerical modelling of the process under consideration with the use of the PC will allow determining the optimum values of the mentioned parameters subject to the condition that the potato tubers are not damaged, when they are on the surface of the spiral separator during their cleaning.

The application of various separators and cleaning machines for cleaning the potato heap immediately after its extraction from the soil has stipulated the publication of considerable numbers of books and papers in various scientists (Peters, 1997; Petrov, 2004; Veerman & Wustman, 2005; Bishop et al., 2012; Wang et al., 2017). That being the case, significant part of the published papers are concerned with the conditions that ensure the stable motion of potato tubers on the separating surfaces of the cleaning machines and the guaranteed sifting (removal) of soil impurities and plant debris from the separation zone (Feller et al., 1987; Misener & McLeod, 1989; Ichiki et al., 2013; Bulgakov et al., 2018a; 2018b).

Authors developed a design of the spiral potato separator (Fig. 1), which includes the assembly of three spirals mounted each on its drive shaft with the other end free (cantilevered). The potato heap to be separated is fed on them from above, which results in a significant part of soil impurities being immediately sifted down. Meanwhile, the potato tubers are entrained by the coils of spirals and transported along their axes, provided that the coils of spiral springs do not entrain impurities, while the said coils are capable of self-cleaning from the stuck wet soil in the process of their operation. The field testing of the potato heap separator under consideration has shown positive results Bulgakov et al., 2017), which provides the basis for further investigation of the described process with the aim of optimising the design and kinematic parameters of the new separating appliance.

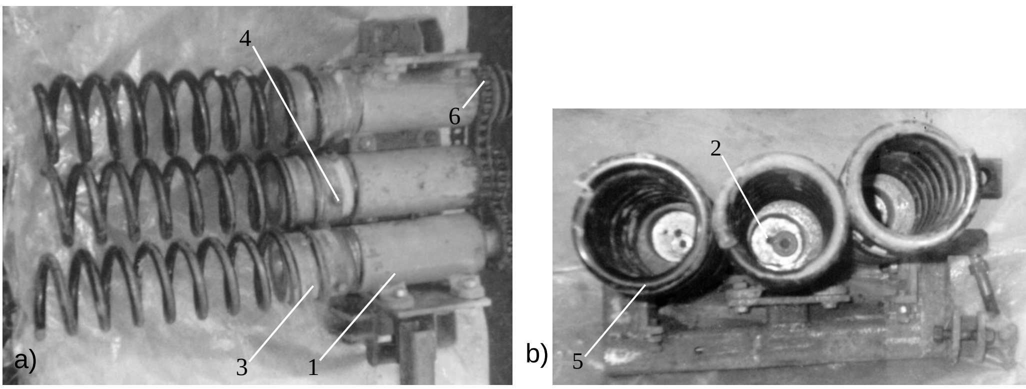

Figure 1. The spiral potato heap separator: a) top view; b) side view. 1 – bearing pedestal; 2 – hub; 3 – bearing ring; 4 – fastener; 5 – cleaning spiral; 6 – sprocket wheel.

The aim of the study is to determine the design and kinematic parameters of the improved design of the spiral potato separator, which ensure the high quality of cleaning and rule out any damage to the tubers, basing on the development of a new theory of the potato tuber's motion on the separator's surface.

MATERIALS AND METHODS

In order to construct the analytical mathematical model of the potato tuber's motion on the spiral separator's surface, it is necessary first to identify the said tuber with a material point, which is approximated by a solid sphere with a mass of m and a radius of r_b. A schematic model will be constructed basing on the analysis of various modes of the relative motion of a single potato tuber, i.e. a material point, on the surface of the spiral separator (Fig. 2). The latter is represented by the two cantilevered driven spirals 1 and 2 rotating about their longitudinal axes at equal angular velocities of ω. Thereby, one end of each spiral is attached rigidly to its drive shaft, the second end is free. The winding senses of the spirals 1 and 2 are shown by the arrows. The identical pitch S of both windings is shown in Fig. 1. Initially, the potato tuber's body in the form of the material point designated by the letter C, which has, as it was indicated earlier, a radius of r_b, arrives onto the surface of the first spiral winding 1, which has a specified radius of R and a pitch angle of γ. The spiral winding 1 starts entraining the material point C, i.e. the potato tuber, by its helical line into their joint motion, i.e. in the rotational motion together with the spiral winding itself, and the translational motion along the spiral's axis, i.e. along the direction of its winding.

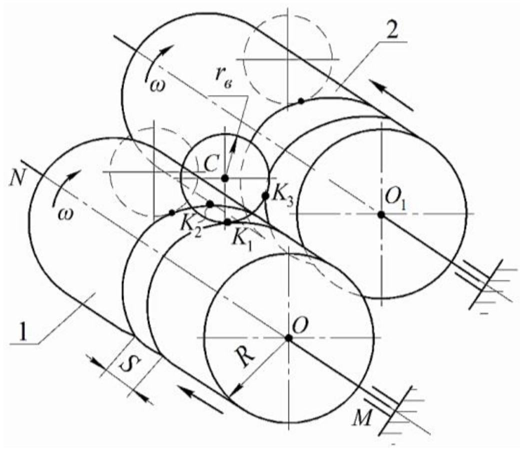

Figure 2. Schematic model of potato tuber's relative motion on surface of spiral separator.

However, as a result of the action of the force of gravity on the potato tuber and the rotation of the spiral 1, the potato tuber will in a very short time reach the trough between the neighbouring spirals 1 and 2. Obviously, within this short time, after its small displacement along the helical line (spiral), the potato tuber will virtually not move along the spiral's longitudinal axis, i.e. the axis MN in this instance. That means that the potato tuber, while residing on the upper side of the spiral 1, cannot be transported to any appreciable distance by the coils of this spiral alone. Therefore, the main advancement of the potato tuber along the MN axis can take place, only when the tuber is in the trough formed by the two neighbouring spirals 1 and 2. Moreover, the duration of the single potato tuber staying at the top, on the coil of only one spiral 1, will be negligibly small, because under the effect of its own weight or by the action of the continuously fed flow of the potato heap to be cleaned the tuber will certainly be pushed forward and down. Hence, detailed analysis is needed for the transportation of potato tubers just in the case, when the tuber has fallen into the trough formed by the two adjacent spirals 1 and 2 of the separator.

At the same time, after the potato tuber falls into the space between the two neighbouring spirals 1 and 2 (Fig. 2), i.e. into the trough, it will surely stay in it and it is unlikely that the tuber immediately ascends to the top of the spiral 2, although, in principle, such a situation cannot be ruled out in view of the rotation of the spiral 2 and the presence of the force of friction between the tuber and the coils of the spiral 2. Nevertheless, it is fair to say that the more probable scenario is, when the potato tuber under the action of the friction force, despite being possibly captured by the coils of the spiral 2 and drawn into the joint motion, very soon rolls or slides down either back into the same trough or into the next trough between the spirals 2 and 3. Summing up, the potato tuber's motion along the trough between the coils of the spirals 1 and 2 without any breakaways will be considered.

It is obvious that, upon reaching the certain critical angular velocity of ω in the rotation of the spiral 1, the potato tuber can take off from the surface of the spiral 1 and fly over all the three spirals, but that case ought to be regarded as a sufficiently rare one and it should be investigated separately.

Whereas in case of the potato tuber's motion on the coils of the spiral 1 without breaking away followed by its falling down into the trough between the spirals 1 and 2, the spiral 2 serves as the thrust surface that prevents the potato tuber from moving (perpendicular to the MN axis (effectively, on the surface of the spiral 2).

As the potato tuber, while residing in the mentioned trough between the spirals 1 and 2, at the same time stays between two adjacent coils of the spiral 1 that continues to rotate, the said coils slipping on the tuber's surface, but restraining the tuber on both sides and retaining it in the groove between them, move it along the MN axis.

It makes no difference for the potato tuber's translation along the MN axis, whether the tuber moves along the helical groove formed by the two adjacent coils or the tuber is quiescent and the groove moves along the tuber. Since the spiral 2 rotates with the same sense as the spiral 1 and the coils of both the spirals wind identically, the coil of the spiral 2 thrusting against the potato tuber slips on its surface, acting as a thrust surface.

Thus, the contact between the potato tuber and the surfaces of the spirals 1 and 2 during the tuber's translation along the MN axis occurs at the three points K_1, K_2 and K_3, as shown in Fig. 2.

But, the translational motion of the potato tuber along the MN axis is only theoretically close to straight-line motion (basing on the purely geometrical properties of the helical line). In effect, due to a number of random factors, in particular, due to the variable mass of the separated potato heap passing on the surface of all the three spirals, the said spirals perform linear, at a first approximation, oscillations on a vertical line, i.e. perpendicular to the MN axis, which contribute to the sifting of the soil fed together with the potato tubers and other plant residues as well as the cleaning of the tubers' side surfaces from the stuck soil. In this process, the potato tubers perform three-dimensional oscillations about their centres of mass, and in some cases also angular displacements about some of their axes. Evidently, the said oscillations and angular displacements are of random nature. But, for the most part, the potato tubers situated on the surfaces of the separator's spiral springs perform together with the spirals linear translational oscillations oriented vertically, i.e. perpendicular to the MN axis.

Nevertheless, the principal motion of the potato tuber is its translational displacement along the MN axis (i.e. along the trough between the spirals 1 and 2) under the action of the reaction forces applied by the helical groove or, to be more accurate, by the coil that pushes against the potato tuber, propelling it along the MN axis. The said helical groove acts as the constraint that shapes, for its part, the line of the normal reaction force applied to the potato tuber during its translation along the MN axis, and the equation of that line should be taken as the equation of constraint. Apparently, the main cleanup of the potato tubers from the stuck soil and the sifting of soil and other foreign materials from the potato heap fed for separation take place during the translation of potato tubers along the MN axis alongside with the oscillations of the spirals.

Therefore, it is reasonable first to investigate the process of the translation of a potato tuber situated in the trough between the two spirals under the action of the spirals' helical coils.

RESULTS AND DISCUSSION

In order to generate the analytical mathematical model of the mentioned process, the equivalent schematic model of the interaction between the potato tuber and the surfaces of the above-mentioned separator spiral coils (Fig. 3) has to be set up. In the case under consideration, the potato tuber resides in the trough between the spirals 1 and 2, and on the spiral 1 it is situated in the space between two adjacent coils, its surface supported by both the spiral coils. It is easily evident that, enumerating the two above-mentioned coils in the direction of the tuber's progression along the MN axis, the first coil acts as the pushing element, the second coil acts as the bearing part. The coil of the spiral 2, as it was already pointed out earlier, acts as the thrust part. Hence, as can be seen in Fig. 2 and Fig. 3, at the points of the spirals' contacts with the tuber's surface (its shape being close to spherical) K_1, K_2 and K_3 the normal reaction forces N_1, N_2 and N_3, respectively, are applied. The force of gravity acting on the tuber $\bar{G}$ is applied to the potato tuber's centre of mass (point C) and is vectored vertically down.

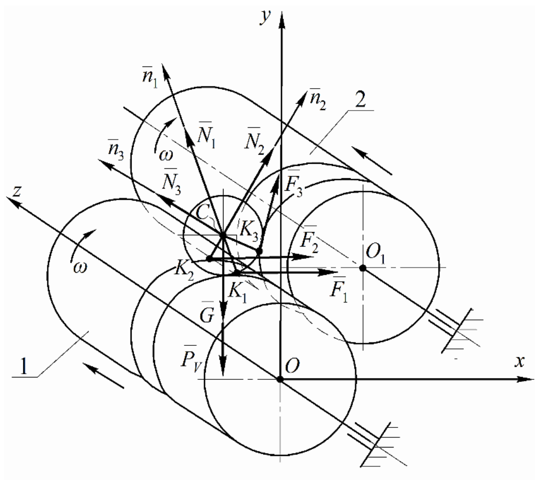

Figure 3. Equivalent schematic model of interaction between potato tuber's body and spiral separator's surface.

The potato tuber's motion under the action of the system of forces shown in the equivalent schematic model (Fig. 3) will be investigated with reference to the fixed Cartesian coordinate system xOyz with its origin (point O) situated on the MN longitudinal axis of the spiral 1, its axis Oz coinciding with the MN longitudinal axis of the spiral 1, the axis Oy being directed vertically up and the axis Ox being directed to the right and contained in the spiral's cross-section plane.

After selecting the coordinate system, the forces applied to the potato tuber, as shown in Fig. 3, have to be described.

They are, first of all: N_1, N_2 and N_3 – the normal reaction forces exerted by the surfaces of the coils of the spirals 1 and 2, respectively, vectored along the common normal lines on the surfaces of the coils and the tuber at the points of contact K_1, K_2 and K_3, respectively, their vectors crossing the tuber's centre (point C). Thus, their lines of action intersect at the point C.

F_1, F_2 and F_3 – friction forces, which are generated, when the coils of the spirals 1 and 2 as well as the spiral 3, respectively, slip on the surface of the potato tuber at the points of contact K_1, K_2 and K_3, respectively. They are vectored in the same directions, as the spirals' senses of rotation, along the common tangents of the coils and the surface of the potato tuber.

As is known, the F_i forces of sliding friction are expressed as follows:

$$F_i = f \cdot N_i, \;\; i = 1,2,3, \tag{1}$$

where f – coefficient of sliding friction for the potato tuber sliding on the spiral's material (most often spring steel). In case of potato tubers, it can be assumed that $f = 0.2…0.3$ (Guo & Campanella, 2017).

G – potato tuber's force of gravity (N), which can be found, as is known, from the following expression:

$$G = mg \tag{2}$$

where m – mass of the potato tuber (kg); g – gravity acceleration (m s^{-2}).

$\bar{P}_V$ – force of the fed potato heap's dynamic action on the spiral separator that causes the spiral's bending (bending force), vectored vertically down.

The first step is to set up the potato tuber's equation of motion in vector notation on the basis of the constructed equivalent schematic model (Fig. 2):

$$m\bar{a} = \bar{G} + \bar{N}_1 + \bar{N}_2 + \bar{N}_3 + \bar{F}_1 + \bar{F}_2 + \bar{F}_3 + \bar{P}_V, \tag{3}$$

where $\bar{\alpha}$ – potato tuber's translation acceleration under the action of the described system of forces (m s^{-2}).

In terms of the projections on the axes of the fixed Cartesian coordinate system xOyz, the vector Eq. (3) takes the following form:

$$\left.\begin{aligned}
m\ddot{x} &= N_1\cos\left(x,\hat{\bar{n}}_1\right) + N_2\cos\left(x,\hat{\bar{n}}_2\right) + N_3\cos\left(x,\hat{\bar{n}}_3\right) - F_1\cos\left(x,\hat{\bar{V}}_1\right) - \\
&\quad - F_2\cos\left(x,\hat{\bar{V}}_2\right) - F_3\cos\left(x,\hat{\bar{V}}_3\right), \\
m\ddot{y} &= N_1\cos\left(y,\hat{\bar{n}}_1\right) + N_2\cos\left(y,\hat{\bar{n}}_2\right) + N_3\cos\left(y,\hat{\bar{n}}_3\right) - F_1\cos\left(y,\hat{\bar{V}}_1\right) - \\
&\quad - F_2\cos\left(y,\hat{\bar{V}}_2\right) - F_3\cos\left(y,\hat{\bar{V}}_3\right) - G - P_V, \\
m\ddot{z} &= N_1\cos\left(z,\hat{\bar{n}}_1\right) + N_2\cos\left(z,\hat{\bar{n}}_2\right) + N_3\cos\left(z,\hat{\bar{n}}_3\right) - F_1\cos\left(z,\hat{\bar{V}}_1\right) - \\
&\quad - F_2\cos\left(z,\hat{\bar{V}}_2\right) - F_3\cos\left(z,\hat{\bar{V}}_3\right).
\end{aligned}\right\} \tag{4}$$

In order to simplify the obtained system of differential Eq. (4), it is assumed that the potato tuber sits symmetrically in the trough between the spirals 1 and 2, i.e. its centre of mass (point C) is located in the middle of the said trough. In that event, as may be inferred from Fig. 2, the following is obtained:

$$
\left.\begin{aligned}
m\ddot{x} &= (N_1+N_2)\cos\left(x,\hat{\bar{n}}_1\right) - N_3\cos\left(x,\hat{\bar{n}}_3\right) - \\
&\quad -(F_1+F_2)\cos\left(x,\hat{\bar{V}}_1\right) - F_3\cos\left(x,\hat{\bar{V}}_3\right), \\
m\ddot{y} &= (N_1+N_2)\cos\left(y,\hat{\bar{n}}_1\right) + N_3\cos\left(y,\hat{\bar{n}}_3\right) - \\
&\quad -(F_1+F_2)\cos\left(y,\hat{\bar{V}}_1\right) - F_3\cos\left(y,\hat{\bar{V}}_3\right) - G - P_V, \\
m\ddot{z} &= (N_1-N_2)\cos\left(z,\hat{\bar{n}}_1\right) + N_3\cos\left(z,\hat{\bar{n}}_3\right) - \\
&\quad -(F_1+F_2)\cos\left(z,\hat{\bar{V}}_1\right) - F_3\cos\left(z,\hat{\bar{V}}_3\right).
\end{aligned}\right\} \qquad (5)
$$

where $\bar{n}_1, \bar{n}_2, \bar{n}_3$ – common normal lines on the surfaces of the coils and the tuber at the points of contact K_1, K_2 and K_3, respectively; $\bar{V}_1, \bar{V}_2, \bar{V}_3$ – velocity vectors of the potato tuber's relative motion along the spirals' coils at the points of contact K_1, K_2 and K_3, respectively, vectored along the common tangents of the surfaces of the coils and the potato tuber in the directions opposite to the coils' circumferential velocities at the points of contact.

The next step is to determine the direction cosines of the angles between the axes of the coordinate system xOyz and the normal lines on the coils' surfaces at the K_1, K_2 and K_3 points of contact between the potato tuber and the coils of the spirals 1 and 2 included in the system of differential Eq. (5).

The direction cosines $\cos\left(x,\hat{\bar{n}}_i\right)$, $\cos\left(y,\hat{\bar{n}}_i\right)$, $\cos\left(z,\hat{\bar{n}}_i\right)$, $i = 1, 2, 3$, are defined by the following dependencies:

$$
\begin{aligned}
\cos\left(x,\hat{\bar{n}}_i\right) &= \frac{\partial f_k}{\partial x}\cdot(\Delta f_k)^{-1}, \\
\cos\left(y,\hat{\bar{n}}_i\right) &= \frac{\partial f_k}{\partial y}\cdot(\Delta f_k)^{-1}, \\
\cos\left(z,\hat{\bar{n}}_i\right) &= \frac{\partial f_k}{\partial z}\cdot(\Delta f_k)^{-1}, \\
i &= 1, 2, 3;\ k = 1, 2,
\end{aligned} \qquad (6)
$$

where Δf_k – modulus of gradient of the function $f_k = f_k(x, y, z)$ determined from the following expression:

$$
\Delta f_k = \sqrt{\left(\frac{\partial f_k}{\partial x}\right)^2 + \left(\frac{\partial f_k}{\partial y}\right)^2 + \left(\frac{\partial f_k}{\partial z}\right)^2},\ k = 1, 2 \qquad (7)
$$

$f_k = f_k(x, y, z)$, $k = 1, 2$ – equation of constraint that corresponds to the equation of surface of the spiral winding.

For the cylindrical spiral 1 with the specified dimensions and the longitudinal axis coinciding with the coordinate axis Oz, the equation of constraint in the Cartesian coordinate system xOyz appears as:

$$f_1 = \frac{S^2}{4\pi^2}\left[\frac{x\cdot\sin\frac{2\pi z}{S} - y\cdot\cos\frac{2\pi z}{S}}{\sqrt{x^2+y^2}}\right]\cdot\cos\left(\frac{S}{2\pi\sqrt{x^2+y^2}}\right)+ \tag{8}$$

$$+\left(\sqrt{x^2+y^2}-R\right)^2 - r^2 = 0.$$

Since the longitudinal axis of symmetry of the spiral 2 is offset to the right along the Ox axis by the centre-to-centre distance equal to *a*, its equation of constraint in the Cartesian coordinate system xOyz appears as follows:

$$f_2 = \frac{S^2}{4\pi^2}\left[\frac{(x-a)\sin\frac{2\pi z}{S} - y\cdot\cos\frac{2\pi z}{S}}{\sqrt{(x-a)^2+y^2}}\right]\cos\left(\frac{S}{2\pi\sqrt{(x-a)^2+y^2}}\right)+ \tag{9}$$

$$+\left[\sqrt{(x-a)^2+y^2}-R\right]^2 - r^2 = 0,$$

where S – spiral winding pitch.

At this stage, it is necessary first to determine the relevant partial derivatives and the gradient of the function that represents the equation of constraint. In order to achieve that, the equations of constraints (8) and (9) have to be differentiated with respect to the *x, y, z* variables, then, in the obtained expressions, the *x*, *y* and *z* variables have to be substituted by their parametric expressions, which will be determined as follows. According to Krause & Minkin (2005), the parametric equations of the helical lines (coils) of the spirals 1 and 2 have to be written down. They appear as follows:

– for the spiral 1:

$$\left.\begin{aligned} x &= R\cos(\psi_{01}+\psi),\\ y &= R\sin(\psi_{01}+\psi),\\ z &= -S\psi\cdot(2\pi)^{-1}, \end{aligned}\right\} \tag{10}$$

– for the spiral 2:

$$\left.\begin{aligned} x &= a + R\cos(\psi_{02}+\psi),\\ y &= R\sin(\psi_{02}-\psi),\\ z &= -S\psi\cdot(2\pi)^{-1}, \end{aligned}\right\} \tag{11}$$

where R – radius of the spiral; $\psi = \omega t$ – independent angular parameter of the spiral, which defines the position of the cross-section within the spiral's length; ψ_{01}, ψ_{02} – initial values of the independent angular parameters of the spirals 1 and 2, respectively, at the initial instant $t = 0$; a – centre-to-centre distance between the spirals 1 and 2.

Considering the fact that the corresponding cross-section of the spiral 2 (in the place of contact of the mentioned spirals with the potato tuber at the points K_1, K_2 and K_3 is displaced by an angle of π with respect to the angular parameter of the spiral 1, the following initial values of the angular parameters are assumed:

$$\psi_{01} = 0,\ \ \psi_{02} = \pi. \tag{12}$$

Thereupon, the parametric Eq. (10) and (11), subject to (12), take the following form:

– for the spiral 1:

$$\left.\begin{aligned} x &= R\cos(\omega t), \\ y &= R\sin(\omega t), \\ z &= -S\omega t\cdot(2\pi)^{-1}, \end{aligned}\right\} \tag{13}$$

– for the spiral 2:

$$\left.\begin{aligned} x &= a + R\cos(\omega t + \pi), \\ y &= R\sin(\omega t + \pi), \\ z &= -S\omega t\cdot(2\pi)^{-1}, \end{aligned}\right\} \tag{14}$$

or

$$\left.\begin{aligned} x &= a - R\cos(\omega t), \\ y &= -R\sin(\omega t), \\ z &= -S\omega t\cdot(2\pi)^{-1}. \end{aligned}\right\} \tag{15}$$

As a result of the above-mentioned operations of differentiating the constraint equations and substituting the variables x, y and z in the obtained values of partial derivatives by their parametric expressions (13) and (15), the following expressions are obtained for the partial derivatives in the parametric form:

$$\frac{\partial f_1}{\partial x} = \frac{\partial f_2}{\partial x} = A\sin(\omega t) + B\cos(\omega t)\cdot\sin(2\omega t), \tag{16}$$

$$\frac{\partial f_1}{\partial y} = \frac{\partial f_2}{\partial y} = A\cos(\omega t) + B\sin(\omega t)\cdot\sin(2\omega t), \tag{17}$$

$$\frac{\partial f_1}{\partial z} = C\cdot\cos(2\omega t), \tag{18}$$

$$\frac{\partial f_2}{\partial z} = -C\cdot\cos(2\omega t), \tag{19}$$

where

$$A = -\frac{S^2}{4\pi^2 R}\cdot\cos\left(\frac{S}{2\pi R}\right), \tag{20}$$

$$B = \frac{S^2}{4\pi^2 R}\cdot\cos\left(\frac{S}{2\pi R}\right) - \frac{S^3}{8\pi^3 R^2}\cdot\sin\left(\frac{S}{2\pi R}\right), \tag{21}$$

$$C = \frac{S}{2\pi}\cdot\cos\left(\frac{S}{2\pi R}\right). \tag{22}$$

Thereat, the gradients of the functions $f_1(x,y,z)$and $f_2(x,y,z)$ are equal and, according to (7), are determined by the following formula:

$$\Delta f_1 = \Delta f_2 = \sqrt{\left[A\sin(\omega t) + B\cos(\omega t)\cdot\sin(2\omega t)\right]^2 + \left[A\cos(\omega t) + B\sin(\omega t)\cdot\sin(2\omega t)\right]^2 + C^2\cos^2(2\omega t)}. \tag{23}$$

Taking into account the expressions (6) and (16)–(23), finally, the target values of the direction cosines of the angles between the coordinate axes and the spiral coils' normal reaction forces at the K_1, K_2 and K_3 points of contact between the potato tuber and the surfaces of coils of the spirals 1 and 2 are obtained:

$$\cos\left(x,\hat{\bar{n}}_1\right) = \cos\left(x,\hat{\bar{n}}_2\right) = -\cos\left(x,\hat{\bar{n}}_3\right) = \frac{A\sin(\omega t) + B\cos(\omega t)\cdot\sin(2\omega t)}{\sqrt{\left[A\sin(\omega t) + B\cos(\omega t)\cdot\sin(2\omega t)\right]^2 + \left[A\cos(\omega t) + B\sin(\omega t)\cdot\sin(2\omega t)\right]^2 + C^2\cos^2(2\omega t)}}, \tag{24}$$

$$\cos\left(y,\hat{\bar{n}}_1\right) = \cos\left(y,\hat{\bar{n}}_2\right) = \cos\left(y,\hat{\bar{n}}_3\right) = \frac{A\cos(\omega t) + B\sin(\omega t)\cdot\sin(2\omega t)}{\sqrt{\left[A\sin(\omega t) + B\cos(\omega t)\cdot\sin(2\omega t)\right]^2 + \left[A\cos(\omega t) + B\sin(\omega t)\cdot\sin(2\omega t)\right]^2 + C^2\cos^2(2\omega t)}}, \tag{25}$$

$$\cos\left(z,\hat{\bar{n}}_1\right) = -\cos\left(z,\hat{\bar{n}}_2\right) = \cos\left(z,\hat{\bar{n}}_3\right) = \frac{C\cdot\cos(2\omega t)}{\sqrt{\left[A\sin(\omega t) + B\cos(\omega t)\cdot\sin(2\omega t)\right]^2 + \left[A\cos(\omega t) + B\sin(\omega t)\cdot\sin(2\omega t)\right]^2 + C^2\cos^2(2\omega t)}}. \tag{26}$$

Further, the cosines of the angles between the vectors of the relative velocity of the potato tuber's motion along the spiral windings at the points of contact K_1, K_2 and K_3 and the coordinate axes Ox, Oy and Oz, i.e. the values $\cos\left(x,\hat{\bar{V}_i}\right)$, $\cos\left(y,\hat{\bar{V}_i}\right)$ and $\cos\left(z,\hat{\bar{V}_i}\right)$, i = 1, 2, 3, have to be determined.

Since the velocity vectors $\bar{V}_1$ and $\bar{V}_2$ are collinear, the following holds true: $\cos\left(x,\hat{\bar{V}_2}\right)=\cos\left(x,\hat{\bar{V}_1}\right)$, $\cos\left(y,\hat{\bar{V}_2}\right)=\cos\left(y,\hat{\bar{V}_1}\right)$, $\cos\left(z,\hat{\bar{V}_2}\right)=\cos\left(z,\hat{\bar{V}_1}\right)$.

The direction cosines $\cos\left(x,\hat{\bar{V}_i}\right)$, $\cos\left(y,\hat{\bar{V}_i}\right)$ and $\cos\left(z,\hat{\bar{V}_i}\right)$ can be found with the use of the following expressions (Vasilenko, 1996):

$$\begin{aligned}
&\cos\left(x,\hat{\bar{V}_i}\right)=\frac{\dot{x}}{V_i}=\frac{\dot{x}}{\sqrt{\dot{x}^2+\dot{y}^2+\dot{z}^2}},\\
&\cos\left(y,\hat{\bar{V}_i}\right)=\frac{\dot{y}}{V_i}=\frac{\dot{y}}{\sqrt{\dot{x}^2+\dot{y}^2+\dot{z}^2}},\\
&\cos\left(z,\hat{\bar{V}_i}\right)=\frac{\dot{z}}{V_i}=\frac{\dot{z}}{\sqrt{\dot{x}^2+\dot{y}^2+\dot{z}^2}},\\
&i=1,2,3.
\end{aligned} \tag{27}$$

For that purpose, the velocities $\bar{V}_i$ =1, 2, 3, of the potato tuber's relative motion along the coils of the spirals 1 and 2 , respectively, have to be determined. That requires differentiating the systems of Eq. (13) and (15) on time *t*. The following is obtained for the spiral 1:

$$\left.\begin{aligned}
\dot{x}&=-R\omega\cdot\sin(\omega t),\\
\dot{y}&=R\omega\cdot\cos(\omega t),\\
\dot{z}&=-S\omega\cdot(2\pi)^{-1},
\end{aligned}\right\} \tag{28}$$

and for the spiral 2:

$$\left.\begin{aligned}
\dot{x}&=R\omega\cdot\sin(\omega t),\\
\dot{y}&=-R\omega\cdot\cos(\omega t),\\
\dot{z}&=-S\omega\cdot(2\pi)^{-1}.
\end{aligned}\right\} \tag{29}$$

The systems of Eq. (28) and (29) represent the formulae for finding the projections of the circumferential velocities of the points on coils during the rotation of the spirals 1 and 2, respectively, on the coordinate axes Ox, Oy and Oz.

Considering the fact that the velocities $\bar{V}_i$, i =1, 2, 3, of the potato tuber's relative motion along the coils are vectored in opposition to the vectors of the circumferential velocities of the points on coils, the projections of their vectors on the coordinate axes Ox, Oy and Oz are opposite in sign, therefore, the systems of Eq. (28) and (29) take the following form:

$$\left.\begin{aligned}\dot{x} &= R\omega\cdot\sin(\omega t),\\ \dot{y} &= -R\omega\cdot\cos(\omega t),\\ \dot{z} &= S\omega\cdot(2\pi)^{-1},\end{aligned}\right\} \tag{30}$$

and

$$\left.\begin{aligned}\dot{x} &= -R\omega\cdot\sin(\omega t),\\ \dot{y} &= R\omega\cdot\cos(\omega t),\\ \dot{z} &= S\omega\cdot(2\pi)^{-1},\end{aligned}\right\} \tag{31}$$

Hence, the velocity modulus of the potato tuber's relative motion along the spirals' coils is equal to:

$$V_i = \sqrt{\dot{x}^2 + \dot{y}^2 + \dot{z}^2}, \quad i = 1, 2, 3, \tag{32}$$

or, after substituting the values (30) and (31) and carrying out the corresponding transformations, the following is obtained:

$$V_i = \frac{\omega}{2\pi}\sqrt{4\pi^2 R^2 + S^2}, \quad i = 1, 2, 3\cdot \tag{33}$$

Thereafter, in accordance with the expressions (27), the required cosines of the angles between the vectors $\bar{V}_i$, i =1, 2, 3, and coordinate axes Ox, Oy and Oz are finally obtained. They appear as follows:

$$\cos\left(x,\hat{\bar{V}_1}\right) = \cos\left(x,\hat{\bar{V}_2}\right) = \frac{2\pi R\cdot\sin(\omega t)}{\sqrt{4\pi^2 R^2 + S^2}}, \tag{34}$$

$$\cos\left(y,\hat{\bar{V}_1}\right) = \cos\left(y,\hat{\bar{V}_2}\right) = -\frac{2\pi R\cdot\cos(\omega t)}{\sqrt{4\pi^2 R^2 + S^2}}, \tag{35}$$

$$\cos\left(z,\hat{\bar{V}_1}\right) = \cos\left(z,\hat{\bar{V}_2}\right) = \frac{S}{\sqrt{4\pi^2 R^2 + S^2}}, \tag{36}$$

$$\cos\left(x,\hat{\bar{V}_3}\right) = -\frac{2\pi R\cdot\sin(\omega t)}{\sqrt{4\pi^2 R^2 + S^2}}, \tag{37}$$

$$\cos\left(y,\hat{\bar{V}_3}\right) = \frac{2\pi R\cdot\cos(\omega t)}{\sqrt{4\pi^2 R^2 + S^2}}, \tag{38}$$

$$\cos\left(z,\hat{\bar{V}_3}\right) = \frac{S}{\sqrt{4\pi^2 R^2 + S^2}}\cdot \tag{39}$$

By substituting the expressions (24)–(26) and (34)–(39) in the system of differential Eq. (5), the following system of differential equations is obtained:

$$\left.\begin{aligned}
m\ddot{x} &= \left(N_1+N_2-N_3\right)\times \\
&\times\frac{A\sin(\omega t)+B\cos(\omega t)\cdot\sin(2\omega t)}{\sqrt{\left[A\sin(\omega t)+B\cos(\omega t)\cdot\sin(2\omega t)\right]^2+\left[A\cos(\omega t)+B\sin(\omega t)\cdot\sin(2\omega t)\right]^2+C^2\cos^2(2\omega t)}}- \\
&-\left(F_1+F_2+F_3\right)\frac{2\pi R\sin(\omega t)}{\sqrt{4\pi^2R^2+S^2}}, \\
m\ddot{y} &= \left(N_1+N_2+N_3\right)\times \\
&\times\frac{A\cos(\omega t)+B\sin(\omega t)\cdot\sin(2\omega t)}{\sqrt{\left[A\sin(\omega t)+B\cos(\omega t)\cdot\sin(2\omega t)\right]^2+\left[A\cos(\omega t)+B\sin(\omega t)\cdot\sin(2\omega t)\right]^2+C^2\cos^2(2\omega t)}}- \\
&-\left(-F_1-F_2+F_3\right)\frac{2\pi R\cos(\omega t)}{\sqrt{4\pi^2R^2+S^2}}-G-P_V, \\
m\ddot{z} &= \left(N_1-N_2+N_3\right)\times \\
&\times\frac{C\cos(2\omega t)}{\sqrt{\left[A\sin(\omega t)+B\cos(\omega t)\cdot\sin(2\omega t)\right]^2+\left[A\cos(\omega t)+B\sin(\omega t)\cdot\sin(2\omega t)\right]^2+C^2\cos^2(2\omega t)}}- \\
&-\left(F_1+F_2+F_3\right)\frac{S}{\sqrt{4\pi^2R^2+S^2}},
\end{aligned}\right\} \quad (40)$$

where the coefficients *A*, *B* and *C* are determined in accordance with the expressions (20), (21) and (22), respectively.

Thus, the system of differential Eq. (40) has been obtained, which describes the potato tuber's motion under the action of the rotating spirals' coils in the absolute coordinate system xOyz, when the tuber resides in the trough between the adjacent spirals.

Meanwhile, as the spirals' rotation is characterised by constant angular velocities of, $\omega = \text{const}$, the potato tuber under the conditions of such steady-state motion moves at a constant velocity of $\bar{V}_i,\ i = 1, 2, 3,$ relative to the surfaces of coils of the spirals 1 and 2, which velocity can be found from the expression (33). But, in the absolute coordinate system the projections of the potato tuber's velocity will be as follows: $V_x = V_y = 0$ and $V_z = S\omega \cdot (2\pi) = \text{const}$, because the potato tuber in the form of a material point moves only along the Oz axis.

Thereby, the $\ddot{x}$, $\ddot{y}$ and $\ddot{z}$ accelerations of the tuber along the three coordinate axes Ox, Oy and Oz can be considered as equal to zero. Hence, putting the left-hand sides of the differential equations in the system (40) to zero, in view of the formula (1), the following system of linear algebraic equations in the unknown quantities N_1, N_2 and N_3 with variable coefficients is obtained:

$$\left.\begin{aligned}
&(N_1+N_2-N_3)\frac{A\sin(\omega t)+B\cos(\omega t)\cdot\sin(2\omega t)}{\sqrt{\left[A\sin(\omega t)+B\cos(\omega t)\cdot\sin(2\omega t)\right]^2+\left[A\cos(\omega t)+B\sin(\omega t)\cdot\sin(2\omega t)\right]^2+C^2\cos^2(2\omega t)}}-\\
&-(fN_1+fN_2+fN_3)\frac{2\pi R\sin(\omega t)}{\sqrt{4\pi^2R^2+S^2}}=0,\\
&(N_1+N_2+N_3)\frac{A\cos(\omega t)+B\sin(\omega t)\cdot\sin(2\omega t)}{\sqrt{\left[A\sin(\omega t)+B\cos(\omega t)\cdot\sin(2\omega t)\right]^2+\left[A\cos(\omega t)+B\sin(\omega t)\cdot\sin(2\omega t)\right]^2+C^2\cos^2(2\omega t)}}-\\
&-(-fN_1-fN_2+fN_3)\frac{2\pi R\cos(\omega t)}{\sqrt{4\pi^2R^2+S^2}}-mg-P_V=0,\\
&(N_1-N_2+N_3)\frac{C\cos(2\omega t)}{\sqrt{\left[A\sin(\omega t)+B\cos(\omega t)\cdot\sin(2\omega t)\right]^2+\left[A\cos(\omega t)+B\sin(\omega t)\cdot\sin(2\omega t)\right]^2+C^2\cos^2(2\omega t)}}-\\
&-(fN_1+fN_2+fN_3)\frac{S}{\sqrt{4\pi^2R^2+S^2}}=0.
\end{aligned}\right\}\quad(41)$$

In essence, the system of Eq. (41) comprises the equations of the potato tuber's equilibrium, when it resides in the trough between the adjacent separator spirals 1 and 2 in contact with the coils of these spirals at the points K_1, K_2 and K_3 (Fig. 1) at the random instant of time t. The fulfilment of the conditions set by (41) ensures the theoretically stable position of the potato tuber in the trough with the constant points of contact K_1, K_2 and K_3 over the period of its translation along the spiral's longitudinal axis, i.e. the axis Oz, up to the moment of its final departure from the spirals.

In this case, the potato tuber, as already mentioned, moves at a constant velocity of $V_z = S\omega\cdot(2\pi)^{-1}$ along the Oz axis up to the point of its departure from the spirals onto the discharge conveyor.

The system of Eq. (41) can be solved analytically with the use of Cramer's rule. In order to do that, the system is to be transformed into the form that allows applying the said method. Hence, the following designations are introduced:

$$\frac{A\sin(\omega t)+B\cos(\omega t)\cdot\sin(2\omega t)}{\sqrt{\left[A\sin(\omega t)+B\cos(\omega t)\cdot\sin(2\omega t)\right]^2+\left[A\cos(\omega t)+B\sin(\omega t)\cdot\sin(2\omega t)\right]^2+C^2\cos^2(2\omega t)}}=A_1 \tag{42}$$

$$\frac{A\cos(\omega t)+B\sin(\omega t)\cdot\sin(2\omega t)}{\sqrt{\left[A\sin(\omega t)+B\cos(\omega t)\cdot\sin(2\omega t)\right]^2+\left[A\cos(\omega t)+B\sin(\omega t)\cdot\sin(2\omega t)\right]^2+C^2\cos^2(2\omega t)}}=A_2 \tag{43}$$

$$\frac{C\cos(2\omega t)}{\sqrt{\left[A\sin(\omega t)+B\cos(\omega t)\cdot\sin(2\omega t)\right]^2+\left[A\cos(\omega t)+B\sin(\omega t)\cdot\sin(2\omega t)\right]^2+C^2\cos^2(2\omega t)}}=A_3 \tag{44}$$

$$\frac{2\pi R\sin(\omega t)}{\sqrt{4\pi^2R^2+S^2}}=B_1 \tag{45}$$

$$\frac{2\pi R\cos(\omega t)}{\sqrt{4\pi^2R^2+S^2}}=B_2 \tag{46}$$

$$\frac{S}{\sqrt{4\pi^2R^2+S^2}}=B_3\cdot \tag{47}$$

Substituting the expressions (42–47) in the system of Eq. (41), the following system of equations is obtained:

$$\left.\begin{aligned}&(N_1+N_2-N_3)A_1-(fN_1+fN_2+fN_3)B_1=0,\\&(N_1+N_2+N_3)A_2-(-fN_1-fN_2+fN_3)B_2=mg+P_V,\\&(N_1-N_2+N_3)A_3-(fN_1+fN_2+fN_3)B_3=0.\end{aligned}\right\} \tag{48}$$

After certain transformations, the system of equations suitable for solving with the use of Cramer's rule is obtained:

$$\left.\begin{aligned}&(A_1-fB_1)N_1+(A_1-fB_1)N_2+(-A_1-fB_1)N_3=0,\\&(A_2+fB_2)N_1+(A_2+fB_2)N_2+(A_2-fB_2)N_3=mg+P_V,\\&(A_3-fB_3)N_1+(-A_3-fB_3)N_2+(A_3-fB_3)N_3=0.\end{aligned}\right\} \tag{49}$$

The principal determinant of the system (49) has to be written down. It is as follows:

$$\Delta = \begin{vmatrix} A_1 - fB_1 & A_1 - fB_1 & -A_1 - fB_1 \\ A_2 + fB_2 & A_2 + fB_2 & A_2 - fB_2 \\ A_3 - fB_3 & -A_3 - fB_3 & A_3 - fB_3 \end{vmatrix}. \quad (50)$$

The next step is to write down the determinants Δ_i required for finding the unknown quantities N_i, i =1, 2, 3:

$$\Delta_1 = \begin{vmatrix} 0 & A_1 - fB_1 & -A_1 - fB_1 \\ mg + P_V & A_2 + fB_2 & A_2 - fB_2 \\ 0 & -A_3 - fB_3 & A_3 - fB_3 \end{vmatrix}, \quad (51)$$

$$\Delta_2 = \begin{vmatrix} A_1 - fB_1 & 0 & -A_1 - fB_1 \\ A_2 + fB_2 & mg + P_V & A_2 - fB_2 \\ A_3 - fB_3 & 0 & A_3 - fB_3 \end{vmatrix}, \quad (52)$$

$$\Delta_3 = \begin{vmatrix} A_1 - fB_1 & A_1 - fB_1 & 0 \\ A_2 + fB_2 & A_2 + fB_2 & mg + P_V \\ A_3 - fB_3 & -A_3 - fB_3 & 0 \end{vmatrix}. \quad (53)$$

Then, pursuant to Cramer's rule, the following solution of the system of equations is obtained:

$$N_1 = \frac{\Delta_1}{\Delta}, \; N_2 = \frac{\Delta_2}{\Delta} \text{ and } N_3 = \frac{\Delta_3}{\Delta}. \quad (54)$$

The obtained values of the normal reaction forces N_1, N_2 and N_3 provide for the stable position of the potato tuber during its translation along the longitudinal axes of the separator spirals.

The necessary and sufficient condition of the existence and uniqueness of a solution for the system of Eq. (49) and, hence, also (41), is the system's principal determinant not being equal to zero, i.e. the condition that $\Delta \neq 0$.

The next stage in the development of the mathematical model for the process of cleaning potatoes on the surface of the spiral separator is the compilation of the computer programme and the numerical solution of the obtained system of Eq. (49), which describes the motion of the potato tuber on the surface of the spiral separator, with the use of the PC. That would enable finding the optimum parameters of the spiral separator. Further, it is also necessary to investigate analytically the possible angular displacements of the potato tuber about the axes that pass through its centre of mass during its stay on the surface of the spiral separator under the action of the moments produced by the friction forces.

CONCLUSIONS

1. An analytical mathematical model has been developed for the process of cleaning potatoes on cantilevered cleaning spirals. The model allows determining the efficient design and kinematic parameters of the spiral separator with the use of analytical methods.

2. It has been established that the main work process of the transportation and cleaning of potato tubers takes place in the troughs between two adjacent spirals of the separator.

3. As a result of the analytical investigation, the system of linear equations of the potato tuber's motion, which, in effect, are the equations of the relative equilibrium of the tuber's position in the trough between the coils of two adjacent spirals, has been generated.

4. Solving the obtained system of equations on the basis of Cramer's rule and with the use of the PC will make it possible to plot the graphical dependencies that show the effect of the spiral separator's design and kinematic parameters on the behaviour of the process of separating the potato heap and cleaning the tubers from stuck soil.

REFERENCES

Bishop, C., Rees, D., Cheema, M.U.A., Harper, G. & Stroud, G. 2012. *Potatoes*. Crop Post-Harvest: Science and Technology: Perishables. Book Chapter, pp. 334–359.

Bulgakov, V., Ivanovs, S., Adamchuk, V. & Ihnatiev, Y. 2017. Investigation of the influence of the parameters of the experimental spiral potato heap separator on the quality of work. *Agronomy Research* **15**(1), 44–54.

Bulgakov, V., Nikolaenko, S., Adamchuk, V., Ruzhylo, Z. & Olt, J. 2018a. Theory of retaining potato bodies during operation of spiral separator. *Agronomy Research* **16**(1), 41–51.

Bulgakov, V., Nikolaenko, S., Adamchuk, V., Ruzhylo, Z. & Olt, J. 2018b. Theory of impact interaction between potato bodies and rebounding conveyor. *Agronomy Research* **16**(1), 52–64.

Feller, R., Margolin, E., Hetzroni, A. & Galili, N. 1987. Impingement angle and product interference effects on clod separation. *Transactions of the American Society of Agricultural Engineers* **30**(2), 357–360.

Guo, W. & Campanella, O.H. 2017. A relaxation model based on the application of fractional calculus for describing the viscoelastic behavior of potato tubers. Transactions of the *ASABE* **60**(1), 259–264.

Ichiki, H., Nguyen Van, N. & Yoshinaga, K. 2013. Stone-clod separation and its application to potato in Hokkaido. *Engineering in AgricultureEnvironment and Food* **6**(2), 77–85.

Krause, F. & Minkin, A. 2005. Research on shaftless screw conveyors. *Bulk Solids Handling* **25**(2), 92–100.

Misener, G.C. & McLeod, C.D. 1989. Resource efficient approach to potato-stone-clod separation. *AMA, Agricultural Mechanization in Asia, Africa and Latin America* **20**(2), 33–36.

Peters, R. 1997. Damage of potato tubers: A Review. *Potato Research* **39**(Spec. Issue), 479–484.

Petrov, G. 2004. *Potato harvesting machines*. Mashinostroenije, Moskow, 320 pp (in Russian).

Vasilenko, P.M. 1996. *Introduction to agricultural mechanics*. Kiev, Agricultural Education, 252 pp.

Veerman, A. & Wustman, R. 2005. *Present state and future prospects of potato storage technology*. Potato in Progress: Science Meets Practice, Book Chapter, pp. 179–189.

Wang, X., Sun, J., Xu, Y., Li, X. & Cheng, P. 2017. Design and experiment of potato cleaning and sorting machine. *Nongye Jixie Xuebao/Transactions of the Chinese Society for Agricultural Machinery* **48**(10), 316–322 and 279.

Agronomy Research **16**(4), 1607–1613, 2018
https://doi.org/10.15159/AR.18.150

Effect of PTO- driven tillage machines on soil particles transfer

M. Buřič, P. Novák* and J. Hůla

Czech University of Life Sciences Prague, Faculty of Engineering, Kamýcká 129, CZ165 21 Prague 6 – Suchdol, Czech Republic
*Correspondence: novakpetr@tf.czu.cz

Abstract. Displacement of soil particles by erosion can be seen as a major threat to the quality of agricultural land in the conditions of Czech Republic. While the effects of water and wind erosion have long been investigated and reported, the effect of soil tillage technology on soil particles translocation are relatively new area of agriculture research. Soil tillage may contribute to the undesirable translocation of soil particles towards lower-lying parts of fields especially on slopes. The effect of soil tillage implements on soil particle translocation has not been sufficiently explained yet. The object of this research was to assess the influence of PTO (power takeoff)-driven tillage machines on soil particle translocation during secondary tillage (soil preparation). Measurements to determine the displacement of soil particles were performed in location Nesperská Lhota in the Central Bohemia Region. Measurements were performed on a sandy loam cambisol after harvest winter cereals (winter wheat). To indicate displacement of soil particles was used grit of white limestone (size 10–16 mm). Limestone was put down into the trench with known position orthogonal to the direction of working operations. Subsequently were performed working operations in the specified sequence. Limestone particles were counted and weighed in each section. It was detected by measuring the different nature of displacement for each machine. Statistical significance of differences in the weight of translocated particles was evaluated for different type of machines.

Key words: tillage erosion, soil tillage, seedbed preparation.

INTRODUCTION

Tillage erosion is presently regarded as a serious phenomenon that contributes to the degradation of soil fertility (Govers et al., 1999; Logsdon, 2013). In some areas, tillage erosion can be a greater risk than water erosion. Van Oost et al. (2006) report that about half of the arable land in Canada is damaged by tillage soil erosion (soil translocation more than 6 Mg ha^{-1} yr^{-1}), while only 15% of arable land is damaged by water erosion. Due to repeated soil tillage operations, soil particles gradually move in downslope direction. Soil particles are removed from areas where slope is increasing (convex) to areas where slope is decreasing – concave (Papiernik, 2009). Machines for soil tillage are characterized by different intensity on the soil and their undesirable displacement. The literature gives as more aggressive and potentially erosive effects of mouldboard ploughs and chisel tillers. Van Muysen & Govers (2002), Van Muysen et al. (2006) and Li et al. (2007) reported that in general there was considerably more information about the effects of primary soil tillage on soil particle translocation than in secondary soil tillage. Soil tillage machines are characterized by varying intensity on the soil and their undesirable displacement.

Serious displacement of soil particles can also be caused by secondary soil tillage. Tiessen et al. (2007) found that secondary tillage can be equally as erosive as conventional primary tillage with use the mouldboard plough. The authors emphasize the importance of tillage speed and depth. Soil damage is increasing when the secondary soil tillage is repeated during the seedbed preparation.

Displacement of soil particles by machines with active powered working tools has been relatively little studied. Van Muysen & Govers (2002) investigated the displacement of soil particles using rotary harrow and seeder combination. The relativery high value of transport coefficient *k* was rather surprising (123 kg m^{-1} per tillage operation). Tillage depth is relatively low for cultivation with the harrow-seeder combination. Tillage at shallow depth of an unconsolidated soil causes not only large displacement of soil particles, but high variation in displacement distances of soil particles too. The analysis indicates that powered tools move quantities of soil particles, resulting in tillage erosion.

MATERIALS AND METHODS

An experiment was established at the location of Nesperská Lhota in Central Bohemia for the purpose of assessment of soil particles translocation. The experiment was focused on measurement of the influence of PTO- driven tillage machines on the translocation of soil particles during seedbed preparation (secondary soil tillage). On the experimental field was sandy-loam cambisol.

At the beginning of August 2017 winter wheat was harvested (yield 5.8 t ha^{-1}) and the straw was crushed. Subsequently, the field was cultivated by a disc harrow. After emergence of shattered seeds, the field was ploughed to a depth of 0.22 m paralleled to the contours at the beginning of September. After the soil subsided, measurements were carried out during the second half of September. Firstly, soil tillage was conducted by a levelling bars and harrow. Three grooves (each for one machine tested) were then created (see Fig. 1).

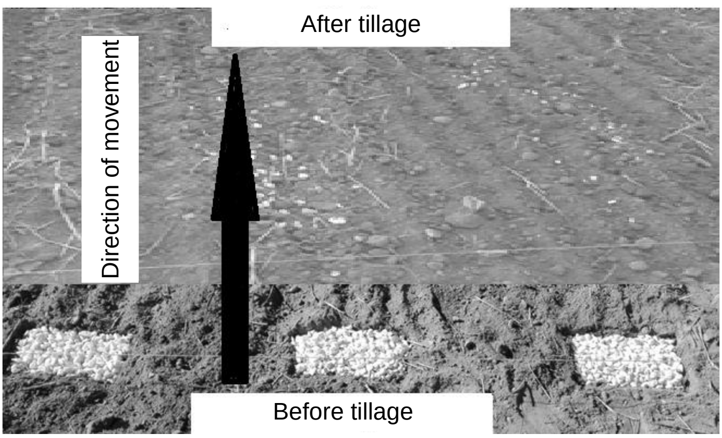

Figure 1. Experimental scheme.

Topsoil displacement of limestone grit with the fraction size of 12–16 mm was the indicator. Grits were placed into 3 created grooves of 0.33 m in length, 0.10 m in depth (soil tillage depth) and 0.20 m in width. The longer side of all grooves was perpendicular to the direction of the all machines movement. After the grooves had been created and filled with limestone grit, the measured place was passed through by individually machines for secondary soil tillage.

The machines that were chosen to measure the translocation of soil particles in the operations of secondary soil tillage:Vitkovice H 180 rotary cultivator of working width 1.8 m, Amazone Re Vario 401 oscillating harrows of working width 4 m and Rabe Werk 250 power harrows of working width 2.5 m. Working speeds were chosen according to typical speeds for a given machine design: 4 km h^{-1} (rotary cultivator), 6.5 km h^{-1} (oscillating harrows), 6.5 km h^{-1} (power harrows).

Individual grits (tracers) were picked by hand in 0.3 m sections. In a crosswise direction each section was divided into 3 parts (3 grooves in one line- 3 repeats). All grits from the given section were weighed. Kopecky cylinders with the volume of 100 cm^3 were taken to determine the basic physical properties of soil. Soil moisture was measured with a Theta Probe sensor (Delta Devices) in a layer of tilled soil. Data were processed using the programmes MS Excel (Microsoft Corp., USA) and Statistica 12 (Statsoft Inc., USA). It was used descriptive statistics and anova.

Table 1 shows the basic physical soil properties. The values of reduced bulk density and porosity are typical for soil kind in the experimental field. The values of porosity indicate a higher content of macro pores, which is a result of recent soil tillage (ploughing).

Table 1 shows the basic physical soil properties. The values of reduced bulk density and porosity are typical for soil kind in the experimental field. The values of porosity indicate a higher content of macro pores, which is a result of recent soil tillage (ploughing).

Table 1. Soil bulk density and total porosity before secondary tillage

Depth, m	Bulk density, g cm^{-3}	Porosity, % vol.
0.05–0.10	1.34	47.2
0.10–0.15	1.37	46.1

RESULTS AND DISCUSSION

The first evaluated machine was an Amazone oscillating harrows of the working width 4 m. The machine had a conventional 2 rows design. A groove of 0.10 m in depth was made and it contained crushed limestone. Subsequently, the tractor with the harrows passed the groove while the groove centre was in the middle of the working width of the machine. The evaluation of acquired data shows a noticeable translocation of particles in the direction of the machine movement. Fig. 1 shows the curve representing the average values of translocation in the particular segments (per 0.3 m). There is a steep fall in the weight of translocated particles at a longer distance from the original location. The relationship of the tracer weight to a distance from the original location can be described by a power function. The graph shows that the particles are translocated by the spikes of the harrows to short and middle distances. The most distant tracers were found out at a distance of more than 4.50 m. Novák & Hůla (2017a) found power functions for moving the particles during secondary tillage. In their research they used combinator to secondary soil tillage on a slope. They found a very strong relationship.

Further measurements were done after the soil tillage operation with a power harrows cultivator of the working width 2.5 m. Fig. 2 shows a relation of the weight of translocated tracers to a distance from the original location. To express this relation a power model of the function was used again. For this machine the most distant tracers were found at a distance 5.27 m. The weight of displaced particles again drops rapidly with the distance from the original site Character of the movement can also be affected by plant residues in the subsurface layer of soil.

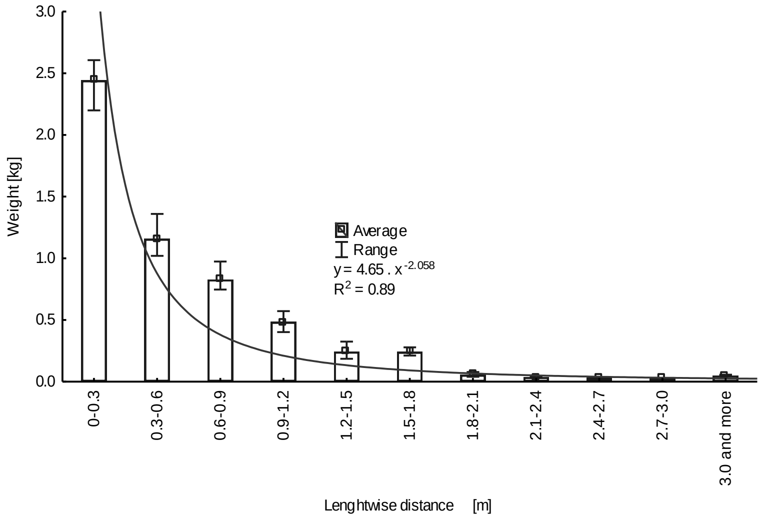

Figure 2. Translocation of tracers – oscillating harrows.

Table 2 contains a comparison of both machines. For comparison, the Tukey HSD test was used at a significance level of 0.05. The table shows average values, homogeneous groups are indexed. It can be seen from the table that in most sections a statistically significant difference was recorded. It is true that the oscillating harrows have less effect on the longitudinal movement of the particles than the power harrows. This is due to the smaller effect of working tools. Comparison took place at the same work speed, depth and soil conditions.

The third machine evaluated with regard to the translocation of soil particles was a Vitkovice rotary cultivator (see Fig. 4). The type of particle translocation

Table 2. Average translocation of particles (g) with a power harrows in a lengthwise direction and marked out homogeneous groups (Tukey's HSD test)

Distance, m	Power harrows	Oscillating harrows
0–0.3	3.24^a	2.48^b
0.3–0.6	0.95^a	1.19^a
0.6–0.9	0.49^a	0.88^b
0.9–1.2	0.95^a	0.51^b
1.2–1.5	0.89^a	0.32^b
1.5–1.8	0.46^a	0.33^a
1.8–2.1	0.41^a	0.11^b
2.1–2.4	0.23^a	0.09^b
2.4–2.7	0.19^a	0.08^b
2.7–3.0	0.16^a	0.06^b
3.0 and more	0.24^a	0.03^b

Homogeneous groups are marked by letters a, b.

was completely different from preceding measurements (Fig. 3). The reason is the turning of working tools. The rotating knives throw the parts of the soil backwards. The displacement of the particles is thus not deducted in the direction of movement but against it. Rotary cultivators are the only soil cultivation machines with this ability. The particle translocation can be successfully described by the quadratic function. The quadratic function was used by the Hůla et al. (2015) to describe the movement of soil particles when using the plow for primary soil cultivation. Character of the movement was in this case due to the reversal of the soil layer by the plow working tools. In this case, it is caused by throwing the particles through the rotor of the machine. Particles most likely hit the machine cover and then down to the ground. This is the most probable distance of about 0.6 m. Less particles then remain in their original location, or they reach a greater distance.

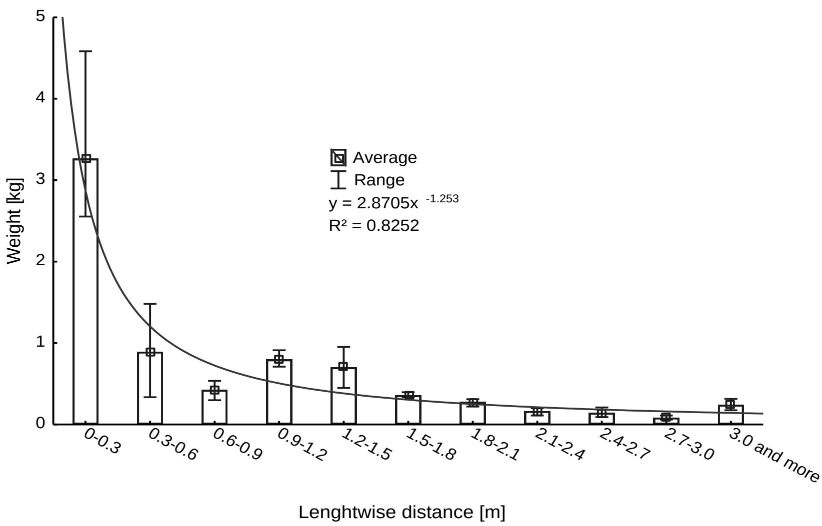

Figure 3. Translocation of tracers – power harrows.

The results of the measurement of soil particles displacement by machines with powered working tools confirmed the findings of other authors partly. Novák & Hůla (2017b) found a significant displacement during repeated secondary soil tillage. They also confirmed the conclusions of their earlier study (Hůla & Novák, 2016) .Rotary harrow and driven oscillating harrow moved the soil particles in the driving direction similar to the pre-sowing machines with non-powered working tools. These results are basically consistent with findings reported by Van Muysen & Govers (2002). Also, the results of Tiessen et al. (2007) were confirmed: secondary tillage implements can be equally as erosive as conventional primary tillage implements, for example mouldboard plough. A totally different character of the soil particles displacement was found when working with the horizontal rotary blade tiller. Translocation of soil particles was in a direction opposite to the machine movement direction. It can be a positive effect in driving in downslope direction. However, it is not possible to assume the use of the horizontal rotary blade tiller as a corrective measure on soils with symptoms of tillage erosion.

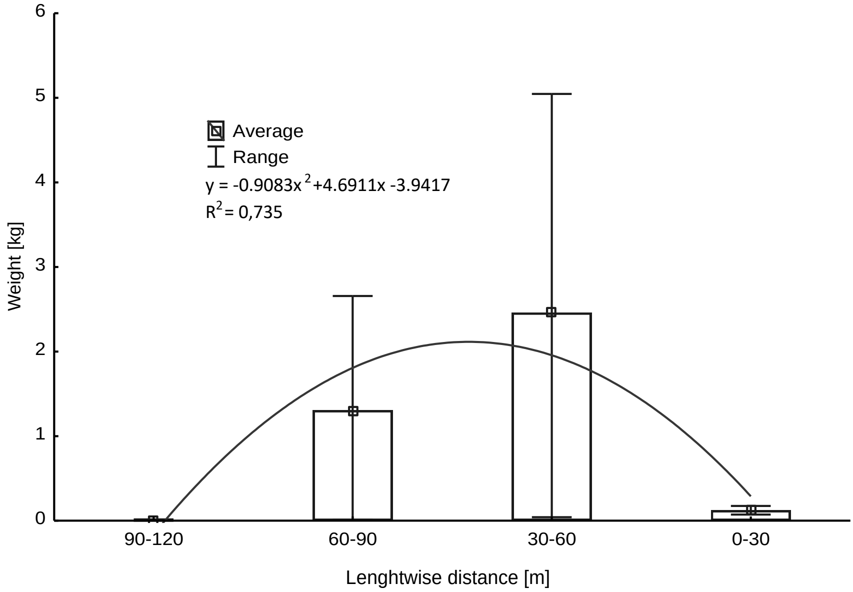

Figure 4. Translocation of tracers –rotary cultivator.

Overall, it is possible to agree with Van Muysen & Govers (2002) conclusions: powered tools move quantities of soil material. Therefore it is necessary to obtain further results of research on the erosivity of powered tools.

In practise, powered harrows and oscillating harrows are in combination with seeder machines, which further increases the erosive effect of these machines sets.

CONCLUSIONS

The results of measuring the translocation of soil particles document the fact that soil tillage may translocate soil particles to a different extent both in the direction of the machine movement and in a crosswise direction. Tillage erosion can thus contribute to soil erosion as well as water or wind. The selection of machines (not only PTO driven) for soil tillage can substantially influence the intensity of soil translocation. The results of the experiment demonstrate the significant effect of PTO driven machinery on the translocation of soil particles. It was recorded entirely different character of translocations when using a rotary cultivator. For two other tested machines, the character of the soil particles translocation was similar.

ACKNOWLEDGEMENTS. Supported by the Ministry of Agriculture of the Czech Republic – Project No. QJ1520028 and by the Czech University of Life Sciences Prague, Project No. IGA 31160/1312/3117.

REFERENCES

Govers, G., Lobb, D.A. & Quine, T.A. 1999. Tillage erosion and translocation: emergence of new paradigm in soil erosion research. *Soil & Tillage Research* **51**, 167–174.

Li, S., Lobb, D.A. & Lindstrom, M.J. 2007. Tillage translocation and tillage erosion in cereal-based production in Manitoba, Canada. *Soil & Tillage Research* **94**, 164–182.

Logsdon, S.D. 2013. Depth dependence of chisel plow tillage erosion. *Soil & Tillage Research* **128**, 119–124.

Hůla, J. & Novák, P. 2016. Translocation of soil particles during primary soil tillage. *Agronomy Research* **14**(2), 392–399.

Novák, P. & Hůla, J. 2017a. The influence of sloping land on soil particle translocation during secondary tillage . *Agronomy Research* **15**(3), 799–805.

Novák, P. & Hůla, J. 2017b. Translocation of the upper soil layer in multiple operations of seedbed preparation. *Research in Agricultural Engineering* **63**, Special Issue, 46–52.

Papiernik, S.K., Schumacher, T.E., Lobb, D.A., Lindstrom, M.J., Lieser, M.L., Eynard, A. & Schumacher, J.A. 2009. Soil properties and productivity as affected by topsoil movement within an eroded landform. *Soil & Tillage Research* **102**, 67–77.

Tiessen, K.H.D., Lobb, D.A., Mehuys, G.R., Rees, H.W. 2007. Tillage erosion within potato production in Atlantic Canada: II. Erosivity of primary and secondary tillage operations. *Soil & Tillage Research* **95**, 320–331.

Van Muysen, W. & Govers, G. 2002. Soil displacement and tillage erosion during secondary tillage operations: the case of rotary harrow and seeding equipment. *Soil & Tillage Research* **65**, 185–191.

Van Muysen, W.V., Oost, K.V. & Govers, G. 2006. Soil translocation resulting from multiple passes of tillage under normal field operating conditions. *Soil & Tillage Research* **87**, 218–230.

Van Oost, K., Govers, G., de Alba, S. & Quine, T.A. 2006. Tillage erosion: a review of controlling factors and implications for soil quality. *Progress in Physical Geography* **30**(4), 443–466.

Agronomy Research **16**(4), 1614–1621, 2018
https://doi.org/10.15159/AR.18.158

Analysis of indoor temperature in the workshop building during the summer: a pilot study

D.V. Cao* and P. Kic

Czech University of Life Sciences Prague, Faculty of Engineering, Department of Technological Equipment of Buildings, Kamýcká 129, CZ165 21 Prague, Czech Republic
*Correspondence: caodoan2006@gmail.com

Abstract. The aim of this paper is the presentation of measurements' results and the calculation method for analysis and evaluation of climate conditions as well for using of natural illuminance in two large simple buildings during summer which could be used to calculate power demand for the air cooling to reduce the indoor temperature caused by solar radiation. In this research, we carried out experiments of measuring the indoor temperature at level of working place which is 1.1 m, in two similar large workshops with floor area 260 m^2 and height 6.5 m, during several hot summer days. The indoor conditions were strongly influenced by the solar radiation as the buildings have large wall and roof windows. The indoor air temperatures in the first building achieved 39.5 °C, which caused the heat stress for workers. The indoor air temperatures in the second building achieved only 29.5 °C. The calculated power demand for the air cooling to reduce the indoor temperature to 25 °C is 25.6 kW in the first building, the cooling power for second building is 14.9 kW. We investigated measured construction of the workshop and we set up the formula in order to calculate thermal balance. The measurement results and calculated results in two buildings are compared and summarized in the tables and in the graphs for analysis. As a general conclusion, it must be said that solar radiation has a big influence on the air temperature and methods of passive air-conditioning should be more applied also on the production buildings in industry, agriculture and other branches of civil engineering to release heat increasing air temperature inside the building.

Key words: air conditioning, inside temperature, solar radiation, thermal balance.

INTRODUCTION

Indoor temperature is part of the indoor environmental quality component that is influenced by the climatic condition and construction of place (Randall, 2006). A successful indoor environment greatly depends on an understanding of the environmental factors, including building design and setting (Yeang, 2006).

The thermal performance of the building envelope can make a significant contribution to decrease the needed energy. So, it is important to insulate the envelope of the building. The determination of the temperature of the walls that constitute the building envelope may be considered as an essential part of an efficient building design. The thermal performance of an opaque wall depends on how well its materials transfer the heat flux through it, and the weather conditions (Bellahcene et al., 2017). The building envelopes propose an essential element between occupied building spaces and weather conditions. Thermal insulation in the walls is often designed for static performance based on its thermal resistance (Karlsson et al., 2013).

The influence of outdoor climate on indoor climate, especially during summer, has been well investigated (Quinn et al., 2014). Indoor temperature is mainly influenced by outdoor, but its diurnal course is inhibited due to the physical characteristics of the building (Höppe, 1993). When direct solar radiation enters a room through the windows, the additional thermal load needs to be considered (La Gennusa et al., 2005). Studies by, for example, Höppe (1993) and Melikov et al. (2013) indicate that air velocity influences the convective heat transfer and therefore improves the thermal sensation, especially at high room temperatures and humidity levels.

High average air temperature and solar radiation during the summer indicate that cooling demand would be dominant. Abundant wind around the year offers a great potential for passive cooling and indoor air quality improvement (Fleury, 1980; Bahadori, 1986).

Passive cooling includes techniques for solar and heat control, heat modulation and heat dissipation using naturally driven phenomena such as natural ventilation, radiative cooling, evaporative cooling and ground cooling (Cook, 1990; Santamouris & Kolokotsa, 2013). It is useful for improving thermal comfort in low-energy buildings. Since cooling efficiency of passive techniques is closely associated with environmental conditions, local vernacular architecture has become invaluable reference in recent studies (Kimura, 1994). Problems and principles of passive cooling and application in agricultural buildings are solved in several studies (Conti et al., 2016; Týbl & Kic, 2016; Kic, 2017; Leso et al., 2017).

Based on these results and those of further studies, the assessment and improvment of indoor climate condition, especially temperature cause by solar radiation and convective heat transfer should be more considered.

The aim of the calculation method used in this paper is to analyze the indoor conditions in large simple buildings for workers during some days in the summer. We carried out inside and outside measurement of temperature humidity and light intensity. The places of measurement are two workshops which have similar dimensions but different roof windows and wall windows. The results of measurement will show the influence of solar radiation on the inside temperature in the different constructions of the buildings. Afterwards we can compare internal climate conditions to recommended values to evaluate how the roof and wall windows influence on the temperature and intensity of illuminance in the two workshops. The next part of this research paper is to set up formulas in order to calculate the demand of power for the air cooling to reduce the indoor temperature or intensity of air flow to maintain the same inside and outside temperature.

MATERIALS AND METHODS

The authors carried out experiments of measuring the indoor temperature at level of working place which is 1.1 m, in two similar large workshops with floor area 260 m^2 and height 6.5 m, during several hot summer days. The indoor conditions were strongly influenced by the solar radiation as the buildings have large wall and roof windows. The first building (WS1) has 54 m^2 of wall windows and 81 m^2 of roof windows, the second building (WS2) has only 34 m^2 of wall windows and 28.5 m^2 of roof windows.

Air temperatures and relative humidity were measured by data loggers Comet System ZTH65 outside and inside the buildings with registration at intervals of 15 minutes during ten days (long-time measurement). Parameters of ZTH65 are: temperature operative range –30 to +70 °C with accuracy ± 0.4 °C and operative range of relative humidity 5–95% with accuracy ± 2.5%.

During the long-measurement in the two workshops, natural ventilation and forced ventilation were not used; the workshops did not have air conditioning. Therefore, the inside temperature in the two workshops is always higher than outside temperature. In this search work, we set up formulas in order to calculate the required cooling power in the recommended values in relevant standards and supply air flow to keep inside temperature at the level of outside temperature.

For calculation of the required cooling power we use the following heat balance general equation:

$$Q_s + Q_w - Q_c = Q_a \tag{1}$$

where Q_s – total heat gain by solar radiation, W; Q_c – total heat loss by convection, W; Q_w – total heat gain through the walls, W; Q_a – power consumption of air conditioning, W.

We calculated the required supply air flow by the following general equation:

$$Q_s + Q_w - Q_c = Q_v \tag{2}$$

$$V_{air} = \frac{Q_v}{\rho \cdot C \cdot (t_i - t_e)} \cdot 3{,}600 \tag{3}$$

where Q_v – energy loss with ventilation, W; V_{air} – required supply air flow, $m^3 h^{-1}$; ρ – density of the air, $kg\,m^{-3}$; C – specific heat capacity of the air, $J\,kg^{-1} \cdot K^{-1}$; t_i – internal temperature, °C; t_e – temperature of the supply air, °C.

We set up the Eqs (1), (2) and (3) in the program Mathcad and then we put measurement's data of construction and data in weather station to the equations. We showed obtained results in the graphs below.

We also evaluate the light in the two workshops by using daylight factor. The different translucent area of buildings resulted in different daylight factors, which were measured by lux meter TECPEL 536. The daylight factor is visual and light condition in interior. It shows the quantitative criterion of luminous state of the environment. The daylight can be calculated according to the Eq. (4).

$$e = \frac{E_m}{E_H} \cdot 100 \tag{4}$$

where e – daylight factor, %; E_m – illuminance of the given plane in the interior, lx; E_H – simultaneous unshadowed external horizontal illuminance, lx.

The obtained results of air temperature and relative humidity as well as the daylight measurements were processed by Excel software and verified by statistical software Statistica 12 *(ANOVA* and *TUKEY HSD Test*) to recognise if the differences between the results in both workshops are significant. Different superscript letters (*a*, *b*) in common are significantly different from each other in the columns of the tables *(ANOVA; Tukey HSD Test;* $P \leq 0.05$*)*, e.g. if there are the same superscript letters in the columns (workshops WS1 and WS2) it means the differences between the values in workshops are not statistically significant at the significance level of *0.05*.

RESULTS AND DISCUSSION

The measurement results in research work show and analyse outdoor and indoor temperature together with relative humidity of the air in the two workshop buildings during the summer when the rooms were without ventilation and air conditioning. Then, the obtained results were compared with the values recommended in relevant standards.

The results of long-time measurement of temperature and relative humidity of the air in the two workshops are presented in Table 1. The average external temperature was 18.7 ± 4.4 °C, average external relative humidity was 53.4 ± 16.6% during research period.

The results of this measurement show that the differences between both workshops in terms of internal air temperature as well as relative humidity are statistically significant at the significance level of *0.05* during the research period.

The air temperature in the two workshops during the whole measured period and the temperatures in both workshops are higher than outdoor temperatures (the average temperature was 18.7 °C outside, 25.6 °C in WS2, 31.8 °C in WS1). The optimal temperature for workers in the summer is between 23 to 26 °C, which has not been reached in this period even during the external outdoor temperature. It shows that in the summer, when the workshop does not have ventilation or the cooling power, working place influences the heat stress for workers in the WS2.

Table 1. Results of measurement and statistical evaluation of internal temperature t_i, internal relative humidity RH_i in workshops WS1, WS2. Different letters (*a, b*) in the superscript are the sign of high significant difference (*ANOVA; Tukey HSD Test*; *P ≤ 0.05*) between the conditions in the workshops

Parameter	Workshop	
	WS1	WS2
t_i ± SD, °C	31.8 ± 2.8^a	25.6 ± 1.6^b
RH_i ± SD, %	28.6 ± 3.5^a	36.5 ± 3.9^b

SD – Standard deviation.

From the measurement results, the air temperature in the WS2 is lower than in the WS1. The reduction of roof windows area and the improvement of the shape of windows in the WS2, contribute to reduce the impact of solar radiation on the indoor thermal comfort and reduce the inside temperature during the highest external temperatures. This construction in the WS2 would help to reduce the heat stress for workers.

Average values and standard deviation show that the relative humidity in the WS1 and WS2 is lower and more stable than outside. As in other building, the air moisture does not cause major problems in terms of microclimatic comfort. Recommended maximum relative humidity 70% was not exceeded in the two workshops. It is good for workers and for equipment. The minimal recommended indoor relative humidity is 30%. The low relative humidity 28.6% in the workshop WS1 is below this recommended value. It corresponds with the psychometric changes of the air inside the workshop with very high internal temperature.

For the next comparison of temperature values, the external temperature and temperature in the two workshops during 24 hours of the day are summarized in Fig. 1.

From the Fig. 1 we can see that, the highest temperature in the two workshops is from 2 pm to 5 pm which is around 1 hour later than the highest outside temperature. Then the temperature in the night (from 8 pm to 6 am) is lower because the solar radiation didn't impact the workshops. This two phenomena happened by heat accumulation from the walls, floor and roof of the building. Outside air temperature decreased but construction of this building released energy from day temperature. Therefore, the inside temperature is always higher than outside.

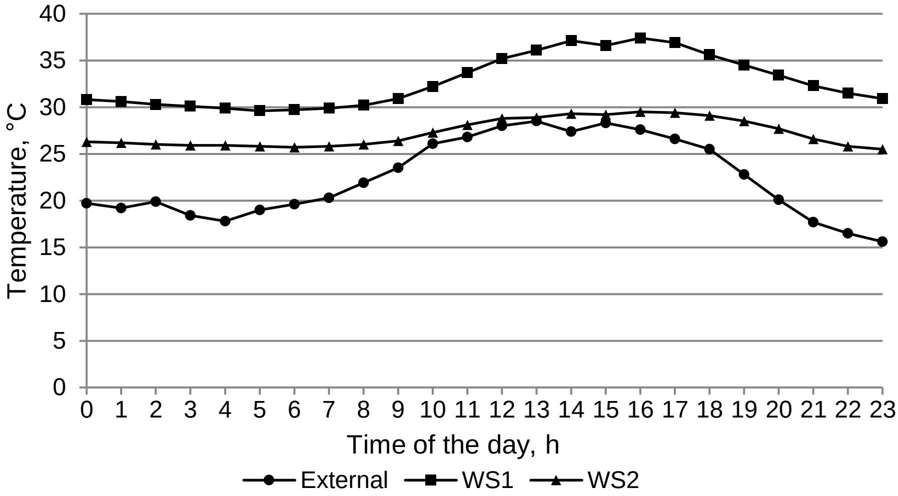

Figure 1. External temperature and temperature in the two workshops during 24 hours of the day.

In this case, we can use air conditioning equipment or forced ventilation to reduce inside temperature to the standard values. By calculation of energy balance, we can calculate the required cooling power or required forced ventilation in two workshops. The calculated results are showed in the Figs 2 and 3.

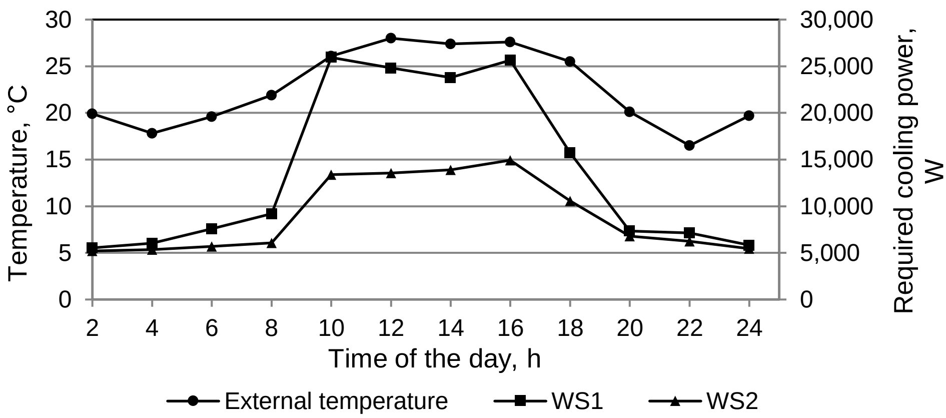

Figure 2. External temperature and required cooling power in the two workshops during 24 hours of the day.

In Fig. 2 is showed the required cooling power to keep inside temperature at 25 °C. In this case, the required cooling power in the WS1 is higher than in WS2 about 11 kW at the extreme outside temperature (between 12 am to 4 pm). From the night to the morning, the required cooling power decreases gradually and is nearly the same in two workshops.

In case of calculation of required ventilation to keep the same temperature inside and outside and to evacuate heat gain, the obtained results are showed in the Fig. 3. At the extreme outside temperature, the required ventilation in the WS2 is higher than in the WS1. The reason is because of the (3) equation. In this time, the outside temperature is 28 °C and the inside is 28.8 °C, therefore the temperature difference is only about 0.8 °C. It shows that, when the temperature of supply air and exhaust air is similar, we have to use the big intensive ventilation to decrease inside temperature. Therefore, we should not use forced ventilation when temperature of supply air and exhaust air are similar.

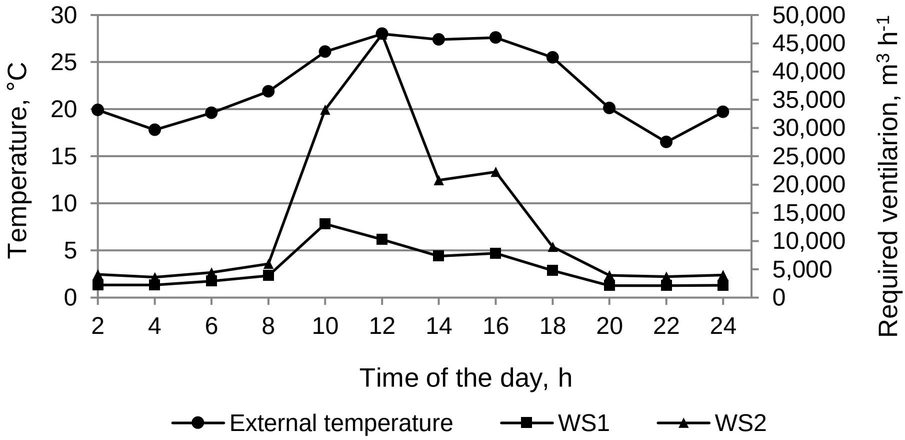

Figure 3. External temperature and required ventilation in the two workshops during 24 hours of the day.

The comparison of both workshops from the point of view of area covered by the roof windows and wall windows and measured values of illuminance in two workshops and calculated daylight factors e are presented in the Table 2. During the time of illuminance's measurement, the average measured simultaneous non shaded external horizontal illuminance E_H was approximately 27,000 lx.

Table 2. Results of measurement of the illuminance and calculated daylight factor e in two workshops WS1, WS2 during the short time with the area of roof and wall windows. The same letter (*a*) in the superscript is the sign that there is not high significant difference (*ANOVA; Tukey HSD Test*; $P \leq 0.05$) between the daylight factors in the workshops

	Area of the roof windows m^2	Area of the wall windows m^2	Average measured illuminance lx ± SD	Daylight factor e % ± SD
WS1	81	54	2,491 ± 1,451	9.2 ± 5.4[a]
WS2	28.5	34	1,590 ± 1,435	5.9 ± 5.3[a]

SD – Standard deviation.

The average daylight factor e = 9.2% in the workshop WS1 is bigger than e = 5.9%. The difference between the daylight factors was evaluated statistically and surprisingly the difference is not significant at the significance level of *0.05*. It can be explained by the large standard deviations of the measured values of illuminance.

The mean daylight factor in the first workshop was 9.2% and in the second workshop 5.9%. According to the visual activity class IV in both workshops demanded daylight factor is 5%. The area of roof window of the WS2 is smaller than in WS1, therefore average measured illuminance in the WS2 is lower than in the WS1. We can say that, in the case of no air conditioning or ventilation, if the area of roof window decreases, temperature also decreases and the intensity of illuminance is lower, nevertheless not significantly.

CONCLUSIONS

Solar radiation is the main factor that influences the inside temperature in the two workshops. The temperature in WS2 is lower than in WS1 because the WS1 has bigger roof and wall window that absorb solar radiation and makes heat higher inside the building.

In the building WS1, when the inside air was not cooled or ventilated, the inside temperature (average 31.7 °C) exceeded recommended temperature (between 23 °C to 26 °C). This produces heat stress for workers inside the workshop.

In the night-time, the roof did not absorb solar radiation, however the inside temperature was still higher than outside. The reason for this phenomenon is the heat accumulation in the walls, roof, floor and all equipment in the workshops. These absorb heat in the day-time, and during the night release heat increasing air temperature inside the building.

The calculated power demand for the air cooling to reduce the indoor temperature to 25 °C is 25.6 kW in the first building, the cooling power for second building is 14,9 kW. The construction properties of the WP2 allow saving energy consumption for air conditioning or ventilation, but at the same time cause the increase of required energy for illuminance.

REFERENCES

Bahadori, M.N. 1986. Natural air-conditioning system. *Advances in Solar Energy* **3**, 283–356. Plenum Press, New York.

Bellahcene, L., Cheknane, A., Bekkouche, SMA. & Sahel, D. 2017. The effect of the thermal inertia on the thermal transfer in building wall. *International conference on advances in energy systems and environmental engineering* **22** (in Poland).

Conti, L., Barbari, M. & Monti, M. 2016. Design of sustainable agricultural buildings: A case study of a wine cellar in Tuscany, Italy. *Buildings* **6**(2), 1–8.

Cook, J. 1990. The state of passive cooling research. *Passive Cooling*, ed. J. Cook, Chapter 7, 539–569. The MIT Press, Cambridge, MA.

Fleury, B. 1980. Ventilative cooling: State of the art. *Proceeding of Workshop on Passive Cooling*. Italy, 2–4 April, 123–133.

Höppe, P.R. 1993. Indoor climate. *Experientia* **49**, 775–779.

Karlsson, J., Wadso, L. & Oberg, M. 2013. A conceptual model that simulates the influence of thermal inertia in building structures. *Energy and Buildings* **60**, 146–151.

Kic, P. 2017. Effect of construction shape and materials on indoor microclimatic conditions inside the cowsheds in dairy farms. *Agronomy Research* **15**(2), 426–434.
Kimura, K. 1994. Vernacular technologies applied to modern architecture. *Renew. Energy* **5**(Part II), 900–907.
La Gennusa, M., Nucara, A., Rizzo, G. & Scaccianoce, G. 2005. The calculation of the mean radiant temperature of a subject exposed to the solar radiation - a generalised algorithm. *Building and Environment* **40**, March, 367–375.
Leso, L., Morshed, W., Conti, L. & Barbari, M. 2017. Evaluating thermal performance of experimental building solutions designed for livestock housing: The effect of greenery systems. *Agronomy Research* **15**(1), 239–248.
Melikov, A.K., Skwarczynski, M.A., Kaczmarczyk, J. & Zabecky, J. 2013. Use of personalized ventilation for improving health, comfort, and performance at high room temperature and humidity. *Indoor Air* **23**, 250–263.
Quinn, A., Tamerius, J.D., Perzanowski, M., Jacobson, J.S., Goldstein, I., Acosta, L. & Shaman, J. 2014. Predicting indoor heat exposure risk during extreme heat events. *Science of The Total Environment* **490**, 686–693.
Randall, T. 2006. Environmental Design (3th ed.). New York: Taylor & Francis Inc. Robinson.
Santamouris, M. & Kolokotsa, D. 2013. Passive cooling dissipation techniques for buildings and other structures: the state of the art. *Energy and Building* **57**, 74–94.
Týbl, J. & Kic, P. 2016. Thermal properties and reduction of energy consumption of buildings. *Agronomy Research* **14**, 1222–1231.
Yeang, K. 2006. Ecodesign-a manual for ecological design. London: Wiley-Academy.

Agronomy Research **16**(4), 1622–1629, 2018
https://doi.org/10.15159/AR.18.163

Extended use of Sphagnum peat as a biosorbent for Zn(II): repetitious sorption-desorption process

V. Denisova*, K. Tihomirova and L. Mezule

Riga Technical University, Research Centre for Civil Engineering, Water Research Laboratory, P. Valdena street 1-204, LV-1048 Riga, Latvia
*Correspondence: viktorija.denisova@rtu.lv

Abstract. In this study, continuous biosorption-desorption cycles in a fixed-bed column were performed to evaluate the extended use of sphagnum peat as biosorbent material to remove Zn(II) ions from aqueous solutions. Biosorption-desorption studies revealed that the sphagnum peat as biosorbent could be regenerated using 0.1M HCl as eluting agent with more than 70% recovery in four successive biosorption-desorption cycles. The results showed that the sphagnum peat should be used as an alternative, effective and low-cost biosorbent for Zn(II) ions removal from polluted aqueous solution.

Key words: biosorption-desorption process, fixed-bed column, zinc, sphagnum peat.

INTRODUCTION

Heavy metal pollution is a serious environmental problem and represents a threat to human and ecosystem due to its toxic effect and accumulation tendency throughout the food chain. Wastewaters from a variety of industry are an important source of environmental pollution due to their high content of heavy metal such as cadmium, copper, chromium, lead and zinc. They may induce human health hazards through contact with contaminated surface or drinking water in result of emission of the untreated industrial wastewater discharged into the aquatic ecosystem (Kobielska et al., 2018). Therefore, the removal of heavy metal ions from aqueous solutions is necessary and very important.

Zn(II) is an essential micronutrient for human health and is involved in numerous biological routes within the human body, however, it is also toxic at levels of 100–500 mg per day (Volesky & Holan, 1995; Chapman, 2006). At high concentration it may cause damages to human health such as respiratory diseases, coughing and problems like abdominal pain, vomiting and nausea (Plum et al., 2010). In recent years, the removal of Zn(II) ions from wastewater has gained a significant attention due to the need to protect the environment (Parmar & Thakur, 2013). Zinc (Zn(II)) is widely used in industrial activities like mining, manufacturing and production of products such as batteries, wood, ceramics, textiles, paints and fertilizers (Katsou et al., 2010).

Various techniques have been applied to remove heavy metal ions from wastewaters, e.g., coagulation, chemical precipitation, ion exchange, membrane filtration, electrochemical treatment, reverse osmosis and adsorption (Carolin et al., 2017). Biosorption is an alternative technology employing low cost filtration materials like orange peel (Liang et al., 2011), cocoa pod husk (Njoku, 2014), pine bark (Cutillas-Barreiro et al., 2016), hay (Tihomirova et al., 2017) and palm kernel shell (Karri & Sahu, 2018) for removal of toxic metals from industrial wastewaters. Another inexpensive and widely available natural biosorbent is sphagnum peat. Despite being defined as a slowly renewable fuel material (Crill et al., 2000), the main advantages of sphagnum peat as biosorbent are free availability in large quantities in temperate climate zones and high biosorption capacity which has demonstrated a high uptake capacity of dissolved Zn(II) (Denisova et al., 2017). Nevertheless, currently biosorption is mainly carried out in batch systems, but from a practical point of view, dynamic fixed-bed column studies are necessary to demonstrate the practical applicability for industrial wastewater treatment (Jin et al., 2018). The desorption performance or the biosorbent regeneration is important for cost-effective implementation of the biosorption process in fixed-bed column operation. The regeneration process is related to the repeated reuse of the biosorbent with minimum loss of efficiency. Thus, the regeneration process can minimise the need of new adsorbent and reduce the utilization problem of used biomass; therefore, desorption studies are important to evaluate biosorbent recycling and metal recovery (Akar et al., 2009; Rizzuti et al., 2015).

The aim of this research was to investigate the regeneration potential of sphagnum peat for enhanced Zn(II) removal and subsequent recovery by successive biosorption-desorption process in a continuous fixed-bed column.

MATERIALS AND METHODS

Preparation of the biosorbent

Commercialsphagnum peat moss (AS EESTI TURBATOOTED, Estonian peat products Ltd, Estonia) was used in the biosorption-desorption experiments as a biosorbent. It had an organic matter content of 98%, ash content of 2% and pH values ranged from 3.6–4.4 after rinsing with tap water. Humification degree wasH2-H4 according to the von Post scale (von Post, 1924).

Preparation of Zn(II) solution

The synthetic Zn(II) ion solution was prepared by dissolving the appropriate quantity of $ZnSO_4 \cdot 7H_2O$ (Reachem Slovakia, Slovakia) in tap water to achieve Zn(II) concentrations of 100 mg L^{-1}. The concentration was determined by Atomic Absorption Spectrometer (AAS) (Aanalyst 200, Perkin Elmer, USA) with air-acetylene flame.

Biosorption experiments

Continuous biosorption experiments were performed in up-flow fixed-bed column. The glass column with 3.2 cm inner diameter and 30 cm length was filled with 40 g of dry sphagnum peat to obtain a bed depth of 25 cm. Stainless steel sieves with a mesh size of 220 μm were installed at both top and bottom of the packed glass column in order to avoid the washing out of biosorbent material. Before the first experiments, the biosorbent material was intensively washed with tap water for 24 h using continuous up-flow at a flow rate of 15 mL min^{-1} by peristaltic pump (MasterFlex L/, model 77202-50, Cole-Parmer Instrument Co.) to remove brown-coloured water and small particles of dirt.

After this washing procedure, synthetic Zn(II) ion solution with an initial concentration of 100 mg L^{-1} at pH 6.6 ± 0.1 was fed through the up-flow fixed-bed column with the same flow rate as used in washing procedure. All the experiments were carried out at room temperature (22 ± 2 °C).

Samples of Zn(II) solution were collected periodically from the top of the column (Fig. 1, a) and acidified with a concentrated nitric acid (HNO_3 65%, Lach-Ner Ltd., Czech Republic) to obtain a concentration of 2% v v^{-1} HNO_3; then the samples were filtered with 0.45 μm membrane filter (Filtropur S, Sarstedt, Germany). Afterwards, the samples were analysed for the remaining Zn(II) concentrations by using flame AAS. The pH, conductivity and temperature of the influent and effluent of collected samples were measured by using digital benchtop meter (inoLab® Multi 9420 IDS, WTW, Germany). Each experiment was performed in triplicate, and the average results are reported in this study.

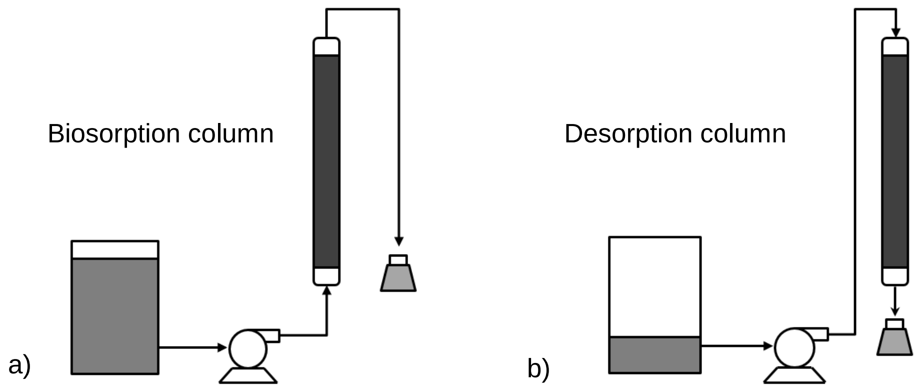

Figure 1. Schematic diagram of the experimental set-up for a continuous process in a fixed-bed: a) biosorption; b) desorption column.

The biosorption efficiency of the fixed-bed column can be described through the breakthrough curve concept when equilibrium between influent and effluent Zn(II) ion concentration is achieved (99% of an initial Zn(II) concentration).

The maximum column capacity q_{total} (mg), the total mass of metal ions acquired by the biosorbent in fixed-bed column experiments can be calculated by the following equation (Martin-Lara et al., 2012):

$$q_{total} = \frac{Q}{1{,}000} \int_{t=0}^{t=t_{total}} (C_0 - C_t)dt \qquad (1)$$

where C_0 – the influent metal concentration (mg L^{-1}); C_t – is the effluent metal concentration (mg L^{-1}); Q – the flow rate of Zn(II) ion solution which passed through the column (mL min^{-1}).

The total metal removal efficiency (%) at the breakthrough can be calculated as:

$$\text{Removalefficiency (\%)} = \frac{q_{total}}{m_{total}} \cdot 100 \qquad (2)$$

where q_{total} – total mass of metal adsorbed into biosorbent (mg); m_{total} – the total amount of metal ions sent to the column (mg).

The biosorption capacity q_e (mg g^{-1}), the amount of Zn(II) adsorbed (mg) per unit dry weight of biosorbent can be determined using the following equation:

$$q_e = \frac{q_{total}}{m} \quad (3)$$

where m – the total mass of biosorbent in the column (g).

Regeneration of biosorbent

Zn(II) containing biosorbent was regenerated using 1.2 L of 0.1M hydrochloric acid (HCl) as eluting agent. The acid was fed into the top of the fixed-bed column (Fig. 1, b) at the same flow rate used in the biosorption cycle. The effluent samples were collected from the bottom of the column after every bed volume or 200 mL. All samples were analysed with the same procedure as used in biosorption experiments.

After metal elution, the biosorbent was washed thoroughly byup-flow tap water until pH 6.5 and reused for next cycle of biosorption. The biosorption-desorption process was continued for six cycles.

The efficiency of Zn(II) removal or desorption yieldwas calculated from the ratio of the amount of Zn(II) ions desorbed and the total Zn(II) ions adsorbed into the biosorbent in a fixed-bed column using the following equation:

$$\text{Desorption yield (\%)} = \frac{\text{Amount of Zn(II) ions desorbed}}{\text{Amount of Zn(II) ions biosorbed}} \cdot 100 \quad (4)$$

The surface structure of the biosorbent material, before and after Zn(II) successive biosorption-desorption experiments, were characterized by a stereo microscope (Zeiss Stemi 508, Germany).

Statistical analysis

In order to ensure the accuracy and reproducibility of the collected data, all biosorption-desorption experiments were performed in triplicate. Microsoft Excel 2013 *t-test* (two tailed distribution) and ANOVA single parameter tool (significance level, $p \leq 0.05$) were used in data analysis.

RESULTS AND DISCUSSION

The regeneration of the biosorbent is one of the key factors in demonstrating the practical applicability of biosorbent use in industrial wastewater treatment. Different types of eluent agents have been used for recovery of the adsorbed heavy metal ions from biosorbent materials. Akar et al. (2009) regenerated *Symphoricarpusalbus* biomass from Pb(II) in five biosorption-desorption cycles using 0.01M HNO_3 solution; Martin-Lara et al. (2012) showed good efficiency for Pb(II) removal using 0.3M HCl from acid-treated olive stone; Jin et al. (2018) and Freitas et al. (2018) used 0.1M HNO_3 as eluting agent and showed a good reusability of Cd(II), Cu(II) and Ag(II) for *Pleurotusostreatus* spent substrate and Verde-lodo bentonite. Here removal of Zn(II) ions from the sphagnum peat with the smallest possible volume of an eluting solution was evaluated to reduce the aggressive effect of the acidic eluent on binding sites of biosorbent (Hammaini et al., 2007). Moreover, lower amounts of chemicals required for the process will facilitate its cost-efficiency.

In the present study, successive biosorption-desorption cycles of Zn(II) by sphagnum peat were repeated six times. The effect of repetitious sorption-desorption process on Zn(II) removal was shown in Fig. 2. The results showed that the highest removal efficiency of Zn(II) was 99% in the first four successive biosorption-desorption cycles within 48 hours. These results indicate that the sphagnum peat sorption capacity was exhausted after 48 hours. Based on this observation, an equilibrium time of 48 hours was considered as a maximum contact time for biosorption process. The average biosorption capacity of sphagnum peat was 47 ± 11 mg Zn(II) g^{-1}. No significant difference ($p > 0.05$) was observed between four successive biosorption-desorption cycles.

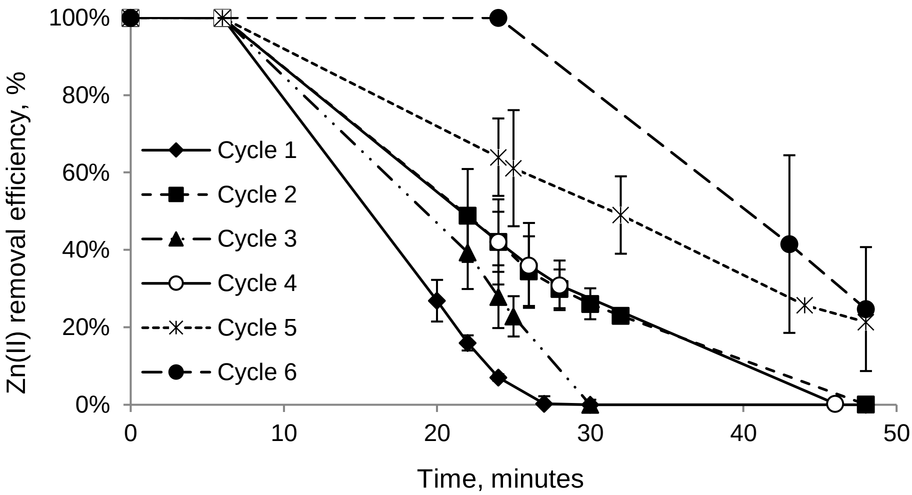

Figure 2. The effect of biosorption cycle number on Zn(II) removal efficiency by sphagnum peat. The initial Zn(II) concentration – 100 mg L^{-1}. The data represent the average values of three experiments for each biosorption experiment cycle and the correlation coefficients (R^2) were from 0.962 to 0.989. The error bars represent the standard deviation (SD).

The sorption capacity of sphagnum peat increased in the following two biosorption-desorption cycles. At the same time, the increase in biosorption time to more than 50 hours did not allowed to recover of the adsorbed metal.

The overall recovery was $1{,}608 \pm 42$ mg of Zn(II) per L of 0.1M HCl used for desorption (around 71% from the total amount of adsorbed Zn(II) during four biosorption-desorption cycle). The maximum desorbed concentration of Zn(II) was achieved in the first 40 minutes by using 0.6 L or 3 fixed-bed column volume of 0.1M HCl (Fig. 3).

The results showed that the maximum desorption efficiency was achieved 93% after first biosorption-desorption cycle (Fig. 4). The desorbed concentrations of Zn(II) from sphagnum peat were $1{,}573 \pm 39$ mg L^{-1}. No significant difference ($p > 0.05$) was observed of desorbed concentration of Zn(II) during 80 minutes of desorption process. And during the next 3 desorption cycles, the amount of desorbed Zn(II) decreased to 60%, but during next two cycles decreased with cycle number (Fig. 4).

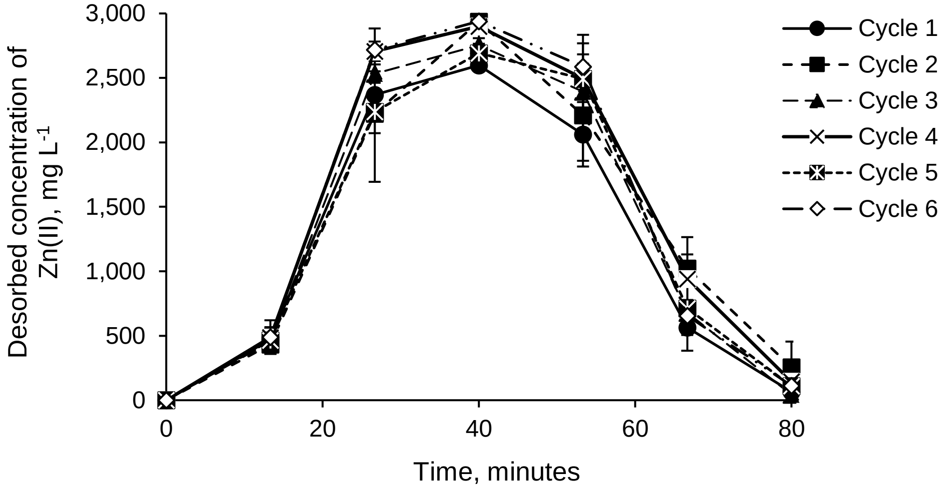

Figure 3. The desorbed concentration of Zn(II) from sphagnum peat during 80 minutes by using 0.1M HCl. The initial Zn(II) concentration – 100 mg L^{-1}. The data represent the average values of three experiments for each biosorption experiment cycle. The error bars represent the standard deviation (SD).

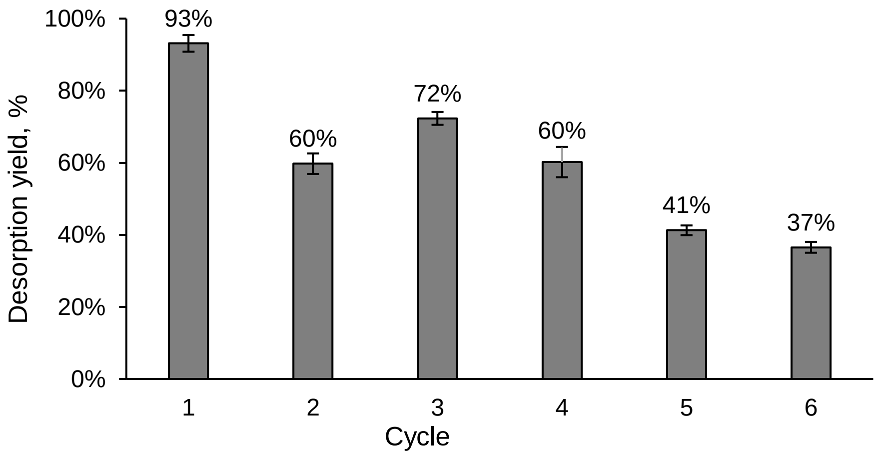

Figure 4. Percentage of Zn(II) desorbed from sphagnum peat in successive biosorption-desorption cycles by using 0.1M HCl as eluting agent. The data represent the average values of three experiments for each biosorption-desorption cycle. The error bars represent the standard deviation (SD).

The results showed that 0.1M HCl as eluting agent allows to remove the loaded Zn(II) ions from the column in a short period of time and had suitable efficiency in the sphagnum peat recovery. Other eluting agents are possible, however, wide availability, price and good test results set HCl as a superior eluting agent.

In order to characterize the biosorbent surface structure, micrographs with stereo microscope were taken before (Fig. 5, a) and after (Fig. 5, b) the Zn(II) regeneration with 0.1M HCl to verify any changes.

Micrographs with a 2.0 x magnification (Fig. 5) indicated some deformation and tendency of sphagnum peat particles to granulate. The biomass before Zn(II) biosorption-desorption cycles had smaller particle size (Fig. 5, a).

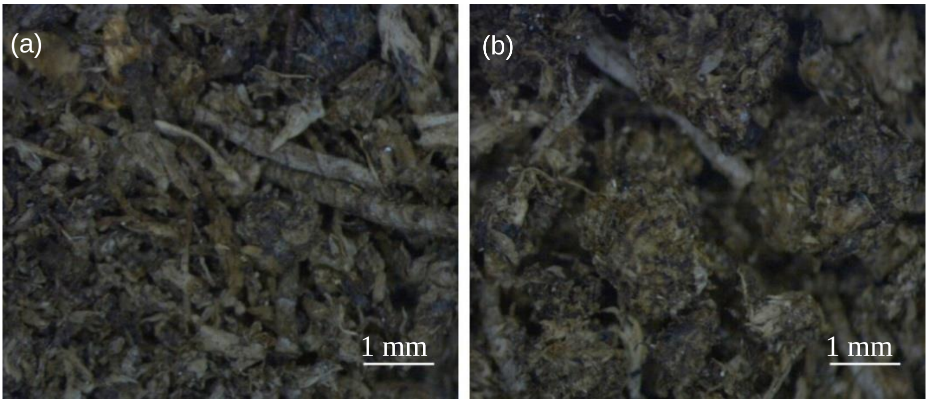

Figure 5. Micrograph (2.0 x magnification) of sphagnum peat surface before (a) and after (b) Zn(II) biosorption-desorption cycles.

To further demonstrate the applicability of sphagnum peat and its re-use upgrades in the technological process are advisable. This could include immobilization onto granular adsorbent to limit a blockage in the column and to increase Zn(II) removal efficiency. Moreover, the possible over-extensive use of the resource should be evaluated due to its specific classification (Crill et al., 2000).

CONCLUSIONS

The results of this study indicated that the sphagnum peat can be successfully used for biosorption in continuous fixed-bed column. Biosorption and desorption cycles were carried out and revealed that the maximum successive number of cycles with 0.1M HCl as efficient eluent were four.

The regenerated sphagnum peat characterization demonstrated tendency to granulate, although no further changes were observed in adsorbent material surface.

ACKNOWLEDGEMENTS. This work has been funded by IPP3: INNO INDIGO Programme Project B-LIQ ‘Development of an Integrated Process for Conversion of Biomass to Affordable Liquid Biofuel’, No. ES/RTD/2017/18 (PVS ID 2802).

REFERENCES

Akar, S.T., Gorgulu, A., Anilan, B., Kaynak, Z. & Akar, T. 2009. Investigation of the biosorption characteristics of lead(II) ions onto *Symphoricarpusalbus*: Batch and dynamic flow studies. *Journal of Hazardous Materials* **165**, 126–133.

Carolin, C.F., Kumar, P.S., Saravanan, A., Joshiba, G.J. & Naushad, M. 2017. Efficient techniques for the removal of toxic heavy metals from aquatic environment: A review. *Journal of Environmental Chemical Engineering* **5**, 2782–2799.

Chapman, D. 2006. *Water Quality Assessments: A guide to the use of biota, sediments and waterin environmental monitoring*. Taylor & Francis London, United Kingdom, Second Edition, 626 pp.

Crill, P., Hargreaves, K. & Korhola, A. 2000. *The role of peat in Finnish greenhouse gas balances.* Ministry of Trade and Industry **32**(1), Helsinki, Finland, 71 pp.

Cutillas-Barreiro, L., Paradelo, R., Igrexas-Soto, A., Nunez-Delgado, A., Fernandez-Sanjurjo, M.J., Alvarez-Rodriguez, E., Garrote, G., Novoa-Munoz, J.C. & Arias-Estevez, M. 2016. Valorization of biosorbent obtained from a forestry waste: Competitive adsorption, desorption and transport of Cd, Cu, Ni, Pb and Zn. *Ecotoxicology and Environmental Safety* **131**, 118–126.

Denisova, V., Tihomirova, K. & Mezule, L. 2017. Biosorption of Zn(II) by Sphagnum peat. *Chemical Engineering Transactions* **57**, 385–390.

Freitas, E.D., Almeida, H.J., Almeida Neto, A.F. & Vieira, M.G.A. 2018. Continuous adsorption of silver and copper by Verde-lodo bentonite in a fixed bed flow-through column. *Journal of Cleaner Production* **171**, 613–621.

Hammaini, A., Gonzalez, F., Ballester, A., Blazquez, M.L. & Munoz, J.A. 2007. Biosorption of heavy metals by activated sludge and their desorption characteristics. *Journal of Environmental Management* **84**, 419–426.

Jin, Y., Teng, C., Yu, S., Song, T., Dong, L., Liang, J., Bai, X., Liu, X., Hu, X. & Qu, J. 2018. Batch and fixed-bed biosorption of Cd(II) from aqueous solution using immobilized *Pleurotusostreatus* spent substrate. *Chemosphere* **191**, 799–808.

Karri, R.R. & Sahu, J.N. 2018. Modeling and optimization by particle swarm embedded neural network for adsorption of zinc (II) by palm kernel shell based activated carbon from aqueous environment. *Journal of Environmental Management* **206**, 178–191.

Katsou, E., Malamis, S. & Haralambous, K. 2010. Examination of zinc uptake in a combined system using sludge, minerals and ultrafiltration membranes. *Journal of Hazardous Materials* **182**, 27–38.

Kobielska, P.A., Howarth, A.J., Farha, O.K. & Nayak, S. 2018. Metal-organic frameworks for heavy metal removal from water. *Coordination Chemistry Reviews* **358**, 92–107.

Liang, S., Guo, X. & Tian, Q. 2011. Adsorption of Pb^{2+} and Zn^{2+} from aqueous solutions by sulfured orange peel. *Desalination* **275**, 212–216.

Martin-Lara, M.A., Blazquez, G., Ronda, A., Rodriguez, I.L. & Calero, M. 2012. Multiple biosorption-desorption cycles in a fixed-bed column for Pb(II) removal by acid-treated olive stone. *Journal of Industrial and Engineering Chemistry* **18**, 1006–1012.

Njoku, V.O. 2014. Biosorption potential of cocoa pod husk for the removal of Zn(II) from aqueous phase. *Journal of Environmental Chemical Engineering* **2**, 881–887.

Parmar, M. & Thakur, L.S. 2013. Heavy metal Cu, Ni and Zn: Toxity, health hazards and their removal techniques by low cost adsorbent: A short overview. *International journal of plant, animal and environmental sciences* **3**(3), 143–157.

Plum, L.M., Rink, L. & Haase, H. 2010. The essential toxin: impact of zinc on human health. *International Journal of Environmental Research and Public Health* **7**(4), 1342–1365.

Rizzuti, A.M., Ellis, F.L., Cosme, L.W. & Cohen, A.D. 2015. Biosorption of mercury from aqueous solutions using highly characterised peats. *Mires and Peat* **16**, 1–7.

Tihomirova, K., Denisova, V., Jaundzema, L. & Mezule, L. 2017. Hydrolysed biomass waste as a potential biosorbent of zinc from water. *Agronomy Research* **15**(3), 905–914.

Volesky, B. & Holan, Z.R. 1995. Biosorption of heavy metals. *Biotechnology progress* **11**(3), 235–250.

von Post, L. 1924. Das Dasgenetische System der organogenenBuldungenSchwedens. Memoires sur la nomenclature et la classification des sols. *Comité International de Pédologie IV*, Communication **22**, 287–304.

Agronomy Research **16**(4), 1630–1641, 2018
https://doi.org/10.15159/AR.18.179

Assessment of potato plant development from Minitubers

I. Dimante[1,2,*] and Z. Gaile[1]

[1]Latvia University of Life Sciences and Technologies, Faculty of Agriculture, Liela street 2, LV 3001 Jelgava, Latvia
[2]Institute of Agricultural Resources and Economics, Priekuli Research centre, Zinatnes street 2, LV 4126 Priekuli, Latvia
[*]Correspondence: ilze.dimante@arei.lv

Abstract. In production of minitubers, manipulation of their weight by modifying production method is common. Under field conditions plant development from minitubers can be affected by their weight, as well as cultivar. This objective of this study was to compare plant development from four minituber weight classes (MtC) (3 to 4.99 g, 5 to 9.99 g, 10 to 19.99 g, and > 20 g) with broken apical dominance of cultivars 'Monta', 'Prelma' and 'Mandaga'. 'Prelma' and 'Mandaga' had a similar development pattern, and minitubers > 20 g required significantly less growing degree days (GDD) to emerge than minitubers from the lightest classes. The heaviest minitubers needed on average 176 GDD for 50% emergence and 207 GDD were needed for the lightest class. The difference in GDD between the marginal MtC was more pronounced in period between 50 and 80% emergence. MtC did not affect the final rate of emergence. Number of above ground stems (1.4–4.0) was significantly affected by MtC. 'Monta' had significantly different development – delayed emergence, lower emergence rate, less above ground stems, faster canopy closure. Our study showed that plant development was significantly affected by MtC and cultivar. Differences between MtC were more pronounced under adverse meteorological conditions.

Key words: Field performance, non-emergence, potato ageing, number of stems, GDD.

INTRODUCTION

Minitubers are small tubers produced from in vitro derived potato plantlets (Struik, 2007) in protected environments at the initial stage of potato (*Solanum tuberosum*) seed production worldwide. The average weight of minitubers is affected by the production technology. Minituber field performance can be significantly affected by their weight (Struik & Lommen, 1999; Barry et al., 2001). Therefore, it is relevant to know the minimal minituber weight appropriate for further field multiplication under particular conditions.

Plant emergence is an important phase of potato development. In regions, where potatoes are planted relatively late and cloudiness is common, plants capture less global radiation than would be desirable (Haverkort & Struik, 2015). The highest level of solar radiation, which is a key factor for photosynthesis, is reached in May and June. Therefore, in Northern Regions, fast emergence of plants and quick canopy closure are crucial for the further growth and yield formation under short growing season conditions.

Time to emergence in days after planting (DAP) can be very variable and tubers of different physiological status may have a different lag period between planting and emergence. Lag period decreases with increasing temperature (Firman et al., 1992). Delayed emergence and slow initial growth is typical for plants developing from minitubers. Thus, Fulladolsa et al. (2017) reported a 14 day delay in comparison to conventional tubers. Moreover, the smaller the minituber is, the longer dormancy it has and it can affect plant emergence (Hagman, 1990; Lommen & Struik, 1994). Hagman (1990) compared minitubers with 10 and 30 mm diameters and observed significantly delayed emergence of the smaller ones.

The main environmental factor driving potato emergence is temperature (Haverkort et al., 2015). The growing degree days (GDD) approach may be an accurate way to discriminate the differences in plant emergence between cultivars and weight classes of minitubers (MtC) over two and more growing seasons. The necessary amount of GDD for emergence of minitubers in the field is not widely studied.

One of the main traits defining the physiological status of the seed tuber and potato plant growth vigour is number of stems per emerged plant. The number of stems is a crucial trait as it influences tuber number both per plant and per unit area. Genotype and seed size are the factors most likely affecting the stem number per plant (Struik et al., 1990). In addition, stem number can be reduced when apical dominance of the sprouts is not broken (Wurr et al., 2001).

Few studies on field performance of minitubers involve the assessment of the number of stems. Additionally it is rarely known if sprout apical dominance has been broken.

Minitubers produce significantly less stems than conventional tubers (Lommen & Struik, 1994; Gopal et al., 2002). In previous studies, one plant from minituber produced 1–2 stems (Lommen & Struik, 1994; Külen et al., 2011), while in other studies 2– stems (Gopal et al., 2002; Ozkaynak & Samanci, 2006) were produced.

The canopy closure (or ground cover) phase characterizes radiation interception, which reaches 100% only when full ground cover is established (MacKerron & Waister, 1985; Haverkort et al., 2015). Advanced canopy closure can give a relative increase in potential yield (MacKerron & Waister, 1985; Haverkort & Struik, 2015). Development of the canopy can be estimated as DAP or days after emergence (DAE). Plant emergence is the most appropriate starting point for assessing further phases of potato development including canopy closure (O'Brien et al., 1998).

Little information exists on the field performance of minitubers in Northern Europe and in Baltic states in particular. Planting of minitubers can be conducted relatively late in this region and growing season is very short. Heavy virus pressure caused by ware potato production traditions in hobby gardens is limiting factor for potato seed production in Baltic states. Less field generations of potato seed can help solving this obstacle The production of large quanities of minitubers with good field performance can reduce number of field multiplication generations and increase availabilty of high quality potato seed of locally breed cultivars.. The objective of this study was aimed to compare plant development of minitubers from three cultivars and four weight classes with broken apical dominance.

MATERIALS AND METHODS

A three year (2014–2016) study was carried out at Priekuli Research Centre (PRC) of Institute of Agricultural Resources and Economics, Latvia (57°18′ N, 25°20′ E). Three cultivars of different maturity bred in PRC were used for the study ('Monta' – early, 'Prelma' – medium early and 'Mandaga' – medium late).

Minitubers were obtained from *in vitro* plantlets grown in fertilized peat in greenhouses of PRC. Minitubers were stored nine months including seven months cold storage (3 °C). Two weeks before planting, minitubers were de-sprouted and then pre-sprouted under diffused natural light.

Each year, minitubers of weight classes 3 to 4.99 g, 5 to 9.99 g, 10 to 19.99 g, and > 20 g were planted by hand in a sandy loam soil in the second part of May. Winter cereals were used as the previous crop in all three years.

A randomized split-plot design was used with the cultivar as the main plot and MtC as the subplot. The trial was replicated three times in 2014 and four times in 2015 and 2016. Minitubers were planted at 0.7 m between rows using 0.2 m in-row spacing. Each sub-plot consisted of 48 minitubers (12 tubers × 4 rows). Plant development was evaluated only in two inner rows in order to avoid possible effect of the competition between plots.

Fertilizers were broadcasted on the surface of the field one week before planting at the rate of 60 kg N ha^{-1}, 55 kg P_2O_5 ha^{-1} and 90 kg K_2O ha^{-1}. Broadcasting of the fertilizers was followed by the deep tillage. Plant protection measures were performed as needed and were aligned with the integrated pest management practice.

Plant emergence was assessed two to three times a week and the date of the emergence was considered when 50% of plants in the plot were visible above the soil surface (MacKerron & Waister, 1985). Observations of emergence were continued at previously mentioned intervals up to 50 days after planting (DAP) to determine the final number of emerged plants. Simultaneously, the number of days to 80% emergence (E80%) was assessed to evaluate further plant development. Plant emergence rate was recalculated to GDD starting from the 2nd day after planting. As plant emergence was assessed in early mornings, the recorded date of emegence was excluded from the calculation of GDD.

Canopy closure was estimated when at least 90% of plants met within rows and data were recorded as days after 50% emergence (DAE50%). Data on GDD was added to analysis only for the reference, as the GDD approach for prediction of canopy development fits better under conditions not subjected to environmental stresses (Haverkort et al., 2015).

The canonical formula for GDD calculation was applied according to McMaster & Wilhelm (1997), and 2 °C was used as a base temperature (Tbase) for pre-sprouted tubers (MacKerron & Waister, 1985).

The number of above ground stems was determined for each sub-plot two weeks before harvesting.

Effects of the two main factors – cultivar and MtC were determined by analysis of variance (ANOVA) using SPSS version 18.0. The LSD test at $\alpha = 0.05$ probability level was used to compare group differences. The effect of growing year was treated as a random factor. When the appropriateness of GDD approach was examined, one way ANOVA on year effects was performed.

RESULTS AND DISCUSSION

Plant emergence

Time to E50% and E80% expressed both in DAP and GDD was significantly affected by cultivar ($P < 0.001$) and MtC ($P < 0.05$). The largest proportion of variation was attributed to the effect of cultivar (36–61%), while MtC explained only 5–9% of variation.

P-values presented in Table 1 confirm the significant effect of growing year on time to plant emergence for all studied cultivars when expressed in DAP. This confirms the statement that time to emergence can be very variable between years (Firman et al., 1992) and temperature is the main factor driving plant emergence (Haverkort et al., 2015). Table 1 shows that GDD approach can be more conservative to describe the time required for potato emergence, as the effect of the growing year was not significant for two cultivars

Table 1. *P*-values for the effect of growing year on plant emergence to 50%, to 80% and within rows canopy closure expressed in DAP and GDD for three cultivars

Cultivar	E50%		E80%		Canopy closure within rows	
	DAP	GDD	DAP	GDD	DAE50%	GDDAE50%
Monta	< 0.001	< 0.001	< 0.001	< 0.001	< 0.001	< 0.001
Prelma	< 0.001	**0.618**	< 0.001	**0.285**	< 0.001	< 0.001
Mandaga	< 0.001	**0.389**	< 0.001	**0.425**	< 0.001	< 0.001

For all cultivars, it took more days to emerge in 2015 (Fig. 1), when mean air temperature in the end of May and in the beginning of June was lower when compared with that in other years and the long term average data. Minitubers of all weight classes below 20 g of ‘Prelma’ and ‘Mandaga’ had significantly ($P < 0.05$) lower emergence rate 20 DAP than MtC > 20 g. MtC did not affect emergence rate of ‘Monta’ significantly up to 30 DAP in 2015. All MtC of ’Monta’ continued to emerge after 30 DAP and minitubers from two largest weight clases had significantly higher emergence rate at 41 DAP. In 2014, due to higher than average air temperature, plants emerged very rapidly and no effect of MtC of ’Prelma’ and ’Mandaga’ was observed on emergence rate in any of the evaluated periods (Fig. 1). In 2016, emergence was also fast, however, a significant effect of MtC was observed 20 DAP for ’Monta’ and ’Prelma’. However, this effect was not as pronounced as in 2015. In general, MtC had a more clear effect on differences of plant emergence pattern when weather was cold. Differences between MtC were observed until 20 DAP, but shortly before 30 DAP only insignificant differences remained in 2015 and 2016. Only for ‘Prelma’ in 2015 and for ‘Monta’ in 2016 was the effect of MtC on plant emergence rate 30 DAP still significant ($P < 0.05$).

No significant differences in emergence to 50% and to 80% expressed in GDD were observed for ‘Prelma’ and ‘Mandaga’ between the years (Table 1). These results agree with a statement by Haverkort (2007) that some developmental processes including sprout growth have constant rates to reach a certain phase. However, due to unexplained factors ‘Monta’ showed an atypical growth response as significantly more ($P < 0.001$) GDD were required by Monta on 2015 than on other years of the study to emerge both to E50% and E80%.

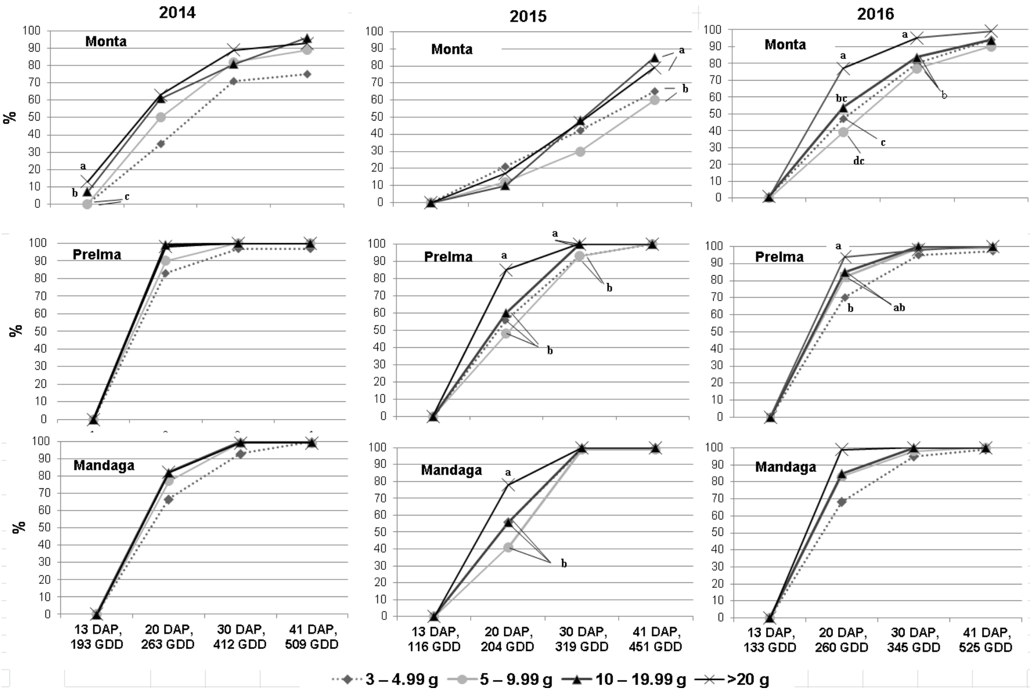

Figure 1. Emergence (%) pattern of plants from minitubers depending on cultivar and weight class of minitubers. *Different letters indicate significant differences (P < 0.05) between weight classes of minitubers within cultivar and within year. Samplings not marked with letters are not significantly different.*

GDD accumulated by plants to reach E50% and E80% was significantly ($P < 0.001$) affected by cultivar and MtC. 'Monta' differed significantly from 'Prelma' and 'Mandaga'. The two latter cultivars accumulated similar amount of GDD to E50% and to E80% (Fig. 2). The interaction between the main factors was not significant ($P = 0.992$ and $P = 0.993$ respectively).

Plants from each MtC of 'Monta' accumulated significantly more GDD (on average 83 GDD more) to reach E50% than plants of 'Prelma' and 'Mandaga'. The difference in GDD became even more pronounced for E80% (on average 136 GDD more needed for 'Monta'). The effect of cultivar corresponds to previous findings showing a genotype effect on accumulated GDD needed to reach certain development phases (Streck et al., 2007). In a study with conventional tubers Jefferies & MacKerron (1987) found on average 378 GDD required for 'Maris Piper' to reach E50% with Tbase 0 °C in formula. Similar results have been published by O'Brien et al. (1998). Even when their data is recalculated to Tbase 2 °C, the value (~ 271–298) is still higher than average number of GDD in our study. Only GDD to E50% for three lightest MtC of 'Monta' can be compared to those obtained by Jefferies & MacKerron (1987) and O'Brien et al. (1998). These remarkable differences could be affected by cultivar. In addition, the storage temperature did not exceed 4 °C in both examples and no information on sprout development is provided. Firman et al. (1992) reported that well sprouted cold tubers can reduce thermal time by 60 GDD (Tbase 1 °C), but pre-warmed tubers (no data on sprouting specified) can reduce thermal time by 15 GDD (Tbase 1 °C). Consequently, we can assume that planting of well sprouted and warm tubers can reduce GDD requirement even more. This explains relatively small requirement of GDD even for smaller minitubers to emerge in our experiment.

We found that significantly more GDD for emergence of ‘Monta’ in comparison with other cultivars were required only by minitubers. In experiments where conventional tubers are used, ‘Monta’ does not have delayed emergence in comparison with ’Prelma’ and medium late cultivars (Dr. I. Skrabule, PRC, personal communication). The actual storage conditions, storage time and relatively big size of minitubers often causes early sprouting. As only minitubers without sprouts can be certified, then common practice under described conditions is removing (de-sprouting) of the etiolated sprouts. During the de-sprouting the apical dominance is broken and this help increase the number of stems under the field conditions. However, the effect of early sprouting on field performance of some cultivars can be negative (Struik et al., 2006). Before de-sprouting, shrinkage of minitubers of ’Monta’ was quite pronounced. Besides, minitubers had quite strongly established etiolated sprouts. These may be signs of advanced ageing and early cultivars are prone to very high rate of ageing (Struik et al., 2006). Possibly minitubers of ‘Monta’ are more sensitive to storage conditions than conventional tubers.

Emergence of lighter minitubers to E50% was delayed in comparison to heavier minitubers (Fig. 2). Lighter tubers have longer dormancy (Van Ittersum, 1992), therefore, they are physiologically younger and emerge later than heavier ones as reported by Knowles & Knowles (2006), Oliveira et al. (2014) and other researchers. Our study confirms previously described associations on minitubers as well.

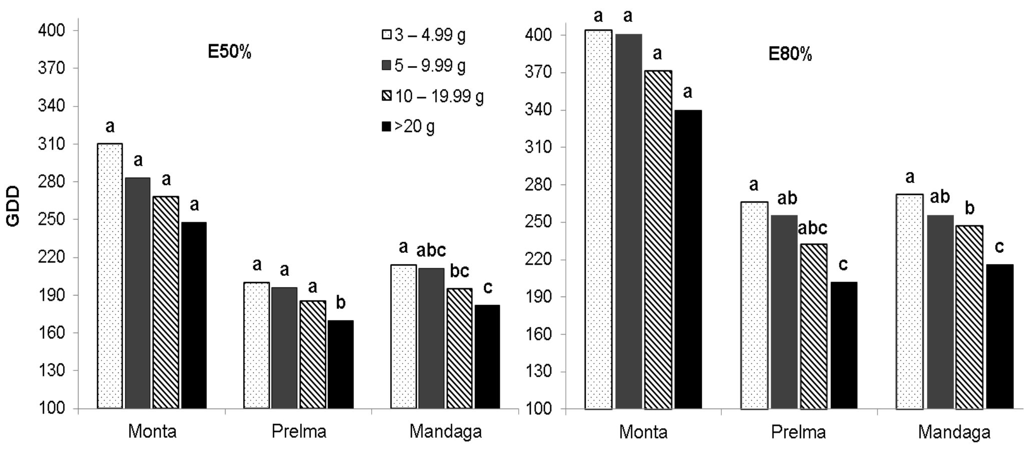

Figure 2. Accumulated GDD to 50% emergence (E50%) and 80% emergence (E80%) (*Different letters indicate significant differences (P < 0.05) between weight classes of minitubers within cultivar. Analysis was done separately for E50% and E80%*).

For ‘Prelma’ and ‘Mandaga’ the emergence gap to E80% between the lightest and heaviest minitubers was more pronounced than from planting to E50% (Fig. 3). It took longer for the remaining smaller minitubers to emerge from E50% to E80%. Thus, the difference between marginal MtC of ‘Prelma’ in GDD value to E80% increased two times when compared to difference in GDD value to E50%. Performance on ‘Mandaga’ was similar to that of ‘Prelma’. Our results agree with Lommen & Struik (1994) who found that more time is needed for lightest minitubers to emerge after E50%. A similar difference pattern in emergence to E50% and E80% was observed for ‘Monta’.

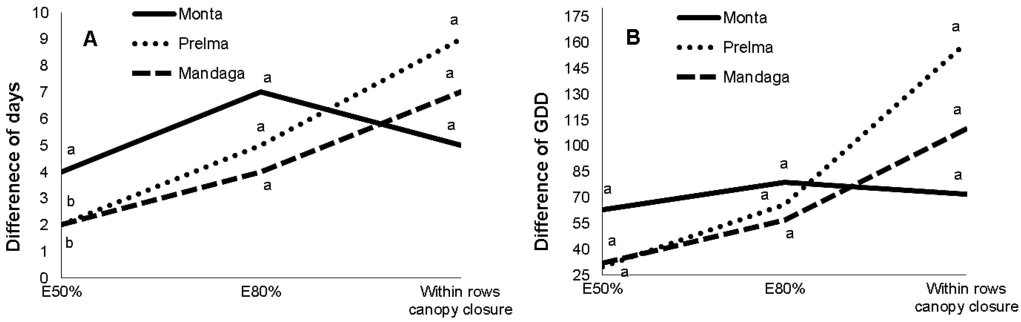

Figure 3. Difference in days (A) and GDD (B) between the smallest (3–4.99 g) and the largest (> 20 g) weight class of minitubers required to reach E50%, E80% after planting (emergence gap) and to reach within rows canopy closure after emergence (canopy closure gap). *Different letters indicate significant differences (P < 0.05) between cultivars within the observation.*

In research by Allen et al. (1992), time to E50% of smaller conventional tubers increased with planting depth. Fulladolsa et al. (2017) agrees, as in their study, rows were hilled after the time when most of the conventional tubers had emerged. Authors assume that hilling may delay emergence of minitubers despite of shallower planting. Our study is partly in line with this statement. In the case of ‘Prelma’ and ‘Mandaga’, minitubers from smaller MtC usually emerged to E80% only after the hilling, while during all study years for ‘Prelma’ and two years for ‘Mandaga’ minitubers from the MtC > 20 g emerged before hilling. All MtC of ‘Monta’ emerged to E50% mostly after hilling, therefore hilling does not explain differences in emergence gap between the smallest and largest MtC.

Percentage of emerged plants of ‘Prelma’ and ‘Mandaga’ was not significantly affected by growing year, and MtC (Table 2). In contrast, significantly less plants of cultivar ‘Monta’ emerged in 2015 when compared with other years, and the significant effect of MtC on plant emergence rate was observed in 2015 (Table 2).

Table 2. Percentage of emerged plants produced by minitubers of five weight classes, 2014–2016

Weight class of minitubers, g	**Emerged plants 50 DAP, %**				Means within weight class of minitubers
	Monta		Prelma	Mandaga	
	2015	2014–2016	2014–2016	2014–2016	
3–4.99	68[b]	**82**[a]	**99**[a]	**99**[a]	93[a]
5–9.99	66[b]	**82**[a]	**100**[a]	**99**[a]	94[a]
10–19.99	86[a]	**92**[a]	**100**[a]	**100**[a]	97[a]
➢ 20	84[a]	**92**[a]	**100**[a]	**100**[a]	97[a]
Means within cultivar	**87.0**[A]		**99.8**[B]	**99.5**[B]	×

Different letters indicate significant differences (P < 0.05) between data within column. Different capital letters indicate significant differences (P < 0.05) between means within cultivar.

Results on percentage of emerged plants partly agree with those of Lommen & Struik (1994) and Barry et al. (2001) who did not find a significant effect of weight of planted minitubers on percentage of plants emergence and reported 82–100% emergence depending on growing season.

The low emergence rate of cultivar ‘Monta’, especially in 2015 (Table 2), when only 66–86% of plants emerged, may be explained by the physiological status of planted minitubers. A phenomenon, the so called “non-emergence” of too old tubers, has been previously demonstrated (Bodlaender & Marinus, 1987; Oliveira et al., 2014). Hagman (1990), as well, found this phenomenon investigating minitubers. Bodlaender & Marinus (1987) and Hagman (1990) found that non-emergence was significantly affected by cultivar. Nutrition reserves of minitubers can be lost during sprout formation (Lommen & Struik, 1993) and probably due to early sprouting and subsequent de-sprouting, ‘Monta’ had a lower emergence rate than other cultivars. A significantly lower percentage of emerged plants from two lighter MtC in comparison to two heavier MtC confirmed this assumption. However, minitubers of ‘Monta’ had slower emergence as well and this is in contrast to findings reporting earlier emergence of older tubers (Knowles & Knowles, 2006; Oliveira et al., 2014). These contradictions do not allow us to claim that minitubers of ‘Monta’ were too old to have good emergence rate. More research on this cultivar is necessary.

Number of above ground stems

The main factors (cultivar and MtC) explained more than 77% of the variance in number of above ground stems, MtC being a dominant factor determining 59% of variance. Significant interaction between the main factors was found ($P < 0.001$).

Mean values within MtC over cultivars (Table 3) were similar to those obtained by Gopal et al. (2002), Ozkaynak & Samanci (2006), and Wrobel (2015). Relatively large minitubers were used in the mentioned studies (20–30 g, up to 18 g and 15–30 mm respectively), which resulted in 1.3–5.0 stems per plant depending on cultivar. Heavier minitubers produced significantly more main stems (Ozkaynak & Samanci, 2006). In contrast, only 1–2 stems per plant and no significant differences between different MtC were reported in the study of Lommen & Struik (1994), when very small minitubers were used (0.13–3.99 g).

Table 3. Above ground stems per emerged plant depending on MtC and cultivar, 2014–2016

Weight class of minitubers, g	Number of above ground stems per emerged plant			Means within weight class of minitubers
	Monta	Prelma	Mandaga	
3–4.99	1.4^{c}	1.6^{d}	1.7^{d}	**1.6^{d}**
5–9.99	1.5^{c}	2.0^{c}	2.2^{c}	**1.9^{c}**
10–19.99	1.8^{b}	2.7^{b}	2.9^{b}	**2.4^{b}**
> 20	2.4^{a}	4.0^{a}	3.9^{a}	**3.4^{a}**
Means within cultivar	1.8^{A}	2.6^{B}	2.7^{B}	×

Different letters indicate significant differences (P < 0.05) between data within columns. Different capital letters indicate significant differences (P < 0.05) between means within cultivar.

In our study, the number of above ground stems increased significantly with the increase of MtC both over cultivars and within each cultivar. Heavier tubers are physiologically older, therefore, usually have more stems (Knowles & Knowles, 2006; Oliveira et al., 2014).

Canopy closure

Full ground cover was observed only in few plots over the three study years, therefore, canopy closure within rows were assessed to compare plant development after emergence.

Time to within rows canopy closure expressed in DAE50% was significantly determined by cultivar and MtC ($P < 0.001$). No significant interaction between main factors was detected ($P = 0.652$). Across cultivars and MtC means less time for within rows canopy closure was required in 2015, when plants had significantly delayed E50% expressed in DAP. In 2014 and 2016, on average 39 DAE50% were required to reach within rows canopy closure, while significantly more GDD were accumulated in 2016 when compared to 2014 (556 and 445 GDD respectively). This tendency was similar for all cultivars and all MtC separately, except MtC > 20 g of 'Prelma'. These results confirm the statement that thermal time approach to estimate canopy closure is not consistent (Streck et al., 2007). In the last 10 days of June 2016, 85.6 mm of rain (309% of long term average precipitation) was recorded and 58 mm fell during 24 hours. Heavy rainfall caused water logging in field and plant development slowed down, despite optimal temperature.

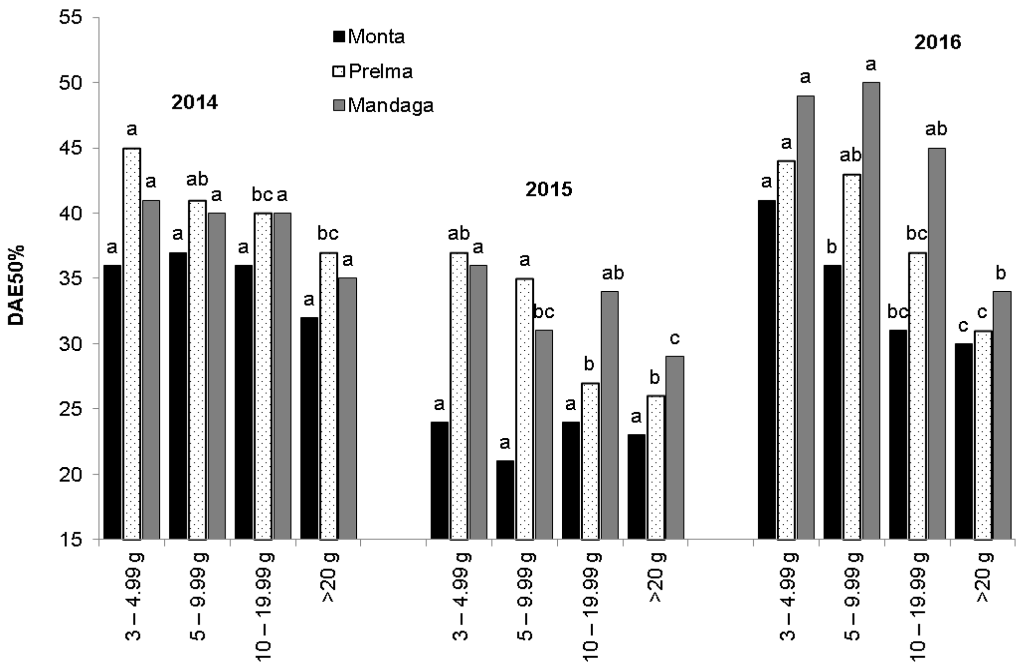

Figure 4. Time to within rows canopy closure expressed in DAE50%. *Different letters indicate significant differences (P < 0.05) between MtC within cultivar and within year*.

Data in Fig. 4 shows faster within rows canopy closure of plants grown from heavier minitubers, however, these differences in all years of the study were significant only for ‘Prelma’ ($P < 0.05$), while for ’ Monta’ significant effect of MtC on canopy closure was observed only in 2016, but for ’Mandaga’ in 2015 and 2016. Barry et al. (2001) reported that plants from smaller minitubers may have a 14 day delay in ground cover when expressed in DAP, or they even do not reach full ground cover. Similarly our results showed DAE delay for the MtC 3–4.99 g (10, 8, 5 days for ‘Prelma’, ‘Mandaga’, ‘Monta’, respectively). Radouani & Lauer (2015) did not find significant differences in ground cover 30 DAP depending on minitubers size. They used 15–20 g and heavier minitubers. Our results agree with theirs, because even for ‘Prelma’ significant differences between two heavier MtC were not found.

Despite the significant delay of plant emergence of ‘Monta’, the earliness of this cultivar became apparent when plants reached 90% within row canopy closure in fewer days after E50% than plants of ‘Prelma’ and ‘Mandaga’.

The difference between the marginal MtC of ‘Prelma’ and ‘Mandaga’ in DAE50% to within row canopy closure was more pronounced than it was to emergence (Fig. 3) Stem development of lighter minitubers became slower mostly because the tuber nutrition reserves were spent during the emergence (Lommen & Struik, 1994) and the mother tuber role was lost earlier. Results for ‘Monta’ were not consistent with other cultivars tested.

CONCLUSIONS

This study showed that the effect of weight class of minitubers on plant development was more pronounced under adverse meteorological conditions when minitubers from the lightest classes had much slower initial growth. Overall this study showed that plants from lighter minitubers had slower emergence and canopy closure (even if not significant), and less above ground stems. Nevertheless, the final emergence rate was not significantly affected by the weight class of minitubers.

The significantly different response of ‘Monta’ relative to the other cultivars tested revealed the necessity for studying each cultivar for minitubers field performance in detail. Moreover, this early cultivar showed an unforeseen response such as more days after planting and more GDD required to emerge, when compared to medium early ’Prelma’ and medium late cultivar ’Mandaga’. Moreover, ’Monta’ had significantly lower emergance rate and non- emergence phenomenon was observed especially in 2015. More attention should be given to the storage of ‘Monta’ minitubers to slow the ageing.

ACKNOWLEDGEMENTS. The authors thank Dr. Ilze Skrabule for her great support in organizing the field trials and valuable advices during data assessment. We greatly acknowledge the role of Potato tissue culture laboratory technical staff in growing of minitubers and in assistance during the field trials and data collection.

REFERENCES

Allen, E.J., O'Brien, P.J. & Firman, D. 1992. An evaluation of small seed for ware-potato production. *The Journal Of Agricultural Science* **118**(2), 185–193. http://doi.org/10.1017/S0021859600068775

Barry, P., Clancy, P.C. & Molloy, M. 2001. The effect of seed size and planting depth on the yield of seed potatoes grown from minitubers. *Irish Journal of Agricultural and Food Research* **40**(1), 71–81.

Bodlaender, K.B.A. & Marinus, J. 1987. Effect of physiological age on growth vigour of seed potatoes of two cultivars. 3. Effect on plant growth under controlled conditions. *Potato Research* **30**(3), 423–440. http://doi.org/10.1007/BF02361920

Firman, D.M., O'Brien, P.J. & Allen, E.J. 1992. Predicting the emergence of potato sprouts. *Journalof Agricultural Science* **118**(1), 55–61. http://doi.org/doi:10.1017/S0021859600068003

Fulladolsa, A.C., LaPlant, K.E., Groves, R.L. & Charkowski, A.O. 2017. Potato plants grown from minitubers are delayed in maturity and lower in yield, but are not at a higher risk of potato virus Y infection than plants grown from conventional seed. *American Journal of Potato Research*, *Online* **12**. http://doi.org/10.1007/s12230-017-9613-1

Gopal, J., Kumar, R. & Kang, G.S. 2002. The effectiveness of using a minituber crop for selection of agronomic characters in potato breeding programmes. *Potato Research* **45**, 145–151.

Hagman, J. 1990. *Micropropagation of potatoes: Comparisons of different methods*. SLU/Repro, Uppsala, 94 pp.

Haverkort, A.J. 2007. The canon of potato science: 46. Potato crop modelling. *Potato Research* **50**(3–4), 399–402. http://doi.org/10.1007/s11540-008-9064-7

Haverkort, A.J., Franke, A.C. & Steyn, J.M. 2015. A Robust Potato Model: LINTUL-POTATO-DSS. *Potato Research* **58**, 313–327. http://doi.org/10.1007/s11540-015-9303-7

Haverkort, A.J. & Struik, P.C. 2015. Yield levels of potato crops: recent achievements and future prospects. *Field Crops Research* **182**, 76–85. http://doi.org/10.1016/j.fcr.2015.06.002

Jefferies, R.A. & MacKerron, D.K.L. 1987. Thermal time as a non-destructive method of estimating tuber initiation in potatoes. *Journal of Agricultural Science* **108**, 249–252.

Knowles, N.R. & Knowles, L.O. 2006. Manipulating stem number, tuber set, and yield relationships for northern- and southern-grown potato seed lots. *Crop Science* **46**(1), 284–296. http://doi.org/10.2135/cropsci2005.05-0078

Külen, O., Stushnoff, C., Davidson, R.D. & Holm, D.G. 2011. Gibberellic Acid and Ethephon Alter Potato Minituber Bud Dormancy and Improve Seed Tuber Yield. *American Journal of Potato Research* **88**(2), 167–174. http://doi.org/10.1007/s12230-010-9178-8

Lommen, W.J.M. & Struik, P.C. 1993. Performance of potato minitubers in a controlled environment after different storage periods. *Potato Research* **36**(4), 283–292. http://doi.org/10.1007/BF02361794

Lommen, W.J.M. & Struik, P.C. 1994. Field performance of potato minitubers with different fresh weights and conventional seed tubers: Crop establishment and yield formation. *Potato Research* **37**(3), 301–313.

MacKerron, D.K.L. & Waister, P.D. 1985. A simple model of potato growth and yield. Part I. Model development and sensitivity analysis. *Agricultural and Forest Meteorology* **34**(2–3), 241–252.

McMaster, G.S. & Wilhelm, W.W. 1997. Growing degree-days: one equation, two interpretations. *Agricultural and Forest Meteorology* **87**, 291–300.

O'Brien, P.J., Allen, E.J. & Firman, D.M. 1998. A review of some studies into tuber initiation in potato (Solanum tuberosum) crops. *The Journal of Agricultural Science* **130**(3), 251–270. http://doi.org/doi:null

Oliveira, J.S., Moot, D.J. & Brown, H.E. 2014. Seed potato physiological age and crop establishment. *Agronomy NewZealand* **44**, 85–93.
Ozkaynak, E. & Samanci, B. 2006. Field performance of potato minituber weights at different planting dates. *Archives of Agronomy and Soil Science* **52**(3), 333–338. http://doi.org/10.1080/03650340600676552
Radouani, A. & Lauer, F.I. 2015. Field performance of cultivars Nicola and Russet Burbank micro and minitubers. *American Journal of Potato Research* **92**(2), 298–302. http://doi.org/10.1007/s12230-014-9421-9
Streck, N.A., de Paula, F.L.M., Bisognin, D.A., Heldwein, A.B. & Dellai, J. 2007. Simulating the development of field grown potato (Solanum tuberosum L.). *Agricultural and Forest Meteorology* **142**(1), 1–11. http://doi.org/10.1016/j.agrformet.2006.09.012
Struik, P.C., Haverkort, A.J., Vreugdenhil, D., Bus, C.B. & Dankert, R. 1990. Manipulation of tuber-size distribution of a potato crop. *Potato Research* **33**(4), 417–432. http://doi.org/10.1007/BF02358019
Struik, P.C. & Lommen, W.J. M.1999. Improving the field performance of micro-and minitubers. *Potato Research* **42**(3–4), 559–568. http://doi.org/10.1007/BF02358172
Struik, P.C., van der Putten, P.E.L., Caldiz, D.O. & Scholte, K. 2006. Response of stored potato seed tubers from contrasting cultivars to accumulated day-degrees. *Crop Science* **46**(3), 1156–1168. http://doi.org/10.2135/cropsci2005.08-0267
Van Ittersum, M.K. 1992. Variation in the duration of tuber dormancy within a seed potato lot. *Potato Research* **35**(3), 261–269. http://doi.org/10.1007/BF02357706
Wrobel, S. 2015. Assessment of potato microtuber and in vitro plantlet seed multiplication in field conditions – Growth, development and yield. *Field Crops Research* **178**, 26–33. http://doi.org/10.1016/j.fcr.2015.03.011
Wurr, D.C.E., Fellows, J.R., Akehurst, J.M., Hambidge, A.J. & Lynn, J.R. 2001. The effect of cultural and environmental factors on potato seed tuber morphology and subsequent sprout and stem development. *Journal of Agricultural Science* **136**, 55–63. http://doi.org/10.1017/S0021859600008431

Agronomy Research **16**(4), 1642–1648, 2018
https://doi.org/10.15159/AR.18.172

Suitability of Common nettle (*Urticadioica*) and Canadian goldenrod (*Solidagocanadensis*) for methane production

V. Dubrovskis*, I. Plume and I. Straume

Latvia University of Life Sciences and Technologies, Faculty of Engineering, Institute of Energetics, Cakstesblvd. 5, LV3001 Jelgava, Latvia
*Correspondence: vilisd@inbox.lv

Abstract. Support for biogas production in Latvia was decreased. There is an urgent need to investigate the suitability of various inexpensive renewable biomass resources for energy production. Also, itis necessary to explore the possibilities to improve the anaerobic fermentation process with the help of various catalysts. Biocatalyst Metaferm produced in Latvia was used in previous studies with other biomass and showed increase in biogas and methane production. The article shows the results of studies on biogas (methane) production from chopped fresh Common nettle (*Urtica dioica*) and Canadian goldenrod (*Solidago canadensis*) biomass and effect of catalyst Metaferm in anaerobic fermentation process. The anaerobic digestion process was performed in 0.75 L laboratory digesters, operated in batch mode (38 ± 1.0 °C, 35 days). The average specific biogas or methane production per unit of dry organic matter added (DOM) from Common nettle was 0.709 L g^{-1}_{DOM} or was 0.324 L g^{-1}_{DOM} respectively. Average specific biogas or methane volume produced from chopped Canadian goldenrod in anaerobic fermentation was 0.548 L g^{-1}_{DOM} or 0.267 L g^{-1}_{DOM} respectively. Average biogas or methane yield from digestion of chopped Common nettle with 1 mL Metaferm was 0.752 L g^{-1}_{DOM} or 0.328 L g^{-1}_{DOM} respectively. Average specific biogas or methane yield from anaerobic fermentation of chopped Canadian goldenrod with 1 mL Metaferm was 0.624 L g^{-1}_{DOM} or 0.276 L g^{-1}_{DOM} respectively. Adding of catalyst Metaferm increases methane yield from chopped nettle or Canadian goldenrod by 1.2% or 3.4% respectively. All investigated biomass resources can be used for methane production.

Key words: anaerobic digestion, biogas, Canadian goldenrod, methane, nettle.

INTRODUCTION

In recent years, several measures have been implemented in Latvia to reduce the support for biogas production, such as the introduction of a 9% profit margin, without taking into account large initial capital investments and high interest rates on bank loans. Raw material prices have also increased. The financial situation of the producers of biogas has deteriorated and some owners have already ceased operation of biogas plant. Therefore, the use of new, inexpensive raw biomass would be very important for them.

There are land areas in Latvia that are not well managed. Such areas were overgrown with wild plants, e.g. with Common nettle and, more recently, with Canadian goldenrod. Canadian Golden alpine or Canadian goldenrod (*Solidago canadensis*) is the species within *Curculidae* family that has a natural distribution area in North America, but now it is spread as invasive plant across Europe, including Latvia. In Latvia, this plant is spreading widely, forming dense groups in lawns, set-aside lands, along railways and roads. The Canadian goldenrod is a perennial herb with a height of 70–150 cm. A lot of leaves are located on the stem densely up to hop cones, which is quite dense with yellow flowers. The plant blooms from July to September (Klavins, 2018).

Common nettle or Stinging nettle (*Urtica dioica*) is a perennial Common nettle family herb (60–170 cm in height). This is one of the best–known herb within nettle's genus. The natural spread area is Europe, Asia, North Africa and North America. Common nettles, when in contact with humans or other animals, injects histamine and other chemicals into the skin, causing burning pain. The roots are long, yellowish. Leaves are ellipsoidal with linear bracts and are richly covered with pitchforks. The herb has lot of flowers that manifestly exceeds the length of the leaf stalk. The plant blooms from June to October (Klavins, 2018).

There is less literature data on the use of Common nettles for the production of biogas. Some (Statistics handbook Austria, 2005; Cropgen, 2011) show that nettles are a good raw material providing 120–420 m^3 t^{-1} per unit of dry organic matter or 605–3,780 m^3 ha^{-1} per year. Lehtomaki (2006) calculated that 3,000–5,000 $m^3 ha^{-1}$ of methane per year could be obtained from Common nettles or 30–50 MWh ha^{-1} energy per year. Other authors (Wellinger et al., 2013) have reported dry matter yield 6–10 t_{DM} ha^{-1}, methane 2,200–3,600 m^3 ha^{-1} per year, and energy 21–35 MWh ha^{-1} per year.

Information on use of Canadian goldenrod for biogas production also can be found in literature (Oleszek & Krzeminska, 2017).These authors analyse the suitability of common goldenrod plants as mono–substrates and co–substrates for biogas production. Furthermore, the role of bioactive compounds included in the biomass of this plant species was investigated. The results showed that the common goldenrod species produces lower biogas and methane yields than maize silage. The methane yield from Goldenrod was 127 L kg^{-1}_{DOM}, from maize silage 241 L kg^{-1}_{DOM} and from Goldenrod with maize silage 214L kg^{-1}_{DOM}. However, the anaerobic fermentation of Goldenrod and maize mixture(1:1) resulted in approximately 9.5% higher biogas yield and 16.6% higher methane yield compared to the theoretical yields estimated for two mono–substrates. A statistically significant increase in biogas production efficiency resulted from more favourable C : N ratio and by the influence of bioactive compounds contained in Canadian Goldenrod biomass. The addition of Goldenrod crude extract into maize silage caused 30% increase in the biogas yield approximately. This effect may be associated with a positive impact of biologically active substances on microorganisms or with a decrease in redox potential of the fermenting mass.

Several publications have documented the biogas yields from invasive varieties of *S. canadensis* and *S. gigantea* (Seppälä et al., 2013). These studies stated that these species are productive and cheap substrates that are worthy of interest. Generally, to achieve the highest profitability in biogas production, low–cost substrates with high methane potential are selected. Cultivated or wild perennials are increasingly considered for this purpose and can be an additional source of feedstock for biogas plants. Desirable features of wild perennials are high yield at low soil fertility requirements. To avoid competition with land for food and feed production, fallows for cultivation of perennials could be considered due to its large areas, which are estimated at 8.3 Mha (million hectare) in EU–15 by year 2030 (Seppälä et al., 2013). Such lands are overgrown mostly by invasive plants (such as goldenrods), which are characterised by great tolerance to habitat conditions. As stated by (Young et al., 2011), insufficient research has been conducted on existing (non-cultivated) bioenergy sources (such as invasive plant species) from non-crop agricultural land areas.

Metaferm, created and produced in Latvia is substance, which induce biological processes. Metaferm contain multi enzymes, microelements and B group vitamins as well growing stimulators. Our previous studies shows that use of catalyst Metaferm has a positive effect on methane yield in anaerobic fermentation process of some biomass (Dubrovskis & Plume, 2015).

The aim of this study is to evaluate the suitability of Canadian goldenrod and Common nettle as substrates for biogas production and clarify whether the addition of biocatalyst Metaferm (made in Latvia) in substrates leads to positive effect. Furthermore, the role of bioactive compounds included in this plant biomass should be clarified.

MATERIALS AND METHODS

The methodology described below and similar with German VDI 4630 guideline and the German Methodenhandbuch Energetische Biomassenutzung (Thran, 2010) were used for the present study.

Freshly (15.09.2017) picked from meadow near our laboratory samples of Common nettle and Canadian goldenrod (whole plants without roots) were finely (2–10 mm chunks) chopped and used for anaerobic fermentation experiments. Average samples were taken and it's the chemicals compositions were determined in the LUA laboratory according to the standardized methodology ISO 6496:1999. For each group of raw materials an average sample was taken and the total dry matter, organic dry matter and ashes content were measured.

The analysis were performed according to standard methods. Each group's raw material was thoroughly weighed carefully. All bioreactors (volume of 0.75 L) were filled with the same amount (500.0 g) of inoculums (digestate from a continuous working laboratory bioreactor with almost finished cows manure). Two bioreactors were filled with inoculums only as control. The others bioreactors were filled in with inoculums and biomass sample (20.0 g) with/without catalyst Metaferm (see Table 1).

Chopped Common nettles (20.0 g) (15% flowers, 56% leaves and 29% stalks) were filled in bioreactors R2-R5 (without Metaferm), and in bioreactors R6–R8 (with 1 mL Metaferm). Chopped Canadian goldenrods (20.0 g) (17% flowers, 64% leaves and 19% stalks) were filled in bioreactors R9–R11 (without Metaferm), and in bioreactors R12–R15 (with 1 mL Metaferm).

Bioreactors were filled with substrate and placed in a heated chamber (Memmert model). Gas from each bioreactor was directed into separate storage gas bag located outside the heated chamber.

Dry matter (TS) and organic dry matter (DOM) was determined by investigation of initial biomass sample weight and dry weight by using scales Shimazu at 105 °C and by investigation of ashes content help by furnace (Nabertherm model) burning the samples at 550 °C according to special heating cycle. All substrates were prepared, carefully mixed, and all sealed bioreactors were put in heated chamber in same time before anaerobic digestion. Composition of gases collected in storage bag was analysed with the gas analyser (GA 2000 model). The percentage of oxygen, carbon dioxide, methane and hydrogen sulphide were registered. Substrate pH value was measured before and after finishing of anaerobic fermentation process, using pH meter (PP–50 model) with accessories. Scales (Kern KFB 16KO2 model) was used for weighting of substrate before anaerobic processing and for weighting of digestate after finishing of fermentation process.

The accuracy of the measurements was ± 0.025 L for gas volume, ± 0.1 °C for temperature and ± 0.02 for pH. Methane (CH_4), carbon dioxide (CO), oxygen (O_2) and hydrogen sulphide (H_2S) content in biogas was measured periodically. Weights Kern FKB 16KO2 with accuracy ± 0.2 g was used for measurement of total weight of substrates, and the unit Shimazu with accuracy ± 0.001 g was used for weighting of biomass samples to obtain total solids and dry organic matter content.

Fermentation process was provided with single filling in batch mode until biogas emission ceases (35 days). Final digestate was weighed, and dry matter and ashes were investigated to determine organic dry matter content. Total biogas and methane production values were calculated using the biogas normal volumes and quality parameters obtained from gas collected in the gas storage bag for each bioreactor (Becker et al 2007).

Experimental data were recorded in the experimental log and also stored in computer.

RESULTS AND DISCUSSION

The data on sample analysis and on amount of biogas and methane produced was estimated for all 16 bioreactors, and average results were calculated.

The results of raw material analyses before anaerobic digestion are shown in Table 1.

Weight of raw material in Table 1 is provided with error value depending on accuracy of respective weight measuring instrument used. Weight of total solids (TS) and dry organic matter (DOM) in Table 1 is provided with accuracy ± 0.001 g.

Table 1. Results of analysis of raw materials

Bioreactor	Raw material	Weight g	pH	TS %	TS g	ASH %	DOM %	DOM g
R1; R16	IN	500 ± 0.2	7.69	2.01	10.050	19.61	80.39	8.079
R2–R5	CN	20 ± 0.001		21.81	4.362	20.83	79.17	3.453
R2–R5	IN+CN	520 ± 0.2	7.35	2.77	14.412	19.98	80.02	11.532
R6–R8	IN+CN+MF	521 ± 0.2	7.36	2.78	14.483	19.99	80.01	11.588
R9–R11	CG	20 ± 0.001		34.33	6.866	8.99	91.01	6.249
R9–R11	IN+CG	520 ± 0.2		3.20	16.916	13.77	86.23	14.328
R12–R15	IN+CG+MF	521 ± 0.2		3.20	16.682	13.79	86.21	14.382

Abbreviations: TS – total solids; ASH – ashes; DOM – dry organic matter; IN – inoculums; CN – Common nettle; CG – Canadian goldenrod; MF – Metaferm.

Both inoculum substrates in control bioreactors (R1, R16) have low dry matter content as almost finished digestate were used for inoculums.

As it can be seen from the raw material (Table 1) Canadian goldenrod biomass has a relatively high dry matter and organic dry matter content. This is explained due to the fact that the stems part of the plant was also used, and this part has less moisture content compared to the fresh leaves or flowers. The Common nettle biomass had higher moisture content, because their stem contains more juice. The natural proportions (by the weight) of the three main components of the plant – stem, leaves and flowers – were observed during filling in each bioreactor.

This raw material, containing a lot of organic dry matter and also juice, is well suited for biogas production. Biogas and methane yields from Common nettle and Canadian goldenrod are shown in Table 2.

Table 2. Biogas and methane yields from Common nettle and Canadian goldenrod

Reactor	Raw material	Biogas, L	Biogas, L g^{-1}_{DOM}	Methane, aver. %	Methane, L	Methane, L g^{-1}_{DOM}
R1	IN500	0.00	0.00	0.00	0.00	0.00
R16	IN500	0.20	0.025	8,00	0.016	0.020
R2	IN500+CN20	2.50	0.724	37.71	0.943	0.273
R3	IN500+CN20	2.20	0.637	50.23	1.105	0.320
R4	IN500+CN20	2.40	0.695	48.06	1.154	0.334
R5	IN500+CN20	2.70	0.781	47.38	1.277	0.370
	Aver. R2–R4	**2.45**	**0.709**	**45.85**	**1.120**	**0.324**
	± st.dev.	**± 0.21**	**± 0.06**	**± 5.56**	**± 0.14**	**± 0.04**
R6	IN500+CN20+MF1	2.50	0.724	45.02	1.124	0.326
R7	IN500+CN20+MF1	2.60	0.752	43.75	1.137	0.329
R8	IN500+CN20+MF1	2.70	0.781	42.13	1.137	0.329
	Aver. R5–R8	**2.60**	**0.75**	**43.60**	**1.133**	**0.328**
	± st.dev.	**± 0.10**	**± 0.03**	**± 1.45**	**± 0.01**	**± 0.01**
R9	IN500+CG20	4.20	0.672	44.79	1.882	0.301
R10	IN500+CG20	3.40	0.544	42.83	1.461	0.233
R11	IN500+CG20	3.30	0.528	49.62	1.636	0.262
R12	IN500+CG20	2.80	0.448	60.94	1.708	0.273
	Aver. R9–R11	**3.43**	**0.548**	**49.55**	**1.67**	**0.267**
	± st.dev.	**± 0.58**	**± 0.09**	**± 8.11**	**± 0.17**	**± 0.03**
R13	IN500+CG20+MF1	3.90	0.62	42.79	1.670	0.267
R14	IN500+CG20+MF1	3.80	0.608	47.04	1.789	0.286
R15	IN500+CG20+MF1	4.00	0.640	42.81	1.71	0.274
	Aver. R12–R15	**3.90**	**0.624**	**44.21**	**1.723**	**0.276**
	± st.dev.	**± 0.10**	**± 0.02**	**± 2.45**	**± 0.06**	**± 0.01**

Note: Biogas and methane values for bioreactors 2–15 with fresh source biomass are provided with already subtracted average biogas and methane values obtained from reactors 1 and 16.

Abbreviation: L g^{-1}_{DOM} – litres per 1 g dry organic matter added (added fresh organic matter into inoculum).

Usually, pre-shredding of raw material significantly increases methane yields. This could be explained by the fact that the raw materials studied were better distributed by the anaerobic digestion process because the microbial access to the raw material was better. Compared to literature (Lehtomaki, 2006), the methane yield from Common nettles is medium (Table 2).

Methane production from the Canadian goldenrod was much higher, compared to results reported by Polish researchers (Oleszek & Krzeminska, 2017). This is explained by fact that Polish researchers used silage from Canadian goldenrod.

Specific biogas and methane gases volumes obtained from bioreactors R2–R15 are presented in Fig. 1.

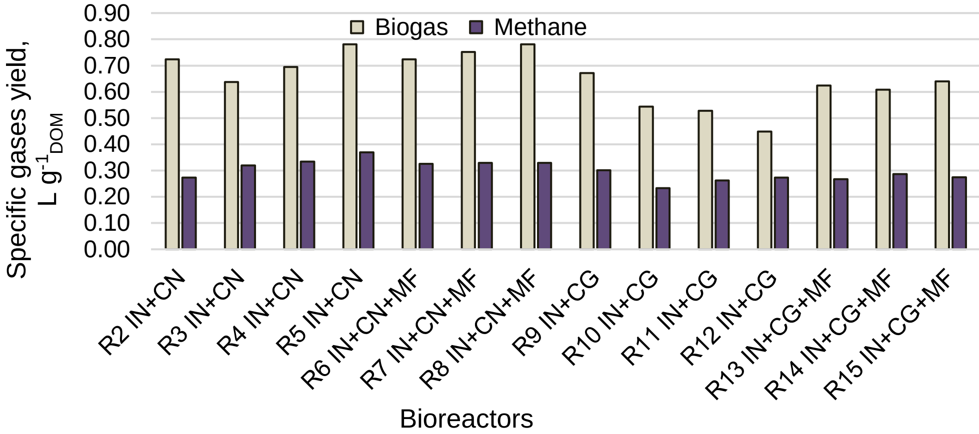

Figure 1. Specific biogas and methane yields from bioreactors filled with Common nettles and Canadian goldenrods.

The figure shows the best methane yield from bioreactor R5. It can be explained with better microbes association in used inoculum filled in this bioreactor.

Average methane volumes and methane percentage in biogas for groups of bioreactors with Common nettle and Canadian goldenrod biomass are shown in Fig. 2.

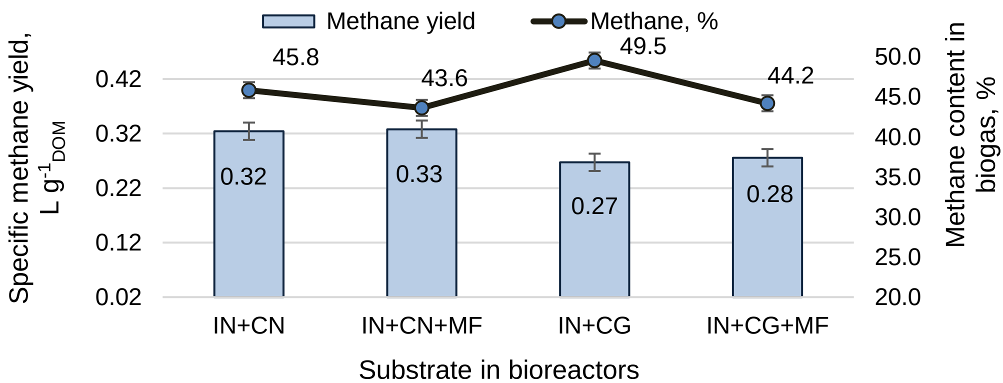

Figure 2. Average specific methane yields and methane percentage for groups of bioreactors with Common nettle and Canadian goldenrod substrates without and with added Metaferm.

Fig. 2 shows the average methane content in biogas from Common nettle biomass in biogas was 45.8% and the average methane content in biogas from Canadian goldenrod was 49.5%. These are lower methane contents compare with often used in biogas plants raw materials (for example maize silage).These contents are higher for both plants, if used Metaferm. It can be explained by the fact that there used fresh raw materials.

The total methane yield from Common nettle with Metaferm was higher by 1.2% compared to Common nettle substrate without Metaferm. A slight increase could be explained by the fact that there are already enough bioactive substances in the substrate without Metaferm. Adding of 1 mL catalyst Metaferm to substrate with Canadian goldenrod increased methane yield by 3.4%.

CONCLUSIONS

The average specific methane yield from Common nettle biomass substrate was 0.324 L g^{-1}_{DOM}. The result is good, similar that obtainable from maize silage. It convinces that fresh Common nettle can substitute maize silage for some month's period in summer. The average specific methane yield from Canadian goldenrod biomass was 0.267 L g^{-1}_{DOM}, which is better than from manure, but expectations in improving of high methane production were not met.

The addition of Metaferm increased the specific methane yield slightly. Using this biocatalyst for Common nettle and Canadian goldenrod fresh biomass cannot be economically. Such level of increased methane yield in Latvian conditions do not justify the application costs of Metaferm.

The results of the study show that nettle and Canadian goldenrod can be used as raw materials for the production of methane.

In future studies, it would be desirable to clarify the effect of different pre-treatment (treatment with acids, bases, chrushing degree) methods on the anaerobic fermentation of investigated biomass.

ACKNOWLEDGEMENTS. This work has been supported by the Latvian National Research Programme LATENERGI.

REFERENCES

Becker, K., Dowler, H. & Meckel, H. 2007. *Faustzahlen biogas* (Calculations of biogas). Publisher Kuratorium für Technik und Bauwesen in der Landwirtschaft, Darmstadt, 181 pp. (in German).

Klavins, A. 2018. The Latvian Nature Encyclopaedia. *www.latvijasdaba.lv* Accessed: January 25, 2018 (in Latvian).

Lehtomaki, A. 2006. Biogas from energy crops and crops residues. *Doctoral thesis*, University of Jyvaskyla, 94 pp.

Oleszek, M. & Krzeminska, I. 2017. Enhancement of Biogas Production by Co-Digestion of Maize Silage with Common Goldenrod Rich in Biologically Active Compounds. *Bio Resources* **12**(1), 704–714.

Sepal, M., Laine, A. & Rental, J. 2013. Screening of novel plants for biogas production in northern conditions. *Bio resource Technology* **139**, 355–362.

Statistics handbook Austria. 2005. *Statistic Austria*. Vienna Austria. Austrian statistical Office: www.statistik.at/web_en/statistics/index.htm.

Thran, D. 2010. *Methodenhandbuch Energetische Biomassenutzung* (Methods Manual Energetic use of biomass), Leipzig, 93 pp.

VDI 4630. 2006. Vergärung organischer Stoffe Substrat charakterisierung, Probenahme, Stoffdatenerhebung, Gärversuche. *Verein Deutscher Ingenieure* (Fermentation of organic substances Substrate characterization, sampling, substance data collection, fermentation tests. German engineers). Düsseldorf, pp. 48. (in German).

Wellinger, A., Murphy, J. & Baxter, D. 2013. *The biogas handbook*. Woodhead Publishing 512 pp.

Young, S., Gopalakrishnan, G. & Keshwani, D. 2011. Invasive plant species as potential bioenergy producers and carbon contributors. *Journal of Soil and Water Conservation*, **66**(2), 45–50.

Agronomy Research **16**(4), 1649–1659, 2018
https://doi.org/10.15159/AR.18.190

Agronomic evaluation of a Colombian passion fruit (*Passiflora edulis* Sims) germplasm collection

C.H. Galeano Mendoza[1,*], I. Cerón-Souza[2] and L.V. Arango[1]

[1]Centro de Investigación Palmira, Corporación Colombiana de Investigación Agropecuaria – AGROSAVIA, Diagonal a la intersección de la Carrera 36A con Calle 23, Palmira, Valle del Cauca, Colombia
[2]Centro de Investigación Tibaitatá, Corporación Colombiana de investigación Agropecuaria – AGROSAVIA, Km 14 vía Bogotá-Mosquera, Cundinamarca, Colombia
[*]Correspondence: cgaleano@corpoica.org.co

Abstract. Passion fruit (*Passiflora edulis* Sims) is one of the most promissory crops in Colombia with approximately 7,400 ha cultivated, an average production of 89,000 t and an average yield of 15 t ha^{-1}. However, low yields as well as harvest problems including fruit quality, generate important losses, mainly due to lack of improved cultivars with particular characteristics for each market (fresh consumption, agroindustry) and specific adaptations to biotic and abiotic stress factors in producer areas. Therefore, as a pre-breeding phase, this study aimed at characterizing preliminary the production and physiochemical characteristics of 60 passion fruit germplasm accessions maintained in Corporación Colombiana de Investigación Agropecuaria (AGROSAVIA). We cultivated these accessions in the field for 22 months between 2014 and 2015, measuring 17 variables associated to both yield production and fruit quality. We analysed data using phenetic and multivariate methods to establish levels of genetic diversity. Additionally, we constructed a selection index (SI) with the most informative variables to select individuals according to fruit weight, shape and colour, as well as juice percentage. Results of genetic grouping and principal components showed a broad genetic diversity across the working collection, without any population substructure. Fruit volume, pulp and seed weight were the variables that explained 80% of the phenotypic variation. Finally, we identified 30 promissory accessions as parental for the first cycle of recurrent selection using the SI. We conclude that this core collection represents the diversity included in the working collection with promissory accessions to initiate an intra-population recurrent selection program.

Key words: passion fruit, plant breeding, selection index, genetic diversity, germplasm collection.

INTRODUCTION

Passion fruit (*Passiflora edulis* Sims) belongs to the genus *Passiflora* L. that is one of the most important genera in economic terms of the Passifloraceae botanical family. This gender comprises a wide diversity with ca. 530 species, all with an American origin (Yockteng et al., 2011). Colombia is the country with the most extensive *Passiflora* diversity worldwide with 162 species, followed by Brazil with 127 species (Ocampo et al., 2010). Nevertheless, the materials with the highest economic importance for Colombia are the two botanical forms of *P. edulis* Sims, f. edulis Sims (gulupa) and f. *flavicarpa* Degener (passion fruit or maracuyá). Some authors prefer to simplify the taxonomy of both forms, using only the name *P. edulis* Sims (Bernacci et al., 2008). However, in this study, we recognize passion fruit and gulupa as different botanical forms as stated by Ocampo & Coppens (2017).

Passion fruit is a diploid ($n = 9$) self-incompatible species with extensive cross-pollination mediated mainly by insects (Bruckner et al., 1995). The genetic diversity within *P. edulis* worldwide has been evaluated using morphological descriptors and agronomic characteristics (Meletti et al., 2005a; Abreu et al., 2009). Moreover, several microsatellite molecular markers have been used (Oliveira et al., 2005; dos Santos et al., 2011; Cerqueira-Silva et al., 2014b; Araya et al., 2017). In Colombia, the genetic diversity of *P. edulis* has partially been studied using molecular markers as random amplified microsatellites (RAM) and amplified fragment length polymorphisms (AFLP) in gulupa (*P. edulis* f. *edulis*) (Fonseca-Trujillo et al., 2009; Ortiz et al., 2012). Furthermore, in yellow passion fruit (*P. edulis* f. *flavicarpa*), a preliminary diversity analysis was carried out in materials collected in producer regions assessing physicochemical fruit characteristics (Ocampo et al., 2013) and using single sequence repeat (SSR) molecular markers (Ocampo et al., 2017). Additionally, pre-breeding activities have been carried out to evaluate compatibility between interspecific crossings among commercial and wild cultivars (Ocampo et al., 2016).

In Colombia during 2015, approximately 7,400 ha were cultivated with passion fruit obtaining a production of 89 thousand tons, being the departments of Huila, Meta and Valle del Cauca the main producers with an average yield of 15 t ha^{-1} (MADR, 2017). In contrast, Brazil shows a cultivated area that is more than six times larger (51,187 ha) than in Colombia with a production that is ten times higher, i.e. 921,275 t (IBGE, 2016), and a potential yield for new cultivars of 50 t ha^{-1} (Meletti et al., 2005b). In Colombia, one of the reasons for the low productivity is the lack of improved cultivars, either explicitly adapted to each producer zone with better response to biotic and abiotic stress factors or with specific characteristics for each market (i.e. fresh consumption or agroindustry) (Quintero et al., 2012). Moreover, the first and unique cultivars registered in the 1970s in Colombia were selections called Hawai, Brasil, and Venezuela. Since then, no research in plant breeding in this species has been carried out (Jaramillo et al., 2009). Currently, AGROSAVIA is interested in starting a breeding program in passion fruit using its working collection. However, this collection is not well conserved nor characterized. Therefore, the aim of this study was to characterize for the first time the passion fruit working collection maintained in AGROSAVIA and provide insights about the most promissory materials identified for future breeding programs.

MATERIALS AND METHODS

Study site and variables measured

During 2014, 1,313 passion fruit plants were obtained from seeds belonging to 60 accessions maintained in the working collection of AGROSAVIA (Corpoica). This material was previously not conserved or characterized properly, and therefore, we performed this first assessment with the material available, i.e. without repetitions or any experimental design in the field. The field trial was stablished in Centro de Investigación

Palmira of Corpoica (AGROSAVIA), located in the department of Valle del Cauca, between January 2014 and October 2015. The study site has an average annual temperature of 24 °C, a mean annual precipitation of 1,032 mm, an average relative humidity of 72%, an average sunshine of 5.8 hours day^{-1}, and a wind speed of 1.5 m s^{-1}; climatic variables were calculated using data collected from a meteorological station located on site.

Once plants were obtained, they were stablished in a deep Vertisol soil, with a clay-loam texture, good fertility conditions and rich in organic matter. Moreover, plants were cultivated using a trellis system establishing a distance of 2.5 m between plants, and 1.5 m between rows (Jaramillo et al. (2009). Two variables related to yield components, including total plant production and number of fruits per plant, were registered in the entire population. Finally, a random subgroup of 295 plants was selected for fruit quality evaluation including 15 variables. Among these, fruit colour (i.e. scale from one to ten, where one is white and ten is yellow), fruit shape (diameter in mm/height in mm ratio), fruit volume (mL), fruit density (g mL^{-1}), peel thickness (mm), and peel weight (g). Moreover, pulp weight (g), seed weight (g), juice weight (g), juice (%), Brix degrees (°Brix), acidity (%), vitamin C (%), juice pH and average fruit weight (g).

Statistical analysis

A principal component analysis (PCA) and grouping was carried out with the software NTSYS-pc® version 2.02 g (Rohlf, 1990), standardizing the data with the function *STAND.* Principal components were identified with the *EIGEN* and *PCA* functions. Moreover, Pearson's correlation and variance-covariance matrices were constructed using the *CORR* and *VAVCOV* functions, respectively. For grouping analysis, each genotype was considered as an operational taxonomic unit (OTU), and a dissimilarity matrix was constructed with an average taxonomic distance using the function *DIST*. Furthermore, we grouped and constructed a dendrogram with the *UPGMA* function. For the principal coordinate analysis, we used a similarity matrix with the algorithms *DCENTER* and *EIGEN*. Finally, we developed a selection index based on yield and market requirements using the Eq. 1:

$$SI = P(0.4) + J(0.2) + S(0.2) + C(0.2) \quad (1)$$

where *P* is fruit weight per plant, *J* is juice percentage, *S* is fruit length and width relation, and *C* is fruit colour.

RESULTS AND DISCUSSION

The primary goal of this study was to characterize for the first time the production and physiochemical characteristics of 60 passion fruit germplasm accessions maintained in AGROSAVIA. We found a considerable variation associated with the number of plants within each accession (Fig. 1). We obtained on average 21 plants per accession. In some cases, only one plant per accession was obtained (e.g. 12.2Cenicafe, 40.5Cenicafe, 5.1Cenicafe, 7.1Cenicafe and La Union S1P3). In comparison, accessions that came from collections with masal selection as La Union 2/2 and La Union 1/2 (L. Arango, 2017 personal communication) showed the highest number of individuals, i.e. 167 and 120 plants, respectively. We found that seed viability and adaptation during their initial crop growth phases are probably the main factors associated with the considerable variation observed in the phenotypic characteristics in our data. The diversity in germination patterns observed across different passion fruit populations is due to the effect of the exterior seed layer that limits water absorption, and therefore, inhibits germination (Santos et al., 2015). Consequently, to achieve uniform germination in passion fruit seeds, it is necessary to use several treatments with warm water, sulphuric acid and sucrose (Ghosh et al., 2017).

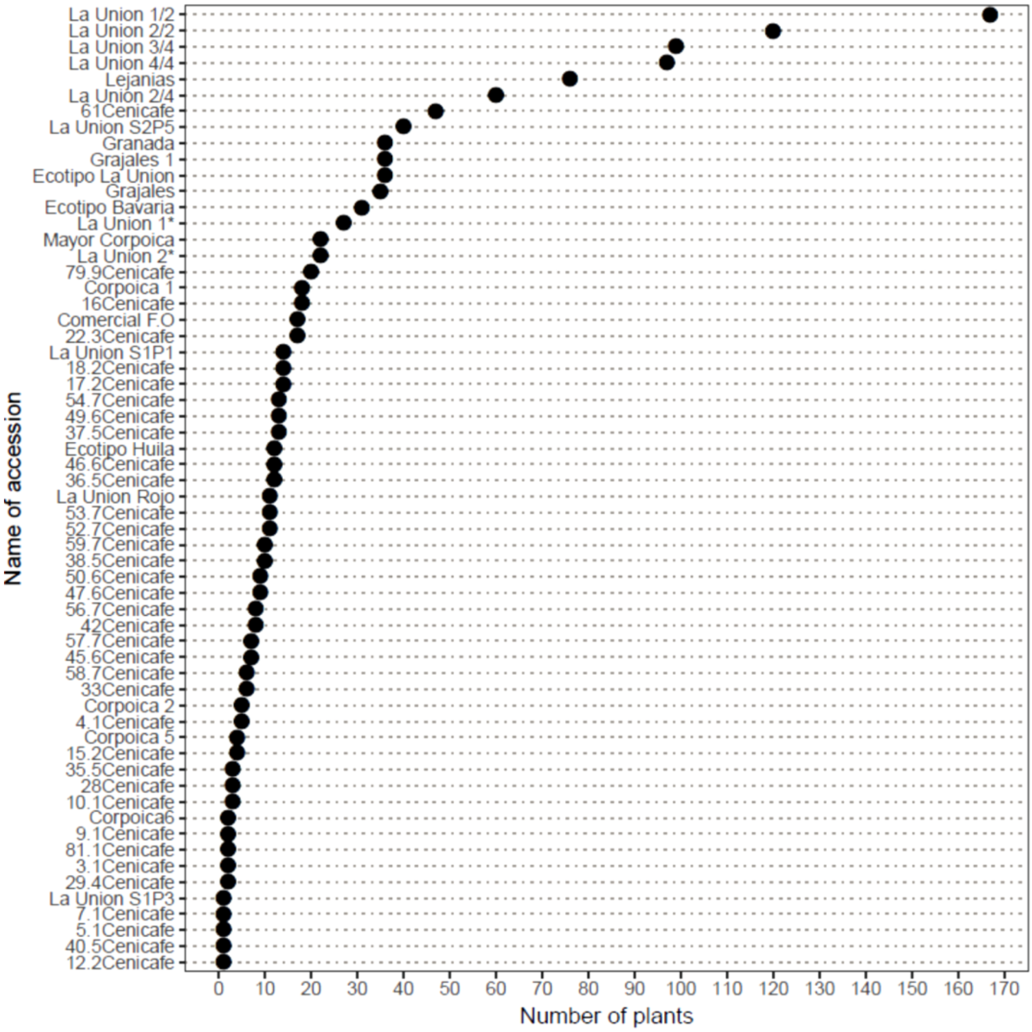

Figure 1. Total number of plants per accession (n = 60) from the *Passiflora edulis* working collection of AGROSAVIA assessed in this study.

Regarding the two yield components considered (i.e., plant weight and fruit number) as well as the 15 variables associated with fruit quality, we found a wide variation in the data (Fig. 2). This variation is mainly due to their forced cross-pollination condition. Therefore, passion fruit populations are heterogeneous and heterozygous. In the case of plant weight, the average found in our collection was 5.9 kg with variation ranging from 0.2 kg to 19 kg. These results show materials that can potentially reach up to 50 t ha^{-1}, similarly to the maximum yield obtained by improved hybrid materials from Brazil (Meletti et al., 2005b). However, detailed studies with controlled pollination must be carried out to establish heritability in a broad and narrow sense, and in this way, establish recurrent selection schemes that will be used to achieve a higher genetic gain (Gonçalves et al., 2007). Similarly, the broad variation of fruit quality traits, such as Brix degrees, acidity and percentage of juice within this working population is very important to develop new cultivars for the agroindustry and the fresh market. Therefore, further studies evaluating the environmental stability of these traits as well as other nutrition properties such as antioxidant potential have to be developed to increase nutritional value as a functional food (dos Reis et al., 2018).

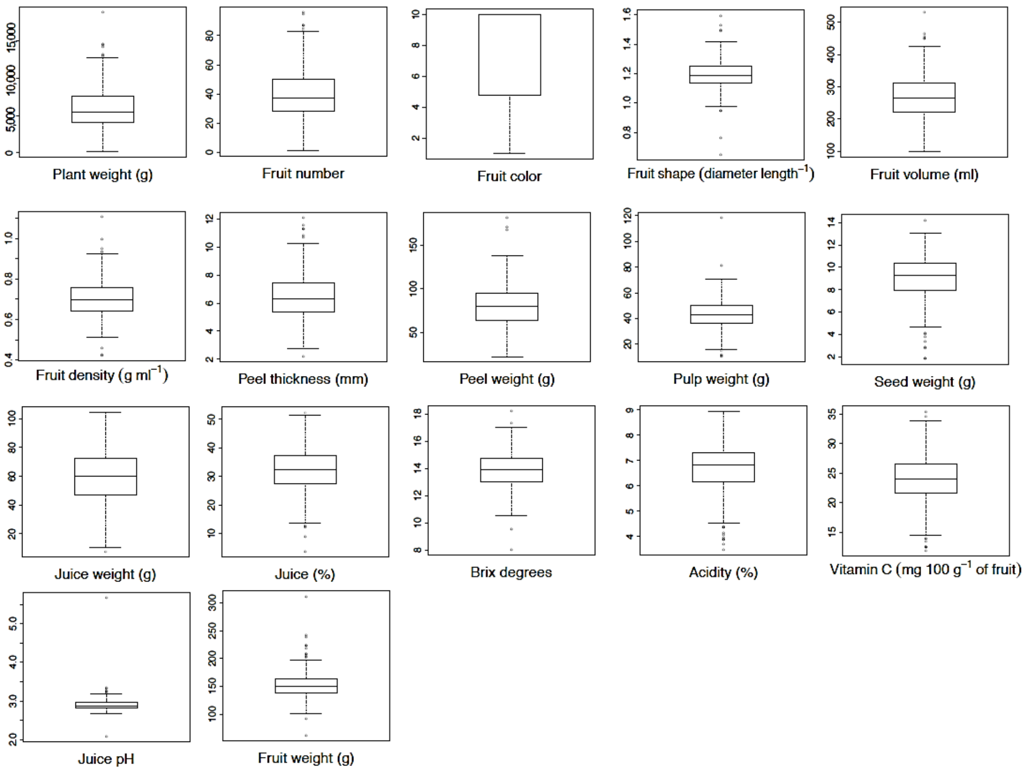

Figure 2. Box plots for each of the 17 variables measured in the *Passiflora edulis* working collection of Agrosavia.

Principal component analysis for fruit quality characteristics (Table 1) shows that variables like fruit volume, peel weight, pulp weight, seed weight, juice weight and peel thickness explain best the first component (PC1). For the second component (PC2), the variables juice weight, juice percentage, and total weight are the ones that have more relevance. We found a positive correlation between the seven variables that explain much better the principal component analysis with high ranges varying from 0.1 to 0.75. However, juice (%) is negatively correlated with four variables (i.e. fruit volume, peel thickness, peel weight and pulp weight with a range from -0.07 to -0.45) (Fig. 3, A).

The analysis of 25 morpho-agronomic descriptors to identify improved cultivars in Brazil showed similar results (Fonseca, 2017). In this study, seed weight and peel thickness were highlighted as the most important variables that explained the phenotypic variation. Additionally, in the first genetic diversity screening of a Colombian passion fruit collection carried out through the evaluation of 40 accessions, peel thickness and seed weight were also the variables that explained most of the variability (Ocampo et al., 2013). Further studies in a diversity panel as well as with a segregating population will establish possible heterotic groups in passion fruit and the subsequent use of hybrid vigour in new cultivars (Silva et al., 2014).

Table 1. Principal component analysis for 17 yield and fruit quality variables measured in passion fruit. Bold values indicate the variables that explain each component

Variable	PC1	PC2	PC3
Fruit colour	0.095	0.135	0.161
Fruit shape	-0.323	0.101	0.174
Fruit volume	**0.858**	-0.060	0.099
Fruit density	-0.038	0.086	0.248
Peel thickness	**0.501**	-0.385	-0.239
Peel weight	**0.777**	-0.445	-0.160
Pulp weight	**0.781**	0.099	0.093
Seed weight	**0.785**	0.126	0.123
Juice weight	**0.623**	**0.509**	0.465
Juice percentage	-0.091	**0.693**	**0.557**
Brix degrees	0.181	0.239	0.147
Acidity %	0.174	0.000	-0.253
Vitamin C	0.188	-0.093	-0.371
Juice pH	-0.025	-0.145	0.099
Total weight	0.184	**0.674**	-0.644
Number of fruits	0.081	0.687	-0.685
Fruit weight	0.323	-0.077	0.203

Despite the genetic variability that was seen using fruit quality features, the PCA analysis did not show a defined structure within the population (Fig. 3, B). Similar results using molecular markers show the low genetic structure in passion fruit mostly due to self-incompatibility and cross-pollination (Ocampo et al., 2017). However, this information is useful to select genetically contrasting materials that can be used as parental to increase segregation in following generations. Additionally, because of the selection pressure that these materials have suffered to select the best plants, much of the phenotypic variability is due to environmental effects with a narrow genetic base. Therefore, any pre-breeding and breeding program in passion fruit must start with the collection, conservation, and characterization of new materials in both *ex situ* and *in situ* germplasm banks. After this process has been carried out and the information has been analysed, it is possible to identify a core collection which represents the minimum number of materials with the highest allelic variability (Cerqueira-Silva et al., 2014a). Recent studies have used SSR markers with high polymorphism and with a broad genome coverage as a complementary tool for characterization of the genotypic diversity within the *Passiflora* genus (Araya et al., 2017).

There are two possibilities to increase the genetic diversity bases of passion fruit in a pre-breeding program. The first strategy is to search for wild materials to increase the allelic variability of this botanical form. This strategy has been used in gulupa (Ortiz et al., 2012). Alternatively, a second strategy is to cross passion fruit with closest species. Fortunately, in Colombia, the following high compatible interspecific crosses have been identified as viable: *P. edulis* f. *flavicarpa* × *P. vitifolia*, *P. alata* and *P. cincinnata*; *P. maliformis* × *P. caerulea*; and *P. edulis* f. *edulis* × *P. edulis* f. (Ocampo et al., 2016).

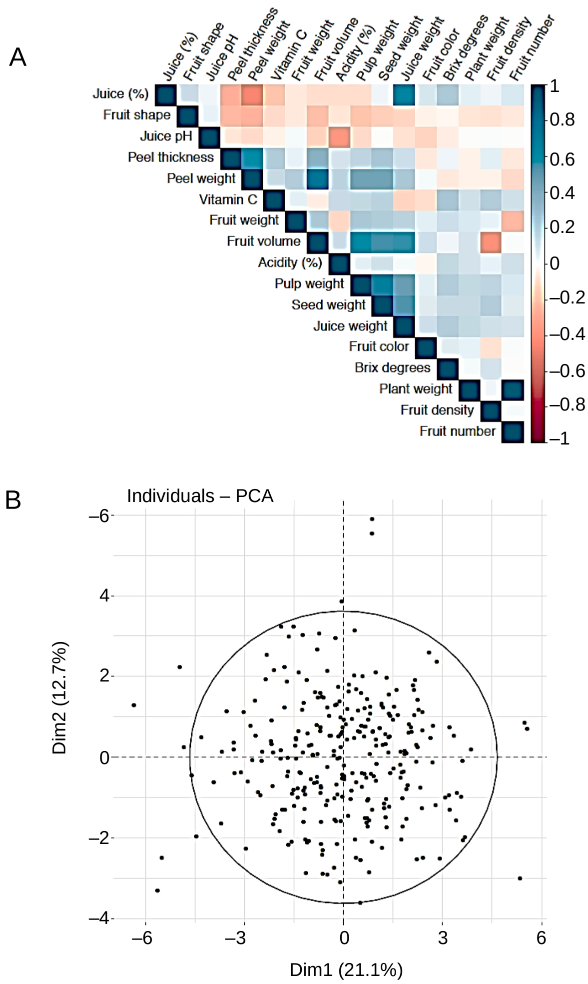

Figure 3. A – Correlation analysis among 17 variables analysed in the passion fruit collection; B – Variation of individuals in the two PCA dimensions that explains the data showing no evidence of subpopulation structure.

Finally, the SI analysis allowed us to identify 30 accessions from the working collection with most desirable characteristics to continue with the next recombination and/or selection cycle. Five of the materials with the highest SI were 38.5Cenicafe, 18.2Cenicafe, LaUnion 2/4, Lejanias, and Grajales with values of 2.09, 1.93, 1.44, 1.40 and 1.29, respectively (Fig. 4). Furthermore, with a selection pressure of 10%, thirty of the best-improved materials showed a SI superior to 0.65. The use of SI has been critical in plant breeding and particularly in passion fruit progeny evaluations. Furthermore, non-parametric SI have shown good gain predictions that are superior, in a balanced way, among the characteristics assessed (Silva & Viana, 2012). Moreover, SI give us the possibility to complement these results with future molecular analyses and response trials to specific biotic stresses. For example, Cerqueira-Silva et al. (2015) used 23 SSR markers together with plant response values (incidence and severity) for anthracnose, scab and passion fruit woodiness virus (PWV) to select the most promissory materials.

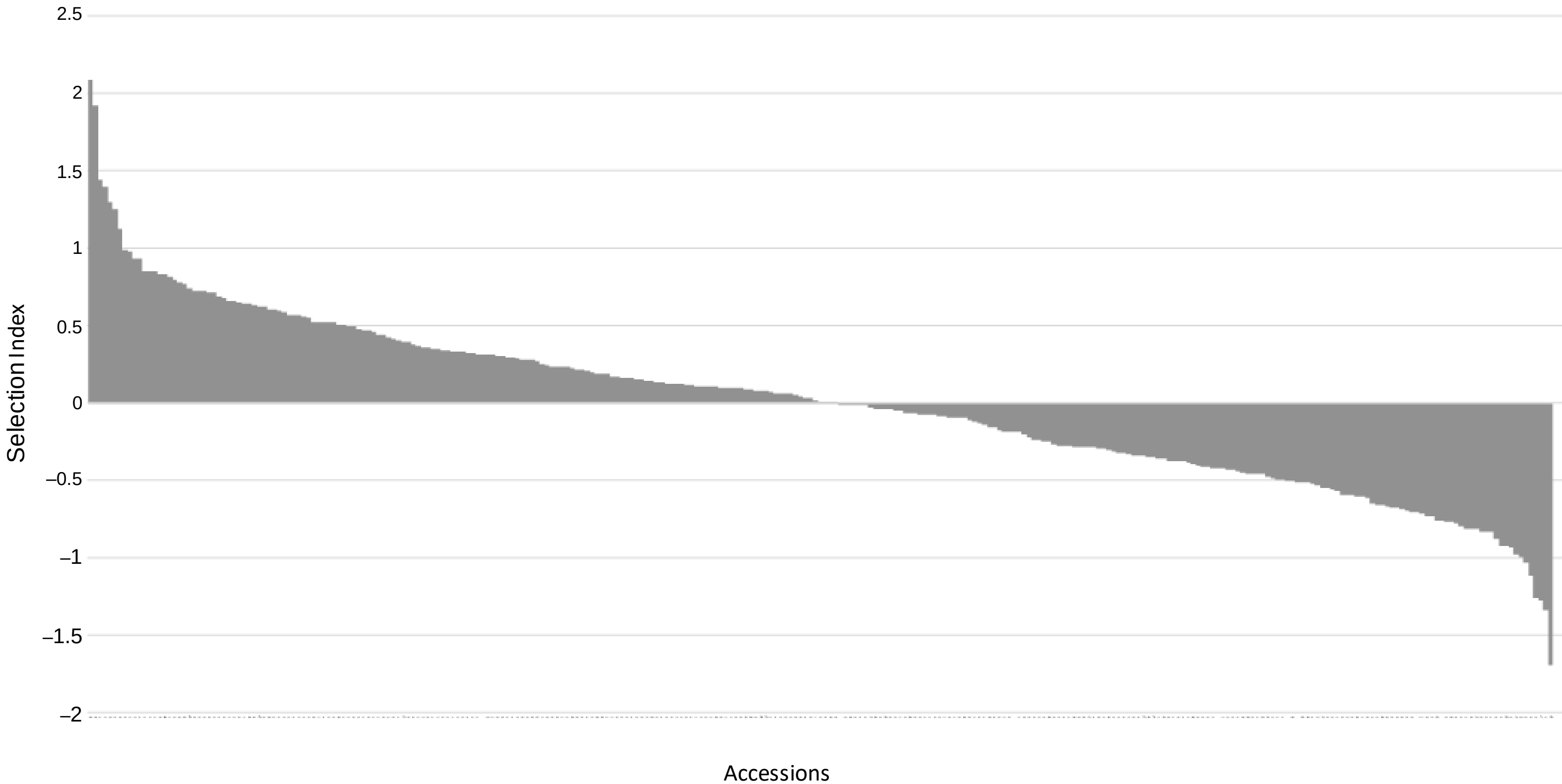

Figure 4. Selection index of 295 passion fruit plants that represent the diversity of 60 accessions from the working collection of Agrosavia (Corpoica).

CONCLUSIONS

This study allowed us to establish for the first time the genetic diversity of the passion fruit germplasm collection of AGROSAVIA (Corpoica). We found a high diversity across 60 accessions including 17 variables associated to yield production and fruit quality. Despite this variability, we did not find evidence of population substructure within the collection. Therefore, we selected the 30 most promissory accessions to be used in the first recurrent selection cycle plan as part of a future breeding program for this species in Colombia. These accessions and their progenies are going to be genotyped across the genome and combined with current agronomic characterization to estimate their breeding values (GEBV), and reduce selection cycles in a future selection process (Viana et al., 2017).

ACKNOWLEDGEMENTS. The authors wish to thank Ministerio de Agricultura y Desarrollo Rural (MADR) of Colombia for financing this study. We are also grateful to Victor Alexander Balanta and Yaneth Patricia Ramos for their dedication during and beyond the operative work in the greenhouse and field. In addition, we wish to thank the Editor and Reviewers for their very helpful input and suggestions.

REFERENCES

Abreu, S.P.M., Peixoto, J.R., Junqueira, N.T.V. & Sousa, M.A.F. 2009. Características agronômicas de seis genótipos de maracujazeiro-azedo cultivados no Distrito Federal. *Rev. Bras. Frutic.* **31**, 920–924.

Araya, S., Martins, A.M., Junqueira, N.T.V., Costa, A.M., Faleiro, F.G. & Ferreira, M.E. 2017. Microsatellite marker development by partial sequencing of the sour passion fruit genome (*Passiflora edulis* Sims). *BMC Genomics*. **18**, 549.

Bernacci, L.C., Soares-Scott, M.D., Junqueira, N.T.V., Passos, I.R.S. & Meletti, L.M.M. 2008. *Passiflora edulis* Sims: the correct taxonomic way to cite the yellow passion fruit (and of others colors). *Rev. Bras. Frutic.* **30**, 566–576.

Bruckner, C.H., Casali, V.W.D., de Moraes, C.F., Regazzi, A.J. & da Silva, E.A.M. 1995. Self-incompatibility in passion fruit (*Passiflora edulis* Sims). *ISHS*, 45–58.

Cerqueira-Silva, C.B.M., Jesus, O.N., Oliveira, E.J., Santos, E.S.L. & Souza, A.P. 2015. Characterization and selection of passion fruit (yellow and purple) accessions based on molecular markers and disease reactions for use in breeding programs. *Euphytica* **202**, 345–359.

Cerqueira-Silva, C.B.M., Santos, E.S.L., Jesus, O.N., Vieira, J.G.P., Mori, G.M., Corrêa, R.X. & Souza, A.P. 2014a. Molecular genetic variability of commercial and wild accessions of passion fruit (*Passiflora* spp.) targeting *ex situ* conservation and breeding. *Int. J. Mol. Sci.* **15**, 22933–22959.

Cerqueira-Silva, C.B.M, Santos, E.S.L., Vieira, J.G.P., Mori, G.M., Jesus, O.N., Corrêa, R.X. & Souza, A.P. 2014b. New microsatellite markers for wild and commercial species of Passiflora (Passifloraceae) and cross-amplification. *Appl.Plant Sci*. **2**, apps.1300061.

dos Reis, L.C.R, Facco, E.M.P., Salvador, M., Flôres, S.H. & de Oliveira Rios, A. 2018. Antioxidant potential and physicochemical characterization of yellow, purple and orange passion fruit. *Journal of Food Science and Technology*. doi:10.1007/s13197-018-3190-2

dos Santos, L.F., de Oliveira, E.J., dos Santos, Silva. A., de Carvalho, F.M., Costa, J.L. & Pádua, J.G. 2011. ISSR markers as a tool for the assessment of genetic diversity in Passiflora. *Biochem. Gen.* **49**, 540–554.

Fonseca-Trujillo, N., Márquez-Cardona, M.P., Moreno-Osorio, J.H., Terán-Pérez, W. & Schuler-García, I. 2009. Caracterización molecular de materiales cultivados de gulupa (*Passiflora edulis* f. *edulis*). *Univ. Sci.* **14**, 6. http://dx.doi.org/10.11144/javeriana.SC14-2-3.cmdm (in Spanish).

Fonseca, K. 2017. Descriptors validation, characterization and genetic diversity of cultivar and wild passion fruit. Faculdade de agronomia e medicina veterinária. Universidade de Brasília, Brasilia, 95 pp. (in Portuguese).

Ghosh, A., Dey, K. F. & Dey, A. 2017. Effects of different pre-germination treatment methods on the germination and seedling growth of yellow passion Fruit (*Passiflora edulis* var. *flavicarpa*). *Int. J. Curr. Microbiol. App. Sci*. **6**, 630–636.

Gonçalves, G.M., Viana, A.P., Bezerra Neto, F.V., Pereira, M.G. & Pereira, T.N.S. 2007. Selection and heritability in the prediction of genetic gain in yellow passion fruit. *Pes. Agropec. Bras.* **42**, 193–198 (in Portuguese).

IBGE. 2016. Séries históricas e estatísticas: lavoura permanente – quantida de produzida. IBGE, Brasil.

Jaramillo, J., Cardenas, J. & Orozco, J. 2009. *Colombian passion fruit* (*Passiflora edulis)* f*ield handbook*. Corpoica, Palmira, Colombia, 80 pp. (in Spanish).

MADR. 2017. Municipal Agricultural Evaluations - EVA. In: Prospectiva OdPy (ed). MADR, Colombia, 50 pp. (in Spanish).

Meletti, L.M.M., Soares-Scott, M.D. & Bernacci, L.C. 2005a. Phenotypic characterization of three selections of red passion fruit (*Passiflora edulis* Sims). *Rev. Bras. Frutic.* **27**, 268–272 (in Portuguese).

Meletti, l.M.M., Soares-Scott, M.D., Bernacci, L.C. & Passos, I.R. 2005b. Passion fruit plant breeding: past and future. In: Faleiro FG, Junqueira NTV, Braga MF (eds) Passion fruit: germplasm and plant breeding , Planaltina, DF, pp. 55–78 (in Portuguese).

Ocampo, J., Arias, J.C. & Urrea, R. 2016. Interspecific hybridization between cultivated and wild species of genus *Passiflora* L. *Euphytica* **209**, 395–408.

Ocampo, J. & Coppens, G. 2017. Morphological characterization in the genus *Passiflora* L.: an approach to understanding its complex variability. *Plant Syst. Evol.* **303**, 531–558.

Ocampo, J., Acosta-Barón, N. & Hernández-Fernández, J. 2017. Variability and genetic structure of yellow passion fruit (*Passiflora edulis* f. *flavicarpa* Degener) in Colombia using microsatellite DNA markers. *Agron. Colomb*. **35**(2), 15. doi:10.15446/agron.colomb.v35n2.59973

Ocampo, J., D'Eeckenbrugge, G. & Jarvis, A. 2010. Distribution of the genus *Passiflora* L. diversity in Colombia and its potential as an indicator for biodiversity management on the coffee growing zone. *Diversity,* **2**, 1158–1180.

Ocampo, J., Urrea, R., Wyckhuys, K. & Salazar, M. 2013. Exploration of the genetic variability of yellow passion fruit (*Passiflora edulis* f. *flavicarpa* Degener) as basis for a breeding program in Colombia. *Acta Agron.* **62**(4), 352–360 (in Spanish).

Oliveira, E.J., Pádua, J.G., Zucchi, M.I., Camargo, L.E.A., Fungaro, M.H.P. & Vieira, M.L.C. 2005. Development and characterization of microsatellite markers from the yellow passion fruit (*Passiflora edulis* f. *flavicarpa*). *Mol. Ecol. Notes* **5**, 331–333.

Ortiz, D.C., Bohórquez, A., Duque, M.C., Tohme, J., Cuéllar, D. & Mosquera Vásquez, T. 2012. Evaluating purple passion fruit (*Passiflora edulis* Sims f. *edulis*) genetic variability in individuals from commercial plantations in Colombia. *Gen. Res. Crop Evol.* **59**, 1089–1099.

Quintero, E., Lopez, I. & Kondo, T. 2012. Manejo integrado de plagas como estrategia para el control de la mosca del botón floral del maracuyá *Dasiops inedulis* Steyskal (Diptera: Lonchaeidae). Revista Corpoica – Ciencia y Tecnología Agropecuaria **13**, 31–40.

Rohlf, F. 1990. Numerical taxonomy and multivariate analysis system (NTSYS-pc). Departament of Ecology and Evolution, New York, 43 pp.

Santos, C.E.M., Morgado, M.A.D.O., Matias, R.G.P., Wagner Júnior, A. & Bruckner, C.H. 2015. Germination and emergence of passion fruit (*Passiflora edulis*) seeds obtained by self- and open-pollination. *Acta Sci-Agron.* **37**, 489–493.

Silva, F.H.L., Viana, A.P., Ferreira, R.T., Freitas, J.C.O., Santos, J.O. & Rodrigues, D.L. 2014. Measurement of genetic diversity in progenies of sour passion fruit by ward-mlm methodology: a strategy for heterotic group formation. *Cienc. Agrotec.* **38**, 240–246.

Silva, M.G.M. & Viana, A.P. 2012. Alternatives of selection in a yellow passion fruit population under intrapopulation recurrent selection. *Rev. Bras. Frutic.* **34**, 525–531 (in Portuguese).

Viana, A.P., de Lima e Silva, F.H., Glória, L.S., Ribeiro, R.M., Krause, W. & Boechat, M.S.B. 2017. Implementing genomic selection in sour passion fruit population. *Euphytica* **213**, 228.

Yockteng, R., d'Eeckenbrugge, G.C. & Souza-Chies, T.T. 2011. Passiflora. In: Kole C (ed) Wild Crop Relatives: Genomic and Breeding Resources: Tropical and Subtropical Fruits. Springer Berlin Heidelberg, Berlin, Heidelberg, pp 129–171.

Agronomy Research **16**(4), 1660–1667, 2018
https://doi.org/10.15159/AR.18.167

Study of effect of arbuscular mycorrhiza (*Glomus intraradices*) fungus on wheat under nickel stress

A. Heydarian[1], H.R. Tohidi Moghadam[1], T.W. Donath[2] and M. Sohrabi[2,*]

[1]Islamic Azad University Varamin- Pishva Branch, Department of Agronomy, IR 33817-74895 Varamin, Iran
[2]Kiel University, Department of Landscape Ecology, Institute for Natural Resource Conservation, Olshausenstr. 75, DE24118 Kiel, Germany
[*]Correspondence: msohrabi@ecology.uni-kiel.de

Abstract. In many regions of the world soils are contaminated with heavy metals and therefore restricted in their use. For instance, the absorption of nickel (Ni) in the tissue of plants increase the plant's metabolism and cause physiological disorders or even death. Arbuscular mycorrhizal fungi are known to enhance the tolerance of host plants to abiotic and biotic stress. Thus, we investigated the potential of the arbuscular mycorrhizal fungi *Glomus intraradices* to mitigate deleterious effects of Ni in wheat. The experiment was conducted using four levels of Ni (0, 60, 120 and 180 mg per kg of soil) and two levels of mycorrhizal fungi application (with and without *Glomus intraradices*). Nickel stress significantly decreased seed number per spike, thousand-seed weight, seed yield per plant, concentration of chlorophyll a and b. At the same time, we found increased catalase (CAT) enzyme activity and dityrosine (DT) treatments. Mycorrhizal fungi application attenuated Ni effects, i.e. fungal presence increased seed number per spike, thousand-seed weight, chlorophyll a and b. Furthermore mycorrhizal fungi application reduce CAT enzyme activity and DT. In general, our results suggest that mycorrhizal fungi application reduces harmful effects of Ni stress in wheat.

Key words: CAT, chlorophyll, dityrosine, mycorrhizal fungi, nickel.

INTRODUCTION

Soil contamination with heavy metals as a result of human activities such as mining, metallurgical processes and application of fertilizers, pesticides and fungicides in agriculture is a serious threat for ecosystems and human health. Particularly when food crops are grown on contaminated soil, heavy metals may enter the human food chain (Dixi et al., 2001; Sheetal et al., 2016). The transfer and accumulation of heavy metals in soil-plant systems is impress by multiple factors (Wang et al., 2017). Here we test, whether mycorrhizal fungi may be used to reduce the heavy metal uptake by wheat and thus may pose a possibility to grow crops on heavy metal contaminated soils without challenging human health. Among the heavy metals, Nickel (Ni) is an essential micronutrient for plant growth and development (Eskew et al., 1983). However, it becomes toxic at high concentrations, Excess Ni disturbs photosynthesis and membrane function (Moya et al., 1993; Madhava Rao & Sresty, 2000; Boominathan & Doran, 2002). High condensation of Ni, excite the production of reactive oxygen species (ROS) such as superoxide ion (O^{2-}) and hydrogen peroxide (H_2O_2) at cellular level. (Gajewska & Sklodowska, 2007) and caused oxidative stress by membrane lipid peroxidation (Baccouch et al., 1998). The most obvious symptoms of Ni-toxicity, the inhibition of growth, chlorosis, necrosis and wilting have been reported not only for wild but also crop plants such as cabbage or wheat (Pandey & Sharma 2002; Gajewska et al., 2006). The symbiosis between plants and arbuscular mycorrhiza (*Glomeromycota*) is one of the most substantial interactions between plants and microorganisms in the soil For the plant this coexistence leads to strengthened absorption of nutrients such as phosphorus, nitrogen and micronutrients through mycelium (Kapulnik & Douds, 2000; Javaid, 2009) and in exchange host plants provide carbohydrates to the fungi (Smith & Read, 2008). An enhanced phosphorus concentration in plants, in turn, raises photosynthesis rate and carbohydrates production (Parádi et al., 2003). Yet, arbuscular mycorrhizal fungi not only assist host plants in absorbing nutrients, but also improve their tolerance against environmental abiotic factors such heavy metals (Jahromi et al., 2008).

An improved tolerance against heavy metals is achieved by arbuscular mycorrhizal fungi binding heavy metals to their cell walls (Hildebrandt et al., 2007) and emit glomalin (Gonzalez-Chavez et al., 2004). Moreover, mycorrhiza fungi participate in nontoxic formation through symbiosis with plants to accumulate heavy metals in plant root (Joner & Leyval, 1997). The performance of these fungi in soils contaminated with heavy metals have been fulfilled by several studies (Khan et al., 2000; Abdel Latef, 2011; Miransari, 2011; Abdel Latef, 2013). In general, mycorrhizal fungi improve mineral nutrient balance, especially rare nutrients, stimulate their uptake when the nutrients amount is low and inhibit their absorption when amount of nutrients is high. The aim of this study was to determine Ni distribution in shoot and root of wheat grown under Ni contaminated soil, and to understand if mycorrhizal fungi application presents a potential strategy for immobilizing Ni, thus reducing its deleterious effects in wheat. We particularly hypothesized that the application of the arbuscular mycorrhizal fungi *Glomus intraradices* to wheat (i) lowers the inhibition of seed germination as well as, (ii) growth and development, and (iii) the decrease in yield of wheat when grown in nickel contaminated soil.

MATERIAL AND METHODS

The experiment was conducted in a greenhouse at Varamin- Pishva, Iran, in 2016. It followed a completely randomized 4 × 2 factorial design, with three replicates per treatment combination. The soil of the experimental site was a clay loam one, with a montmorillonite clay type, low in nitrogen (0.06–0.07%), low in organic matter (0.56–0.60), and alkaline in reaction with pH of 7.2 and Ec = 0.66 dS m^{-1}. The soil texture was sandy loam, with 10% of neutralizing substances. For the experiment, sterilized field soil (autoclaved at 121 °C and pressure of 15 atmospheres for one hour , before being used as culture soils) was used to prepare four levels of Ni-contamination (0, 60, 120 and 180 mg of Ni chloride per 1 kg of soil) and filled in 30 x 30 cm plastic pots. For the second treatment factor, the top layer of the soil of half of the pots was inoculated with 2 g of Glomus intraradices spores and fungal propagules inoculum (purchased from Biotech Turan Company, Semnan, Iran) just before seed sowing. Each pot was fitted with ten seeds of cultivar Pishtaz before placing it in the controlled environment. The room was equipped with cool white fluorescent lamps. Room air temperature was 20–22 °C, during the 16/8 h light/dark photoperiod. Photosynthetically active radiation at the top of the canopy was 400 μmol m^{-2} s^{-1}, during the light photoperiod. Relative humidity in the room was 70%. Plants were hand irrigated daily until optimal field capacity was reached. The field capacity was determined by slowly saturating four soil-filled pots until water started to drip from the bottom. Pots were covered and allowed to drain for 24 h and then weighted. The average weight was the definition of field capacity and the pots were kept watered to this weight. At seed filling stage, flag leaves were collected and immediately frozen in liquid nitrogen and stored at 80 °C until further laboratory analyses. At physiological maturity stage, plants were harvested at the soil surface and seed per spike counted and weighted to determine thousand seed weight and seed yield per plant. Chlorophyll was extracted by 80% acetone according to Arnon (1949). The extracts were filtrated, and chlorophyll a and b content were determined by spectrophotometer (model Cintra 6 GBC; GBC Scientific Equipment, Dandenong, Victoria, Australia) at 645 nm and 663 nm. The content of chlorophyll was expressed as mg × g^{-1} of fresh weight. Catalase activity was estimated by the Cakmak & Horst (1991) method. The reaction mixture contained 100 μl of crude extract, 500 μl of 10 mM H_2O_2 and 1,400 μl of 25 mM sodium phosphate buffer. Catalase activity was estimated by recording the absorbance reduction at 240 nm, for 1 min, using a spectrophotometer.

Dityrosine was estimated by the Amado et al. (1984) method. Leaf samples were homogenized with 5 mL of 0.16 M Tris-phosphate, pH 7.5. The plant tissue homogenate was centrifuged at 5,000 g for 60 min to remove debris. o,o-dityrosine was recovered by gradient elution from the C-18 column (Econosil C18, 250 mm × 10 mm) and was analyzed by reversed-phase HPLC with simultaneous UV-detection (280 nm). A gradient was formed from 10 mM ammonium acetate, adjusted to pH 4.5 with acetic acid, and methanol, starting with 1% methanol and increasing to 10% over 30 min. A standard dityrosine sample was prepared according to Amado et al. (1984). Dityrosine was quantified by assuming that its generation from the reaction of tyrosine with horseradish peroxidase in the presence of H_2O_2 was quantitative (using the extinction coefficient e315 = 4.5 mM^{-1} cm^{-1} at pH 7.5). From each treatment, one gram of dried tissue (root and shoot) was placed in an electrical oven at 480 °C for 5 h. After cooling, obtained ash was solved in 10 mL 10% nitric acid. After filtering, the solution was poured in plastic tubes and the amount Ni in roots and shoots were analyzed by atomic absorption spectroscopy (Model GBC 932 plus) (Reeves et al., 1996).

All data were analyzed by analysis of variance using the GLM procedure in SAS (SAS Institute Inc., 2002). The assumptions of the variance analyses were tested by checking if the residuals were random, homogenous, with a normal distribution and a mean of about zero. The significance of differences among means was carried out using Duncan's multiple range test at $p < 0.05$.

RESULTS AND DISCUSSION

The main effects of Ni and fungus were significant on all measured traits (Table 1). The interaction between Ni and fungus was significant on CAT enzyme activity (Table 1). The lowest seed number per spike, 1,000 seed weight and seed yield per plant were obtained when wheat plants were exposure to 180 mg $NiCl_2$ (Table 2).

Table 1. Analysis of variance on wheat attributes affected by nickel stress and mycorrhizal fungi

S.O.V	d.f	Seed number per spike	Thousand seed weight	Seed yield per plant	Chlorophyll a	Chlorophyll b	Catalase enzyme activity	Dityrosine
Ni	3	55.38**	65.40**	44.57**	0.205**	0.003**	16,030.35**	10.37**
Myc	1	5.22**	91.26**	6.38*	0.035**	0.005**	2,338.20**	0.752**
Ni* Myc	3	0.21ns	2.27ns	0.35ns	0.0001ns	0.00001ns	280.25*	0.057ns
Error	16	0.47	6.76	1.69	0.0003	0.00006	53.98	0.028
C.V (%)		1.73	6.77	6.02	1.46	1.61	5.35	2.45

*, ** and ns significant at 0.05, 0.01 percentage and no significant, Myc = Mycorrhiza, Ni = nickel.

Table 2. Comparison of main means wheat attributes affected by nickel stress condition and mycorrhizal fungi

Treatment	Seed number per spike	Thousand seed weight (g)	Seed yield per plant (g)	Chlorophyll a (mg g^{-1}FW)	Chlorophyll b (mg g^{-1}FW)	Catalase enzyme activity (ΔA mg pro.min^{-1})	Dityrosine (nmol g^{-1} FW)
Nickel concentration							
0	43.31a	42.15a	11.04a	1.576a	0.540a	74.22d	5.24d
60	41.58b	40.11a	9.51a	1.368b	0.500b	116.63c	6.48c
120	37.65c	36.36b	7.14b	1.236c	0.495b	170.59b	7.59b
180	37.05c	35.00b	4.82c	1.151d	0.485c	187.30a	8.23a
Mycorrhiza							
-	39.43b	36.45b	7.61b	1.295b	0.490b	147.06a	7.06a
+	40.36a	40.35a	8.64a	1.371a	0.520a	127.31b	6.71b

Treatment means followed by the same letter within each common are not significantly different ($P < 0.05$) according to Duncan's Multiple Range test.

Plants grown in Ni contaminated soil showed visible symptoms of injury reflected in terms of chlorosis, growth inhibition and browning of root tips. The lowest seed number per spike, 1,000 seed weight and seed yield per plant were obtained when no mycorrhizal fungus was applied, while the highest seed number per spike, 1,000 seed weight and seed yield per plant were obtained by treating the soil with mycorrhizal fungus (Table 2). Increased water and nutrients absorption after the application of mycorrhizal fungus may explain the increase in seed number per spike, thousand seed weight and seed yield per plant. In addition, arbuscular mycorrhizal fungi may also increase plant growth by improving nutrition through increasing water uptake and reduced soil compaction (Gaur & Adholeya, 2004). The present study showed that chlorophyll a and b production decreased when wheat plants were exposure to 180 mg $NiCl_2$ (Table 2). The plants response to Ni in the soil seems to be closely linked to the chlorophyll activity, since the highest levels of chlorophyll-a and chlorophyll-b were obtained when the plants were colonized with mycorrhizal fungus (Table 2 and Fig. 2). Analogously, several authors report decreased chlorophyll contents in the leaves of Ni-exposed plants (Pandey & Sharma, 2002; Seregin & Kozhevnikova, 2006; Gajewska & Sklodowska, 2007). Dhir et al. (2009) assumes that this decline in chlorophyll levels might be due to a lower Fe content, reduced efficiency of enzymes involved in chlorophyll biosynthesis and replacement of central Mg^{2+}-molecules in chlorophyll by heavy metals. Accordingly, earlier research already suggested that some heavy metals disable the biosynthesis of chlorophyll (Ouzounidou, 1995).

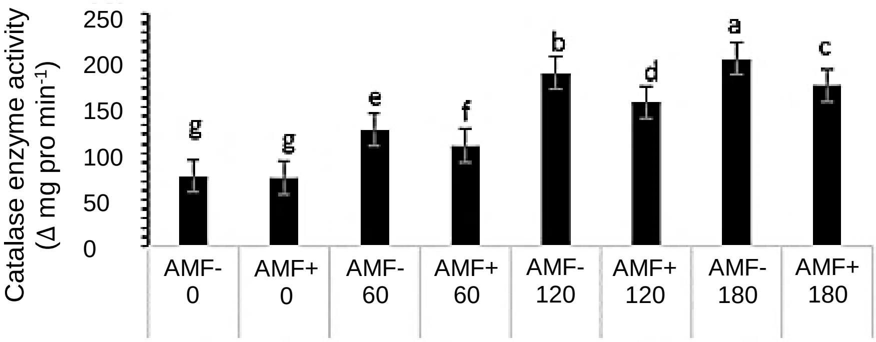

Figure 1. Interaction between nickel stress condition and mycorrhizal fungi on CAT enzyme activity- Nickel-chloride concentrations (0, 60, 120 or 180 mg per kg of soil) and presence (AMF+) or absence (AMF-) of arbuscular mycorrhizal fungi. Presented are the mean ± SE.

Sohrabi et al. (2018) also reported that the Pb-contamination caused a significant decrease in total chlorophyll contents. The lowest CAT enzyme activity was obtained when mycorrhizal fungus was applied, also according to our results the highest CAT enzyme activity was obtained when wheat plants were exposure to $NiCl_2$ concentration with 180 mg per kg of soil (Table 2 and Fig. 1). The results showed that the highest dityrosine content was observed in wheat plants exposed to 180 mg $NiCl_2$ per kg of soil (Table 2). CAT enzyme activity increases when plants have to increase their defense activity against oxidative stress. Consequently, several researchers have reported an increase in CAT activity under heavy metal stress, e.g. Cd, Hg, Ni, Pb and Fe (Ma, 2000; Pang et al., 2001; Yang et al., 2001; Parlak, 2016). The primary response of plants to heavy metal stress is the generation of ROS upon exposure to high levels of heavy metals that which destroys chlorophyll molecules by ROS, reducing photosynthesis and growth (Wojtaszek, 1997; Halliwell & Gutteridge, 1998; Feda et al., 2004; Mithofer et al., 2004). Again, stress through heavy metals was – as indicated by a low CAT enzyme activity – lowest when mycorrhizal fungus was applied (Table 2 and Fig. 1). The capability of arbuscular mycorrhiza to lower stress plants experience when exposed to heavy metals relies on the fungi's ability to produce Glomalin (Arriagada et al., 2005). This insoluble glycoprotein, which is produced by the hyphae, was shown to bind potentially toxic elements including heavy metals (Gonzalez-Chavez et al., 2004).

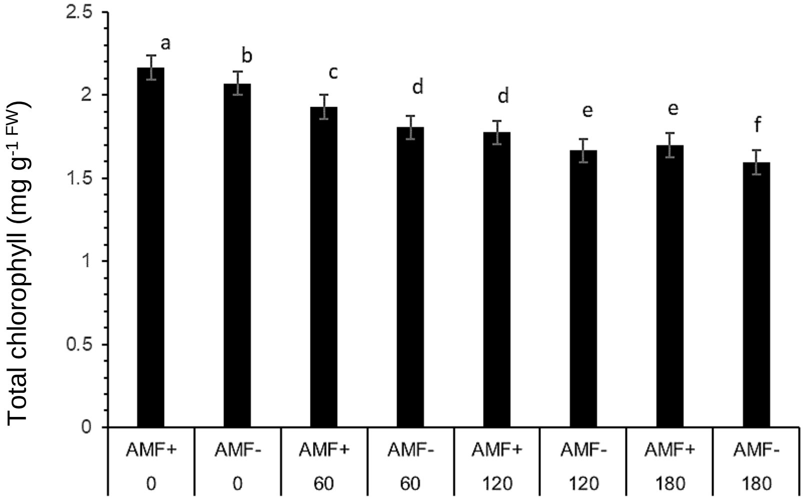

Figure. 2. Interaction between nickel stress condition and mycorrhizal fungi total chlorophyll (mg $g^{-1\ FW}$) activity- Nickel-chloride concentrations (0, 60, 120 or 180 mg per kg of soil) and presence (AMF+) or absence (AMF-) of arbuscular mycorrhizal fungi. Presented are the means ± SE.

CONCLUSION

In conclusion, evidence is now accumulating that mycorrhizal fungus can filter out toxic heavy metals and thus keep them away from the plants. The results of this study showed that inoculation with Glomus. intraradices increases wheat resistance against Ni stress and improves seed yield under Ni stress.

REFERENCES

Abdel Latef, A.A. 2011. Influence of arbuscular mycorrhizal fungi and copper on growth, accumulation of osmolyte, mineral nutrition and antioxidant enzyme activity of pepper (*Capsicum annuum* L.). *Mycorrhiza* **21**, 495–503.

Abdel Latef, A.A. 2013. Growth and some physiological activities of pepper (*Capsicum annuum* L.) in response to cadmium stress and mycorrhizal symbiosis. *Journal of Agricultural Science and Technology* **15**, 1437–1448.

Amado, R., Aeschbach, R. & Neukom, H. 1984. Dityrosine: *in vitro* production and characterization. *Methods Enzymol* **107**, 377–388.

Arnon, D.I. 1949. Copper enzymes in isolated chloroplasts, polyphenoloxidase in *Beta vulgaris*. *Plant Physiology* **24**, 1–15.

Arriagada, C.A., Herrera, M.A. & Ocampo, J.A. 2005. Contribution of arbuscular mycorrhizal and saprobe fungi to the tolerance of *Eucalyptus globulus* to Pb. *Water Air and Soil Pollution* **166**, 31–47.

Baccouch, S., Chaoui, A. & El Ferjani, E. 1998. Nickel-induced oxidative damage and antioxidant responses in *Zea mays* shoots. *Plant Physiology and Biochemistry* **36**, 689–694.

Baccouch, S., Chaoui, A. & El Ferjani, E. 2001. Nickel toxicity induces oxidative damage in Zea mays roots. *Journal of Plant Nutrition* **24**, 1085–1097.

Boominathan, R. & Doran, P.M. 2002. Ni-induced oxidative stress in roots of the Ni hyperaccumulator, *Alyssum bertolonii*. *New Phytologist* **156**, 205–215.

Cakmak, I. & Horst, W. 1991. Effect of aluminium on lipid peroxidation, superoxide dismutase, catalase and peroxidase activities in root tip of soybean (*Glysin max*). *Plant Physiology* **83**, 463–468.

Dhir, B., Sharmila, P., Saradhi, P.P. & Nasim, S.A. 2009. Physiological and antioxidantresponses of *Salvinia natans* exposed to chromium-rich wastewater. *Ecotoxicology and Environmental Safety* **72**, 1790–1797.

Dixi, V., Pandey, V. & Shyam, R. 2001. Differential antioxidative responses to heavy metal in roots and leaves of pea (*Pisum sativum L*. CV. Azad). *Journal of Experimental Botany* **52**, 1101–1109.

Eskew, D.L., Welch, R.M. & Norvell, W.A. 1983. Nickel an essential micronutrient for legumes and possibly all higher plants. *Science* **222**, 621–623.

Feda, E.A., Kevin, J.B. & Colin, J.B. 2004. Metal catalyzed oxidation of tyrosine residues by different oxidation systems of copper/hydrogen peroxide. *Journal of Inorganic Biochemistry* **98**, 173–84.

Gajewska, E., Sklodowska, M., Slaba, M. & Mazur, J. 2006. Effect of nickel on antioxidative enzyme activities, proline and chlorophyll contents in wheat shoots. *Biologia Plantarum* **50**, 653–659.

Gajewska, E. & Sklodowska, M. 2007. Effect of nickel on ROS content and antioxidative enzyme activities in wheat leaves. *Biometals* **20**, 27–36.

Gaur, A. & Adholeya, A. 2004. Prospects of arbuscular mycorrhizal fungi in phytoremediation of heavy metal contaminated soils. *Current Science* **86**, 528–534.

Gonzalez-Chavez, M., Carrillo-Gonzalez, R., Wright, S. & Nichols, K. 2004. The role of glomalin, a protein produced by arbuscular mycorrhizal fungi, in sequestering potentially toxic elements. *Environmental Pollution* **130**, 317–323.

Halliwell, B. & Gutteridge, J.M.C. 1998. Mechanisms of damage to cellular targets by oxidative stress: lipid peroxidation. Chap 4. In: Halliwell B and Gutteridge JMC (eds.). Free radicals in biology and medicine. *Oxford Science Publication*, 284–306.

Hildebrandt, U., Regvar, M. & Bothe, H. 2007. Arbuscular mycorrhiza and heavy metal tolerance. *Phytochemistry* **68**, 139–146.

Jahromi, F., Aroca, R., Porcel, R. & Ruiz-Lozano, J. M. 2008. Influence of salinity on the in vitro development of *Glomus intraradices* and on the in vivo physiological and molecular responses of mycorrhizal lettuce plants. *Microbial Ecology* **55**, 45–53.

Javaid, A. 2009. Arbuscular mycorrhizal mediated nutrition in plants. *Journal of Plant Nutrition* **32**, 1595–1618.

Joner, E. & Leyval, C. 1997. Uptake of ^{109}Cd by roots and hyphae of a *Glomus mosseae*/*Trifolium subterraneum* mycorrhiza from soil amended with high and low concentrations of cadmium. *New Phytologist* **135**, 353–360.

Kapulnik, Y. & Douds, D. 2000. Arbuscular mycorrhizas: physiology and function. *Published 30th by Springer*, pp. 307–343.

Khan, A.G., Knek, C. & Chaudhry, T.M. 2000. Role of plants, mycorrhizae and phytochelation in heavy metal contaminated land remedian. *Chemosphere* **41**, 197–207.
Ma, J. 2000. Effects of Ni pollution on wheat seedling growth and the index of physiology and biochemistry. *Journal of the Hebei Vocation Teachers College* **14**, 17–20.
Madhava Rao, K.V. & Sresty, T.V.S. 2000. Antioxidative parameters in the seedlings ofpigeonpea (*Cajanus cajan* (L.) *Millspaugh*) in response to Zn and Ni stresses. *Plant Science* **157** 113–128.
Miransari, M. 2011. Hyper-accumulators, arbuscular mycorrhizal fungi and stress of heavy metals. *Biotechnology Advances* **29**, 645–653.
Mithofer, A., Schulze, B. & Boland, W. 2004. Biotic and heavy metal stress response in plants: evidence for common signals. *FEBS Letters* **566**, 1–5.
Moya, J.L., Ros, R. & Picazo, I. 1993. Influence of cadmium and nickel on growth, net photosynthesis and carbohydrate distribution in rice plants. *Photosynthesis Research* **36**, 75–80.
Ouzounidou, G. 1995. Cu-ions mediated changes in growth, chlorophyll and other ion contents in a Cu- tolerant *Koeleria splendens*. *Biologia Plantarum* **37**, 71–78.
Pandey, N. & Sharma, C.P. 2002. Effect of heavy metals Co^{2+}, Ni^{2+} and Cd^{2+} on growth and metabolism of cabbage. *Plant Science* **163**, 753–758.
Pang, X., Wang, D. & Peng, A. 2001. Effect of lead stress on the activity of antioxidant enzymes in wheat seedling. *Environmental Science, Beijing* **22**, 108–112.
Parádi, I., Bratek, Z. & Láng, F. 2003. Influence of arbuscular mycorrhiza and phosphorus supply on polyamine content, growth and photosynthesis of *Plantago lanceolata*. *Biologia Plantarum* **46**, 563–569.
Parlak, K.U. 2016. Effect of nickel on growth and biochemical characteristics of wheat (*Triticum aestivum* L.) seedlings. *NJAS – Wageningen Journal of Life Sciences* **76**, 1–5.
Reeves, R., Baker, A., Bgrhidi, A. & Berazain, R. 1996. Nickel-accumulating plants from the ancient serpentine soils of Cuba. *New Phytologist* **133**, 217–224.
SAS Institute Inc. 2002. The SAS System for Windows, Release 9.0. *Statistical Analysis Systems Institute*, Cary, NC, USA.
Sheetal, K.R., Singh, S.D., Anand, A. & Prasad, S. 2016. Heavy metal accumulation and effects on growth, biomass and physiological processes in mustard. *Indian Journal of Plant Physiology* **21**(2), 219–223.
Seregin, I.V. & Kozhevnikova, A.D. 2006. Physiological role of nickel and its toxic effects on higher plants. *Fiziologiya Rastenii* **53**, 285–308.
Sohrabi, M., Tohidi-Moghadam, H.M., Donath, TW & Ghooshchi, F. 2018. Investigating the probable consequences of super absorbent polymer and mycorrhizal fungi to reduce detrimental effects of lead on wheat (*Triticum aestivum* L.). *Agronomy Research*: accepted. https://doi.org/10.15159/AR.18.009
Smith, S. & Read, D. 2008. Mycorrhizal symbiosis 3rd Edition. *Academic Press*, London, 800 pp. (in England).
Wang, SH., Wu, W., Liu, F., Liao, R. & Hu, Y. 2017. Accumulation of heavy metals in soil-crop systems: a review for wheat and corn. *Environmental Science and Pollution Research* **24**, 15209–15225.
Wojtaszek, P. 1997. Oxidative burst: an early plant response to pathogen infection. *Biochemical Journal* **322**, 681–692.
Yang, D., Shi, G. & Song, D. 2001. The resistance reaction of *Brasenia schreberi* winter-bud to Cr^{6+} pollution. *Journal of Lake Sciences* **13**, 169–174.

Agronomy Research **16**(4), 1668–1676, 2018
https://doi.org/10.15159/AR.18.171

Assessment of the actual hand position on the steering wheel for drivers of passenger cars while driving

M. Hruška

Czech University of Life Sciences, Faculty of Engineering, Department of Technological Equipment of Building, Kamýcká 129, CZ165 21 Prague 6, Czech Republic
*Correspondence: jabko@tf.czu.cz

Abstract. This work deals with the assessment of the actual position of the hands on the steering wheel of drivers of passenger cars in specific driving modes. The findings are compared with the location that is generally considered to be optimal in terms of both active and passive safety, and the long-term effects on the health of the driver. The research described in this work was carried out on a sample of randomly selected drivers in the Czech Republic. For all of the measurements, one identical neutral passenger middle-class vehicle, with which none of the test subjects had previous experience, was selected. The reason for this research was to model a normal situation where the driver controls a vehicle with his hands on the steering wheel in a position that is only the result of his or her own intuition and the subjective sense of the driver's comfort. On the basis, of a statistical evaluation of the obtained data, it was found that the introductory hypothesis, which states that a significant part of the tested sample of drivers holds the steering wheel in an unsuitable manner, can be confirmed. This fact negatively impacts not only on the reduction of active and passive safety, but also affects the health of drivers who drive a large amount of kilometres annually. The results of this work can be used in the design of cabs and modern passenger car systems that will be able to motivate the driver to hold the steering wheel in an optimal way. This will directly affect road safety and positively influence the health of drivers.

Key words: driver, posture, hands, steering wheel, age, gender.

INTRODUCTION

Today, the ergonomic design of passenger car cabins is a key part of the design process of a new vehicle (Wang et al., 2007; Bhise, 2012). An optimally ergonomically-designed driver's seat plays a major role particularly in the field of vehicle safety (Reed, 1998). Modern multifunctional steering wheels and hand rests provide a direct link between the driver and the machine, and the optimal design of these elements directly affects the driver's feelings and well-being, and thereby the safety of the vehicle's operation (Chang & Chen, 2016).

The position of the driver's hand on the steering wheel is important from several points of view, but these are in some ways contradictory. They include, for example, active safety requirements, subjective feelings of comfort, passive safety, and others. This work seeks to ascertain and evaluate the actual position of drivers' hands that they most often occupy during long, calm trips on major roads or motorways. The work compares the acquired data with values that are described as optimal (Hault-Dubrulle et al., 2010), and the differences obtained are assessed mainly from a physiological and medical point of view. The work is also concerned with the position of the grip on the load on specific muscle groups, in particular in the area of the lumbar spine.

A great deal of research focuses on measuring the position of the driver's hand on the steering wheel (Schmidt et al., 2015), and such research is mostly focused on the impact of grip on passive safety and the subsequent type and extent of injury during an accident. This most often consists of measurements in laboratory conditions and on special measuring seats (Schiro et al., 2013). This work obtains accurate data from a real environment, where the monitored subject is not stressed by the laboratory environment and sits in the actual vehicle, and is therefore able to take up the position that is used in normal operation.

There is a relatively high degree of consensus among experts on the issue of optimum steering wheel grip values. The optimal value is generally specified, according to the analogue clock face with the position of the left hand on the nine, and the right hand on the three while the driver holds the steering wheel with both hands (Hault-Dubrulle et al., 2010; Schiro et al., 2013). The primary objective of this work is to find out how large a percentage of drivers from the tested sample do not observe these grip values, and what the most commonly used values actually are.

Some ergonomics studies (Hruška & Jindra, 2016) showed that there is a link between gender, as well as the age of the driver and his or her ability to control the vehicle and adjust its controls. The secondary objective of this work is therefore to verify the hypothesis that there is a correlation between age, gender, mileage driven and correct steering wheel grip.

MATERIALS AND METHODS

Participants

A total of 100 participants (39 women and 61 men) were obtained for the measurements, all of them from the university environment – students or graduates of technical or economic orientation. The age of the participants ranged from 18 to 65 years (the average age was 29 years). It was clearly required and verified that all of the participants had a driving license authorizing the driving of passenger cars. All of the participants were also in good health and had no restrictions in the locomotive apparatus.

Table 1. Number of tested persons and their parameters in relation to the measurements

	Amount	Age			Number of driven km (thousands of km)		
		Average	Minimum	Maximum	Average	Minimum	Maximum
Men	61	30	19	65	192	5	800
Women	39	27	18	52	68	5	400
Total	100	29	18	65	144	5	800

Test environment

The test vehicle that was chosen was the Mercedes Benz C220d model series 2016, with standard interior features and steering on the left. The vehicle was equipped with modern longitudinally-adjustable seats with mechanical movement in the longitudinal direction and with the electronic positioning of the seat height, seat inclination and backrest inclination (Fig. 1). All of the tested persons marked the range of seat and steering wheel position settings as sufficient. The features included a mechanically adjustable steering wheel with a classical cross-sectional arm (Fig. 1). The vehicle can be characterized as a standard mid-class sedan with a classical steering wheel design.

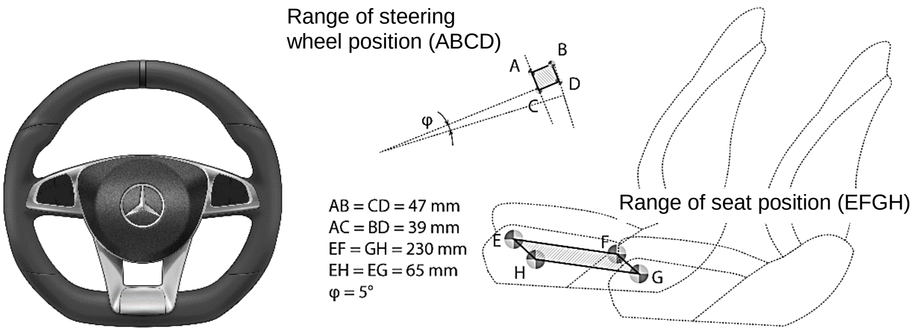

Figure 1. Seat and steering wheel position ranges, and the shape of the steering wheel in the test vehicle.

The vehicle was placed in a laboratory under constant light conditions at constant temperature and stable noise load so that all of participants in the experiment had the same external conditions (Fig. 2). During the measurements, the driver's door was closed to allow the test subject to use the left arm rest.

Figure 2. Test subject in the measuring vehicle with hands in the optimal position L9-R3.

Data Collection Procedures

None of the tested persons had any previous experience with the test car, but all of the tested persons were using the same steering wheel concept that the test vehicle had at the time of the vehicle measurement. Each tested person was thoroughly trained and familiarized with the seat and steering wheel control systems before getting into the measuring vehicle. After getting into the test vehicle, each tested person was given enough time to test out and understand all of the functions necessary to control the seat and steering wheel position. Prior to the measurement, each tested person was asked whether he or she considered his position in the vehicle to be comfortable and whether this position was as near as possible to the position they normally occupy in a vehicle.

The test subjects were also asked to grip the steering wheel in the way in which they were used to and in a truly relaxed position during usual traffic on a major road outside a city. The position of the hands was subsequently coded as L1-L12 or R1-R12, or a combination of both positions, when the steering wheel was gripped by both hands (Fig. 3). However, in practice, because other values were not measured, the left hand values were measured only on the left part of the L7-L12 sphere, and for the right hand on the right part of the R1-R6 sphere.

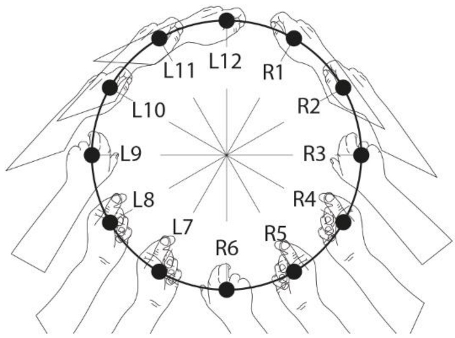

Figure 3. Scheme of the positions of individual grips according to the analogue clock face.

The active data collection described above, where the test subject is directly in the vehicle and is able try out the investigated hand position on the steering wheel, was evaluated as the better than the normal questionnaire method. As part of the aforementioned measurements, during the primary collection of statistical data (age, mileage driven, etc.), the tested persons were also asked about the position of the hands on the steering wheel. However, after getting into the vehicle, nearly 70% of the tested persons corrected or clarified this data, in particular due to the effect of mechanical memory, where the test subjects better realized the position in which they ordinarily drive. For the reasons described above, only the data obtained directly by measurements in the vehicle are therefore used for statistical evaluation.

RESULTS AND DISCUSSION

The results obtained during the measurements were statistically processed and evaluated using pivot tables, the Pearson's chi-squared test and the Anova method. The percentage representation of individual positions obtained from the measured data, regardless of whether the steering wheel is held in one hand or both, are shown in Table 2 and Fig. 4. The data shows that some of the steering wheel grip positions, such as position R3, differ substantially for both genders, whereas the opposite position, L9, indicates roughly the same results for both genders. These differences are explained below based on demonstrated right or left hand preferences depending on gender.

Table 2. The resulting values of grip percentage representation in individual positions

Item	L7	L8	L9	L10	L11	L12	R1	R2	R3	R4	R5	R6
Both genders	14.9%	5.3%	43.6%	26.6%	6.4%	3.2%	1.7%	27.1%	54.2%	5.1%	10.2%	1.7%
Women	12.8%	0.0%	48.7%	38.5%	0.0%	0.0%	0.0%	11.0%	16.0%	0.0%	2.0%	0.0%
Men	16.4%	9.1%	40.0%	18.2%	10.9%	5.5%	3.3%	16.7%	53.3%	10.0%	13.3%	3.3%

Interesting are the differences in the upper positions L11, L12 and R1, where women do not use these positions at all. This fact can be explained mainly by lower values of anthropometric data in women compared to the same parameters in men. Another possible explanation is the need to use more steering forces on the steering wheel at these positions, given the longer lever, which may be less comfortable for women (Tilley, 2002).

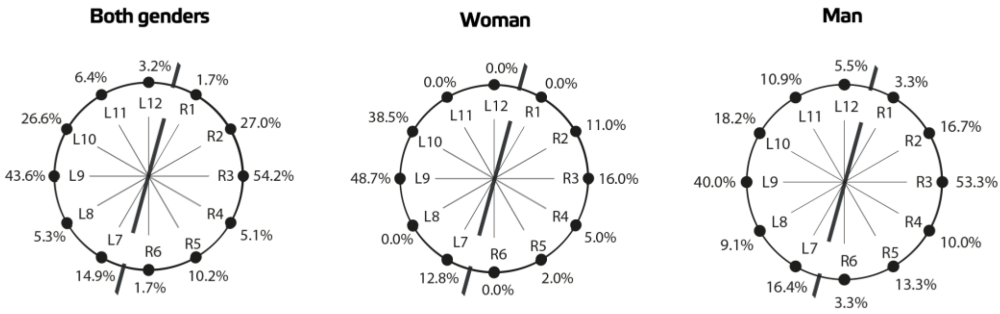

Figure 4. Schematic depiction of the resulting grip percentage representation values in individual positions.

Note: The values in percentages are calculated separately for the left and right hand.

The percentage representation of the steering wheel grip method using only the left or right hand, or both hands at once, and depending on gender, is shown in Table 3. Here, it is evident that women prefer to hold the steering wheel with both hands, which is also confirmed below by Pearson's chi-squared test (Table 4).

If women hold a steering wheel with one hand, they significantly prefer the left hand, and they do not use the right hand at all when steering. Even in the case of men, it is evident that when driving with only one hand, they use the left hand. This can be explained by the fact that all of the test subjects exclusively drive cars with steering on the left and the shift lever is on the right side of the car. This may lead to the preferred use of the left hand for steering while the driver is restrained by the right hand on the central armrest and the right hand is placed on the gear lever. In this respect, it would be interesting to supplement the results presented in this work with further follow-up research that would identify the same data for persons using only vehicles with the steering on the right side. This would make it possible to specify this influence more closely.

Table 3. Method of holding the steering wheel depending on gender

	Left hand only	Right hand only	Both hands
Both genders	41.0%	6.0%	53.0%
Women	25.6%	0.0%	74.4%
Men	50.82%	9.84%	39.34%

Table 4. Data evaluation using a Pearson's chi-squared test

Degrees of freedom	X^2	Critical value	Cramer's V	Significance level
1	11.7	3.84	0.342	0.05

In order to confirm the hypotheses defined above, it was necessary to subject the measured results to a statistical analysis. Pearson's chi-squared dependency test was used in order to test the dependency between the gender of the tested persons and the optimal value of the spontaneously chosen angle.

Table 5 shows the input data for evaluating the statistical significance of how the steering wheel is held depending on the gender of the tested persons. As the default source for further statistical processing, a pivot table (Table 5) with two degrees of freedom was used, distinguishing separate grips with left and right hand. Because the number of subjects who steered using only the right hand was insufficient, it was necessary to reduce the degree of freedom and merge the subjects with those who steered with any one hand and those who steered with both hands. Using Pearson's chi-squared dependence test, the value of X^2 (11.71) was calculated, which is significantly higher than the critical value (3.84), confirming the primary input hypothesis that the method of holding the steering wheel is dependent on gender.

Table 5. Input data for statistical evaluation of the dependence of steering wheel grip on gender

	Left only	Right only	Both hands	Sum
men	31	6	24	61
women	10	0	29	39
both genders	41	6	53	100

The rate of grip dependency on gender was further verified by Cramer's V (0.342). Based on the calculated values, the dependence of the grip on the steering wheel on gender can be considered significant. The explanation of the difference in gripping a steering wheel between women and men can be sought out in particular in the different settings of the relative position of the steering wheel and the top of the body for each gender. As was ascertained in other research (Hruška & Jindra, 2016), women have a tendency to sit closer to the steering wheel and to have more bent and relaxed hands. This is due to differences in the anthropometric parameters of men and women (Tilley 2002; Wang et al., 2007), but also in the psychological level, as women tend to approach driving more responsibly (Bergdahl, 2005) and try to observe the generally recommended position of L9R3, even at the cost of lower subjective comfort.

Tables 6, 7 and 8 show the most frequently represented combinations when the test subject holds the steering wheel with both hands. It can be seen that in this case, the results for both men and women are very similar, and the differences occur mainly in the frequency of individual combinations. When steering with both hands, most of the subjects mainly use the L9R3 or L10R2 position, which is strongly represented mainly by women.

Table 6. The most represented combinations of hand position without gender differences

	L7	L8	L9	L10	L11
R1	0	0	0	0	1
R2	0	0	1	15	0
R3	0	0	30	0	0
R4	1	0	0	0	0
R5	4	1	0	0	0

The Mann Whitney U test statistical method at a significance level of 0.05 was used to assess secondary hypotheses that assess the dependence of the way a steering wheel is gripped on experience (driven mileage) and age.

Table 7. The most represented combinations of hand positions for women

	L7	L8	L9	L10	L11
R1	0	0	0	0	0
R2	0	0	0	11	0
R3	0	0	16	0	0
R4	0	0	0	0	0
R5	2	0	0	0	0

Table 8. The most represented combinations of hand positions for men

	L7	L8	L9	L10	L11
R1	0	0	0	0	1
R2	0	0	1	4	0
R3	0	0	14	0	0
R4	1	0	0	0	0
R5	2	1	0	0	0

The *p-value*, calculated by the Mann-Whitney test, which determines the order of the respondents by mileage divided by the way the steering wheel is held, is 0.001. Since this value is less than the chosen significance level of 0.05, it can be confirmed that the method of holding the steering wheel is related to mileage. Drivers who have a higher mileage drive more often with one hand (Table 9).

The *p-value*, calculated by the Mann-Whitney test for the age-based respondents, divided by the way the steering wheel is held, is 0.068. Since this value is higher than the chosen significance level of 0.05, it can be said that the steering angle of the steering wheel is not statistically significant with the age of the respondents (Table 10).

Table 9. Dependence of steering wheel grip method on the number of driven km using the Mann Whitney U test method

Steering wheel grip	Number of subjects	Average km	*p-value*
One hand	47	177.6	0.001
both hands	53	113.3	

Table 10. Dependence of steering wheel grip method on the age of subjects using the Mann Whitney U test method

Steering wheel grip	Number of subjects	Average age	*p-value*
One hand	47	30.2	0.068
both hands	53	28.1	

The above results must also be interpreted from the point of view of the effects on the health of the driver, in particular for professional drivers or for drivers who travel long distances; it is for these drivers that the aforementioned data is essential as a factor that has a long-term effect on their health condition.

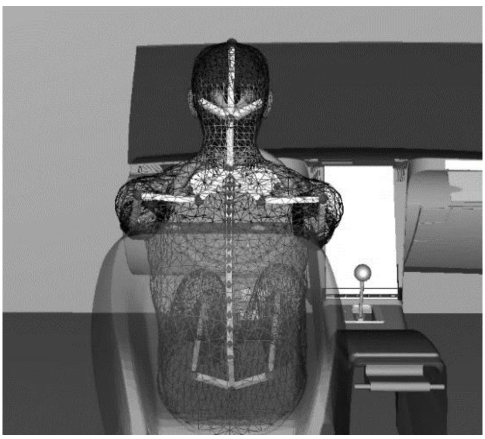

Figure 5. Driver gripping the steering wheel in position L9R3.

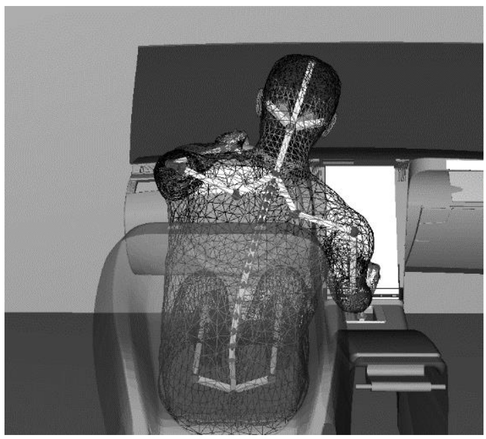

Figure 6. Driver gripping the steering wheel in position L12.

While observing test subjects during the measurements, it became clear that every subject who does not grip the steering wheel with both hands, will necessarily be subject to a certain degree of rotation of the upper half of the body. If we assess the aforementioned steering wheel grip position from the viewpoint of the impact on the health of the driver, it should be noted, that the worst steering wheel grip positions are L11, L12 and R1. In order to simply evaluate of these positions, the Tecnomatix Jack program was used, in which the L9R3 (Fig. 5) and the L12 (Fig. 6) positions were simulated for a 95 percentile man in a general middle class sedan. In Figs 5 and 6, it is quite clear that in drivers who only grip the steering wheel with the left hand in the least suitable position, L12, there is significant lateroflexia with significant muscle strain, in particular *m. quadratus lumborum, m. obliquus externus abdominis, m. obliquus internus abdominis and m. erector spinae.* Long-term driving in such a position can lead to pain in the lumbar spine and, in extreme cases, to permanent damage to the postural system (Véle, 1995; Havlíčková, 1999). In contrast, the driver in Fig. 5, who holds the steering wheel with both hands in the L9R3 position, is sitting upright and the load on the muscle groups in the lumbar spine is uniform in this case. As can be seen from the above results (Table 2), the above described inappropriate positions are occupied exclusively by men, and it can therefore be stated that the influence of the inappropriate position of the steering wheel grip on health condition will be significantly greater for men than for women.

CONCLUSIONS

In this work, a large amount of valuable primary data was obtained from a relatively homogeneous group of respondents, which may be statistically interesting in terms of possible comparisons with other statistics that could be obtained from respondents with other parameters such as different education, age, etc. By dividing the data by means of pivot tables, it was found that when driving, a statistically significant group of respondents gripped the steering wheel in a way that cannot be labelled as optimal on the basis of the selected comparative parameters.

This finding could be used for the further development of passenger car cabins, where the modelling of the interior could create conditions wherein the driver is not forced to find a subjectively comfortable grip of the steering wheel which, however, cannot be described as optimal for the above reasons (Hault-Dubrulle et al., 2010; Schiro et al., 2013,). This would eliminate the human factor, which is imperfect in these cases of subjective judgment.

On the basis of the above results, it can be further stated that the primary hypothesis mentioned in the introduction of the thesis has been fully confirmed. There are statistically significant differences in how men and women grip the steering wheel when driving in calm traffic outside cities. The explanation of this phenomenon can be seen in the generally more responsible approach of women to driving a car (Vágnerová, 2007), but also in the fact that men are able to relax more freely in the vehicle and occupy an instinctively relaxed position (Wilson, 1999, Bergdahl, 2005).

The secondary hypotheses, specified in the introduction to this work, were partially demonstrated, only in the case of the dependence on the method of holding the steering wheel on mileage. In the case of dependence on holding the steering wheel on respondent's ages, some dependence was found, but it cannot be considered valid due to insufficient statistical evidence.

The results presented in this paper could serve as a basis for further research that could help to further refine the aforementioned findings. The data and hypotheses presented in this paper could serve as ancillary factors in the design of vehicles with regard to potential customer target groups.

The contribution of this work can also be seen in the number of test subjects and gender factor involvement. Another benefit of this work is the provision of valid data for further follow-up research in which the above results could be clarified or supplemented by data obtained from field investigations or, for example, from environments where vehicles with the steering on the right prevail, thereby excluding or confirming some other hypotheses which came from this research.

REFERENCES

Bhise, V. 2012. *Ergonomics in the automotive design process*. Taylor & Francis Group, 309 pp. ISBN 978-1-4398-4210-2

Bergdahl, J. 2005. Sex differences in attitudes toward driving: A survey. *The Social Science Journal* **42**, 595–601. ISSN 03623319

Chang, Yu-M. & Chen, Ch.W. 2016. Kansei assessment of the constituent elements and the overall interrelations in car steering wheel design. *International Journal of Industrial Ergonomics* [online] **56**, 97–105. ISSN 01698141

Hault-Debrulle, A., Robache, F., Paxaux, M.P. & Morvan, H. 2010. Determination of pre-impact occupant postures and analysis of consequences on injury outcome. Part I: A driving simulator study. *Accident Analysis & Prevention* [online], 66–74. ISSN 00014575

Havlíčková L. 1999. *Physiology of physical strain I: General part* (*Fyziologie tělesné zátěže I: obecná část).* Praha: Karolinum, 203 pp. ISBN 9788071848752

Hruška, M. & Jindra, P. 2016. Ability to handle unfamiliar systems in passenger cars according to driver skills. *Agronomy Research* **14**(5), 1601–1608.

Reed, M.P. 1998. *Statistical and Biomechanical Prediction of Automobile Driving. Ph.D. Dissertation*..University of Michigan. USA, 235 pp.

Schiro, J., Gabrielli, F., Pudlo, P. & Barbier, F. 2013. Steering wheel hand position in low-speed maneuvers. Transportation Research Part F: *Traffic Psychology and Behaviour* [online], 133–145. ISSN 13698478

Schmidt, S., Seiberl, W. & Schwirtz, A. 2015. Influence of different shoulder-elbow configurations on steering precision and steering velocity in automotive context. *Applied Ergonomics* [online] 176–183. ISSN 00036870

Tilley, A.R. 2002. *The measure of man and woman: human factors in design*. Rev. ed. New York: Wiley, 98 pp. ISBN 04-710-9955-4

Vágnerová, M. 2007. *Introduction to psychology (Základy psychologie).* Karolinum, 356 pp. ISBN 80-246-0841-3

Véle, F. 1995. *Kinesiology of postural system (Kineziologie posturálního systému)*. Karolinum, 83 pp. ISBN 80-7184-297-4

Wilson, R. 1999. *The MIT Encyclopedia of the Cognitive Sciences*. Cambridge, Massachusetts, 964 pp.

Wang, M.J.J., Wu, W.Y., Lin, K.C., Yang, S.N. & Lu, J.M. 2007. Automated anthropometric data collection from three-dimensional digital human models. *International Journal of Advanced Manufacturing Technology* **32**, 109–115.

Agronomy Research **16**(4), 1677–1685, 2018
https://doi.org/10.15159/AR.18.193

Effect of environmental temperature on bending strength of the finger jointed aspen lumber

J. Iejavs[1], U. Spulle[2,*], V. Jakovlevs[2], E. Buksans[2] and A. Zelmenis[3]

[1]Forest and Wood Products Research and Development Institute, Dobeles iela 41, LV–3001 Jelgava, Latvia
[2]Latvia University of Life Sciences and Technologies, Forest faculty, Department of Wood Processing, Dobeles iela 41, LV–3001 Jelgava, Latvia
[3]"4 Plus" Ltd. Abula iela 6B, LV–4201 Valmiera; Merķeļa iela 20, LV–4301 Alūksne, Latvia
[*]Correspondence: uldis.spulle@llu.lv

Abstract. Glued sauna wall boards are used as non–load–bearing structures. These products are subject to aggressive microclimate impact and very often for the gluing in length and width thermoplastic polyvinyl acetate adhesives (PVAC) are used.
In the performed research sauna wall boards made of common aspen (*Populus tremula* L.) with mean wood moisture content 8% were used. For the gluing in length with finger joint PVAC glue of D4 (LVS EN 204) group was used.
The aim of the research is identifying the impact of the environmental temperature on the strength of finger jointed aspen timber in 4 point static bending (in compliance with standard LVS EN 408). As a result of the study it was established, that after holding the finger jointed testing pieces visible in flat wise for 3 hours at the temperature of 100 °C, the mean bending strength decreased by 56% or 31.7 MPa in comparison to that held in the standard atmosphere. In case of the aspen timber with finger joints visible in edge wise held for 3 hours at the temperature of 100 °C, the bending strength decreased by 60% or 29.3 MPa in comparison to the testing pieces of the same type held in the standard atmosphere.

Key words: thermoplastic glue, sauna wall board, temperature effect.

INTRODUCTION

Glued timber has experienced a major growth of consumption during the last 15 years. The main reason for this is the availability of raw materials, the low energy consumption of the production process and the attractive price of the end product. Glued timber has turned from being just a decorative material into broadly used basic structural material with essential advantages in comparison to steel or concrete (Kociņš, 2007). The popularity of wood gluing can be explained by its several essential advantages, for example, the increased sizes in all directions and possibilities to produce different 3D structural building elements – curved, twisted etc. The possibility of constructing robust connections minimising deformations of the elements to be connected presents another essential advantage. Also timber materials of small dimensions and lower quality can be used for production of glued structures. Irrespective of the natural dimension of timber, glued structures of virtually unlimited cross section, any rational profile and length can be produced. Maximum mechanisation of the technological process, convenient transportation of glued materials and their low weight complies with the modern construction requirements (Ulpe & Kupče, 1991).

The finger joints are better than the slope connection which is usually applied for gluing of plywood and peeled veneers. For stretched and bent elements the finger joint is more secure as the glued surface area is bigger. However, in the finger joints mainly shear stress and minor tension stresses can be found. The contact is constructed based on the assessment that the stress levels in the glue would not reach the ultimate strength before timber reaches it. By using the finger joints the timber can not only extend, it can also be connected under an angle (Ulpe & Kupče, 1991).

Geometric parameters of finger joints (Fig. 1) and dimensions of the material have a considerable impact upon the strength of the finger joints (Thelanderson & Larsen, 2003). In the elements of non–load–bearing structures PVAC glues which are resistant to temperature up to 110 °C and even up to 145 °C when modifications are most often used, moreover, if the two-component dispersion glue is used. The connections of PVAC glue do not dissolve in water, however, they swell and lose their strength considerably. Humidity and water resistance depends on the chemical composition of glues (Kūliņš, 2004). PVAC glues are physically hardening glues with high adhesion and, depending on application, they are characterised by high strength in both dry and very wet service conditions. Plasticisers from 10 to 50% can be added to PVAC glues. They maintain flexibility of the glue connection even at low temperatures (Zeppenfeld & Grunwald, 2005).

Similar to increase of moisture content in timber, increase of timber temperature decreases the mechanical properties. It is important to investigate the mechanical properties of timber as the timber temperature increases. However, from the point of view of drying it is important to identify the mechanical properties as the timber moisture content decreases within the temperature range from 10 to 140 °C. In order not to decrease the mechanical properties of timber without causing the chemical destruction of timber, at the timber moisture content of 70% and above the temperature may not be increased above 45 °C. Along with the temperature increase, the moisture conductivity increases considerably. When temperature increases from 20 to 60 °C and then up to 80 °C, the moisture conductivity rate in tangential direction for fibres increases, and in case of aspen wood this increase is 3.8 and 7.1 times (Tuherm, 2007). However, if the temperature increases above 40 °C, the stability of the glue connection decreases considerably. Chemical reactions of the timber take place under the impact of moisture and temperature. The lower the moisture the higher the temperature may be without reducing the mechanical properties of timber. Moisture and temperature are closely interacting. At a constant moisture content and temperature lover than 150 °C, mechanical properties are approximately linearly related to temperature (Wood Handbook, 2010). Also Peter Niemz and Walter Ulrich Sonderegger carried out that increased temperature are decreasing the mechanical properties of wood (Niemz & Sonderegger, 2017). The reduction of strength is also affected by duration when timber is kept in the environmental temperature. Repeated drying and moistening of timber also have a negative impact on the physical and mechanical properties of timber. As well the temperature impact is one of the most important properties of glued timber elements

(Sedliačik & Šmidriaková, 2012). Previous research made by authors Ján Sedliačik and Mariá Šmidriaková (Sedliačik & Šmidriaková, 2012) shows that bending strength of glued finger joints made out of beech (*Fagus sylvatica* L.) and spruce (*Picea abies* L.) with 1-component polyurethane (PUR) and 2-component melamine–urea–formaldehyde (MUF) glues at increased temperature up to 110 °C, decreases.

From the point of view of the national economy, in Latvia aspen is the timber with the highest potential following pine, birch and spruce. It has the best application when it is used for interior finish of sauna, as well as other interior finish works and structures with humidity up to 15%. Aspen has a shorter lifetime in outdoor conditions. Aspen is characterised by the lifetime which is among the longest ones if the moisture content does not exceed 9%. Considering the practical operational conditions, aspen is the species of timber with lowest resistance to biological impact, following linden. It is characteristic for aspen that at the age of cutting 40% of aspen has been affected by rot (Tuherm, 2007). Aspen timber can be used for sauna wall board thanks to its low density. Due to its low density, aspen has high heat capacity, however, comparatively low heat conductivity. Last couple of year's sauna wall board production companies are trying to fulfil requirements of the customers to make longer and wider wall boards with higher quality surface. The lower quality of aspen timber requires to glue these elements in length, width and height. Due to health hazards in formaldehyde emissions from glues with base of these, there is one possibility to use PVAC glues for common products (Sedliačik & Šmidriaková, 2012).

The aim of the research to investigate the influence of the environmental temperature to the finger jointed aspen lumber glued with PVAC glue.

MATERIALS AND METHODS

The dimensions of the cross section of produced aspen (*Populus tremula* L.) lumbers were 28×74 mm. They were industrially dried till moisture content 8%. Glued products of this type are used for production of sauna wall and cladding boards. After drying, all the visually identified defects of wood were cut out (cracks, knots and rot), thus obtaining defect–free lumber with the nominal length of 700 mm and was cut in half. Before finger joints and jointing were made, from connection side of finger joints of the each lumber specimen was cut for identification of the moisture content and density. At the ends of lumber finger joints were industrially produced. For one part of the testing pieces finger joints was visible in the flat wise and for the other part in the edge wise (Fig. 1) (Jokerst, 1981).

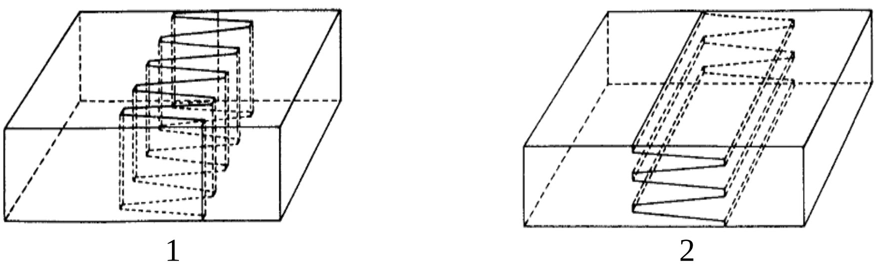

Figure 1. View of Finger Joints: 1 – flat wise; 2 – edge wise (Jokerst, 1981).

As both parts of the glued lumber elements were produced from the same aspen lumber, the impact of the differences of moisture content and density of different lumber in bending strength of the glued finger joints has been minimised.

Production of finger joints is based on the operational properties of the selected products. The rated geometric parameters of produced finger joints and testing piece are presented in (Fig. 2).

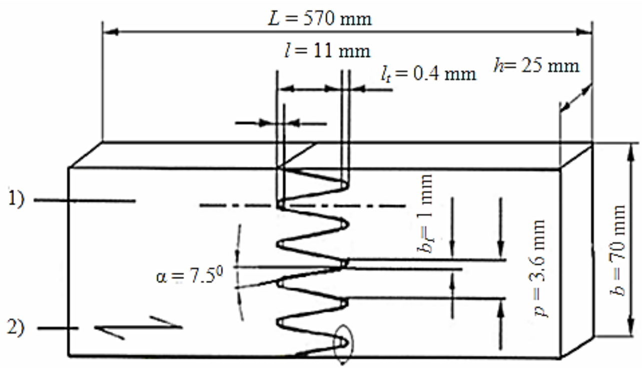

Figure 2. Linear and angle parameters of the finger joint: *l* – length of fingers; *p* – step of fingers; b_t – width of the finger; l_t – tolerance of the finger joints end; α – side angle of the finger joint; *L* – length of testing piece; *h* – thickness of the testing piece; *b* – width of the piece; 1) – way of symmetry of the finger joint; 2) – fibre direction of the testing piece (DIN68140EErl ND, 1981).

In the research polyvinyl acetate glue D4 group (EN 204) was used which is one component glue broadly used by wood processing companies for gluing window and door components. The method of application of glue was by soaking lumber elements and the glue consumption in testing pieces was identified by weighing for each individual testing piece. The scale with accuracy of 0.01 g was used for weighing the testing pieces.

The open holding time of lumber elements after application of glue was 15 to 20 seconds. The gluing surface area was identified for both the finger joints produced in the flat wise and it was 8,725 mm^2, as well as edge wise and it was 7,175 mm^2.

Within the developed research 75 glued testing pieces with finger joint in flat wise and 75 with finger joint in edge wise were produced. Also one group with 15 testing pieces with no finger joints as reference testing pieces was made for testing in standard atmosphere (air temperature 20 ± 3 °C; air humidity 65 ± 5%). For investigation of the influence of the environmental temperature to finger joint mechanical properties followed temperature levels 20, 40, 60, 80 and 100 °C were selected. For each of temperature groups 15 testing pieces were selected.

For gluing with finger joints, the laboratory hydraulic press was used after application of glue (Fig. 3). The pressing

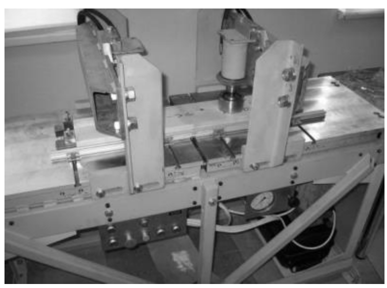

Figure 3. Equipment for gluing finger joints.

was done by first applying vertically slight pressure to the lumber element flat wise and then adding pressure horizontally from the both ends of the testing pieces. The total closed holding time was 30 seconds. Gluing of testing pieces was performed by the end pressure 1.7 MPa and the holding time in the press under the pressure for 2 seconds. The holding time was controlled by using a chronometer.

Testing pieces with finger joint visible on both the flat and edge wise, following their production and gluing, were stored for 168 hours in a conditioning chamber, under standard climate conditions at environmental temperature 20 ± 2 °C and relative air humidity 65 ± 5%, until stable timber moisture content and complete hardening of glue. Testing pieces were placed in the conditioning chamber after their marking by maintaining small distances between them to ensure air circulation around each testing piece. Following conditioning testing pieces divided into their preliminary treatment groups, were placed in heating ovens for starting heating.. Testing pieces were held at the above mentioned temperatures for 3 hours in order for heat to penetrate thoroughly. Testing pieces were placed in the oven with small distances between them in order to secure that heat penetrates throughout the whole cross–section of the material.

The reference testing pieces were produced from aspen lumber with the length of 570 mm, free of any visible wood defects (knots, splits and fibre distortion) in order to prevent any impact upon properties in testing. The initial moisture content of reference testing pieces was 8%. The reference testing pieces were conditioned at the standard atmosphere in a conditioning chamber until obtaining constant mass.

Following production of all the testing pieces and holding them under specific temperature, the mechanical properties were determined under four–point statistic bending in compliance with the requirements of standard LVS EN 408 (EN 408, 2003). It was done after taking out testing piece by piece from oven with specific temperature and test them in standard atmosphere and room temperature.

For all testing pieces both thickness and width was determined at the distance of approximately 40 mm from the finger joint by means of a sliding calliper with the accuracy of up to 0.1 mm. The measuring ruler with the accuracy 1 mm was used for determining the length of a testing pieces.

Investigation of the moisture content prior to gluing and at the moment of test was performed in compliance with the methodology of standard EN 13183–1 (EN 13183–1, 2003).

After investigation of testing pieces in bending, moisture content specimen were cut from them again in order to determine the difference of moisture after testing. Specimens for determining moisture content were cut as close as possible to the breaking place.

The same cut specimens used for determining moisture content were also used for determining the density of the specimens. The timber density prior to gluing and after drying was determined in compliance with standard ISO 13061-2 (ISO 13061-2, 2014).

The mean arithmetic values, standard deviations and the statistically significant correlations for sets of testing pieces and specimens were determined by using the statistic calculation methodology (Arhipova & Bāliņa, 2006). MS Excel software was used for summary and statistic processing of end results.

RESULTS AND DISCUSSION

The mean application of the glue for finger joints produced in the flat wise is 194 g m^{-2}, and for finger joints produced in the edge wise is 237 g m^{-2} (Table 1). By pressing the lumber elements together, more glue was pressed out from finger joints produced in the flat wise, which explains the reason why the glue application is lower.

Table 1. Glue application and physical properties (mean values and standard deviations) of tested pieces

Test/ Temperature groups	Mean density (standard deviation), kg m^{-3}		Mean moisture content (standard deviation), %		Mean glue application (standard deviation), g m^{-2}	
	Flat wise	Edge wise	Flat wise	Edge wise	Flat wise	Edge wise
Temp. 20 °C	458 (48)	464 (31)	8.2 (0.95)	7.8 (0.26)	198 (18.4)	238 (31.8)
Temp. 40 °C	453 (57)	465 (27)	8.8 (1.13)	7.9 (0.30)	198 (20.0)	239 (38.5)
Temp. 60 °C	449 (49)	471 (31)	8.3 (0.72)	7.9 (0.20)	187 (26.7)	230 (35.2)
Temp. 80 °C	448 (42)	445 (27)	7.7 (1.22)	8.1 (0.41)	191 (24.3)	233 (37.5)
Temp. 100 °C	436 (48)	464 (22)	7.6 (0.86)	7.9 (0.39)	198 (18.2)	242 (28.7)
Ref. solid wood	458 (72)		8.3 (0.72)		-	

The glue application was determined by weighing each testing piece prior to and after gluing. In both cases, when the produced finger joints are glued, the margins of optimum glue application as declared by the manufacturer were exceeded by gluing the material along the face and connected it along the thickness. As in case of the finger joints the end timber is glued, higher glue consumption than in case of gluing materials along thickness is permitted. Both on the flat and on edge wise the minimum and maximum glue application was determined. The minimum application is 140 g m^{-2} and the maximum application is 321 g m^{-2}. The statistically significant correlation between the glue application and the static bending strength for all ten groups was not found ($p > 0.05$).

Following conditioning under standard atmosphere, upon checking the reference testing pieces in four point bending, the obtained mean bending strength is 76.3 MPa. This value is used as the maximum bending strength value of the relevant material for comparing the other testing pieces.

In case of the finger joint visible in the flat wise of the testing piece, following conditioning under the standard atmosphere, the obtained mean bending strength is 57.1 MPa. As compared with the reference testing pieces (solid wood), they withstand up to 75% of the values of the bending strength of aspen reference testing pieces. In case finger joints are visible in the edge wise, the mean bending strength is 48.7 MPa. They withstand up to 64% of the values of the bending strength of aspen reference testing pieces (Fig. 4).

The temperature impact upon the bending strength aspen finger joints produced in the flat wise is presented in (Fig. 4).

There is a strict not linear functionally negative correlation between the environmental temperature and the bending strength of aspen finger joints produced in the flat wise and it is described by the logarithmic correlation coefficient 0.9.

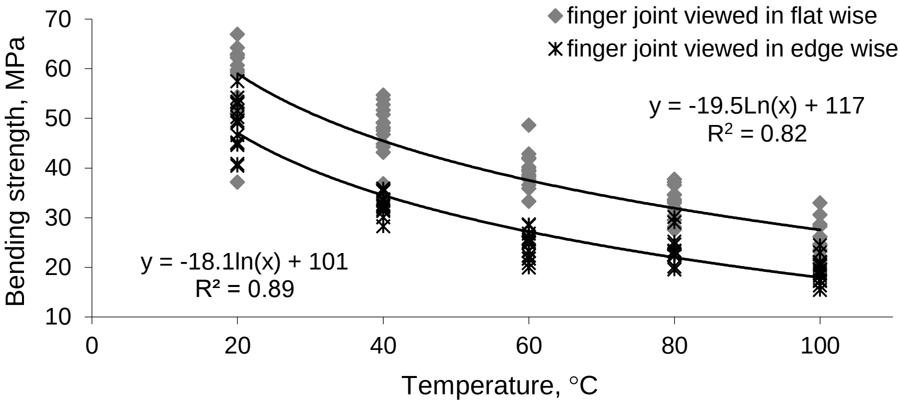

Figure 4. Temperature influence to bending strength of the aspen finger joints.

There is a strict not linear functionally negative correlation between the environmental temperature and the bending strength of aspen finger joints produced in the edge wise and it is described by the logarithmic correlation coefficient 0.9. As the environmental temperature of aspen finger joints increases, the bending strength decreases, both cases.

When sauna wall boards are longitudinally glued by using finger joints and PVAC, in case of both types of production of finger joints, under increased temperature (100 °C), a considerable decrease (exceeding 50%) of the bending strength should be expected in comparison to the bending strength of sauna wall boards under standard atmosphere.

Several conclusions can be drawn in the result of analysis of the impact of aspen density prior to gluing upon the bending strength of finger jointed aspen sauna wall boards. Following conditioning of testing pieces in the standard atmosphere, there is a medium strict and functionally positive correlation between the density and the bending strength of the finger jointed aspen sauna wall boards and it is described by the linear correlation coefficients 0.7 (in case of testing pieces with the finger joint produced in the flat wise) and 0.5 (in case of testing pieces with the finger joint produced in the edge wise). The strong correlation between the density and the bending strength for all ten groups was found ($p < 0.05$).

It follows from the above that if aspen timber with higher density is chosen for finger jointing of sauna wall boards, following conditioning of the glued material in the standard conditioning atmosphere, materials with higher bending strength will be obtained. In the result of analysis of density upon the bending strength of finger jointed sauna wall boards held in high temperature it can be concluded that there are weak correlations between the density of aspen timber prior to gluing and the bending strength of aspen sauna wall boards after holding them in high temperatures, the linear correlation coefficients being below 0.5. In the result of comparing the bending strength of sauna wall boards at holding temperature levels 20 and 100 °C, it can be seen that the impact of aspen timber density upon the bending strength of finger jointed lumber tends to decrease. In case of both type of production of finger joints, following holding in temperature of 100 °C, a trend can be seen that as aspen timber density prior to gluing increases the bending strength decreases.

Based on the results of the research, we can conclude that temperature impact to the aspen finger jointed wall boards glued with PVAC are showing the same tendencies as it is described in previous research where PUR and MUF glues were used, increased temperature up to 110 °C decreasing the bending strength of finger jointed spruce wood (Sedliačik & Šmidriaková, 2012). Within carried research this type of the PVAC glue had to be considered separately, as it is classified as thermoplastic glues used for non–load–bearing structures.

Results of research done by institute ETH Zurich has shown strength reduction differences if using adhesives that fulfil current approval criteria for the use in load-bearing timber components (Frangi et al., 2012). Sauna wall boards elements are not classified as load – bearing timber components, but even using there are used under short term loads, it could be recommend to use that type of glue for that kind of application.

CONCLUSIONS

1. The outcome of research shows that glued joints may be the weakest points of finger jointed aspen sauna wall boards under conditions of increased temperature.

2. Regression diagrams of bending strength of the tested finger joints (visible in flat or edge wise), glued with PVAC glue, in the both cases shows no linear tendencies when environmental temperature increases from 20 to 100 °C.

3. The thermoplastics glues can be used for finger jointing of aspen wood in case the environmental temperature of the used connections don't increases more than 80 °C, in other case bending strength of connection decreases more than 50%.

4. In order to obtain materials with a higher bending strength, following conditioning of longitudinal glued material in the standard atmosphere, aspen timber with higher density should be chosen, strong correlation between the density and the bending strength for all ten groups was found ($p < 0.05$).

5. For sauna wall elements with higher bending strength, finger joints viewed in flat wise should be used, for less visible joints, finger joints viewed in edge wise should be used. For investigation of influence of the temperature to the finger joints for several cycles weathering tests should be done.

ACKNOWLEDGEMENTS. Research was carried out within the project 'Technology validation of the latest bonding and decorative, protective treatment for high value-added wood products production', Central Finance and Contracting Agency (CFCA), project No. 1.2.1.1/16/A/009 co-financed by the European Union within the Project framework of the European Regional Development Fund.

NACIONĀLAIS ATTĪSTĪBAS PLĀNS 2020

EIROPAS SAVIENĪBA
Eiropas Savienības struktūrfondi un Kohēzijas fonds

IEGULDĪJUMS TAVĀ NĀKOTNĒ

REFERENCES

Arhipova, I. & Bāliņa, S. 2006. *Statistics in Economics. Solutions with SPSS and Microsoft Excel*. Computer Science Centre, Rīga, 352 pp. (in Latvian).

Classification of thermoplastic wood adhesives for non–structural applications: LVS EN 204:2016 (2016) Available at: https://www.lvs.lv/lv/products/132874, 6 April 2018.

Frangi, A., Bertocchi, M., Clauß, S. & Niemz, P. 2012. Mechanical behaviour of finger joints at elevated temperatures. *Wood Science and Technology*. Volume 46, Issue 5, Springer Berlin Heidelberg, Berlin, pp. 793–812.

Jokerst, R. 1981. *Finger–Jointed wood products*. United States Department of agriculture, forest service, 26 pp.

Kociņš, J. 2007. *Timber in constructions*. Stilus, Rīga, 255 pp. (in Latvian).

Kūliņš, L. 2004. *Production of the Glued Wood Materials*. KTC, Jelgava, 246 pp. (in Latvian).

Moisture content of a piece of sawn timber–Part 1: Determination by oven dry method. LVS EN 13183-1:2003 (2003). Available at: https://www.lvs.lv/lv/products/12389, 6 April 2018.

Niemz, P. & Sonderegger, W.U. 2017. *Wood Physics. Physics of wood and wood-based materials*. Carl Hanser Verlag, München, 580 pp. (in German).

Physical and mechanical properties of wood–Test methods for small clear wood specimens – Part 2: Determination of density for physical and mechanical tests ISO 13061–2:2014 (2014) Available: https://www.iso.org/obp/ui/#iso:std:60064:en, 17 April 2018.

Sedliačik, J. & Šmidriaková, M. Heat resistance of adhesive joints for wood constructions. *Acta Facultatis Xylologiae Zvolen*, **54**(2), Technická univerzita vo Zvolene, Zvolen, 2012, pp. 87–94.

Thelanderson, S. & Larsen, H.J. 2003. *Timber Engineering*. John Wiley & Sons Ltd., England, 466 pp.

Timber finger Jointing DIN68140EErl ND 1981. 1981. Available at: https://www.din.de/en/getting-involved/standards-committees/nhm/standards/wdc-beuth:din21:3535060, 17 April 2018 (in German).

Timber structures. Structural timber and glued laminated timber. Determination of some physical and mechanical properties: LVS EN 408+A1:2012. 2012. Available at: https://www.lvs.lv/lv/products/32434, 6 April 2018.

Tuherm, H. 2007. *Mechanical machining of the hardwoods and development of the new products*. Research report. 2007. Latvia University of Agriculture, Jelgava, 116 pp. (in Latvian).

Ulpe, J. & Kupče, L. 1991. *Wood and plastics constructions: study material for students of Riga Technical University, industrial and civil engineering specialties*. Zvaigzne, Rīga, 303 pp. (in Latvian).

Zeppenfeld, G. & Grunwald, D. 2005. *Adhesives for timber and furniture industry*, 352 pp. (in German).

Wood Handbook. *Wood as an Engineering Material 2010*. Forest Product Society, Madison, 509 pp.

Agronomy Research **16**(4), 1686–1697, 2018
https://doi.org/10.15159/AR.18.154

Mathematical description of loading curves and deformation energy of bulk oil palm kernels

A. Kabutey[1,*], D. Herak[1], C. Mizera[1] and P. Hrabe[2]

[1]Czech University of Life Sciences Prague, Faculty of Engineering, Department of Mechanical Engineering, Kamycka 129, CZ16521 Prague, Czech Republic
[2]Czech University of Life Sciences Prague, Faculty of Engineering, Department of Material Sciences and Manufacturing Technology, Kamycka 129, CZ16521 Prague, Czech Republic
[*]Correspondence: kabutey@tf.czu.cz

Abstract. The study aimed at describing the experimental and theoretical relationships between the force and deformation curves as well as the deformation energy of bulk oil palm kernels under compression loading. Vessel diameters of 60, 80 and 100 mm with initial pressing heights of the bulk kernels measured at 40, 60 and 80 mm were examined by applying a maximum compressive force of 200 kN and a speed of 5 mm min^{-1}. For the theoretical description of the force and deformation curves, the tangent curve mathematical model was applied using the MathCAD 14 software where the force coefficient of mechanical behaviour, *A* (kN), the deformation coefficient of mechanical behaviour, *B* (mm^{-1}) and the fitting curve function exponent, *n* (-) were determined respectively. The determined coefficients in addition to the maximum deformation values obtained from the compression test were used for the estimation of the theoretical or analytical deformation energy. The determined regression models expressing the deformation, numerical energy and theoretical energy as well as the tangent model coefficients *A* and *B* dependent on the vessel diameter and pressing height were statistically significant ($P < 0.05$) or (*F*-ratio > *F*-critical). Improving the mechanical pressing of oil extraction for both domestic and industrial applications still remain a concern of researchers and engineers.

Key words: bulk oil palm kernels, vegetable oil, compression test, force-deformation curves, theoretical models.

INTRODUCTION

The oil palm fruit produces two types of oils namely palm oil and palm kernel oil. The palm oil is derived from the fibrous mesocarp while the palm kernel oil is obtained from the nut or seed of the palm fruit. The palm kernel oil is a triglyceride of a complex mixture of fatty acids with lauric and oleic acids as major fatty acids (Hadi et al., 2009; Septevani et al., 2015). The palm kernel oil contributes about 10% of the quantity of palm oil produced which is useful for both domestic and industrial purposes (Okoye et al., 2008; Vincent et al., 2014). The mechanical pressing which includes hydraulic press, screw press and the rolling press is the most common method for oil extraction due to several advantages including chemical-free and protein-rich meal, simple in construction and easy operation and maintenance (Mrema & McNulty, 1985; Okoye et al., 2008).

However, the process leaves about 8–14% of the residual oil in the seedcake compared to the solvent method which is able to extract over 98% of oil but it is a very complex process and high in cost (Bamgboye & Adejuno, 2007; Deli et al., 2011). As a result of the inefficiency associated with the mechanical pressing, there have been some considerable studies on its optimization in terms of the oil recovery efficiency and energy requirement (Tindale & Hill-Hass, 1976; Bredesson, 1993; Bargale et al., 1999). These studies focused on the process variables such as the pressure, temperature and moisture content as well as physical treatments such as size reduction, cracking, dehulling; thermal treatments such as preheating, dry extrusion; and hydrothermal treatment such as steaming, hot water soaking, blanching and flaking. Based on these processing steps, the oil recovery has improved from 50% to 80% (Singh & Bargale, 2000; Okoye et al., 2008).

In order to achieve suitable operation of the mechanical pressing for oil extraction, it is important also to examine the mechanical behaviour, the force and deformation curves and deformation energy of the bulk oilseeds, nuts or kernels in linear compression loading (Herak et al., 2012; Kabutey et al., 2013; Divišová et al., 2014; Akangbe & Herak, 2017; Kabutey et al., 2017). There is also the need to describe mathematically the linear compression process to predict the oil expression behaviour in mechanical pressing (Mrema & McNulty, 1985; Herak et al., 2013a; Sigalingging et al., 2014, Sigalingging et al., 2015). This knowledge, nevertheless, is very limited in the literature. Therefore, the study aimed at describing the experimental and theoretical relationships between the force and deformation curves and deformation energy of bulk oil palm kernels under compression loading.

MATERIALS AND METHOD

Sample and compression test

Bulk oil palm kernels purchased from Afosu/Abirim in the Birim North District in the Eastern Region of Southern Ghana were used for the compression test. The universal compression testing machine (ZDM 50, Czech Republic) and pressing vessels of diameters of 60, 80 and 100 mm with a plunger were used for the compression test. The initial pressing heights of the samples were measured at 40, 60 and 80 mm for all vessel diameters and loaded by applying a maximum compressive force of 200 kN and a speed of 5 mm min^{-1}.

Parameters determined

The moisture content of the samples was determined using the conventional method (ISI, 1996). From Eq. (1) (Blahovec, 2008), the moisture content was calculated to be 9% w.b.

$$M_C = \frac{m_a - m_b}{m_a} \cdot 100 \qquad (1)$$

where M_C is the percentage moisture content in wet basis (% w.b.); m_a and m_b are the masses of samples before and after oven drying at a temperature of 105 °C and a drying time of 17 h.

The percentage kernel oil yield was determined as the ratio of the mass of kernel oil (the difference between the mass of initial height of bulk kernels and mass of bulk kernels cake) to that of the mass of initial pressing height multiplied by 100 as given by Eq. (2) (Deli et al., 2011).

$$O_Y = \frac{O_w}{O_m} \cdot 100 \quad (2)$$

where O_Y is the percentage kernel oil (%); O_w is the mass of bulk kernels oil (g) and O_m is the mass of initial pressing height of bulk kernels (g).

The numerical or experimental deformation energy, N_{de} of the bulk kernels was also calculated using Eq. (3) (Herak et al., 2013a; Akangbe & Herak, 2017).

$$N_{de} = \sum_{n=0}^{n=i-1} \left[\left(\frac{F_{n+1} + F_n}{2} \right) \cdot (x_{n+1} - x_n) \right] \quad (3)$$

where N_{de} is the numerical deformation energy (J); $F_{n+1} + F_n$ and $x_{n+1} - x_n$ are the values of the force (N) and deformation (mm), *n* is the number of data points and *i* is the number of subsections of the deformation axis (-).

The theoretical description of force and deformation curve was done by using the tangent curve mathematical model (Herak et al., 2013a; Sigalingging et al., 2014, Sigalingging et al., 2015) as given in Eq. (4) as follows:

$$F(x) = A \cdot (\tan(B \cdot x))^n \quad (4)$$

where *F* is the force (N); *x* is the deformation (mm); *A* is the force coefficient of mechanical behaviour (N); *B* is the deformation coefficient of mechanical behaviour (mm^{-1}), *n* is the fitting curve function exponent (-).

The theoretical or analytical deformation energy, T_{de} was determined by Eq. (5) which is the integral of Eq. (4) for *n* = 1 as follows:

$$\int F(x)dx \to -\frac{A \cdot ln(\cos(B \cdot x))}{B} \quad (5)$$

Statistical analysis

The calculated parameters were analysed using the STATISTICA 13 software (Statsoft, 2013) by employing the multiple regression procedure. The theoretical data analysis, that is, the determination of the coefficients *A*, *B* and *n* of the tangent curve mathematical model Eq. (4) and their statistical evaluation was done using the MathCAD 14 software (Marquardt, 1963; Pritchard, 1998; Mathsoft, 2014).

RESULTS AND DISCUSSION

The amounts of mass of kernel oil and percentage kernel oil of bulk oil palm kernels measured at pressing heights of 40, 60 and 80 mm in vessel diameters of 60, 80 and 100 mm are presented in Table 1. The increase in bulk kernels pressing heights and vessel diameters linearly increased the output kernel oil. The calculated percentage kernel oil at a maximum compressive force of 200 kN and a speed of 5 mm min^{-1}, however, showed both increasing and decreasing trends with the increase in bulk kernels pressing heights and vessel diameters. The literature indicates that pressure, temperature, pressing time, speed and moisture content are other processing factors influencing the percentage oil yield (Khan & Hanna, 1983; Mrema and McNulty, 1985; Deli et al., 2011). The varying combinations of these processing factors need to be studied extensively under compression loading to determine their optimum amounts.

Table 1. Calculated amounts of bulk kernels oil yield (Mean ± Standard Deviation)

Variables (mm)	Mass of bulk kernels* (g)	Mass of bulk kernel cake** (g)	Mass of kernel oil (g)	Kernel oil yield (%)
D = 60				
H = 40	65.7 ± 0.0	56.5 ± 0.3	9.2 ± 0.3	14.1 ± 0.4
H = 60	102.5 ± 0.7	86.4 ± 0.3	16.1 ± 0.4	15.7 ± 0.3
H = 80	135.4 ± 1.4	116.1 ± 0.0	19.4 ± 1.4	14.3 ± 0.9
D = 80				
H = 40	122.1 ± 2.3	110.6 ± 4.1	11.3 ± 1.7	9.3 ± 1.5
H = 60	180.3 ± 125	161.5 ± 0.2	18.8 ± 1.4	10.4 ± 0.7
H = 80	234.7 ± 1.7	210.7 ± 2.6	23.9 ± 1.1	10.2 ± 0.5
D =100				
H = 40	187.1 ± 4.2	171.9 ± 4.4	15.1 ± 0.2	8.1 ± 0.3
H = 60	281.5 ± 0.8	259.4 ± 1.1	22.1 ± 1.8	7.9 ± 0.6
H = 80	374.7 ± 2.7	329.7 ± 1.8	45.0 ± 4.5	12.0 ± 1.1

D is the pressing vessel diameter (mm); *H* is the pressing height of bulk kernels (mm); * is the mass of bulk kernels before pressing; ** is the mass of bulk kernels cake after pressing.

The values of the deformation, numerical energy and theoretical energy increased along with the increase in bulk kernels pressing heights and vessel diameters as shown in Table 2. The box plots of these relationships are shown in Figs 1 and 2.

The results were statistically significant where F-ratio > F-critical or P-value < 0.05 as presented in Table 3. The coefficients of determination (R^2) were 0.98, 0.96 and 0.94 respectively.The expressions of the deformation, D_{fm} (mm), numerical energy, N_{de} (J) and theoretical energy, T_{de} (J) dependent on the vessel diameter, D (mm) and pressing height, H (mm) are described in Eqs. 6, 7 and 8 as follows:

Table 2. Calculated amounts of bulk kernels deformation and deformation energy (Mean ± Standard Deviation)

Variables	Deformation	Deformation energy (J)	
(mm)	D_{fm} (mm)	Numerical, N_{de}	Theoretical, T_{de}
D = 60			
H = 40	25.6 ± 0.3	689.3 ± 10.9	780.4 ± 33.7
H = 60	38.1 ± 0.5	985.8 ± 25.1	950.8 ± 23.7
H = 80	50.1 ± 0.0	1,239.2 ± 42.0	1,241.0 ± 67.9
D = 80			
H = 40	23.2 ± 1.0	876.0 ± 2.3	874.9 ± 10.8
H = 60	35.3 ± 0.4	1,285.2 ± 8.8	1,266.0 ± 1.4
H = 80	45.5 ± 0.4	1,612.7 ± 16.2	1,595.5 ± 91.2
D =100			
H = 40	23.7 ± 0.4	1,073.9 ± 30.3	1,105.0 ± 18.4
H = 60	33.8 ± 0.2	1,561.4 ± 34.9	1,541.5 ± 7.8
H = 80	41.7 ± 0.4	2,045.5 ± 50.4	2,092.0 ± 33.9

D is the pressing vessel diameter (mm), *H* is the pressing height of bulk kernels (mm).

$$D_{fm} = 12.6 - 0.12 \cdot D + 0.54 \cdot H \quad (6)$$

$$N_{de} = -1{,}043.6 + 14.7 \cdot D + 18.8 \cdot H \quad (7)$$

$$T_{de} = -989.7 + 14.7 \cdot D + 18.1 \cdot H \quad (8)$$

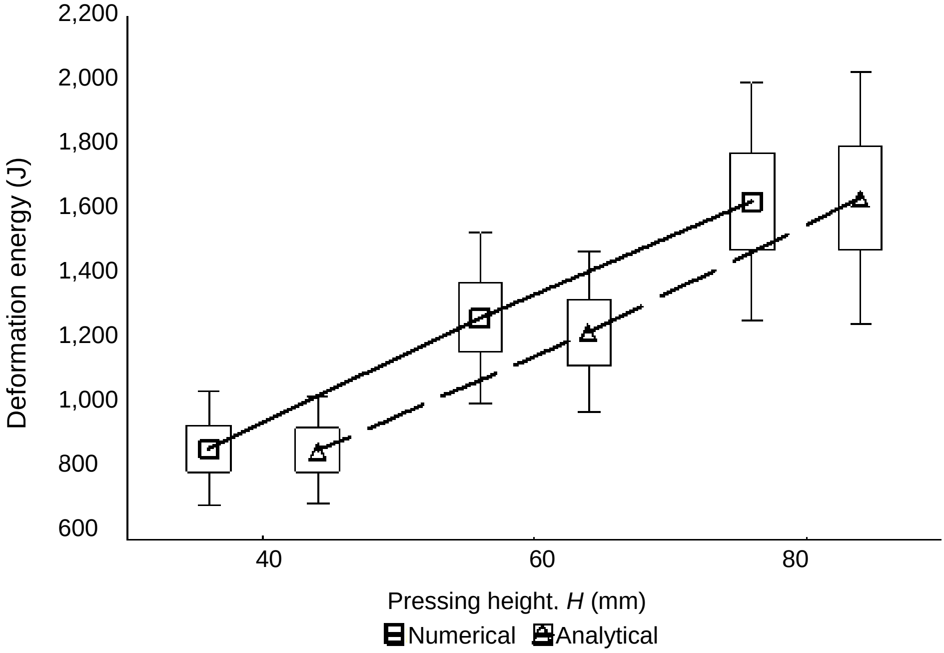

Figure 1. Comparison between numerical and analytical deformation energy based on the bulk samples pressing height.

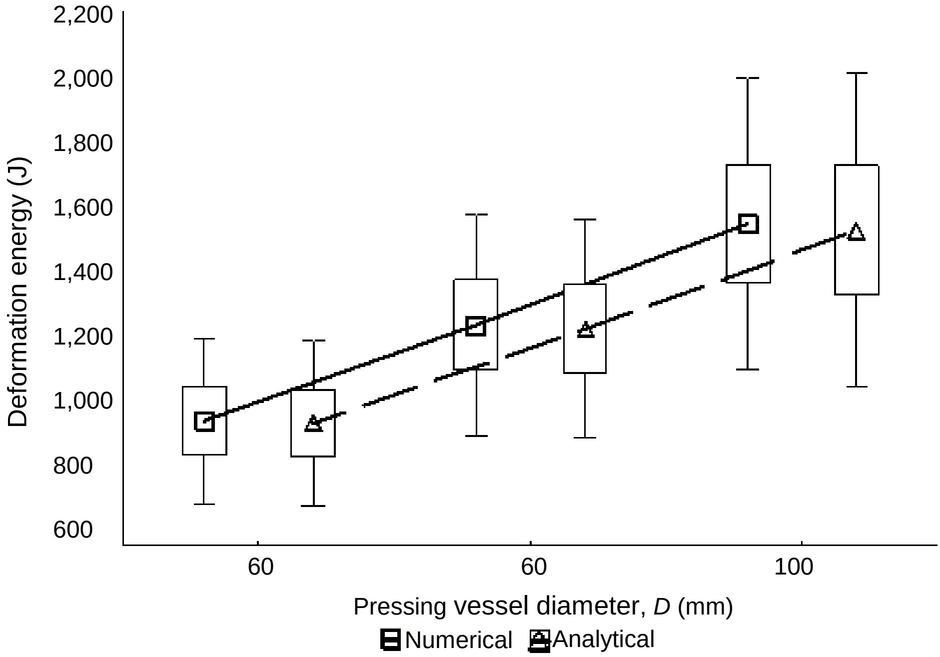

Figure 2. Comparison between numerical and analytical deformation energy based on the pressing vessel diameter.

The experimental and theoretical descriptions of the force and deformation curves of the bulk oil palm kernels for vessel diameters (D = 60, 80 and 100 mm) in relation to bulk kernels pressing heights (H = 40, 60 and 80 mm) are illustrated in Figs 3–5. All the curves showed a smooth curve characteristic which is important for analysing the deformation energy both experimentally and theoretically (Divišová et al., 2014; Kabutey et al., 2014; Sigalingging et al., 2014, Sigalingging et al., 2015). The smooth curve behaviour is also vital for understanding the required energy demand for the oil point and percentage oil yield (Faborade & Favier, 1996; Herak et al., 2010, 2013b).

Table 3. Statistical values of regression analysis of the calculated variables

Calculated parameters	F-ratio (-)	F-critical (-)	P-value (-)	R^2 (-)
D_{fm} (mm)	377.65	3.63	< 0.05	0.98
N_{de} (J)	205.67	3.63	< 0.05	0.96
T_{de} (J)	113.97	3.63	< 0.05	0.94

F-ratio > F-critical or P-value < 0.05 is significant (Statsoft, 2013). F-ratio is the value of the F test (-); F-critical is the critical value that compares a pair of models (-); P-value is the significance level used for testing a statistical hypothesis (-); R^2 is the coefficient of determination (-).

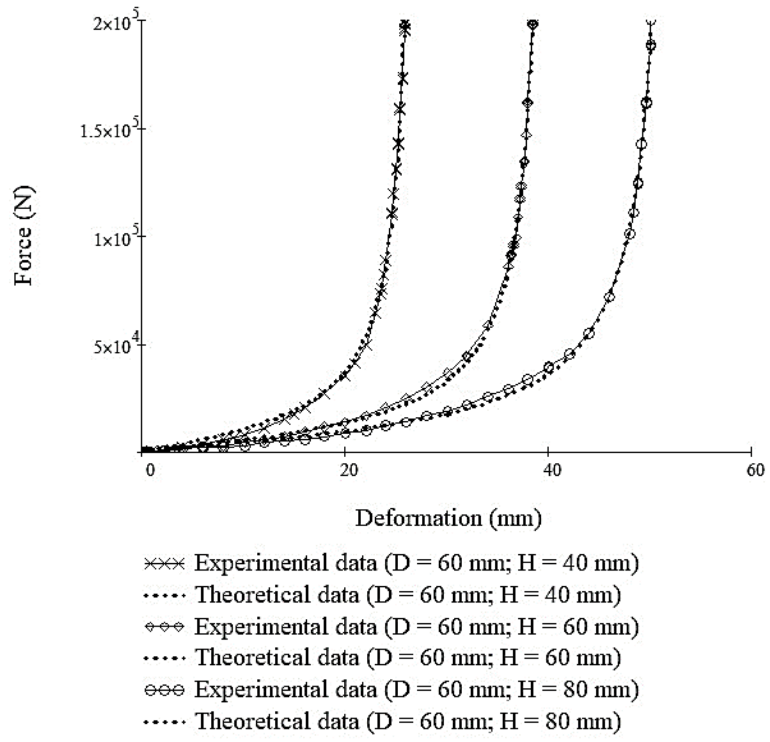

Figure 3. Experimental and theoretical descriptions of the force and deformation of bulk oil palm kernels for vessel diameter, (D = 60 mm) in relation to pressing heights, (H = 40, 60 and 80 mm).

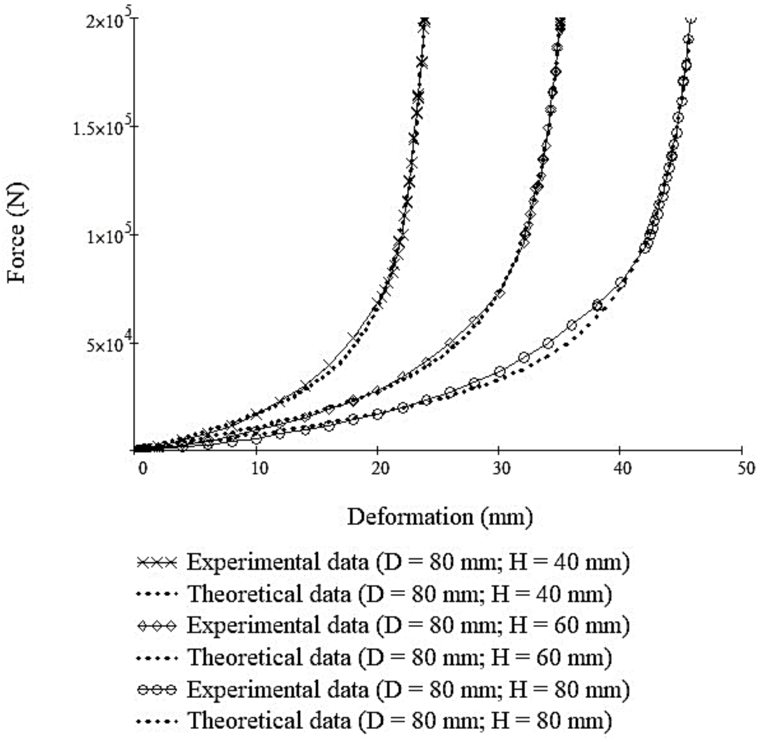

Figure 4. Experimental and theoretical descriptions of the force and deformation of bulk oil palm kernels for vessel diameter, (D = 80 mm) in relation to pressing heights, (H = 40, 60 and 80 mm).

The determined coefficients of the tangent curve mathematical model; A, B and n using Eq. 4 are given in Table 4. Their statistical values are also given in Table 5. The results were statistically significant (P > 0.05) or (F-ratio < F-critical) (Mathsoft, 2014). These determined coefficients together with the deformation values (Table 2) can be used to describe theoretically the experimental relationship between the force and deformation curves of bulk oil palm kernels compressed at a maximum compressive force of 200 kN and a speed of 5 min min^{-1}.

Table 4. Determined coefficients of the tangent curve model (Mean ± Standard Deviation)

Variables (mm)	A (N)	B (mm^{-1})	N (-)
D = 60			
H = 40	18,280.0 ± 2,262.7	0.058 ± 0.0	1
H = 60	15,030.0 ± 1,640.5	0.039 ± 0.0	1
H = 80	13,785.0 ± 685.9	0.030 ± 0.0	1
D = 80			
H = 40	26,175.0 ± 1,887.9	0.063 ± 0.0	1
H = 60	24,630.0 ± 1,513.2	0.041 ± 0.0	1
H = 80	23,540.0 ± 212.1	0.032 ± 0.0	1
D =100			
H = 40	39,485.0 ± 261.6	0.058 ± 0.0	1
H = 60	39,075.0 ± 1,364.7	0.041 ± 0.0	1
H = 80	44,140.0 ± 466.7	0.033 ± 0.0	1

A is the force coefficient of mechanical behaviour (N); B is the deformation coefficient of mechanical behaviour (mm^{-1}); n is the fitting curve function exponent (-).

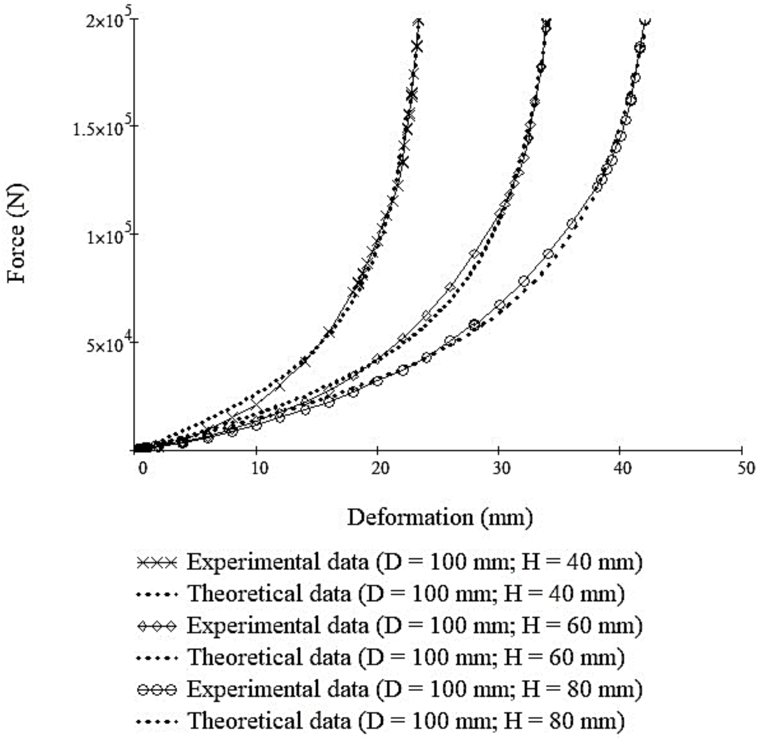

Figure 5. Experimental and theoretical descriptions of the force and deformation of bulk oil palm kernels for vessel diameter, (D = 100 mm) in relation to pressing heights, (H = 40, 60 and 80 mm).

Table 5. Statistical values of the ANOVA analysis of the tangent model coefficients (Mean ± Standard Deviation)

Tangent model coefficients	*F*-ratio (-)	*F*-critical (-)	*P*-value (-)	R^2 (-)
A, *B*, *n* (*D* = 60)				
H = 40	0.019 ± 0.006	3.858 ± 0.007	0.889 ± 0.019	0.998 ± 0.001
H = 60	0.003 ± 0.004	3.848 ± 0.000	0.964 ± 0.036	0.999 ± 0.001
H = 80	0.0001 ± 0.0001	3.862 ± 0.000	0.995 ± 0.003	0.999 ± 0.000
A, *B*, *n* (*D* = 80)				
H = 40	0.002 ± 0.00	3.848 ± 0.000	0.963 ± 0.001	0.999 ± 0.001
H = 60	0.002 ± 0.001	3.848 ± 0.001	0.964 ± 0.007	0.999 ± 0.001
H = 80	0.0001 ± 0.00	3.847 ± 0.000	0.991 ± 0.002	0.999 ± 0.000
A, *B*, *n* (*D* = 100)				
H = 40	0.028 ± 0.035	3.848 ± 0.000	0.886 ± 0.095	0.999 ± 0.001
H = 60	0.020 ± 0.006	3.848 ± 0.000	0.888 ± 0.169	0.999 ± 0.000
H = 80	0.018 ± 0.022	3.848 ± 0.000	0.906 ± 0.072	0.999 ± 0.000

F-ratio < *F*-critical or *P*-value > 0.05 is significant (Mathsoft, 2014).

The regression equations of the tangent model coefficients *A* (N) and *B* (mm^{-1}) of the tangent curve model for the fitting function exponent, $n = 1$ are described in Eqs. 9 and 10 dependent on the vessel diameter *D* and pressing height *H*. The whole models statistical values were significant ($P < 0.05$) or (*F*-ratio > *F*-critical). The coefficients of determination (R^2) of the determined models were 0.94 and 0.99 (Table 6).

$$A = -22{,}039.2 + 630 \cdot D - 20.6 \cdot H \quad (9)$$

$$B = 0.09428 + 0.0009 \cdot D - 0.0023 \cdot H - 0.000005 \cdot D^2 + 0.000013 \cdot H^2 \quad (10)$$

The force coefficient of mechanical behaviour, *A* (N) and the deformation coefficient of mechanical behaviour, *B* (mm^{-1}) dependency on the pressing vessel diameter in relation to the pressing height are displayed in Figs 6 and 7 respectively. It can be seen that the force coefficient of mechanical behaviour increased linearly with increasing pressing heights and vessel diameters while the deformation coefficient of mechanical behaviour was suitably fitted by a polynomial function.

Table 6. Statistical values of regression analysis of the tangent model coefficients *A* and *B*

Tangent model coefficients	*F*-ratio (-)	*F*-critical (-)	*P*-value (-)	R^2 (-)
A	115.37	3.63	< 0.05	0.94
B	372.53	3.63	< 0.05	0.99

A is the force coefficient of mechanical behaviour (N); *B* is the deformation coefficient of mechanical behaviour (mm^{-1}) (Statsoft, 2013).

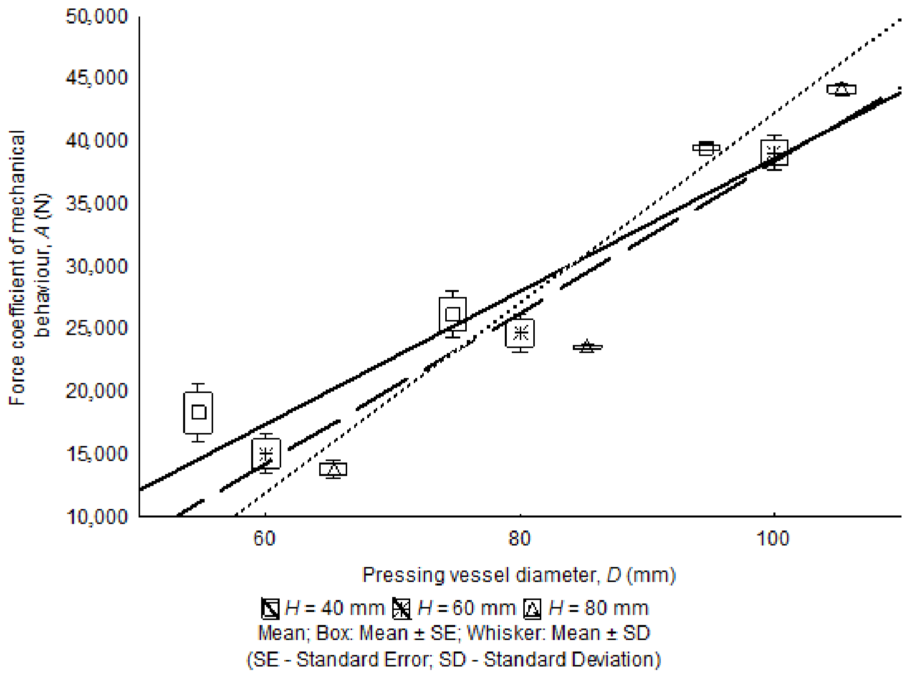

Figure 6. Force coefficient of mechanical behaviour, *A* (N) versus pressing vessel diameter, *D* (mm) in relation to bulk samples pressing heights, *H* (mm).

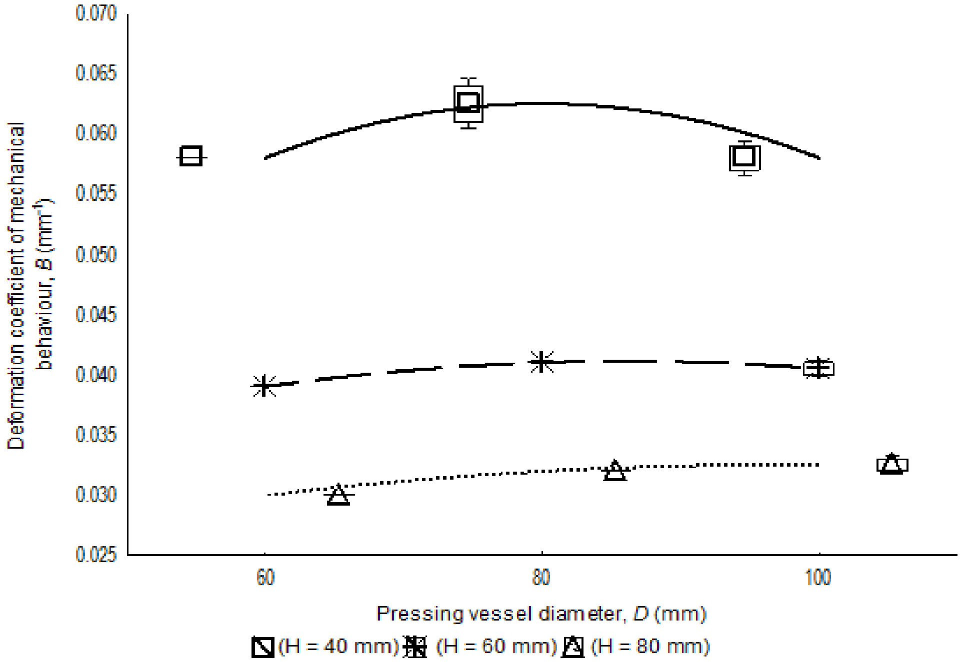

Figure 7. Deformation coefficient of mechanical behaviour, *B* (mm^{-1}) versus pressing vessel diameter, *D* (mm) in relation to bulk kernels pressing heights, *H* (mm).

CONCLUSIONS

The experimental dependency between the force and deformation curves of bulk oil palm kernels at pressing heights of 40, 60 and 80 mm and vessel diameters of 60, 80 and 100 mm were described theoretically using the tangent curve mathematical model. The statistical values of the ANOVA analysis of the tangent curve model coefficients namely the force coefficient of mechanical behaviour, *A* (N), the deformation coefficient of mechanical behaviour, *B* (mm^{-1}) and the fitting curve function exponent, *n* (-) were significant ($P > 0.05$) or (F-ratio < F-critical) based on the MathCAD 14 software. Regression equations of the deformation, numerical energy, theoretical energy, force coefficient of mechanical behaviour and deformation coefficient of mechanical behaviour dependent on the pressing height and vessel diameter were determined. Their statistical values from the regression analysis were also significant ($P < 0.05$) or (F-ratio > F-critical) based on the STATISTICA 13 software. At a maximum force of 200 kN and speed of 5 mm min^{-1}, the fitting curve function exponent, *n* of the tangent curve mathematical model for describing bulk oil palm kernels was found to be 1. This information is important for analyzing or predicting the oil expression behaviour involving the mechanical screw presses.

ACKNOWLEDGEMENT. The research was financially supported by the Internal Grant Agency of Faculty of Engineering, Czech University of Life Sciences Prague, grant number: 2017: 31130/ 1312/ 3111.

REFERENCES

Akangbe, O.L. & Herak, D. 2017. Mechanical behaviour of selected bulk oilseeds under compression loading. *Agronomy Research* **15**(S1), 941–951.

Bamgboye, A.I. & Adejumo, A.O.D. 2007. Development of a sunflower oil expeller. *Agricultural Engineering International*: *the CIGR Ejournal* **9**, 1–6.

Bargale, P.C., Ford, R.J., Sosulski, F.W., Wulfsohn, D. & Irudayaraj, J.I. 1999. Mechanical oil expression from extruded soybean. *Journal of American Chemists' Society* **76**(2), 223–229.

Blahovec, J. 2008. *Agromaterials Study Guide*. Prague, Czech University of Life Sciences Prague: 7 pp.

Bredesson, D.K. 1993. Mechanical oil extraction. *Journal of the American Oil Chemists' Society* **60**, 211–213.

Deli, S., Farah Masturah, M., Tajul Aris, Y. & Wan Nadiah, W.A., 2011. The effects of physical parameters of the screw press oil expeller on oil yield from *Nigella sativa* L. seeds. *Journal International Food Research* **18**(4), 1367–1373.

Divišová, M., Herák, D., Kabutey, A., Sigalingging, R. & Svatoňová, T. 2014. Deformation curve characteristics of rapeseeds and sunflower seeds under compression loading. *Scientia Agriculturae Bohemica* **45**(3), 180–186.

Faborade, M.O. & Favier, J.F. 1996. Identification and significance of the oil-point in seed-oil expression. *Journal of Agricultural Engineering Research* **65**, 335–345.

Hadi, S., Ahmad, D. & Akande, F.B. 2009. Determination of the bruise indexes of oil palm fruits. *Journal of Food Engineering* **95**, 322–326.

Herak, D., Gurdil, G., Sedlacek, A., Dajbych, O. & Simanjuntak, S. 2010. Energy demands for pressing Jatropha curcas L. seeds. *Biosystems Engineering* **106**, 527–534.

Herak, D., Kabutey, A. & Hrabe, P. 2013b. Oil point determination of *Jatropha curcas* L. bulk seeds under compression loading. *Biosystems Engineering* **116**(4), 470–477.

Herák, D., Kabutey, A., Divišová, M. & Simanjuntak, S. 2013a. Mathematical model of mechanical behaviour of Jatropha curcas L. seeds under compression loading. *Biosystems Engineering* **114**(3), 279–288.

Herak, D., Kabutey, A., Divisova, M. & Svatonova, T. 2012. Comparison of the Mechanical Behaviour of Selected Oilseeds under Compression Loading. *Not Bot Horti Agrobo* **40**(2), 227–232.

ISI, 1996. Indian standard methods for analysis of oilseeds, IS: 3579. New Delhi: Indian Standard Institute.

Kabutey, A., Divišova, M., Sedlaček, L., Boatri, W.E., Svatonová, T. & Sigalingging, R. 2013. Mechanical behaviour of oil palm kernels (*Elaeis guineensis*). *Scientia Agriculturae Bohemica* **44**(1), 19–23.

Kabutey, A., Herak, D., Choteborsky, R., Mizera, C., Sigalingging, R. & Akangbe, O.L. 2017. Oil point and mechanical behaviour of oil palm kernels in linear compression. *International Agrophysics* **31**(3), 351–356.

Kabutey, A., Herák, D., Dajbych, O., Boatri, W.E. & Sigalingging, R. 2014. Deformation energy of Jatropha curcas L. seeds under compression loading. *Research in Agricultural Engineering*, **60**(2), 68–74.

Khan, L.M. & Hanna, M.A. 1983. Expression of Oil from Oilseeds – A Review. *Journal of Agricultural Engineering Research* **28**, 495–503.

Marquardt, D.W. 1963. An algorithm for the least-squares estimation of nonlinear parameters, SIAM. *Journal of Applied Mathematics* **11**(2), 431–441.

Mathsoft., 2014. Parametric Technology Corporation, Needham, MA02494, USA.

Mrema, G.C. & McNulty, P.B. 1985. Mathematical model of mechanical oil expression from oilseeds. *Journal of Agricultural Engineering Research* **31**(5), 361–370.

Okoye, C.N., Jiang, J. & Hui, L.Y. 2008. Design and development of secondary controlled industrial palm kernel nut vegetable oil expeller plant for energy saving and recuperation. *Journal of Food Engineering* **87**, 578–590.

Pritchard, P.J. 1998. Mathcad: A tool for engineering problem solving. McGraw-Hill Science Engineering. Septevani, A.A., Evans, D.A.C., Chaleat, C., Martin, D.J. & Annamalai, P.K. 2015. A systematic study substituting polyether polyol with palm kernel oil based polyester polyol in rigid polyurethane foam. *Industrial Crops & Products* **66**, 16–26.

Septevani, A.A., Evans, D.A.C., Chaleat, C., Martin, D.J. & Annamalai, P.K. 2015. A systematic study substituting polyether polyol with palm kernel oil based polyester polyol in rigid polyurethane foam. *Industrial Cropas and Products* **66**, 16–26.

Sigalingging, R., Herák, D., Kabutey, A., Čestmír, M. & Divišová, M. 2014. Tangent curve function description of mechanical behaviour of bulk oilseeds: A review, *Scientia Agriculturae Bohemica* **45**(4), 259–264.

Sigalingging, R., Herák, D., Kabutey, A., Dajbych, O., Hrabě, P. & Mizera, C. 2015. Application of a tangent curve mathematical model for analysis of the mechanical behaviour of sunflower bulk seeds. *International Agrophysics* **29**(4), 517–524.

Singh, J. & Bargale, P.C. 2000. Development of a small capacity double stage compression screw press for oil expression. *Journal of Food Engineering* **43**, 75–82.

Statsoft., 2013. Inc. Tulsa, OK74104, USA.

Tindale, L.H. & Hill-Hass, S.R. 1976. Current equipment for mechanical oil extraction. *Journal of the American Oil Chemists' Society* **53**, 265–270.

Vincent, C.J., Shamsudin, R. & Baharuddin, A.S. 2014. Pre-treatment of oil palm fruits: A review. *Journal of Food Engineering* **143**, 123–131.

Agronomy Research **16**(4), 1698–1707, 2018
https://doi.org/10.15159/AR.18.168

Efficiency of the use of field beans in fattening lambs

D. Kairisa* and E. Aplocina

Latvia University of Life Sciences and Technologies, Faculty of Agriculture, Institute of Agrobiotechnology, Liela street 2, LV 3001 Jelgava, Latvia
*Correspondence: daina.kairisa@llu.lv

Abstract. The breeding and feeding of self produced pulses to livestock is one of the important directions of research for reducing the production costs of livestock products. Experiment on the effective using of the field beans to lambs for fattening was arranged in three replications using the Latvian Dark-headed breed male lambs. The mixture of concentrated feed consisted of 50% of bean and 50% of oat. Lambs were weighed at the starting and ending of the trial. Carcass quality was assessed according to the European standard for the classification of carcasses of sheep. The fattening period lasted from 37 to 94 days, on average 63 ± 3.6 days. The average live weight gain per day was 247.4 ± 13.85 g, and live weight increased on average by 15.3 ± 0.94 kg. Significantly higher ($P < 0.05$) growth rate during fattening period reached lambs of 3rd group, where lambs started fattening above 27 kg of live weight, reaching a 276.8 ± 26.26 g daily live weight gain. The quality of the obtained carcasses was an average, and score for musculature was from R to O class, but the average score for fat deposition was from 3 to 4 points. The mixture of field beans and oats provided 19.3% of crude protein and 12.1 MJ of metabolizable energy 1 kg of dry matter, and its unlimited feeding provided medium lamb's growth rate. The level of feed conversion was 7.56 kg of dry matter.

Key words: beans, lamb, fattening, slaughter, carcass.

INTRODUCTION

Well-balanced and optimized nutrition of lambs is important precondition in breeding and production of lamb meat in high quality. For this purpose it is necessity for extra feeding of suckle lambs and optimal feeding after weaning with the aim to get live weight gain to 200 g per day and more. Shortage of different nutrients at first can lead to lower clip and quality of wool, amount and quality of meat, feed conversion for production of meat and wool, and to growth of suckle lambs finally (Kairisa & Selegovska, 2004).

In Latvia the basic feed for sheep is hay of good quality and concentrates. According Boughalmi & Araba (2016) studies, fattened lambs have a higher carcass weight and dressing percentage if the feed ration consists from concentrated feed and hay, as compared to ration which consist from concentrated feed and pasture grass. The best hay is hay from natural meadows (Latvietis, 2013). Concentrates mostly consist of barley, oats and wheat, which can be supplemented by protein feed, minerals and vitamins. Not only imported soya bean but also other protein crops – field beans

(*Vicia faba* L.), peas, lupines, vetches – are excellent forage because of their high protein content.

The most common protein feed for livestock is field beans which are an excellent source of both protein and energy for ruminants. The protein content of field beans is 29.6%, the soluble protein is 14.97%, undegraded intake protein (UIP) is 44.18% of crude protein (Osmane et al., 2015). The protein is extensively and rapidly degradable in the rumen and protein not degraded in the rumen should be accessible later in the intestinal tract (Ramos-Morales et al., 2010). Some heat treatments of beans can increase the proportion of protein that by-passes digestion in the rumen, but there is much variability in this effect and ultimately in how heat treatments affect animal performance (Yu et al., 2004). Compared to cereals, the content of lysine in field beans is relatively high and the contents of the sulphur-containing amino acids cysteine and methionine are low (Crepon et al., 2010). Min et al (2015) experiments have shown that phytochemical plant tannins can modify the fatty acid composition of meat, thus indirectly affecting its colour stability, antioxidant status and shelf life (Luciano et al., 2009) Tannins in field beans are located mainly in the hull. The presence of some tannins with field beans can protect protein from degradation in the rumen but allow it be subsequently digested post-ruminally (Martinez et al., 2004). They can also have beneficial effects in reducing bloat and enteric methane, and in providing an anthelminthic effect. However, high concentrations of some tannins can reduce feed intake and thus animal performance (Butter et al., 1999). Antinutritional substances in field beans are not currently considered problematic for fully-developed ruminants (Melicharová et al., 2009).

According Sinclair et al. (1991) increasing the dietary protein level resulted in an increase in cold carcass weight, chest width, carcass protein content, *M. longissimus dorsi* depth and fatness class and weight of liver and kidney. The use of field beans in varying proportions, in replacement of soybean meal and sunflower meal, did not affect lamb performance (Caballero et al., 1992). Moreover, carcasses from lambs fed field beans showed lower fatness than those from lambs fed soybean cake or lentil diets. According investigation of Boukhris et al. (2013) average daily gain of lambs was similar for all dietary treatments, which included soya bean or field bean. However, lambs fed by concentrates comprising 100 g kg^{1} field bean had the lowest proportion of fat in the carcass than that for lambs which received 200 g kg^{1} field bean or just soya as protein source. Unlimited feeding lead to lower carcass weight and dressing percentage compared to lambs that received limited amount of concentrated feed (Karaca et al., 2016).

As sheep is a ruminant, the feeding of sheep is very similar to feeding of cow. Therefore profitable sheep breeding is not possible without complete nutrition. As most lambs require 10–14 kg of feed to produce 2 kg of liveweight (1 kg of carcase weight), ration costs are a major issue within a feedlotting program (Duddy et al., 2016).

The objective of this study was assessing the suitability of field beans in lamb finishing diets.

MATERIALS AND METHODS

A study on the possibilities of feeding of field beans to lambs was carried out in collaboration with the Latvian Sheep Breeders Association at the breeding control station in three replications. The study was carried out in the autumn and winter period, using the Latvian Dark-headed male lambs born in the middle of summer (late June or July) in 2014, 2015 and 2016. 19 lambs were purchased after weaning from mothers 3 to 3.5 months old with a live weight of 19.8 kg to 30.2 kg. They were placed by 3 or 4 in one pen in outdoor shed, and the straw was used as bedding material. For research purposes and analyzing of data they were divided into 3 research groups according their live weight. Mixture of ryegrass and clover 2nd cut hay and grain meal was fed unlimited, and the amount of consumed food was regularly counted. Water was provided from the automatic water bowls. The fattening of lambs started after a two week adaptation period. Based on the fact that lambs with higher live weight are able to consume a larger amount of feed (Nutrient requirements ..., 2007), data from the study were analyzed taking into account the lambs' live weight at the beginning of fattening (Table 1).

Table 1. The research scheme

Research groups	Live weight of lambs at the beginning of fattening, kg	Number of lambs
1.	till 25	6
2.	25–27	6
3.	above 27	7

In order to bring the main nutrient content closer to the concentrated feed mix, the bean and oat meal mixture was in equal proportion to 50% and 50%. The following feed nutrient biochemical parameters were analyzed before the start of the trial according with generally accepted methods of analysis: dry matter (DM) according ISO 6496:1999 method; neutral detergent fiber (NDF) according LVS EN ISO 16472:2006; acid detergent fiber (ADF) according LVS EN ISO 13906:2008; crude protein (CP) according LVS EN ISO 5983-2:2009; calcium (Ca) according LVS EN ISO 6869:2002; phosphorus (P) according ISO 6491:1998; ash according ISO 5984:2002/Cor 1:2005, but metabolizable energy (ME) was calculated in laboratory based on the results of the ADF analysis (Rohweder, 1984; Ositis, 1996). The quality indicators for nutrients were determined by the accredited laboratory of Agronomic analysis of the Latvia University of Agriculture.

Lambs were weighted at the start and end of the study. Using the obtained live weight results, the absolute increase in live weight per day (A) were calculated by formula (1):

$$A = \frac{Wt - Wo}{t} \quad (1)$$

where W_t – live weight at the end of the period, kg; W_0 – live weight at the beginning of the period, kg; t – period, days.

Lambs were slaughtered in a certified slaughterhouse, reaching at least 40 kg of live weight. Before slaughtering of lambs, 12-hour fasting period was applied without limiting of water intake. After slaughter of lambs, chilled carcases (24 hours after slaughter) were weighed and the carcass dressing (K) was calculated according to the formula (2):

$$K = \frac{Km}{Wk} \cdot 100 \quad (2)$$

where K – carcass dressing, %; Wk – live weight before slaughtering, kg; Km – carcass weight, kg.

The carcase quality was assessed according to the European Standard for the Classification of Sheep Carcasses (Markovic et al., 2014), where EUROP letter designations were used to indicate musculature development. The evaluation of the obtained data is based on the numerical values: E – excellent (1), U – very well developed (2), R – good (3), O – average (4), P – weak (5). The level of fat stratification is designated by numbers from 1 to 5, where 1 – very low, 2 – low, 3 – medium high, 4 – high, 5 – very high. Using the tape measure, the length of the carcase and the thigh girth were measured. The cold carcasses were weighed and sawed into two symmetrical sides along backbone. One side was divided into the main tissue components: muscle, bone, fat and connective tissue. Using the obtained results, the tissue ratio was calculated: meat (muscle + fat) and bone, muscle and fat, muscle and bone.

The data obtained in the study were analyzed using mathematical methods of data processing. The average values of the characteristics, the standard error and the coefficient of variation are calculated. The significance of the average values difference is determined by the t-test. The small letters of the Latin alphabet: a, b, c were used to indicate the significance of the differences ($P < 0.05$) between the study groups.

RESULTS AND DISCUSSION

The results summarized in Table 2 show, there were no significant differences in the number of lambs at birth or in age at the beginning of fattening. A significant difference ($P < 0.05$) was observed in live weight of lambs at the beginning of study, which indirectly indicates the milk productivity of sheep mothers as well as feeding management of lambs on farms.

The chemical composition of the grain meal mixture is summarized in Table 3.

Table 2. Litter size, age and live weight of lambs at the beginning of fattening

Research group	Litter size	Age, days	Live weight, kg
	$\bar{x} \pm S_{\bar{x}}$		
1.	1.83 ± 0.307^a	90 ± 4.8^a	22.5 ± 0.70^a
2.	2.00 ± 0.258^a	91 ± 3.5^a	26.3 ± 0.25^b
3.	1.86 ± 0.143^a	97 ± 5.1^a	28.0 ± 0.41^c

$^{a, b, c}$ – values followed by different letters are significantly different between groups ($P < 0.05$).

Table 3. Chemical composition of grain meal mixture (n = 3)

Indices	DM, %	In dry matter						
		CP, g	NDF, g	ADF, g	ME[1], MJ	Ash, g	Ca, g	P, g
Average	89.5	193.5	194.6	136.9	12.1	54.5	5.6	5.4
Standard error	0.40	6.36	8.83	19.05	0.12	2.43	0.46	0.52
Min.	88.8	183.2	184	105.4	12.5	50.4	4.8	4.5
Max.	90.1	205.1	212.1	171.2	11.7	58.8	6.4	6.3
Variation V, %	0.8	5.7	7.9	24.1	1.7	7.7	14.3	16.8

[1] Calculated as: Metabolizable energy (ME) MJ kg^{-1} dry matter = 0.155 × TDN, where TDN is total digestible nutrients, % in dry matter (Ositis, 1996) and %TDN = 88.9 - (0.779 × ADF%) (Rohweder, 1984).

According to Barzdina & Kairisa (2016), the average daily gain for Romanov and Dorper crossbread lambs is 291 g. To reach the planned 40 kg live weight prior to slaughtering of lambs, the fattening period lasted from 37 to 94 days, on average 63 ± 3.6 days. During Barzdina & Kairisa (2016) research, the average live weight gain per day was 247.4 ± 13.85 g, and live weight increased on average by 15.3 ± 0.94 kg during fattening period.

In our study a significantly shorter fattening period was observed to lambs in groups 2 and 3 (Table 4). First group lambs were fed on average by 26 days longer than in group 3 and by 16 days longer than lambs of 2nd group (P <0.05). During the study, the live weight of 1st group lambs increased by an average of 16.8 ± 1.47 kg.

Table 4. Fattening period and live weight gain of lambs

Research group	Fattening period, days	Live weigt gain per period, kg	Live weight gain per day, g
	$\bar{x} \pm S_{\bar{x}}$		
1.	78 ± 3.8[a]	16.8 ± 1.47[a]	218.0 ± 18.74[a]
2.	62 ± 6.2[b]	14.7 ± 1.80[a]	242.4 ± 22.18[ab]
3.	52 ± 4.3[b]	14.6 ± 1.74[a]	276.8 ± 26.26[b]

[a, b] – values followed by different letters are significantly different between groups (P < 0.05).

Significantly higher growth rate during fattening period reached lambs of 3rd group, reaching a 276.8 ± 26.26 g daily live weight gain. The difference in live weight gain between the first and third group lambs is 58.8 g (P < 0.05) per day. The age of 1st group lambs at the end of fattening period was 178 days, but the age of 3rd group lambs was only 160 days. The difference in live weight gain is because the younger lambs have a higher growth rate than older lambs.

The average age of the lambs prior to slaughter was 167 ± 4.6 days and average live weight was 42.8 ± 0.77 kg (Table 5). 3rd group lambs were slaughtered by 18 days younger – on age of 160 ± 9.3 days with an average of 44.8 ± 1.40 kg live weight. There is significant difference (P < 0.05) in live weight at the end of fattening period between 1st and 3rd groups of lambs, and also in live weight prior to slaughter between 1st and 3rd groups and between 2nd and 3rd groups of lambs.

Table 5. Age and live weight of lambs prior to slaughter, cold carcass weight and carcass dressing

Research group	Age at the end of fattening, days	Live weight at the end of fattening, kg	Live weight prior to slaughter, kg	Cold carcass weight, kg	Carcass dressing, %
	$\bar{x} \pm S_{\bar{x}}$				
1.	178 ± 5.2[a]	40.7 ± 0.56[a]	39.5 ± 0.55[a]	18.2 ± 0.40[a]	45.9 ± 0.53[a]
2.	164 ± 7.4[a]	42.4 ± 1.35[ab]	40.9 ± 1.32[a]	18.8 ± 0.74[a]	45.9 ± 0.90[a]
3.	160 ± 9.3[a]	44.8 ± 1.40[b]	43.5 ± 1.25[b]	19.5 ± 0.79[a]	44.8 ± 1.09[a]

[a, b] – values followed by different letters are significantly different between groups (P < 0.05).

According Kairisa & Barzdina (2016a) research, the age prior to slaughter of Latvian dark-headed lambs fed by concentrated feed was similar – 165 days, but lambs were on average by 8.1 kg heavier, reaching 50.7 kg of live weight before slaughter and carcass dressing was 44.8%. In our trial 24 hours after the end of fattening period, carcass weight loss was an average of 3% before slaughter. There was no significant difference between the weight of the cold carcasses and the calculated carcass dressing of all study groups. The lowest carcass dressing percentage was obtained from one of the lambs of the 3rd group, only 39.7%, but the largest for one of the lamb in the 2nd group – 48.1%. It should be noted that the lambs were not cut before slaughter, resulting in the weight of skin for some lambs reaching 7 kg or 15% of live weight.

The results of carcass quality assessment are summarized in Table 6. None of the qualitative characteristics of the carcasses have shoved significant differences due to the fact that the cold carcass weight in all study groups was quite similar from 18.2 kg (group 1) to 19.5 kg (group 3). The obtained results on the length of the carcass and the thigh girth conform with the previously published ones, where the length of carcasses of the Dark-headed lambs was on average 72.2 to 75.3 cm, and the thigh girth from 67.6 to 70.0 cm (Kairisa & Barzdina, 2016b). In general, the development of muscle tissue of four carcasses (21%) was estimated by the O class (moderately developed), but the others (79%) with the R class (well developed). The fat cover for 5 carcasses (26%) was estimated at 3 points, while the remaining (74%) at 4 points, which means that the carcasses are with high level of fat stratification.

Table 6. The quality indices of lambs carcasses

Research group	Carcass lenght, cm	Thigh girth, cm	Fat layer at the 13th rib, mm	Development of muscles, points	Fat stratification, points
	$\bar{x} \pm S_{\bar{x}}$				
1.	71.2 ± 1.22	62.2 ± 0.91	2.9 ± 0.27	3.33 ± 0.167	4.00 ± 0.000
2.	70.2 ± 2.14	62.7 ± 2.47	3.2 ± 0.48	3.25 ± 0.171	3.67 ± 0.211
3.	75.0 ± 3.65	66.1 ± 3.38	2.4 ± 0.21	3.29 ± 0.184	3.57 ± 0.202

From the obtained results, it was concluded that lamb carcasses of group 1 had a weaker musculature compared to carcasses from other groups and a higher fat cover. According to Barzdina & Kairisa (2006) research, muscular tissue development in Latvian Dark headed lamb carcass in 50 cases corresponded to class R and in 50% cases to class O. In our investigation 79% of carcasses were evaluated according to class R. According to the assessment of fat tissue stratification, 74% of carcasses were estimated at 4 points, which indicated on quite well muscular tissue development and too high fat tissue stratification in carcass. Results of research with Estonian whitehead sheep shows that in 53.7% cases muscular tissue assessment in lamb carcass correspond to class R, but assessment of fat tissue stratification indicates that in 65.1% cases it is above 2 (Piirsalu, 2003; Piirsalu & Mettis, 2005).

In the carcasses of all lambs the proportion of muscle tissue was 52.3% on average, the fat content was 21.4%, and the bone density was 25.7%. The proportion of the carcass tissue parts is summarized in Table 7. The obtained results show that a larger proportion of muscle tissue was in the carcasses of lambs in 1st group, and the lowest in carcasses of 2nd group lambs.

Table 7. Proportion of carcass tissues, %

Research group	Muscles	Fats	Bones
	$\bar{x} \pm S_{\bar{x}}$		
1.	53.3 ± 1.05^{a}	19.8 ± 1.02^{a}	26.5 ± 0.32^{a}
2.	51.2 ± 0.77^{a}	23.4 ± 1.41^{b}	24.9 ± 0.96^{a}
3.	52.4 ± 0.99^{a}	21.2 ± 1.24^{ab}	25.8 ± 0.61^{a}

Although the visually estimated fat content of lambs of the group 1 was the highest –an average of 4 points, however, the total carcase fat content was lower, on average 19.8%, which is 3.6% ($P < 0.05$) less than of group 2 and 1.4% lesser than of lamb's carcasses of group 3. 1st group lambs had longer fattening period, they reach slaughter weight later and during this period the formation of muscle tissue was more intense than the formation of fat tissue.

The results of carcass tissue ratio are summarized in Table 8. In the study, the average meat and bone ratio of all lamb carcasses was 2.9, muscle and fat 2.5, but muscle and bone 2.0. The highest proportion of meat and bone, as well as muscle and bone was obtained for carcasses of lambs of group 2, due to the fact that the carcasses of this group had the smallest part of bones – 24.9% and the largest part of fat – 23.4%, but these differences are not significant ($P > 0.05$). The best muscle and fat ratio of the carcasses was at first group.

The most important indicator for lamb's breeders is the feed consumption of lambs what resulted in live weight gain. The consumption of feed for 1 kg of live weight gain indicates the conversion of feed, or the use of nutrients in the lamb body. During the study, for the 1 kg of live weight gain lambs consumed in average 3.33 kg of grass hay and 5.21 kg of concentrated feed, totally 7.56 kg of feed dry matter, indicating a worse conversion of feed compared to a Barzdina & Kairisa (2015) study on unlimited feeding of concentrated feed. In this study, dietary intake for 1 kg of live weight gain was 3.00 kg of hay and 4.7 kg of concentrated feed. In a study in Iran (Majdoub-Mathlouthi at al., 2013), in feeding of Barabarine lamb by unlimited amount of oat straw and 600 g of concentrated feed in ration, consisted from soya bean cake, wheat bran, corn grains and mineral feed, feed conversion rate was 9.3 units. Feeding of alfalfa hay for an unlimited diet for lambs of the Sufolk breed, the feed conversion ratio was 9.17 (Phillips et al., 2002). The studies of other authors (Emailizadeh et al., 2012; Khevani et al., 2014) indicate the feed conversion rate from 4.0 to 7.4, which is quite close to our study.

Table 8. Ratio of lambs carcass parts

Research group	Meat / bone	Muscle / fat	Muscle / bone
	$\bar{x} \pm S_{\bar{x}}$		
1.	2.76 ± 0.044	2.73 ± 0.171	2.01 ± 0.050
2.	3.03 ± 0.148	2.25 ± 0.205	2.07 ± 0.079
3.	2.86 ± 0.096	2.53 ± 0.175	2.03 ± 0.059

CONCLUSIONS

The research resulted in new knowledge about the possibilities of using field beans in diet of fattening lambs. A mixture of concentrated feed, created by using the 50% of field beans and 50% of oats, provided one kg of dry matter with 193.5 g of crude protein and 12.1 MJ of metabolizable energy. Unlimited feeding of this concentrated feed to Latvian dark-headed lambs provided an average of 247.4 g of live weight gain per day without any digestion disorders in lambs. Significantly better fattening results are obtained with lambs starting fattening at 3 months of age with live weight above 27 kg. Lambs of this group compared to 1st group lambs had a significantly shorter fattening period – 52 days, which is by 26 days less ($P < 0.05$), resulting in a significantly higher increase in live weight gain per day – 276.8 g, which is by 58.8 g higher ($P < 0.05$). The study did not show any significant differences in carcase quality assessment, but a significantly higher proportion of fat was obtained for 2nd group lamb carcasses, on average 23.4%. The quality of the obtained carcasses is moderate, muscle tissue development is in the R and O classes (79% of carcasses were evaluated according to class R), but the fat tissue stratification is from 3 to 4 points (74% of carcasses were estimated at 4 points), which indicated on quite well muscular tissue development and too high fat tissue stratification in carcass. In future researchers have the task to conduct experiments with the aim of improving quality of carcass obtained from Latvian dark-headed lambs. For the production of one kg of live weight gain 3.33 kg of grass hay and 5.21 kg of grain meal mixture, or 7.56 kg of dry matter, were consumed.

ACKNOWLEDGEMENTS. Financial support for the research project was provided by Latvia Ministry of Agriculture.

REFERENCES

Barzdina, D. & Kairisa, D. 2006. Carcass quality analysis in Latvian Darkhead sheep. *Veterinaria ir zootechnika* **36**(58), 11–16.

Barzdina, D. & Kairisa, D. 2015. Latvian Dark-headed breed lambs growth parameter analysis. In *Līdzsvarota lauksaimniecība*, Jelgava, Latvija, pp. 172–177.

Barzdina, D. & Kairisa, D. 2016. Fattening result analysis of Romanov and Dorper crossbred lambs. In *16th International multidisciplinary scientific geoconference*. Austria, Hofburg, pp. 657–664.

Boughalmi, A. & Araba, A. 2016. Effect of feeding management from grass to concentrate feed on growth, carcass characteristics, meat quality and fatty acid profile to Timahdite lamb breed. *Small Ruminant Research* **144**, 158–163.

Boukhris, H., Damergi, C. & Najjar, T. 2013. Growth performances and carcass composition of Barbarine lambs: Effect of the substitution rate of soya bean cake by faba beans (Vicia faba). In: Ben Salem H. (ed.) & López-Francos A. (ed.). *Feeding and management strategies to improve livestock productivity, welfare and product quality under climate change*. Zaragoza: CIHEAM / INRAT / OEP / IRESA / FAO, pp. 223–228.

Butter, N.L., Dawson, J.M. & Buttery, P.J. 1999. Effects of dietary tannins on ruminants. In Caygill, J.C. & Mueller-Harvey, I. (ed.). *Secondary Plant Products – antinutritional and beneficial actions in animal feeding.* Nottingham University Press, pp. 51–70.

Caballero, R., Rioperez, J., Fernandez, E., Marin, M.T. & Fernandez, C. 1992. A note on the use of field beans (*Vicia faba*) in lamb finishing diets. *Anim. Prod*. **54**, 441–444.

Crépon, K., Marget, P., Peyronnet, C., Carrouée, B., Arese, P. & Duc, G. 2010. Nutritional value of faba bean (*Vicia faba L.*) seeds for food and feed. *Field Crops Research* **115**, 329–339.

Duddy, G., Shards, C., Bell, A., Hegarty, R. & Casburn, G. 2016. Feedlotting lambs. Primefact 523, 2nd ed. www.dpi.nsw.gov.au/factsheets.

Esmailizadeh, A.K., Nemati, M. & Mokhtari, M.S. 2012. Fattening performance of purebred and crossbred lambs from fat-tailed Kurdi ewes mated to four iaranian native ram breeds. *Tropical animal health and production J*. **44**, 217–223.

ISO 6491:1998. Animal feeding stuffs. Determination of phosphorus content. ISO/TC34/SC10, ICS: 65.120, ed.2, 7 pp.

ISO 5984: 2002/Cor.1:2005. Animal feeding stuffs. Determination of crude ash. ISO/TC34, Food products SC 10 ed.3, 10 pp.

ISO 6496:1999. Animal feeding stuffs. Determination of moisture and other volatile matter content. ISO/TC34/SC10, ICS: 65.120, ed.2, 7 pp.

Kairisa, D. & Barzdina, D. 2016a. Quality evaluation of fattening lambs using ultrasonic scanner Mindray Dp-50 Vet. In *15th International scientific conference "Engineering for rural development"*, Jelgava, Latvia, **15**, pp. 750–755.

Kairisa, D. & Barzdina, D. 2016b. Different age analysis of fattening results of Latvian Blackhead breed lamb. In *Līdzsvarota lauksaimniecība,* Jelgava, Latvija, pp. 168.–173.

Kairisa, D. & Selegovska, E. 2004. Importance of balanced feeding in the breeding of young sheep. *Veterinaria ir zootechnika* **27**(49), 70–74.
Karaca, S., Yilmaz, A., Kor, A., Bingol, M. & Keskin, S. 2016. Effect of different feeding systems on the fattening performance, slaughter-carcass characteristics and meat quality in lambs. *Indian Journal of Animal Research* **50**(4), 595–600.
Khewani, T.Al., Shaker, M.M. & Al-Olofi, S. 2014. Fattening ability and carcass value of Dhamari and Tehami ram lambs, F1 crossbreeds of Dhamari x Tehami in Yemen. *Tropical animal health and production J*. **46**(8), 1363–1370.
Latvietis, J. 1995. *Requirement for sheep feeding* (*Aitu ēdināšanas normas)*. Jelgava: LLU, 23 pp. (in Latvian).
Latvietis, J. 2013. *Fodder (Lopbarība)*. Jelgava, LLU, 308 pp, (in Latvian).
Löhle, K. & Leucht, W. 1997. *Goats and sheep* (*Ziegen und Schefe*). Stuttgart: Ulmer, 84 pp. (in German).
Luciano, G., Monahan, F.J., Vasta, V., Biondi, L., Lanza, M. & Priolo, A. 2009. Dietary tannins improve lamb meat colour stability. *Meat Sci.* **81**, 120–125.
LVS EN ISO 13906:2008. Animal feeding stuffs. Determination of acid detergent fibre (ADF) and acid detergent lignin (ADL) contents. ISO 13906:2008, ISO/TC34/SC10, 17 pp.
LVS EN ISO 16472:2006. Animal feeding stuffs. Determination of amylase-treated neutral detergent fibre content. ISO 16472:2006, ISO/TC34/SC10, 15 pp.
LVS EN ISO 5983-2:2009. Animal feeding stuffs. Determination of nitrogen content and calculation of crude protein content. ISO 5983-2:2009, ISO/TC34/SC10, ICS: 65.120, ed. 2. part 2, 15 pp.
LVS EN ISO 6869:2002. Animal feeding stuffs. Determination of calcium, magnesium and sodium. ISO 6869:2000, ISO/TC34/SC10, ed.1, 15 pp.
Majdoub-Mathlouthi, L., Saïd, B., Say, A. & Kraiem, K. 2013. Effect of Concentrate Level and Slaughter Body Weight on Growth Performances, Carcass Traits and Meat Quality of Barbarine Lambs Fed Oat Hay Based Diet. *Meat science* **93**(3), 557–563.
Markovic, B., Bjelanovic, M., Vucic, G., Berg, P. & Egelandsdal, B. 2014. Comparision of carcass sharacteristics and meat quality of Norwegian White sheep breed with two Western Balkan Pramenka sheep breeds. *Agriculture and Forestry Journal*, Podgorica **60**(1), 53–61.
Martinez, T.F., Moyano, F.J., Diaz, M., Barroso, F.G. & Alarcón, F.J. 2004. Ruminal degradation of tannin-treated legume meals. *Science of Food and Agriculture* **84**, 1979–1987.
Melicharová, V., Pechová, A., Dvorak, R. & Pavlata, L. 2009. Performance and metabolism of dairy cows fed bean seeds (Vicia faba) with different levels of anti-nutritional substances. *Acta Veterinaria Brno* **78**, 57–66.
Min, B.R., Solaiman, S., Taha, E. & Lee, J. 2015. Effect of plant tannin-containing diet on fatty acid profile in meat goats. *J. Anim. Nutr*. **1**, 1–7.
Nutrient Requirements of small ruminants: sheep, goats, cervids and New World camelids. 2007. Committee on Animal Nutrition, NRC, The National academy press, 362 pp.
Ositis, U. 1996. *Feedstaffs energy and protein assessment systems in different states of the World* (*Barības līdzekļu enerģētiskās un proteīna vērtēšanas sistēmas dažādās pasaules valstīs)*. Jelgava: LLU, 95 pp. (In Latvian).
Osmane, B., Konosonoka, I.H. & Cerina, S. 2015. Assessment of legumes quality (Tauriņziežu kvalitātes vērtējums). *Saimnieks* **5**, 82–84 (in Latvian).
Phillips, W.A., Reuter, R.R., Brown, M.A., Fitch, J.Q., Rao, S.R. & Mayeux, H. 2002. Growth and Performance of Lambs Fed a Finishing Diet Containing Either Alfalfa or Kenaf as the Roughage Source. *Small Ruminant Research* **46**, 75–79.

Piirsalu, P. 2003. The quality of meat from the carcasses of Estonian breeds of cheep classified according to the EUROP grading system. In *Proceedings of the 9th Baltic animal breeding conference*. Sigulda, pp. 115–120.

Piirsalu, P. & Mettis, K. 2005. Factors affecting sheep meat quality of the Estonian whiteface breed of sheep classified acording to the SEUROP granding system. In *Proceedings of the 11th Baltic animal breeding conference.* Palanga, pp. 137–140.

Ramos-Morales, E., Sanz-Sampelayo, M.R. & Molina-Alcaide, E. 2010. Nutritive evaluation of legume seeds for ruminant feeding. *Animal Physiology and Animal Nutrition* **94**, 55–64.

Rohweder, D.A. 1984. Estimating forage hay quality. *In* National Alfalfa hay quality testing workshop. Chicago, IL, March 22–23, pp. 31–37.

Sinclair, L.A., Galbraith, H.J. & Scaife, R. 1991. Effect of dietary protein concentration and cimaterol on growth and body composition of entire male lambs. *Animal Feed Science and Technology* **34**(3–4), 181–192.

Yu, P., Tamminga, S., Egan, A.R. & Christensen, D.A. 2004. Probing equivocal effects of heat processing of legume seeds on performance of ruminants. *Asian-Australasian Journal of Animal Sciences* **17**, 869–876.

Agronomy Research **16**(4), 1708–1719, 2018
https://doi.org/10.15159/AR.18.170

Faults and the physical workload in sawing and packing-related woodworking processes when considering potential ergonomic solutions

H. Kalkis[1,2,*], Z. Roja[3] and S. Babris[4]

[1]Riga Stradiņš University, Faculty of European Studies, Dzirciema street 16, LV-1007 Riga, Latvia
[2]University of Latvia, Faculty of Business Management and Economics, Aspazijas blvd 5, LV-1050 Riga, Latvia
[3]University of Latvia, Ergonomic Research Centre, Jelgavas street 1, LV-1004 Riga, Latvia
[4]BA School of Business and Finance, K. Valdemara 161, LV-1013 Riga, Latvia
[*]Correspondence: henrijs.kalkis@gmail.com

Abstract. The forest sector is a high-risk economic sector in Latvia, one in which manual work, awkward postures, the tightening up of individual muscle groups, and work monotony still exists. The aim of this study was to analyse the physical workload and fault modes, and their effects on the sawing and packing processes in woodworking when considering potential ergonomic solutions. Results show that packing operators and saw operators alike are exposed to severe loads, and these results coincide with survey results in which employees in these professions complain about the physical load and mention lower back pain. Fault modes and their effects on the sawing and packing processes were analysed using Failure Mode and Effects Analysis, and the main errors which were revealed in packing operations were related to machinery and lifting equipment, as well as to ergonomics and errors involving the human factor. The risk priority was calculated in terms of a figure. Financial indices were compared before and after any potential improvement in the sawing and packing processes. Analysis proves that investments in the improvement of ergonomics in relation to the automation of the production process saves human resources and is economically favourable when it comes to ensuring the sustainable development of the business in question.

Key words: ergonomics, load, forest sector, operations, failure modes.

INTRODUCTION

In Latvia, the forest sector plays a vital role in the development of the national economy, employing between 45,000–50,000 people as it does. The forest sector comprises the forestry and wood industries. It is a high-risk economic sector, one in which manual work still exists. According to recent statistics, occupational illnesses are caused by ergonomic risks at work such as heavy manual work, awkward postures, the tightening-up of individual muscle groups, work monotony, lifting and moving heavy loads, work intensity, repetitive movements, and so on. According to the research that has been carried out by other authors, the most common occupational illnesses are carpal tunnel syndrome (NIOSH, 2004), arthritis in the wrists, back pain spondylosis, osteochondritis (Rossignol et al., 2005; Garg et al., 2007), hearing impairment (Robinson et al., 2015) and, quite often, obstructive pulmonary diseases (Carosso et al., 1987; Mandryk et al., 1999; Soytas, 2006; Thepaksorn et al., 2017).

Production processes in the century of modern industrialisation are closely related to the human factor. The human factor refers to the existence of a human interaction with technology, equipment, and the daily working environment (Sanders & McCormick, 1992).

Musculoskeletal disorders (MSD) are associated with high costs to employers such as absenteeism, lost productivity, increased health care, disability, and compensation costs for workers. Work-related MSD cases are more severe than the average non-fatal injury or illness (Bernard, 1997). As observed by Adei & Kunfaa (2007) in their study of wood processing industries in Ghana, occupational exposure to ergonomic hazards in the wood-processing industries were due mainly to lifting weights and uncomfortable posture during working hours. Workers had to remain in a standing position for as long as seven hours of an eight-hour shift, and back pain was the main complaint that resulted from awkward work postures such as prolonged standing, bending, or kneeling.

Rather often, a number of new businesses at the start of their activities, particularly small or medium-sized businesses, do not have a clear long-term business strategy, and have not yet developed a system which would ensure balanced interaction between technological processes, human resources, and the environment. Having something like this in place would facilitate the quality of their final product, ensuring that it corresponds to the needs of their clients and enabling them to compete successfully in a progressive business environment on the local market and in foreign markets as well. Successful competition, based on free market principles, is the basis of any state economics. Scientists point out that 'progressive work and a progressive business environment mean continuous, dynamic development and reform, as well as investment in technology and human resources' (Kramer et al., 2007). Therefore it is essential that new forms and methods are sought out in order to facilitate work productivity and increase the economic effectiveness of the organisation, and not decreasing product quality and retaining human resources. In the development of contemporary technology, the human factor and ergonomics both play a significant role in raising levels of work productivity. Around the world, there is a good deal of research available concerning the well-being of employees in an organisation and perfection of technology (Drury & Fox, 1976; Dul & Neumann, 2009). The significance of the human factor in the management and control of process quality has been proven. In particularly it is justified in the work of 'Ergonomics in total quality management: how can we sell ergonomics to management?' (Lee, 2005), in which employee participation is emphasised: employees are the first to evaluate their work, after that the problems are analysed by specially-organised expert groups which work out suggestions for improving the work. Such an approach increases work productivity, decreases the costs involved in the work, and improves safety at work. The process is part of ergonomics management, which has the aim of adjusting work process for an employee, changing their behaviour in a positive direction, and particularly emphasising their loyalty to the organisation. Nowadays ergonomics management in organisations, as well as process management, are of great significance in business to ensure the effectiveness of the organisation. This is a new approach to business, one in which the ergonomic aspects and values are taken into account in terms of business strategy, which includes ensuring the provision of adequate process management and the profitability of the business. The costs involved in ergonomic measures or solutions are easily understandable, as they are fixed financial means for improving the equipment being used, the acquisition of more modern equipment, the training of employees, etc. At the same time, evaluating benefits is more difficult, as they are related to a decrease in costs due to illnesses being suffered by employees, reduced losses due to goods not being produced within a certain time period, and so on. In addition, there are benefits which are difficult to convert into monetary value: the satisfaction of employees, loyalty to the business, etc. The costs involved in the provision of ergonomic solutions can be single (in terms of capital investments) and long-term. If the equipment and spare parts are produced on-the-spot, the costs are determined by using accounting information and personnel costs. Work will not be effective and process quality will not be achieved if an employee does not receive due attention. This is one of the most significant factors which can positively influence work effectiveness, the competitive ability of the business, and the satisfaction levels of clients (Brown et al., 2001). Global industrialisation and modern technology not only increases work effectiveness, but rather often causes problems which are of an ergonomic character such as, for example, work-related muscular-skeletal disorders (WRMSD).

The aim of this study was to analyse physical workload, fault modes, and the effects of these in terms of the sawing and packing processes in woodworking while considering potential ergonomic solutions.

MATERIALS AND METHODS

The research was carried out at a medium-sized woodworking business with a total of 86 employees. The background factors for the subjects are presented in Table 1.

For the research twelve saw operators and nine assembly operators were selected – all male, all right-handers of various age groups with a length of service which ranged from less than a year to 25 years. The mean age for saw operators was 36.7 ± 4.3, but for packing operators it was 33.4 ± 3.7. The selection criteria for being involved in the research were as follows: in the compulsory health check-up no health problems had been found which were due to the heavy physical manual work, and all of the subjects selected agreed to participate in the study.

Table 1. Background factors for the subjects, with standard deviation (SD) and range

Occupation (length of service)	n	Mean age ±SD	Range
Saw operators	12	36.7 ± 4.3	20–58
(0–5 years)	4	25.5 ± 7.5	20–32
(6–15 years)	4	34.6 ± 3.1	25–41
(> 15 years)	4	46.2 ± 6.9	29–58
Packing operators	9	33.4 ± 3.7	19–61
(0–5 years)	3	24.2 ± 2.5	19–26
(6–15 years)	3	36.4 ± 4.0	25–38
(> 15 years)	3	43.8 ± 3.2	32–61

Job requirements for saw operators were as follows: sawing logs into planks on a horizontal, one-ribbon saw. As part of this process, the operator manually pushes the saw in order to produce the planks. Then two operators manually take the plank off the ribbon. The other process that was studied is packing. During the packing process, operators manually lift and move the materials, piling them in big packs. Then each ready pack is wrapped with polythene and a binding hoop (involving manual work). The amount of packing work is not regular – it depends on the amount of units that have been produced.

In order to include employees in any improvement in their working conditions and to discover what the employees involved think of the existing working conditions, a questionnaire was worked out. It included questions which covered the physical load at work, work intensity, and the psychosocial working conditions (the weight of the mass to be lifted, lifting frequency, whether the mass is easy to grip, whether the working space is sufficient and one's body position is comfortable, and whether the task to be performed corresponds to the employee's abilities). The questionnaire also included questions covering the working environment (restricted work posture, uneven floors, microclimate parameters, and lightning), and psychosocial risks (the conformity of rest break frequency with the work being carried out, unexpected changes in workload, errors at work, defective production, bad relations with the line manager, a lack of support from colleagues, and insufficient training, plus leisure time activities: smoking, alcohol consumption, and physical activities).

The Key Indicator Method was used to determine physical workload, and to assess the lifting, holding, and carrying of heavy loads, and also to analyse manual handling operations (Steinberg & Caffier, 1998; Klussmann et al., 2010).

By means of this method it is possible to identify overloaded lifting activities or the moving of heavy loads, or the carrying out of other dynamic operations. When this method is applied, actions which are related to the moving of heavy loads are assessed using points, including the length of the physical workload (in terms of hours), the weight of the object to be moved (in terms of kilogrammes), the state of the worker's body, and the conditions in which the work is carried out.

According to the Key Indicator Method, the total workload score can be calculated as follows:

$$WL = (M + S + A) \times I \tag{1}$$

where WL – workload (total score); M – value points which are dependent upon the weight of the load to be moved; S – value points which are dependent upon the position of the body during the performance of operations; A – value points which are dependent upon the working conditions; I – value points which are dependent upon the length of a work shift. As the investigation was carried out for multiple workers, the details collected were statistically analysed and mean values were calculated with a standard deviation (SD) for each value point.

The identification criteria for physical load is also taken into account and, according to this method, four categories can be deduced to demark the levels of hard work (light, moderate, hard, and very hard). These are shown in Table 2.

Fault modes and their effects on the sawing and packing processes were analysed by using Failure Mode and Effects Analysis (FMEA) (Tague, 2004; American Society for Quality, 2013). Today FMEA is widely used in various fields such as, for example, the automotive, nuclear, healthcare, and manufacturing industries (Juang et al., 2016).

Table 2. Key Indicator Method workload assessment criteria with categories showing levels of hard work

Description	Points	Risk height
Minimum physical load no significant endangerment to health	< 10	I
Increased physical load. Overload possible for persons of low physical ability (workers over 40 or younger than 21; 'beginners'	10 to 25	II
Significantly increased physical load. Overload possible for persons of normal physical ability	25 to 50	III
Physical overload possible for everyone	> 50	IV

Levels of danger and the priority level for these faults are determined by the Risk Priority Figure (RPF). The RPF is a mathematical calculation of the numerical 'Severity, Probability, and Detection' ratings and is calculated by using this formula:

$$RPF = (Severity) \times (Probability) \times (Detection) \quad (2)$$

The three risk factors, severity, probability, and detection are estimated with the help of a value scale which ranges from one to ten (Pillay & Wang, 2003). The RPF is used to prioritise items that require additional planning or action. The higher the RPF value of a failure mode, the higher is the degree of priority for any necessary improvements.

Evaluation points according to the FMEA method were determined for the following elements: 1) processes; 2) possible type of fault in process; 3) possible effects of the fault; 4) possible reasons for the fault; 5) existing management; 6) improvement action for suggested ergonomics.

FMEA has been carried out using the computer program, Xfmea, which was produced by the American corporation, 'ReliaSoft', which allowed the potential RPF to be calculated if the manual work is substituted by an automatic process (Reliasoft XFMEA software, 2011).

Cost-benefit calculations in relation to occupational health and safety issues (Devisilov, 2007) were carried out additionally in order to analyse potential economic effectiveness if ergonomic solutions are introduced into the sawing and packing processes in a woodworking enterprise. Losses (S_j) were compared before and after the institution of ergonomic solutions, evaluating costs, or providing compensation in cases of accidents, trauma, or occupational illnesses. Losses (Z_n) due to production which has not been carried out, or which has been delayed or returned before any ergonomic solutions were determined; total losses (S) were determined due to capital investments (A) for economically-improved systems and exploitation (L), as was any increase in business profits (ΔP), annual economic effectiveness (EG), and the absolute economic effectiveness of potential investments (EA) were determined. In calculations, the formulas given by the methodology for an assessment of economic effectiveness were used (Devisilov, 2007).

RESULTS AND DISCUSSION

Questionnaire results

Those employees who were involved in the study were divided into two groups: saw operators (n = 12) and packing operators (n = 9) by age and length of service in the profession. Saw operators (n = 12) were aged between 20–58 with a length of service of 33.33% of workers between zero to five years, 33.33% between six to fifteen years, and 33.33% of more than fifteen years. Packing operators (n = 9) were aged between nineteen and 61, with a length of service in the profession of 33.33% for workers between zero to five years, 33.33% between six to fifteen years, and 33.33% of more than fifteen years.

In summarising the acquired questionnaire results it was concluded that employees in the sawing and packing processes were mainly subjected to the following ergonomic risks: heavy manual work (72%), physical load (54%), repeated and frequent movements of the arms and body, and awkward work postures (47%). Nearly all employees (83%) recognised that the aforementioned ergonomic risks were increased by other risks in the work environment (such as chemicals, noise, vibration, and lighting), and that the work is intensive, and that the short breaks that are permitted at work are insufficient. The saw operators lift and move heavy loads of a weight that is between 10–20 kg, between 200–250 times within a single shift, while the packing operators lift and move heavy loads weighing between 50–60 kg, between 150–160 times within a shift. The lower back, legs, and arms are exposed to physical loads during the work process. Stress at work was mentioned by 24% of the employees who were asked. A total of 76% of participants in both of the groups being studied indicated high requirements at work, a lack of management support and low levels of monitoring of the work process, errors at work, and defective production. Nearly all of the participants (86%) admitted smoking and imbibing alcohol in moderate doses in their leisure time. They do not carry out any physical activities. A total of 87% of participants considered that in order to lighten the manual work, the introduction of mechanisation is necessary in the sawing and packing processes. Only 13% of workers considered that the number of employees should be increased.

Physical load analysis

Using the Key Indicator Method, a total assessment of workload was carried out and the degree of risk R_d was determined (see Table 3).

Table 3. Key Indicator Method results (L – load weight, P – work posture, C – work conditions, I – work intensity), standard deviation (SD), workload score (WL), risk degree (R_d)

Professions	L±SD	P±SD	C±SD	I±SD	WL	Risk degree R_d **I – V**	Potential Risk degree R_d **I – V**
	Number of points						
Saw operators (n = 12)	4.4 ± 1.3	3.5 ± 1.8	1.3 ± 0.7	3.1 ± 1.6	32.98	**III**	**II**
Packaging operators (n = 9)	3.6 ± 1.9	4.2 ± 1.3	1.6 ± 0.4	3.6 ± 1.8	32.34	**III**	**II**

In evaluating the physical load, it should be noted that packing operators and saw operators are exposed to severe loads which correspond to ‘Risk Degree 3’. This coincides with survey results in which employees of these professions complained of physical load and mentioned pain in the lower back. More often at their work places, defective production occurs or the work cycle is delayed due to accidents. This results in a decrease in the amount of materials being produced and a reduction of the economic effectiveness of the business. Therefore, improvements or modernisation are needed in a number of production processes. Ergonomic measures could create opportunities for the essential improvement of working conditions for packing and saw operators. In the process of sawing wood with a one-ribbon saw, the operator pushes the saw, sawing one plank at a time; removing the sawn timber is something that has not been mechanised; this is manual work. While changing the equipment to a frame-saw with an automated log-feed and plank-sorting line, the mechanisation of the work process is achieved which is something that is much more effective, ie. the amount of produced materials grows almost fifteen times and the time used in sawing 90 m^3 of timber decreases threefold. In one packing process in production, two employees are involved who manually lift and pack the ready product (140 times in a shift, moving stacks of planks with a total mass of between 40–50 kg). In introducing an automated hoist, the same work could be carried out by just one employee. The physical load in the work process would be significantly reduced, since a packer would not need to manually lift heavy stacks of planks. The number of movements which involve bending the body, which in the existing process rather often reaches more than a thousand movements in a shift, would also decrease. Apart from that, due to the introduction of ergonomic measures, productivity would rise by nearly four times, while packing work which involves 100 m^3 of production would require almost five times less time. Our proposals regarding ergonomic improvements conform with similar studies which have been carried out by other authors (Mirka et al., 2002). They determined that ‘productivity benefits which could be drawn from these interventions were also found, but it is felt that the productivity improvements may only be a fraction of those that may result from the long-term utilisation of such interventions by skilled workers attempting to maximise their productivity’. Those ergonomic intervention measures which have been proposed in the study could be effective when it comes to ensuring a reduction of work-related muscular-skeletal diseases (WRMSD) which are related to the work of employees, which is something that has also been suggested by the authors of other studies (Marras et al., 2000; Karsh et al., 2001). The participation of those employees who were involved in the study on ergonomic improvements in the sawing and packing processes promoted ergonomic solutions, which conforms to studies on solutions for ergonomic intervention in relation to employee participation and the continuous introduction of ergonomic solutions in order to decrease incidents of WRMSD (van Eerd et al., 2010; Cantley et al., 2014). In the studies, it is emphasised that the systematic control of ergonomic risks is part of the system of occupational health and safety at work. At the same time, the authors indicate that participants in ergonomic improvements should be knowledgeable, experienced, and trained in ergonomics.

Results from the FMEA method

For the analysis of the potential effectiveness of ergonomic solutions in woodworking operations, the FMEA method was applied and the danger levels involved in and the priority levels for these faults were determined in the sawing and packing processes.

Ergonomic solutions were considered in relation to the installation of a new automated line for sawing the logs, and acquiring new ergonomic hoists in packaging operations.

FMEA, using the computer program, XFMEA, proved the potential effectiveness of ergonomic intervention in the sawing and packing processes. Errors made by the equipment were analysed, along with ergonomic risks and the production process. The FMEA analysis results are summarised in Tables 4 and 5.

Table 4. Risk Priority Figure before and after potential ergonomic solutions being put into place in packing operations

Processes and faults (errors)		RPF before ergonomic solutions				Potential RPF after ergonomic solutions			
Process	Likely kind of fault	Severity	Probability	Detection	RPF	Severity	Probability	Detection	RPF
Packing operations	Equipment:								
	Sorting errors	9	9	8	648	6	5	4	120
	Packing errors	9	8	8	576	8	4	3	96
	Other faults	8	9	8	576	6	5	4	120
	Ergonomics risks:								
	Muscles fatigue	9	9	8	576	7	6	5	210
	Manual handling	9	9	7	392	6	5	5	150
	Other faults	9	6	8	216	5	6	5	150
	Human factor errors								
	Skills, competences	8	8	8	512	8	8	8	512
	Fatigue	9	9	7	567	5	5	4	100
	Other faults	9	6	8	432	5	6	4	120
	Production errors:								
	Scratch faults	9	9	8	648	7	5	6	210
	Design defects	8	9	8	576	7	5	5	175
	Other faults	8	9	8	576	6	7	4	168
Total RPF					6,758	Total RPF			2,131

The FMEA analysis showed that the main errors in packing operations are related to machinery and lifting equipment, as well as to ergonomics and errors involving the human factor. Equipment errors were connected to sorting and packing defects (the RPF was above a score of 500), as well as scratches and design defects which appeared due to inappropriate lifting and moving of the loads (the RPF was above a score of 500). Hence ergonomics risks were analysed along with the main errors which were associated with muscle fatigue and manual handling as well as awkward postures and repetitive movements. These risks influence errors which involve the human factor such as attention, skills, competences, and fatigue levels. Skills and competences depend upon each individual operator and will remain the same even after potential improvements have been carried out. Additional training could improve skills for these employees after ergonomic solutions have been implemented in terms of packing operations (specifically involving automated lifting equipment).

Similarly, the FMEA analysis was applied to sawing operations and the following main errors were found: technology (machinery), ergonomics, the human factor, and production errors. Production and equipment errors (with an RPF above 600) could be significantly minimised if potential improvements could be implemented in terms of a new automated line for sawing the logs (the RPF could be decreased to 150). Similarly, as for packing operations, sawing operations could also see a decrease in ergonomics and errors which involve the human factor. Skills and competences will remain at the same level even after the introduction of an automated sawing line, but could be improved if training were to be provided to employees. A summary of RPF scores before and after potential ergonomic solutions are implemented is shown in Table 5.

Table 5. Risk Priority Figure before and after potential ergonomic solutions

Processes	TOTAL RISK PRIORITY FIGURE (RPF)	
	RPF before ergonomic solutions	Potential RPF after ergonomic solutions
Packing operations	6,758	2,131
Sawing operations	9,364	2,081

The total initial risk priority figure (RPF) was determined which, in the business which was being studied, was: an RPF of 6,758 (packing operations) and 9,364 (sawing operations). This RPF was very high and showed that urgent improvements are needed in terms of work organisation and risk prevention. The potential RPF evaluation suggests that after ergonomic solutions have been implemented and a modernisation of technology has been carried out, ergonomic risks could be reduced: an RPF of 2,131 (packing operations) and 2,268 (sawing operations). This shows that improvements are needed through the introduction of ergonomic solutions which will help to reduce errors in work in terms of the equipment as well as preventing a physical overload by at least three to four times. There is a reason to consider that, together with the introduction of preventive measures, the volume of production and product quality will also increase.

Several authors have successfully applied the FMEA method. For example, the risk priority level was calculated for the failure mode in a manufacturing business and the FMEA has been proposed as a decision-making support tool (Franceschini & Galetto, 2001). The researchers analysed the potential failure modes in manufacturing and chose the greatest failure risk as one that would be the target of improvements. This corresponds to the investigation by the authors which discovered that the risk priority figure can be significantly decreased if the ergonomic solutions are implemented.

Economic calculation analysis of potential ergonomics solutions

Potential economic calculations have been calculated for ergonomic solutions in sawing and packing operations. Financial indices were compared before and after any potential improvement to sawing and packing processes.

The calculation summary for ergonomic solutions in a woodworking business is shown in Table 6.

Table 6. Calculation summary for potential ergonomic solutions

Total losses	Before ergonomic solutions	Potential after ergonomic solutions
	79,000 EUR	22,800 EUR
Potential effectiveness after ergonomic solutions		
annual economic effectiveness or advantage	absolute effectiveness of investments	period of investment payoff
63,000 EUR	0.78	1.28 years

The economic calculation analysis which was carried out in terms of potential ergonomic solutions was made possible by being allowed access to the financial data of the business which was the subject of the study. The results indicate that, after ergonomic solutions have been implemented in sawing and packing operations, annual production rates could increase by 43%. When taking into account potential profits and the expenses being incurred for maintenance and ergonomic solutions (covering maintenance staff, equipment servicing, the acquisition of spare parts, etc), the annual economic effectiveness was determined as being a figure which could reach as high as 63,000 EUR. The calculated absolute economic effect of investments, EA = 0.78, shows that investments in ergonomic solutions will be effective. The period of investment payoff, T, is calculated as being comparatively short, almost a single, with $T = (1/EA) = 1/0.78 = 1.28$ years.

Analysis proves that investments into the improvement of ergonomics in relation to the automation of production process retains human resources and is economically favourable when it comes to ensuring the sustainable development of the business in question.

CONCLUSIONS

Employees in a woodworking company are subjected to heavy levels of manual work, a high physical load, and repeated and frequent movements of the arms and body, as well as awkward work postures. These can all serve to cause rapid tiredness and a lack of attention, which may result in errors in production process and defective production.

An analysis of the effectiveness of ergonomic solutions shows that any business that has introduced ergonomic solutions and has modernised its production process technology can decrease not only the risk of physical overload at work, but can also decrease error types and their consequences, improve the monitoring of the process, and also the quality of the finished products.

Ergonomic solutions in combination with other improvements in woodworking production processes all have a positive effect on productivity levels and are likely to have financial benefits for a business, including a decrease in WRMSD, the promotion of satisfaction in its employees, and an improvement in the company's image.

REFERENCES

Adei, D. & Kunfaa, E.Y. 2007. Occupational health and safety policy in the wood processing industry in Kumasi, Ghana. *Journal of Science and Technology* **27**(2), 151–171.

American Society for Quality. 2013. Failure mode effects analysis (FMEA). *http://www.asq.org/learn-about-quality/process-analysis-tools/overview/fmea.html*. Accessed 15.12.2017

Bernard, B.P. 1997. *Musculoskeletal disorders and workplace factors: a critical review of epidemiologic evidence for work-related musculoskeletal disorders of the neck, upper extremity, and lower back.* U.S. National Institute of Occupational Safety and Health. 590 pp.

Brown, S., Blackmon, K., Cousin, P. & Maylor, H. 2001. *Operations Management. Policy, Practice and Performance Improvement.* Oxford: Butterworth-Heinemann Linacre House, 439 pp.

Cantley, L.F., Taiwo, O.A., Galusha, D., Barbour, R., Slade, M.D., Tessier-Sherman, B. & Cullen, M.R. 2014. Effect of systematic ergonomic hazard identification and control implementation on musculoskeletal disorder and injury risk. *Scandinavian Journal of Work, Environment & Health* **40**(1), 57–65.

Carosso, A., Ruffino, C. & Bugiani, M. 1987. Respiratory diseases in wood workers. *British Journal of Industrial Medicine* **44**, 53–56.

Devisilov, V.A. 2007. *Labour protection*. Forum-Infra-M, pp. 392–402 (in Russian).

Drury, C.G. & Fox, J.G. 1976. Human Reliability in Quality Control. *Applied Ergonomics* **7**, 46 pp.

Dul, J. & Neumann, W.P. 2009. Ergonomics Contributions to Company Strategies. *Applied Ergonomics* **40**, 745–752.

Garg, A., Gerr, F. & Katz, J.N. 2007. Low Back Pain and the Workplace. *Journal of the American Medical Association* **298**(4), 403–404.

Franceschini, F. & Galetto, M. A New Approach for Evaluation of Risk Priorities of Failure Modes in FMEA. 2001. *International Journal of Production Research* **39**(13), 2991–30023.

Jiang, W., Xie, C., Wei, B. & Zhou, D. 2016. A modified method for risk evaluation in failure modes and effects analysis of aircraft turbine rotor blades. *Advances in Mechanical Engineering* **8**, 1–16.

Karsh, B.T., Moro, F.B.P. & Smith, M.J. 2001. The efficacy of workplace ergonomic interventions to control musculoskeletal disorders: A critical analysis of the peer-reviewed literature. *Theoretical Issues in Ergonomics Science* **2**(1), 23–96.

Klussmann, A., Steinberg, U., Liebers, F., Gebhardt, H. & Rieger, M.A. 2010. The Key Indicator Method for Manual Handling Operations (KIM-MHO) – evaluation of a new method for the assessment of working conditions within a cross-sectional study. *BMC Musculoskeletal Disorders* **11**, 272 pp.

Kramer, W.J., Jenkins, B. & Katz, R.S. 2007, The Role of the Information and Communications Technology Sector in Expanding Economic Opportunity. Corporate Social Responsibility Initiative. In: *Report No. 22. Cambridge, MA: Kennedy School of Government, Harvard University,* 52 pp.

Lee, K. 2005. Ergonomics in Total Quality Management: How Can We Sell Ergonomics to Management. *Ergonomics* **48**(5), 547–558.

Mandryk, J., Alwis, K.U. & Hocking, A.D. 1999. Work-related symptoms and dose-response relationships for personal exposures and pulmonary function among woodworkers. *American Journal of Industrial Medicine May* **35**(5), 481–90.

Marras, W.S., Allread, W.G., Burr, D.L. & Fathallah, F.A. 2000. Prospective validation of a low-back disorder risk model and assessment of ergonomic interventions associated with manual materials handling tasks. *Ergonomics* **43**(11), 1866–86.

Mirka, G.A., Smith, C., Shivers, C. & Taylor, J. 2002. Ergonomic interventions for the furniture manufacturing industry. Part IF lift assist devices. *International Journal of Industrial Ergonomics* **29**, 263–273.

National Institute for Occupational Safety (NIOSH). 2004. Carpal tunnel syndrome (CTS). In: *Chapter 2: Fatal and nonfatal injuries, and selected illnesses and conditions. In: Worker health chartbook 2004.* USA, Washington, No. 2004–146, 354 pp.

Pillay, A. & Wang, J. Modified failure mode and effects analysis using approximate reasoning. 2003. *Reliability Engineering & System Safety* **79**, 69–85.

Reliasoft XFMEA software. 2011. *http://www.reliasoft.com/xfmea/features1.htm*. Accessed 23.07.2017

Robinson, T., Whittaker, J., Acharya, A., Singh, D. & Smith, M. 2015. Prevalence of noise-induced hearing loss among woodworkers in Nepal: a pilot study. *International Journal of Occupational and Environmental Health* **21**(1), 14–22.

Rossignol, M., Leclerc, A., Allaert, F.A., Rozenberg, S., Valat, J.P., Avouac, B., Coste, P., Litvak, K. & Hilliquin, P. 2005. *Occupational and Environmental Medicine* **62**, 772–777.

Sanders, M.S. & McCormick, E.J. 1992. *Human factors in engineering and design*. USA, McGraw-Hill, Inc.

Soytas, U. 2006. Physical and Ergonomic Hazards in the Textile, Chemical, Foodl, Metal Products, and Woodworking Industries in Turkey. *International Journal of Occupational and Environmental Health* **12**(1), 35–41.

Steinberg, U. & Caffier, G. 1998. *Methodological issues in the application of load handling Regulation*. Z. Arbwiss **52**(24 NF), pp.101–109 (in German).

Tague, N.R. 2004. *The Quality Toolbox*. ASQ Quality Press, pp. 236–240.

Thepaksorn, P., Thongjerm, S., Incharoen, S. Siriwong, W., Harada, K. & Koizumi, A. 2017. Job safety analysis and hazard identification for work accident prevention in para rubber wood sawmills in southern Thailand. *Journal of Occupational Health* **59**(6), 542–551.

van Eerd, D., Cole, D., Irvin, E., Mahood, Q., Keown, K., Theberge, N., Village, J., St. Vincent, M. & Cullen, K. 2010. Process and implementation of participatory ergonomic interventions: a systematic review. *Journal Ergonomics Volume* **53**(10), 1153–1166.

Agronomy Research **16**(4), 1720–1727, 2018
https://doi.org/10.15159/AR.18.149

Concentration of air-borne microorganisms in sport facilities

P. Kic[1,*], L. Ruzek[2] and E. Popelarova[2]

[1]Czech University of Life Sciences Prague, Faculty of Engineering, Department of Technological Equipment of Buildings, Kamycka 129, CZ165 21 Prague, Czech Republic
[2]Czech University of Life Sciences Prague, Faculty of Agrobiology, Food and Natural Resources, Department of Microbiology, Nutrition and Dietetics, Kamycka 129, CZ165 21 Prague 6, Czech Republic
[*]Correspondence: kic@tf.czu.cz

Abstract. This paper is focused on the microclimatic research in several buildings and rooms used for sport at the University. The attention is paid mainly to the problems of dimensions of space, capacity and activity of sportsmen, and influence of space ventilation. The air samples for microbiological analyses were taken by the microbial air sampler Merck Mas-100 Eco and cultivated by potato-dextrose agar and nutrient agar. Captured microorganisms, are expressed as colony forming units per m^3 (CFU m^{-3}). Measurement results showed that bacteria average quantity was statistically significantly less without students (562 CFU m^{-3}) than with students (1,024 CFU m^{-3}). The students inside the rooms increased the bacteria concentration. From this point of view the ventilation is not adequate for the removal of bacteria from ventilated spaces. From the results we can conclude that the great importance on the air quality in terms of a specific bacteria concentration has the specific volume of the room per one athlete. The worst situation is in rooms with the smallest volume, which has the largest biological load of the space. The lowest quantity of bacteria was in the swimming pool all year round (152 to 300 CFU m^{-3}). The opposite situation was in average quantity of filamentous fungi, which was with students and ventilation (57 CFU m^{-3}) and without students but without ventilation (109 CFU m^{-3}). The pollution of air by fungi was higher without ventilation.

Key words: air, gyms, indoor environment, pollution, swimming pool, ventilation.

INTRODUCTION

This paper is focused on the microclimatic research in different rooms at Czech University of Life Sciences campus. The microbial contamination (bacteria and filamentous fungi including presence of allergenic genus *Cladosporium* and *Aspergillus*) and also main microclimatic parameters of the air (temperature and relative humidity of air) were measured and evaluated in the relation to different performance conditions of tested rooms. The attention is paid to purpose of the rooms, ventilation or air-conditioning.

Many scientific and professional papers emphasize the influence of indoor climate on the human health (Gorny & Dutkiewicz, 2002; Karwowska, 2003; Fisk at al., 2007) and on the comfortable feeling of inhabitant inside the different buildings and rooms (Seppänen at al., 2006).

One of the frequent sources of microorganisms in the air is dust. It is usually also an accompanying sign of higher aerosol contamination by microorganisms. The attention to microbiological pollution is paid in some research works e.g. Bouillard et al. (2005), Orru et al. (2011), Brodka et al. (2012). The methodology and the results of measurements correspond to the research topic, especially to factors that are specific to studied space, e.g. Kic & Růžek (2014).

Results of large research work focused on the problems of seasonal variations of indoor microbial exposures and their relation to temperature, relative humidity, and air exchange rate is described in the publication Frankel et al. (2012). Indoor fungi peaked in summer (median 235 CFU m^{-3}) and were lowest in winter (median 26 CFU m^{-3}). Indoor bacteria peaked in spring (median 2,165 CFU m^{-3}) and were lowest in summer (median 240 CFU m^{-3}). According to the research findings and measurement results Kic et al. (2014), people are the source of bacterial and fungal contamination inside the rooms.

As the university students as well as the staff should be active not only in the study or research but also in the sport activities, it is important to know what the situation inside the sport facilities is. Due to the fact that during sport activities people breathe very intensively, the air inside the rooms should be very clean. The aim of this paper is to present results of microclimatic research focused on the microbiological pollution, biological load by people and influence of ventilation in several rooms used for physical education and sport activities at the Czech University of Life Sciences Prague.

MATERIALS AND METHODS

This research work and measurements of the actual values were carried out in buildings and rooms of Department of Physical Education at the Czech University of Life Sciences Prague. All rooms are situated in two buildings, three of them in the same building (two conventional gyms GA, GB and one fitness centre GC). The first gym GA has the following dimensions: floor area about 540 m^2, volume 4,320 m^3 and it is used mainly for different ball games. The second gym GB has the following dimensions: floor area about 216 m^2, volume 1,728 m^3 and it is used mainly for sports games, floor exercise, aerobics, table tennis, etc. The third gym GC has the following dimensions: floor area about 92 m^2, volume 240 m^3 and it is used as a fitness centre. The last building is swimming pool centre SP (pool is 25 m long), which has the following dimensions: floor area about 640 m^2, volume 4,018 m^3.

A ventilation device is relatively outdated. There are not sensors for measurement and control of temperature, humidity or CO_2. There are only two limit states manually operated by the person: on or off. For technical reasons, it is not possible to measure the ventilation rate of air inlet or outlet in individual rooms. The long air-ducts are located in inaccessible places under the ceiling (height approximately 8 m) and air is distributed air to several rooms at the same time.

The measurements were carried out first when all rooms were empty, without students and without ventilation, several days without cleaning the floors. The same measurements were carried out during the normal function of rooms, with students and with standard ventilation calculated and designed by empirical method according to the ventilation rate per one person (30 m^3 h^{-1} $person^{-1}$). There were following number of persons during the measurement inside the rooms: GA 20 students play floorball, GB 27 students doing aerobic exercise, GC 18 students in fitness training, SP 20 students swim.

Rather important is specific biological load of the sport rooms calculated from the previous data. The summarised values of specific volume of space per one person in the rooms are following: gym GA has 216 m^3 per person, GB has 64 m^3 per person, fitness GC has only 13 m^3 per person and swimming pool SP has 201 m^3 per person.

The air samples for microbiological analyses were taken by the instrument Merck Mas-100 Eco, microbial air sampler with volume 0.200 m^3 air, and cultivated by PDA (potato-dextrose agar OXOID CM 139; 100%) and NA (nutrient agar OXOID CM 003; 100%). Colonies of microorganisms were evaluated after 5 days of incubation. Yeast and filamentous fungi were cultivated at 22 °C, bacteria at 29 °C. Captured microorganisms, which on the culture media formed colonies, were expressed as colony forming units per m^3 (CFU m^{-3}). Measuring devices and equipment technology environment continues to improve and provide a larger volume and more accurate results. New studies are constantly providing fresh information, but there are still many uncertainties. Maybe, new and more precise ideas about the influence on the human health can be discovered. Recommended air pollution limits of the indoor environment by a mixed bacteria population and a mixed filamentous fungi population according to the EUR 14988 EN are presented in the Table 1.

Table 1. Air pollution limits of the indoor environment (living rooms) by a mixed bacteria population and a mixed filamentous fungi population (EUR 14988 EN)

Pollution category	Bacteria CFU m^{-3}	Filamentous fungi CFU m^{-3}
Very low	< 50	< 25
Low	< 100	< 100
Medium	< 500	< 500
High	< 2,000	< 2,000
Very high	> 2,000	> 2,000

The obtained results of air-borne microorganisms measurements were processed by Excel software and verified by statistical software Statistica 12 (*ANOVA* and *TUKEY HSD Test*) to recognise the difference between the results in different rooms of sport centre during the summer and winter measurements. Different superscript letters (a, b, c) in common are significantly different from each other in the columns of the tables *(ANOVA; Tukey HSD Test;* $p \leq 0.05$*)*, e.g. if there are the same superscript letters in the column (rooms GA, GB, GC, SP) it means the differences between the values in rooms or between different states and conditions of the same rom are not statistically significant at the significance level of *0.05*.

The temperature and humidity of surrounding air were measured by sensor FH A646–2 including temperature sensor NTC type N with operative range from –30 to +100 °C with accuracy ± 0.1 K, and air humidity by capacitive sensor with operative range from 5 to 98% with accuracy ± 2%. Furthermore the concentration of CO_2 was measured by the sensor FY A600 with operative range 0–0.5% and accuracy ± 0.01%. The sensors were connected to the data logger ALMEMO 2690–8.

RESULTS AND DISCUSSION

Average values and standard deviations of external temperatures t_e and relative humidity RH_e, internal temperature t_i, relative humidity RH_i and concentration of carbon dioxide in the rooms without students and without ventilation during the summer period are summarized in the Table 2.

Some small differences between the measured values in the investigated areas correspond to slight changes in outdoor air during the measurement and different room dimensions as well as to the different thermal and technical characteristics and properties of these rooms.

The internal temperatures are related to the external mainly in the large gyms GA and GB. The internal temperature is smaller than external temperature in the fitness GC, which is not too large and the massive walls and mass of exercise tools, dumbbells and other equipment manifest as an accumulation mass of energy, so the cold accumulated during the night in this mass decreases slightly during the internal temperature during the day. The internal temperature is higher than the external temperature in the swimming pool SP as it is influenced by the warm water in the pool.

Relative humidity of internal air corresponds to temperature and rather high humidity ratio of external air in the summer. As there is not ventilation, the concentration of CO_2 is slightly higher, which is a rest of polluted air from the previous periods with some people activities.

Table 2. External temperature t_e and relative humidity RH_e, internal temperature t_i, relative humidity RH_i and concentration of carbon dioxide CO_2 in the rooms without students and without ventilation during the summer period

Room	t_e	RH_e	t_i	RH_i	CO_2
	°C ± SD	% ± SD	°C ± SD	% ± SD	ppm ± SD
GA	25.2 ± 0.2	51.8 ± 0.8	25.9 ± 0.1	56.2 ± 0.4	568 ± 11
GB	25.9 ± 0.2	48.5 ± 1.7	25.9 ± 0	55.8 ± 0.4	518 ± 10
GC	26.5 ± 0.1	44.4 ± 0.3	26.1 ± 0.1	57.2 ± 0.6	654 ± 20
SP	26.9 ± 0.1	42.6 ± 0.5	28.9 ± 0.4	53.4 ± 3.0	512 ± 41

SD – Standard deviation.

Table 3. External temperature t_e and relative humidity RH_e, internal temperature t_i, relative humidity RH_i and concentration of carbon dioxide CO_2 in the rooms with students and with ventilation during the winter period

Room	t_e	RH_e	t_i	RH_i	CO_2
	°C ± SD	% ± SD	°C ± SD	% ± SD	ppm ± SD
GA	7.2 ± 0.1	74.1 ± 0.2	22.7 ± 0.1	41.3 ± 3.0	740 ± 10
GB	7.4 ± 0.1	74.4 ± 0.6	21.6 ± 0.1	41.7 ± 1.0	689 ± 56
GC	7.3 ± 0.4	74.3 ± 0.1	22.4 ± 0.1	42.3 ± 0.4	771 ± 8
SP	7.1 ± 0.1	74.8 ± 0.2	27.2 ± 0.2	33.3 ± 0.7	350 ± 0

SD – Standard deviation.

The same external and internal quantities measured in the rooms with students and with ventilation during the winter period are presented in the Table 3. The results show the influence of intensive heating and ventilation in the swimming pool, which caused the highest air temperatures but also the lowest relative humidity and lowest CO_2 concentration.

The internal temperatures, relative humidity and CO_2 concentration in all gyms are in suitable range. Temperatures are increased by the heating system of the rooms. Relative humidity is lower than in the summer as the humidity ratio of external air is rather low (see low external temperature). The internal production of water vapour produced by respiration is not influencing the indoor humidity negatively thanks to the ventilation.

Table 4. Results of measurement of microbiological contamination by air-borne microorganisms in summer and winter. Different superscript letters (a, b, c) are the sign of the high significant difference between the rooms GA, GB, GC and SP (*ANOVA*; *Tukey HSD Test*; $p \leq 0.05$)

Room	Bacteria		Filamentous fungi	
	Summer	Winter	Summer	Winter
	CFU m^{-3} ± SD	CFU m^{-3} ± SD	CFU m^{-3} ± SD	CFU m^{-3} ± SD
GA	850 ± 137^{a}	$1,065 \pm 170^{a}$	$118 \pm 12^{a,b}$	45 ± 3^{a}
GB	467 ± 39^{b}	$1,433 \pm 179^{a}$	$115 \pm 20^{a,b}$	58 ± 28^{a}
GC	778 ± 54^{a}	$1,297 \pm 84^{a}$	133 ± 16^{a}	70 ± 7^{a}
SP	152 ± 39^{c}	300 ± 223^{b}	70 ± 20^{b}	55 ± 3^{a}

SD – Standard deviation.

Table 4 shows that the air pollution by biological contaminants is comparable in gym GA and fitness GC, which is according to EUR 14988 EN high (500-2000 CFU m^{-3}) in the case of bacteria during the summer. Different superscript letters (a, b, c) are the sign of the high significant difference between the rooms. The same letter (e.g. a) in lines of the same columns means, that there is not significant difference between values which were measured in different rooms.

The concentration of bacteria in gym GB and swimming pool SP is medium. The lowest quantity of bacteria is in the swimming pool SP.

It is also medium pollution in the case of filamentous fungi (100-500 CFU m^{-3}) in summer. The concentration of filamentous fungi was low (25–100 CFU m^{-3}) in all sport rooms during the winter. The lowest quantity of fungi was also in the swimming pool SP. The presence of conidia of filamentous fungi in the indoor environment is due to their presence in the incoming outdoor air. The inlet air is less polluted by the conidia of filamentous fungi in the winter. Their main source of filamentous fungi are necrotizing parts of plants, and those are few in the winter.

Prussin & Linsey (2015) identified eight major sources of airborne microorganisms in the built environment: humans, pets, plants, plumbing systems, heating, ventilation, and airconditioning systems, mold, dust resuspension and the outdoor environment.

Khan & Karuppayil (2012) recognized different sources of air-borne microorganisms in indoor environment. Our research carried out in the sport facilities eliminated other indoor factors. The arrangement of equipment was the same in summer (without students) and in winter (with students). The number of bacteria increases with the number of people present in both gyms GA and GB, in the fitness GC as well as in the swimming pool SP. Summer is a period without education, with a minimum number of people using gyms or fitness, but in winter it's the opposite. Many students and other clients come to gyms especially during the winter to strengthen their health and increase resistance to the expected respiratory problems. However, during sports activities, the air is heavily polluted with the finest dust particles (PM_1 and $PM_{2.5}$), which can penetrate into the lungs. The finest dust can contain biological contaminants.

The cleanest environment in terms of air pollution by biological contaminants has a swimming pool all year round. It can be caused by chlorine, which is released in a negligible amount from the water, and also by the ventilation. The right side of the pool with windows and ventilation system had during the whole year significantly lower values of biological contaminants than the left side without windows. The described situation well reflects the standard deviation, especially in case of bacteria in winter.

To study the influence of ventilation on the occurrence of microorganisms in the rooms there are statistically evaluated the differences between the ventilated and not ventilated spaces. The comparison of bacteria concentration and fungi concentration between the room without ventilation in summer and the same room with ventilation in winter are presented in the Table 5. The same letter (e.g. a) in both columns of the same line means, that there is not significant difference between both values. E.g. there is not significant difference between the bacteria concentrations in GA in summer and winter measurements. The difference of filamentous fungi concentration in GA in summer and winter measurements are significant.

Table 5. Results of measurement of microbiological contamination by air-borne microorganisms in summer and winter. Different superscript letters (a, b) are the sign of the high significant difference between the results measured in the not-ventilated (Summer) and ventilated (Winter) of the same room (*ANOVA*; *Tukey HSD Test*; $p \leq 0.05$)

Room	Bacteria		Filamentous fungi	
	Summer	Winter	Summer	Winter
	CFU m^{-3} ± SD	CFU m^{-3} ± SD	CFU m^{-3} ± SD	CFU m^{-3} ± SD
GA	850 ± 137^a	$1,065 \pm 170^a$	118 ± 12^a	45 ± 3^b
GB	467 ± 39^a	$1,433 \pm 179^b$	115 ± 20^a	58 ± 28^a
GC	778 ± 54^a	$1,297 \pm 84^b$	133 ± 16^a	70 ± 7^b
SP	152 ± 39^a	300 ± 223^a	70 ± 20^a	55 ± 3^a

SD – Standard deviation.

As already mentioned, people are the source of bacterial and fungal contamination inside the rooms. The results in the Table 5 show that regardless of ventilation, during the winter with the presence of people in all spaces, the concentration of bacteria was higher than in the summer, without people. From this point of view the ventilation is not adequate for the removal of bacteria from ventilated spaces. From the results we can conclude that the great importance on the air quality in terms of a specific bacteria concentration has the specific volume of the room per one athlete. The worst situation is in rooms with the smallest volume, which has the largest biological load of the space.

Statistical evaluation showed that significantly higher concentrations of bacteria are only in the smaller GB gym and in the fitness GC. Higher concentrations of bacteria in the large gym GA and in pool SP were not statistically confirmed. This result can be explained by the positive effect of ventilation.

Another is the situation in these rooms with regard to the occurrence of a fungi. In all rooms the concentration of fungi has decreased in the winter, which can be explained by the positive influence of ventilation, the supply of fresh clean air and the removal of contaminated air out.

It can be concluded from this comparison that intensive ventilation has a positive effect on reduction of the microorganisms' concentration of in space. Intensive ventilation is necessary, especially in smaller rooms, with higher numbers of actively moving people.

Table 6 is focus on the presence of allergenic filamentous fungi (*Cladosporium* and *Aspergillus*). Different superscript letters (a, b, c) are the sign of the high significant difference between the rooms. The same letter (e.g. a) in lines of the same columns means, that there is not significant difference between values which were measured in different rooms. *Cladosporium* reached nearly 30% of all isolated filamentous fungi in the gym GA, surprisingly in winter. In other cases, its representation was lower (12–17%). However, its presence in the indoor air of the sports facilities may be potentially dangerous for students and other sportsmen. *Cladosporium* presents was negligible (< 4%) in both gyms (GA, GB) and fitness GC in the summer. Only in swimming pool SP *Cladosporium* occurred almost in 24% of filamentous fungi.

Table 6. Results of measurement of microbiological contamination by allergenic filamentous fungi *Cladosporium* and *Aspergillus* in summer and winter. Different superscript letters (a, b) are the sign of the high significant difference between rooms (*ANOVA*; *Tukey HSD Test*; $p \leq 0.05$)

Room	*Cladosporium*		*Aspergillus*	
	Summer	Winter	Summer	Winter
	CFU m^{-3} ± SD	CFU m^{-3} ± SD	CFU m^{-3} ± SD	CFU m^{-3} ± SD
GA	0.0 ± 0.0^{a}	8.3 ± 4.4^{a}	18.3 ± 5.6^{a}	1.7 ± 2.2^{a}
GB	$1.7 \pm 2.2^{a,b}$	13.3 ± 7.8^{a}	3.3 ± 4.4^{b}	0.0 ± 0.0^{a}
GC	$5.0 \pm 6.7^{a,b}$	10.3 ± 6.7^{a}	3.3 ± 2.2^{b}	1.7 ± 2.2^{a}
SP	16.7 ± 5.6^{b}	8.3 ± 5.6^{a}	0.0 ± 0.0^{b}	0.0 ± 0.0^{a}

SD – Standard deviation.

The genus *Aspergillus* was found only in gyms (GA, GB) and fitness (GC), not in the swimming pool SP in summer. Attention should be paid to his 16% presence in the gym GA, in other sports facilities (GB and GC), its share was only 2–3%. In winter the genus *Aspergillus* was not present at gym GB and swimming pool SP. The source in gyms GA and fitness GC was probably not in the air drawn from the outside.

Large differences between the sampling points (see SD) mean that there is no relation to the ventilation and outside air.

CONCLUSIONS

The results of measurements in the University sport facilities showed that:

- The average pollution by bacteria in all gyms was rather high during the summer without students, without ventilation and without cleaning of the rooms. The presents of students even increased the bacteria concentration several times despite intensive ventilation during the winter period.
- The lowest quantity of bacteria was in the swimming pool all year round.

- Very big influence on the indoor air cleanness and reduction of air pollution has the intensive ventilation. Intensive ventilation is more important if the room has small dimensions and number of sportsmen is high.
- The pollution of air by fungi was higher during the summer period without students but without cleaning and without ventilation. Sufficient ventilation by fresh and clean air caused lower pollution by fungi in all rooms during the winter period in spite of students' activities.

The pollution by air-born microorganisms in sports facilities can be considered as significant. It is necessary to continue in this research and focus attention mainly on filamentous fungi. From the practical point of view it is possible to recommend an improvement of the air-conditioning system function, which should be equipped with automatic control and sensors for measurement of temperature, relative humidity and CO_2.

REFERENCES

Bouillard, L., Michel, O., Dramaix, M. & Devleeschouwer, M. 2005. Bacterial contamination of indoor air, surafaces, and settled dust, and related dust endotoxin concentrations in healthy office builgings. *Ann. Agric. Environ. Med*. **12**, 187–192.

Brodka, K., Sowiak, M., Kozajda, A., Cyprowski, M. & Szadkowska-Stanczyk, I. 2012. Biological contamination in office buildings related to ventilation/air conditioning system. *Medycyna Pracy* **63**(3), 303–315 (in Polish).

EUR 14988 EN. 1993. European collaborative action on urban air, indoor environment and human exposure reports. Report No 12. Biological particles in indoor environment. 81 pp.

Fisk, W.J., Gomez, Q.L. & Mendell, M.J. 2007. Meta-analyse of the associations of respiratory health effects with dampness and mold in homes. *Indoor Air* **17**, 284–296.

Frankel, M., Beko, G., Timm, M., Gustavsen, S., Hansen, E.W. & Madsen, A.M. 2012. Seasonal variations of indoor microbial exposures and their relation to temperature, relative humidity, and air exchange rate. *Applied and Environmental Microbiology* **78**(23), 8289–8297.

Gorny, R.L. & Dutkiewicz, J. 2002. Bacterial and fungal aerosols in indoor environment in Central and Eastern European countries. *Annals of Agricultural and Environmental Medicine* **9**, 17–23.

Karwowska, E. 2003. Microbiological air contamination in some educational settings. *Polish Journal of Environmental Studies* **12**, 181–185.

Khan, A.A.H. & Karuppayil, S.M. 2012. Fungal pollution of indoor environments and its management. *Saudi Journal of Biological Sciences* **19**, 405–426.

Kic, P. & Růžek, L. 2014. Microbiological environment in special rooms of University campus. *Agronomy Research* **12**(3), 837–842.

Kic, P., Ruzek, L. & Popelarova, E. 2014. Air-conditioning and microbiological environment in the lecture room. *Scientia Agriculturae Bohemica* **45**(2), 104–109.

Orru, H., Teinemaa, E., Lai, T., Tamm, T., Kaasik, M., Kimmel, V., Kangur, K., Merisalu, E. & Forsberg, B. 2011. Health impact assessment of particulate pollution in Tallinn using fine spatial resolution and modeling techniques. *Air Qual Atmos Health* **4**, 247–258.

Prussin II, A.J. & Linsey, C.M. 2015. Sources of airborne microorganisms in the built Environment. *Microbiome* **3**:78. https://doi.org/10.1186/s40168-015-0144-z

Seppänen, O., Fisk, W.J. & Lei, Q.H. 2006. Ventilation and performance in office work. *Indoor Air* **16**, 28–36.

Agronomy Research **16**(4), 1728–1741, 2018
https://doi.org/10.15159/AR.18.156

Effect of drying technologies on bioactive compounds maintenance in pumpkin by-products

D. Kļava, S. Kampuse*, L. Tomsone, T. Kince and L. Ozola

Latvia University of Life Sciences and Technologies, Faculty of Food Technology, Riga street 22, LV-3004 Jelgava, Latvia
*Correspondence: skampuse@inbox.lv

Abstract. During the pumpkin processing large amounts of waste material as a combination of pumpkin peel, seeds and the flesh between seeds has produced. Therefore it is important to investigate the possibilities for using the pumpkin residues. The aim of this research was to investigate the effect of different drying technologies on maintenance of bioactive compounds in pumpkin by-products. Two pumpkin residue products of Hubard group pumpkins were used to obtain pumpkin powder: residue products formed in the process of extracting industrial pumpkin purée by heating it in a heat exchanger and treating through a sieve of pulpier; residues resulting from pumpkin juice extraction process mechanically pressed from fresh, chopped pumpkins. In order to be able to choose the most suitable drying technology pumpkin by-products were dried in the microwave-vacuum, convective (at 40, 50, 70 and 80 °C) and freeze-drying type dryers. For all samples total carotenes, the ascorbic acid, total phenols content (TPC) and antiradical activity ($DPPH^{\cdot}$, $ABTS^{\cdot}+$) were determined by using standard methods. The highest total carotenes content was retained in freeze-dried pumpkin powders. The most suitable drying method for obtaining pumpkin powder with the highest ascorbic acid, total phenolic content and antiradical activity is drying in convective type drying at 80 °C temperature.

Key words: pumpkin residues, ascorbic acid, total phenols, carotenoids, drying technologies.

INTRODUCTION

As it is mentioned by several authors the nutritional value of pumpkin fruits is high. In the fresh pumpkin fruit total carotene content ranges from 2 to 10 mg 100 g^{-1}, vitamins C and E account for 9–10 mg 100 g^{-1} and 1.03–1.06 mg 100 g^{-1}, respectively (Terazawa et al., 2001; Nawirska et al., 2009; Ghabos et al., 2016). Pumpkin fruit is also a valuable source of other vitamins, e.g., B6, K, thiamine, and riboflavin, as well as minerals, e.g., potassium, phosphorus, magnesium, iron and selenium. Pumpkin flesh is a delicious and fully appreciated additive in a diversity of products for children and adults. Pumpkin fruits are processed to obtain juice, pomace, pickles and dried products (Nawirska et al., 2009). But one of the important problems is that pumpkin processing causes large amounts of waste which are consist of a combination of pumpkin peel, seeds and the flesh between seeds. One of the promising possibilities for reuse of pumpkin residues is drying and getting of pumpkin powder or flour.

Within the investigations of pumpkin powder scientists found that moisture, protein, fat, fiber and carbohydrate percentage of the pumpkin powder were around 6.01, 3.73, 1.32, 2.91 and 78.73%, respectively. β-carotene content of the powder was around 7.30 mg $100g^{-1}$ (Das & Banerjee, 2015).

One of the oldest methods for food preservation is drying, which consists of removing water from the product in order to provide microbiological safety (Mitra et al., 2012; Horuz & Maskan, 2015; Saengrayap et al., 2015; Ghabos et al., 2016). The most popular and traditional drying method is convective hot air drying. The method itself is a low-cost one, but has the disadvantage of entailing a time-consuming process. During contact with oxygen that is present in the air, the product becomes exposed to high temperature for a long time, and such exposure reduces the content of some valuable components which readily undergo oxidation at elevated temperature. (Lozano et al., 1983; Ghabos et al., 2016).

Drying process can cause changes in food surface characteristics which lead to color changes. Changes attributed to carotenoids and other pigments can also be caused by heat and oxidation during drying. In particular, higher drying temperatures and longer drying times were seen to facilitate greater pigment losses (Noor Aziah & Komathi, 2009; Roongruangsri & Bronlund, 2016). It is believed that drying at lower temperatures provides less nutritional loss (Galoburda & Rakčejeva, 2008). In the study of Roongruangsri & Bronlund (2016) the total carotenoid content of dried pumpkin powder produced at 70 °C (about 17.66 μg g^{-1} dry weight) was found to be significantly lower ($P \leq 0.05$) when compared to powders produced at 50 and 60 °C (about 25.99 and 16.42 μg g^{-1} dry weight, respectively). Moreover, the dried pumpkin powder produced at 70 °C showed the highest percentage of decrease in carotenoid content compared to those produced at drying temperatures of 50 and 60 °C.

Products that have been dried in microwave-vacuum dryer or freeze-dryer have biger pores, retains better structure of the plant-based product cells, while air-dried products break down the cells and form a denser structure.

Scientific research has shown that after microwave-vacuum drying, food colour, flavour, nutrients and other biologically active ingredients that are sensitive to thermal treatment and oxidation are much better preserved compared to convective drying (Scaman & Durance, 2005; Galoburda & Rakcejeva, 2008).

In the production of food, vacuum freeze-drying can be used to obtain high-quality porous products, as there is less loss of biologically active compounds and flavour compared to convective drying, the colour, shape and structure of the product are better preserved (Food Industry Technological Equipment, 2000). The products are low density and have a very good rehydration capability.

The aim of this research was to investigate the effect of different drying technologies on maintenance of bioactive compounds in pumpkin by-products.

MATERIALS AND METHODS

Two pumpkin residue products of Hubard group pumpkins were used to obtain pumpkin powder:

1) Residue products formed in the process of extracting industrial pumpkin purée by heating it in a heat exchanger at 99–100 °C temperature for 3–5 min, and treating through a sieves of pulpier (Steamed sample);

2) Residues resulting from pumpkin juice extraction process mechanically pressed from fresh, chopped pumpkins (Freshly-pressed sample).

Both types of by-products were stored in the freezer (-20 ± 2) °C before further processing for 2 mounths. In order to be able to choose the most suitable drying technology pumpkin by-products were dried in the microwave-vacuum dryer ‘Musson-1’ (Ingredient, Russia), convective dryer using ‘Memmert’ Universal Oven UF55 and UF160 (Memmert GmbH+Co.KG, Germany at 40, 50, 70 and 80 °C) and freeze-drying type using vacuum freeze-dryer FT333 (Armfield Ltd, Ringwood England).

The abbreviated terms (Table 1) were used in the part of the results for the different types of drying.

Table 1. The identification of samples

No	Description	Code
1.	Frozen untreated pumpkin residues	Fresh
2.	Died in microwave-vacuum dryer	MW
3.	Drying in vacuum-freeze-dryer	FD
4.	Dried in convective hot air dryer 40 °C	C-40
5.	Dried in convective hot air dryer 50 °C	C-50
6.	Dried in convective hot air dryer 70 °C	C-70
7.	Dried in convective hot air dryer 80 °C	C-80

For all samples total carotenes, the ascorbic acid, total phenols content (TPC) and antiradical activity (DPPH$^{\cdot}$, ABTS$^{\cdot}$+) were determined.

The ascorbic acid content (mg 100 g^{-1}) was experimentally determined using iodometric method: 5 g of the sample was added to 100 mL of 6% oxalic acid, 1 min crushed with a blender and filtered through a paper filter. Then add 2 mL of 1% starch solution to the 10 ml of filtrate and titrate with 0.05 M J_2 (Jansons, 2006).

The amount of vitamin C in each sample was determined in three replicates. The content of ascorbic acid in the sample is calculated according to formula:

$$C = 5{,}000 \frac{V_{sample}}{m \cdot V_{\mathrm{stan}dard}} \qquad (1)$$

where 5,000 – the coefficient; V_{sample} – amount of 0.05M iodine used for titration, mL; $V_{standart}$ – Use of 0.05M iodine solution in 25 mL standard solution, titration, mL.

The carotene content (mg 100g^{-1}) was determined by weighing 1–2 g of the crushed sample on analytical scales, adding 20 mL of 96% ethanol and stirring on a magnetic stirrer (MS01). After stirring for 15 minutes, add 25 mL of petroleum ether (with boiling temperature 80–110 °C) and continue to stir for 1 hour, then the sample was placed in a dark place until a complete formation of two layers, where the upper yellow-coloured layer contains carotenes which was analysed by Jenway 6705 UV / Vis spectrophotometer at a wavelength of 440 nm, taking petroleum ether as a control solution. The carotenoids content of each sample was determined in two replications. Grading schedule was established with potassium dichromate and carotene equivalent (KE) was found. The content of carotenes was calculated according to the formula (2) (Методы биохимического ..., 1987, Ozola et al., 2017):

$$X = \frac{0.208 \times 25 \times KE}{36 \times a} \quad (2)$$

where 0.208, 25 and 36 coefficients; m – sample weight, g; KE-carotene equivalent, which is the amount of potassium dichromate at the measured absorption.

The total phenols in dried pumpkin powders determined spectrophotometrically by 'JENWAY 6705 UV' spectrophotometer at a wavelength of 765 nm using Singleton et al. (1999) method also described by Priecina & Kārkliņa (2014) with some modifications. Weight 3 g of pumpkin residue powder, add 20 mL of ethanol/water mixture (80 : 20), place the glass on a magnetic stirrer, and leave to stir for 2 hours. After the mixing, the sample in another conical flask was filtered through a paper filter until the sample was completely filtered. The filtered samples were collected in a 25-mL volumetric flasks and filled with solvent to the mark. In three separate flasks 0.5 mL of the extract were measured, 2.5 mL of Folin-Ciocalteu phenol reagent diluted 10 times with distilled water was added, after 5 minutes 2 mL of 7.5% Na_2CO_3 was added too, mixed and withstood 30 min Gallic acid equivalent was used to quantify the total polyphenols content. The total phenol content of the test samples was expressed as milligrams of gallic acid equivalent per 100 grams of dry sample weight (mg GAE 100 g^{-1} DW) (Singleton et al., 1999; Priecina & Kārkliņa, 2014).

The analyses were done in three replications.

For determination of antioxidant activity in the samples 2.2 diphenyl picyrylhydrazine (DPPH) and 2,2′-azino-bis(3-ethylbenz-thiazoline-6-sulfonic) acid ($ABTS^{\bullet+}$) radicals were used.

The determination of DPPH antiradical activity was performed on the basis of (Yu et al., 2003) with some modifications:

Place 0.5 mL of the test solution in a cuvettes;

Add 3.5 mL of freshly prepared DPPH solution (0.004 g DPPH per 100 mL of ethanol);

Leave in a dark place at room temperature 30 minutes;

The results were read on a JENWAY 6300 spectrophotometer at a wavelength of 517 nm (Priecina & Kārkliņa, 2014). For the quantitative expression of antiradical activity, the Trolox equivalent of 6 hydroxyl 2,5,7,8 tetramethylchromo-carboxylic acid was used. The Trolox calibration curve was created and, using the read-out absorbance, the antiradical activity in the analyzed samples was expressed in mg Trolox equivalent per 100 grams of sample dry matter (mg Trolox 100 g^{-1} DW) (Priecina & Kārkliņa, 2014).

The radical scavenging activity (RSA) of extracts was also measured by 2,2′-azino-bis(3-ethylbenz-thiazoline-6-sulfonic) acid ($ABTS^{\bullet+}$) radical cation assay (Re et al., 1999). For the assessment of extracts, the $ABTS^{\bullet+}$ solution was diluted with a phosphate buffer solution to obtain the absorbance of 0.800 ± 0.030 at 734 nm. The RSA was expressed as TE 100 g^{-1} DW of plant material (Kampuse et al., 2016).

RESULTS AND DISCUSSION

Total carotene content

Frozen residues

The total carotene content in the raw material varied from 18.31 ± 0.4 mg 100 g^{-1} dry matter (fresh, frozen parts of pumpkin residues) up to 20.51 ± 0.25 mg 100 g^{-1} dry matter (steamed, frozen pumpkin residues), showing a significant increase ($P < 0.05$) in the initial values for steamed samples.

Pumpkin powder made from steamed, frozen pumpkin residues

There was a significant difference ($P < 0.05$) between total carotene content in pumpkin powder dried in convective, microwave-vacuum and freeze-dryer. Also, significant differences ($P < 0.05$) between the total carotene content of dried pumpkin powder in convective dryer at various temperature regimes were observed. The highest total carotene content was retained in freeze-drying system dried pumpkin powders. In total, the carotene content in pumpkin powders varied from 10.04 ± 0.31 mg per 100 g^{-1} dry matter (using convective drying at 80 °C) to 20.84 ± 0.89 mg 100 g^{-1} dry matter (using drying in a freeze-dryer) (Fig. 1).

Comparing pumpkin powder dried at different temperature regimes of convective dryer, their total carotene content significantly decreased ($P < 0.05$) with increasing temperature (comparing drying at 40 °C and 80 °C decreased by 42%).

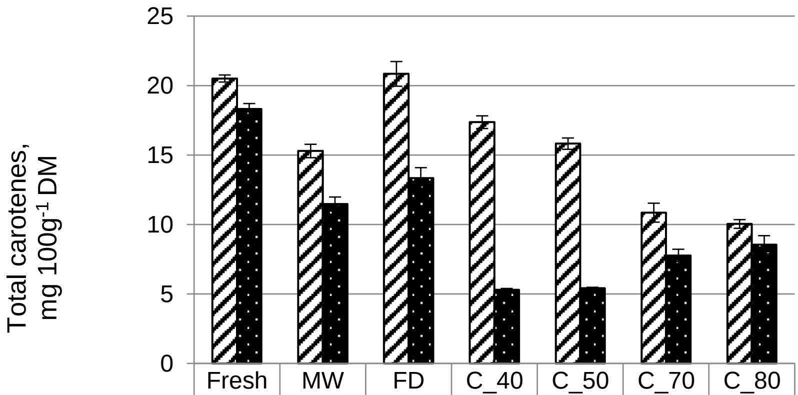

	Fresh	MW	FD	C_40	C_50	C_70	C_80
Steamed	20.51	15.29	20.84	17.36	15.82	10.85	10.04
Freshly-pressed	18.31	11.47	13.34	5.31	5.42	7.77	8.54

Figure 1. The comparison of total carotenes content in pumpkin powder obtained in different drying regimes.

Pumpkin powder made from fresh, frozen residues

Changes in the content of carotenes in pumpkin powders made from fresh, frozen residues were similar to those observed from steamed residues. Similarly to the samples described above, there were significant differences ($P < 0.05$) between the total carotene content in samples of convective, microwave-vacuum drying and drying in vacuum freeze-dryer. Also, significant differences ($P < 0.05$) between the total carotene content of dried pumpkin powder in convective dryer at various temperature regimes were observed but the interesting was fact that the highest total carotenes content was observed to C-80 sample, and total carotene content significantly increased ($P < 0.05$) with increasing temperature, which was a completely different tendency from the powders derived from steamed residues. This relationship can be explained by the activity of different enzymes in these two different samples: for the steamed sample enzymes activity was completely inactivated before drying, while in the freshly-pressed sample enzymes were still active at the start of the drying. It is proved also by other authors that during drying process polyphenoloxidasis activity remains still high for longer periods when the drying temperature is between 55–60 °C, whereas shorter exposure period is needed to inactivate enzymes at temperatures between 75–80 °C (Arslan et al., 1998; Sonawane & Arya, 2014).

The highest total carotene content was retained in freeze-dried samples, although the results were significantly lower compared to steamed powders. In total, the carotene content in these pumpkin powders varied from 5.31 ± 0.09 mg per 100 g^{-1} of dry matter (using convective dryer at 40 °C) to 13.34 ± 0.75 mg per 100 g^{-1} of dry matter (using drying in a freeze-dryer) (Fig. 1). A total reduction in carotene content compared to a frozen, no dried pumpkin residues ranged from 27% (using freeze-drying method) to 71% (using drying in a convective dryer 40 °C). In the study of Roongruangsri & Bronlund (2016) the carotenoid degradation was observed from 18 to 56% using convective drying at 50, 60 and 70 °C temperatures. Within the increase of temperature, the total amount of carotenoids also decreased in this investigation which coincides with our data of steamed pumpkin residues dried in convective dryer but opposite to the results of freshly-pressed by-products. There is no unanimous opinion about the influence of temperature to the degradation of carotenoids. In the study with drying of cassava roots authors (Onyenwoke et al., 2015) concluded the following statement: 'Drying at High Temperature Short Time (HTST) retained more TCC on average, than Low Temperature long Time (LTLT) as was observed during tray drying at temperature range between 80–95 °C for 1hour and 55–70 °C for 2 hours'.

Ascorbic acid content

Frozen residues

The content of ascorbic acid or vitamin C was relatively low in raw pumpkin residues. Its content ranged from 17.20 ± 0.02 mg 100 g^{-1} of dry matter (freshly-pressed pumpkin residues) to 25.43 ± 0.69 mg per 100 g^{-1} of dry matter (steamed pumpkin residues), showing a significant ($P < 0.05$) higher initial values for steamed sample. Also, all dried samples derived from steamed residues were with higher ascorbic acid content than from freshly-pressed.

Pumpkin powder made from steamed pumpkin residues

A slight significant difference ($P < 0.05$) of pumpkin powder ascorbic acid content was observed between convective hot air, microwave vacuum drying and vacuum freeze-dying techniques. Also, the difference between the contents of ascorbic acid of convective dried samples in different temperature regimes was significant ($P < 0.05$). The highest content of vitamin C was retained in a samples dried at 80 °C temperature. In general, the content of C vitamin in pumpkin powders varied from 5.78 ± 0.57 mg of 100 g^{-1} of dry matter (using microwave-vacuum dryer) to 12.10 ± 0.69 mg of 100 g^{-1} of dry matter (using a convective dryer at 80 °C) (Fig. 2).

After drying, all pumpkin powders had a decrease in ascorbic acid content compared to raw sample ranging from 52% (using convective dryer at 80 °C) to 77% (using microwave-vacuum drying).

Pumpkin powder made from freshly-pressed residues

Comparing the changes in ascorbic acid content from freshly-pressed residue powders there were no significant differences between different drying methods and regimes. In general, the content of ascorbic acid in these pumpkin powders varied from 5.03 ± 0.04 mg of 100 g^{-1} of dry matter (using vacuum freeze-drying) to 7.77 ± 0.09 mg of 100 g^{-1} of dry matter (using drying in a convective dryer at 80 °C) (Fig. 2).

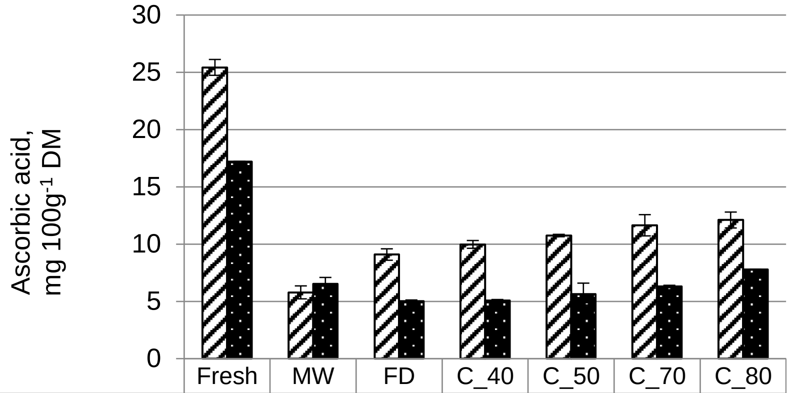

	Fresh	MW	FD	C_40	C_50	C_70	C_80
Steamed	25.43	5.78	9.09	9.97	10.75	11.64	12.10
Freshly-pressed	17.20	6.53	5.03	5.08	5.63	6.30	7.77

Figure 2. The comparison of ascorbic acid content in pumpkin powder obtained in different drying regimes.

The obtained results proved that there is no big influence of drying technology to the ascorbic acid content because of big instability of this vitamin in such crashed residue mass. Also by the observations of other authors the vitamin C is the most unstable bioactive compound because it oxidases easily during different processing operations and storage. The degradation of vitamin C is influenced by temperature, pH, the presence of metal ions, enzymes, water, light and the time of product heating (Machlin, 1991).

Total phenol content (TPC)

Frozen residues

The content of total phenols in frozen residues varied from 135.59 ± 3.94 mg per Gallic acid equivalent (GAE) of 100 g^{-1} dry matter (freshly-pressed pumpkin residues) up to 179.67 ± 10.90 mg GAE 100 g^{-1} dry matter (steamed pumpkin residues), and the differences were significant ($P < 0.05$) (Fig. 3). These data are similar to the data mentioned in literature about the total phenols content in fresh pumpkins of different cultivars (Biesiada et al., 2011).

Pumpkin powder made from steamed pumpkin residues

The highest content of total phenols was in powder dried in convective dryer. Overall, the total phenol content in pumpkin powders varied from 159.14 ± 8.70 mg

GAE per 100 g^{-1} dry matter (using microwave-vacuum drying) to 383.04 ± 10.31 mg GAE per 100 g^{-1} dry matter (using drying in a convective dryer at 80 °C). The total phenol content in steamed pumpkin residues were similar or higher than in fresh samples what is similar to the findings of Yang et al. (2010) with drying of blanched sweet potatoes.

There was no significant difference between the total phenol content in microwave-vacuum dryer and freeze-dryer dried pumpkin powders ($P > 0.05$). In contrast, the difference between the total phenol content in the convective dryer in different temperature regimes dried pumpkin powder was significant ($P < 0.05$), and, with increasing drying temperature, the total content of phenols in pumpkin powders also increased (compared to a drying of 40 °C and 80 °C increase was even 65%) (Fig. 3). In case of phenolic compounds, the investigations showed that with treatment in higher temperatures and shorter time it is possible to get dried product with higher total phenol content. The release of active enzymes could cause enzymatic degradation and lose extractable phenolics (Tomsone & Kruma, 2014) what could be the main reason of lower total phenol content in dried freshly-pressed residues.

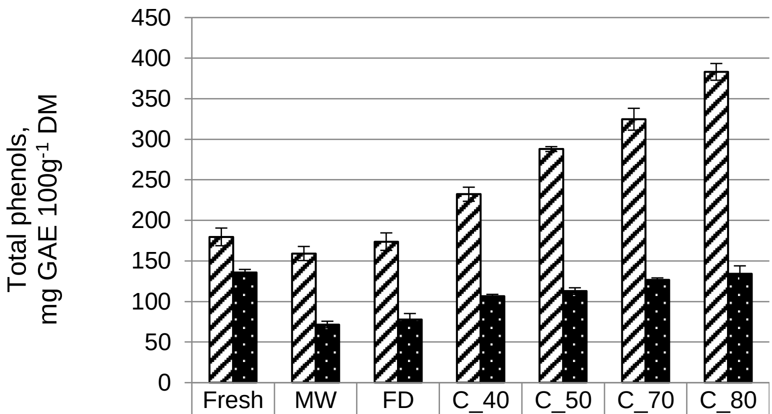

	Fresh	MW	FD	C_40	C_50	C_70	C_80
Steamed	179.67	159.14	173.80	232.20	287.89	324.66	383.04
Freshly-pressed	135.59	71.62	77.65	106.72	112.79	126.60	134.22

Figure 3. The comparison of total phenol content in pumpkin powder obtained in different drying regimes.

Pumpkin powder made from freshly-pressed residues

Comparing the total phenol content, there were significant differences ($P < 0.05$) found between dried pumpkin powders obtained with different dryers and in different temperature regimes. Similarly to powders from steamed residues, the highest content of total phenols was in convective dryer obtained pumpkin powder. Overall, the total phenol content in pumpkin powders varied from 71.62 ± 4.06 mg GAE per 100 g^{-1} dry matter (using microwave-vacuum dryer) to 134.22 ± 9.74 mg GAE per 100 g^{-1} dry matter (using drying in a convective dryer at 80 °C).

There was no significant difference between the total phenol content in microwave-vacuum dryer and vacuum freeze-dryer dried pumpkin powder ($P > 0.05$). In contrast, the total phenol content in different temperature regimes obtained samples of convective dryer increased within increasing the drying temperatures (compared to a drying of 40 °C and 80 °C increase was 26%). Significant differences were not detected (*P* > 0.05) when dried at 40 °C and 50 °C, and dried at 70 °C and 80 °C.

Compared to frozen raw residues, the smallest reduction in total phenols was in convective dried pumpkin powder, where it decreased by 1% (80 °C) to 21% (40 °C).

As it is also reported by Aydin & Gocmen (2015) oven drying increased phenolic contents and bioaccessible phenolics (1,237.457 mg of GAE 100 g^{-1} DW, respectively) in comparison with freeze-drying. Higher total phenols content after drying and grinding of pumpkin powder comparing with fresh samples could be explained with better extraction of phenolic compounds from the flour with particles of very small size while in steamed in freshly-pressed pumpkin residues the size of particles was much bigger. Another reason of increasing phenolic compounds with increasing the temperature could be the activity of enzymes in the freshly-pressed pumpkin residues. To avoid enzymatic oxidation from polyphenol oxidases, samples may need to be heated to a temperature of more than 90 °C for a few minutes. These enzymes catalyze the oxidation of phenols to quinones with subsequent nonenzymatic rapid polymerization. These oxidases can also be inhibited by lowering the pH to below 4.0 (Murkovic, 2003). As it is reported by Rabadan-Chavez & Lugo-Cervantes (2018) in the studies with cocoa beans the roasting in high temperatures of well-fermented cocoa beans significantly affected the levels of phenolic compounds. Procyanidins (mainly procyanidin dimers B1, B2, B5, and procyanidin trimer C1) and anthocyanins showed extensive degradation due to hydrolysis, oxidation, or condensation reactions under the effect of high temperatures, elevated humidity, and enhanced exposure to oxygen. A similar trend has been observed for epicatechin, which showed intensive oxidation or degradation during the roasting process. But it has been observed also that the content of catechin increased during the roasting process. It has been attributed to the degradation of procyanidins into (+)-catechin and (−)-epicatechin, combined with the epimerization of (−)-epicatechin into (−)-catechin, due to high temperatures of roasting (Rabadan-Chavez & Lugo-Cervantes, 2018). It means that the total amount of phenolic compouns is dependent from the composition of phenolic compounds of each food product. Therefore, more studies are necessary to evaluate the composition of pumpkin residue powders.

Antiradical scavenging activity

2.2-diphenyl-1-picrylhydrazyl- (DPPH) reagent antiradical scavenging activity

Frozen residues

The DPPH antiradical activity in the fresh samples varied from 4.16 ± 0.11 mM, converted to Trolox equivalent (TE) 100 g^{-1} dry matter (Freshly-pressed pumpkin residues) to 5.46 ± 0.35 mM TE per 100 g^{-1} dry matter (steamed pumpkin residues). Among these DPPH antiradical activity indices, significant (*P* < 0.05) differences were observed (Fig. 4).

Pumpkin powder made from steamed pumpkin residues

The highest DPPH antiradical activity was in convective dried pumpkin powder. Generally, the antiradical activity of DPPH in pumpkin powders varied from 8.69 ± 0.24 mM TE per 100 g^{-1} dry matter (using microwave-vacuum dryer) to 17.61 ± 0.56 mM TE per 100 g^{-1} dry matter (using convective drying at 80 °C) (Fig. 4), and it was much higher than the antiradical activity of fresh samples. Similar results also were reported in Nakhon et al. (2017) comparison of fresh pumpkin and pumpkin flour. In this experiment pumpkin flour exhibited greater antioxidant activities (DPPH, ABTS and FRAP), but had lower β-carotene than fresh pumpkin (Nakhon et al., 2017).

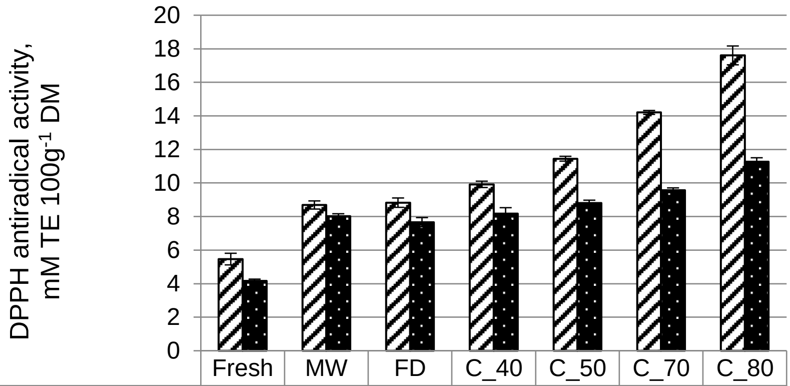

	Fresh	MW	FD	C_40	C_50	C_70	C_80
Steamed	5.46	8.69	8.83	9.92	11.45	14.20	17.61
Freshly-pressed	4.16	8.02	7.67	8.17	8.81	9.56	11.27

Figure 4. The comparison of antiradical activity (DPPH) in pumpkin powder obtained in different drying regimes.

Comparing the DPPH antiradical activity between the microwave-vacuum dried, freeze-dried, and convective dried in different temperature regimes pumpkin powders, there were found significant ($P < 0.05$) differences. But there was no significant difference ($P < 0.05$) between DPPH antiradical activity in microwave-vacuum drying and freeze-drying methods obtained pumpkin powder. In contrast, the antiradical activity of DPPH for dry pumpkin powders dried in convective dryer in different temperature regimes was significant ($P < 0.05$), with an increase in drying temperature, DPPH antiradical activity in pumpkin powders also increased like it was also with phenols.

The DPPH antiradical activity of the microwave-vacuum dried pumpkin powder increased by 59%, of freeze-dried pumpkin powder increased by 61%, for convective dried pumpkin powder increase was even from 81% (40 °C) to 222% (80 °C). As the DPPH antiradical activity has a high correlation with total phenol content the increase of DPPH antiradical activity could be explained with the increase of phenols in dried powders compared to fresh, frozen residues. Also in in the investigations of Hossain et al. (2010) drying of herbs has been found to be a very useful technique for increasing the amount of phenolic compounds and antioxidant capacity of the extracts. Among the drying methods tested, air-drying was found to be the best method for all the samples while freeze-drying and vacuum-oven drying showed lower phenol content and antiradical activity (Hossain et al., 2010).

Pumpkin powder made from freshly-pressed residues

Comparing the DPPH antiradical activity between the microwave-vacuum dried, freeze-dried, and convective dried in different temperature regimes pumpkin powders, there were significant ($P < 0.05$) differences. The highest DPPH antiradical activity similarly as in steamed sample was in convective dried pumpkin powder. The antiradical activity of DPPH in pumpkin powders varied from 7.67 ± 0.27 mM TE per 100 g^{-1} dry matter (using freeze-dryer) to 11.27 ± 0.24 mM TE per 100 g^{-1} dry matter (using drying in a convective dryer at 80 °C) (Fig. 4).

The antiradical activity of DPPH for dry pumpkin powders dried in convective dryer in different temperature regimes was significant ($P < 0.05$), and as the drying temperature increased, the antiradical activity of DPPH in pumpkin powders also increased (compared to a drying of 40 °C and 80 °C increase was 38%).

The lowest increase in DPPH antiradical activity was for freeze-dried pumpkin powder (increased by 84%), for microwave-vacuum dried pumpkin powder increase was 90%, but for convective dried powder increase was from 96% (40 °C) to 170% (80 °C).

Similar results in comparison of two drying methods also scientists Que et al. (2008) found. Hot air-dried pumpkin flour showed stronger antioxidant activities than freeze-dried flour. The percentage inhibition of peroxidation in linoleic acid system by 15 mg mL−1 extracts from hot air-dried and freeze-dried pumpkin flours was found to be 92.4% and 86.1% after 120 h of incubation, respectively (Que et al., 2008).

2.2-azino-bis (3-etilbenztiazolin-6-sulphonic acid) (ABTS+) reagent antiradical scavenging activity

Frozen residues

The $ABTS^+$ antiradical activity in fresh samples ranged from 11.22 ± 0.88 mM, converted to Trolox equivalent (TE) 100 g^{-1} dry matter (freshly-pressed residues) to 12.66 ± 1.04 mM TE per 100 g^{-1} dry matter (steamed, frozen pumpkin residues). There was no significant difference ($P < 0.05$) among these $ABTS^+$ antiradical activity indices.

Pumpkin powder made from steamed pumpkin residues

Comparing the DPPH antiradical activity between the microwave-vacuum dried, freeze-dried, and convective dried in different temperature regimes pumpkin powders, there were found significant ($P < 0.05$) differences. The overall tendencies for changes of $ABTS^+$ antiradical activity were similar as to DPPH antiradical activity. The highest $ABTS^+$ antiradical activity was in convective dried pumpkin powder. In general, the antiradical activity of $ABTS^+$ in pumpkin powders varied from 5.93 ± 0.92 mM TE per 100 g^{-1} dry matter (using freeze-dryer) to 54.91 ± 1.23 mM TE per 100 g^{-1} dry matter (using drying in a convective dryer at 80 °C).

$ABTS^+$ Antiradical activity decreased by 53% for freeze-dried pumpkin powder. In the case of microwave vacuum drying, this activity increased by 98%, while for convective dried powder increase was from 177% (40 °C) to 333% (80 °C).

Pumpkin powder made from freshly-pressed residues

The tendences for changes of $ABTS^+$ antiradical activity for pumpkin powder made from freshly-pressed residues were similar to samples made from steamed residues, only the absolute values were much lower (Fig. 5). Overall, the antiradical activity of $ABTS^+$ reagent in pumpkin powders varied from 2.86 ± 0.17 mM TE per 100 g^{-1} dry matter (using freeze-dryer) to 24.94 ± 1.06 mM TE per 100 g^{-1} dry matter (using drying in a convective dryer at 80 °C).

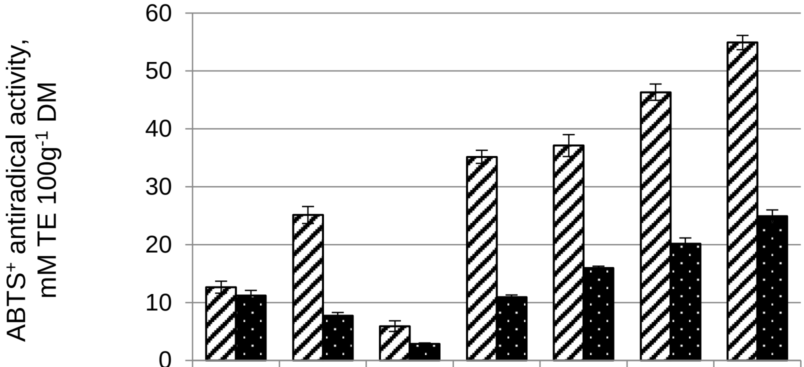

	Fresh	MW	FD	C_40	C_50	C_70	C_80
Steamed	12.66	25.12	5.93	35.17	37.12	46.34	54.91
Freshly-pressed	11.22	7.72	2.86	10.91	15.98	20.17	24.94

Figure 5. The comparison of antiradical activity (DPPH) in pumpkin powder obtained in different drying regimes.

With the rissing of temperature $ABTS^+$ antiradical activity in pumpkin powders also increased.

CONCLUSIONS

The highest total carotenes content retains in freeze-dried pumpkin powders. The most suitable drying method for obtaining pumpkin powder with the highest ascorbic acid, total phenolic content and antiradical activity is drying in convective type dryer at 80 °C temperature. But it is still unclear the mechanism of formation of phenolic compounds during drying of pumpkin by-products at higher temperatures, and some more investigations are necessary for evaluation of formation and degradation processes of different phenolic compunds and antiradical activity affected by temperature.

ACKNOWLEDGEMENTS. To contract No SB/L – 1/17 (3.2-10/2017/LLU/25-02.05.2017) with company 'SKAI BLTIJA'.

REFERENCES

Arslan, O., Temur, A. & Tozlu, I. 1998. Polyphenol oxidase from Malatya Apricot (*Prunus armeniaca L). Journal of Agricultural and Food Chemistry* **46**, 1239–1271.

Aydin, E. & Duygu, G. 2015. The influences of drying method and metabisulfite pre-treatment on the color, functional properties and phenolic acids contents and bioaccessibility of pumpkin flour. *LWT - Food Science and Technology* **6**(1), 385–392.

Biesiada, A., Nawirska, A., Kucharska, A. & Sokól-Letowska, A. 2011. Chemical Composition Of Pumpkin Fruit Depending On Cultivar And Storage. *Ecological Chemistry and Engineering* **18**(1), 9–18.

Das, S. & Banerjee, S. 2015. Production of pumpkin powder and its utilization in bakery products development: a review. *International Journal of Research in Engineering and Technology* **4**(5), 478–481.

Food Idustry technologycal equipment. 2000. (Pārtikas rūpniecības tehnoloģiskās iekārtas) L. Dukaļskas red. Jelgava: LLU PTF, 525 pp. (in Latvian).
Galoburda, R. & Rakčejeva, T. 2008. *The alternative processes of food processing* (Pārtikas pārstrādes alternatīvie procesi). Jelgava: LLU, 94 pp. (in Latvian).
Ghaboos, S.H.H., Ardabili, S.M.S., Kashaninejad, M., Asadi, G. & Aalami, M. 2016. Combined infrared-vacuum drying of pumpkin slices. *Journal of Food Science and Technology* **53**(5), 2380–2388.
Horuz, E. & Maskan, M. 2015. Hot air and microwave drying of pomegranate (*Punica granatum* L.) arils. *Journal of Food Science and Technology* **52**(1), 285–293.
Hossain, C., Barry-Ryan, A.B., Martin-Diana, N.P. & Brunton, M.B. 2010. Effect of drying method on the antioxidant capacity of six *Lamiaceae* herbs. *Food Chemistry* **123**, 85–91.
Jansons, E. 2006. *Theoretical background of analytical chemistry* (Analītiskās ķīmijas teorētiskie pamati), LU Akadēmiskais apgāds, 307 pp. (in Latvian).
Kampuse, S., Tomsone, L. Krūma, Z., Šabovics, M. & Skrabule, I. 2016. Effect of lovage phenolics to formation of acrylamide in French fries. *Agronomy Research* **14**(S2), 1315–1327.
Lozano, J.E., Rotstein, E. & Urbicain, M.J. 1983. Shrinkage, porosity and bulk density of foodstuffs at changing moisture contents. *Journal of Food Science* **48**, 1497–1502.
Machlin, L.J. 1991. *Handbook of Vitamins. 2nd ed.*, New York; Basel Marcel: Dekker, Inc., 595 pp.
Mitra, J., Shrivastava, S. & Rao, P. 2012. Onion dehydration: a review. *Journal of Food Science and Technology* **49**(3), 267–277.
Murkovic, M. 2003. Phenolic Compounds. In: Caballero, B., Finglas, P. & Toldra, F. (eds) *Encyclopedia of Food Sciences and Nutrition. 2nd ed.*, Academic Press, New York, pp. 4507–4514.
Nakhon, P.P.S., Jangchud, K., Jangchud, A. & Prinyawiwatkul, W. 2017. Comparisons of physicochemical properties and antioxidant activities among pumpkin (*Cucurbita moschata* L.) flour and isolated starches from fresh pumpkin or flour. *International Journal of Food Science & Technology* **52**(11),·2436–2444.
Nawirska, A., Figiel, A., Kucharska, A.Z., Sokół-Łętowska, A. & Biesiada, A. 2009. Drying kinetics and quality parameters of pumpkin slices dehydrated using different methods. *Journal of Food Engineering* **94**(1), 14–20.
Noor Aziah, A. & Komathi, C. 2009. Physicochemical and functional properties of peeled and unpeeled pumpkin flour. *Journal of Food Science* **74**(7), 328–333.
Onyenwoke, C.A., Ojo, C.C., Omodamiro, R.M., Egesi, C.N. & Simonyan, K.J. 2015. Effect of Drying Methods on Total Carotenoids Content Retention in Pro- Vitamin A High Quality Cassava Flour . *Umudike Journal of Engineering and technology* **1**(2), 1–9.
Ozola, L., Kampuse, S. & Galoburda, R. 2017. The effect of high-pressure processing on enteral food made from fresh or semi-finished ingredients. *FoodBalt 2017: 11th Baltic conference on food science and technology 'Food science and technology in a changing world': conference proceedings*, Jelgava, LLU, 80–85.
Priecina, L. & Kārkliņa, D. 2014. Natural Antioxidant Changes in Fresh and Dried Spiecies and Vegetables International *Journal of Biological, Biomolecular, Agricultural, Food and Bioechnical Engineering* **8**(5), 492–496.
Que, F., Mao, L., Fang, X. & Wu, T. 2008. Comparison of hot air-drying and freeze-drying on the physicochemical properties and antioxidant activities of pumpkin (*Cucurbita moschata Duch*.) flours. *International Journal of Food Science & Technology* **43**, 1195–1201.
Rabadan-Chavez, G. & Lugo-Cervantes, E. 2018. Phenolic Compounds in Cocoa and Chocolate. In: Leo, M.L., Nollet, J., Gutierrez-Uribe, A. (eds) *Phenolic Compounds in Food. Characterization and Analysis.* Taylor & Francis Group, LLC, pp. 375–389.

Re, R., Pellegrini, N., Proteggente, A., Pannala, A., Yang, M., Rice-Evans, C. 1999 Antioxidant activity applying an improved ABTS radical cation decolorization assay. *Free Radical Biology and Medicine* **26**, 1231–1237.

Roongruangsri, W. & Bronlund, J.E. 2016. Effect of air-drying temperature on physico-chemical, powder properties and sorption characteristics of pumpkin powders. *International Food Research Journal* **23**(3), 962–972.

Saengrayap, R., Tansakul, A. & Mittal, G.S. 2015. Effect of far-infrared radiation assisted microwave-vacuum drying on drying characteristics and quality of red chilli. *Journal of Food Science and Technology* **52**(5), 2610–2621.

Scaman, C.H. & Durance, T.D. 2005. Combined Microwave Vacuum-drying. In: Sun. D.W. (ed) *Emerging technologies for Food Processing*. Elsevier: Academic Press, New York, pp. 507–533.

Singleton, V.L., Orthofer, R. & Lamuela-Raventos, R.M. 1999. Analysis of total phenols and other oxidation substrates and antioxidants by means of FolinCiocalteu reagent. *Method in Enzymology* **299**, 152–178.

Sonawane, S.K. & Arya, S.S. 2015. Effect of drying and storage on bioactive components of jambhul and wood apple. *Journal of Food Science and Technology* **52**(5), 2833–2841.

Terazawa, Y., Ito, K., Masuda, R. & Yoshida, K. 2001. Changes in carbohydrate composition in pumpkins (Cucurbita maxima) (kabocha) during fruit growth. *Journal of the Japanese Society for Horticultural Science* **70**(5), 656–658.

Tomsone, L. & Kruma, Z. 2014 Influence of freezing and drying on the phenol content and antioxidant activity of horseradish and lovage. *Proc. Conf. FoodBalt 2014*, Jelgava, Latvia, pp. 192–197.

Yang, J., Chen, J., Zhao, Y. & Mao, L. 2010. Effects of Drying Processes on the Antioxidant Properties in Sweet Potatoes. *Agricultural Sciences in China* **9**(10), 1522–1529.

Yu, L., Perret, J., Harris, M., Wilson, J. & Haley, S. 2003. Antioxidant Properties of Bran Extracts from ‘Akron’ Wheat Grown at Different Locations. *Journal of Agricultural and Food Chemistry* **51**, 1566–1570.

Ермаков, А.И. 1987. Methods of biochemical analysesof plants (Методы биохимического исследования растений). Под ред. А.И.Ермакова, Ленинград, ВО «Агропромиздат», pp. 112–113 (in Russian).

Agronomy Research **16**(4), 1742–1751, 2018
https://doi.org/10.15159/AR.18.162

Biostability of cotton fibers with different natural colors and selection

O. Kotomenkova[1,*] and A. Vinogradova[1,2,*]

[1]Peter the Great St. Petersburg Polytechnic University, Institute of Industrial Management, Economics and Trade, High economic and trade school, Polytechnicheskaya street 29, RU195251 St. Petersburg, Russia
[2]Saint Petersburg National Research University of Information Technologies, Mechanics and Optics, Faculty of Technological Management and Innovation, Kronverksky Prospect 49, RU197101 St. Petersburg, Russia
[*]Correspondence: kot-og@yandex.ru; ann-vin@yandex.ru

Abstract. Biodamageability is one of the weak sides of the cotton-plant fiber. Economic loss from the cotton damage caused by microorganisms is significant. Toxic chemical compounds are used to preserve the cotton fiber. This has a negative impact on environment and cotton consumers. The degree of the cotton biodamage depends on selection variety, types of cultivation, storage conditions and other factors. One of the directions in cotton planting is selection of the boll-stained cotton. It was established that naturally colored cotton of different varieties has high biostability. It allows to product hypoallergenic, eco-friendly textile and reduces impact on the environment. The purpose of the work is stability evaluation for microbiological damage of different cotton varieties including those naturally colored during long-term storage in different temperature and humidity conditions. The research lasted for 10 years. The species composition of the cotton microflora was determined, the impact of fiber on microorganisms and dynamics of samples biodamage was studied in the work. The results obtained show preservation of microflora viability on cotton fiber when storing it under normal conditions for a long-term period. With an increase in temperature and humidity necessary for microorganisms' growth, the fiber destruction processes are amplified. It was established that cotton damage degree depends on the regimes and terms of its storage as well as the color of the fiber. Nature-colored cotton is more resistant for microorganisms, some varieties inhibit the growth of mold fungi.

Key words: biostability, cotton fibers.

INTRODUCTION

One of the directions in the field of cotton breeding is the creation of boll-stained cotton selections. The research of nature-colored cotton was subject of a number of works (Elesini et al., 2002; Grigoryev & Illarionova, 2009; Pekhtasheva et al., 2012). The usage of nature-colored cotton is capable of producing ecologically clean textiles and eases-off the environment thanks to refusal to use synthetic dyestuff.

The problem of lint is its biological damageability. Economic damage from cotton damage with microorganisms reaches sizeable amounts (Yermilova, 1991). To save lint, toxic chemical mixtures are often applied. It is negative for the environment and consumers of cotton goods. The grade of cotton biological damage depends on elite selection, ways of cultivation, storage conditions and other factors.

Many authors mentioned in their works higher biostability of nature-colored cotton in separate grades compared to white cotton (Grigoryev & Illarionova, 2009; Pekhtasheva et al., 2012).

The purpose of the work was stability assessment of cotton fibers of different grades with white and nature-colored fiber to microbiological damages on long storage in various conditions of temperature and humidity. The species composition of cotton flora, dynamics of biological damage of samples was defined, and influence of fibers on microorganisms was studied in the work.

MATERIALS AND METHODS

As objects of the research, samples of cotton fibers with green, beige, brown nature-color were chosen. Also a sample of white cotton from selection 175-F was investigated.

For a research of questions of fibers and microorganisms' interaction bacterium and the microfunguses were used, as they had an ability to damage cotton fibers and their goods. These are bacterium – Bacillus subtilis, Basillus pumilus, Pseudomonas fluorescens, Erwinia herbicola, Bacillus sp. and microfunguses – Aspergillus niger, Aspergillus terreus, Penicillium variabili, Penicillium cyclopium, Penicillium chrysogenum, Chaetomium globosum.

The effect of fibers on microorganisms was assessed with a method of agar plates in a direct impact of fibers on live cells of bacterium and mushrooms growing on the growing medium (meat-peptonic agar for bacterium and a wort agar for mushrooms). For this purpose, 10 mg of a fiber with a mass rolled into a ball were put into the center of a Petri dish on a growing medium, inoculated in a definite form of a microorganism. To control it, the cups sown with bacterium or mushrooms but without a fiber pattern were used. The inoculation of equal number of microbe cells was provided in each dish. This was made with the help of prior preparation of clean culture of microorganism dilutions in sterile physiological solution. This dilution contained 1 billion microbe cells per 1 mL of suspension (10 Turbidity units) which was controlled according to turbidity standards. Then 1 mL of the received suspension was put into a Petri dish and spread evenly on the agar plate surface. Thus, a solidly even growth of a microbe colony was obtained in all dishes. Crops were thermostated at a temperature of 30 °C within one day for bacterium and 7 days at a temperature of 26 °C for mushrooms. The degree of microorganisms' sensitivity to fibers was determined by the presence/absense of a sterile zone around the species and by the solidity change in the microbic colonies growth in the dishes with fibres as compared with test ones. The tests were carried out for each type of cotton fiber and each microbic culture in five replications.

Production of microorganisms from samples of cotton fibers and determination of their quantity were carried out by a seeding technique on dense growing mediums of washouts from fibers (Kotomenkova & Vinogradova, 2007). Identification of microorganisms was carried out by standard techniques using determinants of bacterium and microfunguses.

The research of samples biostability has been conducted during 10 years. The biostability degree of cotton fibers in relation to microscopic flora which is spontaneously found on them during the plant growth from the environment (the so-called ‘spontaneous microscopic flora’) was evaluated.

The first stage was carried out in 2006. After the initial damage of cotton fibres was determined, they were placed for storage in various conditions.

The first species series was kept in a climatic chamber during 30 days, under the conditions which were most favorable for the microorganisms’ growth (air temperature of 26–30 °C, relative humidity was 90–100%).

The second species series was put for long-term storage under normal conditions (air temperature 18–22 °C, the relative humidity was 60–65%) for 10 years. After the 10-year storage, the species were returned to the conditions which were favorable for microorganisms’ development.

To evaluate the biostability of cotton fibers, their structure condition was determined at the beginning of the experiment and after each storage stage.

The degree of fibers damage was determined by the optical microscopy method, with application of MIKMED-5 microscope (LOMO, Russia).

For biostability research samples of cotton fibers were cultivated in a climatic chamber for 30 days under normal conditions of storage (air temperature was 18–22 °C, relative air humidity was 65%) and under optimal conditions for growth and reproduction of microorganisms (air temperature was 26–30 °C, relative air humidity was 90–100%).

Damage degree of fibers was determined by a light-microscopical method. At the same time, types of changes of fiber composition were revealed with the subsequent measure calculation of biological destruction according to the following formula (1) (Yermilova, 1991):

$$k = 0.002x_1 + 0.025x_2 + 0.255x_3 \qquad (1)$$

where k – is an indicator of biological destruction of a fiber; x_1, x_2, x_3 – is a quantity of damage by classes A, B and C respectively; k_1, k_2, k_3 – are coefficients of weightiness of damages by classes A, B and C.

Damages of Class A include the first changes in fibers surface: fouling by microorganisms and their metabolites, surface unevenness and small cracks.

Class B unites stronger destruction manifestations: deep cracks, swelling, thinning out, side damages.

Class C includes fibers exfoliation, deep local side damage and fibers degradation.

The value of a destruction indicator $K \leq 0.3$ corresponds to the initial changes of a fiber surface which do not affect its internal composition; in the range of $0.3 < K \leq 3.55$; not only a surface is destructed, but internal sites of fibers, which is followed by initial changes of its composition; in the range of $3.55 < K$ is a deep biological destruction of fibers at all levels (Yermilova, 1991).

The fibers structure changes under the influence of microorganisms were studied with the use of electronic microscopy (PEM) and infra-red spectroscopy (FTIR).

For the study of the thin structure of cotton fibers surface an electronic microscope JSM-T200 (JEOL, Japan) was used. The material was assembled on the table and sputtered with gold in vacuum. Each preparation was examined in 20–30 fields of vision; the most characteristic changes were photoed.

Infra-red fibers spectra were taken on a double-beam spectrometer UR-10 (Carlzeiss Jena, Germany) with retrievable automatic prisms. The spectra were taken in a wave number range from 400 to 4,000 cm^{-1}. The samples were prepared according to a moulding technique. Potassium bromide was applied as a moulding matrix. The fiber weight quantity constituted 5 mg.

Structure changes of damaged fibers were evaluated by comparing the IR-spectra parameters (the changes in the width, shape and size of the absorption band) before and after they have been influenced by microorganisms. The IR-spectra decoding was exercised on the basis of research works in the given sphere.

Processing of results was carried out by means of methods of mathematical statistics.

RESULTS AND DISCUSSION

When fibers and microorganisms cooperate the influence is of a bilateral character. Its results largely determine the textile fiber biostability in the process of its storage and operation.

In this respect, the research results should be divided into three parts:

The microorganisms' reactions to the fibers' impact

The results of impact assessment of the studied samples of cotton fibers on bacterium and microfunguses are presented in Table 1. All the considered microorganisms are the disruptors of cotton.

Table 1. The effect of fiber on bacterium and microfunguses

Microorganisms	Diameter of a growth inhibition zone, mm the color of cotton fiber			
	green	brown	beige	white
1. Bacterium				
Bacillus subtilis	0	0	0	0
Basillus pumilus	0	0	0	0
Pseudomonas fluorescens	0	0	0	0
Erwinia Herbicola	0	0	0	0
Basillus sp.	0	0	0	0
2. Microfunguses				
Aspergillus niger	0	0	0	0
Aspergillus terreus	growth intensity decrease*	growth intensity decrease*	growth intensity decrease*	growth intensity decrease*
Penicillium variabili	0	0	0	0
Penicillium cyclopium	0	0	growth intensity decrease*	0
Penicillium chrysogenum	0	0	growth intensity decrease*	0
Chaetomium globosum	0	0	growth intensity decrease*	0

Note: Decrease of growth intensity as compared to growth in a test group.

The analysis of results shows that self-colored cotton does not possess an antibacterial action.

At the same time, it is established that a beige fiber suppresses growth of microfunguses of *Penicillium cyclopium, Penicillium chrysogenum, Chaetomium globosum* a little. All studied cotton fibers suppress growth of Aspergillus terreus.

White fiber of the cultivated types and the majority of modern cotton grades are the result of a longtime selection.

Fiber of wild species of a cotton is beige or pinkish to bronze (Gossypium anomalum Wawra et Peyr.), yellowish (Gossypium areysianum Defl.), light brown (Gossypium harknessii Brandg.), brown (Gossypium triphyllum Hohr.), dark brown (Gossypium armourianum Kearney.), brownish (Gossypium somalense Hutch.), brownish green (Gossypium klotzschianum Andress.), green (Gossypium sturtianum var. nandawarense (Der.) Fryx.), dark green (Gossypium davidsonii Kell.) tones. As selection practice shows, the sign of a fiber color is connected with his chemical composition, which, in turn, determines durability, and fineness. So, white fiber contains no more than 0.7–0.8% the adipoceratous substances whereas green one contains to 17.0% (Popova & Khafizov, 1985). Color is given to fiber by catechines (aromatic substances from group of flavonoids which oxidation products form the flobafenas, which cause brown, yellow-brown and blackish color and is antiseptic (Grigoryev & Illarionova, 2009).

Hence, the revealed decrease of growth intensity of microfunguses, as compared to the test group, can be a consequence of the fibers' chemical composition peculiarities or of the antagonistic action of the epiphytic bacterial flora contained on fiber. As it is known, the bacteria of the *Bacillus subtilis* group, which are a part of it, produce biologically active connections of antifungal action (Loeffler et al., 1990).

It should be noted that after cultivating the fibers of natural green color on a growing medium with microorganisms the intensity and brightness of green color increased.

The reason of this effect was not studied in the process of the given research. However, the authors consider this effect to be interesting for researchers studying the color of self- colored cotton and its changes.

The study of microorganisms' quantity and species composition on the fibers

The study of microorganisms' quantity and species composition on the cotton fibers was exercised with initial samples, before their biostability test.

The quantity of microorganisms separated from the studied samples of cotton fibers was not equal (Table 2). Most microbial cages are separated from a green cotton fiber, least are separated from with white cotton fiber.

Table 2. The number of live bacterial cells separated from cotton fibers samples

Cotton fiber	Total microbial number, kl g^{-1} of fiber	Cotton fiber	Total microbial number, kl g^{-1} of fiber
green	$3.17 \cdot 10^5$	beige	$2.00 \cdot 10^5$
brown	$1.30 \cdot 10^5$	white	$0.77 \cdot 10^5$

But the number of microorganisms on the fiber is not a direct reason of its biostability (Kremer, 1987).

Among the microorganisms-destructors which are a part of flora separated from samples of cotton fibers epiphytic sporous bacterium of the *Bacillus subtilis* group prevail. The composition of microfunguses is small and quite conformed (Table 3).

Table 3. Mushroom micromycetes separated from control samples of cotton fibers

Cotton fibers	Mushroom micromycetes
green	*Aspergillus niger, Penicillium chrysogenum*
brown	*Aspergillus niger*
beige	*Aspergillus niger, Penicillium chrysogenum, Paecilomyces variotii*
white	*Aspergillus niger*

The study of cotton fibers' biostability, of various colors and selections

The results of the biostability research of cotton fibers upon storage in various temperature-humidity modes are presented in Table 4. Fig. 2 presents a diagram of the destruction indicator changes, which demonstrates the speed of cotton fiber destruction in various storage conditions.

Table 4. Biological damageability of cotton fibers under various storage conditions

Self-color of cotton fibers	Exposing period and conditions					
	2006, 30 days, temperature 26–30 °C humidity 90–100%		2006–2016, 10 years, temperature 18–22 °C humidity 60–65%		2016, 30 days, temperature 26–30 °C humidity 90–100%	
	Fiber destruction indicator, K		Fiber destruction indicator, K		Fiber destruction indicator, K	
	Initial fiber, K_0	Exposed fiber K_n	Initial fiber, K_0	Exposed fiber K_n	Initial fiber, K_0	Exposed fiber K_n
green	0.23	3.11	0.23	0.68	0.68	3.58
brown	0.22	1.59	0.22	0.57	0.57	2.24
beige	0.18	0.42	0.18	0.30	0.30	1.66
white	0.14	0.47	0.14	0.41	0.41	2.33

The composition analysis of initial the self-colored fibers (2006) reveals the presence of overgrowing by microorganisms on all models and (in certain cases) an insignificant streakiness (cracks, deepened surface). Value of a destruction indicator for these fibers is $K \leq 0.3$ that shows initial changes of a fiber surface which do not affect its internal composition. After exposing the cotton fibers, an increased total number of damages and the destruction indicator are revealed at all studied fibers. The green fiber was most severely damaged ($k = 3.11$).

The composition analysis of the initial self-colored fibers (2006) reveals the presence of initial structural changes on all models: overgrowing by microorganisms on all models and (in certain cases) an insignificant streakiness (cracks, deepened surface). The value of a destruction indicator for these fibers is $k \leq 0.3$ that shows initial changes of a fiber surface which do not affect its internal composition.

After exposing the cotton fibers in conditions, favorable for microorganisms' development, during 30 days, an increased total number of damages and the destruction indicator are revealed at all studied fibers. The green fiber was most severely damaged ($k = 3.11$). The values of the destruction indicator of this fiber are close to the limit, characterizing the transition to the third qualitative gradation characterizing deep biological destruction at all compositional fiber levels (Fig. 1).

Microscopic examination of samples shows damage, such as destruction of the wall; almost all the fibers have overgrowing. The brown fiber (k = 1.59) has wall damages. Beige and white fibers have high biostability under these conditions: the values of the destruction indicator do not exceed 0.47 (7 times weaker than the green fiber).

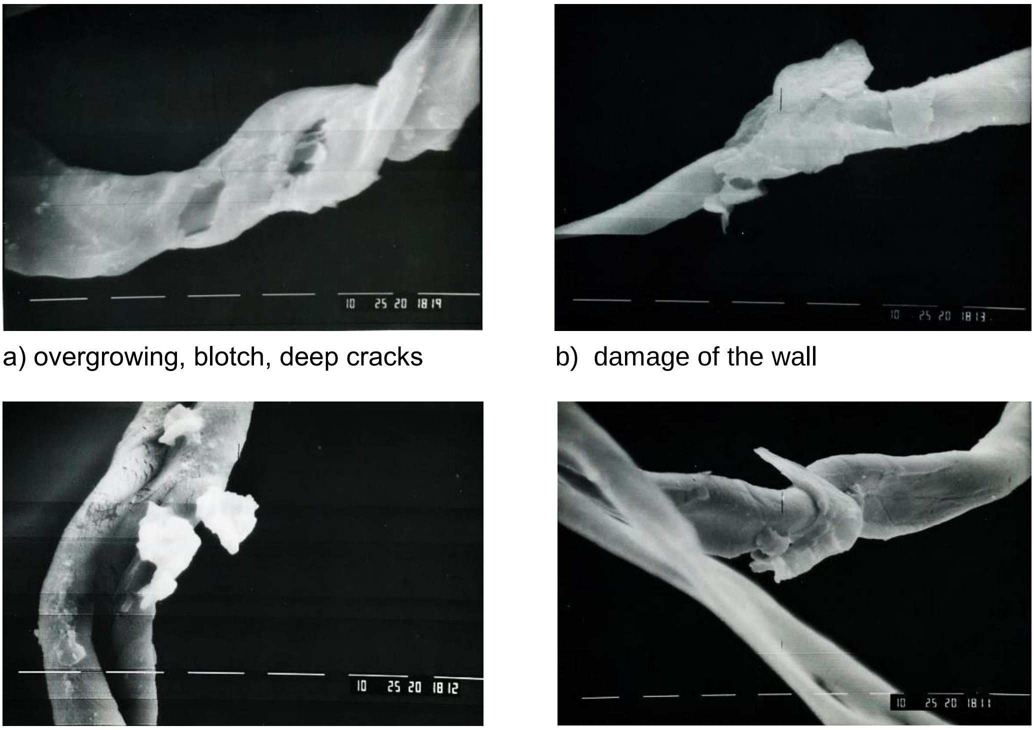

a) overgrowing, blotch, deep cracks

b) damage of the wall

c) overgrowing and blotch

d) cracks and wall damage

Figure 1. Damages of cotton fibers with microorganisms.

Judging by biological destruction the self-colored cotton fibers stored in conditions, optimum for development of microfunguses and bacterium it is possible to arrange the following row: green > brown > white > beige. In comparison with the initial fiber, the green fiber is damaged 13.5 times stronger, and the beige one is damaged only by 2.3 times.

The research of the nature and the degree of damages of the cotton samples stored in normal conditions (air temperature is 18–22 °C, relative humidity of air is 65%) within 10 years (2006–2016) allows to establish the following. The green (k = 0.68) and the brown (k = 0.57) fibers were most severely damaged, there are damages like swelling, stratifications; the beige fiber had only overgrowing and a weak streakiness; the biological destruction indicator for it has remained at the level of boundary values of the beginning of damage (k = 0.3).

Judging by cotton fiber destruction stored in normal conditions within 10 years, it is possible to arrange the following row: green > brown > white > beige, green and white fibers are damaged 3 times more severely, and beige one only by 1.7 times.

With the increase of relative humidity of air up to 90–100% and temperature up to 26–30 °C, the damage rate of fibers suddenly increased: the white one increased almost by 7 times, the beige and green ones increased more than by 5 times, and the brown one increased almost by 4 times. The white cotton has all types of damages: severe streakiness, swellings, the damaged walls, stratifications. The beige and green fibers demonstrate very strong overgrowing and clump of biomass, strong stratification. Brown fiber has only punctate overgrowing, separate swellings and wall damages.

The results of the analysis of infrared ranges of absorption of the studied fibers will be coordinated with the data of the microscopic analysis. The beige fiber has the amorphisation of composition connected with increased hydrophilicity of a sample (area 1,630 of cm^{-1}) and increased proteinous weight due to the growth of microorganisms (the presence of peptide groups in the field of 1,640–1,660 cm^{-1} and 1,540–1,560 cm^{-1}). The brown and white fibers are characterized by deep destruction: a large number of ruptures of molecular chains (1,720–2,900 cm^{1}) and proteinous weight (increased absorption in the field of 1,540–1,560 cm^{-1}). The green fiber has the stronger compositional changes: increased content of carboxyl groups in comparison with the initial one. It demonstrates oxidizing destruction of cellulose, deep amorphisation of fiber as a result of a rupture of the main macromolecules.

The results of the research of dynamics of change of the biological destruction indicator are coordinated with the general damage tendency of cotton fibers by microorganisms (Fig. 2).

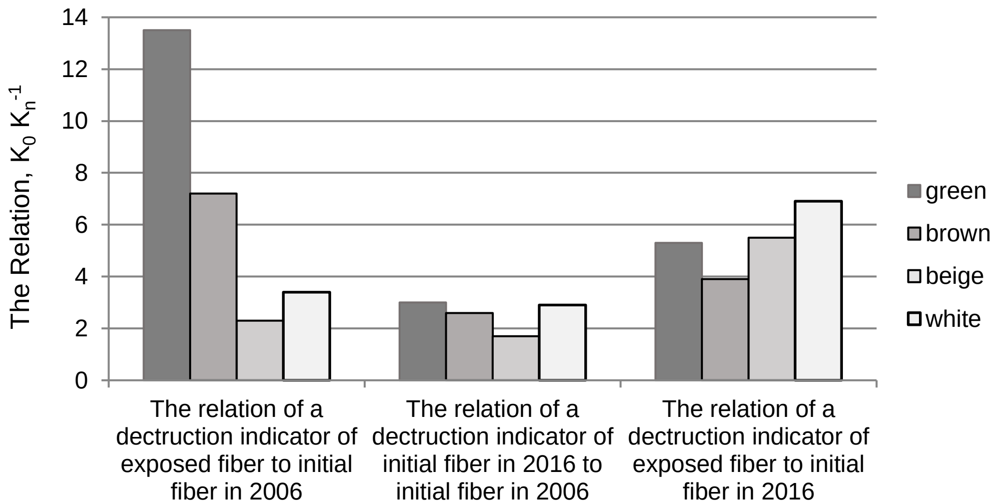

Figure 2. Changes in the cotton fibers' destruction indicator in various storage conditions; K_0 – the initial fiber destruction indicator (start of storage period); K_n – the exposed fiber destruction indicator.

The analysis of the data of Fig. 2 shows that at exposition of fibers in 2006 green fiber has the largest damage speed by microorganisms, brown one is a little smaller. In beige and white fiber, the rate of change in biodegradation speed is the lowest for the present period.

The change in the structure is due to the presence of amorphous sites in cotton fiber, where the thinnest capillary is the penetration channel of microbial enzymes deep into the cellulose composition (Kotomenkova, 2012).

However, at repeated exposition after 10 years in 2016 the damage intensity of all fibers increases approximately equally highly in connection with reclamation of new surfaces by microorganisms, and deepening the biological destruction processes (transition of damages by classes A and B into damages by classes B and C respectively).

CONCLUSIONS

The obtained results lead to the conclusion that self-colored cotton doesn't possess anti-microbe qualities in relation to disrupting microorganisms. However, cotton with self-colored beige fiber cause the decrease of growth intensiveness for particular microfunguses, such as: Aspergillus terreus, Penicillium variabili, Penicillium cyclopium, Penicillium chrysogenum, Chaetomium globosum. The similar activity in relation to Aspergillus terreus is determined for all cotton fibers studied in the paper. The discovered fungistatic activity of beige cotton fiber agrees with the results of its biostability evaluation. This kind of cotton demonstrated the greatest stability against the activity of destructing microorganisms among the studied samples.

Microorganisms included into microflora composition of the studied cotton fibers do not show any species diversity; they are known as disrupting microorganisms for cellulosic materials. The micromycetes isolated from the samples are included into a standard set of species which are used in tests for funginertness.

From cotton fibers of various colors a different number of microbe cells was isolated. Their biggest number was stated in cotton of a natural green color. Green cotton fiber has also the greatest biodamage degree among all studied cotton samples according to the results of biostability testing.

The received results demonstrate preservation of flora viability on cotton fiber during keeping it for a long time in normal conditionns without additional power supplies. Biological destruction of cotton fibers takes place under the normal storage conditions too. Increased temperature and humidity of air necessary for the growth of microorganisms lead to increased processes of fiber destruction. It is established that the damage degree of cotton depends on the modes and the periods of storage and on color of fiber.

The received results can be used in selection of nature-colored cotton, decreasing losses in the process of storage of cotton fiber, improving properties of the produced textiles when modeling processes of biological damageability.

ACKNOWLEDGEMENTS. The authors express their deep gratitude to their supervisor Professor Ermilova, I.A. for the sharing of knowledge and warm attitude, Professor, Botanical Institute of Komarov, V.L. Lebedeva, E.V. for her outstanding work on the identification of microorganisms.

REFERENCES

Elesini, U.S., Čuden, A.P. & Richards, A.F. 2002. Study of the green cotton fibres. *Acta Chim*. **49**, 815−833 (in Slovak).

Grigoryev, S. & Illarionova, K. 2009. Selection of cotton for improving the quality of colored fiber. Moscow. *Agricultural Biology* **3**, 83–87 (in Russian).

Kotomenkova, O.G. 2012. Biodegradability of special materials during storage. *Problems of Economics and management in trade and industry*. No. **2**. pp. 73–81 (in Russian).

Kotomenkova, O.G. & Vinogradova, A.V. 2007. *Security and safety materials for the manufacture of military clothing*. Saratov, Nauka, 80 pp. (in Russian).

Kremer, R.J. 1987. Identity and properties of bacteria inhabiting seeds of selected broadleaf weed species. *Microbial Ecology* **14**(1), 29–37 (in English).

Loeffler, W., Katzer, W. & Kremer, S. 1990. Antibiotics of the Bacillus subtilis group effective against fungi (Gegen Pilze wirksamen Antibiotika der Bacillus subtilis-gruppe). *Forum Mikrobiologie* V. **3**(3). pp. 156–163 (in German).

Popova, P.Ya. & Khafisov, I.K. 1985. Natural color of cotton fiber. In: *Encyclopedia of Cotton Growing*. Tashkent, 306–307 (in Russian).

Pekhtasheva, E., Neverov, A., Zaikov, G. & Sofina, S. 2012. Biostability of natural colored cotton fibers., Kazan, *Bulletin of Kazan Technological University* **15**(5), pp. 110–112 (in Russian).

Yermilova, I.A. 1991. *Theoretical and practical bases of microbial degradation of chemical fibers*. Moscow, 248 pp. (in Russian).

Agronomy Research **16**(4), 1752–1761, 2018
https://doi.org/10.15159/AR.18.151

Field trajectories proposals as a tool for increasing work efficiency and sustainable land management

M. Kroulik[1,*], J. Hula[1] and V. Brant[2]

[1]Czech University of Life Sciences Prague, Faculty of Engineering, Department of Agricultural Machines, Kamycka 129, CZ16500 Prague, Czech Republic
[2]Czech University of Life Sciences Prague, Faculty of Agrobiology, Food and Natural Resources, Department of Agroecology and Biometeorology, Kamycka 129, CZ16500 Prague, Czech Republic
[*]Correspondence: kroulilk@tf.czu.cz

Abstract. Together with the requirement for higher productivity the average performance and the weight of agricultural machines are increasing. Agricultural land is increasingly exposed to pressures caused by agricultural machinery. The heavy agricultural machinery passes across a field are frequently associated with technogenic soil compaction. Soil compaction is one of the main problems of modern agriculture. From the previous measuring of the traffic intensity it was found 86.13% of the total field area was run-over with a machine at least once a year, when using conventional tillage and 63.75% of the total field area was run-over when using direct seeding technology, with dependence on the working width of the machines. Field passes are inevitable in present agriculture. As a result of the increase of total machines weight, it is necessary to optimize the traffic lines trajectories and limit the entries of the machines in the field. At present, the choice of traffic lines direction is based primarily on the experience of drivers or the practice of farmers. There are a number of influences that affect the machine work efficiency. Monitoring of the tractor, on an irregular 8 fields showed the following results. Eight-meter working width tiller or seeder brought shortening of total length of turns at headlands with the change in trajectory azimuth. For purposes of measuring the monitored tractors were equipped with monitoring units ITineris. An overview of the chosen directions of the trajectories and the lengths of working and non-working passes was obtained. Based on the shape of the plot, the trajectory of the lines was also modelled. Suitable traffic lines directions in terms of the ratio of work and non-work passes were searched.
Based on records of real trajectories, the ratio of working and non-working path ranged between 6.3 and 15.2%. It was obvious from the results that the shortening of non-working passes and turns in comparison with the originally chosen trajectory directions was achieved by optimization. This was especially valid for complex shapes of fields. Trajectory optimization leads to a reduction of total length of path in all cases. The reduction in total length of path ranged from 69.7 m to 1,004.8 m. Changing the length of the working path ranged from 10.9 m to 264.9 m with the change in azimuth. The extension was observed in three cases. The highest part on the change of the overall length of the path presented nonworking rides.

Key words: azimuth, optimization, length of rides.

INTRODUCTION

Contemporary farming systems are associated with negative impacts on soil, which damage both production and non-production functions of soils. Agricultural land is exposed to pressures from tractors, harvesters and vehicles. Field passes are unavoidable in today's agriculture. The primary negative consequence of random crossings on field is soil compaction. The fundamental problem of soil compaction changes determination is the correct interpretation of the results because it is a difficult to measure property whose values are influenced by another properties of soil conditions. The undesirable soil compaction due to agricultural passes becomes a worldwide problem (Håkansson et al., 1988; Gysi, 2001; Chamen et al., 2003; Hamza & Anderson, 2005; Chan et al., 2006). Soil compaction is not a seasonal problem, but the traces of undesirable compaction can also be observed over several years. The soil has different compaction resistance – important factors include grain soil distribution, current soil moisture, soil organic matter content and soil structure. Heavy machinery passes are also reflected in the crop yields and can be observed for many years (Radford et al., 2007).

At present, the choice of trajectory direction is based primarily on driver experience or farmer habits. The implementation of field operations significantly influences the energy performance of agricultural production, expressed in terms of fuel consumption (Boxberger & Moitzi, 2008). As Edwards et al. (2017) reported that trajectory optimising provides important benefits for infield operations. The main benefits include reducing labour, costs, fuel consumption and field trafficking intensity. The intensity passes and associated soil compaction with them includes, besides the economic impact, a number of environmental risks like greenhouse gases (GHGs) from fertilised soils (Tullberg et al., 2018) or erosion treat (Li et al., 2007).

Landers (2000) or Jílek & Podpěra (2005) showed that there are a number of influences that affect the efficiency of machine work. The shape of the field, its size, terrain, obstacles and machine working width play a significant role in this respect. In our conditions, fields where two opposite sides are not parallel can be considered as a standard. Brunotte & Fröba (2007) demonstrated the influence of the different shapes of the field on the need for time for ploughing of the field. The need for time ranged from 100% for rectangular plot (aspect ratio 1: 2) to 117.76% for irregular shape. The navigations methods of agricultural machines moving on field, which are influenced by shape and size parameters of soil blocks, including interaction with the relief of the area of interest, have a significant impact on soil degradation processes, especially on soil compaction (Horn et al., 2000; Botta et al., 2006), including the subsequent long-term persistence of this phenomenon (Berisso et al., 2012). The influence of the shape and size of the soil block in interaction with the movement of the machines is then reflected in the economics of the growing systems and consequently in the overall economic efficiency of the agricultural subject.

Also Jin & Tang (2010; 2011) reported that trajectory planning has great potential to find the best infield path which leads to the field operation costs reducing. This potential increases with adoption of agricultural guidance.

Seufert (1995) considers the analysis of the influence of the size and shape of the field in terms of optimizing work operations as one way to increase the productivity of field crops and reducing of energy requirements and consequently the reducing of greenhouse gases emissions (Hameed, 2014). The main aim of the article is the modelling of optimal trajectories with regard to the shape of the field and the impact assessment on the lengths of working and non-working rides. As Oksanen & Visala (2009) mentioned, path planning is an important part of an intelligent agricultural field machine. The machine can be a traditional tractor driven by a human with a navigation system, an autonomous vehicle or a mobile robot.

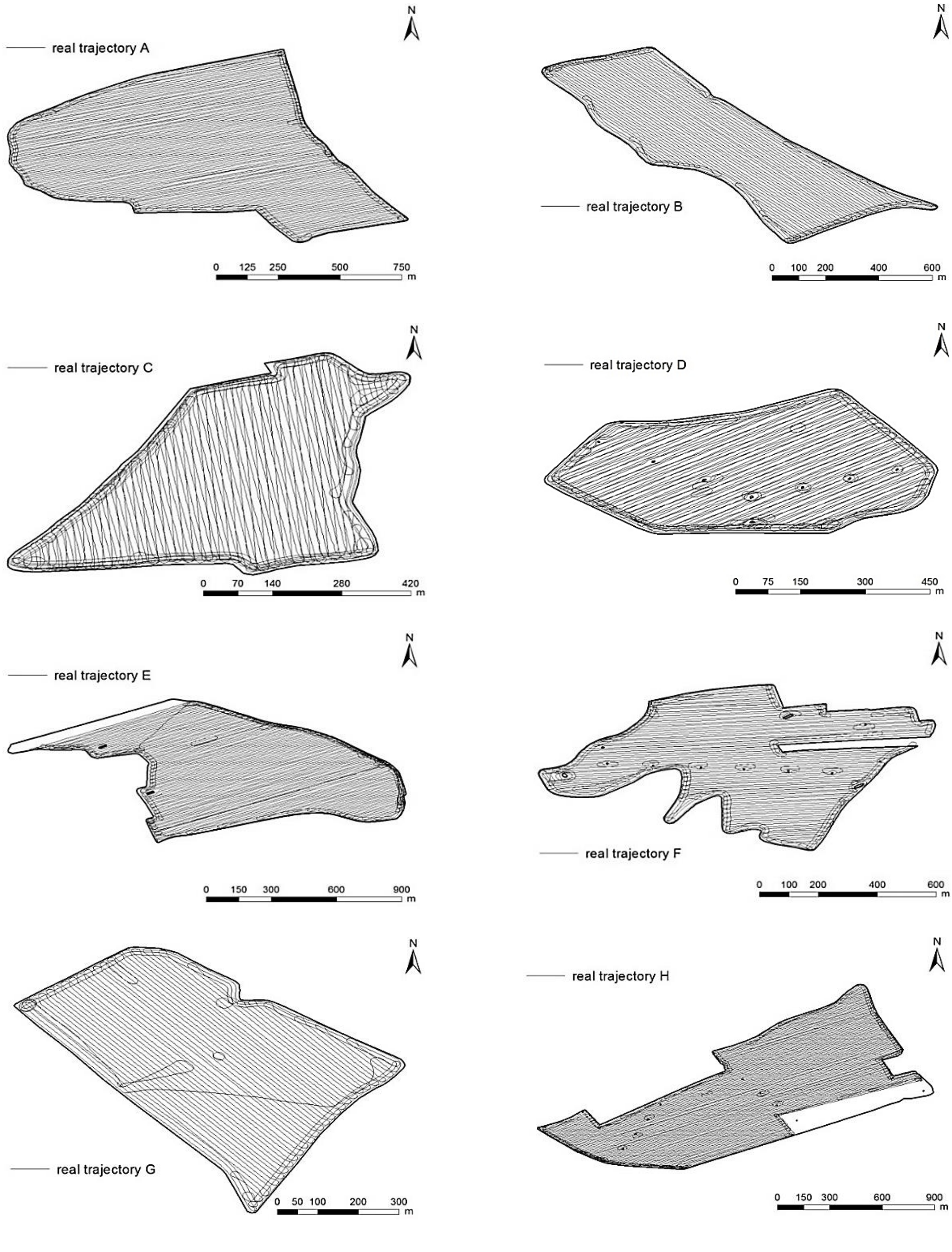

Figure 1. Selected fields and recording of the real direction of machine work trajectories.

MATERIALS AND METHODS

For the evaluation of the movement of machine on field, 8 fields with different shape and acreage were selected. The range of the monitored fields varied from 14.42 to 68.03 ha, (1 ha represents 10,000 m^2).

The tractor was fitted with the ITineris monitoring unit (ITineris Informatikai, Hungary) with a continuous machine position record. On the basis of the driving record, real work trajectories of the machines were obtained (Fig. 1). Data were collected during the work of sowing machine with a working width of 8 m (field A, B, E, F, G, H) and tiller with a working width of 8 m (field C and D).

The next step was the modelling of trajectories for individual fields. The OptiTrail (LeadingFarmers, joint-stock company, Czech Republic) program was used to model the trajectories. For each plot, a total of 180 driving directions were determined with a step of 1°. For the trajectory calculation, the model needs four inputs and parameters, shape of field, which is described by shapefile, working width of machines, number of rides at headlands and minimum turning radius. For the individual trajectories, the lengths of working and non-working rides, length of transport distance, the number of turns and the length of the rides at the headland were calculated. This calculation is created for each azimuth and stored as table. The algorithms attempt to find the shortest possible total path distance for the machine. Direction of the shortest trajectory is stored as A-B line for field guidance. The algorithms attempt to find the shortest possible total path distance for the machine. Direction of the shortest trajectory is stored as A-B line for field guidance. It presents real utilizations of outputs. However the last decision have farmer who decides for trajectory according to the slopes of the fields.

Based on the length of the ride, the most appropriate option was selected and then compared with a variant that was identical to the direction of the ride according to the real record. Software Microsoft office (Microsoft Corporation, Redmond, USA) and ArcGIS 10.4.1 (ESRI, Red lands, USA) were also used.

RESULTS AND DISCUSSION

On the basis of actual trajectory recordings it was possible to determine the real trajectories of work. Based on the model, the parameters of the work rides were calculated for these directions. These values are given in Table 1. For land C and D, lengths were set for two passes due to a double ride during the preparation of the soil. The length of the drive on the headlands for each plot was determined from two hugs of fields.

The ratio between working and non-operating rides ranges from 6.3 to 15.2%. As illustrated by the graph in Fig. 2 with increasing acreage of field the ratio of working and non-working rides has a downward trend. This is consistent with the work of Wagner (2001). He states that the field acreage increasing is associated with a positive effect on reducing the working time per unit area due to a decrease of the time of machine turning. Demmel et al. (2014) report that increasing of the size of the soil block contributes to increasing the efficiency of sugar beet production. On the other hand, the irregular shape of the field may be connected with increase the value of its circumference and thus the occurrence of areas of weed species, which are spread on field around the fringe of fields (Brant et al., 2006; 2008). Increasing the boundaries of field as a contact area with the surrounding landscape increases the risk of application of fertilizers or pesticides outside the boundaries of the field.

Table 1. Model values of travel lengths based on the real azimuth of the rides

Field	Azimuth	Total length of rides, m	Length of working rides, m	Length of turns, m	Number of turns	Length of headland rides, m	Transport, m
A	79°	65,632.14	56,176.61	3,191.88	97	5,905.55	358.10
B	124°	35,223.06	27,662.62	1,842.74	56	5,022.57	695.13
C	165°	21,561.24	15,800.06	2,402.14	73	3,359.04	0.00
	175°	21,698.85	15,835.03	2,237.61	68	3,359.04	267.18
D	65°	20,232.78	15,902.32	1,447.86	44	2,882.59	0.00
	75°	20,599.80	15,993.90	1,283.33	39	2,882.59	439.97
E	72°	58,723.93	48,532.71	2,895.73	88	6,368.83	926.66
F	85°	39,587.26	28,897.48	2,895.73	88	6,744.64	1,049.41
G	130°	27,518.20	21,823.51	1,776.92	54	3,747.85	169.91
H	70°	92,323.62	78,757.01	3,323.51	101	8,382.97	1,860.13

Fechner (2014) has determined the positive effect of optimizing trajectory of work passes to save time when measured on real soil blocks. The most significant time savings resulted from the optimization of trajectories on fields ranging between 10 and 40 ha. On fields with a larger area, the time savings were below 10% compared to the current work rides. In our case, the length of the rides was the main evaluated factor. Fig. 3 shows the changes in working and non-working lengths depending on the selected azimuth. In this example, field D was used.

As can be seen from Fig. 3, the total length of the ride on the field is significantly affected by the number and character of the turns. Transport crossings also contribute to the proportion of non-working rides. This is confirmed by Fechner (2014), which states that optimizing of work trajectories has significantly reduced the need for time to turning of machines at headlands of small and irregular plots. Fig. 4 shows the model trajectory set as optimal, calculated based on the shape of the field.

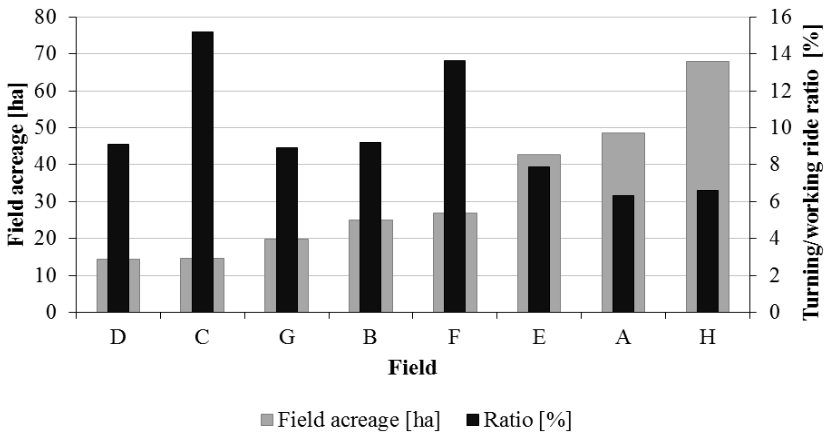

Figure 2. Values of the ratio of working and non-operating rides relative to the land acreage.

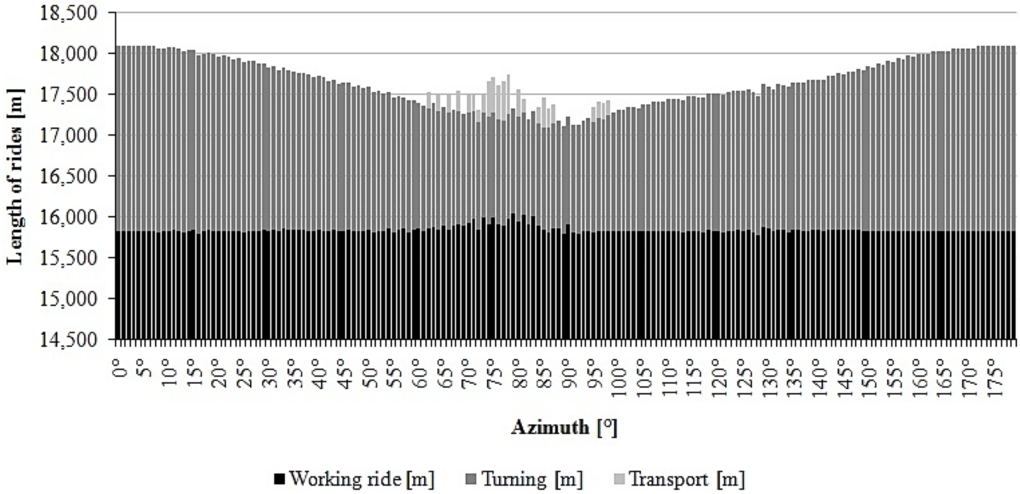

Figure 3. The lengths of working and non-working rides determined for each trajectory azimuth.

It is clear from the outputs that the azimuths of the model trajectories varied from the real routes in all cases. The performance of machines was modified by shape at the same acreage of the soil block. In general, the rectangle with a 1: 2 to 1: 4 aspect ratios is considered to be the optimal shape of the plot in terms of its management. Brunotte & Fröba (2007) stated that the change in shape of the plot from rectangular to irregular shape is associated with an increase in time consumption of more than 17% on a 20 ha field. Fig. 4 shows that the land showed significant shape differences and acreages. The opposite sides were not parallel in all cases. From the operator point of view, it is more difficult to select the optimal driving direction based on an estimate or experience. Table 2 provides an overview of optimized trajectory values. Headland length remains the same. The table shows the ratio of working and non-working rides for individual fields.

Table 2. Values of model rides based on optimized ride azimuths

Field	Azimuth	Total length of rides, m	Length of working rides, m	Length of turns, m	Number of turns	Transport, m	Working and nonworking rides ratio, %
A	90°	65,406.42	56,210.27	3,290.60	100	0.00	5.85
B	153°	34,835.16	27,542.07	2,270.51	69	0.00	9.17
C	45°	20,817.41	15,845.98	1,612.39	49	0.00	10.18
D	89°	20,002.07	15,803.24	1,316.24	40	0.00	8.33
E	73°	58,146.10	48,474.97	2,961.54	90	340.76	6.81
F	83°	39,464.26	28,632.53	2,895.73	88	1,191.36	14.27
G	143°	27,448.53	21,727.31	1,645.30	50	328.07	9.08
H	73°	91,318.82	78,785.44	3,718.38	113	432.02	5.27

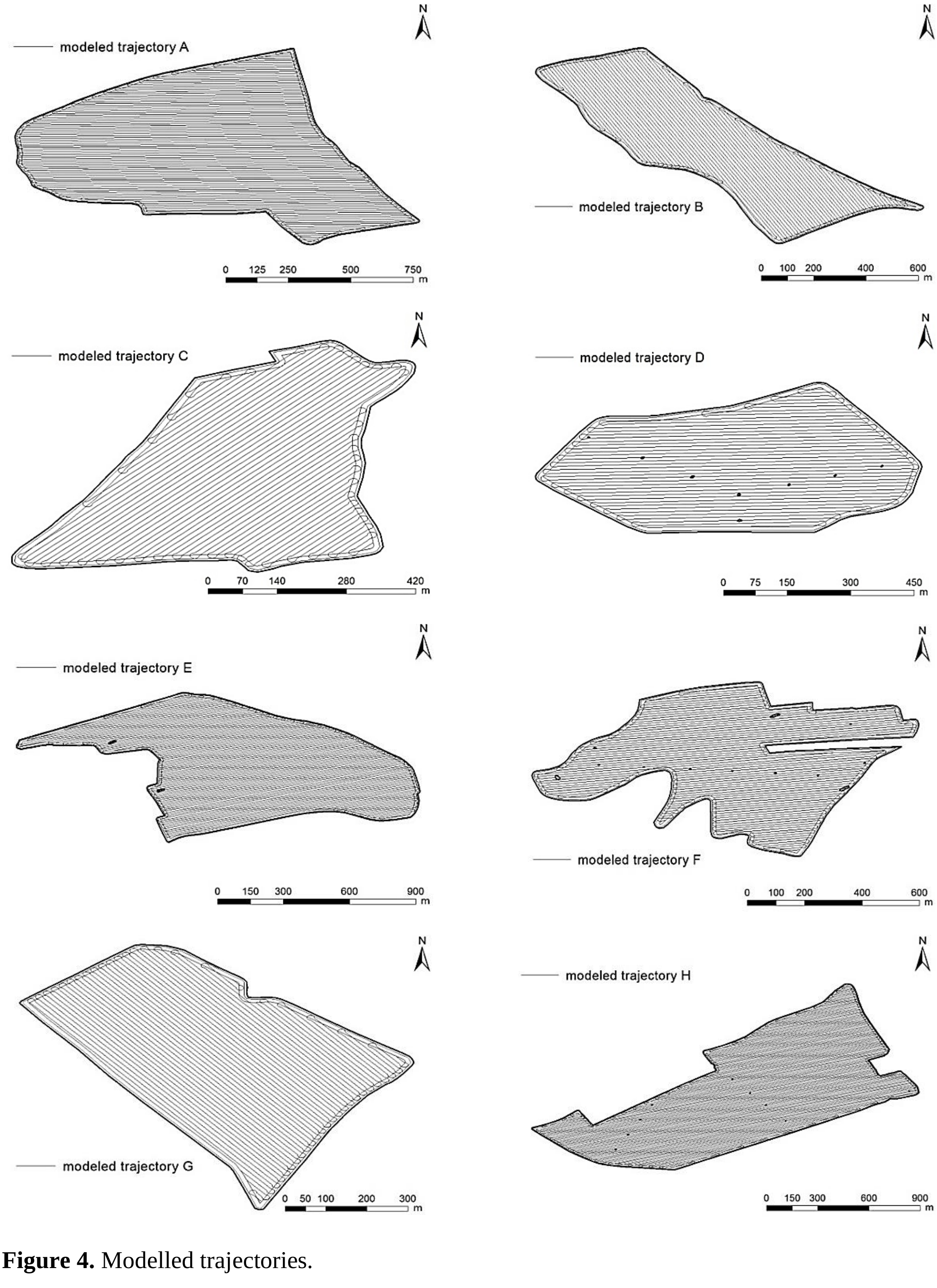

Figure 4. Modelled trajectories.

The number of rotations was reduced and the ratio of working and non-operating rides was improved in comparison with the real situation in all cases with exception of G and F fields. Differences in the ratio between real and model trajectories varied from 7.3 to 35.6%. There was no statistically significant difference between the working and non-operating path ratios of the real record and the model. However, any reduction in costs could ultimately mean economic and also environmental benefits. A slight increase in non-working rides occurred on the fields F and G, however, the total driving length was shortened. Field F presents a complicated shape with a high proportion of turns. The difference in trajectory azimuth was highest for plot C, where the deflection was equal to 120°. For fields B and D, the deflection was 29°, respectively 24°. For other plots, the deflection of the trajectories varied from 1° to 13° against the optimal model. Edwards et al. (2017) also describes a reduction in total journey time when optimizing routes compared to the operator. Bochtis et al. (2013) compared B-patterns against conventional field work patters. They showed reductions in non-working distance up to 58.65% and increases in the area capacity were up to 19.23% when compared with different types of conventional field-work patterns. From the other hand, the rolling terrains of many farms have considerable influence on the design of coverage paths (Jin & Tang, 2011; Hameed et al., 2013; Hameed 2014). Authors presented 3D planning algorithm. As Jin & Tang (2011) presented, the 3D planning algorithm saved 10.3% on headland turning cost during the field tests. Hameed (2014) demonstrates 6.5% reduction in the energy requirements when the driving angle is optimized by taking into account the 3D compared to the case when the applied driving angle is optimized assuming even field areas.

CONCLUSIONS

The results show the direction where modern technical resources can contribute to improving the quality of filed management and reducing adverse effects on soil. The results show that even a minimal change in driving direction can contribute to a reduction in the overall length of the ride on field and also contributes to a reduction in the turning on headlands. This measure contributes to more efficient machine work and reduced soil load. In addition, the results reveal further directions of research activities. The slope of the field does not always allow the optimal direction of the trajectory according to the shape of the plot. Other important elements on the land are, for example, the power lines which need to be bypassed. Route optimization can respect these lines and determine the direction of trajectories. Further work is still needed for the implementation of the sloping model in the calculation of trajectories. Also, from the minimizing of turning and passes point of view of, it seems to be a very interesting topic to align the boundaries of the fields and eliminate the folds from intensive field farming.

ACKNOWLEDGEMENTS. The project was supported by the Grant Agency of the Czech University of Life Sciences Prague (CIGA No. 20163005).

REFERENCES

Berisso, F.E., Schjønning, P., Keller, T., Lamandé, M., Etana, L., de Jonge, W., Iversen, B.V., Arvidsson, J. & Forkman, J. 2012. Persistent effects of subsoil compaction on pore size distribution and gas transport in a loamy soil. *Soil & Tillage Research* **122**, 42–51.

Botta, G.F., Jorajuria, D., Balbuena, R., Ressia, M., Ferrero, C., Rosatto, H. & Tourn, M. 2006. Deep tillage and traffic effects on subsoil compaction and sunflower (*Helianthus annus* L.) yields. *Soil & Tillage Research* **91,** 164–172.

Boxberger, J. & Moitzi, G. 2008. Energieeinsatz in der Landwirtschaft im Wandel, 7–16. In *Energieeffiziente Landwirtschaft. KTBL - Vortragstagung vom 8. bis 9. April 2008 in Fulda*. KTBL, Darmstadt, 248 pp.

Brant, V., Neckář, K., Venclová, V. & Krump, M. 2008. Vorkommen von Conium maculatum L. (Gefleckter Schierling) im Inneren und am Rand von Ackerflächen in der Tschechischen Republik. *Journal of Plant Diseases and Protection,* Special Issue **XXI**, 383–386.

Brant, V., Žamboch, M., Neckář, K. & Venclová, V. 2006. Einfluss der Ackerrandgesellschaften auf die Verunkrautung der Agrophytozönosen durch Arctium tomentosum Mill. (Filzige Klette). *Journal of Plant Diseases and Protection*, Special Issue **XX**, 605–609.

Bochtis, D.D., Sørensen, C.G., Busato, P. & Berruto, R. 2013. Benefits from optimal route planning based on B-patterns. *Biosystems Engineering* **115**(4), 389–395.

Brunotte, J. & Fröba, N. 2007. Schlaggestaltung – kostensenkend und bodenschonend. *KTBL-Schrift 460*. Darmstadt, 178 pp.

Chamen, W.C.T., Alakukku, L., Pires, S., Sommer, C., Spoor, G., Tijink, F.A. & Weisskopf, P. 2003. Prevention strategies for field traffic-induced subsoil compaction: a review: Part 2. Equipment and field practices, *Soil & Tillage Research* **73**, 161–174.

Chan, K.Y., Oates, A., Swan, A.D., Hayes, R.C., Dear, B.S. & Peoples, M. B. 2006. Agronomic consequences of tractor wheel compaction on a clay soil. *Soil & Tillage Research* **89,** 13–21.

Demmel, M., Rothmund, M., Auernhammer, H., Feldmann, J. & Rademacher, T. 2014. Infrastrukturplanung zur Optimierung des Zuckerrübenanbaues in einer Gewanneflur. *Landtechnik* **59,** 36–37.

Edwards, G.T., Hinge, J., Skou-Nielsen, N., Villa-Henriksen, A., Sørensen, C.A.G. & Green, O. 2017. Route planning evaluation of a prototype optimised infield route planner for neutral material flow agricultural operations. *Biosystems Engineering* **153**, 149–157.

Fechner, W. 2014. Einfluss der Hauptbearbeitung auf die Arbeitszeit im Feldbau am Beispiel eines mitteldeutschen Großbetriebes. 19. Arbeitswissenschaftliches Kolloquium des VDI-MEG Arbeitskreises Arbeitswissenschaften im Landbau. *Bornimer Agrartechnische Berichte*. Heft 83. Potsdam-Bornim, Dresden, pp. 22–34.

Gysi, M. 2001. Compaction of a Eutric Cambisol under heavy wheel traffic in Switzerland: field data and a critical state soil mechanics model approach. *Soil & Tillage Research* **61**, 133–142.

Håkansson, I., Voorhees, W.B. & Riley, H. 1988. Vehicle and wheel factors influencing soil compaction and crop response in different traffic regimes. *Soil & Tillage Research* **11**, 239–282.

Hameed, I.A., Bochtis, D.D., Sørensen, C.G., Jensen, A.L. & Larsen, R. 2013. Optimized driving direction based on a three-dimensional field representation. *Computers and electronics in agriculture* **91**, 145–153.

Hameed, I.A. 2014. Intelligent coverage path planning for agricultural robots and autonomous machines on three-dimensional terrain. *Journal of Intelligent & Robotic Systems* **74**(3–4), 965–983.

Hamza, M.A. & Anderson, W.K. 2005. Soil compaction in cropping systems. A review of the nature, causes and possible solutions. *Soil & Tillage Research* **82**, 121–145.

Horn, R., Van den Akker, J.J.H. & Arvidsson, J. 2000. *Subsoil Compaction: Distribution, Processes and Consequences.* Reiskirchen, Germany, Catena Verlag, 462 pp.

Jílek, L. & Podpěra, V. 2005. The effect of the land shape on the energy intensity of operation steps. *Research in Agricultural Engineering* **51**, 134–139.

Jin, J. & Tang, L. 2010. Optimal coverage path planning for arable farming on 2D surfaces. *Transactions of the ASABE* **53**(1), 283–295.

Jin, J. & Tang, L. 2011. Coverage path planning on three-dimensional terrain for arable farming. *Journal of Field Robotics* **28**, 424–440.

Landers, A. 2000. *Farm machinery, selection, investment and management*. Farming Press, United Kingdom, 152 pp.

Li, Y.X., Tullberg, J.N. & Freebairn, D.M. 2007. Wheel traffic and tillage effects on runoff and crop yield. *Soil &Tillage Research* **97**(2), 282–292.

Oksanen, T. & Visala, A. 2009. Coverage path planning algorithms for agricultural field machines. *Journal of Field Robotics* **26**(8), 651–668.

Radford, B.J., Yule, D.F., McGarry, D. & Playford, C. 2007. Amelioration of soil compaction can take 5 years on a Vertisol under no till in the semi-arid subtropics. *Soil & Tillage Research* **97**, 249–255.

Seufert, H. 1995. Kostensparende Lösungen für Stallanlagen. In *Ergebnisse landwirtschaftlicher Forschung*. Justus-Liebig-Universität Gießen 22, pp. 69–94.

Tullberg, J., Antille, D.L., Bluett, C., Eberhard, J. & Scheer, C. 2018. Controlled traffic farming effects on soil emissions of nitrous oxide and methane. *Soil &Tillage Research* **176**, 18–25.

Wagner, P. 2001. Gewannebewirtschaftung – Kosten und Nutzen. In *KTBL Sonderveröffentlichung 034 – Gewannebewirtschaftung*, KTBL, Kuratorium für Technik und Bauwesen in der Landwirtschaft, Darmstadt, pp. 30–41.

Agronomy Research **16**(4), 1762–1770, 2018
https://doi.org/10.15159/AR.18.169

Ergonomic modelling parameters and the influence of ergonomics on planning workplaces

D.G. Maksimov[1,*] and H. Kalkis[2]

[1]Udmurt State University, Institute of Economics and Management, Universitetskaya street 1, bld. 4, RU426034 Izhevsk, Russia
[2]Riga Stradins University, Faculty of European Studies, Dzirciema street 16, LV 1007 Riga, Latvia
[*]Correspondence: maksim.dan.gen@gmail.com

Abstract. Modern economic research divides all economics into structural levels: mega-economics, macroeconomics, meso-economics, micro-economics, and nano-economics. From the point of such traditional divisions, the research is topical in the primary economic structure of society – nano-economics – and thanks to this work operations can be subdivided into workplaces in the form of transformation processes. The aim of the research is to develop ergonomic modelling parameters and to discover the influence of ergonomics on the planning of workplaces based on a case study. The research involved a study of workplace ergonomic planning methods and principles. Solutions for a series of problems which are related to the improvement of workplace ergonomics may be discovered in the following ways: improving work organisation in every workplace by using work process-related micro-elemental methods and a determination of work expenditure, the levels of physical strenuousness involved in the work, the complexity of the work, and the social importance of the workplace. These parameters will allow the workplace quantity characteristics to be discovered, such as in terms of a generalised parameter which conforms to the requirements which describe a workplace, and in terms of operational management via the condition of workplaces and the salary systems being utilised. The research provides a case study in which ergonomic modelling parameters are developed and concrete workplace interventions are introduced.

Key words: human factors, work, workplace, case study, intervention.

INTRODUCTION

The term ‘workplace’ has many interpretations which have a lot in common. The founders of scientific management had no clarity when it came to precisely what constituted a ‘workplace’. They assumed it was an intuitive term, a place in which working activities were carried out (Taylor, 1919; Gastev, 1972; Gastev, 2011).

Over time it became necessary to standardise the term ‘workplace’. In 1943, the American Society of Mechanical Engineers (ASME) focused on the unification of the term ‘workplace’. As a consequence of discussions, the ASME came to the conclusion that the term ‘workplace’ was part of a production space in which an employee carries out their duties.

The International Labour Organisation explains the term 'workplace' as including all places in which workers need to be to carry out their duties or from which they need to be followed in connection with their work where they are directly or indirectly under the direction of their employer (ILO, 2018).

In GOST 12.1.005 (1989), the term 'workplace' is given the following definition: 'a place involving a permanent or temporary stay when working during the course of carrying out one's working activities'. Hence researchers provide several definitions for the term 'workplace', and it may be concluded that in most studies it is a place which is equipped with the necessary technical means so that an employee can carry out any working activity.

In order to further expand the concept of the 'workplace' and move onto the concept of 'ergonomic workplace passport' with the concept of 'the working activities of an individual' which are common to sociology, economics and engineering, with: 'the workplace being an elementary part of the production space in which the allocated means of work, equipment which is required for that work, and the object of the work itself are interrelated with the implementation of individual work processes in accordance with the function of obtaining the product of the work'. The primary scheme for a system in which workplace elements interrelate in accordance with the previously stated definition is shown in Fig. 1.

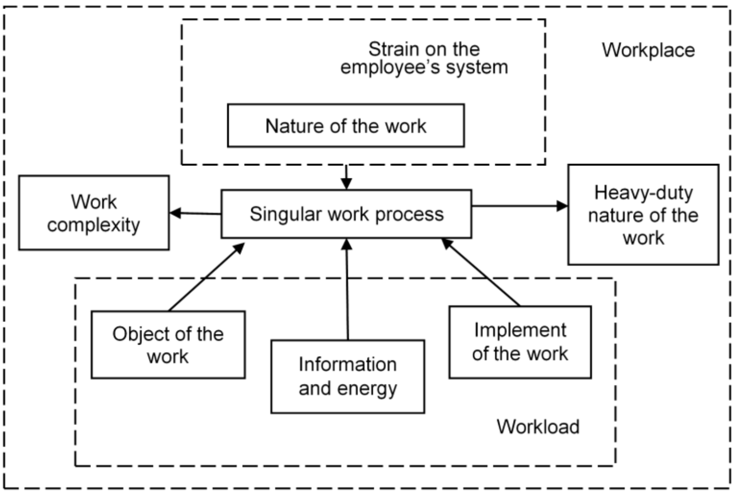

Figure 1. Structural scheme for the workplace (short version).

Successfully implemented and modelled ergonomics for workplaces are very important in terms of the continuous process of improvement, and can result in the optimum functioning of the socio-technical system, one which ensures employee safety at work, psycho-social comfort, improvements in life quality, and providing an influence on one's motivation for the work (Kalkis & Roja, 2016). Hence the implementation of ergonomic modelling parameters which require careful planning and influence analysis.

An ergonomic evaluation of the workplace has been carried out across quite a long period of time because the layout of the workplace is the primary value when creating a physical workplace (Bhattachary, & McGlothlin, 2012). To measure the quality of the workplace the methodology presented in Perevoshchikov (1974; 2015) and Orefkova's work (1990; 2005) were both utilised.

The combination of qualitative, quantitative, emotional, and sanitary-hygienic parameters form the concept, 'the ergonomic workplace passport'.

MATERIALS AND METHODS

All workplaces and all places which must be visited during the course of one's everyday life must have a detailed passport. This has to take the form of an official document. To achieve these objectives, the term 'ergonomic workplace passport' is introduced. This takes into account the qualitative and quantitative characteristics of the workplace and the time spent at work.

Currently, the study focuses on engineering production, and the methodology entitled 'the ergonometric workplace passport' has been developed. Such a methodology provides legal implementation as an integral part of a collective agreement.

The development of methodology entitled 'ergonometric workplace passport' involves various elements that need to be analysed, including the following:

1. The parameters of the object of the work;
2. A list of operations in the workplace;
3. The workplace layout and its ergonomic parameters, including a 3D model creation of the workplace;
4. Work process analysis in the workplace using predetermined motion time systems (PMTS);
5. Calculations for the coefficient levels of physical strenuousness involved in the work , the complexity coefficient, the working conditions coefficient, and the neuro-emotional pressure coefficient in the workplace;
6. The characteristics of the social and production status in the workplace.

In order to be able to determine the quantitative characteristics, the best system to use is one which involves a microelement analysis of time. Microelement standards have their own development processes, and a large number of predetermined motion-time data systems have been developed (known as PMTS). The most prominent of these are as follows:

1. The method time measurement, or MTM (Karger & Walton, 1982; Maynard et al., 2012; De Almeida & Ferreira, 2015);
2. The 'most work measurement time system', or MOST (Zandin, 2002; Deshpande, 2007);
3. MODAPTS (Heyde, 1983; Sullivan et al., 2001).

Perevoshchikova & Orefkova's methods (2005) and unpublished work by the authors was developed on the basis of the MTM and BSM systems, and these are used here to calculate the microelement norms. The methodology includes three additional parameters: mechanical power, the static moment, and logical action.

Currently, on the basis of methods which involve trace elements, an automated system which calculates time allowances has been developed (Genaidy, 1990; Alkan et al., 2016). But these systems only determine the duration of the work process, without affecting the mental characteristics of the work.

In this research, task creation is considered in relation to the 'ergonometric workplace passport'. This is based on a qualitative assessment of working hours in a specific workplace. In order to determine the qualitative and quantitative parameters, the methodology presented by Perevoshchikov (1974; 2015) and Orefkova (1990; 2005) was utilised.

A new method of work measurement system was used, based on findings from a physical performance quantitative assessment, a biomechanical analysis of human work movements, and a work process improvement with an engineering-economic introduction to working standards (Korenev, 1977; BSM, 1989; Orefkov & Perevoschikov, 2005;). Russian copyright registration certificates were obtained which confirmed the existence of software products and their ownership (Maksimov & Perevoschikov, 2014; Maksimov et al., 2015).

The new computer software was developed on the basis of the methodology presented in the article by Maksimov & Kalkis (2016).

RESULTS AND DISCUSSION

Every concrete work process has its own qualitative certainty. This is expressed by a combination of properties, attributes, and parameters which determine the given work process as such. For example, any technological operation is a qualitative manifestation of a single work process.

Therefore the qualitative certainty of work is expressed in a specific individual work process, with multiple processes combining within the scale of a company to define the quality of production.

For practical purposes, the method of dividing jobs and professions into light, moderate, hard, very hard, and heavy-duty categories (Mantoye et al., 1996) is based on physiological, sanitary, and hygienic studies and serves to generalise the practical demands of individual organisations, and it has been used for a relatively long time. At present, when it is required in each concrete case, a scientifically profound approach is required in practically every technological operation which involves the standardisation and organisation of various aspects of the work process. Production requires more precise, detailed standards and methods when it comes to analysing any work process.

The nature of and results from a variety of scientific investigations that have been reported in the press and which link up to aspects of the levels of physical strenuousness involved in the work, along with work strain, and work intensity, if they do not deal with social aspects, may be summarised as follows:

1) the characteristics of work in the physiological aspect is a form of work-related strenuousness;

2) the characteristics of work in terms of the impact imposed by the production environment on the human nervous system are classed as being strain;

3) the value both of the levels of physical strenuousness involved in the work and the work complexity depends upon the material factors and environmental conditions in which the work process is taking place.

In order to be able to study the physiological aspects of an individual in the work process means taking some consideration of the physiological reaction of an individual as a response to competing factors in the work process, such as the object of the work and the instruments being used for that work. Hence it is necessary to analyse and understand the physiology of an organism as a complete system in terms of physiological abstraction and its subordination to the general laws of nature, and it will allow knowledge of the functioning of the human body to be developed in terms of working processes.

The quantitative assessment of categories for the levels of physical strenuousness involved in the work is an holistic process which includes an analysis of interacting physical forces. Several physical conditions of the surrounding environment are then taken into account when carrying out any analysis of the levels of physical strenuousness involved in the work such as, for example, temperature, velocity, air humidity, the chemical composition of air, the level of aerosols in the atmosphere, illumination, noise, vibration, and radiation. By having a huge number of experiments being conducted to measure the energy-related metabolism of an individual in terms of various types of work, a total can be calculated in relation to mechanical work and, as a result of generalisations, a formula can be obtained by which the coefficient of the work can later be determined without resorting to measuring the exchange of human energy. One should take into consideration the fact that the laws of mechanics can be used to calculate external mechanical work.

The process which involves the levels of physical strenuousness involved in the work can be calculated as shown in Formula 1 (Orefkov & Perevoschikov, 2005).

$$H = 0.476 \cdot \left(\frac{A}{4{,}189} + \frac{M_{ave}}{442} + \frac{0.06 \cdot \Delta E_o}{t_0}\right) \qquad (1)$$

where H – the strenuous nature of any technological operation which is currently under research, without size dimensions (relative); A – the mechanical power of the body's locomotor apparatus, J min^{-1}; M_{ave} – the average statistical moment for operation, Hm; t_0 – the total time of the work operation, in seconds; ΔE_o – internal energy expenditure residual for an organism, cal.

For the practical use of the proposed formula, specific methods and guidelines (a manual) were prepared.

The use of the calculation method which involves the levels of physical strenuousness involved in the work and the predetermined motion-time data system allows for an accurate mathematical calculation to be determined in relation to the category of strenuousness involved in the work. Such an approach can confirm the intuitive feelings of individuals when it comes to any imperfections which may exist in the existing formal methods for the evaluation of the levels of physical strenuousness involved in the work.

In the performance of a given type of work, a significant factor is the complexity of the work, something that characterises the intellectual strain of the subject who is involved in carrying out that work. In the research, intellectual strain is understood as being the process of information perception. Work complexity levels serve to influence the speed at which information change is transformed. Information obstacles within the process of perception are objects of attention. An object of attention is a perceived object's specific parameters, and the subject who is involved in carrying out the work establishes continuous contact with it.

In order to quantify any submission of work complexity, the following mathematical formula is used:

$$C_c = \frac{\ln(N_0 - \propto \cdot N_b)}{e^{\left(1 - \frac{\alpha \cdot N_b}{N}\right)}} \cdot \left(\frac{\delta}{\delta_o}\right) \qquad (2)$$

where N – is the total number of algorithmic members in the work process under research, pcs; N_0 – is the quantity of operands in the algorithm for the work process, psc; N_b – the number of logical conditions in the algorithm for the work process, psc; α – the coefficient for the variety of logical conditions; δ – the intensity at which information is processed in the work process which is being researched; δ_o – the intensity at which information is processed in the core work process (the optimum intensity of information processing).

The quantitative evaluation of work complexity is evidenced by the results from the calculation. The calculation of the work expended which takes into account quantitative and qualitative indicators is presented in the following formula:

$$I_{lp} = L = C_h \cdot C_c \cdot C_{cl} \cdot C_{np} \cdot t_o \quad (3)$$

where L – is work input; work·h^{-1}; t_o – is the total time of the work operation, h; C_h – is the coefficient for the levels of strenuousness; C_c – is the complexity coefficient; C_{cl} – is the coefficient for conditions; C_{np} – is the coefficient for neuro-emotional pressure.

The next step in the research was to design the scheme for the system (Fig. 2). The system's operational diagram in Fig. 2 shows the main algorithm which includes the C# programming language and the Visual Studio Community 2017 interactive development environment for modelling software. Firebird (a database server) was chosen to design the database. It is simple to use and makes it possible to create the server.

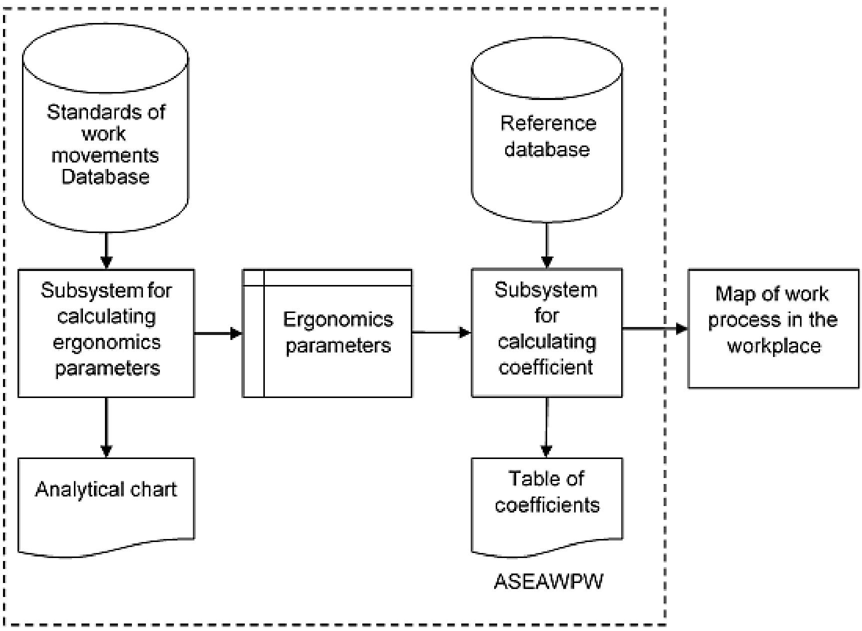

Figure 2. Data showing the ASEAWPW representation (ASEAWPW being the automated system for an ergonomic analysis of work processes in the workplace).

The software product, ‘The automated system of ergonomic analysis for work processes in the workplace’, was used for calculating the complex of work indicators for the work process in conjunction with a database that includes all of the ergonomic dependencies involved in work-related task movements.

The calculations for the computer software were carried out in the following order: (1) the type of work in the workplace is determined. Information is taken from the product’s technological map; (2) gather together information on the method being used to carry out the operation. Information is taken from the product’s technological map; (3) an analysis of primary data; (4) an analysis of basic procedures and transitions; (5) divide transitions into movements and objects of attention; (6) the work process analysis card is filled in. Based on the selected method for trace elements; (7) the work strenuousness coefficient, work complexity coefficient, work conditions coefficient, and neuro-emotional pressure coefficient were determined. The coefficient is determined on the basis of formulae 1 and 2, and with the methodology developed by Orefkov & Perevoschikov (2005); (8) the calculation for the intensity of the work process was carried out. This is a coefficient that is determined on the basis of formula 3.

The main software window is shown in Fig. 3.

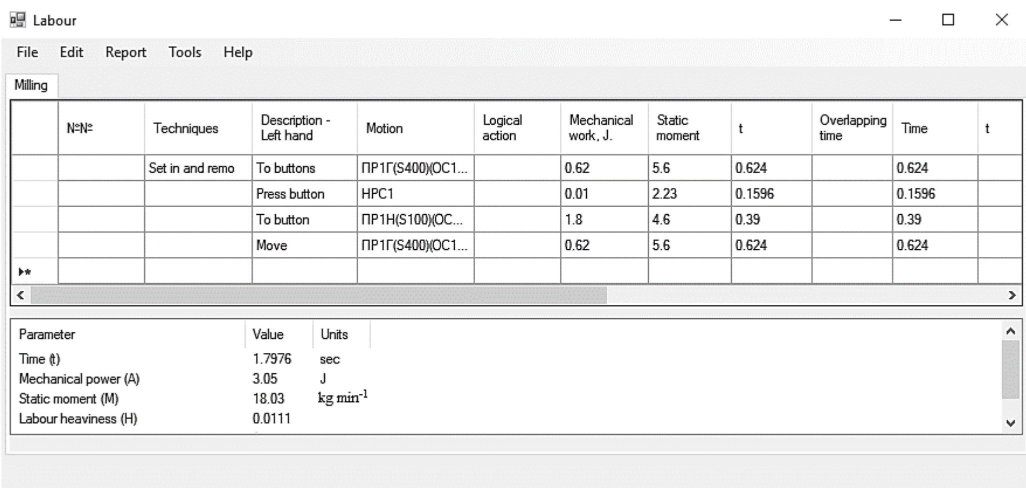

Figure 3. The main program window.

The following table shows some operations that were calculated with the help of the software (Table 1).

Table 1. Work input

Operation	t, time (seconds)	C_h	C_c	L, working hours
Surface grinding of a bracket	28.2	0.71	1.26	0.00698
Milling	27.8	1.03	1.15	0.0091
Boiler diagnosis	29.7	0.58	4.19	0.02005
Milling	17.35	1.21	1.25	0.00729
Machining	99.67	1.22	1.2	0.04053
Turning operation	216	1.2	1.3	0.0936

An analysis of the production operation was carried out using computer software and it gained the results shown below:

1. Operation: milling. information is taken from the product's technological map;
2. Processing a low-speed shaft with a weight of 14.4 kg. Information from a detailed drawing;
3. An analysis of the operation;
4. An analysis of basic procedures and transitions;
5. Cut-up transitions into movements and objects of attention;
6. The data is entered into the program (Fig. 3). Based on the selected trace elements method;
7. Results (the bottom half of fig. 3): total operating time t = 27.8 s; total mechanical work a_0 = 45.54 j; total static moment m_t = 641.9 nms;
8. The coefficient of work strenuousness – C_h = 1.03 (formula 1). The coefficient of work complexity – C_c = 1.15 (formula 2);
9. The coefficient of conditions – $C_{cl} = 1$. The coefficient for neuro-emotional pressure – C_{np} = 1. These factors are not included in the software. A full study should be undertaken of their impact upon the work process;
10. T = 1.03·1.15·1·1·0.0077 = 0.0092 working hours (formula 3).

The data received has been entered into a database and can be used to design an ergonomic passport for a workplace.

The parameters obtained are only a small part of compiling an ergonomic workplace passport, since it is necessary to graphically represent the workplace in question and its interaction with the base of the given labour processes for the company being analysed under specific production conditions.

CONCLUSIONS

The developed methodology, entitled the 'ergonometric workplace passport' can be used in other research and in practical applications in relation to work organisation preventive measures. At the current stage of designing the ergonomic workplace passport, only the first stage is being implemented, involving the option to be able to use computer software when it comes to measuring the quantitative and qualitative parameters of the workplace. It is planned to further refine the basic movement system to determine the energy costs, and to refine the software package for better evaluation results. The most difficult, and most important step, will be to refine the definition of the intellectual complexity of the work being carried out.

REFERENCES

Alkan, B., Ver, D., Ahmad, M., Ahmad, B. & Harrison, R. 2016. A model for complexity assessment in manual assembly operations through predermined motion time systems. *6th cirp conference on assembly technologies and systems (cats).* Procedia CIRP **44**, pp. 429–434.

Bhattachary, A. & McGlothlin, J.D. 2012 *Occupation ergonomics.* CRC Press. 1322 pp.

BSM, *System of standard on basic movement (BSM-1)*, Economics, Moscow 1989, 123 pp. (in Russia).

De Almeida, D. & Ferreira, J.C. 2015. Analysis of the Methods Time Measurement (MTM) Methodology through its Application in Manufacturing Companies. *Flexible Automation and Intelligent Manufacturing* **1**, 2–9.

Deshpande, V.A. 2007. M.O.S.T. – The most advanced work measurement technique. *Journal of Engineering & Technology* **20**, 109–113.

Gastev, A.K. 2011. *Labor installations (Trudovye ustanovki)*. Librocom, Moscow, 344 pp. (in Russia).

Gastev, A.K. 1972. *How need to work. Practical introduction to the science of labor organization.* Economika, Moscow, 478 pp. (in Russia).

GOST 12.1.005. 1989. Occupational safety standards system. General sanitary requirements for working zone air. *http://docs.cntd.ru* accessed 10.01.2018.

Genaidy, A.M., Agrawal, A. & Mital, A. 1990. Computerized predetermined motion-time system in manufacturing industries. *Computer and Industrial Engineering* **18**(4), 571–584.

ILO, International Labour Organization (Convention concerning Occupational Safety and Health and the Working Environment, No. 155) *http://www.ilo.org* accessed 15.01.2018.

Heyde, G.C. 1983. *MODAPTS plus.* Heyde Dynamics, Sydney, 148 pp.

Karger, D.W. & Walton, M.H. 1982. *Advanced Work Measurement*. Industrial Press, New York, 321 pp.

Kalkis, H. & Roja, Z. 2016. Strategic Model for Ergonomics Implementation in Operations Management. *Journal of Ergonomics* **6**(4), 173, 1–5.

Korenev, G.V. 1977 *An Introduction to human mechanics*. Nauka, Moskow, 264 pp. (in Russia).

Maynard, H.B., Schwab, J.L. & Stegemerten, G.J. 2012. *Methods Time Measurement. Literary Licensing*, USA, 302 pp.

Maksimov, D.G. & Kalkis, H. 2016. Software development for Qualimetrical ergonomics of a workplace. *Agronomy Research* **14**(4), pp. 1406–1416.

Maksimov, D.G. & Perevoschikov, Y.S. Avtomatizirovannaya sistema ergonomicheskogo analiza protsessov truda na rabochem meste [Automated system of ergonomic analysis of work processes in the workplace]. The certificate of state registration of software No 2014619839 issued on 23.09.2014.

Maksimov, D.G., Perevoschikov, Y.S. & Orefkov, V.V. Mikroelementnye normativy dlya avtomatizirivannoy sistemy ergonomicheskogo analiza processov truda na rabochem meste [Microelement standards for the automated system of ergonomic analysis of labor processes in the workplace]. *The certificate of state registration of database no. 2015621189* issued on 04.08.2015.

Montoye, H.I., Kemper, W.M., Saris, M. & Wasshburn, R.A. 1996. *Measuring Physical Activity and Energy Expenditure*. Human Kinetics Publishers, Inc. 191 pp.

Orefkov, V.V. & Perevoschikov, Y.S. 2005. *Ergonomics rate fixing of labor*. Publishing House VCUZh, Moscow, 934 pp. (in Russia).

Orefkov, V.V. 1990. *A quantitative assessment of physical performance on the basis of biomechanical analysis of human labor movements*. Dokt, diss. Leningrad, 153 pp. (in Russia).

Perevoschikov, Y.S. 2015. *Labor process (engineering-economic research into working standards)*. Publishing house ‘Udmurt University’, Izhevsk, 331 pp. (in Russia).

Perevoschikov, Y.S., Orefkov, V.V. & Alekseev, B.P. 1992. *A quantitative assessment of labour processes heaviness*. UDSU Publishing House, Izhevsk, 74 pp (In Russia).

Perevoschikov, Y.S. 1974. *Labor process*. Publishing house ‘Udmurtiya’, Izhevsk 222 pp. (in Russia).

Sullivan, B., Carey, P. & Farrell, J. 2001. *Heyde's MODAPTS: A Language of Work*. Jonesboro, AR: Heyde Dynamics Pty, Limited, 218 pp.

Taylor, F.W. 1919. *The Principles of Scientific Management*. New York, London, Harper & Brothers, 156 pp.

Zandin, B. 2002. *MOST Work Measurement Systems*, 3rd Edition. CRC Press, 552 pp.

Agronomy Research **16**(4), 1771–1780, 2018
https://doi.org/10.15159/AR.18.157

Importance of microclimate conditions and CO_2 control in educational buildings: a case study

E. Merisalu[1,*], D. Mugur[1] and P. Kic[2]

[1]Estonian University of Life Sciences Tartu, Institute of Technology, Fr. R. Kreutzwaldi 56/1, EE51014 Tartu, Estonia
[2]Czech University of Life Sciences Prague, Faculty of Engineering, Department of Technological Equipment of Buildings, Kamýcká 129, CZ165 21 Prague, Czech Republic
[*]Correspondence: eda.merisalu@emu.ee

Abstract. Current efforts to minimize energy losses and maximize energy savings for heating of all houses are most often gained by insulating facades and replacing windows. However, these measures can have a significant negative impact on human health and these problems can occur in buildings with a high concentration of people, such as school buildings. The aim of this paper is to analyse the results of measurements of air temperature, relative air humidity and carbon dioxide in winter period in the classrooms of two universities, Estonian University of Life Sciences (EULS) in Tartu and Czech University of Life Sciences (CULS) in Prague. The measurements have carried out in 2017–2018 in eight classrooms of the EULS and two classrooms of the CULS. The external and internal temperature, relative humidity and concentration of carbon dioxide have measured in the classrooms during a few days in the winter period. In the lecture rooms of CULS, when the air conditioning was off, the levels of CO_2 exceeded the recommended levels about two times. The average internal temperature and CO_2 concentrations in the classrooms of EULS follows the norms and refers on good ventilation. The extremely low relative humidity in the classrooms of EULS at $17.1 \pm 2.6\%$ refers to a high risk of allostatic load and respiratory symptoms among students. It is important to pay attention on regular ventilation and relative air humidity control in the teaching rooms, especially with high number of students to prevent seasonal sickness of upper respiratory tract.

Key words: air-conditioning, health impact, lecture rooms, measurement, students.

INTRODUCTION

In the last few decades, the number of studies focusing on the effect of indoor climate conditions on human health has increased rapidly (Fisk at al., 2007; Karottki et al., 2015). In some works, the importance of microclimate for schools' environment (Karwowska, 2003; Kic, 2015) and offices (Seppänen et al., 2006; Tint et al., 2012) is shown. The relationships between the illness, indoor climate and regularity of attendance at a school or office have studied. Inappropriate microclimate may contribute to higher sickness rate and thereby increase the number of days when people do not come to the office or to school. The critical analysis of the research results by Wargocki & Wyon (2017) has demonstrated, that any economic gains achieved by energy conservation in the buildings greatly exceeded the costs, whereby the majority of people reported reduced performance 5–10% for adults and 15–30% for children.

Cross-sectional surveys in many schools in the USA have confirmed that poor ventilation and higher CO_2 levels may play a part in reducing the number of pupils managing to pass language and mathematics tests (Haverinen-Shaughnessy et al., 2011).

In a study of three German Bundeslander (Fromme et al., 2016) the indoor air of 63 day-care centres was analysed for carbon dioxide (CO_2), airborne particulate matter (PM_{10} and $PM_{2.5}$) and volatile organic compounds. The median daily CO_2 concentrations in the individual facilities ranged from 670 ppm to 3,958 ppm (median: 1,297 ppm).

In the areas where people live, air quality deteriorates with substances that enter the air through metabolism, especially by breathing. Exhaled air contains approximately 4% CO_2 and 5% water vapour. It has been revealed that indoor environmental quality significantly influences allostatic load in the body and it can be a predictor for reporting Sick Building Syndrome (SBS) with information on system-specific (neuroendocrine and metabolic) effects (Jung et al., 2014).

Human senses are not able to directly judge the concentration of CO_2, therefore the personal self-assessment of air quality is very unreliable. Humans can approximately sense the CO_2 concentration, since the central nervous system regulates the breathing rate based on blood CO_2 levels (Cummins & Keogh, 2016). The human organism ceases to perceive the concentration of odour after some time, and olfactory organs adapt to the environment in which people find themselves. Certainly everybody knows the situation when a person enters to a small room where already several people are there. When one enters the environment, one smells the stuffy air, but after a while one stops to perceive it as an inconvenience. Once their olfactory organs adapt, one stops to perceive the concentration of odours. However, at a certain concentration, the effect of elevated CO_2 levels is reflected by concentration problems as fatigue, deteriorated attention and mental work. At higher CO_2 concentrations, human fatigue is already increasing and headaches, nausea and breathing problems can occur. Table 1 summarizes the approximate effects of CO_2 on the human organism (Zikan, 2011).

Table 1. Effects of CO_2 on the human organism

Concentration CO_2 (ppm)	Effect on the human organism
about 350	Outdoor environment
up to 1,000	Recommended indoor conditions
1,200–1,500	Recommended maximum level in indoor areas
1,000–2,000	Beginning of fatigue and decreased concentration
2,000–5,000	Beginning of possible headaches
5,000	Maximum safe concentration without health risks
> 5,000	Nausea and increased heart rate
> 15,000	Breathing problems
> 40,000	Possible loss of consciousness

Attention to the CO_2 concentration in classrooms and office rooms has paid in previous studies. According to Heudorf et al. (2009) the levels of CO_2 were very high in all studied schools and could be diminished by intensified ventilation (mean 1,459 to 1,051 ppm). A cross-sectional study in 21 office rooms in Taiwan (2011–2012) showed, that the concentration difference of indoor and outdoor CO_2 (dCO_2) and the ratio of indoor and outdoor CO_2 (CO_2 I/O ratio) levels were a markers of ventilation rate and associated with allostatic load score on the neuroendocrine system, and cough and musculoskeletal pain ($p < 0.05$) (Jung et al., 2014).

An Estonian study held by the Health Board (2015) on indoor air conditions in school classrooms of the renovated and non-renovated buildings showed no differences in room temperature and relative humidity. However, there was a difference in average CO_2 levels, with a higher CO_2 concentration in renovated school buildings (R = 0.204, $p < 0.01$). The effects of indoor air quality (IAQ) problems on school building occupants are often non-specific symptoms rather than well-defined diseases, based on a study by the European Commission (2014). Symptoms commonly attributed to IAQ problems include: eye, nose, throat and skin irritation, sinus congestion, coughing and sneezing, shortness of breath, headaches, and fatigue.

Reinvee et al. (2013) revealed that the Estonian Meteorological measurements (1970–2000) showed an average relative humidity below 20% at indoor temperatures of 21 °C were measured in the winter period from December to March, whereby the effect of humidifiers in EULS teaching rooms increased relative air humidity only by a maximum of 12%. Based on a study by Wolkoff (2018), low relative air humidity increases the transmission and survival of the influenza virus, increases the occurrence of dry eye disease, voice perturbation, body fluid loss, and the symptoms of asthmatics compared to normal relative air humidity. An increased air humidity with hot temperatures increases coughing in allergic rhinitis patients. Increased air humidity also lowers the threshold for smelling odours, the acceptability of the thermal climate and physical performance. Guidelines for healthy environments within European schools stress the importance to promote research and innovation to develop sustainable measures aimed at improving IAQ in the school environment to prevent negative impact on students' health (European Commission, 2014).

The aim of this paper is to analyse the results of measurements of air temperature, relative air humidity and carbon dioxide in winter period in the classrooms of two universities EULS and CULS.

MATERIALS AND METHODS

The first part of this research activity focused on measuring indoor conditions in the lecture rooms of the Faculty of Engineering at the CULS in Prague. It was carried out in the big lecture room A and small seminar room B.

The big lecture room A has a capacity of 121 student places in 11 rows of school desks. The lecture room is stepped and has the following dimensions: length 12.2 m, width from 7.7 m in the lowest point (on blackboard for the presenter) to 9.1 m at the highest (by the entrance) point, the height of the ceiling at the highest point (by the entrance) is 3.2 m and at the lowest point (on blackboard for the presenter) is 4.1 m. The volume is approximately 374 m^3. During the winter, thermal comfort in lecture room A is ensured by warm-water central heating system using classical radiators located on the walls under the windows. Ventilation is only by air conditioning (AC).

Measuring points represent the main characteristic locations on the middle axis of the lecture room, in the central part (sixth bench), which also suitably corresponds to the position between the air inlets. The instruments and sensors installed at the level 1.1 m above the floor. The registration of measured values was in one minute frequency during the whole measured period. Measurements included determination of the quality of indoor air in the lecture room during the different operating modes of AC equipment.

The AC equipment is modular and consists of an inlet section and an outlet section. The inlet part consists of silencers, the filter, the valve chamber, heat exchangers (heater and cooler) and the fan connected to the silencers. The direct cooler is connected to the condenser, the cooling unit that is installed on the roof of the lecture room. A steam humidifier connected to the drinking water is used for humidification. The outlet part consists of the silencer, the filter, the valve and the fan. The AC system was designed with a fresh air inflow of V_e = 4,520 $m^3 h^{-1}$ and an air outflow of V_i = 4,083 $m^3 h^{-1}$ (small overpressure). The ventilation rate per person is about 37 $m^3 h^{-1}$ if the lecture room is filled to capacity. The air change rate is 12 h^{-1}. A rotary regenerative heat exchanger is installed between the inlet and outlet sections for heat recovery from the exhaust air. The regenerator is an industrial product in which the matrix (heat transfer surface) is in a disk form and air flows axially.

Filtration of fresh and exhaust air is through the pleated filters made from the Firon Special G 460 non-woven polyester fabric. This material is G 3 class filter for coarse dust according to the international classification of air filters. According to the previous information and old international standards, this material should be used for elimination of particles over 10 μm.

All parts of the AC equipment are installed on the support frame. Air supply to the lecture room is via pipes with silencers and diffuser inlets in the ceiling, spread uniformly in the ceiling of the room. The air outlet is in the front of the lecture room with two wall grilles in the corner over the blackboard. AC operation is regulated automatically according to the internal temperature, but it was controlled manually during the measurement, to suit the intended experiment.

The small seminar room B has a capacity of 30 student places in 5 rows of school desks. The seminar room has the following dimensions: length 9.2 m, width 5.8 m, height 3.3 m. The volume is approximately 176 m^3. There is a central system of surface heating by water pipeline installed in the floor and ceiling of the whole building. Ventilation is only by opening of windows, there is no active ventilation.

The thermal comfort in the rooms was continuously measured during the experiment by the sensor FHA 646–21 including the temperature sensor NTC type N with an operative range from –30 to +100 °C with an accuracy of ± 0.1 °C, and the air humidity by a capacitive sensor with an operative range from 5 to 98% with an accuracy of ± 2%. Furthermore, the concentration of CO_2 was measured by the sensor FY A600 with an operative range from 0 to 0.5% and an accuracy of ± 0.01%. All of the data was measured continuously and stored to the measuring instrument ALMEMO 2690–8 at one minute intervals (Table 2).

Table 2. Technical parameters of the measuring device, used in CULS Prague

Parameters	Air temperature, °C	Relative air humidity, %	Carbon dioxide, ppm
Measurement ranges	From -30 to 100	From 5 to 98	From 0 to 5,000
Resolution	0.01	0.01	1
Accuracy	± 0.1	± 2.0	± 100

The CO_2 measurements were conducted in both lecture rooms during the winter period with students under normal teaching conditions inside the lecture room. There were 40 students in lecture room A. The measurement period simulated real conditions, with the AC switched off for 20 minutes and then switched on for 50 minutes during the experiment. Usually, teachers switch the AC on in the beginning of lecture. However, sometimes the AC is off for a longer time. It mainly happens in the winter.

The measurements in the small seminar room B were in normal teaching conditions. The first period was the 12-minute break with windows open, then followed the class with 20 students inside and with only several small windows partly opened. More windows were opened after 60 minutes. After the next 20 minutes the class was over and a 30-minute break started with partly opened windows before another class.

The measurements in the classrooms of the Institute of Technology of EULS were carried out in the 2018 winter, where the outside temperatures during the night were from −9 °C to −14 °C and during the day −1 °C to −4 °C. The measurements were taken in a 3-hour period in the morning on 2 separate days.

The data includes the results of measurements collected from eight teaching rooms described in Table 3.

Table 3. Main characteristic parameters of tested classrooms in EULS Tartu

Lecture room	Volume (m^3)	Maximum number of students, n
A109	169	24
A112	158	15
A208	164	15
A220	158	16
A308	102	6
A312	155	14
A403	103	24
A404	156	15

All of the classrooms are equipped by the comfort AC that forwards the microclimate information and CO_2 levels of the rooms to the central system of the whole building. This AC system includes the heating, cooling, air distribution and control system. Each room has its own sensors for measurement of temperature, relative humidity of air and CO_2 concentrations. Each room also has classical radiators located on the walls under the windows, heated by the warm-water central heating system. The occupants of those rooms can control the temperature from the control panel, the central system regulates the ventilation based on CO_2 levels.

The measurements were taken from 5 points in each room. The rooms were divided into 4 quadrants and the centre of each quadrant was taken as a measurement point. Also, the centre of each room was also taken as a measurement point. Measurements were taken from two heights: 0.1 m and 1.1 m. Each point was measured 3 times for 1 minute, the averages of those results are used in calculations. CO_2 measurements were recorded 3 times for 1 minute from the control panel, which receives data from two wall sensors, which were placed on opposite walls in the rooms.

The measurements of air temperature and relative air humidity in the EULS teaching rooms were taken by the COMET S3120 (Table 4).

Table 4. Technical parameters of the measuring device, used in EULS Tartu

Parameters	Air temperature, °C	Relative air humidity, %
Measurement ranges	From -30 °C to +70 °C	0 to 100 %RH
Resolution	0.1 °C	0.1%
Accuracy	± 0.4 °C	±2.5% from 5 °C to 95% at 23 °C

Measurement accuracy (error) of the equipment for air temperature is ± 0.4 °C and for relative air humidity is ± 2.5% relative humidity from 5% to 95% at 23 °C. These figures are based on the data available from the manufacturer.

RESULTS AND DISCUSSION

The results of the microclimate measurements in lecture rooms A and B during winter are summarized and presented in the Table 5 and Figs 1–2. Table 5 presents the results in both lecture rooms during different measurement times and different ventilation conditions.

Table 5. Average external temperature t_e, internal temperature t_i, relative humidity RH_i and concentration of carbon dioxide (CO_2) in the rooms during the measured periods

Measured quantity	Unit	Lecture room A		Seminar room B		
		AC off	AC on	Break	Seminar	Break
t_e	°C ± SD	1.6 ± 0.6	3.4 ± 0.3	4.4 ± 0.2	4.4 ± 0.2	5.5 ± 0.3
t_i	°C ± SD	22.7 ± 0.1	22.7 ± 0.1	22.9 ± 0.1	25.0 ± 1.0	21.5 ± 0.2
RH_i	% ± SD	38.9 ± 0.4	30.2 ± 2.3	29.6 ± 0.8	36.4 ± 2.1	31.3 ± 1.3
CO_2	ppm ± SD	2,075 ± 98	862 ± 427	495 ± 15	1,573 ± 500	616 ± 108

AC – air conditioning; SD – standard deviation.

The highest CO_2 levels were measured during the classes with higher student attendance and when the AC was switched off. In comparison, CO_2 levels were the lowest during break periods and when the AC was switched on. It is clear from Table 5 that in lecture room A the recommended indoor CO_2 level of 1,000 ppm was exceeded. When the AC was off, the levels of CO_2 exceeded the recommended levels about two times. Based on the CO_2 concentration on Fig. 1 it is obvious that the initial CO_2 level was very high (approximately 1,840 ppm). Due to the metabolism by breathing in the lecture room, it increased further to 2,260 ppm. The students and the lecturer did not perceive the worsening of the IAQ due to the slow gradual increase.

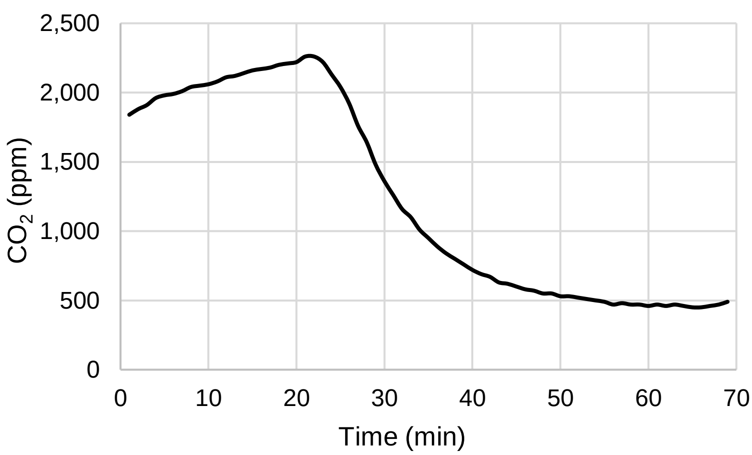

Figure 1. The course of CO_2 concentration during the measurement in the lecture room A.

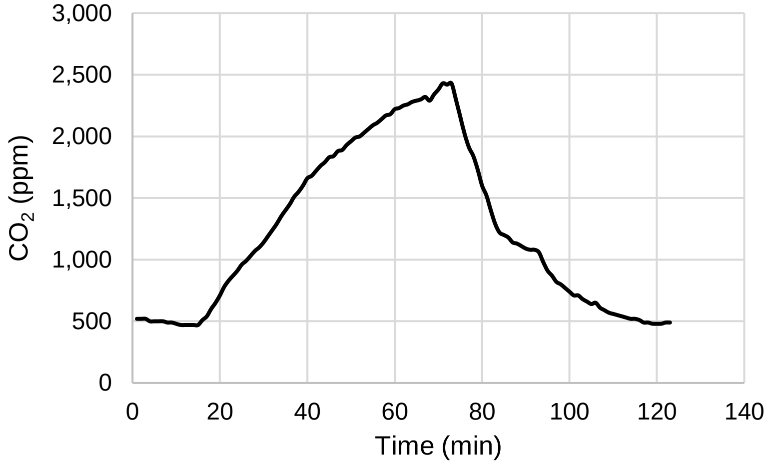

Figure 2. The course of CO_2 concentration during the measurement in the seminar room B.

When the AC was switched on, CO_2 concentration started to decrease immediately, and it slowly stabilized around 450 to 500 ppm. Significant fluctuations of CO_2 concentrations resulted in a high standard deviation value.

However, relative air humidity was on a suitable level throughout the whole measurement period. At the beginning it was at approximately 39%. When AC was switched on, it dropped to about 30% because the outside air supplied to the lecture room had a lower absolute humidity. After it was warmed, the relative humidity decreased considerably due to a higher humidity capacity of warmer air.

The air temperature was close to the desired temperature of +22 °C. At this value of +22 °C, heating and air conditioning should keep the internal temperature stable. Variations in the air temperature for the whole period were relatively small (see standard deviation value). From the thermal comfort point of view, neither the students nor the lecturer in the lecture room felt uncomfortable. Therefore, under normal conditions, the AC usually remains switched off.

According to the results in Table 3, it is clear the concentration of CO_2 was relatively low (approximately 500 ppm) inside seminar room B during the break before the lesson. Due to the large number of people (20 students and the lecturer), the CO_2 concentration rapidly increased to 2,430 ppm. Relative humidity gradually increased from about 30% to 36%. Also, the air temperature gradually increased from 23 °C to 25 °C. By that time, the indoor environment was unpleasant for many people, therefore the windows were fully opened.

By intensive ventilation through the opened windows the CO_2 concentration was gradually reduced from 2,430 ppm to 480 ppm. At the same time, the relative humidity decreased from 36% to 31% and the temperature dropped from +25 °C to +21.5 °C. If the classes last for a longer time, a similar cycle of varying ventilation intensity can be observed; windows are closed again because students sitting near the windows suffer from drafts and cold temperatures. Then the CO_2 concentration starts to rapidly rise again.

The results of microclimatic parameters and carbon dioxide (CO_2) measured in the rooms in the Institute of Technology, EULS are presented in Table 6.

Table 6. Average external (t_e, °C) and internal air temperature (t_i, °C) with the standard deviation, relative air humidity (RH_i, %) with the standard deviation and concentration of CO_2 (ppm) in the EULS teaching rooms during the winter period 2018

Lecture room	t_e, °C	t_i, °C	±SD	RH_i, %	±SD	CO_2, ppm
A109	-4	24.9	0.3	17.7	0.4	300
A112	-3	24.3	0.1	17.4	1.1	492
A208	-3	24.3	0.3	19.8	0.1	481
A220	-2	23.8	0.1	20.8	0.8	426
A308	-2	24.5	0.1	16.7	0.4	652
A312	-2	23.1	0.0	17.1	0.2	560
A403	-1	22.6	0.1	15.9	0.3	782
A404	-1	24.9	0.1	11.9	0.1	203
Mean ± SD	-2.3 ± 2.1	24.1 ± 0.9		17.1 ± 2.6		487 ± 185

t_e – external temperature; t_i – internal temperature; RH_i – relative humidity; SD – standard deviation.

The mean values measured in all rooms presented in Table 6 show, that the AC is functioning well based on the temperature and the concentration of CO_2.

The average indoor temperature measured from 1.1 m height, t_i = 24.1 ± 0.8 °C didn't differ from the results measured from 0.1 m height, t_i = 24.1 ± 0.8 °C. The results follows the values required by the Act of Health Protection Requirements for Schools (2013) (AHPRS), which dictates the different required microclimate levels for the lecture rooms and other teaching spaces.

The average relative humidity in the classrooms of EULS at height of 1.1 m 17.2 ± 2.6% and at height 0.1 m 16.7 ± 2.2% is extremely low. The value required by AHPRS is between 40 to 60% and between 25 to 60% during winter. The measurements were taken during winter, when the absolute humidity of external air is extremely low, but we can clearly see that the relative air humidity does not follow the values required by the AHPRS.

The indoor humidity production by evaporation and respiration is also very low, as there is usually a small number of students in classrooms and there are no other water vapour sources. The increase of relative humidity could be achieved only by the air humidification, which is rather complicated and expensive.

The low relative humidity in teaching rooms during winter has a negative health impact on people with chronic respiratory diseases, allergies and asthmatic symptoms. Sore eyes and voice problems are some of the more common symptoms among teachers (Simberg et al., 2009).

The Madureira et al. (2015) study in 20 public primary schools in Portugal showed that indoor air pollutants, some even at low exposure levels, are related to the development of respiratory symptoms among schoolchildren. High levels of volatile organic compounds (VOC), acetaldehyde, $PM_{2.5}$ and PM_{10} in the air were associated with higher odds of wheezing in children.

The values obtained from the CO_2 sensors are very important but based on the large standard deviation in the results, we can assume that the sensor need to be calibrated regularly. There are two sensors installed in each room. The data presented in Table 6 is the average value of the sensors monitoring the CO_2 concentration in the room. They were usually placed where the majority of students are sitting and the pollution by CO_2 is the highest. The mean CO_2 concentration of 487 ± 185 ppm in all rooms is excellent, it is lower than the required limit of 1,000 ppm. The lowest value in the room A404 is probably caused by faulty calibration, which should be provided regularly according to the manufacturers' instructions. The highest value in the room A403 could have been caused by a high number of students in the small room and by some AC control, as the mean temperature of +22.6 °C is the lowest value from all measured rooms. The automatic control of AC controls the rate of ventilation with the aim to reduce the heat losses by the ventilation system.

In Estonia, there are certain requirements for the microclimate, as required by the AHPRS. These dictate that the air temperature in classrooms must be at least 19 °C and the upper limit for CO_2 concentration doesn't exceed 1,000 ppm. Nevertheless, in the classrooms in the Institute of Technology, EULS the mean CO_2 value (782 ppm) and the air temperature values followed the AHPRS.

CONCLUSIONS

The results of main indoor parameters measurements presented in this paper show that during the winter period the CO_2 concentrations exceed the recommended maximum values inside the lecture rooms of the CULS in Prague. The temperature inside the lecture rooms and classrooms is only slightly increased (an increase of about 1K), but the concentration of CO_2 grew rapidly. The smaller the volume of the classroom and the greater the number of students in it is, the faster the indoor environment worsens. The reaction of the people inside the rooms is disproportionately slow. The natural or forced ventilation controlled by people (usually teacher) is therefore not sufficient. Impaired quality of the indoor environment therefore reduces the concentration of students and increases the transmission risk of infectious diseases.

The measurements in the lecture rooms in the Institute of Technology, EULS, confirmed the positive influence of CO_2 control together with temperature control. The measurement and regulation of these parameters allowed for the optimal indoor conditions for classes. The low relative humidity in winter period is still an ineluctable problem. The improvement could only be achieved by vapour humidification. Low relative humidity in classrooms during the winter may reduce learning efficiency when the eyes tend to dry and tire more easily and the lecturers' voice is under a higher strain. It could be a serious problem for the students in larger classes, since the low relative humidity allows the flu and other respiratory diseases to survive longer and spread more easily.

It is important to regularly monitor the air humidity, air temperature and CO_2 levels in the lecture rooms of both observed universities (EULS and CULS) and to regulate the AC system and humidifiers accordingly.

REFERENCES

European Commission. 2014. *Guidelines for healthy environments within European schools*. Ed. by: Kephalopoulos, S., Csobod, E., Bruinen de Bruin, Y., de Oliveira Fernandes, E. Publication Office of European Union. Luxembourg.

Cummins, E.P. & Keogh, C.E. 2016. Respiratory gases and the regulation of transcription. *Exp. Physiol.* **101**(8), 986–1002.

Fisk, W.J., Gomez, Q.L. & Mendell, M.J. 2007. Meta-analyse of the associations of respiratory health effects with dampness and mold in homes. *Indoor Air* **17**, 284–296.

Fromme, H., Lahrz, T., Burkhardt, R., Fembacher, L., Kraft, M., Sievering, S., Kadler, D. & Dietrich, S. 2016. Indoor air quality in German day care centres - carbon dioxide (CO_2), volatile organic compounds (VOC) and fine dust - LUPE 3. *Gefahrstoffe Reinhaltung der Luft* **76**(3), 55–61.

Haverinen-Shaughnessy, U., Moschandreas, D. & Shaughnessy, R. 2011. Association between substandard classroom ventilation rates and students' academic achievement. *Indoor Air* **212**, 121–131.

Heudorf, U., Neitzert, V. & Spark, J. 2009. Particulate matter and carbon dioxide in classrooms – The impact of cleaning and ventilation. *Int. J. Hyg. Environ. Health* **212**, 45–55.

Jung, C.C., Liang, H.H., Lee, H.L., Hsu, N.Y. & Su, H.J. 2014. Allostatic Load model associated with Indoor Environmental Quality and Sick Building Syndrome among office workers. *PlosOne* **9**(4), e95791.

Karottki, D.G., Spilak, M., Frederiksen, M., Andersen, Z.J., Madsen, A.M., Ketzel, M., Massling, A., Gunnarsen, L., Møller, P. & Loft, S. 2015. Indoor and outdoor exposure to ultrafine, fine and microbiologically derived particulate matter related to cardiovascular and respiratory effects in a panel of elderly urban citizens. *International journal of environmental research and public health* **12**, 1667–1686.

Karwowska, E. 2003. Microbiological air contamination in some educational settings. *Polish Journal of Environmental Studies* **12**, 181–185.

Keskkonnatervise Uuringute Keskus 2015. A study of the indoor air quality of renovated and unrenovated school building in Tallinn. Edited by: Tuulik, K., Harzia, H., Karajeva, G. 105 pp. (in Estonian).

Kic, P. 2015. Dust pollution in university offices. *Agronomy Research* **13**(3), 759–764.

Madureira, J., Paciencia, I., Rufo, J., Ramos, E., Barros, H., Teixeira, J.P. & Fernandes, E.O. 2015. Indoor air quality in schools and its relationship with children's respiratory symptoms. *Atmospheric Environment* **118**, 145–156.

Seppänen, O., Fisk, W.J. & Lei, Q.H. 2006. Ventilation and performance in office work. *Indoor Air* **16**, 28–36.

Riigi Teataja. 2013. Health Protection Requirements for Schools (AHPRS). *https://www.riigiteataja.ee/akt/131052013012?leiaKehtiv*. Accessed 10.04.2018 (in Estonian).

Reinvee, M., Uiga, J., Tärgla, T., Pikk, P. & Annuk, A. 2013. Exploring the effect of carbon dioxide demand controlled ventilation system on air humidity. *Agronomy Research* **11**(2), 463–470.

Simberg, T., Santtila, S., Soveri, P., Varjonen, A., Sala, M.E. & Sandnabba, N.K. 2009. Exploring genetic and environmental effects in dysphonia: a twin study. *J. Speech Lang. Hear. Res.* **62**, 153–163.

Tint, P., Traumann, A., Pille, V., Tuulik-Leisi,V.R. & Tuulik, V. 2012. Computer users´ health risks caused by the simultaneous influence of inadequate indoor climate and monotonous work. *Agronomy Research* **10**(1), 261–268.

Zikan, Z. 2011. Carbon dioxide – secret enemy. *http://vetrani.tzb-info.cz/vnitrni-prostredi/7132-oxid-uhlicity-utajeny-nepritel.* Accessed 29.1.2018 (in Czech).

Wargocki, P. & Wyon, D.P. 2017. Ten questions concerning thermal and indoor air quality effects on the performance of office work and schoolwork. *Building and Environment* **112**, 359–366.

Wolkoff, P. 2018. Indoor air humidity, air quality, and health – An overview. *International Journal of Hygiene and Environmental Health. https://doi.org/10.1016/j.ijheh.2018.01.015* Accessed 10.04.2018.

Agronomy Research **16**(4), 1781–1795, 2018
https://doi.org/10.15159/AR.18.164

The influence of drying method to the changes of bioactive compounds in lingonberry by-products

L. Ozola* and S. Kampuse

Latvia University of Life Sciences and Technologies, Faculty of Food Technology, Riga street 22, LV-3004 Jelgava, Latvia
*Correspondence: lieneozola8@inbox.lv

Abstract. The aim of this research was to evaluate the effect of different drying methods on industrially obtained lingonberry pulp juice by-products. For investigations, by-product was dried using hot air dryer (at temperatures 80 °C, 60 °C and 40 °C), microwave-vacuum dryer and freeze-dryer. The freshly defrosted by-product was used as control. All samples were analysed on the basis of their moisture content, colourimetric attributes (CIE L*a*b* colour system), content of vitamin C (iodometric method), content of total carotenes (TC), total phenol content (TPC), total anthocyanin content (TA) and antiradical activity (DPPH, $ABTS^+$).
The obtained data on content of vitamin C showed a 10% decrease between control and sample dried in hot air at 80 °C. Similar changes were noticed with total anthocyanin content, the lowest amount was also foun in this sample (306.72 ± 18.32 mg 100 g^{-1} DW). Total carotenes content was higher in freeze-dried sample (5.61 ± 0.16 mg 100 g^{-1} DW) which was very close to control sample. A significant loss of total phenol content was noticed after drying, up to 80%, similar tendencies were noticed with changes of antiradical activity. After evaluating the obtained data, the use of hot air dryer at 80 °C temperature resulted in the lowest amount of vitamin C and anthocyanins in lingonberry by-products, which makes this method unsuitable for drying by-products of these berries. However, vacuum assisted microwave drying and freeze drying showed less damaging impact on dried material.

Key words: air drying, antioxidant activity, freeze-drying, microwave-vacuum drying, *Vaccinium vitis-idaea.*

INTRODUCTION

Lingonberry (*Vaccinium vitis-idaea L.*), also known in English as partridgeberry, is a wild, perennial, evergreen dwarf shrub that has red edible berries. Berries from this plant are commonly used in Europe, especially the Northern hemisphere (Alam et al., 2016; Alam et al., 2018). These berries have been considered to have health promoting properties, due to their biochemical content. Lingonberries are a great source of different phenolic substances, vitamins and minerals (Kivimäki et al., 2012; Kivimäki et al., 2013). Mainly their health benefits have been connected to the rich content of polyphenols that are secondary metabolites in plants that consist of one or more aromatic rings and hydroxyl groups. Polyphenols in plants and also human body are important, because they protect them from external factors such as pathogens and UV-radiation. Regular intake of dietary flavonoids can decrease the risk factors of cardiovascular diseases and low-grade inflammation, polyphenols also are known to have positive effects on glucose homeostasis and they inhibit activation of platelets (Kivimäki et al., 2011; Kivimäki et al., 2012; Kivimäki et al., 2013). Also it needs to be taken into consideration that environmental factors like growth place, light, humidity, UV radiation and post-harvest processing (storing, pressing, pasteurization, drying, etc.) are all contributing factors to polyphenolic content of berries (Kivimäki et al., 2012).

In Latvia, lingonberries are consumed in several ways, they can be eaten fresh, frozen and stored for winter, used as decorative element in confectionery, jams, jellies, alcoholic and non-alcoholic drinks. However, for wider use, these berries have a very intense sour and bitter taste, due to the high amounts of organic acids, especially citric acid, which leads to a pH below 4. There is also a high amount of sugars, but the sweetness is masked by acids (Viljanen et al., 2014).

In food manufacturing the use of raw materials, including lingonberries as sufficiently as possible, is a very topical issue. There is a growing interest on creating new products from fruit waste products, which allows to utilize as much of the raw material as possible. One of the ways to process vegetable, fruit and berry by-poducts is to dry them. There are several food drying methods that could be potentially useful, however in this paper we will compare hot air drying (HAD), vacuum freeze-drying (VFD) and microwave-vacuum drying (MWVD).

Food stuff drying is one of the oldest and most commonly known food processing methods that is based on evaporation of free and loosely-bound water from inside the solid material into atmosphere. One of the most known and widely used drying methods is hot-air drying (HAD) or convective drying. In this method, hot air, that has low relative humidity, meets the surface of drying material that transfers t inside the product primarily by conduction. Then the liquid migrates onto the material surface and is transported away by air convection (Karam et al., 2016).

An alternative drying method to HAD is lyophilisation or freeze-drying (FD), this is a gentle dehydration method, which produces high-value dried products. This method is appealing because of its ability to maintain product colour, shape, aroma, nutritional value and overall quality. FD has two steps, in the first step product is frozen (-20 °C) and in the second step a controlled amount of heat (from -2 °C to -10 °C) under vacuum (VFD) or at atmospheric pressure (atmospheric freeze-drying) is applied to promote sublimation i.e. water change from solid to gas without passing through the liquid phase (Karam et al., 2016). Freeze drying can be carried out under vacuum, then heat will be supplied by surface heat exchange if required and evaporated moisture condensed on cold surface, but in case of atmospheric freeze-drying the product will be dried with air.

Microwave-vacuum drying (MWVD) is a fairly new method that has been introduced to replace hot-air drying. The basis of this method is microwave drying (MWD), where the first stage of drying is a heating-up period in which microwave energy is converted into thermal energy inside the moist product and the product temperature increases with time. The second stage is a called a rapid drying period during which thermal energy is used for moisture evaporization and transfer. The last stage is a reduced drying rate period where the local moisture is reduced to a point that the energy needed for moisture vaporization is lower than the thermal energy induced by microwaves. Applying microwave energy under vacuum is suitable for heat-sensitive products like fruits, vegetables and berries. This is also a drying method with efficiency of more energy and improved product quality (Karam et al., 2016).

All three drying methods for this study were chosen for several reasons. HAD was chosen, because this is a very traditional and widely used drying method. VFD is much newer approach and in many other studies, VFD has been proven to be less damaging towards food stuff biochemical content and sensory qualities. MWVD is also a rather new drying method, but mostly gained attention because of its short product drying time.

However, there is still little information found in literature about the influence of different drying techniques to the biochemical composition and quality of concrete products. Therefore, the aim of this research was to evaluate the effect of different drying methods on industrially obtained lingonberry pulp juice by-products. For this research the obtained by-product pulp was dried using HAD (80 °C, 60 °C, 40 °C), VFD and MWVD. To have more homogeneous samples, the dried samples were made into powders before analysis on moisture content, colour, and content of vitamin C, total carotenes, phenols, anthocyanins and antiradical scavenging activity. A frozen by-product (skin, seeds, etc.) was used as control.

MATERIAL AND METHODS

Sample preparation

Lingonberry (*Vaccinium vitis-idaea*) by-product as pulp was obtained from a local Latvian fruit, berry and vegetable product manufacturer Ltd 'KEEFA' in September 2017, but the by-product drying and analysing was done in November 2017 in Latvia University of Agriculture, Faculty of Food technology, Jelgava. The overall research plan can be seen in Fig. 1.

Lingonberry by-product (seeds, skin etc.) was obtained from industrially prepared lingonberry pulp juice as shown in Fig. 1 and stored frozen at -20 ± 2 °C for 1 month before drying and further testing.

For by-product drying, the obtained material was defrosted and divided into six parts. To each part a different drying method was applied and one was left as a control sample for comparison of data. Depending on drying method, abbreviations were used to identify all of the samples that can be seen in Table 1.

Table 1. The identification of samples

Sample name	Drying method
Control	no drying applied (defrosted lingonberry by-products)
HAD80	hot air drying at 80 °C
HAD60	hot air drying at 60 °C
HAD40	hot air drying at 40 °C
VFD	vacuum freeze-drying
MWVD	microwave-vacuum drying

Hot air drying (HAD) of by-products was done using 'Memmert' Universal Oven UF55 (Memmert, Germany) where by-products were dried at 80 °C for 6 h and 60 °C for 12 h and UF160 (Memmert, Germany) by-products dried at 40 °C for 16 h. The end point for product drying was based on personal experience, touch and visual product observation. By-product drying was stopped when material reached the appropriate degree of dryness for the production of powder.

Vacuum freeze-drying (VFD) was done using vacuum freeze-dryer FT33 (Armfield Ltd, Ringwood England). Sample was frozen in air freezer at -22 ± 2 °C temperature before drying. The temperature in condensation chamber was up to -40 °C and the pressure 20 Pa, drying time was up to 48 h.

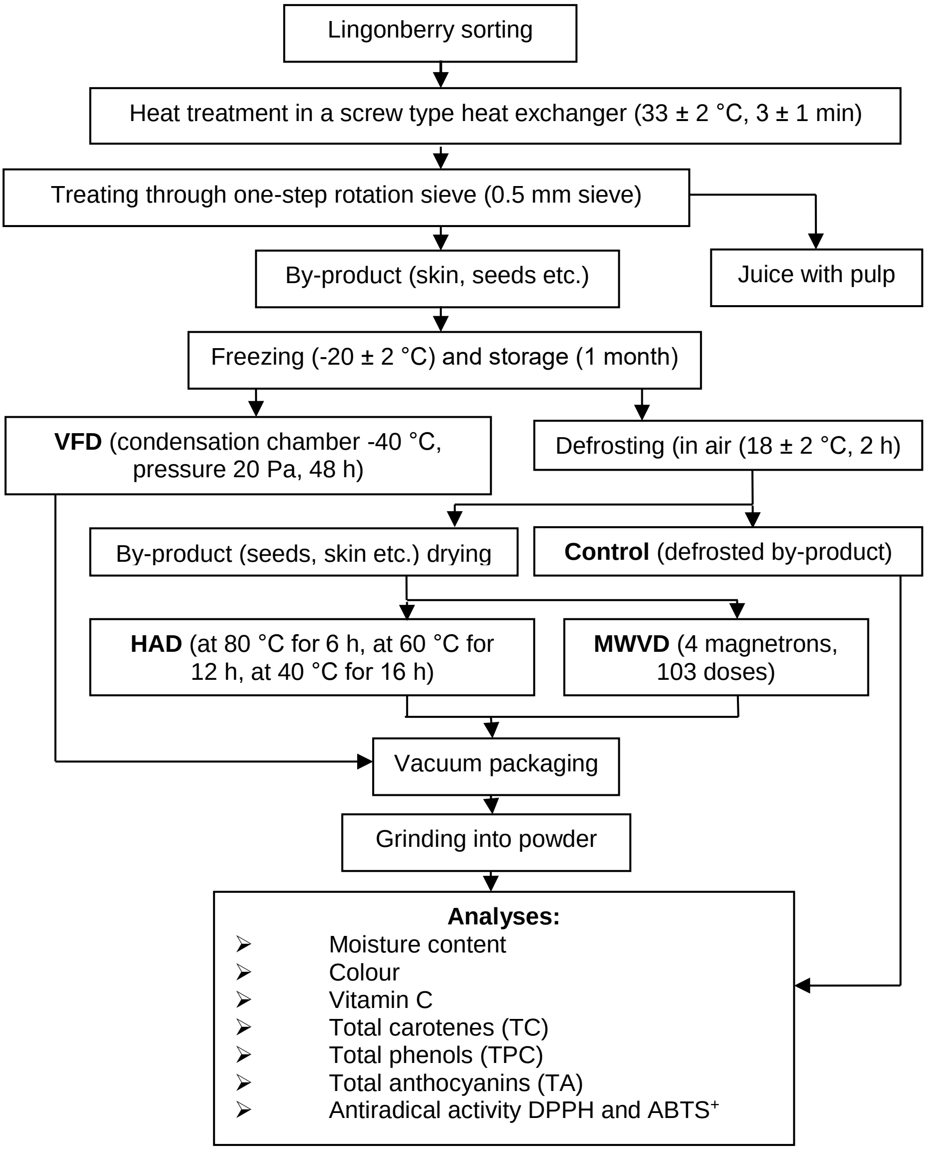

Figure 1. Overall research plan.

Microwave-vacuum drying (MWVD) was done using 'Musson-1' (Ingredient, Russia). The necessary amount of microwave energy (magnetron minutes) was calculated using empirical formulas when the initial moisture of the product is known (78%) and the final is estimated (8%) (Dorofejeva et al., 2011). For sample drying one cycle with four stages was carried out. The number of magnetrons was decreased along the drying process with subsequent doses, starting at 4 magnetrons and 50 doses, following by 3 magnetrons and 30 doses, 2 magnetrons and 13 doses and finally 1 magnetron 10 doses. The pressure in dryer was from 7.466 kPa to 9.332 kPa, cylinder rotation speed was 6 rpm.

All dried samples were vacuum-packaged to protect from air moisture absorption and for analysing purposes milled into powder to create a more homogenous sample. For milling electric Knifetec Mill 'Foss' (FOSS Analytical AB, Sweden) was used, samples were milled for 10 s and kept in LDPE zipped bags. A frozen by-product pulp was used as control and all samples were analysed on their moisture content, colour, and content of vitamin C, total carotenes, total phenol content, total anthocyanins and antiradical activity.

Chemicals and reagents

The chemical analyses of tested samples were carried using the following chemicals and reagents. Oxalic acid dehydrate (126.07 g mol^{-1}), L(+)-Ascorbic acid (176.13 g mol^{-1}), Petroleum ether 80/110, Potassium dichromate, Hydrochloric acid 35-38% (36.46 g mol^{-1}), Sodium carbonate anhydrous (105.99 g mol^{-1}), Potassium persulfate (270.33 g mol^{-1}), Potassium chloride (74.56 g mol^{-1}), Sodium chloride (58.44 g mol^{-1}), di-Sodium hydrogen phosphate anhydrous (141.96 g mol^{-1}), Potassium phosphate monobasic (136.09 g mol^{-1}) and Sodium hydroxide 0.1 N (40.00 g mol^{-1}) were purchased from Chempur (Poland). Iodine concentrate (0.05 mol L^{-1}) FIXANAL was obtained from Fluka Analytical, Sigma-Aldrich (Poland), Starch powder, soluble, ACS (for iodometry) was purchased from Alfa Aesara GmbH & Co KG (Germany). 2,2-Diphenyl-1-picrylhydrazyl was purchased from Sigma-Aldric (Germany), (±)-6-Hydroxil-2,5,7,8-tetra -methylchfomane-2-carboxylic acid was purchased from Sigma-Aldrich (Russian Federation). 2,2'-Azino-bis (3-ethylbenzothiazoline-6-sulfonic acid) diammonium salt ≥ 98% (HPLC) was purchased from Sigma-Aldrich (China). Folin-Ciocalteu, phenol reagent was obtained from Scharlau (Spain), Gallic acid, 98% was purchased from Acros Organics (Belgium). Additional solvents as ethanol (96%) and ultra pure water were provided by Latvia University of Agriculture (Latvia, Jelgava).

Determination of moisture content

Content of moisture in all samples was determined accordingly to standard ISO 6496:1999. For moisture content detection to control (defrosted) sample approximately 5 g was used, for dry samples 2 g of milled sample each in two replications was dried using 'Memmert' Universal Oven UF55, at 105 °C periodically checking the weight changes during drying process by weighing the sample until minimal changes can be observed. Weight loss was used to calculate the moisture content of the sample.

Determination of vitamin C

Content of vitamin C was determined according to the iodine method as described by Kerch et al. (2011) with some modifications. This method is based on determination of L-ascorbic acid, the reduced form of ascorbic acid. A sample of 25 g for defrosted sample and 5 g for dried, milled samples were poured with 100 mL of 6% solution of oxalic acid, homogenized for 1 min, and filtered. Then, 2 mL of 1% solution of starch was added to 10 mL of filtrate and the filtrate was titrated with 0.05 n iodine solution until change of colour, which does not disappear during 30 s. For standard solution of ascorbic acid, 20 mg of ascorbic acid was dissolved in 100 mL of the same 6% oxalic acid solution, 2 mL of the same 1% starch solution was added to 25 mL of the standard solution and the mixture was titrated. The content of ascorbic acid expressed in milligrams per 100 g DW of product was calculated using Eq. (1), on the basis of four replications (Kerch et al., 2011; Ozola at al., 2017):

$$C = 5{,}000 \cdot \frac{V_{sample}}{m \cdot V_{standard}} \quad (1)$$

where V_{sample} – volume of the iodine solution titrated in a sample, mL; $V_{standard}$ – volume of the iodine solution titrated in a standard solution, mL; m – the amount of sample, g.

Determination of total carotenes

For total carotene determination, a spectrophotometric (UV/VIS spectrophotometer Jenway 6705 (Bibby Scientific Ltd., UK)) method described by Kampuse et al. (2015) with modifications was used. A sample of 2 g for control and 1 g for dried, milled samples was mixed with 20 mL of ethanol and mixed on a magnetic stirrer for 15 min. Further 10 mL of pure water was added to dried samples, to ensure layer formation, and stirred for 10 min after which, 25 mL of petroleum ether was added and stirred for an hour. The absorption of oil layer was measured at 440 nm. The content of TC expressed in milligrams per 100 g^{-1} DW was calculated in three replications (Ozola et al., 2017).

Determination of total anthocyanins (TA)

Total anthocyanin content was determined by spectrophotometric method described by Kerch et al. (2011) with some modifications. A sample of 5 g for control and 1 g for dry samples was mixed with 40 g of ethanol and 1.5 M HCl solution (85 : 15 by volume) and homogenized for 1 min. Then the sample was filtered, and filtrate volume measured. TA where detected on spectrophotometer Jenway 6705 at 540 nm. The sample was diluted until absorption was between 0.6 and 0.8. The content of TA expressed in milligrams per 100 g^{-1} DW was calculated with the Eq. (2).

$$C = \frac{A \cdot v \cdot d \cdot 1{,}000}{980 \cdot m} \quad (2)$$

where A – absorbance, expressed as absorbance units; v – volume of filtrate, mL; d – dilution degree; m – sample weight, g.

Measurements were carried out in two replications (Ozola et al., 2017).

Determination of total phenol content

The detection of total phenol content was achieved according to the Folin-Ciocalteu method (Yu et al., 2003) with modifications. A sample of 2 g for control and 1 g for dry samples was used for extract preparation. To 0.5 mL of extracted sample 2.5 mL of 0.2 N Folin-Ciocalteu reagent that has been diluted ten times with pure water was added. After 5 min 2.0 mL of 7.5% $NaCO_3$ was added, the resulting solution was mixed and allowed to stand for 30 min at 18 ± 1 °C in a dark place (Priecina & Karklina, 2014). Absorption was read at 765 nm using JENWAY 6300 (Banoworld Scientific Ltf., UK) spectrophotometer. Measurements were carried out in six replications from two separately weighed samples, the obtained data were expressed as gallic acid mg equivalent (GAE mg $100g^{-1}$ dry sample) (Ozola et al., 2017).

Determination of antiradical activity (DPPH) and radical scavenging activity ($ABTS^+$)

The antiradical activity of extracts was measured on the basis of scavenging activities of the stable 2,2-diphenil-1-picrylhydrazyl-(DPPH) free radical (Yu et al., 2003) with modifications. To 0.5 mL of extracted sample, 3.5 mL freshly made DPPH solution was added; the mixture was shaken and kept in the dark place at 18 ± 1 °C for 30 min; absorbance was measured at 517 nm using JENWAY 6300 spectrophotometer, measurements were carried out in six replications from two separately weighed samples. For the quantitative expression of antiradical activity, the Trolox equivalent of 6-Hydroxil-2,5,7,8-tetra-methylchfomane-2-carboxylic acid was used. A Trolox calibration curve was created and, using the red-out absorbance, the antiradical activity was expressed as mg Trolox 100 g^{-1} per dry sample (Priecina & Karklina, 2014; Ozola et al., 2017).

The radical scavenging activity of extracts was also measured by $ABTS^+$ radical cation assay as described by Re et al. (1999). A stock solution of 2,2′-azino-bis (3-ethylbenz-thiazoline-6-sulfonic) acid (ABTS) (2 mM) was prepared by dissolving in 50 mL of phosphate buffered saline (PBS) obtained by dissolving 8.18 g sodium chloride (NaCl), 0.27 g potassium dihydrogen phosphate (KH_2PO_4), 1.42 g sodium phosphate dibasic (Na_2HPO_4) and 0.15 g potassium chloride (KCl) in 1 L of ultra pure water. If the pH was lower than 7.4, it was adjusted with sodium hydroxide (NaOH). Ultra pure water was used to prepare 70 mM solution of potassium persulfate ($K_2S_2O_8$). $ABTS^+$ radical cation was produced by reacting 50 mL of ABTS stock solution with 0.2 mL of $K_2S_2O_8$ solution and allowing the mixture to stand in the dark at room temperature (18 ± 1 °C) for 15–16 h before use. The $ABTS^+$ radical was stable in this form for more than 2 days when stored in these conditions. For the assessment of extracts, the $ABTS^+$ solution was diluted with PBS to obtain an absorbance of 0.800 ± 0.030 at 734 nm. 5 mL of $ABTS^+$ solution were mixed with 0.05 mL of extract. The absorbance was read at ambient temperature (18±1 °C) after 10 min. PBS solution was used as a blank sample. For both types of antiradical scavenging activity determination, the obtained data were expressed as millimolar Trolox equivalents per 100 g^{-1} DW of sample (Tomsone et al., 2012).

Colour analysis

Sample colour was determined using colour analyser *ColorTec-PMC* (Accuracy Microsensors, Inc, New York, USA) that captures the reflected light of the object. In this study the L*a*b* colour system was used, developed by CIE (*International Commission for Lighting and Ilumination*) 1976 version (Mokrzycki & Tatol, 2011).

The CIE L*a*b* system is based on opponent colour model: L* black/white, describes overall colour intensity, where 0 means black, and 100 is the maximum light intensity; +a*/-a* red/green; +b*/-b* -yellow/blue (Mokrzycki & Tatol, 2011).

In case of the L*a*b* space, the ΔE difference between two colours is calculated by Eq. (3):

$$\Delta E = \sqrt{(\Delta L^*)^2 + (\Delta a^*)^2 + (\Delta b^*)^2} \quad (3)$$

where ΔE – absolute colour difference; ΔL^* – colour intensity difference; Δa^* – red and green colour difference; Δb^* – yellow and blue colour difference (Mokrzycki & Tatol, 2011). The measurements for colour analysis were carried out in five replications.

Statistical analysis

The obtained data was processed using 'Microsoft Office Excel' 2007 version, differences between the results were analysed using one-factor ANOVA followed by Tukey-Kramer method, The linear correlation analysis was performed to determine the relationship between TPC, DPPH and ABTS, and between colour analyses factor a* and total anthocyanin content. The obtained results were presented as their means with standard errors. Differences among results were considered to be significant if $P < 0.05$ (Ozola et al., 2017).

RESULTS AND DISCUSSION

Sample moisture content

The obtained data on dried lingonberry by-product moisture content showed that before drying on average it was 78.8% per 100 g of product (w/w), but after drying the least proportion of moisture was detected in hot air dried samples (HAD80 and HAD60 mainly), where it was approximately 1.8% (w/w). The moisture content of sample HAD40 on average was 3.8% (w/w), in sample that was vacuum freeze-dried (VFD) approximately 4.6% (w/w), but the highest moisture content 8.6% (w/w) was detected in sample MWVD. The detected moisture in samples show that by using HAD at higher temperatures such as 80 °C and 60 °C can create sample with lower moisture than all of the other tested drying methods. HAD is a much more invasive product drying method due to the higher temperatures and prolonged drying time (Karam et al., 2016). These conditions and the fact that the dried material was shredded might have influenced the higher water loss. This type of dried material has a larger surface, the cellular structure was mechanically damaged and therefore could increase the evaporation of water.

Content of vitamin C, total carotenes and total anthocyanins

The obtained data on content of vitamin C did not show any large differences overall, however significant differences between some samples were detected $P < 0.05$. In the control sample, there was 79.4 ± 2.5 mg 100 g^{-1} DW of vitamin C, which was very close to content of vitamin C in dried samples (Table 2). However significant differences were detected between HAD80 and all other samples. By-product hot air drying at 80 °C significantly decreased the amount of vitamin C in dried sample (72.1 ± 4.5 mg 100 g^{-1} DW). Although the vitamin C content had only decreased by 10%, these findings are consistent with other researcher data showing from 20% to 60% depletion of vitamin C for several agricultural materials (Karam et al., 2016). When evaluating other samples no significant difference were detected within the changes of vitamin C depending on drying method of lingonberry by-products. These findings are consistent when analysing the obtained data from freeze-drying and microwave drying treatments, but less common with hot air drying. However Ali et al. (2016) in their research have found that not only freeze-drying and microwave 100 W drying, but also oven dried at 80 °C guava fruit slices had retained a relatively high amount of vitamin C. Ali et al. (2016) concludes that drying temperature and drying time are key parameters which directly affect the vitamin C concentration in guava. Despite the fact that with lingonberry by-product hot air drying at 80 °C showed the highest decrease, it could be possible that in our case a lower temperature and prolonged drying time had less damaging effect on vitamin C content during drying at 40 °C and 60 °C.

When analysing the data on TC and TA, some differences were noticed in comparison to content of vitamin C. The highest total carotene (Table 2) content was in control sample (5.83 ± 0.24 mg 100 g^{-1} DW), but after drying a significant decrease ($P < 0.05$) was noticed for all drying methods except for vacuum freeze-drying (5.61 ± 0.16 mg 100 g^{-1} DW). HAD at 80 °C showed a TC decrease of 19%, but at 40 °C approximately 23% and on average 33% decrease in total carotene content was in sample HAD60 and MWVD.

Although by-product drying at 80 °C showed a significantly higher ($P < 0.05$) TC content then drying at 60 °C no supporting literature was found to fully explain these results. Moreover the statistical analyses showed no significant differences between HAD80 and HAD40, and between HAD60 and HAD40 (Table 2.)

Table 2. Content of vitamin C, TC and TA in lingonberry by-product powders

Sample	Vitamin C (mg 100 g^{-1} DW)	Total carotenes (mg 100 g^{-1} DW)	Total anthocyanins (mg 100 g^{-1} DW)
Control	79.4 ± 2.5 ^{abcd}	5.83 ± 0.24 ^{a}	566.7 ± 24.4
HAD80	72.1 ± 4.5	4.68 ± 0.34 ^{b}	306.7 ± 18.3 ^{a}
HAD60	79.3 ± 2.5 ^{aefg}	3.94 ± 0.17 ^{cd}	343.0 ± 14.5 ^{abc}
HAD40	84.9 ± 2.9 ^{behj}	4.41 ± 0.17 ^{bce}	387.5 ± 5.0 ^{bde}
MWVD	85.5 ± 2.9 ^{cfhk}	3.95 ± 0.29 ^{de}	412.8 ± 7.2 ^{df}
VFD	84.0 ± 3.3 ^{dgjk}	5.61 ± 0.16 ^{a}	396.2 ± 3.4 ^{cef}

Mean values in each column followed by different letters do not have a significant difference according to Tukey-Kramer method ($P < 0.05$).

Considering the difference in sample preparation before testing could explain the lack of significant difference in content of vitamin C and TC. Control was more of a heterogeneous mass in comparison to dried materials, which were pulverized and thus making them more of a homogenous sample therefore depicting the content of vitamin C and TC in analysed samples more precisely. In addition, control did not have any pre-treatment before analysing so this could allow for further enzymatic activity continuing decreasing the amount of vitamin C until sample was analysed.

The content of total anthocyanins (Table 2) also showed a significant decrease after drying ($P < 0.05$). The highest content of TA after drying was in sample MWVD (412.8 ± 7.2 mg 100 g^{-1} DW) which was 27% less than in control sample. Also a relatively high content of TA was found in samples HAD40 (387.5 ± 5.0 mg 100 g^{-1} DW) and VFD (396.2 ± 3.4 mg 100 g^{-1} DW) showing no significant difference $P < 0.05$, corresponding to 45% decrease in sample HAD80 (306.7 ± 18.3 mg 100 g^{-1} DW).

When comparing the obtained data with literature it has been observed that depending on the product there have been found occasions where carotenoid compounds (lycopen in particularly) were heat-stable, even after severe heat treatment, but in other author researches around 19% of TC decrease had been noticed after air-dried carrot slices, paprika and sweet potatoes (Karam et al., 2016). Not only vitamin C and TC, but also total anthocyanins are highly unstable compounds and changes of these compounds can differ from the product to which drying has been applied. Drying at low temperature might not be effective to inactivate enzyme or might take longer time to inactivate the enzymes which are responsible for the anti-oxidative properties such as ascorbic acid, carotenoid and TPC degradation (Sehrawat et al., 2018), and this could potentially explain the TC changes in lingonberry-by product when HAD was applied.

When looking at the obtained data Table 1 it can be clearly seen that there is a tendency of TA decrease when the drying temperature increases (Ruse et al., 2011). Overall Sehrawat et al. (2018) when drying mango cubes detected higher bioactive compound retention. Oxygen deficient environment had provided a better protective effect form oxidative loss of bioactive compounds as compared to HAD (Sehrawat et al., 2018), these findings are also applyable with our research on lingonberry by-product drying.

Overall according to the obtained data hot air drying at 80 °C had the most effect on degradation of vitamin C and total anthocyanin content. The most suitable drying method for beather retention of TC proved to be VFD, but lingonberry by-product MWVD showed the highest content of vitamin C and TA.

Total phenol content, DPPH and ABTS$^+$

The lingonberry by-product powder TPC as shown in Fig. 2. in control sample was very high but after drying the obtained data showed an average decrease of 80% with no significant differences between the used drying methods ($P < 0.05$).

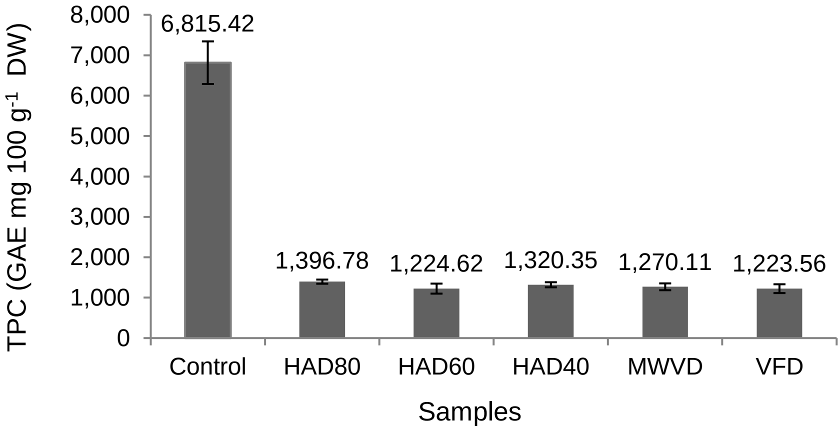

Figure 2. Total phenol content in lingonberry by-product samples (GAE mg 100 g^{-1} DW).

Similar tendencies to TPC were also noticed with antiradical activity, supported by Pearson's coefficient showed a strong correlation $r = 0.9977$ between TPC and DPPH. Also a strong correlation of $r = 0.8585$ was found between TPC and ABTS$^+$, and DPPH and ABTS$^+$ ($r = 0.8628$).

Overall a 60% decrease in antiradical activity was found in all lingonberry-by product powders (Table 2) compared to control ($P < 0.05$), this was also significantly evidenced from ABTS$^+$. Slight difference in DPPH was found between HAD80 (232.67 ± 12.30 mM TE 100g^{-1} DW) and HAD60 (210.14 ± 13.21 mM TE 100g^{-1} DW).

The lowest radical scavenging activity was detected in hot air dried samples (HAD80; HAD60 and HAD40). In sample HAD80 radical scavenging activity had significantly decreased in comparison with control sample, where it was 274.76 ± 12.38 mM TE 100 g^{-1} DW (Table 3). However vacuum freeze-drying showed to be less invasive (215.99 ± 8.06 mM TE 100 g^{-1} DW). Although strong correlation was found between DPPH and $ABTS^+$, the radical scavenging activity showed more significant differences between dried samples in comparison to DPPH (Table 2). No real differences (*P* > 0.05) between samples were found when comparing HAD80 to HAD60, also between HAD60 and HAD40, HAD40 and MWVD, and MWVD compared to FVD.

Table 3. Content of DPPH and $ABTS^+$ in lingonberry by-product powders

Sample	DPPH (mM TE 100g^{-1} DW)	$ABTS^+$ (mM TE 100g^{-1} DW)
Control	551.96 ±20.67	274.76 ± 12.38
HAD80	232.67 ± 12.30 ^{abc}	153.99 ± 12.17 ^{a}
HAD60	210.14 ± 13.21 ^{adef}	170.37 ± 16.57 ^{ab}
HAD40	205.53 ± 8.56 ^{dgh}	180.38 ± 17.70 ^{bc}
MWVD	227.71 ± 20.39 ^{begi}	195.98 ± 9.38 ^{cd}
VFD	220.04 ± 13.03 ^{cfhi}	215.99 ± 8.06 ^{d}

Mean values in each column followed by different letters do not have a significant difference according to Tukey-Kramer method (*P* < 0.05).

(Ek et al., 2006) in their research found 28 phenolic compounds, that included flavonols, anthocyanidins, catechins and their glycosides, and different caffeoyl and ferulic acid conjugates. Although it was not expected from this study to detect such high depletion of TPC after drying it has been reported before that polyphenolics are heat sensitive and prolonged heat treatment causes irreversible chemical changes to phenol content (Guiné et al., 2015). Other contributing factors may include polyphenol binding with other compounds, alterations in their chemical structure, activity of polyphenol ocidase, organic acid content, sugar content and product pH (Guiné et al., 2015).

When evaluating antioxidant activity with DPPH and $ABTS^+$ in plant materials it is possible to obtain varying results. This happens, because of their different working mechanisms of the two assays (Shalaby & Shanab, 2013). DPPH is a stable free radical with an absorption band at 515 nm that is lost when reduced by an antioxidant or a free radical species. But $ABTS^+$ assay measures the relative ability of antioxidant to scavenge the ABTS generated in aqueous phase, as compared with a Trolox standard (Shalaby & Shanab, 2013).

$ABTS^+$ is also known to be useful to determine antioxidant activity of both lipophilic (α-tocopherol, β-carotene) and hydrophilic antioxidants in various matrices. Also reacting rapidly with antioxidants over a wipe pH. However DPPH interactions between antioxidants are also determied by theyr structural conformation and reaction time with DPPH (Martysiak-Żurowska & Wenta, 2012).

In a different study by Michalska et al. (2017), it was also noticed that prolonged exposure to oxygen can considerably affect the compound radical scavenging activity with assay $ABTS^+$, which was noticed when comparing, HAD samples with MWVD and VFD samples where samples were dried in assistance of vacuum. Also Correia et al. (2017) showed that an increase in drying temperature is deleterious to product TPC and antioxidant activity.

Colour analysis

Dried lingonbery by-products were mild into powder and their colourimetric properties were measured (Fig 3.) The obtained data on dried powder analysis showed that there is a slight significant difference in L* factor value and therefore sample MWVD was darker in comparison to HAD80 and VFD. When calculating hue angle values and placing them on CIE L*a*b* 1976 colour wheel the dominant colour for all samples was light red.

The distinct red colour in lingonberries is created by anthocyanins, however compairing lingonberry-by product powder colour analysis factor a* value and total anthocyanin content showed a low correlation r = 0.382.

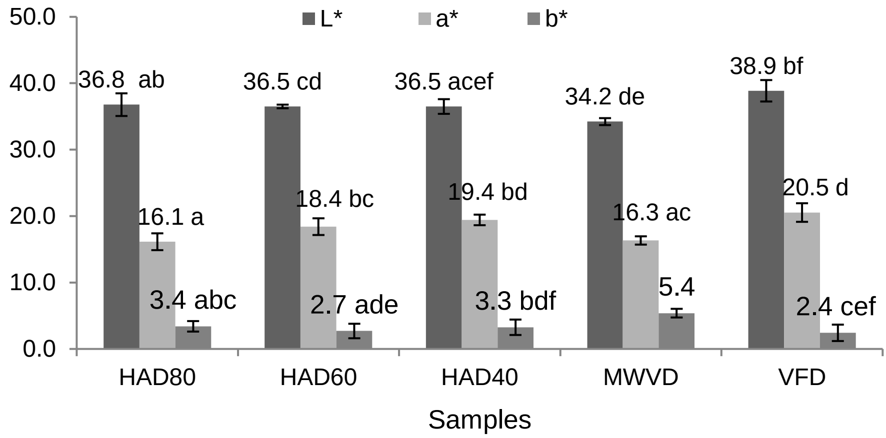

Figure 3. Dried lingonbery by-product colour analysis (CIE L*a*b). Mean values in each row followed by different letters do not have a significant difference according to Tukey-Kramer method ($P < 0.05$).

Mokrzycki & Tatol (2011) described how mathematically it would be possible to determine colour perception and analyse if two samples are different in colour and whether human eyes are able to distinguish them. In CIE L*a*b* system the perceptual colour difference can be determined by ΔE value (Table 4.) where:

$0 < \Delta E < 1$ the observer does not notice the difference;

$1 < \Delta E < 2$ only experienced observer can notice the difference;

$2 < \Delta E < 3.5$ inexperienced observer also notices difference;

$3.5 < \Delta E < 5$ there is a clear difference in colour and it is noticeable;

$5 < \Delta E$ observer notices two different colours (Mokrzycki & Tatol, 2011).

Table 4. Dried lingonberry by-product powder absolute colour difference

Sample	ΔE	ΔE	ΔE	ΔE
HAD80	ΔE with HAD80			
HAD60	2.4	ΔE with HAD60		
HAD40	3.3	1.2	ΔE with HAD40	
MWVD	3.2	4.1	4.4	ΔE with MWVD
VFD	5.0	3.2	2.7	4.7

After calculating ΔE and evaluating colour differences between each sample, the results can be seen in Table 4. The results show that there is no noticale difference between sample HAD60 and HAD40 colour, because absolute colour ddifference between both ΔE values is 1.2. Nevertheless, there is a clear and noticeable difference between HAD80 and VFD also between samples HAD60 and MWVD, HAD40 and MWVD, MWVD and VFD, because $3.5 < \Delta E < 5$. The data coincide with information given in Fig. 3, where microwave-vacuum dried sample is noticeably darker and VFD lighter than other samples.

CONCLUSIONS

In conclusion, of this research it is very difficult to unambiguously advice the most suitable drying method for drying lingonberry pulp juice by-products due to the inconsistencies of the results and lack of significant differences between the used drying methods.

By-product drying at 80 °C coused the highest degradation of vitamin C an total anthocyanin content. More suitable drying methods where vacuum assisted microwave drying and freeze-drying that resulted in better retention of total carotenes, total anthocyanins and vitamin C content.

After by-product drying an 80% degradation of total phenol content was detected which strongly correlated with antiradical activity (DPPH) $r = 0.9977$ and radical scavenging activity ($ABTS^+$) $r = 0.8585$. Because phenols are heat sensitive, drying might have caused changes in their chemical structure, organic acid, sugar content, pH etc. therefore reducing TPC in dried samples, however no significant differences were detected between dried samples ($P > 0.05$).

Vacuum assisted drying methods also showed slightly better retention of DPPH and $ABTS^+$. Similarly, to TPC sample, antiradical activity showed no significant differences between used drying methods, but the highest radical scavenging activity was determined in VFD in contrary the lowest was found in HAD80, however no significant difference was found when compared to HAD60.

In reference to the findings it is possible to say that hot air drying at 80 °C is not the most suitable method for lingonberry by-product drying, however vacuum assisted freeze-drying could be suggested due to the highest retention of vitamin C, total carotenes and by DPPH and $ABTS^+$.

ACKNOWLEDGEMENTS. The research was financed by program 'Scientific Capacity Building LUA' project A05-06 'Development of special dietary foods with high bioavailability'.

REFERENCES

Alam, Z., Morales, H.R. & Roncal, J. 2016. Environmental conditions affect phenolic content and antioxidant capacity of leaves and fruits in wild partridgeberry (*Vaccinium vitis-idaea*). *Botany* **13**, 509–521.

Alam, Z., Roncal, J. & Peña-Castillo, L. 2018. Genetic variation associated with healthy traits and environmental conditions in *Vaccinium vitis-idaea*. *BMC Genomics* **19**(1), 1–13.

Ali, M.A., Yusof, Y.A., Chin, N.L. & Ibrahim, M.N. 2016. Effect of different drying treatments on colour quality and ascorbic acid concentration of guava fruit. *International Food Research Journal* **23**, S155–S161.

Color Models CIELAB. *http://dba.med.sc.edu/price/irf/Adobe_tg/models/cielab.html.* Accessed 14.1.2018

Correia, P.M.R., Guiné, R.P.F., Correia, A.C., Brito, M.F.S., Ribeiro, R.P. 2017. Physical , chemical and sensory properties of kiwi as influenced by drying conditions. *Agricultural Engineering International: CIGR Journal* **19**(3), 203–212.

Dorofejeva, K., Rakcejeva, T., Galoburda, R., Dukalska, L. & Kviesis, J. 2011. Vitamin C content in Latvian cranberries dried in convective and microwave vacuum driers. *Procedia Food Science* **1**, 433–440.

Ek, S., Kartimo, H., Mattila, S. & Tolonen, A. 2006. Characterization of Phenolic Compounds from Lingonberry (*Vaccinium vitis-idaea*). *Journal of Agricultural and Food Chemistry* **54**(26), 9834–9842.

Guiné, R.P.F., Barroca, M.J., Gonçalves, F.J., Alves, M., Oliveira, S. & Correia, P.M.R. 2015. Effect of Drying on Total Phenolic Compounds, Antioxidant Activity, and Kinetics Decay in Pears. *International Journal of Fruit Science* **15**(2), 173–186.

ISO 6496:1999. Animal feeding stuffs – determination of moisture and other volatile matter content. *https://law.resource.org/pub/in/bis/S06/is.iso.6496.1999.pdf*. Accessed 14.1.2018

Kampuse, S., Ozola, L., Straumite, E. & Galoburda, R. 2015. Quality parameters of wheat bread enriched with pumpkin (*Cucurbita Moschata*) by-products. *Acta Universitatis Cibiniensis. Series E: Food Technology* **19**, 3–14.

Karam, M.C., Petit, J., Zimmer, D., Baudelaire Djantou, E. & Scher, J. 2016. Effects of drying and grinding in production of fruit and vegetable powders: A review. *Journal of Food Engineering* **188**, 32–49.

Kerch, G., Sabovics, M., Kruma, Z., Kampuse, S. & Straumite, E. 2011. Effect of chitosan and chitooligosaccharide on vitamin C and polyphenols contents in cherries and strawberries during refrigerated storage. *European Food Research and Technology* **233**, 351–358.

Kivimäki, A.S., Ehlers, P.I., Siltari, A., Turpeinen, A.M., Vapaatalo, H. & Korpela, R. 2012. Lingonberry, cranberry and blackcurrant juices affect mRNA expressions of inflammatory and atherothrombotic markers of SHR in a long-term treatment. *Journal of Functional Foods* **4**, 496–503.

Kivimäki, A.S., Ehlers, P.I., Turpeinen, A.M., Vapaatalo, H. & Korpela, R. 2011. Lingonberry juice improves endothelium-dependent vasodilatation of mesenteric arteries in spontaneously hypertensive rats in a long-term intervention. *Journal of Functional Foods* **3**, 267–274.

Kivimäki, A.S., Siltari, A., Ehlers, P.I., Korpela, R. & Vapaatalo, H. 2013. Lingonberry juice lowers blood pressure of spontaneously hypertensive rats (SHR). *Journal of Functional Foods* **5**, 1432–1440.

Martysiak-Żurowska, D. & Wenta, W. 2012. A comparison of abts and dpph methods for assessing the total antioxidant capacity of human milk. *Acta Sci. Pol. Technol. Aliment* **11**(1), 83–89.

Michalska, A., Wojdyło, A., Lech, K., Łysiak, G.P. & Figiel, A. 2017. Effect of different drying techniques on physical properties, total polyphenols and antioxidant capacity of blackcurrant pomace powders. *LWT - Food Science and Technology* **78**, 114–121.

Mokrzycki, W.S. & Tatol, M. 2011. Colour difference dE- A survey. *Machine Graphics and Vision* **20**, 383–411.

Ozola, L., Kampuse, S. & Galoburda, R. 2017. The effect of high pressure processing on enteral food made from fresh or semi-finished ingredients. In: *11th Baltic Conference on Food Science and Technology.* Foodbalts2017, Latvia, pp. 80–85.

Priecina, L. & Karklina, D. 2014. Natural antioxidant changes in fresh and dried spices and vegetables. *International Journal of Biological, Biomolecular, Agricultural, Food and Biotechnological Engineering* **8**, 492–496.

Re, R., Pellegrini, N., Proteggente, A., Pannala, A., Yang, M. & Rice-Evans, C. 1999 Antioxidant activity applying an improved ABTS radical cation decolorization assay. *Free Radical Biology and Medicine* **26**, 1231–1237.

Ruse, K., Rakscejeva, T., Galoburda, R. & Dukalska, L. 2011. Anthocyanin content in Latvian cranberries dried in convective and microwave vacuum driers. *Food Sciences*, 100–106.

Sehrawat, R., Nema, P.K. & Kaur, B.P. 2018. Quality evaluation and drying characteristics of mango cubes dried using low-pressure superheated steam, vacuum and hot air drying methods. *LWT – Food Science and Technology* **92**, 548–555.

Shalaby, E.A. & Shanab, S.M.M. 2013. Comparison of DPPH and ABTS assays for determining antioxidant potential of water and methanol extracts of *Spirulina platensis*. *Indian Journal of Marine Sciences* **42**(5), 556–564.

Tomsone, L., Kruma, Z. & Galoburda, R. 2012. Comparison of different solvents and extraction methods for isolation of phenolic compounds from horseradish roots *Research for Rural Development* **4**(1), 236–241.

Viljanen, K., Heiniö, R.L., Juvonen, R., Kössö, T. & Puupponen-Pimiä, R. 2014. Relation of sensory perception with chemical composition of bioprocessed lingonberry. *Food Chemistry* **157**, 148–156.

Yu, L., Perret, J., Harris, M., Wilson, J. & Haley, S. 2003. Antioxidant Properties of Bran Extracts from 'Akron' Wheat Grown at Different Locations. *Journal of Agricultural and Food Chemistry* **51**, 1566–1570.

Agronomy Research **16**(4), 1796–1808, 2018
https://doi.org/10.15159/AR.18.177

POST herbicide programme for effective weed control in winter wheat (*Triticum aestivum* L.)

Z. Pacanoski[1] and A. Mehmeti[2,*]

[1]University Ss. Cyril and Methodius, Faculty for Agricultural Sciences and Food, 16-ta Makedonska brigada 3, MK1000 Skopje, Republic of Macedonia
[2]University of Prishtina, Department of Plant Protection, Bill Clinton p.n., XK10000 Prishtina, Republic of Kosovo
[*]Correspondence: arben.mehmeti@uni-pr.edu

Abstract. Field experiments were conducted during two winter wheat-growing seasons to evaluate the efficacy of some new POST herbicides and herbicide combinations for those effective controls of weeds in winter wheat crops in the Republic of Macedonia. The weed population consisted mainly of annual winter and spring and some perennial weeds. Weediness comprised 116 and 208 plants m^{-2} in 2012–2013 and 2013–2014, respectively, in the Skopje region, and 93 and 114 plants m^{-2} in 2012–2013 and 2013–2014, respectively, in the Probištip region. All POST herbicides effectively reduced dominant weeds density (> 93%) in the Skopje region in both years, as well as in the Probištip region in 2012–2013, but not in 2013–2014. In this year, lower temperature directly following application decreased efficacy of POST applied herbicides, which provided control of *Lolium perenne* that was between 76 and 84%; control of *A. ludoviciana* was less than 85%; control of *B. radians* was no more than 83% and no one treatment controlled *P. convolvulus* more than 82%. Wheat yields in the Skopje region were not significant among years for the different POST herbicide applications and ranged between 3,580 and 3,720 kg ha^{-1} in 2012–2013, and between 3,760 and 3,910 kg ha^{-1} in 2013–2014. A significant treatment by year interaction resulted in two distinct years for wheat yields in the Probištip region with POST herbicides. In 2012–2013, wheat yields were between 3,230 and 3,390 kg ha^{-1}, but in 2013–2014, wheat yields ranged from 3,060 to 3,490 kg ha^{-1} and weed-free control showed a significant higher wheat yield compared to all evaluated herbicides.

Key words: efficacy, herbicide, weeds, wheat.

INTRODUCTION

Weed-crop competition is a major factor limiting worldwide production of many crops, including wheat. Weeds are one of the major constraints in wheat production, as they reduce productivity due to competition (Khan et al., 2002; Olesen et al., 2004; Siddiqui et al., 2010) and allelopathy (Gao et al., 2009; Bertholdsson, 2012; Zhang et al., 2016), serve as an alternate host for various insects and fungi by providing habitats for pathogens (Capinera, 2005), and increase harvesting costs (Ozpinar, 2006). According to many authors, weeds cause 17–30% losses in wheat annually (Milberg & Hallgren, 2004; Zand et al., 2007; Rao & Chauhan, 2015). Therefore, the control of weeds is a basic requirement and major component of management in the wheat production system (Nazari et al., 2013). Weed management in wheat is a combination of cultural and herbicidal application (Streit et al., 2003; Chachar et al., 2009; Knežević et al., 2012). Chemical control is the most commonly used and reliable method for controlling weeds in wheat. The importance of this control has been emphasised by various authors (Klein et al., 2006; Frihauf et al., 2010; Geier et al., 2011; Sheikhhasan et al., 2012; Mandal et al., 2014; Mehmood et al., 2014; Mehmeti et al., 2018).

Herbicides registered for weed control in winter wheat in the Republic of Macedonia have significantly changed over the past 4–5 years. Acetolactate synthase (ALS)-inhibiting herbicides are primary herbicides for broadleaf and annual grass weed control in winter wheat. They are widely used because of low environmental impact, low mammalian toxicity, and high efficacy (Khaliq et al., 2011; Reddy et al., 2013). Florasulam, metsulfuron-methyl, tritosulfuron, triasulfuron and tribenuron are registered for weed control in wheat (Kostov & Pacanoski, 2004; Pacanoski & Jankuloski, 2012). These herbicides provide good broadleaf weed control efficacy, but have little to no activity on grass weeds. However, the herbicides pyroxsulam, iodosulfuron-methyl-sodium and mesosulfuron-methyl selectively controls both grass and broadleaf weeds in wheat.

Pyroxsulam is a broad-spectrum herbicide and triazolopyrimidine sulphonamide is labelled for grasses and broadleaf weed control in wheat (Wells, 2008) which was registered in 2011. Herbicides, pyroxsulam as well as the mesosulfuron, iodosulfuron and sulfosulfuron controls wild oat (*Avena fatua* L.), bromes (*Bromus* spp. Scoop.) and rigid ryegrass (*Lolium rigidum* Gaudin) (Wells, 2008). Premixed mesosulfuron-methyl + iodosulfuron-methyl-sodium + diflufenican (Alister OD 180) is another ALS and phytoene dehydrogenase-inhibiting herbicide that was registered in 2014. This herbicide controls certain broad-leaved and grass weeds in wheat (Reza, 2013). Pinoxaden is a newly selective herbicide for annual grass weeds in wheat and barley which was registered in 2012. It belongs to the chemical class of phenylpyrazolines. The herbicide acts by inhibiting the enzym e Acetyl-CoA-Carboxylase (ACCase), interrupting the synthesis of fatty acids and as a final consequence impacts the formation of biomembranes (Hofer et al., 2006). Pinoxaden satisfactorily controls (> 92%) common windgrass (*Apera spica-venti* (L.) Beauv.), slender meadow foxtail (*Alopecurus myosuroides* Huds.) and wild oat (*Avena fatua* L.) (Kieloch et al., 2006).

Taking into consideration the necessity of chemical weed control for stable wheat production, the objective of this study was to investigate the effectiveness of some new POST herbicides and herbicide combinations for effective control of weeds in winter wheat crops in the Republic of Macedonia, and, at the same time, to estimate their influence on wheat yields.

MATERIALS AND METHODS

Field experiments were conducted during two winter wheat-growing seasons in 2012–2013 and 2013–2014 in commercial wheat fields in the Skopje and Probištip wheat-growing regions of northern and north-eastern Macedonia on Fluvisol sandy loam and vertisol, respectively (Filipovski, 2006) (Table 1).

Table 1. Soil characteristics in the wheat-growing regions

Region	Soil	Coarse	Fine sand	Clay+silt	Organic matter	pH-water
		(%)				
Skopje	Fluvisol sandy loam	10.50	63.10	26.40	2.66	6.7
Probištip	Vertisol	3.50	30.00	60.30	2.40	7.2

The wheat was grown following conventional tillage practices. The soil was tilled with a field cultivator prior to sowing. Nitrogen, phosphorus and potassium were applied, as recommended by soil test results. Field experiment were carried out with 'Pobeda' and 'Milenka' winter wheat cultivars, which were sown in a well-prepared seedbed at a seeding rate of 230 and 250 kg ha^{-1} on October 15th, 2012 and October 26th, 2013 in the Skopje region and on October 23rd, 2012 and November 1st, 2013 in the Probištip region, respectively. The experiments were conducted in different sites of the same commercial wheat fields. Herbicides were applied with a CO_2-pressurised backpack sprayer CP-3 calibrated to deliver 300 L ha^{-1} of aqueous solution at 220 kPa.

Herbicides were applied at the end of the wheat-tillering stage (BBCH-scale 28-30). Weeds at the time of treatment were in the following growth stages *Asperugo procumbens* BBCH 30, *Avena ludoviciana* BBCH 23-24, *Lolium perenne* BBCH 28-29, *Bifora radians* BBCH 16-18 and *Polygonum convolvulus* 14-16. The experimental design was a randomised complete block with four replicates and elementary plots 25 m^2. Treatments included Lancelot Super (aminopyralid 300 g a.m. kg^{-1} + florasulam 150 g a.m. kg^{-1}) at 33 g ha^{-1} + Pallas 75 WG (75 g a.m. kg^{-1} pyroxsulam) at 0.25 L ha^{-1}; Alister OD 180 (mesosulfuron-methyl 6.0 g a.i. L^{-1} + iodosulfuron-methyl-sodium 4.5 g a.i. L^{-1} + diflufenican 180 g a.i. L^{-1}) at 0.8 and 1.0 L ha^{-1}; Accurate 20 WG (metsulfuron-methyl 200 g a.i. kg^{-1}) at 30 g ha^{-1}; and Axial 100 EC (pinoxaden, 100 g a.i. L^{-1}) at 0.7 L ha^{-1} and Arat WG (water dispersible granules) (tritosulfuron 250 g a.m. kg^{-1} + dicamba 500 g a.m. kg^{-1}) at 170 g ha^{-1} + Pallas 75 WG (75 g a.m. kg^{-1} pyroxsulam) at 0.25 L ha^{-1}. All herbicides were used in recommended rates. Untreated and weed-free controls were included in the studies as well for comparison. The control plots were left untreated during the entire experimental period. Weed-free control was maintained by hand weeding. Hand weeding was initiated at the emergence of weeds and continued to 28th days after application.

Wheat injury and percent weed control were visually evaluated based on a 0–100% rating scale, where 0 is no injury to wheat plants or no weed control and 100 is complete death of wheat plants or complete control of weeds (Frans et al., 1986). Visual estimates of percent wheat injury were estimated 7 and 21 days after application, based on chlorosis and necrosis for each plot, while weed control efficacy was estimated 28 days after application from a one meter square area with the help of quadrat within each plot at both localities during a 2-year experimental period.

At full maturity, wheat was harvested manually at ground level in an area of 1 m^2 per plot. The yield was determined after harvest based on weights of grain containing 13% moisture.

Maximum and minimum temperatures for 5 days after POST treatments were recorded (Table 2). POST treatments in 2013 were applied at times when herbicide applications typically occur in Macedonian wheat production (Table 2) and, thus, are representative of producer practices and label recommendations. Unusually, in 2014, because of a mild winter, the beginning of wheat vegetation started earlier. POST herbicides were applied at the end of the wheat-tillering stage (BBCH 28-30) on March 22nd in Skopje and on March 26th in the Probištip region, respectively. After application, minimum temperatures in the Probištip region varied and such variability was partially attributed to unfavourable environmental conditions associated with cold night-time temperatures of -1 °C and 0 °C, particularly 48 hours after application (Table 2).

Table 2. Temperature data 5 days after treatment in 2013 and 2014 at the experimental locations

Date	Skopje region				Probištip region			
	2013		2014		2013		2014	
	Temperature (°C)				Temperature (°C)			
	min	max	min	max	min	max	min	max
April 4	10	22	-	-	-	-	-	-
April 5	9	24	-	-	-	-	-	-
April 6	12	23	-	-	-	-	-	-
April 7	9	20	-	-	8	22	-	-
April 8	12	23	-	-	12	25	-	-
April 9	-	-	-	-	10	27	-	-
April 10	-	-	-	-	9	21	-	-
March 23	-	-	6	18	-	-	-	-
March 24	-	-	7	20	-	-	-	-
March 25	-	-	5	17	-	-	-	-
March 26	-	-	6	17	-	-	-	-
March 27	-	-	2	19	-	-	-1	16
March 28	-	-	-	-	-	-	0	15
March 29	-	-	-	-	-	-	3	15
March 30	-	-	-	-	-	-	6	19
March 31							5	19

The data were tested for homogeneity of variance and normality of distribution (Ramsey & Schafer, 1997) and were log-transformed as needed to obtain roughly equal variances and better symmetry before ANOVA was performed. Data were transformed back to their original scale for presentation. Means were separated by using an LSD test at 5% of probability.

RESULTS AND DISCUSSION

Weed control. Efficacy of POST herbicides varied among weed species, treatments and years. Inconsistent weather patterns in the 2 years of study likely influenced the weed control. Temperature, particularly minimum temperature following application, may have contributed to the high performance of POST herbicides in both districts in 2013 and in the Skopje region in 2014 (Table 1). Conversely, unfavourable environmental conditions associated with cold night time temperatures of around 0 °C, particularly 48 hours after application, probably were the most likely reason for the lower efficacy of POST applied herbicides in the control of weeds in the Probištip region in 2014 compared to their application in 2013 (Tables 2 and 3).

Asperugo *procumbens*. *Asperugo procumbens* control in the Skopje region was not significant among years for different POST herbicide applications. In this district, regardless of the year, all POST herbicides provided control of *A. procumbens* between

95 and 100%. However, the greatest control (100%) was achieved with aminopyralid + florasulam + pyroxsulam, mesosulfuron-methyl + iodosulfuron-methyl-sodium + diflufenican (applied at 0.8 and 1.0 L ha^{-1}) and tritosulfuron + dicamba + pyroxsulam in 2012–2013, and with aminopyralid + florasulam + pyroxsulam, mesosulfuron-methyl + iodosulfuron-methyl-sodium + diflufenican applied at 1.0 L ha^{-1} and tritosulfuron + dicamba + pyroxsulam in 2013–2014, respectively (Table 3). Kostov and Pacanoski (2004) reported 98–100% *A. procumbens* control in winter wheat 30 DAT with amidosulfuron + iodosulfuron–methyl–sodium + mefenpyr–diethyl (Sekator) and tritosulfuron + dicamba (Arat WG).

***Lolium perenne*.** *Lolium perenne* control in the Skopje region was not significant among years for different POST herbicide applications. In this region in 2012–2013, all POST herbicides suppressed *L. perenne* 93–100%. Among the POST treatments, only metsulfuron-methyl + pinoxaden showed significantly higher efficacy in control of *L. perenne* compared to all other evaluated herbicides (Table 3). Similar to the previous year, in 2013–2014 all POST applied herbicides controlled *L. perenne* between 94 and 99%. A significant treatment by year interaction resulted in two distinct years for *L. perenne* control in the Probištip region. All POST applied herbicides in 2012–2013 controlled *L. perenne* 95–100%, but only mesosulfuron-methyl + iodosulfuron-methyl-sodium + diflufenican applied at 1.0 L ha^{-1} and metsulfuron-methyl + pinoxaden showed significantly higher efficacy in control of *L. perenne* (99–100%) compared to all other evaluated herbicides (Table 4). In 2013–2014, cold temperature within 48 hours of application could have caused reduced *L. perenne* efficacy. Temperature has been shown to have a large influence on *L. perenne* growth and metabolism (Beevers & Cooper, 1964), and lower temperatures could reduce herbicide uptake. All POST herbicides provided control of this weed between 76 and 84% (Table 4). According to Grey et al. (2012), maximum and most consistent *L. perenne* control (> 90%) occurred with mesosulfuron plus MSO and UAN. Without UAN, control of *L. perenne* with mesosulfuron varied from 44 to 97%. Ellis (2009) reported good POST control of *L. perenne* (> 80%) with pinoxaden, mesosulfuron, flufenacet + metribuzin, and chlorsulfuron + flucarbazone.

***Avena ludoviciana*.** *Avena ludoviciana* control in the Skopje region was not significant among years for different POST herbicide applications. In 2012–2013, all POST herbicides provided control of *A. ludoviciana* between 98 and 100%. Negligible lower efficacy was recorded in 2013–2014. Control of *A. ludoviciana* by POST treatments was above 95%, with only metsulfuron-methyl + pinoxaden providing excellent control (100%) (Table 3). A significant treatment by year interaction resulted in two distinct years for *A. ludoviciana* POST control in the Probištip region In this region in 2012–2013, POST treatments controlled *A. ludoviciana* more than 95%, but the greatest control (100%) was achieved with mesosulfuron-methyl + iodosulfuron-methyl-sodium + diflufenican applied at 1.0 L ha^{-1} and metsulfuron-methyl + pinoxaden. In 2013–2014, POST herbicides' efficacy decreased when a decrease in temperature occurred soon after application. However, *A. ludoviciana* control was less than 85% (Table 4). Pyroxsulam controls important winter annual grass weeds, including *Avena* spp. In North Dakota, pyroxsulam controlled *Avena fatua* L. more effectively when applied at the one- or three-leaf stage than when applied at the five-leaf stage (Hanson & Howatt, 2007).

Table 3. *Asperugo procumbens, Lolium perenne* and *Avena ludoviciana* control (%) 28 days after POST herbicide treatments,in winter wheat in 2012–2013 and 2013–2014 in Skopje region[a-d]

Treatments	Rate (g L ha^{-1})	Skopje region					
		A. procumbens		*L. perenne*		*A. ludoviciana*	
		2012–2013	2013–2014	2012–2013	2013–2014	2012–2013	2013–2014
Untreated control	------	0	0	0	0	0	0
Aminopyralid + florasulam + pyroxsulam	33 + 0.25	100[a]	100[a]	96[b]	95[ab]	100[a]	96[a]
Mesosulfuron-methyl + iodosulfuron-methyl-sodium + diflufenican	0.8	100[a]	95[b]	93[c]	94[b]	98[a]	95[a]
Mesosulfuron-methyl + iodosulfuron-methyl-sodium + diflufenican	1.0	100[a]	100[a]	97[b]	97[ab]	100[a]	98[a]
Metsulfuron-methyl + pinoxaden	30 + 0.7	97[b]	96[b]	100[a]	99[a]	100[a]	100[a]
Tritosulfuron + dicamba + pyroxsulam	170 + 0.25	100[a]	100[a]	97[b]	95[ab]	100[a]	95[a]
LSD 0.05		2.81	3.05	2.97	4.41	2.11	5.29
Random effect interactions POST herbicides treatment x year		NS		NS		NS	

[a] Abbreviation: POST – posteemergence; NS – not significant; [b] POST treatments were applied at wheat BBCH 28-30, *Asperugo procumbens* BBCH 30, *Avena ludoviciana* BBCH 23-24, and *Lolium perenne* BBCH 28-29; [c] Weed control efficacy was estimated 28 DAA; [d] Means followed by the same letter within a column are not significantly different according to Fisher's Protected LSD at $P < 0.05$.

Table 4. *Lolium perenne* , *Avena ludoviciana*, *Bifora radians* and *Polygonum convolvulus* control (%) 28 days after POST herbicide treatments in winter wheat in Probištip region in 2012–2013 and 2013–2014

Treatments	Rate (g L ha^{-1})	Probištip region							
		L. perenne		*A. ludoviciana*		*B. radians*		*P. convolvulus*	
		2012–2013	2013–2014	2012–2013	2013–2014	2012–2013	2013–2014	2012–2013	2013–2014
Untreated control	------	0	0	0	0	0	0	0	0
Aminopyralid + florasulam + pyroxsulam	33 + 0.25	97[b]	78[ab]	97[b]	80[ab]	100[a]	83[a]	100[a]	81[a]
Mesosulfuron-methyl + iodosulfuron-methyl-sodium + diflufenican	0.8	95[b]	76[b]	95[b]	78[b]	97[b]	80[ab]	98[b]	79[a]
Mesosulfuron-methyl + iodosulfuron-methyl-sodium + diflufenican	1.0	99[a]	82[ab]	100[a]	85[a]	100[a]	82[ab]	100[a]	82[a]
Metsulfuron-methyl + pinoxaden	30 + 0.7	100[a]	84[a]	100[a]	85[a]	100[a]	79[b]	100[a]	78[a]
Tritosulfuron + dicamba + pyroxsulam	170 + 0.25	95[b]	80[ab]	98[ab]	82[ab]	100[a]	82[ab]	100[a]	82[a]
LSD 0.05		2.77	7.07	2.08	6.23	1.55	3.64	1.73	4.42
Random effect interactions POST herbicides x year		*		*		*		*	

[a] Abbreviation: POST – posteemergence; * Significant at the 5% level according to a Fisher's protected LSD test at P < 0.05; [b] POST treatments were applied at wheat BBCH 28-30, *Lolium perenne* BBCH 28-29 *Avena ludoviciana* BBCH 23-24, *Bifora radians* BBCH 16-18, *Polygonum convolvulus 14-16*; [c] Weed control efficacy was estimated 28 DAA; [d] Means followed by the same letter within a column are not significantly different according to Fisher's Protected LSD at P < 0.05.

Excellent control of *Avena fatua* with pinoxaden + cloquintocet metyl (5–1.25%), at doses ranging from 20 to 60 g a.i. pinoxaden ha^{-1} applied to two to three leaves and at the beginning of tillering of *Avena fatua*, was reported by Scursoni et al. (2011). Similar results were reported by Hofer et al. (2006). Othello 6% OD (diflufenican 5% + mesosulfuron methyl 0.75% + iodosulfuron–methyl–sodium 0.25% + mefenpyr-diethyl 2.25%) controlled *Avena ludoviciana* more than 95% (Reza, 2013). The same herbicide provided 95% control of *Apera spica-venti* (Vanaga et al., 2010).

***Bifora radians*.** A significant treatment by year interaction resulted in two distinct years for *B. radians* control in the Probištip region with POST herbicides. In this region in 2012–2013, POST treatments provided control of *B. radians* between 97 and 100% (Table 4). In 2013–2014, lower temperature directly following application decreased the likelihood of POST herbicides' efficacy. All POST herbicides provided no more than 83% control of *B. radians* (Table 3). Kostov & Pacanoski (2004) reported 93–98% *B. radians* control in winter wheat 30 DAT with amidosulfuron + iodosulfuron–methyl–sodium + mefenpyr–diethyl (Sekator) and tritosulfuron + dicamba (Arat WG). Florasulam + flumetsulam applied at 50 and 70 mL ha^{-1} provided 92 and 98% control of *B. radians*, respectively (Kostov & Pacanoski, 2007). Effective control of *B. radians* with metsulfuron methyl in winter wheat was reported by Markovic et al. (2005) as well.

***Polygonum convolvulus*.** A significant treatment by year interaction resulted in two distinct years for *P. convolvulus* control in the Probištip region with POST herbicides, as well. In 2012–2013, all POST herbicides suppressed *P. convolvulus* 98–100% (Table 4). No one treatment controlled *P. convolvulus* more than 82% in 2013–2014. In investigations of Sulewska et al. (2012), tritosulfuron + dicamba (Mocarz 75 WG) provided 100% control of *Polygonum* (*Fallopia*) *convolvulus* in maize. Very good control of *Polygonum convolvulus* was observed after application of half of the rate of tribenuron-methyl with adjuvant and amidosulfuron + iodosulfuron in spring barley (Domaradzki & Kieloch, 2009).

Wheat injury. POST herbicides were applied at times when herbicide applications commonly used in Macedonian wheat production system (Table 2) and, thus, are representative of producer practices and label recommendations. However, in 2014 in the Probištip region, minimum temperature varied and such variability was partially attributed to unfavourable environmental conditions associated with cold night time temperatures of -1 °C and 0 °C, particularly 48 hours after application (Table 2). Lower temperatures generally slow crop growth, which results in prolonged herbicide exposure (Rouse & Dittmar, 2013). Negative temperatures directly following POST application caused wheat injury, which ranged from 12–29% across POST treatments 7 days after application (DAA) (Table 5). Wheat injury with tritosulfuron + dicamba + pyroxsulam was more serious (29%). Injuries caused by aminopyralid + florasulam + pyroxsulam, mesosulfuron-methyl + iodosulfuron-methyl-sodium + diflufenican and metsulfuron-methyl + pinoxaden significantly decreased by 7 and 21 DAA (Table 5). However, wheat injury with tritosulfuron + dicamba + pyroxsulam was still evident 21 DAA. Crooks et al. (2004) reported 7–19% injury for mesosulfuron combinations with thifensulfuron when applied at a spray solution rate of 140 L ha^{-1} at Feekes stage 3.0. Bailey et al. (2003) reported 9–24% wheat injury when mesosulfuron was applied at the 2–3 LF (two- to three-leaf wheat at Feekes stage), 2–3 (two- to three-tiller wheat stage) and 4–5 TILL stages (four- to five-tiller wheat stage). Sosnoskie et al. (2009) noted severe wheat injury (up to 40%) when UAN was combined with mesosulfuron application.

Table 5. Wheat plant injury (%) as influenced by POST applied herbicides, and grain yield as influenced by POST applied herbicides in winter wheat in Skopje and Probištip region in 2012–2013 and 2013–2014[a-c]

Treatments	Rate (g L ha^{-1})	Skopje region						Probištip region					
		Wheat injury				Grain yield (kg ha^{-1})		Wheat injury				Grain yield (kg ha^{-1})	
		2012–2013		2013–2014				2012–2013		2013–2014			
		7 DAA	21 DAA	7 DAA	21 DAA	2012–2013	2013–2014	7 DAA	21 DAA	7 DAA	21 DAA	2012–2013	2013–2014
Weed-free control	------	0	0	0	0	3,690[ab]	3,870[a]	0	0	0	0	3,360[ab]	3,490[a]
Aminopyralid + florasulam + pyroxsulam	33 + 0.25	0	0	0	0	3,650[ab]	3,850[ab]	0	0	15	5	3,290[b]	3,120[bc]
Mesosulfuron-methyl + iodosulfuron-methyl-sodium + diflufenican	0.8	0	0	0	0	3,580[b]	3,760[b]	0	0	12	3	3,230[b]	3,060[c]
Mesosulfuron-methyl + iodosulfuron-methyl-sodium + diflufenican	1.0	0	0	0	0	3,700[a]	3,880[a]	0	0	17	6	3,390[ab]	3,210[b]
Metsulfuron-methyl + pinoxaden	30 + 0.7	0	0	0	0	3,720[a]	3,910[a]	0	0	17	5	3,430[a]	3,180[bc]
Tritosulfuron + dicamba + pyroxsulam	170 + 0.25	0	0	0	0	3,670[ab]	3,840[ab]	0	0	29	16	3,340[ab]	3,120[bc]
LSD 0.05						112.8	100.53					99.60	130.72
Random effect interactions POST herbicides x year						NS						*	

[a] Abbreviations: POST – posteemergence; DAA – days after application; NS–not significant; * Significant at the 5% level according to a Fisher's protected LSD test at P<0.05; [b] Herbicide POST treatments included Aminopyralid + florasulam at 33 g ha^{-1} plus Pyroxsulam at 0.25 L ha^{-1}, Mesosulfuron-methyl + iodosulfuron-methyl-sodium + diflufenican at 0.8 and 1.0 L ha^{-1}, Metsulfuron-methyl at 30 g ha^{-1} plus Pinoxaden at 0.7 L ha^{-1}, Tritosulfuron + dicamba at 200 g ha^{-1} plus Pyroxsulam at 0.25 L ha^{-1}; [c] Means followed by the same letter within a column are not significantly different according to Fisher's Protected LSD at P < 0.05.

Hofer et al. (2006) reported 1.5% average wheat phytotoxicity after pinoxaden treatment at the recommended rate. Spring-applied pyroxsulam caused 5–10% wheat injury 5–14 DAT. However, injury was always transient and not detectable by the end of the season (Geier et al., 2011).

Wheat yield. Wheat yields for each treatment in both regions generally reflected overall weed control (Table 5). Wheat yields in the Skopje region were not significant among years for different POST herbicide applications. The lowest yield in 2012–2013 was obtained in plots treated with mesosulfuron-methyl + iodosulfuron-methyl-sodium + diflufenican applied at 0.8 L ha^{-1}. Same herbicide applied at 1.0 L ha^{-1} and metsulfuron-methyl + pinoxaden treatments yielded higher than did the weed-free control, 3,700 and 3,720 kg ha^{-1} respectively. Wheat yields obtained in 2012–2013 from plots treated with aminopyralid + florasulam+ pyroxsulam and tritosulfuron + dicamba + pyroxsulam yielded lower than did the weed-free control, averaging 3,650 and 3,670 kg ha^{-1} respectively (Table 5). In 2013–2014, similar results were obtained. There were significant results in wheat yields between weed-free control and the plots treated with mesosulfuron-methyl + iodosulfuron-methyl-sodium + diflufenican applied at 0.8 L ha^{-1}, averaging 3,870 and 3,760 kg ha^{-1}, respectively. In the same year, wheat yields from plots treated with mesosulfuron-methyl + iodosulfuron-methyl-sodium + diflufenican applied at 1.0 L ha^{-1} and metsulfuron-methyl + pinoxaden yielded higher than did the weed-free control, averaging 3,880 kg ha^{-1} or greater (Table 5). A significant treatment by year interaction resulted in two distinct years for wheat yields in the Probištip region with POST herbicides. In 2012–2013, wheat yields were greater than 3,360 kg ha^{-1} (weed-free control) when mesosulfuron-methyl + iodosulfuron-methyl-sodium + diflufenican and metsulfuron-methyl + pinoxaden were applied at 1.0 L ha^{-1} and 30 g ha^{-1} + 0.7 L ha^{-1}, respectively (3,390 and 3,430 kg ha^{-1}). The wheat yield following mesosulfuron-methyl + iodosulfuron-methyl-sodium + diflufenican application at 0.8 L ha^{-1} was significantly lower (-130 kg ha^{-1}) than that of the weed-free control. Wheat yields in 2012–2013 were not significantly lower for plots treated with aminopyralid+florasulam+pyroxsulam and tritosulfuron + dicamba + pyroxsulam, which yielded lower than did the weed-free control, averaging 3,290 and 3,340 kg ha^{-1} respectively (Table 5). In 2013–2014 wheat yields were more closely related to percent of weeds control, than wheat injury. Only the weed-free control showed a significantly higher wheat yield compared to all evaluated herbicides. However, wheat yields ranged from 3,060 to 3,490 kg ha^{-1}. mesosulfuron-methyl + iodosulfuron-methyl-sodium + diflufenican applied at 0.8 L ha was the lowest-yielding herbicide treatment with 3,060 kg ha^{-1}, whereas metsulfuron-methyl + pinoxaden and mesosulfuron-methyl + iodosulfuron-methyl-sodium + diflufenican applied at 1.0 L ha^{-1} were the highest-yielding herbicide treatments. Yield for these treatments ranged from 3,180–3,210 kg ha^{-1}, and was not significant (Table 5). The same yield was obtained from plots treated with aminopyralid + florasulam + pyroxsulam and tritosulfuron + dicamba + pyroxsulam: 3,120 kg ha^{-1}. A significant negative linear relationship between the winter wheat yield and the numbers of *Apera spica-venti* flowered panicles was reported in a study of Vanaga et al. (2010). According to their results, Alister Grande provided control of *Apera spica-venti* greater than 95% and was the highest-yielding herbicide treatment with 5,596 and 4,732 kg ha^{-1} respectively. Conversely, poor weed control of iodosulfuron + mesosulfuron applied at 18 g a.i. ha^{-1} decreased the grain yield by 42.81 and 51.62% as compared to the weed-free check during both growing seasons, respectively (Malekian et al., 2013). In an investigation of

Dalga et al. (2014) the highest grain yields of 4,700 and 4,455 kg ha^{-1} were obtained in weed-free treatment, followed by that of Pallas 20 g ha^{-1}, which gave grain yields of 4,455 and 4,031 kg ha^{-1} in both experimental localities.

CONCLUSIONS

– Both sites were naturally infested with a high population of *Asperugo procumbens* L., *Lolium perenne* L, *Avena ludoviciana* Dur., *Bifora radians* M.B. and *Polygonum convolvulus* L.
– Weed density in non-treated control plots was 116 and 208 plants m^{-2} in 2012–2013 and 2013–2014, respectively, in the Skopje region, and 93 and 114 plants m^{-2} in 2012–2013 and 2013–2014, respectively, in the Probištip region.
– Efficacy of POST herbicides varied among weed species, treatments and years, respectively. Inconsistent weather patterns in the 2 years of study likely influenced the weed control.
– All investigated POST herbicides effectively reduced dominant weeds in both regions, but mesosulfuron-methyl + iodosulfuron-methyl-sodium + diflufenican (applied at 1.0 L ha^{-1}) and metsulfuron-methyl + pinoxaden showed significantly higher efficacy in control of some weeds compared to the other evaluated herbicides.
– Wheat yields for each treatment in both regions generally reflected overall weed control. Mesosulfuron-methyl + iodosulfuron-methyl-sodium + diflufenican applied at 1.0 L ha^{-1} and metsulfuron-methyl + pinoxaden treatments yielded higher than did the weed-free control and other herbicides, respectively.

REFERENCES

Bailey, W.A., Wilson, H.P. & Hines, T.E. 2003. Influence of AE F13006003 Application Timing on Italian Ryegrass Control. *Weed Tech.* **17**, 842–853.

Beevers, L. & Cooper, J.P. 1964. Influence of Temperature on Growth and Metabolism of Ryegrass Seedlings. *Crop Sci.* **4**, 139–143.

Bertholdsson, N.O. 2012. Allelopathy–A Tool to Improve the Weed Competitive Ability of Wheat with Herbicide-Resistant Black-Grass (*Alopecurus myosuroides* Huds.) *Agronomy* **2**, 284–294.

Capinera, J.L. 2005. Relationships Between Insect Pests and Weeds: An Evolutionary Perspective. *Weed Sci.* **53**(6), 892–901.

Chachar, Q.I., Chachar, M.A. & Chachar, S.D. 2009. Studies on Integrated Weed Management in Wheat (*Triticum aestivum* L.). *J. Agri. and Tech.* **5**, 405–412.

Crooks, H.L., York, A.C. & Jordan, D.L. 2004. Wheat Tolerance to AE F130060 00 plus AE F115008 00 Affected by Time of Application and Rate of the Safener AE F107982. *Weed Tech.* **18**, 841–845.

Dalga, D. Sharma, J.J. & Tana, T. 2014. Evaluation of Herbicides and Their Combinations for Weed Management in Bread Wheat (*Triticum aestivum* L.) in Southern Ethiopia. *Int. J. Nat. Res. Lif. Sci.* **1**(1), 31–47.

Domaradzki, K. & Kieloch, R. 2009. Possibilities of Weed Control in Spring Cereals by Herbicides Applied at Reduced rates. *Polish J. Agr.* **1**, 9–14.

Ellis, A.T. 2009. Control of Italian Ryegrass (*Lolium perenne* L. spp. multiflorum Lam. Husnot) in Wheat (Triticum spp.) and Evaluation of Resistance to Acetyl-CoA Carboxylase Inhibiting Herbicides. *Doctoral thesis,* University of Tennessee.

Filipovski, G. 2006. Soil Classification of the Republic of Macedonia. *MASA*, pp. 313–323.

Frans, R.E., Talbert, R., Marx, D. & Crowley, H. 1986. Experimental Design and Techniques for Measuring and Analyzing Plant Responses to Weed Control Practices. In N. D. Camper ed. Research Methods in Weed Science. 3rd ed. Champaign, IL: *Southern Weed Science Society*, pp. 37–38.

Frihauf, J.C., Stahlman, P.W. & Geier, P.W. 2010. Winter Wheat and Weed Response to Postemergence Saflufenacil Alone and in Mixtures. *Weed Tech.* **24**, 262–268.

Gao, X., Li, M., Gao, Z., Li, C. & Sun, Z. 2009. Allelopathic Effects of *Hemistepta lyrata* on the Germination and Growth of Wheat, Sorghum, Cucumber, Rape, and Radish Seeds. *Weed Bio. Man.* **9**, 243–249.

Geier, P.W., Stahlman, P.W., Peterson, D.E. & Claassen, M.M. 2011. Pyroxsulam Compared with Competitive Standards for Efficacy in Winter Wheat. *Weed Tech.* **25**, 316–321.

Grey, T.L., Cutts, G.S., Sosnoskie, L. & Culpepper, A.S. 2012. Italian Ryegrass (*Lolium perenne*) Control and Winter Wheat Response to POST Herbicides. *Weed Tech.* **26**(4), 644–648.

Hanson, L.K. & Howatt, K.A. 2007. Pyroxsulam Efficacy to Wild Oat Influenced by Application Timing or Adjuvants. *Proceedings of the 62nd North Central Weed Science Society Annual Meeting*. St Lois, MO: NCWSS, pp. 89.

Hofer, U., Muehlebach, M., Hole, S. & Zoschke, A. 2006. Pinoxaden – for Broad Spectrum Grass Weed Management in Cereal Crops. *J. Pla. Dis. and Prot.* **20**, 989–995.

Khaliq, A., Matloob, A., Tanveer, A., Areeb, A., Aslam, F. & Abbas, N. 2011. Reduced Doses of a Sulfonylurea Herbicide for Weed Management in Wheat Fields of Punjab, Pakistan. *Chilean J. Agri. Res.* **71**(3), 424–429.

Khan, I., Hassan, G. & Marwat, K.B. 2002. Efficacy of Different Herbicides for Controlling Weeds in Wheat Crop – II Weed dynamics and herbicides. *Pak. J. Weed Sci. Res*. **8**, 41–47.

Kieloch, R., Domaradzki, K. & Górniak, J. 2006. Pinoxaden – A New Active Ingredient for Grass Weed Control in Cereals of South-West Poland. *J. Pla. Dis. and Prot. Zeitschrift für Pflanzenkrankheiten und Pflanzenschutz Sonderheft* **XX**, 1067–1072.

Klein, R.N., Martin, A.R. & Lyon, D.J. 2006. Annual Broadleaf Weed Control in Winter. Wheat University of Nebraska, *Linkoln Extension, Institute of Agriculture and Natural Resources* NebGuide G1241.

Knežević, M., Baličević, R., Ravlić, M. & Ranogajec, L.J. 2012. Effects of Reduced Herbicide Doses on Annual Weeds and Winter Wheat Yield by Two Tillage System. *Herbologia* **13**(1), 37–46.

Kostov, T. & Pacanoski, Z. 2004. Results of Examinations of Some New Herbicides in Wheat. *Yearbook for Plant Protection* **XV**, 141–152.

Kostov, T. & Pacanoski, Z. 2007. Results of Biological Examinations of Derby-175 in Wheat. *Yearbook for Plant Protection* **XVIII**, 97–100.

Malekian, B., Ghadiri, H., Kazemeini, S.A. & Edalat, M. 2013. Efficacy Evaluation of Sulfosulfuron, Metsulfuron-methyl plus Sulfosulfuron, Mesosulfuron-methyl plus Iodosulfuron-methyl and Iodosulfuron plus Mesosulfuron Herbicides in Winter Wheat (*Triticum aestivum* L.). *Journal Biol. and Env. Sci.* **7**(21), 177–182.

Mandal, M.S.H., Ali, M.H., Amin, A.K.M.R., Masum, S.M. & Mehraj, H. 2014. Assessment of Different Weed Control Methods on Growth and Yield of Wheat. *Int. Agr. and Agr. Res*. **5**(5), 65–73.

Markovic, M., Protic, N., Protic, R. & Jankovic, S. 2005. New Possibilities of Weed Control in Wheat. *Romanian Agri. Res.* **22**, 41–47.

Mehmeti, A., Pacanoski, Z., Fetahaj, R., Kika, A. & Kabashi, B. 2018. Weed Control in Wheat with Post-emergence Herbicides. *Bul. J. Agric. Sci.* **24**(1), 74–79.

Mehmood, Z., Ashiq, M., Noorka, I.R., Ali, A., Tabasum, S. & Iqbal, M.S. 2014. Chemical Control of Monocot Weeds in Wheat (*Triticum aestivum* L.). *American J. Pla. Sci.* **5**, 1272–1276.

Milberg, P. & Hallgren, E. 2004. Yield Loss due to Weeds in Cereals and its Large-Scale Variability in Sweden. *Field Cro. Res.* **86**, 199–209.

Nazari, A.J, Amiri, H., Javadi, M. & Gohlami, M. 2013. Efficiency of Different Herbicides Application for Weed Control in Wheat under Rain Fed Conditions in Iran. *International Journal Agri. and Cro. Sci.* **5**(5), 445–449.

Olesen, J.E., Hansen, P.K., Berntsen, J. & Christensen, S. 2004. Simulation of Above-Ground Suppression of Competing Species and Competition Tolerance in Winter Wheat Varieties. *Field Cro. Res.* **89**, 263–280.

Ozpinar, S. 2006. Effects of Tillage Systems on Weed Population and Economics for Winter Wheat Production under the Mediterranean Dryland Conditions. *Soil and Till. Res.* **87**(1), 1–8.

Pacanoski, Z. & Jankuloski, L. 2012. Response of Winter Wheat Cultivars to 2,4-D + Florasulam Applied at Three Different Growth Stages. *Herbologia* **13**(1), 47–59.

Ramsey, F.L. & Schafer, D.W. 1997. The Statistical Sleuth: A Course in Methods of Data Analysis. Belmont, CA: *Duxbury*. pp. 91–97.

Rao, A.N. & Chauhan, B.S. 2015. Weeds and Weed Management in India – A Review. *Chapter 4 Weed Science in the Asian-Pacific Region*, pp.87–118.

Reddy, S.S., Stahlman, P.W. & Geier, P.W. 2013. Downy Brome (*Bromus tectorum* L.) and Broadleaf Weed Control in Winter Wheat with Acetolactate Synthase-Inhibiting Herbicides. *Agronomy* **3**, 340–348.

Reza, J.M. 2013. Investigatig Efficacy of Othello New Herbicie (Mesosulfuron methyl+Iodosulfuron methyl sodium+ Diflufenican) on Weeds of Wheat Fields. Agricultural Scientific Information and Documentation Centre, *Agricultural Research and Education Organization*. http://agris.fao.org/agris-search/search.do?recordID=IR2015001263 (it is only abstract).

Rouse, C.E. & Dittmar, P.J. 2013. Factors Affecting Herbicide Use in Fruits and Vegetables. Horticultural Sciences Department, Florida Cooperative Extension Service, *Institute of Food and Agricultural Sciences*, University of Florida, pp. 1–5.

Scursoni, J.A., Martín, A., Catanzaro, M.P., Quiroga, J. & Goldar, F. 2011. Evaluation of Post-Emergence Herbicides for the Control of Wild Oat (*Avena fatua* L.) in Wheat and Barley in Argentina. *Crop Protection* **30**(1), 18–23.

Sheikhhasan, M.R.V., Mirshekari, B. & Farahvash, F. 2012. Weed Control in Wheat Fields by Limited Dose of Post-Emergence Herbicides. *World App. Sci. J.* **16**(9), 1243–1246.

Siddiqui, I., Bajwa, R., Huma, Z.E. & Javaid, A. 2010. Effect of Six Problematic Weeds on Growth and Yield of Wheat. *Pak. J. Bot.* **42**(4). 2461–2471.

Sosnoskie, L.M., Culpepper, A.S., York, A.C., Beam, J.B. & Macrae, A.W. 2009. Sequential applications for mesosulfuron and nitrogen needed in wheat. *Weed Tech.* **23**, 404–407.

Streit, B., Rieger, S.B., Stamp, P. & Richner, W. 2003. Weed Populations in Winter Wheat as Affected by Crop Sequence, Intensity of Tillage and Time of Herbicide Application in a Cool and Humid Climate. *Weed Research* **43**, 20–32.

Sulewska, H., Koziara, W., Śmiatacz, K., Szymańska, G. & Panasiewicz, K. 2012. Efficacy of Selected Herbicides in Weed Control of Maize. *Fragm. Agron.* **29**(3), 144–151.

Vanaga, I., Mintale, Z. & Smirnova, O. 2010. Control Possibilities of *Apera spica-venti* (L.) P.Beauv. in Winter Wheat with Autumn and Spring Applications of Herbicides in Latvia. *Agronomy Research* **8** (Special Issue II), 493–498.

Wells, G.S. 2008. Pyroxsulam for Broad-Spectrum Weed Control in Wheat. *Proceedings of the 16th Australian Weeds Conference*. Cairns, Australia: Queensland Weeds Society, pp. 297–299.

Zand, E., Baghestani, M.A., Soufizadeh, S., Eskandari, A., Azar, R.P. & Veysi, M. 2007. Evaluation of Some Newly Registered Herbicides for Weed Control in Wheat (*Triticum aestivum* L.) in Iran. *Crop Protection* **26**, 1349–1358.

Zhang, S.Z., Li, Y.H., Kong, C.H. & Xub, X.H. 2016. Interference of Allelopathic Wheat with Different Weeds. *Pest Man. Sci.* **72**, 172–178.

Agronomy Research **16**(4), 1809–1823, 2018
https://doi.org/10.15159/AR.18.183

Evaluation of greenhouse gas emissions and area of organic soils in cropland and grassland in Latvia – integrated National forest inventory data and soil maps approach

G. Petaja*, M. Okmanis, K. Polmanis, J. Stola, G. Spalva and J. Jansons

Latvian State Forest Research Institute "Silava", Rigas street 111, LV–2169 Salaspils, Latvia
*Correspondence: guna.petaja@silava.lv

Abstract. The aim of the research was to assess distribution of organic soils in farmlands for the time period between 1990 and 2015, as well as to carry out a recalculation of GHG emissions from organic soils in grassland and cropland. We evaluated the area of typical organic soils using digitized soil maps created between 1960s and 1980s there were 183,000 ha of cropland and grassland on organic soils. A selected number of areas on organic soils intersecting with the National forest inventory (NFI) plots were surveyed. We found that 66 ± 10% of surveyed plots still conforms to criteria for organic soils according to Intergovernmental Panel on Climate Change (IPCC) guidelines; in the rest of plots soil organic matter has been mineralized and these areas do not conform to IPCC criteria of organic soils. The following distributionof organic soils was estimated in cropland – 6.3 ± 3.3% in 1990 and 4.1 ± 3.4% in 2015, but in grassland – 11.6 ± 3.6% in 1990 and 7.7 ± 3.9% in 2015. The annual reduction of GHG emissions due to reduction of area of organic soils in cropland in 2015 corresponds to 1,400,000 tonnes CO_2 eq. in comparison to 1990 and in grassland – to 1,100,000 tonnes CO2 eq. The estimated reduction of the GHG emissions due to conversion of organic soils into mineral soils, comparing the average value in 2005–2009 with the projection for 2021–2030 on average will correspond to 313,000 tonnes CO2 eq. annually, however LULUCF sector still won't become a net CO_2 sink according to the GHG inventory data on other land use categories and carbon pools.

Key words: cropland, grassland, GHG emissions, organic soil.

INTRODUCTION

Soil is the largest terrestrial carbon pool and, as such, it can be turned into the largest source of greenhouse gas (GHG) emission from terrestrial ecosystems, depending on land use type and management activities. Globally about 1,220–1,550 Pg of carbon (C) is stored in soils as organic matter to a depth of 1 m and 2,376–2,450 Pg C – to a depth of 2 m. These amounts are significantly higher than C storage in atmosphere and terrestrial plants (Eswaran et al., 1995; Lal, 2004b). Soil organic matter, which consists of carbon-based compounds, influences soil chemical, physical and biological properties. It provides fertility, biological activity and attachment of nutrients to soil adsorption complex and also influences soil structure, air and moisture content. Organic matter also has a significant role in carbon cycle, whereas the carbon cycle along with changes in GHG concentrations is an important component of the biochemical cycle

(FAO, 2004; Nikodemus, 2009; Heikkinen, et al., 2013). Soils with more than 12–18% of organic carbon (approximately 20–30% of organic matter) are considered organic soils (Eggleston et al., 2006). Maintenance of optimal content of soil organic carbon (SOC) secures preconditions for development of healthy forest stands and better plant growth. It also increases net primary production, yieldswater retention capacity and efficiency of fertilizers and irrigation. SOC can reduce plant water stress, erosion, pesticide and nutrient leaching to aquatic ecosystems and mitigates climate change by off-setting anthropogenic emissions through C sequestration in trees and soils (Stoate et al., 2001; Jankauskas et al., 2007; Brock et al., 2011). Most of cropland contains 2–10% of organic matter in topsoil (Bot & Benites, 2005). C content in topsoil is a significant soil quality indicator because content of organic matter is directly proportional to C content in soil (Heikkinen et al., 2013). SOC is also important for ensuring a consistent global food supply. Adoption of SOC conserving agricultural practices can increase food production by 17.6 Mt year^{-1} (Sá et al., 2017).

It is well known that drainage and cultivation of organic soils promotes CO_2 emission from soil, because decomposition rate of organic matter in fertile drained organic soils is relatively high (Maljanen et al., 2010). Soil monitoring results across Europe show a decrease in soil organic carbon stock (Capriel, 2013; Heikkinen et al., 2013), although these results are somewhat controversial (Chapman et al., 2013; Reynolds et al., 2013). In Europe approximately 45% of agricultural lands have low or very low content of organic matter (< 2%). The above-mentioned problem is particularly relevant in countries of Southern Europe, but it is reported in Latvia too (Nikodemus, 2009; Lugato et al., 2014). Climate change is expected to further reduce SOM – it is projected that warmer and wetter climate is likely to increase C losses and thus GHG emissions from organic soils (Jansons et al., 2013; Zeps et al., 2017).

Globally soils contain 1,500 Pg (1 Pg = 1Gt = 10^{15} g) of organic carbon, however the carbon stock is decreasing. Carbon sequestration in soils can be achieved by increasing the flux from the atmosphere to the terrestrial or by slowing down decomposition. One of the best options for soil carbon sinks, is to increase carbon stock in degraded soils (Smith, 2004). Soil degradation is a change in the soil health status resulting in a diminished capacity of the ecosystem to provide goods and services (FAO, 2018). Loss of soil organic matter is an important criterion of soil degradation, as it is vitally important to soil productivity. Decomposition of soil organic matter is encouraged by intensive agricultural practices like deep drainage and ploughing. Ploughing raises the average temperature of soil by mixing oxygen into it and thus contributing to organic matter decay. Also crop cultivation returns less organic matter to the soil than does native vegetation (Fact sheet no. 3: Organic matter decline, 2009). Soil organic matter is also reduced by soil erosion. 18.3 million hectares of agricultural lands in Europe are considered as degraded soils (FAO, 2004).

Agricultural lands can be not only a carbon sink, but also can act a source of GHG emissions. The amount of N_2O and CH_4 emissions from agricultural sector in European Union (EU) is about 465 Mt CO_2 eq. annually (EEA, 2013). The carbon losses from managed organic soils in cropland and grassland in EU countries at the same time equals to 70 Mt of CO_2, according to the latest EU GHG inventory report for 1990–2015, which means if C losses from organic soils were added to the agriculture sector emissions, it would result in a 15% addition to net emissions. Land use type and management practices significantly affect the ratio of input and losses of organic carbon in soil

(Poeplau et al., 2015). Good farming practice is a cost-effective method for decreasing GHG emissions, while ensuring soil quality and food security (Lal, 2004b; 2004a).

The main activities that influence carbon stock in cropland are management of agricultural residues, ploughing, fertilization, selection of crops and intensity of agriculture (continuous or periodical crop cultivation), irrigation, periodical alternation ofcrop cultivation periodically alternates with cultivation of pasture grass and hay. Drainage can significantly (by 28–38% since 1900 in temperate zone alone) reduce carbon stock in organic soils (Armentano & Menges, 1986). It is estimated also that C accumulation in cropland, where ploughing, crop rotation, crop coverage, nutrient input and water management are well-balanced, can reach 200–600 kg ha^{-1} C annually (Lal, 2004a).

Grassland is one of the most widespread types of vegetation globally, that comprises one fifth of world's terrain. It is assumed that 200–300 Pg or about 30% of soil C is stored in grassland (Genxu et al., 2002). In contrary to tendencies of C stock in croplands, long-term results of soil monitoring in Europe show an increase of C content in soil in grassland (Lettens et al., 2005), illustrating the potential for management practices to effectively increase soil C stocks. However, studies in Latvia have demonstrated no difference in C stock in grassland and cropland (Bardule et al., 2017). Other studies show a tendency of increase or retention of soil C stock in natural grasslands in areas, where management activities have taken place without facilitating land degradation, and in improved grasslands, but in degraded grassland areas decrease of C stock was observed (Maia et al., 2009). Good grassland management practices can be used to decrease GHG emissions from soil (Ogle et al., 2004).

According to Kyoto protocol and Decision 2/CMP.6 of the Conference of the Parties reporting of CO_2 removals and GHG emissions caused by management of cropland and grassland in the second commitment period (2013–2020) is voluntary. It is expected that after 2020 reporting of these activities will become mandatory for countries listed in the Annex I of Kyoto protocol, including Latvia (United Nations, 1998). From January 1, 2021, Latvia has to prepare and maintain annual inventory, in which all GHG emissions and CO_2 removals due to cropland and grassland management must be accurately reflected.According to Eggleston et al. (2006) and Hiraishi et al. (2013), calculations of the main sources of GHG emissions and CO_2 removals (key sources) should be done in accordance with scientifically verified national methodologies, but for minor non-CO_2 sources of the emissions the default calculation methods and emission coefficients provided in the guidelines can be used. The land use, including area of organic soils, should be represented in spatially explicated way, which includes 'wall to wall' inventories, as well as statistical inventories like National forest inventories (NFIs). The aim of this study is to assess distribution of organic soils in cropland and grassland for the period between 1990 and 2015, according to NFI data and the digital soil maps elaborated within the scope of the European Economic Area financial instrument funded project 'Promotion of sustainable land resource management by creating a digital soil database', as well to recalculate GHG emissions from drained organic soils in grassland and cropland.

MATERIALS AND METHODS

Analysis of digital soil map data

The plot specific data of the 2nd cycle of NFI (2009–2013) was used to select sample plots with agricultural land use. Only those NFI sample plots were used which have only one land use type within the boundaries of sample plot (500 m^2 circle). The geographical information systems (GIS) layer of NFI was intersected with the digital soil map layer (mapping took place in 1960's – 1980's), to select only those NFI sample plots, which conforms to Intergovernmental Panel on Climate Change (IPCC) organic soil definition (Table 1).

Table 1. Soil types used in selection of organic soils (Kārkliņš, 2016)

No.	Soil type in national classification	Symbol in national soil classification	Approximation to WRB 2014
1.	Alluvial marshy (Aluviālā purva)	AT	Histosols, Fluvisols, Gleysols, Phaenozems
2.	Humic-peaty podzolic gley sod (Trūdaini-kūdrainās velēnu podzolētās gleja)	PGT	Gleysols, Planosols, Stagnosols, Gleyic Podzol, Umbrisols
3.	Bog peat (Augstā purva kūdra)	Ta	Fibric Histosols, Dystric Histic Gleysol
4.	Bog peat gley (Augstā purva kūdras gleja)	Tag	Fibric Histosols, Dystric Histic Gleysol
5.	Transition mire peat (Pārejas purva kūdra)	Tp	Hemic Histosols, Dystric Histic Gleysol
6.	Transition mire peat gley (Pārejas purva kūdras gleja)	Tpg	Hemic Histosols, Dystric Histic Gleysol
7.	Fen peat (Zemā purva kūdra)	Tz	Sapric Histosol, Histic Gleysol
8.	Fen peat gley (Zemā purva kūdras gleja)	Tzg	Sapric Histosol, Histic Gleysol
9.	Humic-peaty gley sod (Trūdaini-kūdrainās velēnu gleja)	VGT	Gleysols, Planosols, Stagnosols

Data conversion to area units was carried out by determination of the total area of NFI sample plots ($8.04\ 10^6\ m^2$) and by dividing it with the total area of Latvia according to data on the total area obtained from GIS Latvia 10.2 map ($64.6\ 10^9\ m^2$). According to this estimate 1 m^2 of a NFI plots corresponds to 0.80 ha of the country area. This figure is later used to extrapolate area of organic soil as well as to determine uncertainty using standard error of proportion.

Field surveys

A set of NFI plots where land use in the 2nd NFI cycle was cropland or grassland and met the criteria of organic soils according to Table 1 was surveyed in autumn of 2016. The number of the NFI plots to be visited was determined according to the preliminary assessment of area of organic soils outside forests using digitized soil maps. According to the assessment there are about 500 NFI plots on organic soils in cropland

and grassland. To represent at least 20% of NFI plots on organic soils in cropland and grassland, 50 NFI plots reported to the Rural Support Service (RSS) as cropland or grassland and 40 NFI plots that were not reported by RSS, but are managed as cropland or grassland and intersects with the polygons of organic soils, were randomly selected. The definitions applied in the National GHG inventory and implemented in the NFI are used in selection. The main difference between grassland and cropland is evidence of ploughing – there should not be signs of ploughing in grassland for at least 20 years. Only complete polygons and plots not bordering with other land use types, were selected for the field survey. Management practices were not considered in the selection, except dominant land use (e.g. cropland or grassland).

Depth of groundwater and thickness of organic rich layer were determined, as well as soil samples from topsoil were collected for analyses in all of the selected plots. Content of total carbon and carbonates (according to ISO 10694:1995 and ISO 10693:1995 standards), as well as soil texture and pH (ISO 11277:2009 and ISO 10390:2005, accordingly) was determined in the soil samples, and compliance with threshold values of organic carbon content for organic soils was determined according to Eggleston et al., 2006. Soil sampling was done to a 20 cm depth according to Penman, 2003. Sampling was carried out during August and October, 2016. Soil samples were collected in 4 replicates of mixed (undefined volume) samples in 13–15 m distance from centre of the NFI plots at 0°, 90°, 180° and 270° from North. Thickness of organic layer was determined in grassland as a border between organic and mineral soil layers and in croplands if it is deeper than mixed topsoil layer. Groundwater level was determined by digging wells in ground until water saturated layer is reached.

Calculation of area of organic soils and greenhouse gas emissions

It is necessary to know the area of organic soils in cropland and grassland to calculate GHG emissions. The current area of organic soils was calculated by multiplying the relative area of organic soils from surveyed plots with the total area of organic soils from digital soil map database (Eq. 1) both for cropland and grassland. It shows the current state of organic soil, assuming that some areas of organic soil, which were mapped in 1960's – 1980's, have turned from organic to mineral soils.

$$A_{2016} = p \cdot A_{database}^{total} \tag{1}$$

where $A2016$ – current total area of organic soils for cropland/grassland, ha; $A_{database}^{total}$ – total area of organic soil for cropland/grassland from digital soil map database, ha; p – relative area of organic soils according to the implemented survey.

The total area of organic soils for cropland and grassland in the digital soil map is assumed to correspond to 1970, which is the approximate mean mapping year. The reduction of area of organic soils since 1970 was calculated by linear interpolation of the area of organic soils in 1970 and 2016.

Annual reduction of area of organic soil was calculated as:

$$\Delta \mathrm{A} = \frac{A_{database}^{total} - A_{2016}}{Y} \tag{2}$$

where ΔA – Annual reduction of area of organic soils, ha; Y – period from soil mapping to field surveys in this study, in this case 46 years.

Emissions from organic soils in cropland and grassland were calculated by multiplying the area of organic soils with IPCC default emission factors (Eq. 3.). Emission factor for temperate region for cropland and for temperate deep drained nutrient rich grassland (7.9 and 6.1 t ha^{-1} C annually, in cropland and grassland, respectively) was used.

$$E_{CO_2} = A_J \cdot EF \tag{3}$$

where E_{CO_2} – CO_2 emissions from cropland/grassland, tonnes CO_2 eq. annually; A_j – area of cropland/grassland in year j, ha; *EF* – IPCC default emissions factor, tonnes CO_2-C ha^{-1} annually. The most conservative assumptions (emission factors for nutrient-rich organic soils in temperate moist climate zone) are used in calculation to avoid underestimation of the emissions and to keep conformity with the methodologies used in the National GHG inventory.

Statistical data analysis

Confidence interval ($\alpha = 0.05$) of sample proportion was calculated according to Eq. 4 to show the uncertainty of the total distribution of organic soils and distribution of organic soils in cropland and grassland.

$$CI_i = Z \cdot \sqrt{\frac{p \cdot (1 - p)}{n}} \tag{4}$$

where CI_i – confidence interval for i value; Z – the probability of normal distribution; p – proportion of the organic soil, %; n – total number of croplands or grasslands assessed.

In order to extrapolate study results to country level to determine uncertainity of distribution of organic soils, two uncertainties were combinedtogether following to the approach in the IPCC guidelines Volume 1 Chapter 3, respectively, uncertainity of relative area of organic soil in in cropland and grassland is combinied with and uncertainty of changes in relative area of organic soils (Eq. 5).

The same approach applied to the whole period.

$$CI_i^{combined} = p \cdot CI_i^{total} + CI_i \tag{5}$$

where CI_i^{total} – confidence interval for proportion of the organic soils from total NFI plots which intersect with layer of soil database; *p* – relative area of the organic soils in the soil database intersecting with NFI plots

RESULTS AND DISCUSSION

Digital soil map data analysis

Digitalized soil maps surveyed between 1960s and 1980s are available for 3,888,000 ha or 60% of the country's area. 58% of areas with soil cartographic data are farmlands, 32.8% – forest.

The total area of organic soils in NFI plots with available soil cartographic material is 505,000 ha or 13%. Half of the organic soils are located in forests and 36% are located in farmlands about 5% are settlements and related infrastructure, mostly drainage systems in agricultural lands or forest lands, and 7% are areas with high groundwater level, respectively rewetted and naturally wet soils. The most common reason of rewetting is deterioration of drainage systems.

Cropland on organic soil is represented in the NFI database with one land use subcategory – cereals; in grassland and extensively cultivated cropland the majority of the area corresponds with the definition of grasslands and pastures, but 17% of the area corresponds to the definition of forest (naturally afforested agricultural land). The total area of farmlands on organic soils is 183,000 ha (8.1% of farmlands).

The most common type of organic soils in cropland and grassland is fen peat soil (*Sapric Histosol* or *Histic Gleysol*), 67%. The proportion of semihydromorphic soils, which canfulfil the criteria of organic soils, is higher in cropland, compared to grassland. According to Latvian soil classification, semihydromorphic soils are soils developed in planes or depressions on fine-textured parent material. Soil profile is water-saturated for a long period within a year including the growing season. This soil class includes Gley, Podzolic-gley and Alluvial soils. All the studied semihydromorphic soils according to WRB-2014 are histosols (Kārkliņš, 2016).

The area of organic soils in cropland and grassland reported in the 2017 GHG inventory report is 142,000 ha (Gancone et al., 2017). The annual CO_2 emissions from organic soils in cropland and grassland according to the latest national GHG inventory report in Latvia equals to 3.7 million tonnes (Gancone et al., 2017). Extrapolation of obtained data on the share of organic soils in the NFI plots (in cropland – 3.3% and in grassland – 10.8%) to the area of cropland and grassland reported in the GHG inventory report would increase the total CO_2 emissions from cropland and grassland on organic soil by 19% (up to 4.3 million tonnes). Such an increase influences the GHG balance in LULUCF sector, as well as in the whole national GHG inventory (14% and 4% increase of GHG emissions, but changes are within the limits of the uncertainty of the default emission factor.

Application of the soil map analysis derived research result on the share of organic soil in cropland and grassland in the GHG inventory would increase GHG emissions in the whole time series from 1990, including 2005–2009, which is set as a potential reference period for the GHG emissions reduction target for grassland and cropland management in 2021–2030.

Assuming that the actual share of organic soils in cropland and grassland is decreasing due to mineralization of organic matter, use of the activity data, which are based on soil maps originated 30–50 years ago would lead to considerable overestimation of the GHG emissions in the reference period, which will be used to set the climate change mitigation targets for grassland and cropland management. A part of organic soils has been mineralized during this time or emits considerably less GHG due to land use changes. In order to improve the accounting of GHG emissions from organic soils the effect of mineralization of organic matter and land use change should be verified and demonstrated with field measurements or modelling data. The main issues to solve are determination of the actual distribution of organic soils in cropland and grassland in NFI plots in Latvia; evaluation of the soil mineralization process to predict GHG emissions from organic soils depending on the depth of organic soil layer and content of organic matter in soil; analysis of land use changes in areas with organic soils, using data about age of forest stands in NFI plots on former arable lands and remote sensing data characterizing conversion of cropland to grassland in 1990–2005; and periodic assessment of soil carbon stock in NFI plots in cropland and grassland on organic soils (once in 5 years by determination of changes in soil carbon content and depth of organics rich layer) to provide field measurement data for verification of the modelled emissions' projections.

Estimated and historical GHG emissions from organic soils can be significantly affected by elaboration of national GHG emission factors for the key sources of emissions, which should be locally verified to ensure compliance of the national GHG inventory with requirements of Kyoto protocol. If emission factors turn out to be significantly smaller than the default values of the IPCC guidelines, like it is approved by studies in forest lands (Lazdiņš et al., 2014; Lupikis & Lazdins, 2015), the net emissions due to management of organic soils will be considerably lower due to a larger area of organic soils in the past.

Survey of organic soils in National forest inventory (NFI) plots

Most of the surveyed plots (84%) are located on grassland. The most common (65%) soil type is fen peat (*Sapric Histosol* or *Histic Gleysol*), which is concentrated mostly in grassland. The most common soil types in cropland are fen peat (*Sapric Histosol* or *Histic Gleysol*) and Humic-peaty gley sod (*Gleysols*, *Planosols* or *Stagnosols*).

Regardless of soil type, groundwater is mostly located below 30 cm, i.e. the majority of the area on organic soils can be characterized as deeply drained according to IPCC (Eggleston et al., 2006). In 74% of the surveyed plots groundwater level is deeper than 30 cm from surface. The exceptions are found in the alluvial plains and glades.

According to the soil carbon content and texture analyses 66 ± 10% of the surveyed areas are organic soils, and the other 34 ± 10% – mineral soils. The majority of historical fen peat soils (*Sapric Histosol* or *Histic Gleysol*) are still classified as organic soil. Only 26 ± 9% of the fen peat soils are mineralized. Transfer from organic to mineral soil (according to IPCC) in the semihydromorphic soils has been found in up to 60 ± 14% of the surveyed areas. Transfer can be explained with a relatively small depth of organic soil layer (< 30 cm) in these soils in the surveyed plots. Soils in cropland have mineralized the most (57 ± 16% from the initial area of organic soil do not meet the IPCC thresholds for organic soils). In grassland 27 ± 12% of areas no longer meet the criteria for organic soil.

Carbon content in soil is the main factor to distinguish organic and mineral soils. Carbon content in mineral soils in the surveyed plots in topsoil (0–20 cm soil layer) is almost 5 times smaller than in the organic soils. But it is still 2 times higher than in mineral soils in Latvia in average (Lazdiņš et al., 2013; Bardule et al., 2017). It means, that the GHG emissions from these soils are most likely continuing regardless of the loosing status of organic soils, however there are no published data substantiating GHG emissions from carbon rich mineral soils in Latvia or surrounding regions with similar conditions.

Assuming that the actual GHG emissions from managed organic soils can be characterized with default emissions' factors (7.9 and 6.1 t ha^{-1} C annually, in cropland and grassland, respectively), it is estimated that the average carbon stock in topsoil (0–20 cm, 285 t ha^{-1} C) of organic soil will decompose in 40 years. Since the average depth of peat layer in cropland and grassland is 57 cm, it is estimated that around 2060 the proportion of organic soil will be reduced by half, comparing with the current situation.

The deepest organic soil layers are found in glades and alluvial planes. Depth of organic soil layer in organic soils in cropland and grassland exceeds 40 cm. In grassland the average depth of organic layer in organic soils is 75 cm, but in croplands it is significantly smaller – 41 cm.

More mineralized soils have been found in areas, where groundwater level is deeper than 30 cm below the surface (37% of cases). Areas, where groundwater is above 30 cm, transfer from organic to mineral soil occurred in 27% of cases.

All plots surveyed in this study were divided into cropland and grassland in order to determine average changes in land use. According to this classification 35 ± 15% of organic soils in cropland and 33 ± 13% of grassland have mineralized. Obtained numbers are used in order to calculate changes in area of organic soil from the moment, when soil mapping was done.

Definition of cropland in IPCC guidelines is different from the NFI definition. A part of grassland is counted as cropland in the GHG inventory (category grasslands in NFI) because these areas are periodically ploughed, but generally maintained as grassland. In order to calculate proportion of organic soils in cropland, a part of organic soils in grassland are counted as organic soils of cropland, by assuming that proportion of organic soils in cropland, which are counted in the NFI as grassland, is similar to the grassland, which belong to the category of grasslands in GHG inventory.

According to above-mentioned assumptions it is estimated that the proportion of organic soils in cropland in 1990 was 6.3 ± 3.3% from the total area, accordingly, more than it is reported now (5.18% of cropland). A part of areas of organic soils have mineralized and the proportion of organic soils in croplands has now dropped to 4.1 ± 3.4%. Similar tendencies have been observed in grasslands. Historically there were 11.6 ± 3.6% organic soils in grassland, but now it has been dropped to 7.7 ± 3.9%. The proportion of organic soils in grassland historically was bigger than the values used in the GHG inventory (5.18% of the grassland area). It can be explained with different criteria for selection of organic soil in earlier reporting (LU Consulting, 2010). The average proportion of organic soils (5.18%) for the GHG inventory was obtained using a different methodological approach – only soils with depth of organics rich layer exceeding 30 cm were considered. Since more detailed information on organic soils is available from the digitalized maps and evaluation of the classification systems applied in different soil inventory cycles, semihydromorphic soils with high content of organic carbon are counted as the organic soils.

Calculations of greenhouse gas (GHG) emissions in cropland and grassland with various inventories

According to the newest GHG inventory report (1990–2015), in 2015 GHG emissions from organic soils in croplands and grassland was 4,135 thousand tonnes CO_2 eq. annually, mostly from cropland (3,276 thousand tonnes CO_2 eq. annually). GHG emissions from grassland have been significantly decreased since 1990 and reached 860 thousand tonnes CO_2 eq. in 2015 because of afforestation of pastures and set-aside areas. The majority of GHG emissions from organic soils in agricultural lands are CO_2, according to GHG inventory data (3,298 thousand tonnes CO_2 eq. in 2015). Methane (CH_4) emissions in croplands come from drainage ditches, but in grassland – from ditches and soil. CH_4 emissions significantly decrease, when groundwater level is below 20 cm (Soosaar et al., 2011), which corresponds with the actual situation of 74% of surveyed plots. It means that in the future it is appropriate to invest in developing methane factors, in order not to overestimate impact of these GHG emissions on climate change in Latvia. A summary of GHG emissions from organic soils is given in Table 2. It is not expected that GHG emissions from organic soils in grassland would significantly increase in future, whereas in croplands a significant increase has been projected, when the cropland areas that have been afforested and transformed to grassland will be returned to production agriculture.

Table 2. Summary of greenhouse gas (GHG) emissions in croplands and grassland in the current inventory, thousand tonnes CO2 eq. annually (Gancone et al., 2017)

Year	1990	1995	2000	2005	2010	2015
CO_2	3,686	3,579	3,441	3,297	3,221	3,298
N_2O	739	719	693	666	651	667
CH_4	195	188	180	171	166	170
total	4,620	4,486	4,313	4,134	4,038	4,135

Application of the study data on distribution of organic soils in cropland and grassland and linear interpolation between the current status and historical distribution of organic soils, a decrease of GHG emissions in cropland in 2015 reaches 300 thousand tonnes CO_2 eq., in comparison to the recent GHG inventory report, but in 1990s the emissions from organic soils significantly increased (in 1990 by 1,000 thousand tonnes CO_2 eq.) due to increase of area of organic soils in the activity data. Total GHG emissions in cropland in 2015 were 3,000 thousand tonnes CO_2 eq. Due to continuous reduction of area of organic soils there is continuous trend in reduction of GHG emissions since 1990. From 1990 to 2015 GHG emissions in croplands decreased by 1,400 thousand tonnes CO_2 eq. annually.

In grassland application of the new activity data on distribution of organic soils also creates continuous decrease of GHG emissions from organic soils after 1990; however, it has to be considered that the total GHG emissions from drained organic soils in grassland would increase by 400 thousand tonnes CO_2 eq. in 2015 in comparison to the recent GHG inventory report and by 1,300 thousand tonnes CO_2 eq. in 1990 due to increase of the share of organic soils. From 1990 to 2015 GHG emissions from organic soils in grassland decreased by 1,100 thousand tonnes CO_2 eq. Summary of difference between currently reported GHG emissions and the recalculated data is provided in Table 3.

Table 3. Difference between recalculated greenhouse gas (GHG) emissions from organic soils in cropland and grassland in comparison with the values reported in GHG inventory report, thousand tonnes CO2 eq. annually (Gancone et al., 2017)

Year	1990	1995	2000	2005	2010	2015
CO_2	1,827	1,475	1,120	790	503	226
N_2O	343	275	207	144	88	32
CH_4	115	94	73	53	37	22
total	2,285	1,844	1,400	988	627	280

Total GHG emissions from organic soil in croplands and grassland, according to the new activity data, in 2015 was 6,900 thousand tonnes CO_2 eq.

Comparing with data reported in the GHG inventory report, application of new activity data on organic soils would significantly increase the net GHG emissions, comparing with the current state. In the recent years recalculated GHG emissions from organic soils in cropland and grassland are decreasing and in following inventories they will be smaller than the currently published forecasts (Ratniece et al., 2017). Further improvements are necessary to clarify proportion of organic soils in cropland and grassland in different periods. It is obvious that share of organic soil in cropland could be bigger in the past due to the fact that the area of cropland was considerably larger and the most of the currently abandoned or periodically cultivated areas were used in production of fodder or other crops. However, farming activities on organic soils in the past still should be evaluated.

A summary of estimates of GHG emissions using the recalculated activity data is provided in Table 4. Comparing recalculated GHG data for the potential reference period for cropland and grassland management (2005–2007) with recalculated data in 2015 (assuming that they are characterizing GHG emissions' in 2016–2020 and onwards, if no changes in activity data takes place), GHG emissions from organic soils will decrease by 313 thousand tonnes CO_2 eq. annually, i.e. in 2021–2030 decrease of GHG emissions will reach about 3,133 thousand tonnes CO_2 eq.

Table 4. Summary of recalculated greenhouse gas (GHG) emissions in cropland and grassland, thousand tonnes CO2 eq. annually (Gancone et al., 2017)

Year	1990	1995	2000	2005	2010	2015
CO_2	5,513	5,054	4,561	4,088	3,724	3,524
N_2O	1,082	994	900	810	739	699
CH_4	310	282	253	224	203	193
total	6,905	6,330	5,713	5,121	4,665	4,415

However, the projected decrease of GHG emissions is not sufficient to change the LULUCF sector in Latvia from source of CO_2 into a sink. Final result of recalculations of the GHG emissions from drained organic soils depends also from land use practices, intensification of agriculture and conversion of grasslands into croplands might result in an increase of GHG emissions from organic soil. Less intensive production whereas may result in larger reduction of GHG emissions. Mineralization of organic soils is another factor affecting GHG emissions in long term prospective.

CONCLUSIONS

1. According to results of the analysis of digitalized soil maps there are 182 thousand ha of cropland and grassland on organic soils. The area of organic soils in cropland and grassland is larger than it is reported in the greenhouse gas (GHG) inventory. The most probable reason for significant difference is different interpretation of semihydromorphic soils in data reported earlier. Application of activity data from digitized soil maps could lead to considerable overestimation of the emissions, because the mineralization of organic matter can considerably reduce area of organic soils in comparison to early 1990s.

2. 66% of the surveyed plots still correspond to Intergovernmental Panel on Climate Change (IPCC) criteria of organic soils, but the rest of soils are already mineralized, although average carbon content in soil is still 2 times higher than the average values in mineral soils in cropland and grassland in Latvia. It means that these soils can still generate GHG emissions in spite of losing status of organic soils. Additional studies determining equilibrium point for carbon content in different soils are necessary to increase accuracy of the emissions' estimates and to improve definition of organic soils.

3. Area of organic soil in cropland is 65% from the initial value, but in grassland – 67% from the initial area of organic soils. Mineralization of organic soils will continue for at least 40 years if linear mineralization rate is considered.

4. As a result of this study the following proportion of organic soils in croplands was determined – 6.3 ± 3.3% in 1990 and 4.1 ± 3.4% in 2015, but in grassland – 11.6 ± 3.6% in 1990 and 7.7 ± 3.9% in 2015.

5. The reduction of GHG emissions from organic soil from 1990 to 2015 due to application of new activity data is 1400 thousand tonnes CO_2 eq. in cropland and 1100 thousand tonnes CO_2 eq. in grassland.

6. Reduction of GHG emissions due to mineralization of organic matter will reach 313 thousand tonnes CO_2 eq. annually in 2021–2030, in comparison with the average values in 2005–2007, but land use, land use change and forestry (LULUCF) sector still will be a net source of GHG emissions.

REFERENCES

Armentano, T.V. & Menges, E.S. 1986. Patterns of change in the carbon balance of organic soil-wetlands of the temperate zone. *J. Ecol*. **74**(3), 755–774.

Bardule, A., Lupikis, A., Butlers, A. & Lazdins, A. 2017. Organic carbon stock in different types of mineral soils in cropland and grassland in Latvia. *Zemdirbyste* **104**(1), 3–8.

Bot, A. & Benites, J. 2005. The importance of soil organic matter: Key to drought-resistant soil and sustained food production. FAO Soils Bulletin No. 80. http://www.fao.org/3/a-a0100e.pdf. Accessed 25.5.2018

Brock, C., Fliessbach, A. & Oberholzer, H. 2011. Relation between soil organic matter and yield levels of nonlegume crops in organic and conventional farming systems. *J. Plant. Nutr. Soil. Sci*. **174**(4), 568–575.

Capriel, P. 2013. Trends in organic carbon and nitrogen contents in agricultural soils in Bavaria (south Germany) between 1986 and 2007: Organic carbon and nitrogen in Bavarian agricultural soils. *Eur. J. Soil. Sci*. **64**(4), 445–454.

Chapman, S.J., Bell, J.S., Campbell, C.D., Hudson, G., Lilly, A., Nolan, A.J., Robertson, A.H.J., Potts, J.M. & Towers, W. 2013. Comparison of soil carbon stocks in Scottish soils between 1978 and 2009: Soil C stocks in Scotland. *Eur. J. Soil. Sci*. **64**(4), 455–465.

EEA. 2013. Trends and projections in Europe. Tracking progress towards Europe's climate and energy targets until 2020. Publications Office of the European Union.

Eggleston, S., Buendia, L., Miwa, K., Ngara, T. & Kiyoto, T. 2006. 2006 IPCC Guidelines for National Greenhouse Gas Inventories. Agriculture, Forestry and Other Land Use. 2006 IPCC Guidelines for National Greenhouse Gas Inventories. Institute for Global Environmental Strategies (IGES), p. 678.

Eswaran, H., Van den Berg, E., Reich, P. & Kimble, J.M. 1995. Global soil C resources. In Lal, R., Kimble, J., Levine, E., Stewart, B.A. (ed.): *Soils and Global Change*, Lewis Publishers, Boca Raton, Florida, pp. 27–43.
Fact sheet no. 3: Organic matter decline (2009), available at: http://eusoils.jrc.ec.europa.eu/projects/SOCO/FactSheets/ENFactSheet-03.pdf Accessed 4 April 2018.
FAO. 2004. Carbon sequestration in dryland soils. World soil resources reports No. **102**. ftp://ftp.fao.org/agl/agll/docs/wsrr102.pdf. Accessed 10. 8.2017.
FAO. 2008. Soil degradation. http://www.fao.org/soils-portal/soil-degradation-restoration/en/. Accessed 10. 8.2017
Gancone, A., Skrebele, A., Līga, R., Ratniece, V., Cakars, I., Siņics, L., Klāvs, G., Gračkova, L., Lazdiņš, A., Butlers, A., Bārdule, A., Lupiķis, A., Bērziņa, L., Degola, L. & Priekulis, J. 2017. Latvia's National Inventory Report Submission under UNFCCC and the Kyoto protocol Common Reporting Formats (CRF) 1990–2015. Ministry of Environmental Protection and Regional Development of the Republic of Latvia, 845 pp.
Genxu, W., Ju, Q., Guodong, C. & Yuanmin, L. 2002. Soil organic carbon pool of grassland soils on the Qinghai-Tibetan Plateau and its global implication. *Sci. Total Environ* **291**(1–3), 207–217.
Heikkinen, J., Ketoja, E., Nuutinen, V. & Regina, K. 2013. Declining trend of carbon in Finnish cropland soils in 1974–2009. *Global Change Biol*. **19**(5), 1456–1469.
Hiraishi, T., Krug, T., Tanabe, K., Srivastava, N., Baasansuren, J., Fukuda, M. & Troxler, T.G. 2013. Revised supplementary methods and good practice guidance arising from the Kyoto Protocol. http://www.ipcc-nggip.iges.or.jp/public/kpsg/pdf/KP_Supplement_Entire_Report.pdf. Accessed 11.8 2017.
Jankauskas, B., Jankauskienė, G. & Fullen, M.A. 2007. Relationships between soil organic matter content and soil erosion severity in Albeluvisols of the Žemaičiai Uplands. *Ekologija* **53**(1), 21–28.
Jansons, Ā., Matisons, R., Baumanis, I., Puriņa, L. 2013. Effect of climatic factors on height increment of Scots pine in experimental plantation in Kalsnava, Latvia. *For. Ecolog. Manag.* **306**, 185–191.
Kārkliņš, A. 2016. Organic soils in the context of calculations of GHG emissions. In *Proceedings Scientifically practical conference Balanced Agriculture*. Jelgava, Latvia, pp. 40–44 (in Latvian).
Lal, R. 2004a. Agricultural activities and the global carbon cycle. *Nutr. Cycl. Agroecosyst*. **70**(2), 103–116.
Lal, R. 2004b. Soil carbon sequestration impacts on global climate change and food security. *Science* **304**(5677), 1623–1627.
Lazdiņš, A., Bārdule, A. & Stola, J. 2013. Preliminary results of evaluation of carbon stock in historical cropland and grassland. In *International Baltic Sea Regional Scientific Conference*. Riga, Latvia, pp. 56–57.
Lazdiņš, A., Lupiķis, A. & Okmanis, M. 2014. Soil carbon stock change due to drainage of a forest stand growing on a transitional bog. Extended abstracts of the CAR-ES network meeting. Vantaa, Finland, pp. 48–50. http://www.metla.fi/julkaisut/workingpapers/2014/mwp316.htm. Accessed 11. 8. 2017.
Lettens, S., Orshoven, J., Wesemael, B., Muys, B. & Perrin, D. 2005. Soil organic carbon changes in landscape units of Belgium between 1960 and 2000 with reference to 1990. *Glob. Change Biol*. **11**(12), 2128–2140.
LU Consulting. 2010. Elaboration of soil and terrain data and simulation of European Commission criteria for determination of less favourable rural areas: summary of project report. Ministry of Agriculture of the Republic of Latvia (in Latvian).

Lugato, E., Bampa, F., Panagos, P., Montanarella, L. & Jones, A. 2014. Potential carbon sequestration of European arable soils estimated by modelling a comprehensive set of management practices. *Glob. Change Biology* **20**(11), 3557–3567.

Lupikis, A. & Lazdins, A. 2015. Results of soil analyses and remote sensing methods in determination of CO_2 emissions from drained organic soils. Knowledge based sector. Riga, Latvia, pp. **50**. https://drive.google.com/file/d/0B_cPAeeFPI52YXBEV3hhM2dWTzA/view?usp=sharing Accessed 10.8 .2017.

Maia, S.M.F., Ogle, S.M., Cerri, C.E.P. & Cerri, C.C. 2009. Effect of grassland management on soil carbon sequestration in Rondônia and Mato Grosso states, Brazil. *Geoderma* **149**(1–2), 84–91.

Maljanen, M., Sigurdsson, B.D., Guðmundsson, J., Óskarsson, H., Huttunen, J.T. & Martikainen, P.J. 2010. Greenhouse gas balances of managed peatlands in the Nordic countries – present knowledge and gaps. *Biogeosciences* **7**(9), 2711–2738.

Nikodemus, O. 2009. Physical geography of Latvia; Geographic condition; Nature of Latvia overview. (in Latvian) <http://latvijas.daba.lv/ainava/> [Accessed 10 08 2017]

Ogle, S.M., Conant, R.T. & Paustian, K. 2004. Deriving grassland management factors for a carbon accounting method developed by the intergovernmental panel on climate change. *Environ. Manage* **33**(4), 474-484.

Penman, J. 2003. Good practice guidance for land use, land-use change and forestry. 2108-11, Institute for Global Environmental Strategies (IGES). http://www.ipcc-nggip.iges.or.jp. Accessed 14. 8. 2017.

Poeplau, C., Bolinder, M.A., Eriksson, J., Lundblad, M. & Kätterer, T. 2015. Positive trends in organic carbon storage in Swedish agricultural soils due to unexpected socio-economic drivers. *Biogeosciences* **12**(11), 3241–3251.

Ratniece, V., Rubene, L., Cakars, I., Siņics, L., Griķe, I., Klāvs, G., Reķis, J., Bērziņa, L., Valujeva, K., Popluga, D., Lazdiņš, A. & Zommere-Rotčenkova, K. 2017. Reporting on policies and measures under article 13 and on projections under article 14 of Regulation (EU) No. 525/2013 of the European Parliament and of the Council, Latvia. Latvia Ministry of the Environmental Protection and Regional Development. http://cdr.eionet.europa.eu/lv/eu/mmr/art04-13-14_lcds_pams_projections/pams/envwqhspw/LV_projections_and_PAMs_2017_Final_1_.pdf. Accessed 10.8. 2017.

Reynolds, B., Chamberlain, P.M., Poskitt, J., Woods, C., Scott, W.A., Rowe, E.C., Robinson, D.A., Frogbrook, Z.L., Keith, A., M., Henrys, P., A., Black, H.I.J. & Emmett, B.A. 2013. Countryside survey: national “Soil Change” 1978–2007 for topsoils in Great Britain – acidity, carbon, and total nitrogen status. *Vadose Zone J.* **12**(2).

Sá, J.C. de M., Lal, R., Cerri, C.C., Lorenz, K., Hungria, M. & de Faccio Carvalho, P.C. 2017. Low-carbon agriculture in South America to mitigate global climate change and advance food security. *Environ. Int*. **98**, 102–112.

Smith, P. 2004. Carbon sequestration in croplands: The potential in Europe and the global context, *Soil Use Manage* **20**, 212–218.

Soil quality - Determination of organic and total carbon after dry combustion (elementary analysis): ISO 10694:1995. 1995. Available at https://www.iso.org/standard/18782.html, 25 May 2018.

Soil quality - Determination of carbonate content -- Volumetric method: ISO 10693:1995. 1995. Available at https://www.iso.org/standard/18781.html, 25 May 2018.

Soil quality - Determination of particle size distribution in mineral soil material - Method by sieving and sedimentation: ISO 11277:2009. 2009. Available at: https://www.iso.org/standard/54151.html, 25 May 2018.
Soil quality - Determination of pH: ISO 10390:2005. 2005. Available at: https://www.iso.org/standard/40879.html, 25 May 2018.
Soosaar, K., Mander, Ü., Maddison, M., Kanal, A., Kull, A., Lõhmus, K., Truu, J. & Augustin, J. 2011. Dynamics of gaseous nitrogen and carbon fluxes in riparian alder forests. *Ecol. Eng*. **37**(1), 40–53.
Stoate, C., Boatman, N., Borralho, R., Carvalho, C.R., Snoo, G.R.D. & Eden, P. 2001. Ecological impacts of arable intensification in Europe. *J. Environ. Manage*. **63**(4), 337–365.
United Nations. 1998. Kyoto protocol to the United Nations framework convention on climate change, 20 pp.
Zeps, M., Jansons, Ā., Matisons, R., Stenvall, N. & Pulkkinen, P. 2017. Growth and cold hardening of European aspen seedlings in response to an altered temperature and soil moisture regime. Agric. For. *Meteorol*. **242**, 47–54.

Agronomy Research **16**(4), 1824–1829, 2018
https://doi.org/10.15159/AR.18.159

Application of conversion model for designing hydrodynamic pumps in turbine mode

M. Polák

Czech University of Life Sciences in Prague, Faculty of Engineering, Kamýcká 129, CZ16521 Praha 6, Czech Republic
Correspondence: karel@tf.czu.cz

Abstract. The use of the smallest water resources has been coming again to the centre of interest in recent years. A water engine – turbine, is the heart of these power plants. This is usually the highest expense for the investor, in terms of cost. The effort is therefore to seek investment less demanding alternatives. One of them is the use of hydrodynamic pumps in reverse turbine operation. This paper provides a methodology for conversion of parameters of the smallest power pumps (micro hydro sites) to turbine operation. The conversion model is based on the results of experimental research at the author's workplace and is suitable for pumps with low specific speeds and outputs. The pump design process for turbine mode is complemented by a practical example for a specific deployment site. This example also serves to verify the accuracy of the conversion model.

Key words: pump as turbine (PAT), conversion model, specific speed, efficiency.

INTRODUCTION

The design of a hydrodynamic pump as turbine (PAT) is based on good knowledge of flow ratios in the reverse operation of the machine. However, compared to a conventional turbine, there are some limitations such as the impossibility of control by means of adjustable guide vanes. But these limitations are counterbalanced by the main advantage of these applications, and that is the price of a machine, that is often much lower than that of a conventional turbine. When designing a PAT, it is necessary to take into account all the specific characteristics and choose a pump from commercial manufacturer's offer that meets all the requirements of the investor. The knowledge of pumps conversion relations for turbine mode is a prerequisite for correct design. A whole range of conversion models was created according to various authors in connection with this issue, for example (Stepanoff, 1957; Childs, 1962; Hancock, 1963; Grover, 1980; Sharma, 1985; Lewinsky, 1987; Schmiedl, 1988; Alatorre-Frenk, 1994; Williams, 1994; Derakhshan & Nourbakhsh, 2008; Güllich, 2008; Nautiyal et al., 2010; Carravetta et al., 2017; Frosina et al., 2017 and Naeimi et al., 2017). These authors, however, proceeded mainly from the experience with large power plants. But small machines have specifics during operation, which complicate the simple transfer of conversion relations for this category or the results achieved by them may differ considerably from reality. One reason is that the efficiency of a pump converted to turbine mode may change. Another reason is the assumption of constant conversion relations across a wide range of specific speeds and pump powers. The author of the article presents his own conversion model here, based on the results of experimental verification of small pumps turbine operation.

MATERIALS AND METHODS

Determining the conversion relations

The starting point for determining the conversion relations was the assumption that the efficiency of the pump changes in the same relation as the specific speed does when changing to a turbine mode. Among others, this results from the requirement to maintain the same circumferential speed of the impeller, or the same speed in both machine modes. This is due to the use of synchronous motors, which can be operated in a generator mode, and the frequency of the electric power grid needs to be maintained for the electricity produced (Bláha et al., 2011). Specific speed by the flowrate is defined by a generally known relation (Melichar et al., 1998; Munson et al., 2006):

$$N_q = N \cdot \frac{Q^{\frac{1}{2}}}{H^{\frac{3}{4}}} \quad (1)$$

where N is shaft speed, Q pump or turbine flowrate and H pump or turbine head. Based on an analysis of the results of the experimental verification, the conversion relations were expressed. The turbine flowrate Q_T and the head H_T are determined from the known hydrotechnical potential of the deployment site. The pump flow rate Q_P is determined from these values using the conversion relation:

$$Q_P = Q_T \cdot \eta_P{}^x \quad (2)$$

and respective pump head H_P:

$$H_P = H_T \cdot \eta_P{}^y \quad (3)$$

where x and y are constants. Their values are in range of $x = 1 \div 1.6$ and $y = 2 \div 2.6$ and they depend on specific speed and size of the pump. The values H_P and Q_P are then used to select a specific pump from the manufacturer's catalogue using the *H*-*Q* characteristics (Polák, 2018).

Example of use of conversion model

Use of the conversion model mentioned above is demonstrated on an example of a particular installation. The principle of the PAT design is to use the multiple approximation method several times until the results of the next step match the results of the previous step.

Example specification: Select a suitable pump from the manufacturer's catalogue for use in turbine mode at a location where the hydrotechnical potential given by flow rate $Q_T = 6.0$ L s^{-1} and net gradient $H_T = 13.5$ m is available.

In the first step of the conversion, it is necessary to determine the specific speed in turbine mode according to Eq. (1). This is based on the requirement for the same shaft speed, i.e. the expected turbine shaft speed will be $N_P = N_T = 1{,}450$ rpm.

$$N_{qT} = N_T \cdot \frac{Q_T^{\frac{1}{2}}}{H_T^{\frac{3}{4}}} = 1{,}450 \cdot \frac{0.006^{\frac{1}{2}}}{13.5^{\frac{3}{4}}} = 16\, rpm \tag{4}$$

The calculated specific speed value is used to predict the efficiency of the pump using the Erhart's diagram in Fig. 1. The diagram represents achievable efficiency of pumps in relation to specific speed (horizontal axis) and flow (vertical axis), i.e pump size. Thick dashed lines represent the values of the example and their intersection indicates the expected efficiency of the pump; here η_{P1} = 56%.

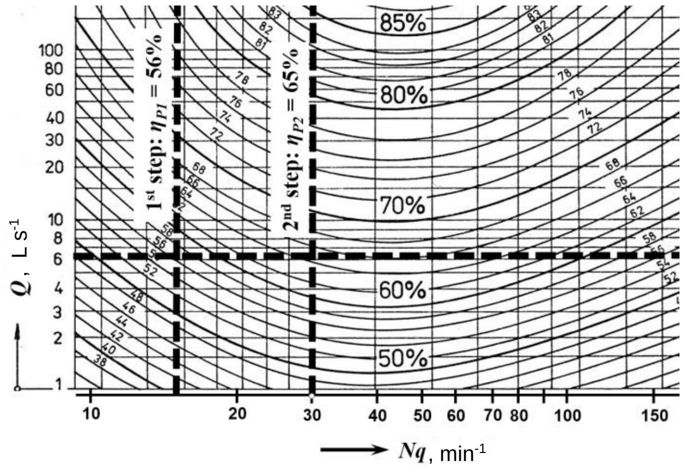

Figure 1. Erhart's diagram (Melichar et al., 1998).

The next step is to calculate the flowrate and pump head according to Eqs (2) and (3) where x and y are constants. Their values are in range of $x = 1 \div 1.6$ and $y = 2 \div 2.6$. For the calculation, their mean value from the interval will be used, i.e. $x = 1.3$ and $y = 2.3$. The pump flowrate will be according to Eq. (2):

$$Q_{P1} = Q_T \cdot \eta_{P1}{}^x = 6 \cdot 0.56^{1.3} = 2.82 \;L\, s^{-1} \tag{5}$$

The pump head will be according to Eq. (3):

$$H_{P1} = H_T \cdot \eta_{P1}{}^y = 13.5 \cdot 0.56^{2.3} = 3.56 \;m \tag{6}$$

Calculation of the pump speed with the values Q_{P1} and H_{T1} will follow:

$$N_{qP1} = N_T \cdot \frac{Q_{P1}{}^{\frac{1}{2}}}{H_{P1}{}^{\frac{3}{4}}} = 1{,}450 \cdot \frac{0.00282^{\frac{1}{2}}}{3.56^{\frac{3}{4}}} = 30\, rpm \tag{7}$$

Following is the second step of the multiple approximation method, when according to the Erhart's diagram the corrected expected pump efficiency is determined using the N_{qP1} value from Eq (7): η_{P2} = 65%. After substituting into Eqs (2) and (3), the corrected pump flowrate Q_{P2} is given:

$$Q_{P2} = Q_{P1} \cdot \eta_{P2}{}^x = 6 \cdot 0.65^{1.3} = 3.43 \;L\, s^{-1} \tag{8}$$

and pump head H_{P2} is given:

$$H_{P2} = H_{P1} \cdot \eta_{P2}{}^{y} = 3.36 \cdot 0.65^{2.3} = 5.01\ m \tag{9}$$

By substituting Q_{P2} and H_{P2} values into Eq. (1), newly corrected value of specific speed N_{qP2} = 25 rpm is obtained. The results of the flowrate or the head calculations from Eqs (5) and (6) or (8) and (9) do not match, which means further correction by repeating the calculations in the next step. However, the corresponding values of Q_{P1} and Q_{P2} or H_{P1} and H_{P2} are already close. This means that these values are already close to real values, so there is more detailed idea of the expected pump parameters. It can be therefore used to select a pump from the manufacturer's catalogue. Assuming $N_P = N_T$ = 1,450 rpm, a pump of the appropriate size can be selected using Q_{P2} = 3.43 L s^{-1} and H_{P2} = 5.01 m – see Fig. 2. This represents a section of *H-Q* field diagram for radial centrifugal pumps from the manufacturer's catalogue where the intersection of dashed lines in the dark grey field indicates the specific pump type and size.

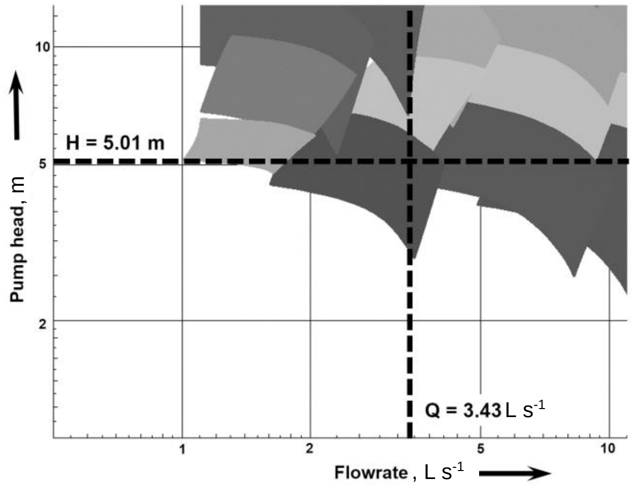

Figure 2. *H-Q* field diagram from the pumps manufacturer's catalogue (ISH Pumps, 2014).

For thus determined pump, the performance characteristics and efficiency can be found in the catalogue. In this case, the efficiency of the pump is η_{P3} = 70%. After substituting this value into Eqs (2) and (3), it can be proceed with the third step in the calculation from which the results are obtained: Q_{P3} = 3.77 L s^{-1} and H_{P3} = 5.94 m. These will be used for calculating specific speed: N_{qP3} = 23 rpm. In the fourth step, the flowrate and head obtained according to Eqs (2) and (3) are Q_{P4} = 3.77 L s^{-1} and H_{P4} = 5.94 m. The results of the fourth step are identical to the results of the third step, so the calculation can be terminated.

Based on the results of the conversion model for the above-mentioned hydrotechnical potential Q_T = 6.0 L s^{-1} and H_T = 13.5 m, the most suitable is a pump with optimum operating parameters: total head H_{P4} = 5.94 m, flowrate Q_{P4} = 3.77 L s^{-1} and shaft speed N_P = 1,450 rpm.

In addition to the above-mentioned basic proposal, an estimation of expected efficiency in the turbine mode can be made:

$$\eta_T = \eta_{P3}\left(1 - \frac{N_{qP3} - N_{qT}}{N_{qP3}}\right) = 0.7\left(1 - \frac{23 - 16}{16}\right) = 0.49 \qquad (10)$$

RESULTS AND DISCUSSION

The validity of the conversion model was verified by comparing the calculated results of the performance parameters with experimentally obtained values measured on the same pump. Verification tests were conducted according to (ČSN EN ISO 9906) on a hydraulic circuit in the Fluid Mechanics laboratory at the Faculty of Engineering, Czech University of Life Sciences Prague (Polák, 2017). Table 1 summarizes the results of the conversion model, the measured performance parameters and their relative difference determined according to:

$$\text{Difference} = 100 \cdot \frac{Model - Reality}{Reality}\ \% \qquad (11)$$

Table 1. Comparison of conversion model with reality

Impeller diameter: D_1, mm	Model	Reality	Difference
Total head: H_T, m	5.94	5.7	+ 4%
Flowrate: Q_T, L s^{-1}	3.77	3.8	- 1%
Shaft speed: N_T, rpm	1450	1450	0
Efficiency: η_T, %	49	48	+ 2%
Specific speed: N_{qT}, rpm	23	24	- 4%

Comparing the results of the conversion model with reality showed very close matching (differences up to 5%) and therefore the author's methodology can be recommended for wider use. Proposed conversion model is suitable for small pumps with a power output of up to 2 kW and a specific speeds up to 40 rpm for which it was primarily designed. The question of determining exact value of conversion factors *x* and *y* for different speeds and outputs remains open for further research.

CONCLUSIONS

Various authors addressed the issue of pump performance parameters conversion for turbine mode in different ways. But their solutions are mostly based on experience with large energy units. However, a simple transfer of these conversions to small devices does not give satisfactory results. The author of the article presents his own methodology which is based on the results of the experimental verification of turbine operation of small pumps. The conversion is performed by multiple approximation method until the results of the consecutive steps match. Besides the conversion of the basic power parameters, an estimate of the expected pump efficiency in turbine mode can also be provided. The method is completed by an illustrative example, which also serves to compare its results with reality. This comparison proved a very good match with reality. The proposed procedure can therefore be recommended for wider use in the area of small pumps with power output of up to 2 kW and specific speed up to 40 rpm for which it was primarily designed.

ACKNOWLEDGEMENTS. This research was supported by project: Activity Proof-of-Concept (No. 99130/1415/4101), Technology Agency of Czech Republic.

REFERENCES

Alatorre-Frenk, C. 1994. Cost minimization in micro hydro systems using pumps-asturbines, *Ph.D. Thesis*, University of Warwick; 1994.

Bláha, J., Melichar, J. & Mosler, P. 2011. Contribution to the use of hydrodynamic pumps as turbines. *Energetika* **5**, 1–5 (in Czech).

Carravetta, A., Houreh, S.D. & Ramos, H.M. 2017. *Pumps as Turbines: Fundamentals and Applications*. Springer, 218 pp.

Childs, S.M. 1962. Convert pumps to turbines and recover HP. *Hydro Carbon Processing and Petroleum Refiner* **41**(10), 173–4.

ČSN EN ISO 9906: Hydrodynamic pumps - Acceptance tests of hydraulic performance parameters - Degrees accuracy of 1, 2 and 3, ČSNI. (in Czech).

Derakhshan, S. & Nourbakhsh, A. 2008. Experimental study of characteristic curves of centrifugal pumps working as turbines in different specific speeds. *Experimental thermal and fluid science* **32**(3), 800–807.

Frosina, E., Buono, D. & Senatore, A. 2017. A performance prediction method for pumps as turbines (PAT) using a computational fluid dynamics (CFD) modeling approach. *Energies* **10**(1), 103.

Grover, K.M. 1980. Conversion of pumps to turbines. Katonah, New York: GSA Inter Corp, pp. 125–138.

Gülich, J.F. 2008. *Centrifugal pumps, 3rd Edition*. Berlin: Springer, ISBN 978-3-642-40113-8.

Hancock, JW. 1663. Centrifugal pump or water turbine. *Pipe Line News* 1963, 25–7.

Lewinsky-Keslitz, HP. 1987. Pumpen als Turbinen fur Kleinkraftwerke. *Wasserwirtschaft* **77**(10), 531–7.

Melichar, J., Vojtek, J. & Bláha, J. 1998. Small hydro turbines, construction and operation. ČVUT, Praha. pp 296 (in Czech).

Munson, B.R., Zouny, D.F. & Okishii, T.H. 2006. *Fundamentals of Fluid Mechanics, Fifth edition*, John Wiley & Sons, Inc., New York, 770 pp. ISBN 0-471-67582-2.

Naeimi, H., Shahabi, M.N. & Mohammadi, S. 2017. A Comparison of Prediction Methods for Design of Pump as Turbine for Small Hydro Plant: Implemented Plant. In: *IOP Conference Series: Earth and Environmental Science.* IOP Publishing.

Nautiyal, H. & Kumar, V. 2010. Reverse running pumps analytical, experimental and computational study: A review. *Renewable and Sustainable Energy Reviews* **14**(7), 2059–2067.

Polák, M. 2017. Experimental evaluation of hydraulic design modifications of radial centrifugal pumps. *Agronomy Research* **15**(SI), 1189–1197.

Polák, M. 2018. Determination of conversion relations for the use of pumps in reverse turbine operation. *Agronomy Research*, In press.

Schmiedl, E. 1988. Serien-Kreiselpumpen im Turbinenbetrieb. Pumpentagung Karlsruhe, 357 pp. (in German).

Sharma, K. 1985. Small hydroelectric project-use of centrifugal pumps as turbines. *Technical report*. Bangalore, India: Kirloskar Electric Co, pp. 14–6.

Stepanoff, A.J. 1957. *Centrifugal and axial flow pumps, design and applications*, John Willy and Sons, Inc., New York 1957, 462 pp.

Williams, AA. 1994. The turbine performance of centrifugal pumps: a comparison of prediction methods. *Proceedings of the IMechE Part A Journal of Power and Energy* **208**, 59–66.

Agronomy Research **16**(4), 1830–1836, 2018
https://doi.org/10.15159/AR.18.180

Farm manure amount calculation using statistical data in Latvia

J. Priekulis[1], A. Aboltins[1,*], A. Laurs[1] and L. Melece[2]

[1]Latvia University of Life Sciences and Technologies, Institute of Agricultural Machinery, Cakstes blvd. 5, LV-3001 Jelgava, Latvia
[2]Institute of Agricultural Resources and Economics, Struktoru street 14, LV-1039 Riga, Latvia
[*]Correspondence: aivars.aboltins@inbox.lv

Abstract. To calculate ammonia emissions caused by production, storage and application of farm manure, it is necessary to know the amount of farm manure obtained in the country and also the kinds of manure. For this purpose, methodology and computer software are developed to calculate the amount of farm manure based on the data of the Central Statistical Bureau, the technology of farm animal handling in the country and the respective valid normative documents. Upon calculating the amount of farm manure produced in Latvia in 2016, it was stated that approximately a half of the manure is litter manure, one third – liquid manure, and one fifth – manure left in the pastures. The most of manure in Latvia (69% of the total amount) is obtained from milk cows, their calves and young stock.

Key words: amount of farm manure, farm animals, statistical data.

INTRODUCTION

Farm manure is an important soil fertilizer. However, production and management of farm manure cause emissions of gases that lead to the greenhouse gas (GHG) effect, ammonia, smells and other unfavorable emissions (Directive 2003/35/EC; Agriculture as an air pollutant source, 2016). Therefore, in all European Union member states annual inventory of GHG emissions as well as ammonia emissions is carried out (UNECE Protocol, 1991; 2006 IPCC Guidelines; EMEP/EEA emission inventory guidebook, 2013). For this purpose, it is necessary to know what amount of farm manure in the country is obtained from every group of farm animals and the proportion of separate kinds of farm manure (litter farm manure, liquid manure, manure left in the pastures).

To determine the amount of farm manure obtained in the country, it is necessary to know the number of animals in every farm animal group and the average farm manure output. Problems are caused by the fact that usually from animals of one animal group several different kinds of farm manure are obtained and the output of farm manure is different. Besides, the statistical data do not reflect the proportion of these kinds of farm manure that are produced in every separate group of farm animals.

Therefore, the aim of the present research is to develop methodology for the calculation of the amount of farm manure produced in the country from every group of farm animals, using the statistical data as well as the coefficients obtained in the research that characterize the technological parameters of farm animal handling: the length of the pasture period, the size of the herd at which the transition from production of litter manure to liquid manure takes place.

MATERIALS AND METHODS

In compliance with the Regulations of the Cabinet of Ministers No 829 in Latvia, farm manure groups are split according to moisture:

- litter farm manure – the content of moisture less than 85%;
- semi-liquid farm manure – the content of moisture 85–90%;
- liquid farm manure –the content of moisture 90–98%;
- slurry – the content of moisture higher than 98%.

The obtained kind of farm manure depends on the group of farm animals, way of handling them and the amount of water added to the farm manure.

If, for instance, dairy cows are kept tied in the stalls, a comparatively large amount of litter is used (2–2.5 kg of straw per one stall per day). In the result, hard litter farm manure is produced. If, in turn, dairy cows are kept in high boxes, the consumption of litter does not exceed 0.5 kg per animal per day. Besides, to the manure collected in the barn the waste water used for washing the dirty floors is also added.

Therefore, in this case liquid manure is produced in the barn. There is also a situation possible that in warm weather the cows are pastured, and then a part of manure is left in the pastures.

In turn, the calves of dairy cows and young stock are kept only on deep litter and liquid manure is not produced in this case.

The general situation of the farm animal groups included in the research and the kinds of the obtained farm manure is summarized in Table 1.

Table 1. Farm animal groups grown in Latvia and kinds of farm manure (Priekulis et al., 2015b)

Farm animal group	Kinds of farm manure			
	Manure left in pastures	Litter manure	Liquid manure, slurry	Manure without litter
Dairy cows	x	x	x	
Calves of dairy cows up to the age of 1 year	x	x		
Young stock of dairy cows 1–2 years old	x	x		
Beef cattle older than 2 years	x	x		
Beef cattle calves up to the age of 1 year	x	x		
Beef young stock 1–2 years old	x	x		
Sows, breeding boars		x	x	
Pigs up to 50 kg (up to 4 months)		x	x	
Breeding gilts and fattened pigs		x	x	
Sheep	x	x		
Goats	x	x		
Horses	x	x		
Laying hens	x	x	x	x
Broilers		x		
Ducks	x	x		
Geese	x	x		

The total amount of farm manure produced by dairy cows is a sum of the total amount of the produced litter farm manure and liquid farm manure as well as the manure left in the pastures.

$$M_g = M_{g.gan} + M_{g.pak} + M_{g.sk}, \quad (1)$$

where M_g – total amount of farm manure produced in the country in the group of dairy cows, kg·year^{-1}; $M_{g.gan}$, $M_{g.pak}$, $M_{g.sk}$ – respective amount of manure left in the pastures, litter manure produced in the barn and liquid manure from dairy cows, kg·year^{-1}.

In accordance to our developed methodology (Priekulis et al., 2015a; Priekulis & Aboltins, 2015), the amount of manure left in the pastures can be calculated according to the following formula, kg year^{-1}

$$M_{g.gan} = k_{g.gan} \cdot Z_g \cdot \frac{\chi_{g.pak}}{100} \cdot q_{g.pak} \cdot \frac{S_{g.sv}}{S_{g.pak}} \quad (2)$$

where $k_{g.gan}$ – coefficient of pasture usage; Z_g – total number of cows according to the statistical data; $\chi_{g.pak}$– percentage of the cows from which litter farm manure is obtained, %; $q_{g.pak}$ – output of litter farm manure at the average milk yield in the country, t year^{-1}; $S_{g.sv}$, $S_{g.pak}$ – average fresh farm manure (mixture of faeces and urine) as well as litter farm manure dry matter content, %.

The amount of litter farm manure produced by dairy cows, kg year^{-1}:

$$M_{g.pak} = (1 - k_{g.gan}) \cdot \frac{\chi_{g.pak}}{100} \cdot Z_g \cdot q_{g.pak}. \quad (3)$$

The amount of liquid farm manure produced by dairy cows, kg·year^{-1}:

$$M_{g.sk} = (1 - \frac{\chi_{g.pak}}{100}) \cdot Z_g \cdot q_{g.sk} \quad (4)$$

where $q_{g.sk}$ – liquid farm manure output from one cow, kg year^{-1}.

The proportion of the animals from which litter farm manure is obtained, i.e. the coefficient $\chi_{g.pak}$ for dairy cows can be calculated according to the formula

$$\chi_{g\ pak} = \frac{Z_{g.pak}}{Z_g} \cdot 100, \quad (5)$$

where $Z_{g.pak}$ – number of cows in the country from which litter farm manure is obtained; Z_g – total number of cows in the country.

The value of this coefficient depends on the level of animal farm modernisation. If all cows are handled in stalls, the coefficient $\chi_{g.pak}$ = 100%, but if all cows are kept in boxes, then the coefficient is $\chi_{g.pak}$ = 0%. Therefore, it is not a constant, but rather a variable value.

To determine this coefficient, the expert method was used (Laurs et al., 2016a; Laurs et al., 2016b), as well as the statistical data from Central Statistical Bureau, available in the country on the percentage of the number of cows depending on the size of the herd.

First of all, by the expert method the following was stated: at what average cow herd size the transition from production of litter farm manure to liquid farm manure takes place. After that the value of the coefficient $\chi_{g.pak}$ was calculated using the statistical data. By means of this methodology, it was stated that in 2016 in Latvia the transition from production of litter farm manure to liquid farm manure took place, if the average size of the herd reached 80 cows, but the value of the coefficient $\chi_{g.pak}$ was 60%.

In turn, the pasture usage coefficient can be calculated using the following formula:

$$k_{g.gan} = \frac{t_{g.gan}}{24 \cdot 365}, \tag{6}$$

where t_{gan} – average length of cow pasturing period, h year^{-1}.

For calculation of this coefficient, also the expert method was used (Laurs et al., 2016a). In the research, it was stated that in Latvia dairy cows are pastured in the average 165 days per year and for 10 hours every day. Therefore, the pasture usage coefficient is 0.188.

In order to calculate the amount of farm manure that can be obtained from calves of milk cows (up to the age of 1 year), it must be considered that calves are kept on deep litter. Therefore, in this case only litter farm manure is produced. Besides, in small farms, where cows are pastured, also calves are pastured. Therefore, the total amount of the farm manure from the calves

$$\sum M_{g.t} = M_{g.t.gan} + M_{g.t.pak}, \tag{7}$$

where $M_{g.t.gan}$, $M_{g.t.pak}$ – amount of manure left in the pastures and the respective amount of litter farm manure produced by calves of dairy cows up to the age of 1 year, kg year^{-1}.

The amount of farm manure left in the pastures

$$M_{g.t.gan} = k_{g.t.gan} \cdot \frac{\chi_{g.pak}}{100} \cdot Z_{g.t} \cdot q_{g.t.pak} \cdot \frac{S_{g.t.sv}}{S_{g.t.pak}} \tag{8}$$

where $k_{g.t.gan}$ – pasture usage coefficient for dairy cow calves up to the age of 1 year (it is assumed to be the same as for dairy cows); $Z_{g.t}$ – total number of dairy cow calves (up to the age of 1 year) according to the statistical data; $q_{g.t.pak}$ – average weighted litter farm manure output from the respective group of calves, kg year^{-1}; $S_{g.t.sv}$, $S_{g.t.pak}$ – average dry matter content of fresh farm manure (mixture of faeces and urine) and litter farm manure for dairy cow calves, %.

The amount of the produced litter farm manure

$$M_{g.t.pak} = (1 - k_{g.t.gan}) \cdot \frac{\chi_{g.pak}}{100} \cdot Z_{g.t} \cdot q_{g.t.pak} + (1 - \frac{\chi_{g.pak}}{100}) \cdot Z_{g.t} \cdot q_{g.t.pak}, \tag{9}$$

A similar approach is used also to calculate the total amount of farm manure for the other farm animal groups as well (Priekulis et al., 2015).

Therefore, to calculate the amount of farm manure produced in the country, the following input data are needed: statistical data on the number of the respective farm animals and their proportion according to the size of the herd, farm manure output norms, the amount of dry matter in farm manure, the results of the expert enquiry on the length of the pasturing period and the size of the herd at which the transition from production of litter farm manure to liquid farm manure or manure without litter (keeping poultry in cage batteries) takes place.

The produced amount of farm manure is calculated using the above given correlations. At first, this amount is calculated for every separate group of farm animals and for every separate kind of farm manure. Summing up the obtained results, the total proportion of the amount of farm manure is obtained.

RESULTS AND DISCUSSION

Using the above described methodology and the data of the Latvian Central Statistical Bureau about the year 2016 the amount of farm manure obtained un Latvia in 2016 and its proportion in groups of farm animals was calculated, Fig. 1.

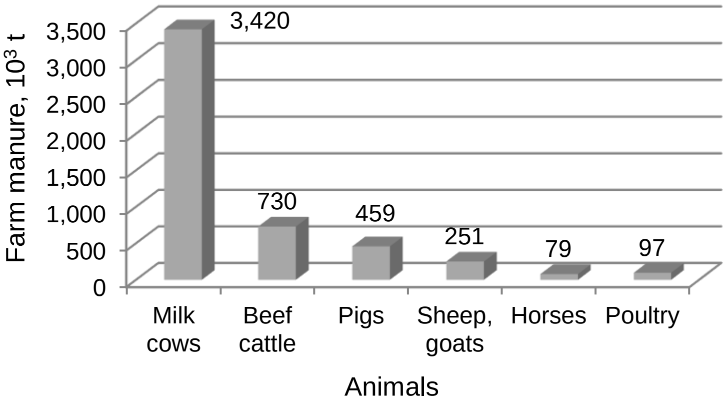

Figure 1. Calculated amount of farm manure (in thousand tons) obtained from farm animals in 2016 in Latvia.

The obtained results show that the largest amount of farm manure is obtained from the group of dairy cows, which includes also calves and young stock (3,420 thousand tons or 67%). A comparatively large amount of farm manure is obtained also from beef cattle and pigs (respectively 14.5% and 9.1% of the total amount), sheep and goats (5.9% in total). In turn, a comparatively small amount of farm manure is obtained from horses and poultry (3.5% in total). The proportion of the kinds of the obtained farm manure is shown in Fig. 2.

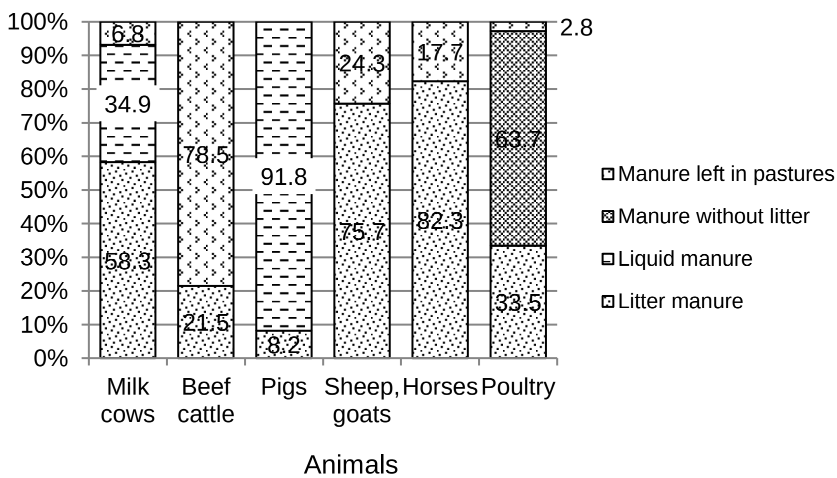

Figure 2. Percentage of kinds of farm manure.

As it was mentioned above, the proportion of farm manure kinds is essentially dependent on the farm animal handling technology. Building new barns and updating the existing ones gradual transition from production of litter farm manure to liquid farm manure takes place. It refers especially to milk farming and pig breeding. If in accordance to our research in 2016 58.3% of the total amount of farm manure in milk farming is litter farm manure, but 34.9% liquid farm manure, it can be planned that this proportion will change every year as the amount of the obtained liquid farm manure will increase.

The total proportion of the kinds of farm animal manure is shown in Fig. 3.

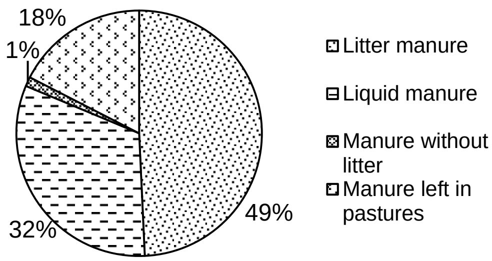

Figure 3. Total proportion of each of the kinds of farm animal manure.

As the figure shows, litter farm manure comprises almost a half (49%) of the total amount of farm manure, liquid farm manure – about one third (32%), but manure left in the pastures – approximately one fifth of the total amount of farm animal manure (18%).

CONCLUSIONS

Methodology for calculation of the amount of farm manure produced in the country from farm animals has been developed based on the statistical data, as well as considering the technological peculiarities of handling animals and the respective normative documents.

It has been stated that approximately 68% of the total amount of farm manure is obtained from dairy cows, their calves and young stock, 14.5% from the total amount of farm manure – from beef cattle, 9% from pigs, but 8.5% from other groups of farm animals.

Approximately a half of the total amount of farm manure is litter farm manure (49%), one third – liquid farm manure (32%) and one fifth (18%) – manure left in the pastures.

REFERENCES

Agriculture as an air pollutant source. Swiss Federal Office for the Environment Internet resource: *https://www.bafu.admin.ch/bafu/de/home/themen/luft/fachinformationen/luftschadstoffquellen/landwirtschaft-als-luftschadstoffquelle.html* Accessed 28.10.2016 (in German).

Central Statistical Bureau data base. Internet resource*: http://data.csb.gov.lv* Accessed 7.12.2017

EMEP/EEA emission inventory guidebook 2013 update July 2015. 3B. Manure management, 65 p

Laurs, A., Priekulis, J., Markovičs, Z. & Aboltins, A. 2016a. Research in farm animal breeding technological parameters. In: *15th International Scientific Conference "Engineering for rural development".* Proceedings, Volume 15. Jelgava, 1054–1058.

Laurs, A., Markovics, Z., Priekulis, J. & Aboltins, A. 2016b. Research in farm management technologies using the expert method. *Agronomy Research* **14**(3), 811–820.

Priekulis, J., Aboltins, A., Laurs, A. & Melece, L. 2015a. Research in manure management in Latvia. In: *14th International Scientific Conference "Engineering for rural development".* Proceedings, Volume 14. Jelgava, 88–93.

Priekulis, J., Laurs, A. & Aplociņa, E. 2015b. Determination of percentage of poultry manure management systems. In: *Problemy intensyfikacji produkcji zwierzęcej na tleochrony środowiska i standardow unii europejskiej.* Monografia pod redakcją naukovą prof. dr hab. inž.W.Romaniuka. Instytut Technologiczno-przyrodniczy w Falentach. Oddział w Warszawie, 169–173.

Priekulis, J. & Aboltins, A. 2015. Calculation methodology for cattle manure management systems based on the 2006 IPCC guidelines. In: *Proceedings of the 25th NJF Congress*. Riga, pp. 274–280.

Proposal for a Directive of the European Parliament and of the Council on the reduction of national emissions of certain atmospheric pollutants and amending Directive 2003/35/EC, COM(2013) 920 final, pp. 20.

Regulations of the Cabinet of Ministers No. 829. Special *Requirements* for the Performance of Polluting Activities in Animal Housing. Effective as of 23 December 2014. Internet resource: *http://m.likumi.lv/doc.php?id=271374* Accessed 7.12.2017.

UNECE (United Nations Economics Commission for Europe) 1991. Protocol to the 1979 convention on long-range transboundary air pollution concerning the control of emission of volatile organic compounds or their transboundary fluxes. *www.unece.org/env/lrtap/full%20text/1991. VOC.e.pdf* Accessed 3.10.2017.

2006 IPCC Guidelines for National Greenhouse Gas Inventories. Chapter 10: *Emissions from Livestock and Manure Management*, pp. 87.

Agronomy Research **16**(4), 1837–1853, 2018
https://doi.org/10.15159/AR.18.161

Optimization of arable land use to guarantee food security in Estonia

R. Põldaru*, A.-H. Viira and J. Roots

Estonian University of Life Sciences, Institute of Economics and Social Sciences, Department of Business Informatics and Econometrics, Fr. R. Kreutzwaldi 1, EE51006 Tartu, Estonia
*Correspondence: Reet.Poldaru@emu.ee

Abstract. Agricultural and food sector has an important role to play in ensuring food security. A competitive agricultural sector warrants food security through increasing level of self-sufficiency in food, and export of surplus production in the sub-branches where it has a comparative advantage. One of the strategic tasks of the state is to secure food supply for the population. To perform this task, the state should estimate if the agricultural producers have the necessary capacity and resources to produce food to meet the needs of population. Mathematical modelling can be used as a tool in solving this analytical problem. The paper demonstrates possibilities of implementing linear programming model in optimizing the use of arable land for ensuring the food demand of Estonian population. The Estonian arable land use optimization model is essentially a static balancing model that simulates the demand and supply of basic food products (meat, dairy products, cereal products and potatoes). The basis for the demand side in the model is Estonian population, divided into 10 groups according to gender and age. The energy and protein needs of the respective population groups are taken into account. The supply side of the model is a typical agricultural production model that guarantees the consistency of crop and livestock farming. The model consists of 163 variables and 178 constraints (equations). The objective of the model is to minimize the use of arable land for field crops to ensure fodder for animal feed, and food for human food consumption. The model is used to analyse various land use strategies. According to the modelling results for ensuring food security of Estonia and to maintain export of dairy products, for which Estonia has a comparative advantage, in the 2016 volume, the total optimal arable land equals to 490,688 ha. There should be 83,600 dairy cows (with average milk yield 9,000 kg cow^{-1}). It is necessary to grow 755,700 piglets per year in order to secure 40 kg of pork per inhabitant. Land use optimization results indicate that Estonian agriculture is able to supply Estonian people with the minimum necessary main food products to guarantee food security, and allows to export essential products (cheese, butter, skimmed milk powder, whole milk powder).

Key words: food security, linear programming model, Estonian agriculture, land use optimization.

INTRODUCTION

Global food security

Food security has been an age-old issue in the human society since people have always worried about the availability and supply of food. Throughout history, agriculture and food production have been among the most important sectors, ensuring food supply for the population. How to guarantee supply of sufficient, safe and nutritious food for everyone? In 2016, there were over 815 million undernourished people around the world (Roser & Ritchie, 2018), indicating that more than 10% of the world's population does not access enough food due to scarce supply, poor infrastructure or low purchasing power. This problem has been intensified by factors such as urbanisation (Miccoli et al., 2016); ageing (Kudo et al., 2015); climate change (Lal, 2013; Misra, 2014), limited resources (both fossil fuels (Naylor & Higgins, 2018) and biological resources such as fertile soil, water (Davis et al., 2016); changes in people's consumption patterns (Kastner et al., 2012; Alexander et al., 2016). These together with increasing global population have created the need to use resources more efficiently, reduce food waste (Koester, 2014), and develop sustainable waste management (Tielens & Candel, 2014; Govindan, 2018).

Food security problems have caused concern around the world. The United Nations (UN) agenda 'Transforming our World: the 2030 Agenda for Sustainable Development' provides guidelines for protecting the people and the planet, and for achieving welfare. Its aim is to integrate the three dimensions of sustainable development – economic, social and environmental – in a balanced and unified manner. Sustainable development goals are interlinked and inseparable, global, and obligatory for all developed countries (UN, 2015; Martin, 2017). Each country must contribute to reaching UN's 17 Sustainable Development Goals through setting their own targets, goals, and priority areas of activity, taking into account the local situation and capacity (Review…, 2016). One of the goals of the sustainable development agenda (Goal 2) is to achieve food security and improved nutrition for everyone, end hunger, and promote sustainable agriculture (UN, 2015). Considering that the EU's Common Agricultural Policy (CAP) aims to create the conditions that enable farmers to fulfil their numerous functions in society, the first of which is provide affordable food for citizens (Agriculture…, 2017) and taking into account the trends of the agricultural policy of the Estonian government (Development…, 2017). Estonia cannot remain a mere spectator of these developments both from national and global viewpoints.

Evolvement of the concept of food security

Food security as a term was first used in the global context during World War II when 44 Heads of State met in the US to discuss the freedom from want in the context of food and agriculture (FAO, 2012a; Hamblin, 2012). Over time, the term food security has meant different things. It has undergone significant development and is understood in various ways. The term food security has evolved from its narrow focus on national and global food availability, now covering several dimensions (Coates, 2013). This is partly due to its multidimensional and multi-sectoral nature (Fairbairn, 2012; Jones et al., 2013; Cafiero et al., 2014; Briones Alonso et al., 2018). As Pinstrup-Andersen (2009) said, 'in its narrowest definition, food security means that enough food is available, whether at the global, national, community, or household level'. Initially, the concept of food security was used to clarify whether a country has access to enough food to meet dietary energy needs (Pinstrup-Andersen, 2009). Food security is generally understood as food availability and access to food in a sufficient quantity and quality required for a healthy life (Aborisade & Bach, 2014).

The widespread definition of food security dates back to the 1996 World Food Summit: 'Food security exists when all people, at all times, have physical, social, and economic access to sufficient, safe, and nutritious food to meet their dietary needs and food preferences for an active and healthy life' (FAO, 2009). This definition consists of four key dimensions. The first dimension is physical availability of food which means there are sufficient quantities of food in different forms. Food availability relates to the supply of food through production, distribution, and trade. The second dimension is access, which is related with the affordability of food within households. Utilization is the third dimension of the food security concept and is related to meeting the nutritional needs of people. The fourth dimension is stability, which means that access to food is guaranteed over time (Jones et al., 2013; van Dijk & Meijerink, 2014; Stringer, 2016; Briones Alonso et al., 2018). Adequate availability is necessary, but does not ensure universal access to sufficient, safe and nutritious food (Barrett, 2010).

Several researchers have further developed the 4-dimensional definition of food security adopted by FAO (2009). Coates (2013) offers five different dimensions to better assess the various aspects of the concept of food security. These alternatives dimensions are a) the sufficiency; b) nutritional adequacy; c) cultural acceptability; d) safety; e) certainty and stability of food. These dimensions can be considered at the global/ national level, at the household level, as well as at the individual level (Coates, 2013). Burchi and De Muro (2016) proposed five different approaches: a) food availability, b) income-based, c) basic needs, d) entitlement, and e) sustainable livelihood. The food availability approach can be used at country or world level and in the agricultural sector, focusing on its production and productivity (Burchi & De Muro, 2016).

Food security is closely linked to food self-sufficiency. National food security was conceived as food self-sufficiency, which means that the country produces food as much as the population demands (Pinstrup-Andersen, 2009; Coates, 2013). Clapp (2017) defines food self-sufficiency as domestic food production that equals or exceeds 100% of the country's food consumption. For assessing a country's self-sufficiency, the ratio (SSR) may be used, which is defined as the percentage of food consumed that is produced domestically. Production, export-import and stocks data are used for calculating the amount of consumed food (Puma et al., 2015). The self-sufficiency ratio is typically calculated for a specific commodity or a class of commodities. FAO recommends that caution be taken when using this ratio for the assessment of food self-sufficiency throughout the country, as it may conceal the situation where the country produces some food abundantly and hopes for imports in order to meet the needs of some other foodstuff (FAO, 2012b).

Food self-sufficiency is primarily related to the availability pillar of food security, focusing on the origin of food or the capacity to produce it domestically and in a sufficient amount (Clapp, 2015).

According to forecasts, the need for a physical availability of food will increase around the world in the coming decades, whereas land resources for food production are limited. In some parts of the world, this presses for a more intensive use of agricultural land, whilst it is important to secure sustainability of agriculture. Verburg et al. (2013) have said that land-based production gives the main biophysical basis for food security and it is therefore an important component in ensuring food security. Hence, land use issues must be taken very seriously also in Estonia, primarily because Estonia's population may be decreasing, but the world's population is still growing rapidly, and is estimated to reach 9.6 billion by 2050 (FAO, 2017). This means that more resources will be needed to satisfy people's primary needs (food, water), and therefore, efficient land use is increasingly important.

Food security in the Estonian context

During past centuries, the volume of agricultural produce in Estonia has been sufficient to provide food for its population and export the surplus production. After Estonia regained its independence in 1991, the country's agricultural land use and production started to decrease, as illustrated by the decrease in the area of agricultural land (Fig. 1). While there was 1,374,000 ha of agricultural land in Estonia in 1992, the area had decreased to 698,200 ha by 2002. In 2016, 1,003,505 ha of agricultural land was in use, i.e. 27% less than in 1992. This means that the use of agricultural land is over ¼ lower than in the first years of independence, but different support measures of the EU's CAP have stimulated the growth of the use of agricultural land by more than 40% by 2016, compared to the lowest point in 2002.

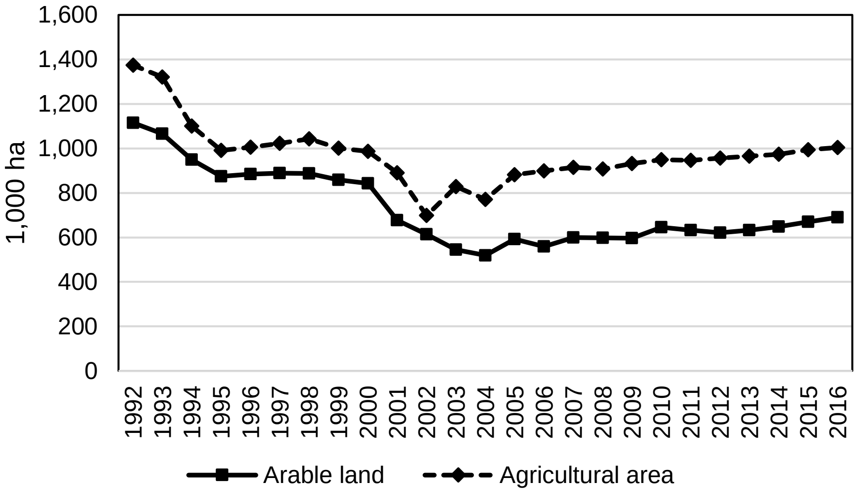

Figure 1. Agricultural land and arable land dynamics in 1992–2016 (SE, 2017; FAOSTAT, 2018).

The area of arable land was in decrease until 2004 (Fig. 1). From 2005, the area of arable land started to increase again and amounted to 690,208 ha in 2016. By 2016, there was 36,918 ha of agricultural land (permanent grassland) not used in agricultural production but maintained in good agricultural and environmental conditions, i.e. land that does not produce agricultural products, thus not producing direct economic added value but provides public goods. As these 36,918 ha of permanent grassland has to be maintained as permanent grassland, added value could be produced via increasing the stock of grazing livestock.

How to make a rational use of existing resources, primarily arable land? Dairy sector is the cornerstone of Estonian agriculture as Estonia is and has been net exporter of milk and dairy products. Hence this study is looking to:

1) define the rational structure of land use in order to ensure food security of the population in terms of the main foodstuffs and the existing production and export volume for milk products (Scenario 1);

2) define the rational structure of land use assuming a significant increase of dairy production and export in the future (Scenario 2).

Expectation for a considerable expansion of the dairy sector is supported by the historical experience. After all, the years 1986–1989 saw nearly 1.3 million tonnes of milk being produced. Around 300 thousand dairy cows were required for this, with average annual milk production per cow slightly above 4,000 kg (SE, 2017). Resources required for such production volumes were already present, i.e. land for producing feed, barns for the cattle and the calves, as well as people and their skills (experience). Although some feed cereals and concentrates were imported from neighbouring Soviet republics, fodder was produced locally, and that arable land is still present and usable in the future.

Various studies have targeted food security issues both at the world scale and at different national levels (Coles et al., 2016; Halldorsdottir & Nicholas, 2016; Peters, et al., 2016; Shepon et al., 2016; Bureau & Swinnen, 2017; Flachowsky et al., 2017; Martin, 2017; Meyfroidt, 2017; Stephens et al., 2017; Sadowski & Baer-Nawrocka, 2018). Different mathematical models have been used in food security modelling (Koh et al., 2013; Davis & D'Odorico, 2015; Chavas, 2017; Qi et al., 2018), including linear programming models (Ward, 2014; Monaco et al., 2016; Sali et al., 2016; Van Kernebeek et al., 2016).

The current study focuses on the physical availability dimension of food security. The use of arable land is optimised in order to define the production capacity of the main foodstuffs and export capacity of dairy products of the Estonian agricultural and food sector. This in turn allows to adjust crop and livestock production in order to ensure the population's food security in terms of the main foodstuffs.

MATERIALS AND METHODS

Estonia's food security and agricultural production capacity were assessed using a linear programming model (Põldaru & Roots, 2012) which has been updated according to changes in the population's structure, consumption habits, and nutritional recommendations for minimal food basket suggested by Estonian nutritional scientists, as well as developments in agriculture (Table ..., 2004; Calculations …, 2016; Estonian ..., 2017; SE, 2017).

Linear programming models are used for solving problems which requirements are represented by linear equations or inequalities, and the purpose of which is clearly expressed and mathematically formulated (Taha, 2003).

The following presents an overview of the linear programming land use optimization model used in the study. The optimization model includes 163 variables that are divided into 7 groups and 178 constraints that are divided into 6 groups (Table 1).

Table 1. Groups of variables and constraints in the optimization model

Groups of variables	Groups of constraints
1. Number of population by gender and age groups (thousands) – 11 variables	1. Population's food demand – 11 constraints
2. Total consumption and production of foodstuffs (tonnes) – 23 variables	2. Food production and consumption – 17 constraints
3. Number of animals (head) – 11 variables	3. The number of animals and structure of livestock farming – 13 constraints
4. Crop sown areas (ha) – 15 variables	4. Feed production – 107 constraints
5. Feed sown areas by animal species (ha) – 67 variables	5. Export product – 8 constraints
6. Cost variables (thousands of euros) – 33 variables	6. Cost – 22 constraints
7. Auxiliary – 3variables	

In case of the given model, the optimization criterion is the minimum sown area of all crops required for the production of foodstuffs – cereal products and food potatoes, and self-produced feed.

Baseline data for the optimisation model is the following:

1. The number of inhabitants in Estonia by sex and age groups (1,315.8 thousand inhabitants), and the calorie and protein requirements of each group. Weighted average demand over all groups is 2,160 kcal of energy and 58 g of protein per capita per day (Estonian …, 2017; SE 2017).

2. Characteristics of eating habits (minimum quantities of meat products, dairy products, cereals, and potatoes consumed per year – a total of 9 different foodstuffs). The minimum consumption amount of these foodstuffs per person are presented in Table 2.

3. Energy content (kcal) and protein content (grams) of primary foodstuffs (9 different foodstuffs).

4. Crop yields (kg ha^{-1}) of 12 different crops, the amount of energy (MJ) and protein (kg) obtained from each hectare.

5. Characteristics of livestock productivity (milk production per cow, slaughter weight of fattening cattle and pigs, meat production from broilers, and egg production per hen per year).

6. Characteristics of the reproduction of animals (the proportion of culled cows per year, the number of calves per one cow, the number of piglets per one sow per year).

7. Yearly energy requirement (MJ) and protein requirement (kg) per year for different species of animals (cattle, pigs, poultry – total of 10 species).

8. The energy content (MJ) and the protein content (kg) of the yield (feed) proposed for feeding different species (10 animal species) obtained from one hectare of feed growing area.

The optimization model uses three equilibrium conditions that ensure balance between production and consumption of agricultural production. Fig. 2, where dashed line ovals visualize the equilibrium conditions depict the main groups of variables and their interaction in order to satisfy the equilibrium conditions and produce results on optimal land use (sown area).

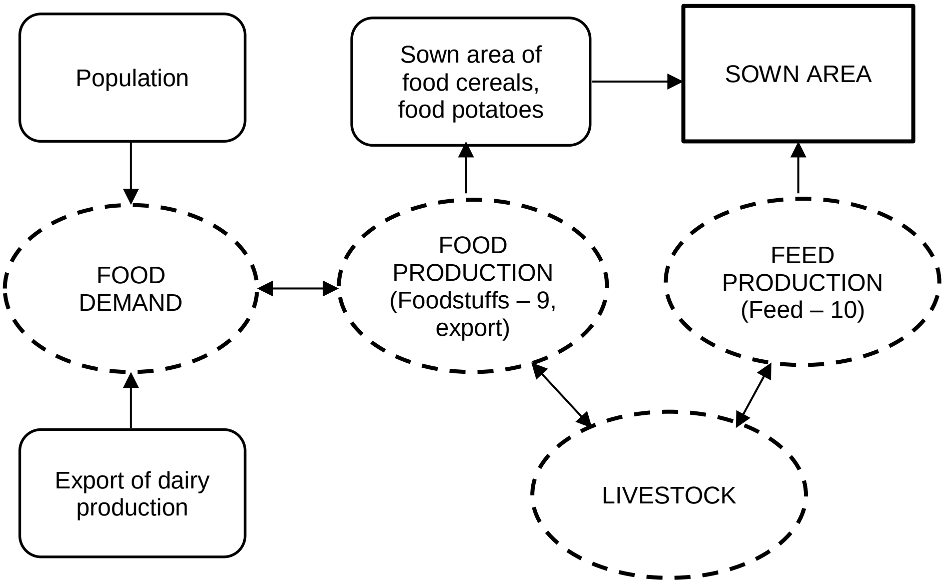

Figure 2. Flow diagram of equilibrium conditions of model.

1. The 1st equilibrium condition (food demand) is based on the population of Estonia and export volumes of dairy products. The supply side consists of estimated amounts of produced foodstuffs. To ensure a balance between consumption and production, the model defines numbers of animals and sown areas (food cereals and food potatoes) required for producing each of the main foodstuffs (Fig. 2). Consumption volumes also determine the numbers of slaughter animals (beef heifers, fattening pigs, and broilers), dairy cattle, and laying hens, which ensure a balance between demand and production (supply).

In modelling dairy production milk is divided in three main components: raw milk, milk protein and milk fat. Produced raw milk (total milk production) is divided into drinking milk, processed milk, and feed for calves and piglets. Milk protein and milk fat obtained from processed milk are the modelling basis (production, consumption and export) of the main products: cheese, butter, whole milk powder (WMP) and skim milk powder (SMP).

2. The 2nd equilibrium condition describes the relation between slaughter animals and slaughter animals (cows, pigs, hens) which satisfies the demand side, i.e. the consumption side, and is in balance with the number of animals produced by the reproductive chain of the respective animal species (supply).

3. The 3rd equilibrium condition describes a balance between feed consumption and production in all animal species. The feeds of all animal species are balanced in terms of the main feed parameters (energy and protein), and are produced in Estonia. There is a different selection of feeds designed for feeding each animal species.

The model has the following limitations:

1. The model is not used for modelling non-agricultural products (aquaculture products), non-local products (coffee, sugar, tea, etc), non-land based foods (honey), fruits, or vegetables.

2. Cereal export and import are not modelled.
3. Only self-produced feeds are used for feeding animals.
4. This study addresses one dimension of food security – food availability and does not take into account the effect of food prices and the purchasing power of various social groups.

This paper provides an analysis of two scenarios:

Scenario 1 defines a rational land use structure in the context of 2017 production conditions with some exceptions:

a) average productivity is 9,000 kg milk per cow,

b) export of dairy products is modelled. Contrary to the actual situation, raw milk export to Latvia and Lithuania is not modelled, but the respective quantity of milk is used for processing to make cheese, butter, WMP, and SMP. Therefore, the results of this scenario do no fully match the current situation in Estonia.

Scenario 2 is used to assess how land use would change if the dairy sector was to increase the production volume considerably:

a) model stipulates a total annual milk production per cow – 10,000 kg,

b) estimated export volumes are chosen so that the estimated total milk production is approximately equal to the total milk production of 1986–1989 (ca 1.3 million tonnes).

The linear programming model is used to identify different land use scenarios which allow to assess how much food the agricultural and food sector are able to produce and export. MS Excel's Premium Solver Pro was used to solve the model.

RESULTS AND DISCUSSION

Consumption of foodstuffs and land use for the food production

Food security and prospective rational land use in Estonia has been analysed using two different scenarios. The modelling results indicate that Estonia's agriculture and food production sector is able to provide the Estonian population with the main foodstuffs (Table 2).

In order to ensure food security, minimum daily energy consumption per person must be 1,700–1,900 kcal (FAO, 2008). The model estimates a daily energy consumption of 2,207 kcal per person, which exceeds the minimum level of food energy and is in line with food consumption recommendations. The consumption of sugar, fish products, cooking oils, fruits and vegetables is added to this amount of energy.

The planned consumption level of protein according to the optimum plan is 97 grams per day. An analysis of the main foodstuffs consumption shows that people tend to exceed the minimum daily requirements of the main foodstuffs in terms of energy and protein.

The analysis of the structure of consumption by consumed calories shows that 1.06×10^{12} kilocalories of energy must be produced to ensure sufficient food for the entire population. Most of the energy (48.6%) is obtained from cereal products, pork (12.9%) is on the second position, leaving drinking milk and drinkable dairy products (10.3%) on the third position.

Cereals are also the largest source of protein (33.8%), pork (19.2%) the second, and drinking milk along with drinkable dairy products (12.1%) the third.

Table 2. Estimated consumption of foodstuffs per year, and agricultural land needed for producing them

Foodstuff	Specified minimum kg per capita	Total t	Calories 10^6 kcal	Percentage of calories %	Protein t	Percentage of protein %	Area ha	Percentage of area %	Calories per m^2 kcal
Beef	9.0	11,777	21,788	2.1	2,355	5.1	14,170	3.6	154
Pork	40.0	52,343	136,616	12.9	8,898	19.2	185,332	47.3	74
Poultry meat	25.0	32,714	45,800	4.3	4,024	8.7	23,834	6.1	192
Eggs (1,000 pcs)	245.0	320,602	39,113	3.7	3,591	7.7	23,598	6.0	166
Milk (products)	130.0	170,115	108,874	10.3	5,614	12.1	41,016	10.5	265
Cheese	10.0	12,432	41,273	3.9	3,481	7.5	22,064	5.6	187
Butter	6.0	7,197	52,611	5.0	216	0.5	19,763	5.0	266
Cereal products	120.0	157,029	515,057	48.6	15,703	33.8	53,821	13.7	957
Potatoes	130.0	170,115	98,667	9.3	2,552	5.5	8,506	2.2	1,160
Total	X	x	1,059,799	100	46,434	100	392,105	100.0	x
Per capita (1,000 kcal, kg)			805		35				

An analysis of the sown areas required for producing the planned foodstuffs demonstrates that 392,105 ha of land must be cultivated in order to feed Estonia's population, i.e. approximately 0.3 ha of land is needed to supply one person with the main foodstuffs (Table 2). The majority of land would be taken up for producing pork, i.e. 185,332 ha, making up 47.5% of the sown area of crop. 13.7% of the sown area of crop would be used for producing food cereals, and 10.5% of the sown area of crop required for feeding the population would be used for producing drinking milk and dairy products made from the latter.

Analysing the amount of energy (the number of calories) produced from one hectare, it appears that the highest amount of energy – 1,160 kcal – is produced from 1 m^2 of potato field, and the lowest amount from 1 m^2 of sown area used for producing pork, i.e. only 74 kcal. 15.7 times less energy is obtained from 1 ha in case of pork production than in case of potato production. Cereals are in the second position when it comes to energy production – 960 kcal m^{-2}.

A similar analysis focusing on protein production shows that the highest amount of protein – 300.0 kg is also produced from one ha of potato field. One ha of sown area used for producing cereal products is on the second position, providing 291.9 kg of protein, and one ha of sown area used for producing poultry is on the third position, providing 168.8 kg of protein.

Sown area of field crops and their structure

Table 3 gives an overview of planned sown areas of field crops and their structure in different scenarios. In the first scenario, the entire planned sown area is 490,689 ha, 61.2% of which is sown area of cereals. In addition to providing a necessary area to guarantee food security to the population (Table 2), such sown area of field crops also guarantees the amount of raw milk production required for producing export dairy products.

The actual sown area of field crops in Estonia was 672,905 ha in 2016 (SE, 2017). Cereals were sown on 351,353 ha which made up 52.2% of the total sown area. Thus, the planned and the real sown areas of crops and their shares differ remarkably. Such big difference of sown areas of field crops is caused by the fact that the sown area of export cereals makes up an important part of the real structure of sown areas of crops. Therefore, the structural indicators presented in Table 3 are not comparable to the indicators of national statistics. 1 million tonnes of cereals were exported in 2015/2016 (SE, 2017). As a result of modelling, 53,821 ha of land is planned as sown area of food cereal, making up 11.0% of the entire sown area of crops, and 21.7% of sown area of the cereal crops.

The estimated sown area of crop in Scenario 2 is 619,928 ha which exceeds the sown area of crop in Scenario 1 by 129,239 ha. Such a large sown area ensures that the production of the dairy sector can be increased to the expected level. Compared to Scenario 1, sown areas of cereal and feed crops are larger. Sown area of cereal crops increased by 38,602 ha, whereas the sown area of all feed cultures increased by 90,638 ha. There were also some changes in the structure of sown areas. The share of feed crops grew from 33.4% to 41.1%.

However, even in the Scenario 2, the sown area of cereals is 18.6% below the actual sown area in 2016. At the same time, in 2016, the self-sufficiency of pork and poultry were 73.5% and 57.4% respectively (SE, 2018). This suggests that if Estonia wants to reduce export of cereals, it should improve its self-sufficiency of pork and poultry and increase pork and poultry production.

Table 3. Planned areas and structure of field crops

Field crop	Scenario 1		Scenario 2		
	Area, ha	Share, %	Area, ha	Share, %	Change, ha
Cereals	248,114	50.6	286,716	46.2	38,602
inc. food cereals	53,821	11.0	53,821	8.7	0
Forage crops	164,069	33.4	254,707	41.1	90,638
multiannual forage crops	24,836	5.1	57,548	9.3	32,712
green fodder	74,709	15.2	113,093	18.2	38,384
inc. mixed hay	17,734	3.6	20,062	3.2	2,327
pasture	54,190	11.0	90,247	14.6	36,057
annual forage crops	2,784	0.6	2,784	0.4	0
succulent feed	64,523	13.1	84,066	13.6	19,543
inc. silage crops	37,553	7.7	57,095	9.2	19,543
potatoes, beets	26,970	5.5	26,970	4.4	0
Food potatoes	8,506	1.7	8,506	1.4	0
Rape	70,000	14.3	70,000	11.3	0
Total	490,689	100.0	619,928	100.0	129,239

In 2016, permanent grassland and fodder crops comprise 48.3% (485,019 ha) of utilised agricultural land. The results of Scenario 1 indicate that 164,069 ha of forage crops are required to ensure self-sufficiency with beef and dairy products, and allow for export of dairy products in 2016 volumes. Increase in milk production in Scenario 2 increase the forage area to 254,707 ha. This suggests that in Scenario 2 approximately 230,000 ha of permanent grassland and/or area of fodder crops could be used to produce beef or even more dairy products for export. Therefore, beef and dairy farming should be developed if Estonia aims to maintain the area of permanent grasslands and keep them in good agricultural and environmental conditions via agricultural production.

Livestock and feed production

Table 4 provides an overview of the estimated number of livestock, sown areas of crops required for producing feeds, as well as energy and protein amounts. The indicators characterising cattle farming are defined on the basis of total milk production. The amount of total milk production is defined on the one hand by the amount of raw milk required for producing dairy products, and on the other hand, the amount of milk that goes for the internal use of agriculture. Total milk production is in balance in terms of demand (consumption) and supply (production). The number of cattle and other indicators characterising the reproduction of cattle are derived from the specified productivity and the required total milk production. In Scenario 1, milk production per cow is 9,000 kg, and in Scenario 2, it is 10,000 kg. The other indicators characterising cattle farming depend directly on the number of cows, and act as a reproductive chain (balancing out the number of cows).

Table 4. Planned number of animals, and feed consumption

	Scenario 1							Scenario 2						
Animal species	No. 1,000	Area 1,000 ha	Share %	Energy 10^6 MJ	Share %	Protein t	Share %	No. 1,000	Area 1,000 ha	Share %	Energy 10^6 MJ	Share %	Protein t	Share %
Dairy cows	83.6	152.3	35.6	7,178	44.4	52.7	38.6	130.7	268.9	48.2	12,451	56.8	95.4	51.9
In-calf heifers	26.8	24.5	5.7	1,030	6.4	10.3	7.5	41.8	38.3	6.9	1,610	7.3	16.1	8.7
Fattening bulls	12.7	9.6	2.2	427	2.6	3.5	2.6	3.3	2.5	0.4	111	0.5	0.9	0.5
Calves	82.0	9.2	2.2	246	1.5	2.8	2.0	128.1	16.6	3.0	645	2.9	4.4	2.4
Fattening pigs	755.7	129.6	30.3	4,715	29.2	35.5	26.1	755.7	123.5	22.2	3,990	18.2	35.5	19.3
Sows	42.8	48.6	11.4	1,261	7.8	14.5	10.7	42.8	48.6	8.7	1,261	5.8	14.5	7.9
Piglets	771.1	7.1	1.7	246	1.5	2.0	1.5	771.1	7.6	1.4	309	1.4	2.0	1.1
Broilers	27.3	20.5	4.8	436	2.7	6.5	4.8	27.3	24.6	4.4	932	4.3	6.5	3.6
Laying hens	1.3	20.2	4.7	456	2.8	6.4	4.7	1.3	20.2	3.6	456	2.1	6.4	3.5
Breeding hens	0.4	6.7	1.6	156	1.0	2.1	1.5	0.4	6.7	1.2	156	0.7	2.1	1.1
Total	X	428.4	100	16,152	100	136.3	100	x	557.6	100	21,921	100	183.8	100

An analysis of indicators related to dairy cattle shows that 83,600 cows (Scenario 1) are enough for producing the necessary quantity of milk. Planned total milk production is 752,465 tonnes. The analysis shows that 730,000 tonnes of milk goes for human consumption (for preparing milk and processed dairy products), with the rest is given to calves and piglets as feed. National statistics show that in 2016, there were 86,100 cows in Estonia, and 783,200 tonnes of milk was produced, meaning that average milk production per cow was 8,878 kg (SE, 2018).

152,300 ha of land must be cultivated to feed the planned 83,600 cows – this is 35.6% of the total sown area of crops required for feed production (428,400 ha). The total amount of energy of feed produced from this sown area is 7,178 million MJ, meaning that 85,900 MJ of energy is produced per one cow per year. The planned amount of energy is in line with normative energy needs, and using the existing feeds fulfils energy and protein needs.

In Scenario 2, the total planned milk production is 1,306,886 tonnes. The number of cows needs to be increased to 130,689 heads to achieve this. 286,900 ha of land must be cultivated to feed the cows. This is 48.6% of the total sown area of crops required for feed production. The total amount of energy of feed produced from this sown area is 12,451 million MJ, meaning that 95,900 MJ of energy is produced per one cow per year. The energy spent on feeding cows makes up 56.8% of the energy used for feeding all animals.

Total pork production is the primary indicator characterising pig farming. Total pork production consists of two parts: the quantity of meat from fattening pigs, and the quantity of meat from slaughtered sows. 755,700 fattening pigs must be reared to produce the quantity of meat required for the population. This exceeds the number of fattening pigs currently being reared in Estonia. According to national statistics, 464,900 fattening pigs were slaughtered in Estonia in 2015 (SE, 2017). Thus, the planned number of fattening pigs exceeds the 2015 level by 1.66 times. The planned sown area of feed crops for feeding fattening pigs is 129,600 ha, which makes up 30.3% of the total sown area of feed crops.

Summary of the main results

Table 5 shows a comparison of the main results of different scenarios, showing that most of the production volume indicators in Scenario 2 exceed the Scenario 1 indicators by 1.16–2.39 times. Such difference is related to the fact that Scenario 2 aimed to model a situation which would describe milk production levels in the years 1986–1989. In Scenario 2, the estimated total milk production is 1,306,886 tonnes, which surpasses the total milk production in Scenario 1 by 1.74 times. To reach this amount, the number of cows must be increased to 130,689, with a milk production of 10,000 kg per cow, which is 1.56 times more cows than in Scenario 1. With an increased number of animals, the total sown area must increase by 1.26 times, the sown area of cereals should increase by 1.16 times, and the sown area of feed crops by 1.55 times. The biggest change in Scenario 2 is the increase of the amount of raw milk required for export dairy products by 2.39 times.

Table 5. Brief comparison of the main results of Scenarios 1 and 2

Indicator	Unit	Scenario 1	Scenario 2	Change
Total sown area	ha	490,688	619,928	1.26
Cereal sown area	ha	248,114	286,716	1.16
Feed crops' sown area	ha	164,069	254,707	1.55
Number of cows	head	83,607	130,689	1.56
Total milk production	t	752,465	1,306,886	1.74
... milk for animal feed	t	22,465	39,018	1.74
... milk for export dairy products	t	386,407	924,275	2.39
… export of cheese	t	15,000	50,000	3.33
… export of butter	t	10,429	25,000	2.40
… export of SMP	t	49,317	87,279	1.77
… export of WMP	t	1,000	2,000	2.00

The optimisation helped to estimate Estonia's agricultural and food sector's capability to produce the main foodstuffs, i.e. it found the optimal crop and livestock structure that ensures availability of domestically produced main foodstuffs for the Estonian population, and the export of dairy products.

CONCLUSIONS

A linear programming model was used for optimisation, with the criterion of optimality being the minimisation of arable land required for producing foodstuffs.

The analysis of the solution results shows that 392,105 ha of arable land is required to supply the Estonian population with the main foodstuffs. This implies an energy use of 2,207 kcal, i.e. approximately 0.3 ha of land is needed to supply one person with the main foodstuffs. In order to supply Estonian residents with sufficient main foodstuffs and to maintain the export of dairy products in 2017 volume, 490,689 ha of land are needed. Increasing dairy production to 1.3 million tonnes per year implies increasing the number of cows up to 130,700 heads and increasing arable land use to 619,928 ha.

Further studies could aim to reduce limitations of this study, analyse the sensitivity of the results with regards to different crop yield levels, consider the export-import of cereals, and assess the impact of changing diets on the agricultural and food production and agricultural land use.

If Estonia aims to maintain it's almost 500,000 ha of permanent grasslands and annual and multi-annual forage crops area and keep these areas in good agricultural and environmental conditions via agricultural production activities, beef and dairy farming and exports should be further developed.

The results of the analysis show that improvements in the self-sufficiency of pork and poultry are needed if Estonia aims to reduce its exports of cereals.

This analysis demonstrated that Estonia's agricultural and food sector has necessary land resources to contribute towards the goal of ensuring food security for the world's population.

REFERENCES

Aborisade, B. & Christian, B. 2014. Assessing the Pillars of Sustainable Food Security. *European International Journal of Science and Technology* **3-4**, 117–125.

Agriculture. A partnership between Europe and farmers. 2017. *European Commission Directorate-General for Communication*. https://publications.europa.eu/en/publication-detail/-/publication f08f5f20-ef62-11e6-8a35 -01aa75ed71a1/. Accessed 10.04.2018.

Alexander, P., Brown, C., Arneth, A., Finnigan, J. & Rounsevell, M.D.A. 2016. Human appropriation of land for food: The role of diet. *Global Environmental Change* **41**, 88–98.

Barrett, C.B. 2010. Measuring Food Insecurity. *Science* **327**, 825–828.

Briones Alonso, E., Cockx, L. & Swinnen, J. 2018. Culture and food security. *Global Food Security*. https://doi.org/10.1016/j.gfs.2018.02.002.

Bureau, J.-C. & Swinnen, J. 2017. EU policies and global food security. *Global Food Security* (in press). https://doi.org/10.1016/j.gfs.2017.12.001.

Burchi, F. & De Muro, P. 2016. From food availability to nutritional capabilities: Advancing food security analysis. *Food Policy* **60**, 10–19.

Cafiero, C., Melgar-Quinonez, H.R., Ballard, T.J. & Kepple, A.W. 2014. Validity and reliability of food security measures. *Annals of the New York Academy of Sciences* **1331**, 230–248.

Calculations gross margin in crop and livestock production. 2016. *http://www.maainfo.ee/data/trykis/kattetulu/KATTETULU2016.pdf* (in Estonian).

Chavas, J.P. 2017. On food security and the economic valuation of food. *Food Policy* **69**, 58–67.

Clapp, J. 2015. Food Self-Sufficiency and International Trade: A False Dichotomy? State of Agricultural Commodity Markets – In Depth. FAO, Rome. *www.fao.org/3/a-i5222e.pdf*.

Clapp, J. 2017. Food self-sufficiency: Making sense of it, and when it makes sense. *Food Policy* **66**, 88–96.

Coates, J. 2013. Build it back better: Deconstructing food security for improved measurement and action. *Global Food Security* **2**, 188–194.

Coles, G.D., Wratten, SD. & Porter, J.R. 2016. Food and nutritional security requires adequate protein as well as energy, delivered from whole-year crop production. *PeerJ*, **4**: e2100 DOI 10.771/peerj.2100.

Davis, K.F. & D'Odorico, P. 2015. Livestock intensification and the influence of dietary change: A calorie-based assessment of competition for crop production. *Science of the Total Environment* **538**, 817–823.

Davis, K.F., Gephart, J.A., Emery, K.A., Leach, A.M., Galloway, J.N. & D'Odorico, P. 2016. Meeting future food demand with current agricultural resources. *Global Environmental Change* **39**, 125–132.

Development plan of the governance area of Estonian Ministry of Rural Affairs 2017–2020. 2017. *https://www.agri.ee/sites/default/files/content/ arengukavad/ ministeerium-valitsemisala-arengukava-2017–2020.pdf*. Accessed 11.04.2018. (in Estonian).

Estonian Nutrition and Physical Activity Recommendations 2015. 2017. National Institute for Health Development. Tallinn. *http://www.tai.ee/en/publications/download/815* (in Estonian).

Fairbairn, M. 2012. Framing transformation: the counter-hegemonic potential of food sovereignty in the US context. *Agriculture and Human Value* **29**, 217–230.

FAO. 2008. FAO methodology for the measurement of food deprivation. Statistics Division. Rome. *http://www.fao.org/fileadmin/templates/ess/documents/food_security_statistics/metadata/undernourishment_methodology.pdf.*

FAO. 2009. Reform of the Committee on World Food Security. CFS:2009/2 Rev.2. *http://www.fao.org/ tempref/docrep/fao/meeting/018/k7197e.pdf*

FAO. 2012a. Coming to terms with terminology: Food security, nutrition security, food security and nutrition, food and nutrition security. *Document CFS 2012/39/4*. Rome: FAO.

FAO. 2012b. FAO Statistical Yearbook 2012. *http://www.fao.org./economic/ess/ess-publications /ess-yearbook/yearbook2012/en/.*

FAO. 2017. The future of food and agriculture – Trends and challenges. Rome. *http://www.fao.org/3/ a-i6583e.pdf*

FAOSTAT. 2018. Online statistical database. *http://www.fao.org/faostat/*. Accessed 7.01.2018.

Govindan, K. 2018. Sustainable consumption and production in the food supply chain: A conceptual framework. *International Journal of Production Economics* **195**, 419–431.

Flachowsky, G., Meyer, U. & Südekum, K-H. 2017. Land Use for Edible Protein of Animal Origin. A Review. *Animals* **7**, 25, 2–19.

Halldorsdottir, T. & Nicholas, K.A. 2016. Local food in Iceland: identifying behavioural barriers to increased production and consumption. *Environmental Research Letters* **11**, 115004.

Hamblin, J.D. 2012. The Vulnerability of nations: Food Security in the Aftermath of World War II. *Global Environment* **10**, 42–65.

Jones, A.D., Ngure, F.M., Pelto, G. & Young, S.L. 2013. What Are We Assessing When We measure Food Security? A compendium and review of Current Metrics. *Advances in Nutrition* **4**, 481–505.

Kastner, T., Rivas, M.J.I., Koch, W. & Nonhebel, S. 2012. Global changes in diets and the consequences for land requirements for food. *Proceedings of the National Academy of Sciences of the United States of America* **109** (18), 6868–6872.

Koester, U. 2014. Food Loss and Waste as an Economic and Policy Problem. *Intereconomi*cs **49**(6), 348–354.

Koh, L.P., Koellner, T. & Ghazoul, J. 2013. Transformative optimisation of agricultural land use to meet future food demands. *PeerJ*. **1**:e1188. DOI 10.7717/peerj.188.

Kudo, S., Mutisya, E. & Nagao, M. 2015. Population Aging: An Emerging Research Agenda for Sustainable Development. *Social sciences* **4**, 940–966.

Lal, R. 2013. Food security in a changing climate. *Ecohydrology & Hydrobiology* **13**, 8–21.

Martin, W. 2017. Agricultural Trade and Food Security. In: *ADBI Working Paper 664*. Tokyo: Asian Development Bank Institute. https://www.adb.org/publications/agriculturaltrade-and-food-security

Meyfroidt, P. 2017. Trade-offs between environment and livelihoods: Bridging the global land use and food security discussions. *Global Food Security* (in press). http://dx.doi.org/ 10.1016/j.gfs.2017.08.001

Miccoli, S., Finucci, F. & Murro, R. 2016. Feeding the Cities Through Urban Agriculture The Community Esteem Value. *Agriculture and Agricultural Sciences Procedia* **8**, 128–134.

Misra, A.K. 2014. Climate change and challenges of water and food security. *International Journal of Sustainable Built Environment* **3**, 153–165.

Monaco, F., Sali, G., Mazzocchi, C. & Corsi, S. 2016. Optimizing agricultural land use options for complying with food demand: evidences from linear programming in a metropolitan area. *AESTIMUM* **68.** Giugno. http://dx.doi.org/10.12128/Aestimum-18725.

Naylor, L. & Higgins, M.M. 2018. The rise in global biodiesel production: Implications for food security. *Global Food Security* **16**, 75–84.

Peters, C.J., Picardy, J., Darrouzet-Nardi, A.F., Wilkins, J.l., Griffin, T.S. & Fick, G.W. 2016. Carrying capacity of U.S. agricultural land: Ten diet scenarios. *Elementa*: *Science of the Anthropocene* **4**, 000116.

Pinstrup-Andersen, P. 2009. Food security: definition and measurement. *Food Security* **1**, 1–7.

Puma, M.J., Bose, S., Chon, S.Y. & Cook, B.I. 2015. Assessing the evolving fragility of the global food system. *Environmental Research Letters* **10**, 024007.

Põldaru, R. & Roots, J. 2012. Using modelling to analyse options for safeguarding food self-sufficiency in Estonia. *Journal of Agricultural Science* **XXIII**(2**)**, 36–44 (in Estonian).

Review on the implementation of the 2030 agenda in Estonia. 2016. *Republic of Estonia Government Office*. Tallinn, 2016. 60 pp.

Roser, M. & Ritchie, H. 2018. Hunger and undernourishment. *https://ourworldindata.org/ hunger-and-undernourishment.* Accessed 15.12.2017.
Qi, X., Fu, Y., Wang, R.Y., Ng, C.N., Dang, H. & He, Y. 2018. Improving the sustainability of agricultural land use: An integrated framework for the conflict between food security and environmental deterioration. *Applied Geography* **90**, 214–223.
Sadowski, A. & Baer-Nawrocka, A. 2018. Food and environmental function in world agriculture - Interdependence or competition? *Land Use Policy* **71**, 578–583.
Sali, G., Monaco, F., Mazzocchi, C. & Corsi, S. 2016. Exploring land use scenarios in metropolitan areas: food balance in a local agricultural system by using a multi-objective optimization model. *Agriculture and Agricultural Science Procedia* **8**, 211–221.
Statistics of Estonia (SE). 2017. Online statistical database. *http://www.stat.ee*. Accessed 15.09.2017.
Statistics of Estonia (SE). 2018. Online statistical database. *http://www.stat.ee*. Accessed 29.01.2018.
Shepon, A., Eshel, G., Noor, E. & Milo, R. 2016. Energy and protein feed-to-food conversion efficiencies in the US and potential food security gains from dietary changes. *Environmental Research Letters* **11**, 105002.
Stephens, E.C., Jones, A.D. & Parsons, D. 2017. Agricultural systems research and global food security in the 21st century: An overview and roadmap for future opportunities. *Agricultural Systems* (in press). https:// doi.org/10.1016/j.agsy.2017.01.011.
Stringer, R. 2016. Food security global overview. In Caraher, M., Coveney, J. (ed/s): *Food Poverty and Insecurity: International Food Inequalities*. Springer. Ch. 2, pp. 11–18.
Table of chemical composition and nutritional value of feeding stuff. 2004. Tartu, 122 pp. (in Estonian).
Taha, H.A. 2003. *Operations Research: An Introduction.* University of Arkansas. Pearson Education, 830 pp.
Tielens, J. & Candel, J. 2014. Reducing food wastage, improving food security? In: *Food & Business Knowledge Platform*. Netherlands, 36 pp.
Van Dijk, M. & Meijerink, G. 2014. A review of global security scenario and assessment studies: results, gaps and research priorities. In: *FOODSECURE*. *Working paper no. 20*. LEI Wageningen UR, 26 pp.
Van Kernebeek, H.R.J., Oosting, S.J., Van Ittersum, M.K., Bikker, P. & De Boer, I.J.M. 2016. Saving land to feed a growing population: consequences for consumption of crop and livestock products. *International Journal of Life Cycle Assessment* **21**, 677–687.
Verburg, P. H., Mertz, O., Erb, K.-H., Haberl, H. & Wu, W. 2013. Land system change and food security: towards multi-scale land system solutions. *Current Opinion in Environmental Sustainability* **5**, 494–502.
Ward, J.D., Ward, P.J., Mantzioris, E. & Saint, C. 2014. Optimising diet decisions and urban agriculture using linear programming. *Food Security* **6**, 701–718.
United Nations (UN). 2015. *Transforming our world: the 2030 Agenda for Sustainable Development*. A/RES/70/1, 41 pp. https://sustainabledevelopment.un.org/post2015/ transformingourworld. Accessed 15.12.2017.

Agronomy Research **16**(4), 1854–1861, 2018
https://doi.org/10.15159/AR.18.206

Morphological and biochemical indicators of *Fusarium oxysporum* f sp. *fragariae* in strawberry crops (*Fragaria* × *ananassa* Duch) in the province of Pichincha, Ecuador

S. Salazar[1], F. Bayas-Morejón[1,*], Z. Niño[2], J. Guevara[1], M. Ruilova[1], O. Merino[1], W. Donato[2] and J. Guamán[1]

[1]Universidad Estatal de Bolívar, Facultad de Ciencias Agropecuarias Recursos Naturales y del Ambiente, Departamento de Investigación. Centro de Investigación y Desarrollo Biotecnológico, EC020150 Guaranda, Ecuador
[2]Universidad Estatal de Bolívar, Facultad de Ciencias Agropecuarias Recursos Naturales y del Ambiente, Departamento de Investigación. Centro de Investigación del Ambiente, EC020150 Guaranda, Ecuador
[*]Correspondence: isba@doctor.upv.es; fbayas@ueb.edu.ec

Abstract. *Fusarium oxysporum* f. sp. *fragariae* is a fungal pathogen, transmitted by soil in crops of strawberry (*Fragaria* × *ananassa* Duch.), which causes wilt disease that, kill the strawberry cultivars. The disease caused by *Fusarium oxysporum* f. sp., *fragariae* is hard to detect as the of the symptoms are similar with other soil-borne diseases. In spite of detection methods targeted *F. oxysporum* using molecular criteria have been developed, they have not been shown to successfully identity the unique identity of *F. oxysporum* strain that causes this disease. In Ecuador, the cultivation of strawberry has acquired great importance for the consumption, promoting the increase of its production. However, the process of importing plant material from producing countries for the purpose of improving production has contributed to the spread of the fungus. The objective of this study was to identify the presence of the *Fusarium oxysporum* f. sp *fragariae* by means of morphometric identification and the application of biochemical methods (BIOLOG) in the province of Pichincha. Fifty-two diseased strawberry plants and 52 asymptomatic plants were analyzed. Of these, 13 isolates were identified by morphometry as *F. oxysporum*. However, through BIOLOG four strains were identified as *F. oxysporum*, 5 as *Fusarium* sp., 2 *F. lateritium*, 1 *F. udum* and 1 strain as *F. sacchari*. The results obtained through the identification and evaluation confirmed the presence of *F. oxysporum* f. sp., *fragariae* in evaluated strawberry cultivars, thus determining the high risk to exist if the pathogen spreads in new plantations in Ecuador.

Key words: *Fusarium oxysporum*, BIOLOG, Morphological Indicators, strawberry.

INTRODUCTION

The big strawberry fruit (*Fragaria* × *ananassa* Duch.) is being cultivated since the year 1800, constituting the starting point of the modern varieties that dominate the world production (López-Aranda et al., 2011).

Its consumption has great acceptance worldwide, as its cultivation has spread to U.S.A, Canada, Mexico, Colombia, Chile, Argentina, Guatemala, Costa Rica, Ecuador and almost entire Europe, generating a growing expansion of consumers, favored by the aerial transport (Fernández, 2005).

Diseases such as Botrytis, grey mould (González et al., 2013) and Fusarium wilt (Koike et al 2009; Henry et al., 2017) infected strawberry. The latter is a very serious disease caused by Fusarium oxysporum f. sp. fragariae. According to Koike et al. (2009), the symptoms consist of foliage wilting, drying and wilting of older leaves, delayed plant growth and reduced fruit production, causing the plants to finally collapse and die. Studies in California by Koike et al. (2009) reported that since 2006, this disease has increased in incidence and severity. The initial problems in 2006 consisted of multiple small patches of infected plants, and by 2009, in some fields, the disease affected large sections. Henry et al. (2017), found infected strawberry population in California of a considerable diversity of F. oxysporun f. sp. fragariae, an indication that horizontal gene transfer might have occurred. This fungus was first reported in Australia in 1965 by Winks & Williams (1965), then in Japan (Takahashi et al., 2003) and Korea (Kim et al., 1982). This pathogen has caused serious losses in strawberry fruit productions fields in Chile (González et al., 2005), Spain (Arroyo et al., 2009), USA (Gordon et al., 2016), Australia (Fang et al., 2012) and in Mexico (Dávalos-González et al., 2016), attributing that its worldwide dissemination is due to its difficult diagnosis (van Diepeningen et al., 2015).

According to Koike & Gordon (2015), the field diagnosis of Fusarium wilt is complicated since other soil-borne diseases also showed very similar symptoms. Methods for detecting F. oxysporum based on molecular criteria have been developed but have not yet been shown to uniquely identify F. oxysporum strain causing strawberry Fusarium wilt. In Ecuador, intensive strawberry cultivation began in 1983, mainly in the province of Pichincha, (Bejarano, 1993). According to the Ministry of Agriculture, Livestock, Aquaculture and Fisheries of Ecuador (MAGAP), this crop constitutes an important socioeconomic alternative for this Province (MAGAP-DPP, 2015). This research is the continuation of the molecular characterization of *Fusarium oxysporum* f. sp. *fragariae* in Pichincha-Ecuador to be able to establish or discard their presence in the country, with the following objectives: to identify the morphology and morphometry of the phytopathogen and to evaluate its biochemistry through the use of the BIOLOG identification system.

MATERIALS AND METHODS

The research work was carried out in the Molecular biology laboratory of the State University of Bolivar, Ecuador. Strawberry plants (*Fragaria* × *ananassa*) were analyzed with 13 inoculums of the pathogenic fungus (*Fusarium* sp.), the treatments are shown in the Table 1.

The microscopic characteristics of the fungus were observed and identified through the use of morphometric keys (Garibaldi et al., 2015), and it was determined with descriptive statistics considering the average lengths of 20 macroconidia (average of maximum and minimum lengths).

Sampling was carried out in strawberry producing areas located in the province of Pichincha, of which 52 plants with symptoms and 52 asymptomatic plants were obtained; these plants were in phases of vegetative development and fruiting stages (Table 2).

Table 1. Treatments used in this work

Treatment	Description
T0:	Strawberry plant without inoculum
T1	Strawberry plant + strain 1
T2	Strawberry plant + strain 2
T3	Strawberry plant + strain 3
T4	Strawberry plant + strain 4
T5	Strawberry plant + strain 5
T6	Strawberry plant + strain 6
T7	Strawberry plant + strain 7
T8	Strawberry plant + strain 8
T9	Strawberry plant + strain 9
T10	Strawberry plant + strain 10
T11	Strawberry plant + strain 11
T12	Strawberry plant + strain 12
T13	Strawberry plant + strain 13

Table 2. Information of the analyzed samples

Cod. Health surveillance	Place of the province	N° of Sample	Sample	Detected pathogens
17-01-85-401	Yaruquí	1	root	*Fusarium* sp.
17-0185-410	El Quinche	1	root	*Fusarium* sp
1/-1	yaruquí	1	Soil / plant	*Rizoctonia* sp
17-2	Yaruquí	1	Soil / plant	*Fusarium* sp
17-3	Yaruquí	1	leaves	*Mycosphaerella* sp
17-4	Yaruquí	1	leaves	*Mycosphaerella* sp
17-7	San Carlos	3	Soil / plant	*Fusarium* sp
17-8	Yaruquí	1	Soil / plant	*Pestalotía* sp
17-9	Yaruquí	2	Soil / plant	*Pestalotía* sp
17-10	Checa	3	Soil / plant	*Fusarium* sp
17-11	Checa	1	leaves	*Mycosphaerella* sp
17-201	Pifo	10	Soil / plant	*Fusarium* sp
17-202	Pifo	3	Soil / plant	*Pestalotía* sp
17-203	Pifo	10	Soil / plant	*Fusarium* sp
17-205	El Quinche	2	Soil / plant	*Pestalotía* sp
17-206	El Quinche	2	Soil / plant	*Pestalotía* sp
17-207	El Quinche	4	Soil / plant	*Pestalotía* sp
17-209	Puembo	1	leaves	*Mycosphaerella* sp
17-210	Puembo	4	Soil / plant	*Fusarium* sp
	TOTAL	52		

The identification method was by isolation on PDA, then it was identified by microscopic observation.

Sowing of plant material and media preparation

Longitudinal cuts of the crown were made and 1–2 cm segments containing areas with or without vascular wilt lesion were removed. After this process, four segments were cultured in Potato dextrose Agar (PDA medium) in triplicate, then incubated at 24 °C for 7 days. The isolates that presented asexual structures of *Fusarium* sp., (conidia, hyphal formation) were selected. On the other hand, 10 g of soil was added in flasks with

90 mL of distilled water, of which, 100 μL of each sample, was cultured in duplicate on PDA agar and incubated for 7 days at 24 °C.

For purification and obtaining monosporic cultures, the PDA cultures were transferred on Malt Extract Agar (MEA), from these pure cultures a suspension of the inoculum was extracted. The suspension was loaded in a Neubauer chamber by counting propagules with the aid of an optical microscope. From this suspension, continuous dilutions were made up to a concentration of 20 propagules / mL of distilled water (macroconidia or microconidia). Finally, the suspension was reseeded on MEA and incubated at 24 °C for 7 days.

Storage of field samples

The samples collected were stored in paper bags with a silica gel envelope and stored in a drying chamber.

Massification of mycelium in liquid medium

In order to obtain a sufficient amount of biomass, two agar blocks of monosporic culture medium were introduced into one flask in duplicate for each isolate. The media was allowed to stand for 5 days. After this period, the solution was filtered using a vacuum pump, the mycelium obtained was rinsed, transferred to eppendorf tubes for storage at -20 °C.

Biochemical evaluation by the BIOLOGY identification system

Pure and monosporic strains were cultured in MEA medium and incubated at 24 °C for 7 days. From this culture, with the help of sterile handle, the mycelium was extracted from the fungus and a suspension of fungi was made. The readings were made by spectrophotometry until a turbidity of 75% ± 2 was obtained for each isolate. Subsequently, the fungus was inoculated into microplates (FF MicroPlate TM), dispensing 100 μL in each of the 96 wells. Microplates were incubated at 24 °C for 7 days, at which time the respective readings were performed, the intervals are shown in the Table 3.

Table 3. Intervals of readings by the BIOLOG system

1° Reading	2° Reading	3° Reading	4° Reading	5° Reading
24 hours	48 hours	72 hours	96 hours	168 hours
8:00	8:00	8:00	8:00	8:00
	13:30	13:30	13:30	
	12:00	12:00	12:00	
	15:00	15:00	15:00	
	17:00	17:00	17:00	

RESULTS AND DISCUSSION

From the total of samples, analyzed after isolation and confirmed by microscopic characteristics, was evidenced in 13 isolates the presence of asexual structures of Fusarium sp., representing 25% of the total samples; In a study carried out by Juber at al. (2014), the incidence of *Fusarium* sp., found in strawberry plants was of 40–60%, these differences are due especially to the environmental characteristics in which the crops are found.

Characteristics of the colony morphology of the 13 isolates planted in PDA

The treatment T1-T4 present pink color; however, the T1 presented a withish-pinkish color in its aerial part and the treatment T2, T3 and T4 a rosy aerial mycelium. The treatments T5, T6, T11-T13 presented a violet color, with a whitish-violet aerial mycelium. The treatments T8 and T9 presented a purple color and in their aerial part whitish mycelium. Whereas, only the T7 treatment presented a yellowish coloration andaerial mycelium different from the others. As far as its growth, a concentric growth was visualized in treatments T4,T5, T6, T7, T10 and T11, and in the rest was a diffuse radial growth (Fig. 1). Similar results were reported by Domsch et al. (2007), of which, the isolates were cultured on PDA and presented different characteristics in color and form of the mycelium.

Figure 1. *Fusarium* colonies showing various colony colors on PDA medium.

According to a study by Quilambaqui, (2005), colonies identified as *Fusarium oxysporum* developed violet or purple mycelium with macroconidia, and another group of Fusarium sp., developed white mycelia that turned to a yellow coloration.

The asexual structures of Fusarium sp. isolated on PDA media are shown in the Fig. 2.

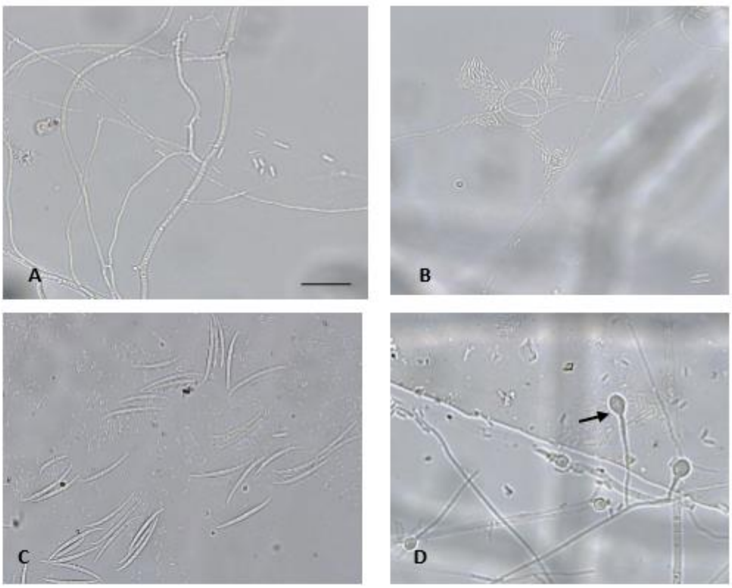

Figure 2. Asexual structures of *Fusarium* sp. isolated on PDA (40X). A: Mycelium; B: Microconidia; C: Macroconidia; D: Chlamydospore (40 µm).

Biochemical evaluation using the BIOLOG identification system

The reading of the color densities in the wells of the sensitivity tests were positive in the treatments T_2, T_5, T_6 and T_{11} for *Fusarium oxysporum*, evidencing a slight difference in the readings between treatments T_5, T_6 and T_{11} due to the absorbance difference. In treatments T_1, T_7, T_8, T_{12} and T_{13}, the limit of detection only indicates at genus level Treatment T_3 and T_9 had 97% identity for *Fusarium lateritium*. The percent results indicated turbidity and colorimetry readings during biochemical reactions between the substrate and the pathogen. On the other hand, a percentage of 99% identity was obtained for *Fusarium sacchari* and 94% for *Fusarium udum* in the treatment T_4 (Table 4).

Table 4. Microplate readings corresponding to the 13 isolates for *Fusarium* sp...

Treatment	Morphometric Identification	Biological Identification	Probability (%)
T1	*Fusarium oxysporum*	*Fusarium* sp.	*
T_2	*Fusarium oxysporum*	*Fusarium oxysporum*	0.99
T_3	*Fusarium oxysporum*	*Fusarium lateritium*	0.97
T_4	*Fusarium oxysporum*	*Fusarium udum*	0.94
T_5	*Fusarium oxysporum*	*Fusarium oxysporum*	0.77
T_6	*Fusarium oxysporum*	*Fusarium oxysporum*	0.78
T_7	*Fusarium oxysporum*	*Fusarium* sp.	*
T_8	*Fusarium oxysporum*	*Fusarium* sp.	*
T_9	*Fusarium oxysporum*	*Fusarium lateritium*	0.97
T_{10}	*Fusarium oxysporum*	*Fusarium sacchari*	0.99
T_{11}	*Fusarium oxysporum*	*Fusarium oxysporum*	0.79
T_{12}	*Fusarium oxysporum*	*Fusarium oxysporum*	*
T_{13}	*Fusarium oxysporum*	*Fusarium* sp.	*

*: No absorbance.

In a study carried out in Sweden by Khalil & Alsanius (2009), they detected five pathogens of vegetable roots, including *Fusarium oxysporum* f.sp. *radicis-lycopersici* and *Fusarium solani,* with a high percentage of identity. Frac et al. (2016), isolated strains of *Fusarium* sp., and identified them by the method of dilutions in filamentous fungi (FF) microplates BIOLOG TM2, but failed to discriminate at the classification level and through this technique also analyzed levels of resistance to fungicides. On the other hand, Gizaw et al. (2017) isolated *Fusarium* species present in the cultivated soil (Rizosfera) and were identified by the BIOLOG technique, being constituted 75% by filamentous fungi of which 16% corresponded to the genus *Fusarium* with the species *F. melanochlorum, F. juruanum, F. avenaceum,* with 62.5% similarity. These results demonstrate in part that the species of *F. oxysporum* are more commonly found in plant materials than in crop soil and that the diversity of *Fusarium* species changes relative to the geographical area.

The BIOLOG identification system method allows diagnose of the possible metabolic patterns of the biochemical profile and the phylogenetic relationship between different isolates, while the pathogen oxidizes the different carbon sources. This diagnosis is related to the manipulation and nature of microorganisms.

On the other hand, no significant statistical differences between the treatments for the distribution were detected, of which there are no differences between the variables. The coefficient of variation was 19.46% tolerable, indicate that it is acceptable for field evaluation. This analysis establishes that the inoculation in the plants was effective both by the concentration of the inoculum and the method performed. The incidence of the disease was determined based on visual symptomatology. In this way, those plants that showed, wilt, necrosis and death of leaves, were considered infected by the pathogen.

CONCLUSIONS

By means of the pathogenesis evaluation, the presence of *Fusarium oxysporum* f sp., *fragariae* that causes the disease in the cultivation of the strawberry in the 13 treatments showing symptomatology of vascular wilt, which determines the presence of this disease in Ecuador. This study represents a first advance study in the recognition of the microbiont associated with the cultivation of strawberry in Ecuador, this determines the importance of the application of biochemical techniques namely using BIOLOG for the detection of the pathogen.

ACKNOWLEDGEMENTS. This work was supported by the 'Departamento de Investigación de la Universidad Estatal de Bolívar'. The authors thank the 'Vicerrectorado Académico y de Investigación and to the debt exchange program Ecuador – Spain, for the support received in carrying out the present work.

REFERENCES

Arroyo, F., Llergo, T., Aguado, A. & Romero., F. 2009. First Report of *Fusarium wilt* Caused by *Fusarium oxysporum on* Strawberry in Spain. *Plant. Dis.* **93**(3), 323. https://doi.org/10.1094/PDIS-93-3-0323B

Bejarano, W. 1993. *New export products, manual of the strawberry*. 1st Ed. PROEXANT, Quito-Ecuador, 119 pp.

Dávalos-González, P.A., Jofre-Garfias, A.E., Díaz-Espino, L.F., Mariscal-Amaro, L.A. & López-Pérez, M.G. 2017. Advances in strawberry breeding in Mexico: genotypes selection with high productivity, good fruit quality, and tolerance to the local viral complex and *Fusarium oxysporum*. *Acta Hortic.* **1156**, 159–166. doi: 10.17660/ActaHortic.2017.1156.23https://doi.org/10.17660/ActaHortic.2017.1156.23

Domsch, K., Gams, W., Anderson, T. 2007. Compendium of soil fungi 2nd. Ed. Die Deutsche Bibliothek- CIP-Einheitsaufnahme, pp. 222–224.

Fang, X., You, M.P. & Barbetti, M.J. 2012. Reduced severity and impact of Fusarium wilt on strawberry by soil pH manipulation, soil organic amendments and crop rotation. *Eur. J. Plant Pathol.* **134**, 619–629. doi: 10.1007 / s10658-012-0042-1

Fernández, J. 2005. Encyclopedia Agricultural and Livestock Practice 2nd Edition Editorial Ocean / Centrum. Mexico, pp. 60961.

Frąc, M., Gryta, A., Oszust, K., Kotowicz, N. 2016. Fast and Accurate Microplate Method (Biolog MT2) for Detection of *Fusarium* Fungicides Resistance / Sensitivity. *Front Microbiol.* **7**, pp.16. doi: 10.3389 / fmicb.2016.00489

Garibaldi, A., Bertetti, D., Pensa, P., Ortu, G. & Gullino, M.L. 2015. First report of *Fusarium oxysporum* causing wilt of Euphorbia mammillaris var. Variegata in Italy. *J. Plant Pathol*. **97** (Supplement), S67–S77.

Gizaw, B., Tsegay, Z., Tefera, G., Aynalem, E., Wassie, M. & Abatneh, E. 2017. Phosphate solubilizing fungi isolated and characterized from Teff rhizosphere soil collected from North Showa zone, Ethiopia. *African J. Microbiol. Res.* **11**(17), 687–696. doi: 10.5897 / AJMR2017.8525

González, F.J, Walls, S. & Mancilla, M. 2005. Detection by PCR-RFLP of *Fusarium oxysporum* f. sp. fragariae causal agent of fusariosis in strawberry. *Mycol. Bulletin* **20**, 63–72.

González, G., Fuentes, Li., Moya-León, M., Sandoval, C. & Herrera, R. 2013. Characterization of two PR genes from *Fragaria chiloensis* in response to *Botrytis cinerea* infection: A comparison with Fragaria x ananassa. *Phys. Mol. Plant. Pathol*. **82**, 73–80. doi.10.1016 / j.pmpp.2013.02.001

Gordon, T.R., Daugovish, O., Koike, S.T., Islas, C., Kirkpatrick, S., Yoshisato, J. & Shaw, D. 2016. Options for Management of Fusarium Wilt of Strawberry in California. *International J. Fruit Sci*. **16**(1), 160–168. doi: 10.1080/15538362.2016.1219294

Henry, P.M., Kirkpatrick, S.C., Islas, C.M., Pastrana, A.M., Yoshisato, J.A., Koike, S.T., Daugovish, O & Gordon, T.R. 2017. The Population of *Fusarium oxysporum* f. sp. *fFragariae,* Cause of Fusarium Wilt of Strawberry, in California. *Plant Dis.* **101**(4), 550–556. https://doi.org/10.1094/PDIS-07-16-1058-RE

Juber, K.S., Al-Juboory, H.H., Al-Juboory, S. 2014. *Fusarium wilt* disease of strawberry caused by *Fusarium oxysporum f*. sp. *fragariae* in Iraq and its control. *J. Exp. Biol. Agric. Sci*. **2**(4), 419–427.

Khalil, S. & Alsanius, W. 2009. Utilization of Carbon Sources by *Pythium*, *Phytophthora* and *Fusarium* Species as Determined by Biolog® Microplate Assay. *The Open Microbiol. J*. **3**, 9–14.

Kim, C., Seo, H., Cho, W. & Kim, S. 1982. Studies on varietal resistance and chemical control to the wilt of strawberry caused by Fusarium oxysporum. Korean J. Plant Protect. 21, 691–67.

Koike, S. & Gordon, T. 2015. Management of Fusarium wilt of strawberry. *Crop. Protect*. **73**, 67–72. doi. 10.1016 / j.cropro.2015.02.003

Koike, S., Kirkpatrick, S.C. & Gordon, T.R. 2009. *Fusarium wilt* of strawberry caused by *Fusarium oxysporum* in California, *APS* **93**(10), pp. 1077. https://doi.org/10.1094/PDIS-93-10-1077A

Leslie, J.Y. & Summerell, B. 2006. *Fusarium* laboratory manual. 1a. Ed. UK. Blackwell Publishing Ltd, pp. 212–219.

López-Aranda, J., Soria, C., Santos, B., Miranda, S., Dominguez, P. & Medina-Mínguez, J. 2011. Strawberry Production in Mild Climates of the World: A Review of Current Cultivar Use. *Int. J. Fruit. Sci*. **11**(3), 232–244. doi. 10.1080 / 15538362.2011.608294

MAGAP-DPP. 2015. Ministry of Agriculture Livestock Aquaculture and Fisheries - Provincial Directorate of Pichincha, Unit for Technological Innovation, Priority Crops, Executive Report, 2015; pp 16. http://sinagap.agricultura.gob.ec/phocadownloadpap/tematicos_zonales/precios_produccion/2016/precios_productor_mayo_2016_zona2.pdf.

Quilambaqui, M.A. 2005. Isolation and identification of species of *Fusarium* spp. Associated with asparagus (*Asparagus officianalis* L.) in five municipalities of Guanajuato, Mexico. *Rev. Tecnol. ESPOL* **18**(1), 135–140.

Takahashi, H., Yoshida, Y., Kanda, H., Furuya, H. & Matsmoto, T. 2003. Breeding of *Fusarium wilt*-resistant strawberry cultivar suitable for field culture in Northern Japan. *Acta Hortic*. **626**, 113–118. doi. 10.17660 / ActaHortic.2003.626.15

Van Diepeningen, A.D., Brankovics, B., Iltes, J., van der Lee & Waalwijk, C. 2015. Diagnosis of *Fusarium* Infections: Approaches to Identification by the Clinical Mycology Laboratory, *Curr. Fungal Infect. Rep.* **9**(3), 135–143. doi. 10.1007 / s12281-015-0225-2

Winks, B. & Williams, Y. 1965. A wilt of strawberry caused by a new form of *Fusarium oxysporum. Queensland J. Agric. Animal. Sci*. **22**, 475–479.

Agronomy Research **16**(4), 1862–1876, 2018
https://doi.org/10.15159/AR.18.153

Human factors and ergonomics in safety management in healthcare: building new relationships

J. Sepp[1,*], K. Reinhold[2], M. Järvis[2] and P. Tint[2]

[1]Tallinn Health Care College, Kännu 67, EE13418 Tallinn, Estonia
[2]Tallinn University of Technology, Ehitajate 5, EE19086 Tallinn, Estonia
[*]Correspondence: jaana.sepp@ttk.ee

Abstract. Human factors are playing an essential role in ensuring occupational health and safety at work. In the healthcare sector, relevant factors include optimizing the interaction of humans with their technical, social working environment, and human characteristics such as knowledge and motivation. Those factors affect the ability to provide good quality of healthcare and safety performance. The aim of this paper is to analyse factors related to safety knowledge, communication and professional competence among caregivers in nursing homes. A group of professionals studied (n = 241, includes nurses and caregivers) completed a validated questionnaire. Descriptive statistics and correlation analyses were applied, using SPSS Statistics 24.

Our study revealed that over half of the respondents possess an occupational certificate and the majority of employers organize regular in-service training at workplaces. Respondents who claimed that in-service trainings are not regular still stated that they generally receive safety and ergonomic related trainings, trainings for working with special equipment. However, only a quarter of respondents have access to occupational safety trainings that focus on specific risks at work.

Based on the results of the study, we emphasize the need of integrating human factors in the safety management system in nursing homes with a special focus on adequate safety training in order to develop necessary skills and knowledge of workers. This would enhance employees' ability to cope successfully with the elderly and people with special needs, to provide safe and high-quality care as well as confidence and the knowledge how successfully they manage conflicts in order to keep good relationships at work.

Key words: competences, healthcare, training, workplace safety.

INTRODUCTION AND THEORETICAL BASIS

Human factors and ergonomics (HFE) are playing an essential role in ensuring occupational health and safety at work that influence workers and their behavior in work-related situations. The need for addressing those factors in healthcare has been recognised by many researchers (Hignett, 2003; Carayon, 2006; Hignett et al., 2013; Valdez et al., 2017). The main topics include optimizing the interaction of humans with their working environment (technical, physical, organizational and social working environment (team, supervisors, culture)) (Moray, 2000), human characteristics such as ability, knowledge, motivation of workers, and commitment to organization (Dul et al., 2012). Management of HFE factors contributes to good quality of healthcare, improvement of patient safety (Carayon, 2010) as well as the prevention of occupational incidents and accidents within the healthcare organization. HFE focuses on the integrated system that includes interaction of humans with their working environment, and whereas in healthcare it is a complex system and environment (Carayon, 2006), focusing on both - on the employee (caregivers) and their safety as well as on a care receiver (patient safety) (Hignett et al., 2013).

In the healthcare, successful safety management within the organization requires the development of safety policies, procedures and structures, followed by the employees as well as a common understanding shared by senior managers and employees that safety is vital for overall performance. In addition, HFE tools and methods are also recommended by researchers (Goodman, 2010; Gutberg & Berta, 2017) as a part of interventions in order to improve patient safety.

The focus of HFE is generally on the improvement of well-being and performance by implementing a hierarchical approach. The improvement of the working environment through systems design is seen as the priority, followed by integrating the human into the system, selecting workers and an effective training that enhances social exchange and organizational learning (Christian et al., 2009) and creates a strong safety culture (Hadjimanolis & Boustras, 2013; Griffin & Hu, 2013).

In today's modern world, researchers emphasize the importance of the development of human resource, professional empowerment and competence of nurses and caregivers in healthcare systems in terms of safety and quality of nursing care (Heydari et al., 2016). Professional competency of nurses composed the central component of a set of skills, knowledge, attitudes, values, and self-efficacy (Levett-Jones et al., 2011), which can elevate nurses' and caregivers' positions among multi-professional teams within healthcare organizations. According to Chang et al. (2012), workers' competency is generally influenced by professional knowledge, reserved work experience, and personal attributes such as change skills, communication skills, qualifications, and experience (Chang et al., 2012) and is strongly related to errors and consequences (Axley, 2008). In addition, Epstein & Hundert (2002) revealed that professional competency might be evaluated according to correct judgment, practice and developed habits in terms of skills used, knowledge, clinical reasoning, shared values, communication, and daily activities.

Inside the organizations, continuous workers training plays also an essential role for health caregivers. The study by Nilsson with colleagues (2014) revealed that acquiring essential competencies by nurses is vital for the quality of everyday nursing practice. The competence level of nurses and training supports them to fulfil their duties effectively, safely, and directly influences the employees' and patients' safety, satisfaction with nursing care and conflict managements (Chan et al., 2014; Ahanchian et al., 2015; Heydari et al., 2016). Organizational learning, teamwork in the unit, feedback, learning from mistakes, communication and blame-free environment are strongly related to patient safety as well as to safety generally (Al-Ahmadi, 2009; Alswat et al., 2017). In healthcare, learning plays a vital role to offer a good quality of care (Ratnapalan & Uleryk, 2014). Legislation points out that training is a meaningful activity for risk prevention and safety and a key component that helps to the change workers' attitudes toward safety and understand their safety responsibility (Grau et al., 2002) and provide organizational effectiveness by HFE (Hignett, 2003; Carayon, 2006; Hignett et al., 2013; Valdez et al., 2017).

Development of professional competence of nurses is meaningful particularly for caregivers who are a part of the hospital system, representing it for patients and their family (Steginga et al., 2005; Ratnapalan & Uleryk, 2014) and providing patient care and living quests. Many scholars report that representatives of this specialty do not, in general. have professional and formal education and enough skills to provide quality care for elderly, sick people or for people with special needs (Salonen, 2009; USDHHS, 2014). Providing good care of patients often involves cognitively and physically difficult work with many work-related psychosocial risk factors, such as quantitative (work load) and emotional demands, workplace and role conflicts that may contribute to high levels of stress as well as burnout amongst nurses (Freimann & Merisalu, 2015). Chang et al. (2012) have found a strong relationship between safety prevention and health hazards, and between safety, health training in a healthcare organization.

Despite many healthcare studies that focus on the efficacy of treatment and practices as well as the importance and relevance of HFE in healthcare, there is a potential for the development of professional competence of nurses and caregivers. In this respect, lack of attention to professional competency of nurses and caregivers can cause problems for healthcare organizations, for example, nurses' poor competency may lead to some undesirable consequences, including nurses' frustration, job dissatisfaction, low job attitudes, including lack of organizational commitment and professional affiliations (Dul, et al., 2012; Hignett et al., 2013; Rajabipour Dehghani, 2013). For those reasons, it is relevant to investigate how human factors are integrated in the current safety management system in healthcare, particularly in nursing homes, in order to understand the interactions among humans and other elements of the system. We examined the relationship between caregivers' professional competency, obtained education and maintained qualifications, safety knowledge, communication, and commitment to safety.

In this article, we share Carayon' (2010) concepts and consider HFE as an innovation that each healthcare organization requires. In particular, focus is on general HFE knowledge provided to its workers, and follows an analytical framework proposed by Carayon et al. (2006) to consider how different components of the system can influence employees' commitment, attitudes and perceptions towards safety in a healthcare organization.

The aim of this paper is to analyse factors related to safety knowledge, communication, commitment to safety and professional competence among nurses and caregivers in nursing homes. We presume that the study will contribute to designing an interactive learning environment, an effective safety training and learning possibilities to integrate HFE into the in-service training activities in healthcare organizations.

MATERIAL AND METHODS

The study group

A simple random was selected from caregivers employed at seven nursing homes in Estonia. In total, 362 questionnaires were sent to nursing homes. The respond rate was 66.6%. Demographic data of the sample are presented in Table 1. It shows that among 241 respondents, 3 or 1.24% were males while 236 or 97.9% were females; information about the gender of one respondent is missing (0.8%). The distribution of respondents according to their age groups shows that 95 employees, composing 39.4%, are in the age group 48–57, followed by 56 employees or 23.2% who are in the age group 58–67, 44 respondents or 18.3% and 29 respondents or 12.1% are in the age group 38–47 and group 28–37, respectively. The rest of 7.1% respondents were spread between the group 18–27 (10 respondents or 4.2%) and the group older than 68 (6 respondents. 2.5%), 1 answer is missing (0.4%). More than a half of the respondents (55.61%) are caregivers, the rest of the respondents are nurses (44.39%) who are engaged in care work in nursing homes.

Table 1. Background information of study participants (*n* = 241)

Demographic variables	Category	Frequency	Proportion
Gender *(n = 241)*	Male	3	1.24
	Female	236	97.93
	Missing	2	0.83
Age *(n = 241)*	18–27	10	4.15
	28–37	29	12.03
	38–47	44	18.26
	48–57	95	39.42
	58–67	56	23.24
	68 and above	6	2.49
	Missing	1	0.41
Occupation *(n = 241)*	Care givers	133	55.61
	Nurse	108	44.39

Methods

The data were collected during the period of January – May 2017. The questionnaire was compiled according to Estonian National Occupational Standard for Care workers (Level 4, the highest level for professional competence of caregivers in Estonia). In order to explore caregivers' perceptions for the educational preparation according to the caregivers' occupational standard that establishes the requirements for working in nursing homes. The questionnaire includes six scales: Scale1 'Necessary skills, knowledge in living quests and patient care'; Scale2 'Necessary skills, knowledge for coping with the elderly and people with special needs'; Scale3 'Communication skills'; Scale4 'First aid'; Scale5 'Professionalism'; Scale6 'Commitment to safety'. Scale6 is not included into the national occupational standard for caregivers. Therefore, we complemented the questionnaire with this issue. The questionnaire was tested in both languages (Estonian and Russian) in two different nursing homes, revised and changed according to the results of piloting.

Description of created scales

The current diagnostic tool was tested for validity and reliability (Table 2). Cronbach α is an estimator of internal consistency. Cronbach alpha provides an assessment of questionnaire consistency; however, values may vary from one, which means best reliability and reliability to zero, which means that reliability is missing. Table 2 illustrates the high and statistically significant reliability coefficient of the following factors: 'Necessary skills, knowledge in living quests and patient care', 'Necessary skills, knowledge for coping with the elderly and people with special needs', and 'Commitment to safety'.

Cronbach's alpha for Scale1 is 0.897, which indicates a high level of internal consistency for this scale. To measure the variable 'Necessary skills, knowledge in living quests and patient care', a combination of questions from 1 to 10 was selected. Cronbach's alpha for Scale2 is 0.877, which indicates a high level of internal consistency for the Scale. To measure the variable, the combination of questions from 11 to 17 was selected. Cronbach's alpha for Scale6 'Commitment to safety' is 0.845, which indicates a high level of internal consistency for the scale. To measure the variable, the combination of questions from 26 to 31 was selected. As the other scales: 'Communication skills', 'First aid' and 'Professionalism' are defined by short lists of questions, the Cronbach's alpha was not calculated for them. But the analyses of the correlation between the questions of these scales were conducted.

As Scale1, 2 and 6 have high and statistically significant reliability coefficient (Table 2), the results of variations of the questions for Scale1, 2 and 6 are described in detail below.

Table 2. Reliability coefficients of the questionnaire for Scales1, 2 and 6

Scale	Cronbach α	M	SD
Scale1. Necessary skills, knowledge in living quests and patient care	0.897	43.42	5.77
Scale2. Necessary skills, knowledge for coping with the elderly and people with special needs	0.877	30.13	3.906
Scale6. Commitment to safety	0.845	25.59	3.806

The results for all specific factors used in the questionnaire are presented in Table 3.

Table 3. Results for the specific factors entered into the analyses

		Scale1	Scale2	Scale3	Scale4	Scale5	Scale6
N	Valid	236	240	241	238	240	234
	Missing	215	211	210	213	211	217
Mean		4.34	4.30	4.09	4.12	4.31	4.27
Std. Error of Mean		.038	.036	.048	.046	.043	.042
Median		4.50	4.43	4.00	4.00	4.33	4.33
Minimum		1.70	1.43	1.00	1.33	1.33	1.00
Maximum		5.00	5.00	5.00	5.00	5.00	5.00

Multiple modes exist. The smallest value is shown.

Respondents' opinions and perception were assessed using a five-point scale. The analyses were prepared using SPSS Statistics 24.0.

All respondents were informed about the aim and procedures of the survey. Every effort was made to ensure the protection of the privacy, confidentiality, and anonymity of individuals and organizations participating in this study.

RESULTS AND DISCUSSION

The first section discusses our general findings, such as results of the analyses of data about the occurrence of occupational disease, workplace stress and availability of safety-related and other additional training among respondents. The second section presents the main results of the study, followed by conclusions and our recommendations.

General findings

Our results revealed that 14.6% of respondents have been diagnosed with occupational diseases, 10% have experienced an occupational accident and 87.9% of the caregivers and nurses claim that their job is stressful (Table 4). Another study conducted by Sepp et al. (2015) in Estonian nursing homes demonstrated that work intensity, lack of time and social support, as well as difficulties in communication with patients influence caregivers' health and well-being.

Our findings also showed that over half (51.7%) of the respondents possess an occupational certificate, which gives a strong reason to credit that those workers may succeed with patient care more effectively than workers without specific vocational training.

Table 4. Characteristics of occupational health and safety aspects among respondents (%, proportion of respondents)

Age group	Occupational disease	Occupational accident	Occupational certificate	Stressful work
Total	14.6	10	51.7	87.9
18–27	-	10	40	60
28–37	24.1	24.1	41.4	82.8
38–47	6.8	9.1	47.7	90.9
48–57	14.7	5.3	48.4	90.5
58–67	17.9	12.5	69.6	87.5
over 68	20	-	33.3	100

Concerning additional trainings reserved by the respondents, the results showed that the majority of employers (82.5%) organize regular in-service training at workplaces (Table 5). Employees who receive regular in-service trainings claimed that those trainings consisted of the following topics: occupational risk and safety, ergonomics, working with special equipment as well as general safety trainings (e.g., fire safety, emergency, evacuation).

Table 5. Results about in-service trainings organized by employers (%, proportion of respondents)

In-service trainings	Respondents' rate
Employers organize regular in-service trainings	82.5
Employers organize occupational risk and safety trainings	79.5
Employees receive ergonomics-related trainings	75.8
Employees receive trainings for working with special equipment	82.9
Employers organize safety trainings (e.g., fire safety)	92.5

It is vital to have regular in-service training in order to strengthen safety behavior, commitment to safety and to improve knowledge about relevant requirement at work. Results of a study by Blair (2004) have demonstrated the core components of safety competency, such as ability to communicate effectively, to accept personal responsibility, to be able to implement and to transport solutions into action, to listen actively and to care, to assess and to evaluate safety effects, to maintain and to share a safety vision, to set goal, and to plan strategic actions. These competencies can be seen as an indicator for human resources development and management and for the development of safety and health training programs (Chang et al., 2012). Trainings for employees need to be planned carefully in order to be practical and effective, to be focused on employees' tasks and everyday work in order to improve workers' skills, performance and quality of working life (Orpen, 1993), their perceptions of quality and safety of care (Gurses et al., 2009).

Relationships between factors

According to our expectations, we found a strong positive correlation (r = .783) at significance level 0.001 between factors Scale1 'Necessary skills, knowledge in living quests and patient care' and Scale2 'Necessary skills, knowledge for coping with the elderly and people with special needs' (see Fig. 1). It means that respondents with higher estimation of their skills, knowledge in living quests and patients care have also higher confidence that they have enough skills, knowledge for coping with the elderly and people with special needs. Professional competency has been proposed as an essential element in the provision of healthcare also by other researchers, for example, Karimi et al. (2017) stated that developing professional competency and organizational commitment is essential for the high-quality and safety in healthcare.

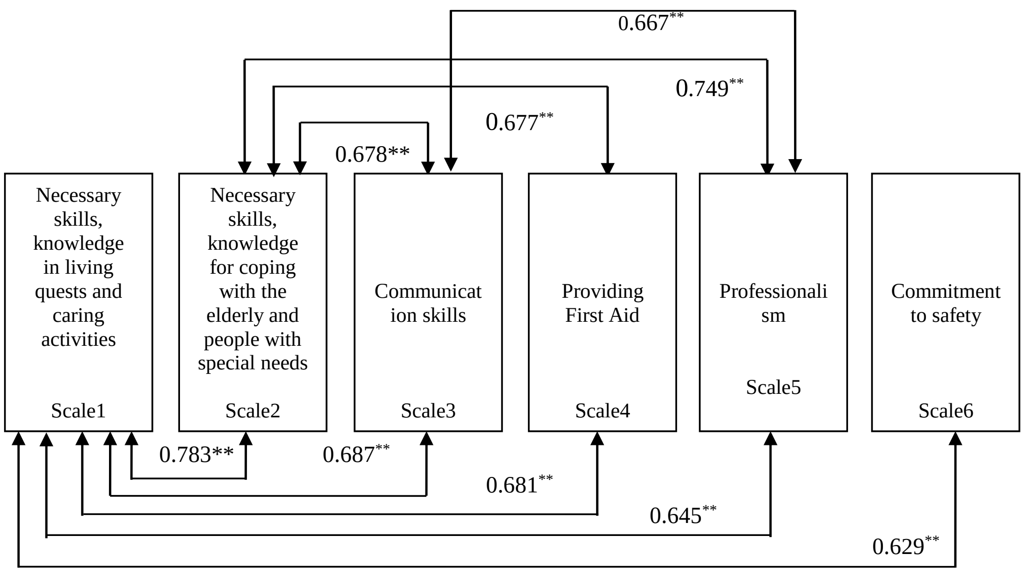

**Statistical significance $p = 0.001$.

Figure 1. Correlations between scales.

In addition, Scale1 ‘Necessary skills, knowledge in living quests and patient care’ has also moderate positive correlations at significance level 0.001 with all other factors Scale3 ‘Communication skills’ (r = .687), Scale4 ‘First aid’ (r = .681), Scale5 ‘Professionalism’ (r = .645) and Scale6 ‘Commitment to safety’ (r = .629). Correlation between Scale1 ‘Necessary skills, knowledge in living quests and patient care’ and Scale3 ‘Communication skills’ shows that confidence in own knowledge and skills about patient care and living quests influences positively employees’ ability to communicate with patients and to find solutions for managing work-related conflicts. Correlation between Scale1 ‘Necessary skills, knowledge in living quests and patient care’ and Scale4 ‘First aid’ shows that employees who estimate their professional skills and knowledge higher than others feel more confident even in emergency situations. Respondents who perceive themselves as a professional with necessary skills and knowledge are more confident about their skills and knowledge also in living quests and patient care. This is confirmed by moderate positive correlation between Scale1 ‘Necessary skills, knowledge in living quests and patient care’ and Scale5 ‘Professionalism’.

Positive moderate correlation between Scale1 ‘Necessary skills, knowledge in living quests and patient care’ and Scale6 ‘Commitment to safety’ may be a reason why respondents who have high estimation of their skills and knowledge tend to be more committed to safety. Vice versa, employees who are more committed to safety have also higher estimation about their knowledge and skills in living quests and patient care. There is also strong positive correlation (r = .749) between factors Scale2 ‘Necessary skills, knowledge for coping with the elderly and people with special needs’ and Scale5 ‘Professionalism’. This means that employees with higher professionalism have higher estimations about their skills and knowledge for coping with the elderly and people with special needs. In addition, Scale2 ‘Necessary skills, knowledge for coping with the elderly and people with special needs’ has also moderate positive correlations with other factors, for instance, Scale3 ‘Communication skills’ (r = .678), Scale4 ‘First aid’ (r = .677), and Scale6 ‘Commitment to safety’ (r = .607).

Moderate positive correlations at significance level 0.001 were obtained between factors Scale3 ‘Communication skills’ and Scale1’ Necessary skills, knowledge in living quests and patient care’ (r = .687), Scale3 ‘Communication skills’ and Scale2 ‘Necessary skills, knowledge for coping with the elderly and people with special needs’ (r = .678), Scale3 ‘Communication skills’, and Scale5 ‘Professionalism’ (r = .667). This means that respondents with higher estimation of their professional knowledge are more confident in communication and willing to be able to solve conflicts more effectively than those employees who estimated those competences lower. These results prove the fact that effective training for health caregivers contributes to many critical aspects during work situations of caregivers and nurses. According to studies by Conner (2014) and Karami et al. (2017), continuous education is also recommended in order to strengthen professional competence of healthcare workers as well as to improve their confidence regarding everyday activities and practice (Orpen, 1993; Steginga et al., 2005), to improve their knowledge about safety, safe and direct patient-centred care (Lakanmaa et al., 2015) as well as enhance job satisfaction and commitment to organization. Another study (Han & Chung, 2015) has demonstrated that health caregivers’ organizational commitment is a vital precondition for the reduction of negative consequences, such as conflicts, exhaustion and turnover within health organization, as well as for mainenance of friendly relationships with co-workers and of patients' health through a positve and supportive relationship to patients (deeper commitment to patients) ad to their families.

Factor Scale4 ‘First Aid’ has moderate positive correlations with factors Scale1 ‘Necessary skills, knowledge in living quests and patient care’ (r = .681) and Scale2 ‘Necessary skills, knowledge for coping with the elderly and people with special needs’ (r = .677) at significance level 0.001. It can be explained that respondents who have high estimation on their knowledge and skills in living quests and patient care, and on skills and knowledge for coping with the elderly and people with special needs are also more confident in their readiness to provide first aid. Respondents who have doubts about their skills and knowledge described in Scales1 and 2 have also doubts in their ability to provide first aid.

There is also moderate positive correlations at significance level 0.001 between factor Scale6 ‘Commitment to safety’ and Scale1 ‘Necessary skills, knowledge in living quests and patient care’ (r = .629), and Scale6 ‘Commitment to safety’ and Scale2 ‘Necessary skills, knowledge for coping with the elderly and people with special needs’ (r = .607) (Table 6). It shows that respondents who have sufficient knowledge and skills required for their work are more likely to contribute to effective cooperation with management and/or with other co-workers in questions related to occupational safety.

Table 6. Relationships between different professional competences of caregivers in Estonia

	Scale	Scale1	Scale2	Scale3	Scale4	Scale5	Scale6
S1	Necessary skills, knowledge in living quests and patient care		.783**	.687**	.681**	.645**	.629**
S2	Necessary skills, knowledge for coping with the elderly and people with special needs			.678**	.677**	.749**	.607**
S3	Communication skills				.593**	.667**	.563**
S4	First aid					.574**	.345**
S5	Professionalism						.536**
S6	Commitment to safety						

**Statistical significance p = 0.001.

Caregivers’ perceptions of their knowledge

Scale1 ‘Necessary skills, knowledge in living quests and patient care’ was measured in the questionnaire by 10 questions (questions 1 to 10). Parameter Scale1 in Table 7 summarizes the results of selected variables included into the factor. The mean of summarized Scale1 variable is 4.34, which is 86.8% of the maximum. The highest level in this scale has question 10, question 8 showed the lowest level. This means that respondents estimate highly their knowledge and skills on patient hygiene and coping in daily life, but they do not feel confident enough to organize patients’ social, rehabilitation and health services. These results indicate that in-service training and vocational training may not give sufficient knowledge to understand fully the system of healthcare with a large spectrum of different tasks, which would be essential in order to be able to give professional advice on clients’ special needs as well as to organize an appropriate patients’ activities by nurses and caregivers.

Table 7. Results of selected variables from Scale1 'Necessary skills, knowledge in living quests and patient care' of the caregivers' professional competences

Questions	Questions											
	Mean	SD	1	2	3	4	5	6	7	8	9	10
1 safe environment	4.32	.824										
2 nursing	4.48	.713	.634**									
3 theory to practice	4.39	.830	.488**	.698**								
4 patient knowledge	4.20	.785	.522**	.481**	.426**							
5 safe medicine taking	4.44	.795	.351**	.532**	.455**	.423**						
6 risk of medicines	4.30	.854	.391**	.449**	.431**	.460**	.746**					
7 helping the nurses	4.46	.737	.344**	.447**	.357**	.416**	.555**	.566**				
8 health services	3.94	.936	.382**	.324**	.368**	.471**	.417**	.457**	.507**			
9 relatives' consulting	4.26	.808	.453**	.488**	.453**	.559**	.493**	.585**	.434**	.541**		
10 patients' hygiene	4.58	.679	.374**	.569**	.446**	.420**	.523**	.449**	.449**	.356**	.487**	
Scale1	4.34	.577	.685**	.770**	.709**	.719**	.755**	.767**	.694**	.683**	.761**	.685**

**Statistical significance *p* = 0.001.

Scale2 'Necessary skills, knowledge for coping with the elderly and people with special needs' includes 7 questions (questions 11 to 17). The mean of the variable of Scale2 was 4.30 (86.0%) and standard deviation 0.558. It has strong uphill linear relationships with questions 12, 14 and 15. This means that respondents understand the importance of having a relevant skills and knowledge for coping with the elderly and people with special needs. There is moderate positive correlation at significance level p<001 between questions 14 and 15, which shows that respondents who have high skills in problem solving tend to know how to motivate elderly patient to try to manage his/her activities independently. In summary, the correlation presented in Table 8 shows that all questions have significance in relation to Scale2.

Scale6 'Commitment to safety' was measured in the questionnaire by 6 questions (questions 26 to 31) (Table 9). The mean of the variable of Scale6 was 4.33 (86.6%) and standard deviation 0.63. We found strong uphill linear relationships with questions 29, 27 and 28, which shows that respondents appreciate their participation and involvement in safety activities as well as the ability to discuss safety issues with management. The most significant correlation was found between questions 28 and 29 (r = .768) at significance level 0.01, which shows that respondents value the management willingness to discuss safety issues. In those cases, workers are motivated eagerly to inform about safety problems as well as to propose safety measures in order to deal with them. This is in line with the study conducted by DeJoy et al. (2017), which has clearly demonstrated that many occupational health problems are generally related to organizational factors.

Akroyd et al. (2007) have addressed the necessary core commitment factors, for example, perceived level of organizational support, management commitment, role of clarity and level of education. According to Farokhzadian et al. (2015), senior managers are responsible for safe working environment, promoting safety and quality care in healthcare organizations.

Table 8. Results of selected variables included into Scale2 'Necessary skills, knowledge for coping with the elderly and people with special needs' of the caregivers' professional competences

Questions/Keywords	Mean	SD	11	12	13	14	15	16	17
11. patients' coping	4.31	.741							
12. patients' daily life support	4.51	.640	.602**						
13. recognition of health problems	4.38	.709	.577**	.580**					
14. patient's problem solving	4.22	.707	.559**	.546**	.637**				
15. patient's independent	4.29	.729	.495**	.509**	.593**	.609**			
16. using the special equipment	4.22	.773	.455**	.571**	.403**	.504**	.515**		
17. work ergonomics	4.19	.830	.407**	.447**	.349**	.348**	.443**	.600**	
Scale2	4.3	.558	.765**	.787**	.768**	.781**	.780**	.767**	.691**

**Statistical significance $p = 0.001$.

Table 9. Results of selected variables included into Scale6 'Commitment to safety' of the caregivers' professional competences

Questions	Questions							
	Mean	SD	26	27	28	29	30	31
26 patients' safety discussions	4.31	.820						
27 safety communications	4.31	.816	.505**					
28 managers discussions	4.29	.861	.343**	.515**				
29 safety proposals	4.27	.816	.397**	.610**	.768**			
30 availability of equipment	4.10	.894	.402**	.512**	.476**	.482**		
31safety trainings	4.29	.834	.445**	.430**	.374**	.373**	.470**	
Scale6	4.33	.634	.684**	.793**	.777**	.807**	.761**	.685**

**Statistical significance $p = 0.001$.

In the analysis of relationships between specific statements, we found a few significant correlations (at significance level $p = 0.001$). The strongest correlations were found between questions 9 (Scale1) and 12 (Scale2) (r = .576), 15 (Scale2) and 17 (Scale2) (r = .559). These relationships mean that if respondents estimate their knowledge and skills highly, they provide good instructions of how to take care of patient's regular needs, provide advice and instructions to the patient´s families as well as support and encourage patients with coping in daily life. In addition, respondents also estimate that they have good knowledge about ergonomics and how to do their job safely. Similarly, there is significant correlation between questions 10 (Scale1) and 12 (Scale2) (r = .546). According to the results, caregivers and nurses who are confident in their knowledge and skills to provide patients' hygiene, and do it safely and effectively, believe that they are also able to provide patients with good instructions for their daily activities.

Previous studies have extensively reported the numerous aspects related to competent and trained employees, such as better safety and health knowledge, skills and experiences (Chang et al., 2012). Additionally, educated and well trained employees tend to discuss safety issues with co-workers more frequently. They also have a better work process across time and better communication and information flow; in addition, they are good in coordinating problems (Horwitz et al., 2009). Another study (Koohi et al., 2013) has demonstrated that trained employees are more committed to organizations and more interested to become involved in the activities beyond their common and pre-determined duties. Our study confirms these previous findings.

In addition, our study showed that training programmes for professional caregivers and nurses should include more extensive knowledge about the general scope of the healthcare system to support competent advice in patients' social, rehabilitation and health services. In addition, more effective training is required how to provide adequate help in emergency situations.

Based on the results of our study, it is required to integrate human factors in safety management of nursing homes with a special focus on adequate safety training and development of necessary skills and knowledge of workers. We also emphasize the need to include the topic of patient safety and worker ergonomics into the national occupational standard as well as in vocational training programs/curriculum. Resulting from our study, we stress the importance of in-service trainings about specific occupational safety issues (e.g., how to use special equipment ergonomically). This would enhance employees' ability to cope successfully with the elderly and people with special needs, to provide safe and high-quality care, to stay confident and to manage conflicts in order to keep good relationships at work.

CONCLUSIONS

The results of our study prove that workers' knowledge, skills and beliefs are essential components for safety and quality in patient care. Resulting from the survey, we can conclude that employees with higher awareness of their professional competence have also higher estimations about their skills and knowledge for coping with the elderly and people with special needs. Respondents who highly estimate their knowledge and skills in living quests and patient care, skills and knowledge for coping with the elderly and people with special needs are also more confident and prepared to provide emergency first aid. We also found that respondents with higher estimation of their professional knowledge are more confident in communication and are able to solve work-related conflicts.

Our results reveal that caregivers and nurses who have high estimation of their skills and knowledge are more committed to safety. We found that respondents who have sufficient knowledge and skills required for their work are more likely to participate in health and safety activities, to discuss topics about occupational safety with co-workers as well as with management. Care givers and nurses who participated in our study emphasized the importance of management commitment to safety in order to be confident to discuss safety problems, suggest safety measures and improvement of working environment. Complementing the national standard with recommended issues (to include safety topic into the curriculum and organize the in-service training) will allow improvement of safety knowledge among caregivers and nurses and will demonstrate that patients' and occupational safety is a priority in all duties in healthcare. We suggest that HFE should be integrated into the in-service training activities in order to enhance safety performance and quality of patient care.

ACKNOWLEDGEMENTS. The acknowledgements should include all people and institutions that have helped to achieve the goals of the research but have not been mentioned as authors.

Funding

This research received funding by Tallinn Health Care College (project Proactive safety management in health care no 1-16/61) in cooperation with Tallinn University of Technology.

REFERENCES

Ahanchian, M.R, Emami Zeydi, A. & Armat, M.R. 2015. Conflict management styles among Iranian critical care nursing staff: a cross-sectional study. *Dimensions of Critical Care Nursing* **34**(3), 140–145. doi. 10.1097/DCC.0000000000000106

Akroyd, D., Jackowski, M.B. & Legg, J.S. 2007. Factors affecting radiographers' organizational commitment. *Radiologic Technology* **78**, 467–475. PMID: 17626229

Al-Ahmadi, T.A. 2009. Measuring Patient Safety Culture in Riyadh's Hospitals: A Comparison between Public and Private Hospitals. *Journal of The Egyptian Public Health Association* **84**(5–6), 479–500.

Alswat, K., Abdalla, R.A.M., Titi, M.A., Bakash, M., Mehmood, F., Zubairi, B., Jamal, D. & El-Jardali, F. 2017. Improving patient safety culture in Saudi Arabia (2012–2015): trending, improvement and benchmarking. *BMC Health Services Research* **17**(1), 516. doi. 10.1186/s12913-017-2461-3

Axley, L. 2008. Competency: A concept analysis. *Nursing Forum* **43**(4), 214–222.

Blair, E.H. 2004. Critical competencies for SH & E Managers – Implications for educators. *Journal of Safety, Health and Environmental Research* **1**(1), 1–13.

Carayon, P. 2006 Human factors of complex sociotechnical systems. *Applied Ergonomics* **37**(4), 525–534.

Carayon, P. 2010. Human Factors in Patient Safety as an Innovation. *Applied Ergonomics* **41**(5), 657–665.

Chan, J.C.Y., Sit, E.N.M. & Lau, W.M. 2014. Conflict management styles, emotional intelligence and implicit theories of personality of nursing students: a cross-sectional study. *Nurse Education Today* **34**(6), 934–939. doi. 10.1016/j.nedt. 2013.10.012

Chang, S.-H., Chen, D.-F. & Wu., T.-C. 2012. Developing a competency model for safety professionals: Correlations between competency and safety functions. *Journal of Safety Research* **43**, 339–350.

Christian, M.S., Bradley, J.C., Wallace, J.C. & Burke, M.J. 2009. Workplace safety: A meta-analysis of the roles of person and situation factors. *Journal of Applied Psychology* **94**(5), 1103–1127.

DeJoy, D.M., Smith, T.D., Woldu, H., Dyal, M.A., Steege, A.L. & Boiano, J.M. 2017. Effects of organizational safety practices and perceived safety climate on PPE usage, engineering controls, and adverse events involving liquid antineoplastic drugs among nurses. *Journal of Occupational and Environmental Hygiene* **14**(7), 485–493. doi. 10.1080/15459624.2017.1285496

Dul, J.R., Bruder, P., Buckle, P., Carayon, P., Falzon, W.S., Marras, J.R., Wilson, B. & van der Doelen. 2012. A Strategy for Human Factors/Ergonomics: Developing the Discipline and Profession. *Ergonomics* **55**(4), 377–395.

Epstein, R.M. & Hundert, E.M. 2002. Defining and assessing professional competence. *Jama* **287**, 226–235.

Farokhzadian, J., Khajouei, R. & Ahmadian, L. 2015. Information seeking and retrieval skills of nurses: Nurses readiness for evidence based practice in hospitals of a medical university in Iran. *International Journal of medical informatics* **84**, 570–577. https://doi.org/10.1016/j.ijmedinf.2015.03.008 PMID: 25936728

Freimann, T. & Merisalu, E. 2015. Work-related psychosocial risk factors and mental health problems amongst nurses at a university hospital in Estonia: A cross-sectional study. *Scandinavian Journal of Public Health* **43**(5), 447–452.

Goodman, G.R. 2010. A Fragmented Patients Safety Concept: The Structure and Culture of Safety Management in Healthcare. *Hospital Topics* **81**(2), 22–29. https://doi.org/10.1080/00185860309598018

Grau, R., Martínez, I.M., Agut, S. & Salanova, M. 2002. Safety attitudes and their relationship to safety training and generalised self-efficacy. *International Journal of Occupational Safety and Ergonomics* **8**(1), 23–35.

Griffin, M.A. & Hu, X. 2013. How leaders differentially motivate safety compliance and safety participation: the role of monitoring, inspiring and learning. *Safety Science* **60**, 196–202.

Gurses, A., Carayon, P. & Wall, M. 2009. Impact of Performance Obstacles on Intensive Care Nurses Workload, Perceive Quality and Safety of Care, and Quality of Working Life. *Health Services Research* **44**(2), 422–443.

Gutberg, J. & Berta, W. 2017. Understanding middle managers' influence in implementing patients safety culture. *BMC Health Service Research* **17**, 582. doi: 10.1186/s12913-017-2533-4

Hadjimanolis, A. & Boustras, G. 2013. Health and safety policies and work attitudes in Cypriot companies. *Safety Science* **52**, 50–56.

Han, K.-S. & Chung, K.-H. 2015. Positive Psychological Capital, Organizational Commitment and Job Stress of Nurses in Small and Medium-Sized Hospitals. *Advanced Science and Technology Letters* **88**, 208–211.

Heydari, A., Kareshki, H. & Armat, M.R. 2016. Is Nurses' Professional Competence Related to Their Personality and Emotional Intelligence? A Cross-Sectional Study. *Journal of Caring Sciences* **5**, 121–132. https://doi.org/10.15171/jcs.2016.013 PMID: 27354976

Hignett, S. 2003. Hospital Ergonomics: A Qualitative Study to Explore the Organisational and Cultural Factors. *Ergonomics* **46**(9), 882–903.

Hignett, S., Carayon, P., Buckle, P. & Catchpole, K. 2013. State of science: human factors and ergonomics in healthcare. *Ergonomics* **56**(10), 1491–1503. doi. 10.1080/00140139.2013.822932

Horwitz, L.I., Meredith, T., Schuur, J.D., San, N.R., Kulkarni, R.G. & Jeng, G.Y. 2009. Dropping the baton: A qualitative analysis of failures during the transition from emergency departments to inpatient care. *Annals of Emergency Medicine* **53**, 701–710.

Karami, A., Farokhzadian, J. & Foroughameri, G. 2017. Nurses' professional competency and organizational commitment: Is it important for human resource management? *PLoS ONE* **12**(11), e0187863. https://doi.org/10.1371/journal.pone.0187863

Koohi, R.Z., Tol, A., Akbari, H.F., Rahimi, F. & Pourreza, A. 2013. Assessing the Relation Between Organizational Climate Components with Organizational Commitment Components among Nurses in Selected Hospitals of TUMS. *Journal of Health Research* **9**, 731–740. http://hsr.mui.ac.ir/ index.php/jhsr/article/view/982.

Lakanmaa, R-T., Suominen, T., Ritmala-Castrén, M., Vahlberg, T. & Leino-Kilpi, H. 2015. Basic Competence of Intensive Care Unit Nurses: Cross-Sectional Survey Study. *BioMed Research International.* http://dx.doi.org/10.1155/2015/536724

Levett-Jones, T., Gersbach, J., Arthur, C. & Roche, J. 2011. Implementing a clinical competency assessment model that promotes critical reflection and ensures nursing graduates' readiness for professional practice. *Nurse Education in Practice* **11**, 64–69. https://doi.org/10.1016/j.nepr.2010.07.004 PMID:20727825

Moray, N. 2000. Culture, politics and ergonomics. *Ergonomics* **43**, 868–868.

Nilsson, J., Johansson, E., Egmar, A.-C., Florin, J., Leksell, J. & Lepp, M. 2014. Development and validation of a new tool measuring nurses self-reported professional competence-The nurse professional competence (NPC) Scale. *Nurse Education Today* **34**(4), 574–580. doi. 10.1016/j.nedt.2013.07.016

Orpen, C. 1993. The effect of time-management training on employee attitude and behaviour: A field experiment. *Journal of Psychology* **128**(4), 393–396.

Rajabipour, A.R. & Dehghani, M. 2013. The relationship between Islamic work ethic and organizational commitment, and job satisfaction. *Journal of Bioethics* **2**, 49–92.

Ratnapalan, S. & Uleryk, E. 2014. Organizational Learning in Health Care Organizations. *System* **2**, 24–33.

Salonen, K. 2009. Home care for older people. Good Practices and Education in six European Countries. EQUIP Project 2007–2009. In: Salonen K, editor. Good practices in home care services in Finland. Tampere: Tampereen Yliopistopaino – Juvenes Print Oy.

Sepp, J., Järvis, M., Tint, P., Siirak, V. & Reinhold, K. 2015. EMG measurements of thumb muscles of nurses and caregivers. *Agronomy Research* **13**(3), 836–845.

Steginga, S.K., Dunn, J., Dewar, A.M., McCarthy, A., Yates, P. & Beadle, G. 2005. Impact of an Intensive Nursing Education Course on Nurses’ Knowledge, Confidence, Attitudes, and Perceived Skills in the Care of Patients With Cancer. *Oncology Nursing Forum* **32**(4), 375–381.

United States Department of Health and Human Services (USDHHS). An Aging U.S. Population and the Health Care Workforce: Factors Affecting the Need for Geriatric Care Workers. Centre for California Health Workforce Studies, University of Chicago; 2006. Retrieved from http://www.raconline.org/ publications/documents/442 Accessed 4 May 2014.

Valdez, R.S., McGuire, K.M. & Rivera, J. 2017. Qualitative ergonomics/human factors research in health care: Current state and future directions. *Applied Ergonomics* **62**, 43–71.

Agronomy Research **16**(4), 1877–1884, 2018
https://doi.org/10.15159/AR.18.165

Additional concentrates do not affect feeding times of cows, but social positions of cows do

M. Soonberg[1,*], M. Kass[1], T. Kaart[2], R. Leming[1] and D.R. Arney[1]

[1]Estonian University of Life Sciences, Department of Animal Nutrition, Fr. R. Kreutzwaldi 46, EE51006 Tartu, Estonia
[2]Estonian University of Life Sciences, Department of Animal Breeding and Biotechnology, Fr. R. Kreutzwaldi 46, EE51006 Tartu, Estonia
[*]Correspondence: maria.soonberg@student.emu.ee

Abstract. In robotic milking dairy systems lack of control over intakes can be problematic for balancing the forage and concentrate portions of diets. This can lead to problems associated with high concentrate intakes and concomitant low forage intakes. To check this as a problem, the feeding behaviour of cows was observed: the number of daily visits to the feed barrier, the duration of these visits and actual feeding, of high and low yielding cows. The cows were robot-milked and fed a ration comprising, separately, concentrate feed from a robot and a feeder, and a grass/clover silage mix forage at the feed barrier. Individual variation in visiting times and times spent at the feed barrier were greater than the effect of level of production. There was no evidence that cows with higher milk yields are differentially motivated to feed from forage. But more dominant cows spent more time feeding than submissive cows.

Key words: behaviour, concentrate feeding, robotic milking, dairy cow.

INTRODUCTION

On dairy farms concentrates are given to cows to increase feed intakes and milk production (Ivemeyer et al., 2014). Concentrate feeding is particularly important in the first weeks immediately after calving when cows go through a period of negative energy balance (Ferris et al., 2003). Currently, concentrate feeding levels in dairy cows' rations are increasing, but so are concentrates' prices, which means they should be used efficiently by producers (Finneran et al., 2012).

There are a wide range of concentrate feeding methods that can be used on farms. Farmers can mix together concentrate with the forage components into a single feed, offer the concentrate portion separately from the forage or combine these two approaches. Whenever the farmer decides to feed concentrates separately from forage there are at least two strategies for this. One option takes account of individual cows' milk yields, and includes the concentrate portion as amounts appropriate to the yield. The second option is to feed the concentrate at a flat rate, which does not take into account the needs of each individual cow (Purcell et al., 2016).

High yielding cows require high levels of concentrate feeds to achieve their maximum potential milk production. Grouping cows based on lactation stage can reduce the problem of differential concentrate feeding requirements in the herd, but farmers must be cautious not to underfeed or overfeed the cows (Mäntysaari et al., 2004). When farmers are not able to group cows by keeping them in different pens, and offering different feed rations in the different pens, one option could be the use of feeding bins, where it is possible to group cows by allowing them to feed from different bins, with different proportions of concentrates to forage, depending on their milk yield. Access to each bin is permitted through cow recognition by a transponder. This means that cows with higher milk yields should receive more concentrates to support their higher production. A second option is to have a feeding barrier and separate concentrate feeding bins where cows receive the concentrate portion of their ration which, as in the previous option, depends on their milk yield and days in milk. Both options require cows to have ID collars fitted with transponders around their necks.

The use of feed bins and individual access by cows is not a perfect solution, as cows can still access the 'wrong' feed bins (Soonberg & Arney, 2014), with highly motivated but lower yielding cows accessing the higher value ration, leading to overcondition in those cows. In addition, where cows are offered concentrates separately from forage, the cows offered higher amounts of concentrates may have a reduced appetite for, and therefore reduced intakes of, forage. This imbalance between concentrate and fibre intakes could have negative effects on degradability, digestion, volatile fatty acid absorption and consequent milk composition and quality. This experiment was designed primarily to investigate whether there is evidence in practice of reduced intakes of forage in the cows which receive the forage and concentrate portions of their diet separately.

If cows are frustrated from satisfying their nutritional needs, or in their motivation to feed, it might be expected that this would be a cause of distress and affect their behaviour. This might affect, in particular, their feeding behaviours and social behaviours (both social and antagonistic behaviours). If therefore cows are identified as having different feeding and social behaviours at different production levels this would suggest an impairment in their level of well-being, and possibly indicate the need for a change in their feeding regime. Feeding behaviour could also be used to estimate the actual intakes and motivation to feed of individual cows.

Our hypothesis for this study was that cows who receive extra concentrate would spend less time feeding on forage when both portions of the ration are offered separately. It was further hypothesised that observation of feeding and social behaviour of dairy cows in a herd could be useful indicators of intakes of dietary rations.

MATERIALS AND METHODS

The study was carried out on the Estonian University of Life Sciences' experimental farm in Märja, Tartumaa, Southern Estonia. Estonia (57°30′ and 59°50′) is in Northern-Europe where dairy cows are mostly kept indoors, either overwinter or all year round.

The university farm houses around 250 cows, including dry cows and youngstock, under a zero grazed system. There are approximately 120 lactating cows at any one time. The lactating cows are divided into two groups. Cows in the first group are milked in a milking parlour and fed a total mixed ration (TMR) from individual feeding bins. Cows in the second group are milked with a forced traffic robotic milking system (DeLaval, 2007). Sample cows were selected from the second group.

The study was run in accordance with the Animal Protection Act of the Republic of Estonia.

Animals and diets

Eight multiparous Estonian Holstein cows (194 + 143.8 days in milk, 30 kg average milk yield, SD 13.1 kg) were selected for the sample group based on the amount of concentrates they received in their diets. Individuals were chosen at random from each of the selected concentrate level dietary groups. The trial was carried out in two groups, each group receiving different amounts of additional concentrate. Four of the sample cows received two or four kg of concentrate feed per day (supplemental concentrate values which were according to the extant practice on the farm and which were according to milk yields), and four cows (control) received no additional concentrate feed from the concentrate feeder. All of the cows were fed a partially mixed ration *ad libitum* and water was freely available at all times from self-filling bowls. The partially mixed ration consisted of a grass and clover silage (63%), and the compound feed was comprised of barley (31%) and rapeseed cake (5%) plus minerals (1%). Additional concentrate was offered at the milking robot, and also from two separate concentrate feed bins, delivered in amounts according to each cow's individual milk yields, to a maximum of half their daily portion per visit.

Forage was provided at a post-and-rail feed barrier three times a day, sufficient to ensure availability of forage was *ad libitum*. Cows were loose housed in an uninsulated building in cubicles (Fig. 1) covered with rubber mattresses. Every day a mixture of peat and sawdust was laid in thin layers on each of the mattresses for additional comfort and to help keep them dry and clean. A mechanical brush (DeLaval, Sweden) was attached to a post in the feeding area where cows could brush themselves. The cows were milked with a milking robot (DeLaval, Sweden), to which the cows had access 24-hours per day.

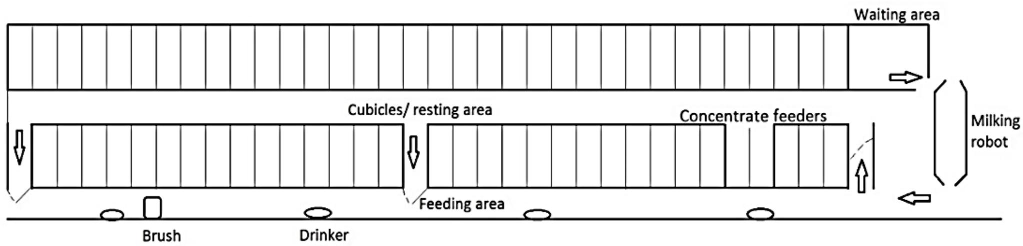

Figure 1. Plan of the housing of the trial cows ('⇒' means movement of cows; '---' indicates one-way gate).

Data collection

Behaviours at the forage feeding area were recorded for three cows in the summer and five in the autumn and winter. Individuals from both groups were presented in both seasons. There were no seasonal differences, average temperature was 9.4 °C with standard deviation of 8.3 °C. Cows behaviour was recorded with video equipment (Sony HDR-PJ580VE, Japan) from an overhead gantry, which was situated directly above the feeding area. Cows were observed such that each cow was observed over 24 hours. Video recordings were analysed by one trained observer playing them back with a

PowerDVD 12. Recordings were made of the starting and ending times of each bout of behaviour. The behavioural parameters recorded were: the time taken by the cows to feed (from the moment of the first apprehension of feed to the moment of the last bite), periods of time spent standing, walking, drinking, grooming (this included the sum of the periods of the time spent allogrooming, being groomed by another and selfgrooming with a mechanical brush). Antagonistic behaviours were also recorded, these included pushing, nudging and intimidating another cow. Pushing was recorded when one cow displaced another cow away from its original position. Nudging meant the aggressor pushed, but did not displace the other cow. Intimidating was recorded when an aggressor cow went close to another cow as if she would start pushing her away but there was no physical contact. When analysing agonistic behaviour, nudging and intimidating data were summed together with the pushing data to form a single antagonistic group of behaviours.

Statistical analyses

Statistical analyses were performed with Microsoft Excel (*t-test* and *F-test*) and with R 3.2.3. Differences between the two groups, were analysed with the *t-test*. Where data were not normally distributed, and could not be normalised by logarithmic transformation, the non-parametric Wilcoxon test was used to identify group differences. A correlation matrix was prepared using the Spearman Correlation coefficients to study the relationships between study variables.

RESULTS AND DISCUSSION

From video recordings, cows receiving no extra concentrate feed had a mean time of feeding of 4 h 40 minutes, walking 17 minutes, standing 1 h 18 minutes and drinking 14 minutes per day. Cows receiving extra concentrate feed fed for 5 h 58 minutes, walked for 24 minutes, stood for 1 h 39 minutes and drank for 11 minutes.

There were no significant differences when comparing the two groups regarding the behaviours observed. However, the cows who received extra concentrate spent more time standing (but not feeding) in the feeding area. Unlike the findings of Nielsen et al., (2010), who reported that cows receiving high concentrate feed fed for a longer period, there was no significant effect of this. More time spent standing in the feeding area might suggest this was so, but it is not evidence for a greater intake of feed, or even a greater time spent feeding itself (Soonberg & Arney, 2014).

From the correlation analyses (Fig. 2), there was a strong correlation between the agonistic behaviour of being pushed away by another cow and standing ($r = 0.889$, $P = 0.004$). Those cows that were pushed away by other cows, spent more of their time standing. It is assumed that the dominant cows were more likely to actively move and find better spots to feed, and push away submissive cows from the feeding barrier. Aggression in dairy cows has been found to be correlated with levels of androgens, and these are both higher in more socially dominant individuals (Bouissou, 1983), a finding confirmed by Phillips & Rind (2001) who identified higher rates of both aggression and allogrooming in socially dominant cows. Submissive cows had less time available for feeding than more dominant cows which indicates that social position may be a factor affecting the feeding times of cows. Such activities can be dependent on time of day and the daily programme of events. DeVries et al. (2004) found that there are more incidents of antagonistic behaviour between cows after milking, while Val-Laillet et al. (2008) showed the greatest displacement of one cow by another at the feed barrier when fresh feed was delivered. So the observation of, and conclusions about, these behaviours should be considered with regard to the time of day of observations.

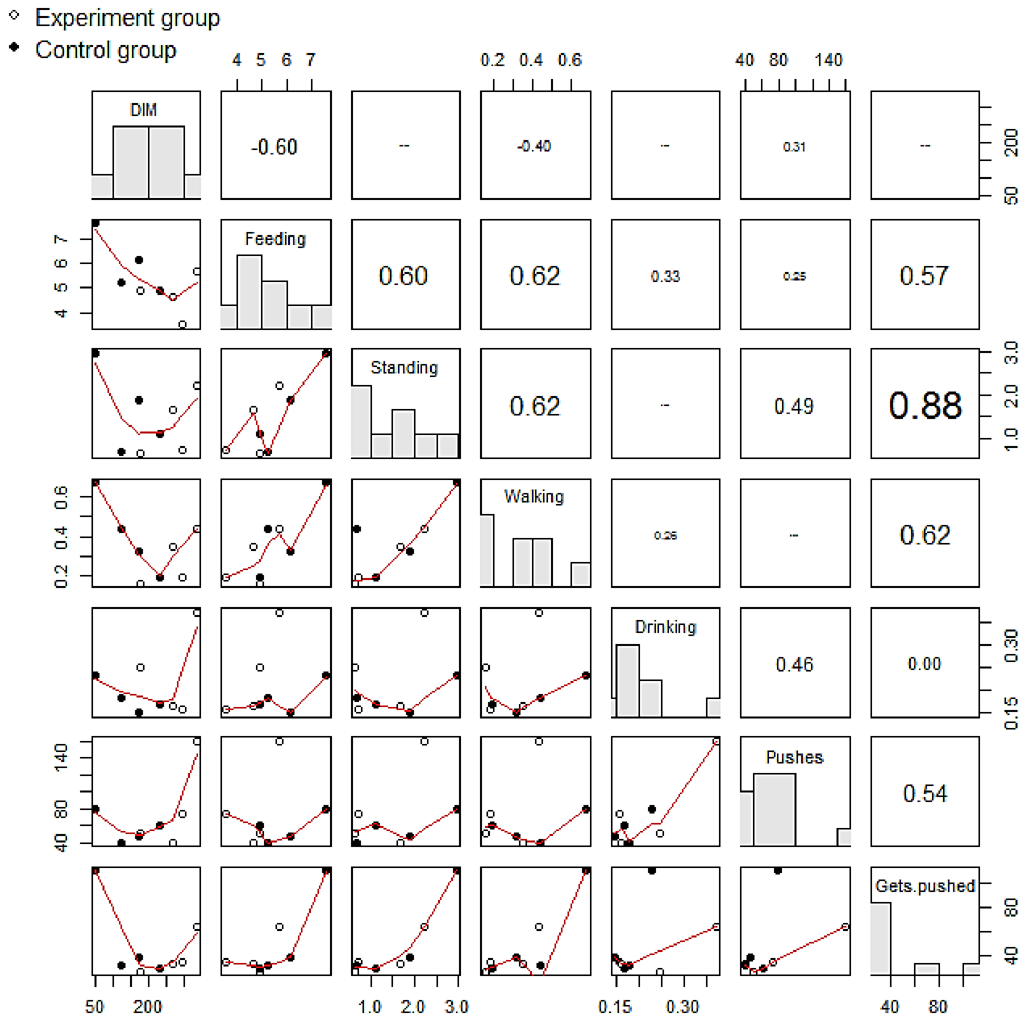

Figure 2. Spearman correlation coefficients of observed behavioural parameters in cows.
In diagonal: distribution of days in milk (DIM), duration of feeding, standing, walking and drinking (hours), and number of pushes and getting pushed per cow in 24 hours; below diagonal: pairwise scatterplots with white and black dots marking the single cows from experiment and control group, respectively, and smoothed red line showing the potential relationship; above diagonal: Spearman correlation coefficients (bigger font corresponds to stronger relationship; only r = 0.88 was statistically significant, p = 0.004*).

There were no significant differences between those cows who received and those cows who did not receive concentrate feed from the concentrate feeder regarding the times spent on each of the behaviours recorded (Table 1).

Table 1. Behavioural observations of cows in the two experimental groups in a 24- hour period. Average (standard deviation), duration of feeding, standing, walking and drinking (hours), and number of pushes and getting pushed per cow in 24 hours in experiment and control group; p-values shows the statistical significance of difference between groups according to Wilcoxon test

Parameters	Group		Standard deviation		P-value
	Control	Experimental	Control	Experimental	
Feeding time, h	5.98	4.68	1.23	0.90	0.200
Standing	1.65	1.31	1.00	0.76	0.686
Walking	0.41	0.28	0.21	0.13	0.343
Drinking	1.18	0.23	0.04	0.10	0.686
Pushes[1]	56.8	81.0	17.2	54.4	0.772
Gets pushed[1]	52.3	39.3	39.4	16.9	0.886

[1] no of incidences.

Neither the feeding time, walking time, nor standing and drinking were affected by additional concentrate feeding between the two groups. Times spent feeding were not different between the groups. There is therefore no evidence that offering additional concentrates separately from the forage had any effect on reducing, or indeed increasing, feeding times of cows.

The individual cow variation was greater than the variation between groups. This may well have been an artefact related to the lactation numbers of the selected cows, which varied from the second to the fourth lactation. In this study, the cows who received concentrate feed were in early to mid-lactation, which would be expected to have a feed consumption higher than those cows in late lactation (Chaplin & Munksgaard, 2001; Nielsen et al., 2010). This agrees with our findings, as the days in milk and time spent feeding were negatively correlated.

Lawrence et al. (2015) investigated total dry matter intakes on high and low concentrate level and found high concentrate cows to have higher total dry matter intake than cows who received less concentrate, but base feed mix intake was not affected by the concentrate amount. The same result could be hypothesised in this study although in a previous study the time that cows feed over a 24- hour period was recorded, which was used to estimate the amounts of feed removed from feed bins over the same period, and no correlation between these two factors was observed (Soonberg & Arney, 2014). Therefore, it was assumed that estimating intakes from time spent feeding is an unreliable measure.

For a cow it is essential to be able to sleep for four hours a day and drowse for around eight hours (Ternman et al., 2012). Submissive cows can remain longer in the feeding area waiting for an opportunity to feed and looking for a free place at the feed barrier where they can feed without disturbance. This may mean that they either consume feed more rapidly while at the feed barrier or feed at times that are not determined by their own motivation to feed but only when they can secure access to feed. This time spent waiting to feed furthermore leaves them less time to rest, which is needed for adequate metabolic system and immune function (Ternman et al., 2012), and lying down is an activity which it is known that dairy cows are highly motivated to do (Munksgaard & Simonsen 1996; Cooper et al., 2007). This deprivation of lying time can leave the cows at a higher risk of poor welfare, associated distress and can lead to problems with individual cows' health.

For the successful farmer, it is important and profitable to consider the accessibility of feed to all of the cows in his herd, including those cows that are submissive. Therefore, more attention should be paid to optimizing the accessibility of feed to submissive cows as well as the herd average cow.

There was no evidence from this study that cows that are given extra concentrate feed separately from forage in their diet spend less time feeding on forage than cows that are not given concentrate. This does not necessarily imply or indicate that they have the same intakes of forage. Additionally, there may have been an effect if the concentrate offered had been of a larger amount than the maximum offered here.

Antagonistic behaviours between cows increased when feed was delivered. Submissive cows spent a longer time in the feeding area than more dominant cows, and received more antagonistic behaviour (pushing, nudging) towards themselves than more dominant cows.

CONCLUSION

This study provides no evidence that cows receiving extra concentrate spend less time feeding on forage when both portions of the ration are offered separately. There was a strong correlation between the agonistic behaviour of being pushed away by another cow and standing, suggesting that submissive cows are prevented from feeding when and for how long as they wish.

The main limiting factors of the study were the relatively small number and large variability of cows. This could have been the reason why almost no differences were discovered between groups. However, several behaviour patterns are clear enough to make general conclusions.

ACKNOWLEDGEMENTS. This study was supported by the Estonian Ministry of Education and Research (institutional research grant IUT 8-1, Fertility and Health in Dairy Cattle).

REFERENCES

Bouissou, M.-F. 1983. Androgens, Aggressive Behaviour and Social Relationships in Higher Mammals. *Hormone Research* **18**, 43–61.

Chaplin, S. & Munksgaard, L. 2001. Evaluation of a simple method for assessment of rising behaviour in tethered dairy cows. *Animal Science* **72**, 191–197.

Cooper, M.D., Arney, D.R. & Phillips, C.J. 2007. Two- or four- hour lying deprivation on the behaviour of lactating dairy cows. *Journal of Dairy Science* **90**, 1149–1158.

DeVries, T.J., von Keyserlingk, M.A.G. & Weary, D.M. 2004. Effect of feeding space on the inter-cow distance, aggression, and feeding behaviour of free-stall housed lactating dairy cows. *Journal of Dairy Science* **87**, 1432–1438.

Ferris, C.P., Gordon, F.J., Patterson, D.C., Mayne, C.S. & McCoy, M.A. 2003. A short-term comparison of the performance of four grassland-based systems of milk production for autumn-calving dairy cows. *Grass and Forage Science* **58**, 192–209.

Finneran, E., Crosson, P., O'Kiely, P., Shalloo, L., Forristal, D. & Wallace, M. 2012. Stochastic simulation of the cost of home-produced feeds for ruminant livestock systems. *The Journal of Agricultural Sciences* **150**, 123–139.

Ivemeyer, S., Walkenhorst, M., Holinger, M., Maeschli, A., Klocke, P., Spengler Neff, A., Staehli, P., Krieger, M. & Notz, C. 2014. Changes in heard health, fertility and production under roughage based feeding conditions with reduced concentrate input in Swiss organic dairy herds. *Livestock Science* **168**, 159–167.

Lawrence, D.C., O'Donovan, M.O., Boland, T.M., Lewis, E. & Kennedy, E. 2015. The effect of concentrate feeding amount and feeding strategy on milk production, dry matter intake, and energy partitioning of autumn-calving Holstein-Friesian cows. *Journal of Dairy Science* **98**, 338–348.

Munksgaard, L. & Simonsen, H. 1996. Behavioural and pituitary- adrenal axis responses of dairy cows to social isolation and deprivation of lying down. *Journal of Animal Science* **74**, 769–778.

Mäntysaari, P., Huhtanen, P., Nousiainen, J. & Virkki, M. 2004. The effect of concentrate crude protein content and feeding strategy of total mixed ration on performance of primiparous dairy cows. *Livestock Production Science* **85**, 223–233.

Nielsen, B.L., Veerkamp, R.F. & Lawrence, A.B. 2010. Effects of genotype, feed type and lactational stage on the time budget of dairy cows. *Acta Agriculturae Scandinavica, Section A- Animal Science* **50**, 272–278.

Phillips, C.J.C. & Rind, M.I. 2001. The Effects on Production and Behavior of Mixing Uniparous and Multiparous Cows. *Journal of Dairy Science* **84**, 2424–2429.

Purcell, P.J., Law, R.A., Gordon, A.W., McGettrick, S.A. & Ferris, C.P. 2016. Effects of concentrate feeding method on the performance of dairy cows in early to mid-lactation. *Journal of Dairy Science* **99**, 2811–2824.

Soonberg, M. & Arney, D.R. 2014. Dairy cow behaviour at individual feeding bins, can we estimate intakes from behavioural observations? *Research for Rural Development, conference* proceedings **1**, 114–117.

Ternman, E., Hänninen, L., Pastell, M., Agenäs, S. & Peetz Nielsen, P. 2012. Sleep in dairy cows recorded with a non-invasive EEG technique. *Applied Animal Behaviour Science* **140**, 25–32.

Val-Laillet, D., de Passille, A.M., Rushen, J. & von Keyserlingk, M.A.G. 2008. The concept of social dominance and the social distribution of feeding-related displacements between cows. *Applied Animal Behaviour Science* **111**, 158–172.

Agronomy Research **16**(4), 1885–1895, 2018
https://doi.org/10.15159/AR.18.155

Modelling of operator's focusing scheme along working hours: Windrowing and cultivating operations

I. Szabó, M. Hushki, Z. Bártfai, A. Lágymányosi and L. Kátai*

Szent István University, Faculty of Mechanical Engineering, Institute of Mechanics and Machinery, Páter K. street 1, HU2100 Gödöllő, Hungary
*Correspondence: katai.laszlo@gek.szie.hu

Abstract. Enhancing productivity and cost reduction are two main targets for any production operation. In the agricultural field; It is the role of researchers to come out with reliable models and make it available to be used in modern farming management organizations as well as to the rural farmers. When it comes to the Human Machine Interface it is essential to assess the system in term of the Human Cantered Design aspects. This research is focusing on the developing simple models for the operator's focusing scheme as a human behaviour inside an off-road vehicle cabin based on the operator's focusing scheme measuring along working hours using proven and up to date technologies. The results of this research provide the decision makers with reliable inputs using proven methodology regarding the change of operator's focusing scheme along working hours in two agricultural operations 'windrowing and cultivating'. Both operations are requiring continuous physical involvement of the operator for checking the attached tool and steering of the vehicle in the planned track, which is directly related to the accumulated passive fatigue as a main contributor of resulted data.

Key words: off-road vehicle, operator's behaviour, eye tracking, focusing scheme, passive fatigue, precision farming.

INTRODUCTION

In continuation of the research work done by (Szabo et al., 2017) regarding Operator's behaviour measuring methodology inside off-road vehicle cabin, this research activities depend on the validated methodology to develop a model representing the change on the resulted operator's focusing scheme along working hours in windrowing and cultivating agricultural operations.

The resulted models from this research are developed to assist the decision-making activity during the planning phase (Man-power, operational procedures, …etc.), which is usually done based on managerial assumptions in the absence of trusted models coming from research and development centres and/or academic sector. (Herdon, 2013) mentioned a very important role of the academic sector improving the development of agricultural operations by problem resolving and developing the recommendations based on the advanced analysis of data to be used in advanced farming processes easily. Therefore; the availability of such models with provide decision makers by a factual based method coming from deterministic data analysis.

Robert (2004) and Xuan (2007) showed that it is essential for the research activities to concentrate on making the necessary studies regarding the resources management to reach the precision farming concept. In this research, one of the targets is to develop dedicated models to different agricultural operations showing the impact of working hours on the accumulated mental and passive physical load. Which might be used directly by rural farming organization as an indicator of the required effort difference between different agricultural operations.

Due to the operational nature of multi-tasking off-road vehicles, operators need to spend long working hours; which increases the level of mental workload leading to human error. Li & Haslegrave (1999) introduced similar conclusion of which the vehicle design should be human oriented in order to maximize comfort and ability to perform the driving task perfectly and safely by reducing the human error possibilities'. Nowadays more and more agricultural machines are equipped with continuous measurement sensors e.g. measurement of soil resistance (Kroulik et al., 2015) to have more exact information on energy demand in order to contribute to the optimization of the production formula during performing his/her duties (i.e. the direction of windrowing based on soil properties). This means that the driver attention is split by many signals.

Operating an off-road vehicle is a complex task, requiring a concurrent execution of various cognitive, physical, sensory and psychomotor skills (Young & Regan, 2007), additionally to control attached tools to perform in-field productive tasks such as agricultural and industrial operations. Ensuring the comfortable ride is considered essential for any vehicle, as well as executing happily and safely requested operational tasks, to that end; the driver ergonomics comes to play as considered as an important parameter that can't be neglected in the design phase of the vehicle (Hsiao et al., 2005).

Tractors are companions for many agriculture workers. Well-designed human – tractor interfaces, such as well-accommodated tractor operator enclosures can enhance operations productivity, comfort and safety (Matthews, 1977; Kaminaka et al., 1985; Liljedahl et al., 1996 and Hsiao et al., 2005).

Many studies have been carried on finding preferred locations of in certain types of tractor controls (Casey & Kiso, 1990), moreover; emphasizing how critical is the placement of controls in some tractors stating that; it creates an impediment to body movement (Hsiao et al., 2005).

When we are talking about automation, it is a general aim to improve comfort and safety (Sheridan, 1992; Endsley, 1996; Fukunaga et al., 1997; Scheding et al., 1999; Shen & Neyens, 2017; Zewdie & Kic, 2017), additionally, it is stated that, in the automated driving condition, driver responses to the safety critical events were slower, especially when engaged in a non-driving task. At the same time in their paper – dealing with driver visual attention (Louw & Merat, 2017) reached a conclusion shows that the drivers understanding of the automated system increases as time progressed, and that scenarios which encourage driver gaze towards the road centre are more likely to increase situation awareness during high levels of automation'.

Generating dependable and deterministic data representing human behaviours inside the workplace using validated method will be beneficial for enhancing current cabin designs as well as the future cabin designs.

Driving is not only a physical task but also visual and mental tasks. The eyes of a driver are indispensable in performing visual tasks such as scanning the road and monitoring in-vehicle devices. Mental tasks are important during driving, and include such factors as understanding vehicle dynamics, making situation-dependent decisions, and judging time/space relationships (Kramer, 1990; De Waard, 1996; Brookhuis & De Waard, 2010 and Marquart et al., 2015) were examined the eye-related measures of drivers' mental workload. The mental workload could be defined as the relation between demands resulted from various tasks to be performed on the operator and his ability to fulfil; with satisfactory; these demands. While (Sporrong et al., 1998) described the mentioned demands as multidimensional, as it involves tasks, operator and system demands together with other factors. Additionally; many studies showed that; the need for well fitted architectural space to the operator's dimensions is considered crucial. The mental workload level is found to be increasing with the time passing.

For the purpose of this research, we focus on passive fatigue. This type of fatigue is characterized by being the indirect product of the human driver's exertion of a set of tasks whose demands are low, monotonous or repetitive (Saxby et al., 2013). These rules out any sort of physical fatigue or mental active fatigue.

(Gonçalves & Bengler, 2015) conducted a study i claims that Highly Automated Driving (HAD) will be commercially available in a near feature, yet human factors issues like the influence of driver state can have a critical impact in the success of this driving paradigm for in road and field safety. It is very likely that Driver State Monitoring Systems (DSMS) will play a bigger role than they have played so far.

MATERIAL AND METHODS

Tobii equipment and software packages

Tobii Pro Glasses 2 is a wearable eye tracker with a wireless live view function for insights in any real-world environment. The ultra-lightweight, user-centric design encourages natural viewing behaviour and ease of use. The system captures data at 50 or 100 Hz. Pro Glasses 2 shows exactly what a person is looking at in real time while moving around in any real-world environment, giving researchers deep and objective insights into human behaviour. Complete unobtrusiveness and Tobii's proprietary 3D eye model technology combine to ensure researchers capture the most natural viewing behaviour and supreme data quality. Quick calibration and system-guided procedures reduce time in the field and make it easy for anyone to start using the system with very little training.

The Real-World Mapping tool integrates into the Pro Glasses Analyzer, streamlining the coding process and dramatically reducing the analysis time. It aggregates and maps data from eye tracking videos to snapshots, allowing immediate visualization of the quantified data or extracting statistics. The powerful post-analysis and visualization tools provide a full spectrum of qualitative and quantitative gaze data analysis and visualizations provides for log events, define areas of interest (AOIs) during the selected time of interest (TOI) from the total recording time, calculate statistics, create heat maps, and export data for further analysis in other software.

MATLAB curve fitting toolbox

The Curve Fitting Toolbox is used to provide the Model of the change on operator's focusing scheme along working hours for the samples collected from windrowing agricultural operation and will be used at later stages to create the models from the samples of the two agricultural operations (windrowing and cultivating).

Implementation steps

The experiment is to be conducted on 3 phases (Fig. 1):

Phase 1: in which the consistency and similarity of the used work field and timing of operations will be ensured. Which applies as well for the experimental execution procedure. Operators are tasked to conduct the same operational procedures along trials. A calibration process for the Tobii glasses 2 is conducted via its dedicated software Tobii glasses controller software. Each operator profile is stored in the software, the software and the equipment have the capability to keep on each operator's profile stored containing the name of the operator and the calibration records, and no recalibration is required to start the next experiment or to restart the recording during the same experiment in case of interruptions.

Phase 2: in which the execution of the experimental trials and data gathering are conducted. The operator is requested to wear special Eye-tracking Tobii glasses 2 providing the operators vision area and defining the point of focusing. Connected to the central station, the recording time is synchronized for all resulted video records.

According to the experiment execution procedure, several areas of interest will be added to matrix storing the representing scheme [M], each element in the matrix will store the accumulated time of operators' glances (gaze) to that area of interest [AM].

Phase 3: in which data analysis and discussion are conducted. The video records are studied and analysed by the research team to decide and document all none beneficial periods that includes abnormal behaviours or reactions to a random external inducer of the operators describing the reason of period exclusion.

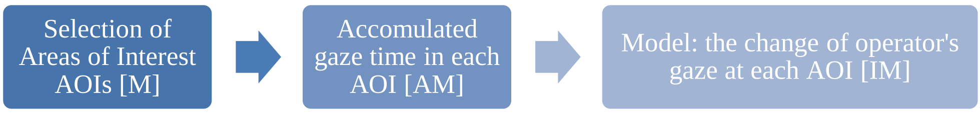

Figure 1. Generating the Change of Operator's focusing scheme along working hours.

Thereafter, the resulted data from the used eye-tracking glasses technology after exclusion procedure is represented in the matrix [AM].

Elements of [AM] are integrated at selected periods of working hours (i.e. at the end of each working hour or based on the nature of the operation) to produce the matrix [IM]k. where k is the selected period number from 1 to K times.

Along working hours, the change of [IM] with increment of k with increment of l will be placed on a graph showing the change of the operator's focusing scheme. Which is the target behaviour studied for each operator along several experimental trials.

Research methodology

To the purpose of this research, the followed methodology is summarized in process map showed in (Fig. 2).

The operator is mandated to wear Tobii glasses and to go through the calibration process whenever a new recording is started. The glasses are connected wirelessly to the windows tablet which is running the Tobii controller software to register the recording information, monitor the real-time view of the operator, conduct the calibration process and to stop, pause and start the recording process.

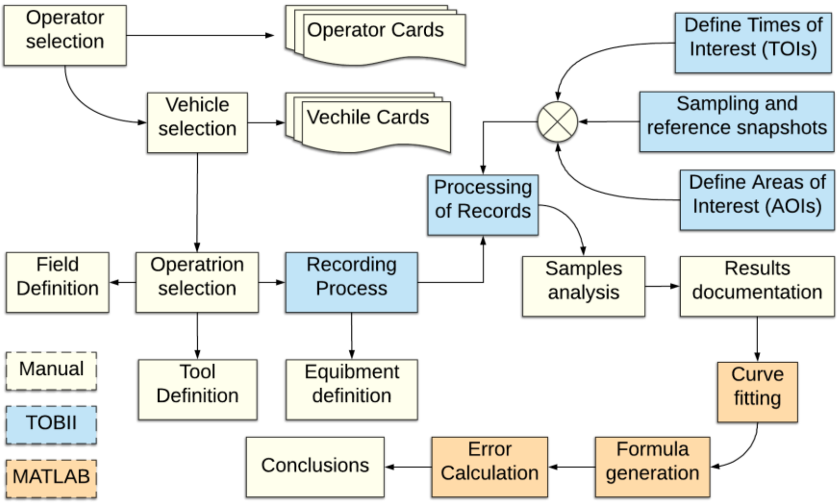

Figure 2. Methodology process map.

Thereafter, the collected video recordings are transferred to the PC which is running the Tobii pro lab software to be analysed using the real-time mapping and available filtering packages to obtain the accumulated times.

Windrowing operation

Windrowing agricultural operation is selected to be the studied operation in this research to produce the model of the change on operator's focusing scheme along working hours. After hay cutting in the agricultural field, windrowing operations are conducted to sort hay into lines in the field. The operation is conducted by specific tools attached to tractors generating hay lines to prepare for the hay baling operation. To the purpose of this research, the used attached tool to the CLAAS tractor (Model: ARES 567 ATZ) is CLAAS LINER 450T (Fig. 3).

Figure 3. CLAAS LINER 450T used for windrowing.

Cultivating operation

The operation is loosening and breaking up of the soil. The soil is cultivated using an attached cultivator (Fig. 4) to destroy weeds and promote growth by increasing soil aeration and water infiltration. Soil being prepared for the planting of a crop is cultivated.

CASE tractor (Model: CASE 7210) (Fig. 5) is selected to the purpose of accommodating the experimental trials. This model has a covered cabin for the operator, which is helpful to control some of experimental conditions (i.e. temperature and humidity inside the cabin) keeping on the consistency of those parameters and conditions.

Figure 4. Cultivating attached tool.

Figure 5. CASE 7210 with attached cultivating tool.

Sampling

To measure the operator's focusing on the AOI during the experimental samples of execution times 11 recording samples are used in windrowing operation and (25) recording samples are used in cultivating operation. Each recording sample (X) represents 600 seconds of the real-time recording of the operator's gaze during the windrowing operation.

Due to the differences between the planned and actual recoding time, each sample is normalized to represent the 600 seconds of recording with a factor (N) not exceeding the 17% of the planned recording time. However, collected snap times on the attached tool is multiplied by the Normalization factor (N) according to the formula:

$$\text{Normalized snap time of (X) sample} = \\ = \text{Normalization factor (N)} \cdot \text{Actual snap time of (X) sample.} \qquad (1)$$

Selection of Areas of interest

To the purpose of this research, the selected area of interest are the attached tools; which require continuous monitoring and checking by turning back; to keep focusing on the passive fatigue of the operator. Reference snapshots are taken for the item in the area of interest form videos recorded by the Tobii Glasses 2 equipment (Fig. 6).

Figure 6. Reference snapshots (windrowing and cultivating tools).

Selection of operator

One operator is selected to wear the eye-tracking equipment. Operator's details are listed in the (Fig. 7). The operator is mandated to spend several minutes inside the selected vehicle cabin during conducting the windrowing operation.

Grebely Csaba	
Age	22 years
Height	184 cm
Weight	78 kg
Experience	5 years

Figure 7. Operator's card.

RESULTS AND DISCUSSION

Measurements and analysis results

After accomplishing the analysis process, the resulted data was exported by Tobii pro lab analyser software to MS Excel sheet. The samples were normalized in accordance to the mentioned normalization formula.

Table 1. Sample Experiment results of windrowing operation

Sample Reference	X value	Tool Snap time (Sec)	N Factor	Time (Normalized) (Sec)	Generated Heat map
10	3	15.17	1.00	15.17	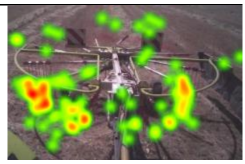
12	5	15.38	0.83	12.82	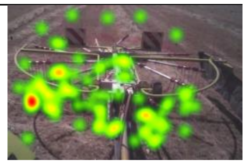
15	8	12	0.86	10.29	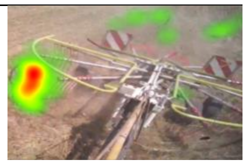
17	3	7.92	1.00	7.92	
18	4	48.72	1.00	48.72	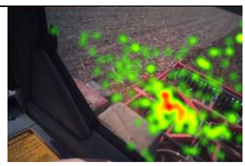

(Table 1) presents sample of exported results for the windrowing operation and cultivating operation, where:

- The sample reference in the original video (column 1); which represents the reference of a certain sample inside the used analyser software (Tobii Pro Lab).
- The sample serial number (X) (column 2); which will represent the X-Axis on the resulted curve.
- The tool snap times in (X) sample (column 3); which will represent the accumulated time of operator's gaze inside the AOI on the Y-Axis on the resulted curve.
- The normalization factor (N) for the sample (X) (column 4).
- The Normalized tool snap times (X*N) (column 5).
- The generated heat map for the sample (X) (column 6); which is a graphical representation for the operator's gaze distribution and accumulated time over the reference image along the sample recording time.

Modelling results

The curve fitting operation is conducted using the MATLAB Curve Fitting Toolbox™, the resulted curves (Fig. 8) for the windrowing and cultivating operations were processed selecting the Linear model (Poly 2) which generates a polynomial equation with the second degree and using Bi-square robust method.

Where

X-Axis represents the samples serial number (1 unit = 600 working seconds); *Y-Axis represents the OFS (Accumulated gaze time on the AOI in seconds)*

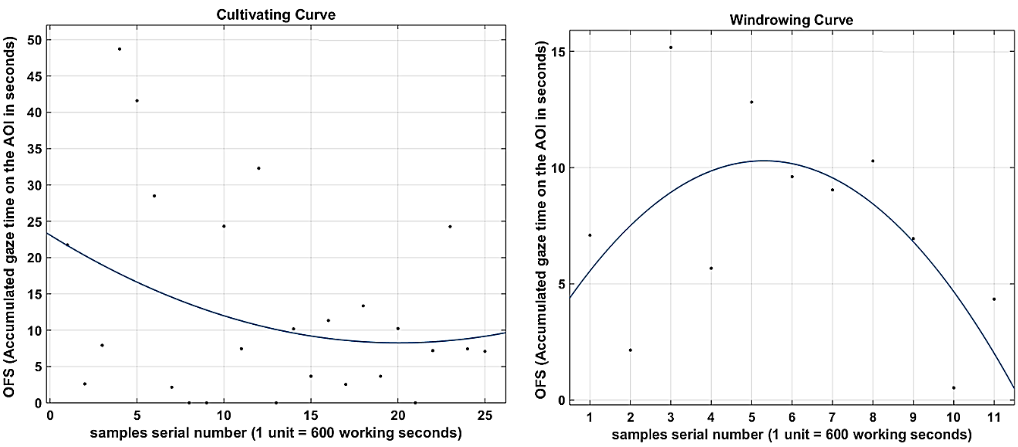

Figure 8. Curve fitting of results.

The resulted models and the goodness of fit is shown in (Table 2), which gave the final equation:

Table 2. Resulted models and the goodness of fit

Windrowing operation model	Cultivating operation model
Linear model Poly2: f(x) = p1*x^2 + p2*x + p3	Linear model Poly2: f(x) = p1*x^2 + p2*x + p3
Coefficients (with 95% confidence bounds): p1 = -2.809 p2 = -1.176 p3 = 10.17	Coefficients (with 95% confidence bounds): p1 = 1.999 p2 = -3.831 p3 = 10.1
Goodness of fit: SSE: 142.5 R-square: 0.2598 Adjusted R-square: 0.07474 RMSE: 4.221	Goodness of fit: SSE: 4083 R-square: 0.0713 Adjusted R-square: -0.01312 RMSE: 13.62

Discussion

The results showed accurate and dependable data of the operator's gaze on selected area of interest. The used equipment and supporting software packages easily defined the time in which the operator paid his attention to the attached windrowing and cultivating tools during working time in operations.

The selection criteria considered the common nature of agricultural operations, the AOI, the use of vehicles, the use of same operational conditions regarding the covered cabin and the use of same operator. Which all contributes to accomplish unified inputs keeping on the realistic implementation behaviour of the operator.

The nature of the selected agricultural operations includes the routine tasks; in which the operator needs to be involved is adding on the mental load due to monitoring of the vehicle track and the accumulated physical fatigue due to checking and monitoring the attached tool.

The resulted models are developed to be used as a simple tool predicting the behaviour of an operator inside the off-road vehicle cabins based on deterministic data analysis. The contribution of the implemented models is expected to assist the decision-making process regarding many aspects (i.e. scheduling of breaking times, working hours and payment estimation). Which make it necessary not to exclude the uncertainties expected to be faced during the real-time implementation of the model. Taking into consideration keeping on the simplicity of the model and not excluding of uncertainties, the resulted models are showing low R^2 Number. However; the resulted models are for the two agricultural operations are found to be the first attempt to modelling the change on operator's focusing scheme along working hours, which is subjected to be improved on a continual base.

CONCLUSIONS

The resulted models showed a notable decrement behaviour in operator's focusing scheme along working hours, which is correlated to the passive fatigue and mental load accumulated along working hours due to the operator contribution to monitor and control the attached back tool on a continual base.

The availability of such models provides the decision makers with dependable and deterministic data to decide on which operation requires more contribution by operators in order to support the developed precision farming concept by dissemination of the resulted modelling results into a simple and reliable way to the rural farming areas.

The resulted models are subjected for further development in the term of the modelling quality. However, it is still usable to provide an indication for comparing different agricultural operations.

REFERENCES

Brookhuis, K. & De Waard, D. 2010. Monitoring drivers' mental workload in driving simulators using physiological measures. *Accident Analysis and Prevention* **42**, 898–903.

Casey, S.M. & Kiso, J.L. 1990. The acceptability of control locations and related features in agricultural tractor cabs. In: *Proceedings of the Human Factors Society 34th annual meeting* (Santa Monica, CA: Human Factors Society), pp. 743–747.

De Waard, D. 1996. The measurement of drivers' mental workload. *Doctoral thesis*, University of Groningen, Haren, Netherlands, pp. 97–107.

Endsley, M.R. 1996. Automation and situation awareness. Automation and Human Performance: *Theory and Applications*, CRC Press. 163–181.

Fukunaga, A., Rabideau, G., Chien, S. & Yan, D. 1997. Towards an application framework for automated planning and scheduling. Aerospace conference. In Proceedings *IEEE*, pp. 411–427.

Gonçalves, J. & Bengler, K. 2015. Driver State Monitoring Systems– Transferable knowledge manual driving to HAD, *AHFE*, pp. 3011–3016.

Herdon, M. 2013. Agroinformatics. University of Debrecen, 5–20. ISBN: 978-963-473-671-4

Hsiao, H., Whitestone, J., Bradtmiller, B., Whisler, R., Zwiener, J., Lafferty, C., Kau, T.Y. & Gross, M. 2005. Anthropometric criteria for design of tractor cabs and protection frames. *Ergonomics* **48**, 323–353.

Kaminaka, M.S. 1985. Research needs in the American agricultural equipment industry. *Applied Ergonomics* **16**(3), 217–220.

Kramer, A. 1990. Physiological metrics of mental workload: A review of recent progress. In D. Damos, (Ed.). 2015. *Multiple-task Performance*. London, Taylor & Francis, pp.279–328.

Kroulik, M., Chyba, J. & Brant, V. 2015. Measurement of tensile force at the fundamental tillage using tractor's built-in sensor and external sensor connected between machines and their comparison. *Agronomy Research* **13**(1), 95–100.

Liljedahl, J.B., Turnquist, P.K., Amith, D.W. & Hoki, M. 1996. *Tractors and Their Power Units*. St. Joseph, MI: American Society of Agricultural Engineers, pp. 226–231.

Li, G. & Haslegrave, C.M. 1999. Seated work postures for manual, visual and combined tasks. *Ergonomics* **42**(8). Taylor and Francis. 1060–1086.

Louw, T. & Merat, N. 2017. Are you in the loop? Using gaze dispersion to understand driver visual attention during vehicle automation. *Transportation Research* Part **C 76**, 35–50.

Marquart, G., Cabrall, C. & Winter, J. 2015: Review of eye-related measures of drivers' mental workload. *Procedia Manufacturing* **3**, 2854–2861.

Matthews, J. 1977. The ergonomics of tractors. *ARC Research Review* **3**, 59–65.

Robert, P. 2004. Agricultural Systems Management: Optimizing Efficiency and Performance. Taylor & Francis. 2004, 3–12. ISBN 0-203-02183-5

Saxby, D.J., Matthews, G., Warm, J.S., Hitchcock, E.M. & Neubauer, C. 2013. Active and passive fatigue in simulated driving: discriminating styles of workload regulation and their safety impacts. *J. Exp. Psychol. Appl.* **19**(4), 287–300.

Scheding, S., Dissanayake, G., Nebot, E.M. & Durrant-Whyte, H. 1999. An experiment in autonomous navigation of an underground mining vehicle. *IEEE Transactions on Robotics and Automation* **15**(1), 85–95.

Shen, S. & Neyens, D.M. 2017. Assessing drivers' response during automated driver support system failures with non-driving tasks. *Journal of Safety Research* **61**, 149–155.
Sheridan, T.B. 1992. Telerobotics, automation, and human supervisory control. MIT Press, pp. 1–10.
Sporrong, H., Palmerud, G., Ka defors, R. & Herberts, P. 1998. The effect of light manual precision work on shoulder muscles-an EMG analysis. *Journal of Electromyography and Kinesiology* **8**, 177–184.
Szabó, I., Hushki, M., Bártfai, Z. & Kátai, L. 2017. Operator's behaviour measuring methodology inside off-road vehicle cabin, operator's focusing scheme. *Agronomy Research* **15**(5), 2172–2182.
Xuan, Z. 2007. Artificial Intelligence and Integrated Intelligent Information Systems: Emerging Technologies and Applications. Idea Group Inc (IGI), 1–75. ISBN 1-59904-249-5.
Young, K. & Regan, M. 2007. Driver distraction: A review of the literature. In: I.J. Faulks, M. Regan, M. Stevenson, J. Brown, A. Porter & J.D. Irwin (Eds.). *Distracted driving*. Sydney, NSW: Australasian College of Road Safety, pp. 379–405.
Zewdie, R. & Kic, P. 2017. Substantial factors influencing drivers' comfort in transportation. *Agronomy Research* **15**(5), 2236–2246.

Agronomy Research **16**(4), 1896–1904, 2018
https://doi.org/10.15159/AR.18.152

The impact of the termination technology of agro-ecological service crops on soil properties in open field vegetable production

K. Tamm[*], I. Bender, E. Nugis, L. Edesi and T. Võsa

Estonian Crop Research Institute, J.Aamisepa 1, EE48309 Jõgeva, Jõgeva Vald, Estonia
[*]Correspondence: kalvi.tamm@etki.ee

Abstract. The agro-ecological service crops (ASC) are introduced in the agro-ecosystems to provide or enhance ecological services, thus promoting the whole soil-plant system equilibrium. To avoid competition with the subsequent cash crops, the growth of the interposed ASC is terminated in advance of the cash crop planting. The traditional, most widespread technique to terminate the ASC is incorporation as green manure into the soil by tillage (GM). However, since tillage includes energy and labour consuming and soil disturbing operations, the use of no/reduced tillage techniques (as the roller crimping technology-RC) has received increasing interest.
An international research consortium (SOILVEG) including Estonian Crop Research Institute, was established in 2015 with the aim to study among others the impact of ASC termination on soil dry bulk density (BD), water content, soil structure and microbiological activity. Data are collected from Estonian trials in 2016 and 2017 at Jõgeva.
The physical properties of 0–40 cm soil layers were determined. Higher BD in soil layers (0–20 cm) of plots with ASC and RC was determined comparing to the GM and control plots. Bigger water content in same layer of plots with ASC and the RC was determined comparing to the GM plots. The use of the ASC-s helped to arise ratio of agronomically preferred soil particles. Microbial activity was estimated by assessing of enzyme dehydrogenase activity in 0–20 cm soil layer. There were no statistically relevant differences in soil dehydrogenase activity (DHA) between the RC and GM treatments.

Key words: agro-ecological service cops (ASC), roller crimping, soil bulk density, soil gravimetric water content, soil structure, soil dehydrogenase activity.

INTRODUCTION

The roller-crimper technology is receiving increasing interest in no-till organic production systems in recent decade as a mean to control weeds, improve soil quality and, reduce labour and fuel costs (Altieri et al., 2011; Luna et al., 2012, Halde et al., 2014). Many studies have shown that the roller-crimper technology and choice of cover crop species influence the weediness of fields and cash crop yield, also soil and plant chemical properties (Mischler et al., 2010; Mirsky et al., 2011; Nord et al., 2012; Canali et al., 2013; Halde et al., 2014). However, the soil physical and biological condition is poorly investigated.

Soil bulk density (BD) plays an important role in crop yield. BD reflects soil ability to function as structural support, has impact on water movement and soil aeration (Arshad et al., 1996; Cresswell & Hamilton, 2002). BD 1.3–1.5 Mg m^{-3} enhances root growth, whereby BD depends on soil texture and the content of organic matter (Guimarães et al., 2002; Tracy et al., 2012). An ideal BD-s for plant growth by soil texture is following: sandy < 1.60, silty < 1.40 and clayey < 1.10 Mg m^{-3}. However, BD values what are for Estonian condition considered to be restricting to root growth are above1.80 Mg m^{-3} for sandy, 1.65 for silty and 1.47 for clayey soil (Arshad et al., 1996).

The tillage practices influence the biological processes in soil through the changes of soil physical properties and distribution of plant residues (Hassink et al., 1993; Miglierina et al., 2000; Bogužas et al., 2010; Carvalho et al., 2010; Janušauskaite, et al., 2013). Soil enzymatic activity is a sensitive indicator to evaluate the influence of different agricultural practices on the soil processes which are carried out by microorganisms (Watts et al., 2010).

The aim of the current study was to investigate the impact of agro-ecological service crops (ASC) and termination technology on soil dry bulk density, water content, structure and microbiological activity.

MATERIALS AND METHODS

Site and soil description and experimental set up

The experiment was carried out on organic field of Estonian Crop Research Institute (58°44'59.41" N, 26°24'54.02" E) in eastern Estonia in 2015 to 2017. The soil of the experimental field was classified as *Calcaric Cambic Phaeozem (Loamic)* clay soil (WRB, 2015). The soil pH_{KCl} was 7.2 and the organic carbon content 2.7%.

Plot size was 4 x 6 m with three replications and 1.5 m stripes between plots (Fig. 1). The field trial was conducted on season 2015/2016 and then switched 50 m to north, to neighbouring trial area on 2016/2017. The precrop on both trial areas was red clover, which was chopped before tillage.

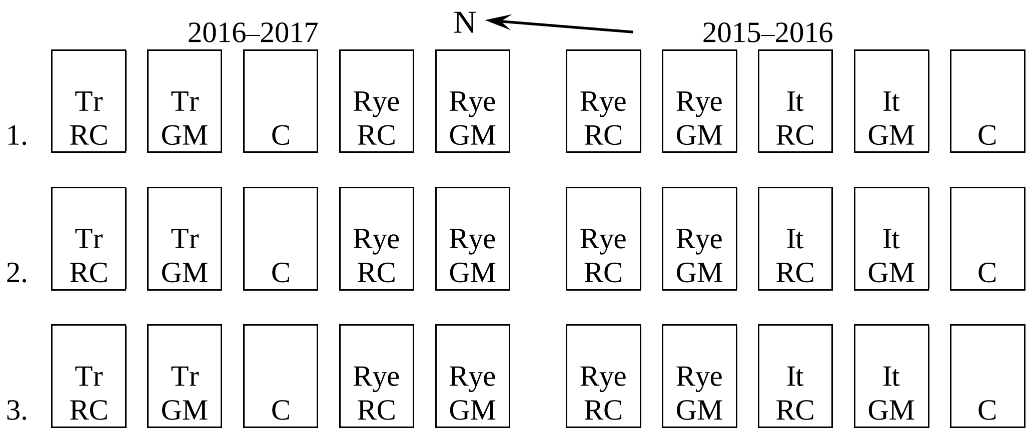

Figure 1. Experimental field design in 2015–2016 and 2016–2017 seasons. Rye – winter rye; It –Italian ryegrass; Tr – winter triticale. C – control, without ASC, RC – the ASC was crimped by roller-crimper, GM – the ASC was chopped by flail mower, incorporated by plough and soil was levelled by tine cultivator; C – control, no ASC, soil was ploughed by plough and levelled by tine cultivator.

Activities on 2015–2016. The first soil tillage on all plots was done after 30 t ha^{-1} solid cattle manure application on the 29^{th} July 2015 with 4-furrow reversible plough (24 cm depth). Cultivating was done with disc cultivator (12–14 cm) on the 9^{th} August and the second time with cultivator with wing tines on the 19^{th} August 2015. The ASC winter rye (*Secale cereale*) `Elvi` 180 kg ha^{-1} and Italian ryegrass (*Lolium multiflorum*) `Talvike` 55 kg ha^{-1} were sown on the 25^{th} August 2015. Control, without ASC (C) was harrowed by rotary harrow (depth 10 cm) on the 4^{th} May 2016. For biomass and C:N ratio measurements the ASC crops were sampled (50 x 50 cm) on the 30^{th} May 2016 and analysed in laboratory of the Estonian University of Life Science department of Soil Science and Agrochemistry. ASC flattening by roller crimper (RC treatment) was done two times on the 6^{th} and four times on the 9^{th} June 2016. Incorporation of the ASC as green manure by chopping and incorporating (GM treatment) with 4-furrow reversible plough (20 cm depth) was made on the 10^{th} June 2016. Control plots and ploughed GM treatment plots were levelled with tine harrow and slat rolls on the 10^{th} June 2016. Cash crop: white cabbage (*Brassica oleracea var. capitata f. alba*) middle-ripening (130 days) cv Jõgeva was planted from 13th to 16th June 2016 by hand. Planting distances were 0.50 m between rows and 0.50 m between plants in the row. Age of the seedlings was 28–30 days. Manual weeding was performed on all treatments on the 25th August. Harvest date was on the 7^{th} October 2016.

Activities on 2016/2017. The first soil tillage on all plots was done after 30 t ha^{-1} solid cattle manure application on the 6^{th} September 2016 with 4-furrow reversible plough (24 cm depth). Cultivating was done with disc cultivator (12–14 cm) on the 7^{th} September. The ASC winter rye (*Secale cereale*) `Elvi/Tulvi` 180 kg ha^{-1} and winter triticale (*Triticosecalium*) `Ruja` 155 kg ha^{-1} were sown on the 8^{th} September 2016. For biomass and C:N ratio measurements the ASC crops were sampled on the 24^{th} May 2017 and analysed. ASC flattening by roller crimper (RC) was done two times on rye and four times (to achieve even termination) on triticale on the 19^{th} June 2017. ASC as green manure (GM) was chopped with flail mower and incorporated with 4-furrow reversible plough (20 cm depth) on the 16^{th} June 2017. Control and GM plots were levelled with tine harrow and slat rolls on the 16^{th} June 2017. Cash crop white cabbage cv Jõgeva was planted on the 19^{th} June 2017 by hand. Planting distances were 0.65 m between rows and 0.50 m between plants in the row. Age of the seedlings was 38 days. All treatments were weeded manually on the 27^{th} July 2017. Harvest date was from the 4^{th} to the 6^{th} October 2017.

Soil bulk density, gravimetric water content and structure

The soil bulk density i.e. BD (Mg m^{-3}), soil gravimetric water content, i.e. GWC (kg kg^{-1}), soil structure K_{str} were assessed in soil layers 0–10, 10–20, 20–30 and 30–40 cm, in October 2016 and 2017. For determination of K_{str} the soil samples of 0–20 cm from three replications were mixed. The BD and GWC were evaluated by Eijkelkamp cylinder (100 cm^3). The soil structure K_{str} (Tamm et al., 2016) was evaluated by USA Standard Testing Sieve and also by method of Swedish University of Agricultural Sciences (Hakansson, 1983; Kritz, 1983) by which the soil has been sieved in laboratory in moist conditions.

The ratio of soil structure K_{str} was calculated as (Tamm et al., 2016):

$$K_{str} = \frac{s_{ps}}{s_{n1}+s_{n2}} \quad (1)$$

where s_{ps} – percentage of soil particles with diameter between 2–4.75 mm (preferred soil structure-*PS*); s_{n1} – percentage of soil particles with diameter < 2 mm (not-preferred soil structure); s_{n2} – percentage of soil particles with diameter > 4.75 mm (also not-preferred soil structure).

The agronomically preferred (0.250–1.0 mm of diameter) and clods (> 9.5 mm of diameter) soil particles at a soil depth 0–20 cm in 2017 were measured in laboratory by air dry soil sieving. After sieving the weight of the soil portions laying on the sieves were weighed and then the relation (%) of the every portion to the total weight was calculated.

Soil dehydrogenase activity

Soil samples (0.2 kg) from each treatment in three replications from the 0–20 cm soil layers with a 16 mm diameter auger were taken on 1.09.2016 and 22.08.2017, during the cabbage growth and almost three month after ASC termination. Samples were sieved (2 mm) and stored at 4 °C until analysis in laboratory. Assessing of soil dehydrogenase activity (DHA) based on Tabatabai (1982). Soil samples (5 g) were incubated at 30 °C for 24 h in the presence of an alternative electron acceptor (triphenyltetrazoliumchloride). The red-tinted product (triphenylformazan) was extracted with acetone and measured in a spectrophotometer at 546 nm.

Data analyses

Observations of soil physical parameters (soil structure, BD, GWC) and dehydrogenase activity based on three sample replicates of related trial plots and soil layers. The data was analyzed by ANOVA. For the soil physical parameters and dehydrogenase activity the Tukey-Kramer Honest Significant Difference (HSD) test was used via the software *JMP 5.0.1.2* (SAS, 2002).

RESULTS AND DISCUSSION

Soil bulk density (BD), gravimetric water content (GWC) and structure(Kstr)

The average soil BD for all trial plots and depths in October of 2016 and 2017 was quite different (Table 1). In both years highest BD was measured in soil layer 30–40 cm. Highest BD occurred in 2016 (20–30 cm layer) in Rye RC plots, where 6 overdrives with the roller crimper was made. Statistical differences between the treatments in depth 0–10, 10–20 and 30–40 cm did not occur during 2016.

The lowest BD occurred in 2017 0–10 cm layer in control plots. In comparison to 2016, in 2017 the BD decreased in 0–10 and 20–30 cm layers of rye RC, rye GM and control plots. In 2016 It RC, It GM and in 2017 Tr RC and Tr GM trial plots the soil BD remained, regardless of the different crops, quite similar in all depths.

During the study the average soil GWC % in 2016 for all treatments and depths was 35.49 % and in 2017 was 31.14 %. In 2016, statistical differences between the treatments did not occur. In 2017 the GWC % in depth 0–10 cm was significantly higher in the RC than in GM and control plots (P = 0.0013).

The soil structure and also agronomical preferred soil particles play an important role in water availability and they form like an architecture of the soil (Hunt & Gilkes, 1992). It is essential to crop production (Bronick & Lal, 2005). Our results show (Table 2) in 2017 a better soil structure coefficient (Kstr) in Rye GM (0.58), Tr GM (0.61) and Control (0.53) treatments. Oppositely, a lowest value (0.21) were found in 2016, on control plot. In 2017, the significantly lowest values had RC plots (Rye RC (0.32) and TrRC (0.26)).

Table 1. Mean values of soil bulk density (BD) and gravimetric water content (GWC) in 2016 and 2017

Depth, cm	Treatment	BD, Mg m^{-3}		CWC %, kg kg^{-1}	
		2016	2017	2016	2017
0–10	Rye RC	1.44^{a}	1.10^{bc}	36.00a	38.13^{a}
	Rye GM	1.34^{a}	1.01^{bc}	34.63^{a}	31.67b
	It /Tr RC	1.41^{a}	1.49^{a}	39.64^{a}	34.87^{ab}
	It/Tr GM	1.34^{a}	1.23^{ab}	35.01a	30.70^{b}
	Control	1.36^{a}	0.80c	38.42^{a}	31.10^{b}
	p > F	*ns*	*0.001*	*ns*	*0.0013*
10–20	Rye RC	1.36^{a}	1.46^{a}	34.74^{a}	35.10^{a}
	Rye GM	1.18^{a}	1.38^{ab}	32.87^{a}	33.33^{ab}
	It /Tr RC	1.27^{a}	1.32^{ab}	34.72^{a}	33.30^{ab}
	It/Tr GM	1.23^{a}	1.25^{b}	33.40^{a}	30.87^{a}b
	Control	1.27^{a}	1.25^{b}	36.96^{a}	29.47^{b}
	p > F	*ns*	*0.0018*	*ns*	*0.0015*
20–30	Rye RC	1.60^{a}	1.00^{abc}	34.68^{a}	31.27^{a}
	Rye GM	1.30^{b}	0.89^{c}	34.03^{a}	33.47^{a}
	It /Tr RC	1.33^{b}	1.51^{a}	36.89^{a}	30.33^{a}
	It/Tr GM	1.37^{ab}	1.47^{ab}	36.64^{a}	32.10^{a}
	Control	1.36^{ab}	0.99^{bc}	39.01^{a}	31.97^{a}
	p > F	*0.029*	*0.006*	*ns*	*ns*
30–40	Rye RC	1.66^{a}	1.66^{a}	33.21^{a}	30.17^{a}
	Rye GM	1.52^{a}	1.73^{a}	36.01^{a}	30.20^{a}
	It /Tr RC	1.59^{a}	1.74^{a}	33.52^{a}	23.43^{a}
	It/Tr GM	1.35^{a}	1.63^{a}	35.02^{a}	23.10^{a}
	Control	1.58^{a}	1.67^{a}	34.36^{a}	28.20^{a}
	p > F	*ns*	*ns*	*ns*	*ns*

Note. Different letters behind the mean values indicate significant differences at $p < 0.05$ (Tukey-Kramer HSD test).

Table 2. Mean values of soil structure (Kstr) in 2016 and 2017; agronomically preferred soil particles (0.250–1.0 mm of diameter) and clods (%) (> 9.5 mm of diameter) at a soil depth 0–20 cm in 2017

Treatment	Kstr		0.250–1.0 mm	> 9.5 mm
	2016	2017	2017	2017
Rye RC	0.29^{ab}	0.32^{b}	2.53^{bc}	55.07^{a}
Rye GM	0.38^{a}	0.58^{a}	4.03^{ab}	44.77^{ab}
It/Tr RC	0.35^{ab}	0.26^{b}	1.97^{c}	59.73^{a}
It/Tr GM	0.29^{ab}	0.61^{a}	5.40^{a}	33.53^{b}
Control	0.21^{b}	0.53^{a}	5.13^{a}	34.73^{b}
p > F	*0.05*	*> 0.001*	*0.004*	*0.002*

Note. Different letters behind the mean values indicate significant differences at $p < 0.05$ (Tukey-Kramer HSD test).

Generally, the dependence between agronomical preferred soil particles and cloddy soil is inverse, which is also confirmed by higher clod-like (> 9.5 mm of diameter) and lower 0.250–1.0 mm soil particles proportion in RC treatments. Higher 0.250–1.0 mm and lower > 9.5 mm soil particles proportion were found in GM plots compared to the RC plots.

Wet clay soils are structurally unstable and have high shrink and swell potential (Blanco-Canqui, & Lal, 2008). Although in 2016, were no clear differences of measured soil physical parameters between the treatments, they became evident in 2017 because the weather was very rainy before the RC termination. In 2016 10 days before RC termination was without any precipitation and during whole previous May was only 3.6 mm rain.

Soil dehydrogenase activity (DHA)

In 2016, the comparison of ASC-s showed that soil DHA was highest in the variant with Italian ryegrass (5.41 TPF μg g^{-1} h^{-1}, $P = 0.007$, Table 3) and lowest in control and rye variants (3.97 and 4.47 TPF μg g^{-1} h^{-1}). In 2017, there were no statistically relevant differences between ASC variants. However, it was possible to observe tendency of higher soil DHA in triticale variant (5.46 TPF μg g^{-1} h^{-1}) than in rye and control variants (4.52 and 5.03 TPF μg g^{-1} h^{-1}). During the growth the plants affect the soil microorganism by physiological and morphological mechanisms as nutrient and water use by plants and by differences in root distribution and exudates (Garbeva et al., 2008; Doornbos et al., 2012). The positive effect of the ASC-s on soil microbial communities associated with crop rhizosphere compared to the bare fallow was also observed by Hacquard et al., 2015. After the cover crops management by the different termination technologies, the organic matter breakdown by microorganisms is largely influenced by C:N ratio. The C:N ratio can limit microbial growth when it is above the threshold value of 25–30 (Biddlestone et al., 1994). In 2016 and in 2017, compared to the plant material C:N ratio of rye (2016 – 35.1 and 2017 – 32.5) the Italian ryegrass (31.3) and triticale (24.2) ratios were lower and therefore were suitable for soil microorganisms.

In 2016 and 2017, the soil DHA in all managements was similar and statistical differences between the RC, GM and Control plots did not occur. As well, there were no statistical differences between the management and the ASC interaction. However, there was tendency that in 2016 and 2017, compared to the Control and rye different managements, the soil DHA was slightly higher in treatments with Italian ryegrass and triticale variants where before the cabbage planting the fresh plant material was rolled down. The reason for this may be that in addition to the rye higher C:N ratio, the rolled or incorporated rye left much bigger mulch layer (902–1,065 DM g m^{-2}) on the soil surface than Italian ryegrass and triticale (378–594 DM g m^{-2}). That might reduce the oxygen availability and a lack of oxygen might reduce the soil DHA, especially on the clay soil. While, Jodaugienė et al., 2010 found in their field experiment in medium clay soil, that the mulch layer thickness 5 or 10 cm had no significant effect on soil hydrolytic enzymes. In our experiment the lower soil enzymatic activity in the variants with larger amounts of mulch may have been due to the coincidence of several inappropriate factors. For example in 2016, this could be caused by the high amount of precipitations during the vegetation period (June – 162 mm; July – 78 mm; August–180 mm) compared to average of 1994–2004 (June – 98 mm; July – 77 mm; August –73 mm).

Table 3. Soil dehydrogenase activity (DHA) at a soil depth 0–20 cm in 2016 and 2017

Factor	Variant	2016	2017
		TPF μg g^{-1} h^{-1}	
ASC	Rye	4.47^{b}	4.52^{a}
	It 2016/Tr 2017,	5.41^{a}	5.46^{a}
	Control	3.97^{b}	5.03^{a}
	p > F	*0.007*	*ns.*
Management	RC	4.94^{a}	5.36^{a}
	GM	4.93^{a}	4.62^{a}
	Control	3.97^{a}	5.03^{a}
	p > F	*ns.*	*ns.*
ASC*Management	Rye RC	4.37^{a}	4.67^{a}
	Rye GM	4.56^{a}	4.36^{a}
	It/Tr RC	5.51^{a}	6.05^{a}
	It/Tr GM	5.30^{a}	4.87^{a}
	Control	3.97^{a}	5.03^{a}
	p > F	*ns.*	*ns.*

Note. Different letters behind the mean values indicate significant differences at $p < 0.05$ (Tukey-Kramer HSD test).

Soil physical properties have significant impact on soil microbial activity, for example Gispert et al. (2013) found soil microbial populations greatest in soils with low bulk density. In present study the soil physical parameters and the soil dehydrogenase activity were not compared because the soils were sampled at a different time.

CONCLUSIONS

The use of the agro-ecological service crops helped to arise ratio of agronomically preferred soil particles. The technology, where the winter rye as ASC was chopped by flail mower, incorporated by plough and after that the soil was levelled by tine cultivator, helped in 2017 to increase the ratio (soil moist sieving) of soil structure. The dependence between agronomically preferred soil particles and cloddy soil was inverse. The sampling period 2016–2017 is quite adequate to make general conclusions about immediate influence of rolling crimping technology method on soil bulk density and gravimetric water content. The tendency of increase of the bulk density with increasing depth was observed on RC rye plots in 2016. However, in 2017 tendency was to the lower bulk densities on GM rye, GM triticale and control plots.

Soil dehydrogenase activity was influenced by the treatment only in 2016, then the dehydrogenase activity was higher in the soils under the ASC Italian ryegrass cultivation than under the winter rye cultivation and in the bare soil. Statistical differences between the roller crimping, chopped/incorporated and plough technology on soil dehydrogenase activity did not occur.

The experiment series could be continued to get more information about the influence of other agro-ecological service crops and termination technology on soil different characteristics.

ACKNOWLEDGEMENTS. This study has been carried out in the frame of the SoilVeg research project 'Improving soil conservation and resource use in organic cropping systems for vegetable production through introduction and management of Agro-ecological Service Crops' and funded in the frame of the Core Organic Plus ERA-NET and Estonian Ministry of Rural Affairs.

REFERENCES

Altieri, M.A., Lana, M.A., Bittencourt, H.V., Kieling, A.S., Comin, J.J. & Lovato, P.E. 2011. Enhancing crop productivity via weed suppression in organic no-till cropping systems in Santa Catarina, Brazil. *Journal of Sustainable Agriculture* **35**, 855–869.

Arshad, M.A., Lowery, B. & Grossman, B. 1996. Physical Tests for Monitoring Soil Quality. In: Doran J.W., Jones A.J., editors. *Methods for assessing soil quality*. Madison, WI, 123–141.

Biddlestone, A.J., Gray, K.R. & Thayanithy, K. 1994. Composting reed beds for aerobic treatment of livestock wastes. In: I.A. Dewi, R.F.E. Axford, I. Fayez, M. Marai and H.M. Oured (Editors), *Pollution in Livestock Production Systems*. CAB International, Wallingford, UK, 345–360.

Blanco-Canqui, H. & Lal, R. 2008. Principles of Soil Conservation. Springer Verlaag, 617 pp.

Bogužas, V., Kairytė, A. & Jodaugienė, D. 2010. Soil physical properties and earthworms as affected by soil tillage systems, straw and green manure management. *Zemdirbyste-Agriculture* **97**(3), 3–14.

Bronick, C.J. & Lal, R. 2005. Soil structure and management: a review. *Geoderma* **24**, 3–22.

Canali, S., Campanelli, G., Ciacci, C., Leteo, F., Testani, E., Montemurro, F. 2013. Conservation tillage strategy based on the roller crimper technology for weed control in Mediterranean vegetable organic cropping systems. *European Journal of Agronomy* **50**, 11–18.

Carvalho, J.L.N., Raucci, G.S., Cerri, C.E.P., Bernoux, M., Feigl, B.J., Wruck, F.J., Cerri, C.C. 2010. Impact of pasture, agriculture and crop-livestock systems on soil C stocks in Brazil. *Soil and Tillage Research* **110**, 175–186.

Cresswell, H.P., Hamilton, G.J, McKenzie, N., Coughlan, K. & Cresswell, H. 2002. Bulk Density and Pore Space Relations. In: *Soil Physical Measurement and Interpretation For Land Evaluation*. (Eds N.J. McKenzie, H.P. Cresswell H.P., K.J. Coughlan) CSIRO Publishing: Collingwood, Victoria, pp. 35–58.

Doornbos, R.F., van Loon, L.C. & Bakker, P.A.H.M. 2012. Impact of root exudates and plant defense signaling on bacterial communities in the rhizosphere. *Agronomy for Sustainable Developmen* **32**, 227–243.

Garbeva, P., Van Elsas, J.D. & Van Veen, J.A. 2008. Rhizosphere microbial community and its response to plant species and soil history. *Plant and Soil* **302**, 19–32.

Gispert, M., Emran, M., Pardini, G., Doni, S. & Ceccanti, B. 2013. The impact of land management and abandonment on soil enzymatic activity, glomalin content and aggregate stability. *Geoderma* **202–203**, 51–61.

Guimarães, C.M., Stone, L.F. & Moreira, J.A.A. 2002. Soil compaction in a bean crop. II. Effect on root and shoot development. *Revista Brasileira de Engenharia Agrícola e Ambiental* **6**, 213–218.

Hacquard, S., Garrido-Oter, R., González, A., Spaepen, S., Ackermann, G., Lebeis, S, McHardy, A.C, Dangl, J.L., Knight R., Ley R. & Schulze-Lefert, P. 2015. Microbiota and host nutrition across plant and animal kingdoms. *Cell Host Microbe* **17**(5), 603–616.

Hakansson, I. (ed.). 1983. Pnysical conditions in cereal seedbeds. A sampling investigation in Swedish spring-sown fields. Reports from the Division of Soil Management nr. 65. Uppsala, 187 pp.

Halde, C.H., Gulden, R.H. & Entz, M.H. 2014. Selecting Cover Crop Mulches for Organic Rotational No-Till Systems in Manitoba, Canada. *Agronomy Journal* **106**(4), 1193–1204.

Hassink, J., Bowman, L.A., Zwart, K.B., Bloem, J. & Brussard, L. 1993. Relationships between soil texture, physical protection of organic matter, soil biota, and C and N mineralization in grassland soils. *Geoderma* **57**, 105–128.

Hunt, N. & Gilkes, B. 1992. *Farm Monitoring Handbook*. UWA, LMS & DSP, 62 pp.

Janušauskaite, D., Kadžienė, G. & Auškalnienė, O. 2013. The influence of tillage on selected biological parameters. The Effect of Tillage System on Soil Microbiota in Relation to Soil Structure. *Polish Journal of Environmental Studies* **22**(5), 1387–1391.

Jodaugienė, D., Pupalienė, R., Sinkevičienė, A., Marcinkevičienė, A., Žebrauskaitė, K., Baltaduonytė, M. & Čepulienė, R. 2010. The influence of organic mulches on soil biological properties. *Zemdirbyste-Agriculture* **97**(2), 33–40.

Kritz, G. 1983. Physical conditions in cereal seedbeds. Reports from the Division of Soil Management. Swedish University of Agricultural Sciences, S-750 07. Uppsala, pp. 25–36.

Luna, J.M., Mitchell, J.P. & Shrestha, A. 2012. Conservation tillage for organic agriculture: evolution toward hybrid systems in the western USA. *Renewable Agriculture and Food Systems* **27**, 21–30.

Miglierina, A.M., Iglesias, J.O., Landriscini, M.R., Galantini, J.A. & Rosell, R.A. 2000. The effects of crop rotation and fertilization on wheat productivity in the Pampean semiarid region of Argentina. 1. Soil physical and chemical properties. *Soil and Tillage Research* **53**, 129–135.

Mirsky, S.B., Curran, W.S., Mortensen, D.M., Ryan, M.R. & Shumway, D.L. 2011. Timing of covercrop management effects on weed suppression in no-till planted soybean using a roller-crimper. *Weed Science* **59**, 380–389.

Mischler, R.A., Curran, W.S., Duiker, S.W. & Hyde, J.A. 2010. Use of a rolled-rye cover crop for weed suppression in no-till soybeans. *Weed Technology* **24**, 253–261.

Nord, E.A, Ryan, M.R, Curran, W.S, Mortensen, D.A, Steven, B. & Mirsky, S.B. 2012. Effects of management type and timing on weed suppression in soybean no-till planted into rolled-crimped cereal rye. *Weed Science* **60**, 624–633.

Tabatabai, M.A. 1982. Soil enzymes. In: Page, A.L., Miller, R.H. & Keeney, D.R. (Eds.) Methods of Soil Analysis, Part 2 Chemical and Microbiological Properties, second ed., vol. **9**. American Society of Agronomy and Soil Science Society of America, Madison, Wisconsin, 903–947.

Tamm, K., Nugis, E., Edesi, L., Lauringson, E., Talgre, L., Viil, P., Plakk, T., Võsa, T., Vettik, R. & Penu, P. 2016. Impact of cultivation method on the soil properties in cereal production. *Agronomy Research* **14**(1), 280–289.

Tracy, S.R., Black, C.R., Roberts, J.A., McNeill, A., Davidson, R., Tester, M., Samec, M., Korosak, D., Sturrock, C. & Mooney, S.J. 2012. Quantifying the effect of soil compaction on three varieties of wheat (*Triticum aestivum* L.) using xray micro computed tomography (CT). *Plant and Soil* **353**, 195–208.

Watts, D.B., Torbert, H.A., Feng, Y. & Prior, S.A. 2010. Soil microbial community dynamics as influenced by composted dairy manure, soil properties, and landscape position. *Soil Science* **175**, 474–486.

WRB. 2015. World reference base for soil resources 2014, update 2015. International soil classification system for naming soils and creating legends for soil maps. *World Soil Resources Reports* No. 106. FAO, Rome.

Agronomy Research **16**(4), 1905–1914, 2018
https://doi.org/10.15159/AR.18.160

Fodder beans and peas in the diet of dairy cows

A. Trūpa[1,*], B. Ošmane[2] and I.H. Konošonoka[2]

[1]Latvia University of Life Sciences and Technologies, Liela iela 2, LV-3001 Jelgava, Latvia
[2]Institute of Agricultural Resources and Economics, Priekuli Research Centre, Zinatnes iela 2, LV-4130 Priekuli, Priekulu parish, Priekulu district, Latvia
[*]Correspondence: aiga.trupa@llu.lv

Abstract. The Holstein-Friesian Black-and-White cows were grouped into four treatments groups according to the analogue principle (n = 4 × 5). Lactating dairy cows were included in the trial in the initial lactation phase with the average milk yield of 23.00 kg per day, fat content 4.10% and 3.20% protein content in milk. The analyses of the chemical composition of legume grains show, that crude protein and undegraded intake protein (UIP) were higher in fodder beans than in peas, respectively 29.97% and 25.04% of dry matter but UIP content, respectively 40.51% and 39.69% of crude protein. There was a total of 17 amino acids detected in legume grains and soybean meal. The highest concentration of arginine, leucine, glutamic acid, aspartic acid and isoleucine was in fodder beans, respectively 0.76%, 0.58%, 0.67%, 0.42% and 0.29% more than in peas. Even though the daily milk yields decreased for all the cow groups during the experiment, which was normal during the lactation period, yet the milk yield decreases for the trial groups. The highest total amount of amino acids in milk was detected in 3rd and 2nd trial cow groups, respectively, 4.00 g kg^{-1} and 3.90 g kg^{-1} which was fed fodder beans and peas. The milk sale and feed cost summary records for the trial that lasted 90 days show that economic efficency of peas plus beans has been positive.

Key words: fodder beans, peas, feed values, amino acids, dairy cows, milk, cost.

INTRODUCTION

Animal supply with healthy feed is a very important factor in the increase of productivity, in rational use of feed and in preservation of animal's health. Moreover, most protein crops are legumes and are therefore very interesting for crop rotation for dairy cow farmers and, overall, for sustainability. The rumen degradability and the soluble fractions (albumins and globulins) of the protein are higher in the grain legumes compared with soybean meals and thus, grain legumes are more suitable as supplements to low-protein forages.

Consequently, livestock farmers worldwide are under increasing pressure to maximise their use of home-grown feeds. So, the cultivation of grain legumes such as, fodder beans (*Vicia faba var. minor*), high protein pea (*Pisum sativum*) on farm could solve the problem and improve the sustainability of the farm (Martini et al., 2008).

Legume grains contain 22–35% proteins, which may provide animal dietary requirements, as well as increase share of local protein sources in feed, diminishing the costs at the same time. Despite all this, the use of inappropriate proteins or amounts may cause an increase in production costs and decrease efficiency. Field beans have relatively high crude protein level and contain a considerable amount of energy in the form of starch, which makes them a unique feed that can be substituted for higher-priced protein and energy commodities like soybean meal (Tufarelli et al., 2012). Field peas are highly digestible and highly fermentable in the rumen, but have a slower starch and protein fermentation rate than several other common feeds. Therefore, fodder beans and peas be used as an important forage legume to enhance feed values for dairy ruminants, especially of importance to today's high yielding dairy cows (Jensen, 2002; Ipharraguerre & Clark, 2005).

The European Union policy on the protection and enhancement of biodiversity on agricultural holdings has contributed to an increase in the area sown with legumes in Latvia. Areas under nitrogen-fixing crops, including fodder beans or field beans and peas, are eligible for financial support regarding environment-friendly agricultural practices; consequently, the total area under field beans in Latvia in the period 2010–2016 increased approximately 11 times (from 2.8 thousand hectares to 31.4 thousand hectares) and that under peas – 7 times (from 1.2 thousand hectares to 8.9 thousand hectares). The sown areas of pulses continue to grow. In 2016, the total area of pulses increased by 32.1%, of which the area of field beans rose by 5.4 thousand hectares or 20.9% (Agriculture of Latvia, 2017).

This means that the growing area under faba beans and peas in Latvia can supply agricultural animals with the necessary amount of protein as well as increase the proportion of domestic proteinrich feedstuffs in the consumption of feed and reduce the production cost of livestock products, i.e. contribute to higher efficiency (Proskina & Cerina, 2017).

The aim of the present research was to investigate the fodder beans and peas in the diets of dairy cows.

MATERIALS AND METHODS

Trials were carried out on the farm 'Upites', Allazu Parish, Allazmuiza Municipality. For the trial, four analogue (according to yield, lactation phase, live weight, fat content and protein content) treatments groups of 20 animals of Holstein-Friesian Black-and-White cows were used in the study. Preparatory period lasted from October 1 to 30, 2015, but feeding trial was carried out from December 2015 to February 2016, i.e. for 90 days. The experimental design is presented in Table 1.

Table 1. Scheme of the trial

Group of cows	Number of cows	Basic feed ration
1st trial	5	BF + 10–12% *Pisum sativum* 'Bruno' + 10 –12% *Vicia faba minor* 'Lielplatone'
2nd trial	5	BF + 20–24% *Pisum sativum* 'Bruno'
3rd trial	5	BF + 20–24% *Vicia faba minor* 'Lielplatone'
4th control	5	BF with soybean meal

The average live weight of cows in all groups were 650 kg the mean age was 3.0 lactations. The cows were in the initial phase of lactation were included in the experiment with the average yield of 23.00 kg per day, fat content 4.10% and protein content 3.20%, lactation days 60–100 ($P > 0.05$). The cows were kept under the tied-housing system, milked twice a day at an interval of 12 hours are kept on the same farm, under equal feeding, housing and exploitation condition.

During the trial, the dairy cows received the basic feed ration (BF) which consisted, calculation per cow per day of: 40 kg silage (grass+legume), 3 kg hay (grass+legume), 4 kg fodder (grains), 4 kg complementary, 0.15 kg mineral additive. In the experimental periood (90 days), the cows all groups were fed the same diet except that the diet of the cows in the control group was supplemented with 1 kg soybean meal that of the 1^{s} trial group with 1.82 kg (0.85+0.97 kg) that of the peas+beans, that of the 2^{nd} group with 1.9 kg peas and that of the 3^{rd} trial group with 1.7 kg beans (Table 2).

Table 2. Dairy cows feeding during the trials

Feedstuffs	Amount, kg	1^{st} trial	2^{nd} trial	3^{rd} trial	4^{th} control
Silage	40	40	40	40	40
Hay	3	3	3	3	3
Concentrated feed	4	4	4	4	4
Complementary feed	4	4	4	4	4
Peas+beans	-	1.82	-	-	-
Peas	-	-	1.9	-	-
Beans	-	-	-	1.7	-
Soybean meal	-	-	-	-	1
Mineral additive	0.15	0.15	0.15	0.15	0.15
Feed ration contains:					
Dry matter, kg	-	21.60	21.70	21.50	20.80
Crude protein, g	-	3,266	3,261	3,276	3,258
NEL, MJ	-	142.7	143.8	139	137.20
Calcium, g	-	153	157	155	162
Phosphorus, g	-	82.0	83.0	85.0	82.0

The feeding ration varied according to each cow's milk yield and physiological state, and was corrected monthly depending on the results of control milk yield, dry period and state of health.

The feeding ration varied according to each cow's milk yield and physiological state, and was corrected monthly depending on the results of control milk yield, dry period and state of health.

When elaborating the feeding rations, we took into consideration the following: amount of feedstuffs, dry matter (DM), net energy for lactation (NEL, MJ), amount of crude protein and macro-elements (Ca, P), (Nutrient Requirements…, 2001). Chemical tests were done in total fifteen samples, beans (n = 5), peas (n = 5) and soybean meal (n = 5). Each cows individual milk yield and whole groups average, content of milk fat and protein was recorded, basing on the control milk yield sheets. Control of the milk yield in cows groups was performed each day, individual milk yields were controled once a month.

A full value nutrition analyses were conducted by the accredited Scientific Laboratory of the Agronomical Analyses under the Latvia University of Agriculture. Amino acid analyses were carried out in Baisogala, Lithuania, in the Institute of Animal Sciences. Chemical analyses of the feed samples was carried out in accordance with the ISO 6498: 1998 standards, dry matter – Feed Analyses met.2.2.1.1: 1993, crude protein – LVS EN ISO 5983-2: 2009, starch – LVS EN ISO 10520:2001, crude fat – ISO 6492:1999, digestible undegraded intake protein (UIP) – calculation method, crude fibre – ISO 5498: 1981, neutral detergent fiber (NDF%) – LVS EN ISO 16472: 2006, acid detergent fiber (ADF%), net energy for lactation (NEL, MJ kg^{-1}) – LVS EN ISO 13906: 2008, crude ash – ISO 5984:2002/Cor 1:2005, calcium – LVS EN ISO 6869: 2002, phosphorus – ISO 6491: 1998 (General requirements for the competence…, 2017) and digestibility (cellulase method) (De Boever et al., 1988). Amino acid tests were performed by means of AccQ Tag technology (Waters Corp., Miliford, MA) and quantified by means of Shimadzu HPLC (low pressure gradient system). Amino acid separation was performed using a Nova-Pak C18, 4 mm, 150 × 3.9 mm (Waters Corp., Miliford, MA) chromatography column at 37 °C. The quantity of milk produced was identified by measuring productivity – standard litres of energy corrected milk, which was calculated by the following formula (Garcia et al., 2006):

$$ECM = \text{Milk yield x } \frac{0.383 \text{ x Milk Fat, \%} + 0.242 \text{ x Milk Protein, \%} + 0.7832}{3.14} \quad (1)$$

where *ECM* – energy corrected milk.

Milk quality analyzes were performed determining the milk fat and protein content, the method ISO 9622-2013 (E) / IDF 141: 2013 (E).

The biometric data was processed using by the computer program *SPSS 16.0*. Data were analyzed by: Mann-Whitney test at significance level 0.05 to define differences in comparison of control group and Wilcoxon signed-rank test to define differences between data at the start and end of the experiment at significance level $P < 0.05$.

RESULTS AND DISCUSSION

Chemical composition of beans, peas and soybean meal

The analysis of feeding rations, consumed by cows during trials, by their chemical content proved that, generally, rations meet the demands of standards. Slight diferences were found in the provision of mineral elements to the all groups cows. The feeding rations statisfied the need of cows for dry matter, feed energy, crude protein, calcium and phosphorus in Table 2.

The chemical composition of fodder beans, peas and soybean meal are presented in Table 3. As can be seen from Table 3 data, the content of dry matter in peas 'Bruno' and fodder beans 'Lielplatone' was high, 90.78% and 90.44% respectively but in soybean meal – 87.41%. Crude protein content was the highest in soybean meal – 50.61% and beans – 29.97%, while in peas – 25.04% of dry matter. Soybean meal had significantly high content of UIP – 73.99% of crude protein. After summarizing reference data, undegraded intake protein (UIP) content in soybean meal in the rumen fluctuates within the range of 75 to 78 per cent (Singh et al., 2012). Relatively high percentage of UIP was also in fodder beans – 40.51%, whereas in peas it was 39.69% of the crude protein.

According to the reference-provided information, the amount of UIP can make up 46% of crude protein content (Batterham & Egan, 1986).

The very soluble nature of the protein in beans that makes them easily degraded in the rumen will provide a pulse of nitrogenous substrate for rumen microbes, and diets need to be formulated to best harness this supply to provide essential amino acids for the ruminant itself (Yu et al., 2004). Meanwhile, the highest ADF content was demonstrated by beans – 11.36%, then peas – 9.59% and the lowest in soybean meal – 6.91%.

Table 3. The chemical composition of fodder beans, peas and soybean meal, on dry matter basis, %

Indicator	Beans (*Vicia faba minor*) 'Lielplatone'	Peas (*Pisum sativum*) 'Bruno'	Soybean meal
Dry matter, %	90.44	90.78	87.41
Crude protein, %	29.97	25.04	50.61
UIP of crude protein, %	40.51	39.69	73.99
Crude fat, %	1.09	1.22	1.60
Starch, %	43.29	48.54	7.62
Crude fiber, %	9.5	7.21	3.57
NDF, %	15.79	20.58	13.98
ADF, %	11.36	9.59	6.91
NEL, MJ kg^{-1}	7.7	7.84	7.89
Crude ash, %	3.61	3.28	1.76
Ca, %	0.12	0.07	0.42
P, %	0.66	0.43	0.71
Digestibility, %	80.00	81.40	81.80

Crude fat concentration in beans is low – 1.09%, in peas 1.22% but highest content of crude fat was in soybean meal – 1.60% of dry matter. The highest content of starch was in peas – 48.54%, beans – 43.29% but the lowest in soybean meal – 7.62% of dry matter. According to the reference data, different soybean sorts have different starch content that varies from 8.11 to 9.40 per cent of dry matter (Batterham & Egan, 1986). The highest crude fiber content was in fodder beans – 9.5% and peas – 7.21% but in soybean meal the content of the crude fiber is relatively low – 3.57%.

NDF content was higher in peas – 20.58% but in beans and soybean meal, NDF content was lower, respectively, by 4.79% and 6.60% of dry matter. Conversely the higher content of ADF showed beans – 11.36%, peas – 9.59% but the lowest content of NDF was in soybean meal – 6.91%.

The energy value (NEL) in peas, beans and soybean meal was at a similar level, respectively – 7.84 MJ kg^{-1} 7.70 MJ kg^{-1} and 7.89 MJ kg^{-1}. The crude ash content was similar to that of beans and peas, 3.61% and 3.28% respectively, which was higher than 1.85% and 1.52% than soybean meal. The highest calcium content was in soybean meal – 0.42% but the lowest in beans – 0.12% and in peas – 0.07% of dry matter. The highest content of phosphorus was for soybean meal – 0.71% and in beans – 0.66% but lower in peas – 0.43% of dry matter.

Digestibility of the analyzed forage was high. The highest rate was demonstrated by soybean meal and peas – 81.80% and 81.40% respectively. Conversely, feeds with high digestibility will often result in a higher feed intake and increased growth (Hongmin et al., 2006).

Amino acids content of beans, peas and soybean meal

There was a total of 17 amino acids detected in legume grains and soybean meal. The highest concentration of arginine, leucine, glutamic acid, aspartic acid and isoleucine was in fodder beans, respectively 0.76%, 0.58%, 0.67%, 0.42% and 0.29% of dry matter more than in peas (Table 4). Methionine, cystine, lysine, threonine, histidine, phenylalanine, tyrozine, glycine, serine and alanine amount in beans and peas was similar. The highest concentration of amino acids was shown soybean meal.

However, compared to cereals, the content of lysine in beans is relatively high and the contents of the sulphur-containing amino acids cysteine and methionine are low. According to reference materials, beans mainly contain lysine, with minor concentrations of methionine and tryptophan (Crepon et al., 2010).

Table 4. The amino acids content, on dry matter basis, %

Amino acids	Beans (*Vicia faba minor*) 'Lielplatone'	Peas (*Pisum sativum*) 'Bruno'	Soybean meal
Methionine	0.21	0.22	0.61
Cystine	0.33	0.30	0.68
Lysine	1.71	1.50	2.80
Threonine	0.97	0.77	1.82
Arginine	2.54	1.78	3.35
Isoleucine	1.14	0.85	2.10
Leucine	2.05	1.47	3.45
Valine	1.21	0.95	2.21
Histidine	0.69	0.50	1.20
Phenylalanine	1.14	1.04	2.32
Tyrosine	0.84	0.64	1.63
Glycine	1.17	0.90	2.00
Serine	1.22	1.01	2.37
Proline	-	0.77	-
Alanine	1.10	0.92	2.06
Aspartic acid	2.82	2.40	5.27
Glutamic acid	4.42	3.75	8.29

Productivity and milk quality during the trial

The cow productivity during the trial is shown in Table 5. Even though the daily milk yields decreased for all the cow groups during the experiment, which was normal during the lactation period, yet the milk yield decreases for the 1^{st}, and 2^{nd} trial groups were smaller – 2.22 kg and 2.10 kg, respectively, compared with the initial stage of the experiment. The greatest decrease in cow productivity was observed for the control group – by 3.98 kg of energy corrected milk but a smaller decrease was observed for the 3^{rd} group – by 0.26 kg of ECM, compared with the initial stage of the experiment ($P < 0.05$). As the cows' productivity decreased during the experimental and lactation period, the fat and protein contents of milk increased in the trial groups, compared with the control group. The fat content of milk slightly increased, on average, by 0.04% in the 3^{rd} and 1^{st} groups and by 0.01% in the 2^{nd} group, compared with the control group, and from 0.33% to 0.37% compared with the initial stage of the experiment. The fat content of milk decreased by 0.36% in the control group, compared with the initial stage of the experiment ($P < 0.05$).

Table 5. Cow productivity during the trial, on average, kg ECM (n = 4 × 5)

Group of cows	November*	December**	January**	February**	Comparison between initial and final values
1st trial	22.7 ± 3.47	23.5 ± 5.21	22.2 ± 3.44	20.5 ± 2.59	-2.22
2nd trial	23.5 ± 5.47	21.6 ± 3.35	21.8 ± 3.16	21.4 ± 4.87	-2.10
3rd trial	20.7 ± 2.23	19.7 ± 1.35	20.3 ± 2.34	20.5 ± 2.58	-0.26
4th control	24.6 ± 6.78	24.9 ± 6.81	21.9 ± 3.38	20.6 ± 2.52	-3.98 ^{S}
p–value (relative to control)					
Group of cows	November*	December**	January**	February**	*P*-value (between initial and final values)
1st trial	0.465	0.600	0.917	0.917	0.225
2nd trial	0.917	0.347	0.917	0.754	0.138
3rd trial	0.251	0.251	0.917	0.916	0.893
4th control	-	-	-	-	0.043^{S}

* initial stage; ^{S} significant differences (P < 0.05); ** trial period.

The research results are similar to the data obtained in Lithuania and USA, where feeding milking cows with peas, the amount of proteins in milk increased the most (Kudlinskiene et al., 2016; Diaz, 2017). The protein content of milk increased in all the experimental groups. The protein content of milk increased average by 0.31% in the 1st group, 0.17% in the 2nd group and 0.27% in the 3rd group, compared with the control group, and by 0.59%, 0.36% and 0.44%, respectively, compared with the initial stage of the experiment (P > 0.05). In a similar research in Italy, it was detected that the amount of proteins in milk increased for the cows that were fed with beans, in contrast with cows that were fed with soybean meal, as we also stated in our field study (Belliere et al., 2008).

The content of total amount of amino acids in milk is shown in Table 6. The total amount of amino acids increased in the milk samples of all the trial groups. The highest increase was found in the bulk milk samples of the 3rd and the 2nd trial group, 4.00 g kg^{-1} and 3.90 g kg^{-1}, respectively. The lowest increase was in the bulk milk samples of the 1st trial group 1.80 g kg^{-1}, respectively, compared with the initial stage of the experiment. However, an increase in the total amount of amino acids was observed in the control group, respectively 2.30 g kg^{-1}. Meanwhile, trial group 3rd, which were fed beans, showed the amount of total amino acids in milk that was 1.70 g kg^{-1} higher than in control group that was fed soybean meal (P < 0.05).

Table 6. The content of total amount of amino acids in milk (n = 4 × 5)

Group of cows	Total amount of amino acids, g kg^{-1}		
	November*	February	Comparison between initial and final values, g kg^{-1}
1st trial	30.2 ± 0.44	32.0 ± 0.68	± 1.80
2nd trial	29.2 ± 0.49	33.1 ± 0.71	± 3.90
3rd trial	30.5 ± 0.37	34.5 ± 0.52	± 4.00
4th control	31.4 ± 0.32	33.7 ± 0.39	± 2.30

* initial stage; ^{S} significant differences (P < 0.05).

The economic efficiency is a key criterion for determining the benefit of one or another feed product fed out. The milk sale and feed cost summary records for the trial that lasted 90 days show that economic efficency of peas plus beans has been positive (Table 7).

Table 7. Milk and feed costs for a cow during the trial of 90 days

Indicator	1st trial	2nd trial	3rd trial	4th control
Milk obtained, kg	9,931.5	9,720	9,090	10,125
Milk wholesale price, EUR kg^{-1}	0.21	0.21	0.21	0.21
Income from milk sales, EUR	2,085.61	2,041.20	1,908.90	2,126.25
Total feed costs per group, EUR	1,313.33	1,330.88	1,296.23	1,366.88
Feed costs per kg of milk yield, EUR kg^{-1}	0.132	0.136	0.142	0.135
Benefit, EUR	772.28	710.32	612.67	759.37
Compared the control	±12.91	-49.05	-146.70	-

The highest economic efficiency in milk production and distribution was shown by group 1st, whose forage included fodder peas+beans, while the lowest efficciency - by group 3rd, which was fed fodder beans. The highest economic efficiency in terms of profit was provided by cows from group 1st – 772.28 EUR, which is 12.91 EUR more than control group.

CONCLUSIONS

1. The obtained results of chemical composition of legume grains the content of dry matter in peas and field beans was high, 90.78% and 90.44% respectively. Crude protein content was the highest in soybean meal – 50.61% and fodder beans – 29.97%, while in peas – 25.04% of dry matter. The highest content of starch was in peas – 48.54%, beans – 43.29% but the lowest in soybean meal – 7.62% of dry matter.

2. Upon the whole, it can be concluded that the highest rate of essential amino acids was detected in soybean meal and fodder beans, while the lowest – in peas.

3. The cow productivity indicators decreased for all the groups, which was normal during the lactation period, yet the daily milk yield decreases for the trial groups were smaller – 2.22 kg, 2.10 kg and 0.26 kg, respectively, compared with the initial stage of the experiment and the control group.

4. The highest total amount of amino acids in milk was detected in 3rd and 2nd trial cow groups, respectively, 4.00 g kg^{-1} and 3.90 g kg^{-1}, which was fed fodder beans and peas but the lowest amino acid amount was detected in trial group 1st – 1.80 g kg^{-1}, which was fed peas plus fodder beans compared with the initial stage of the experiment ($P < 0.05$).

5. The milk sale and feed cost summary records for the trial that lasted 90 days show that economic efficency of peas plus beans has been positive The highest economic efficiency in milk production and distribution was shown by group 1st, which was fed peas+ beans while the lowest efficciency – by group 3rd which was fed fodder beans.

ACKNOWLEDGEMENTS. We acknowledge the scientific research project 'Enhancing of Legumes Growing in Europe through Sustainable Cropping for Protein Supply for Food and Feed' (EUROLEGUME), Agreement No. 613781, provided us with financial support for this research study.

REFERENCES

Agriculture of Latvia. 2017. *http://www.csb.gov.lv/sites/default/files/nr_24_latvijas_lauksaimnieciba_2017_17_00_lv_en.pdf* Accessed 29.01.2018.

Batterham, E.S. & Egan, A.R. 1986. Utilisation of food legumes as feed. http://www.aciar.gov.au/files/node/2214/food_legume_improvement_for_asian_farming_systems_18979.pdf Accessed 14.12.2017.

Belliere, R.S., Casini, M., Giorgetti, A., Lorenzini, G., Lotti, C., Martini, A., Migliorini, P. & Riccio, F. 2008. Production of grain legume crops alternative to soya bean and their use in organic dairy production.

Crépon, K., Marget, P., Peyronnet, C., Carrouée, B., Arese, P. & Duc, G. 2010. Nutritional value of faba bean (*Vicia faba L.*) seeds for food and feed. *Field Crops Research Journal* **115**, 329–339.

De Boever, J.L., Cottyn, B.G., Andries, J.I., Buysse, F.X. & Vanacker, J.M. 1988. The use of a cellulase technique to predict digestibility, metabolizable and net energy of forages. *Animal Feed Science and Technology* **19**, 247–260.

Diaz, F. 2017. Field beans as a protein source for dairy cows. *http://www.allaboutfeed.net/Raw-Materials/Articles/2017/1/Field-peas-as-a-protein-source-for-dairy-cows-81315E* Accessed 18.01.2018.

Garcia, O., Hemme, T., Nho, L.T. & Tra, H.T.H. 2006. The economics of milk production in Hanoi, Vietnam, with particular emphasis on small-scale producers. *PPLPI Working Pape*r, **33**, 39–40.

Hongmin, D., Joe, M. & Tim, A. McAllister. 2006. Emissions from Livestock and Manure Management. In I*PCC Guidelines for National Greenhouse Gas Inventories* **10**, pp. 10–14.

General requirements for the competence of testing and calibration laboratories. 2017. https://www.iso.org/files/live/sites/isoorg/files/store/en/PUB100424.pdf Accessed 07.12.2018

Ipharraguerre, I.R & Clark, J.H. 2005.Varying protein and starch in the diet of dairy cows. *J. Dairy Sci*. **88**, 2556–2570.

Jensen, E.S. 2002. The contribution of grain legumes, currently under-used in the EU, to environment-friendly and sustainable European agriculture, In *Legumes for sustainable agriculture, LINK dissemination event*, Strasbourg, France, pp 28.

Kudlinskiene, I., Gružauskas, R. & Stankevičius, R. 2016. Efects of extruded peas (*Pisum sativum*) on dairy cow's performance, milk composition and sensory properties. *http://www.vetzoo.lsmuni.lt/data/vols/2016/73/pdf/kudlinskiene.pdf* Accessed 20.12.2017.

Martini, A., Migliorini, P., Lorenzini, G., Lotti, C., Rosi Bellière, S., Squilloni, S., Riccio, F., Giorgetti, A. & Casini, M. 2008. Production of grain legume crops alternative to soya bean and their use in organic dairy production.

h*ttp://www.orgprints.org/11957/1/Martini_11957_ed.doc.rgprints.org/view/projects/conference.html* Accessed 03.01.2018.

Nutrient Requirements of Dairy Cattle. 2001. *https://www.nap.edu/catalog/9825/nutrient-requirements-of-dairy-cattle-seventh-revised-edition-2001* Accessed 04.12.2018.

Proskina, L. & Cerina, S. 2017. Economics gains from consumption of legumes in dairy farming. In *16th International Scientific conference ‘Engineering for Rural Development’ Proceeding*. Jelgava, Latvia, pp. 1196–1201.

Singh, D., Kopinski, J. & Takken, A. 2012. Legumes for dairy cattle. *https://www.daf.qld.gov.au/animal-industries/dairy/feed-and-nutrition/legumes* Accessed 18.01.2018.

Tufarelli, V., Khan, R.U. & Laudadio, V. 2012. Evaluating the suitability of field beans as a substitute for soybean meal in early-lactating dairy cow: Production and metabolic responses. *J. Animal Sci*. **83**, 136–140.

Yu, P., Tamminga, S., Egan, A.R. & Christensen, D.A. 2004. Probing equivocal effects of heat processing of legume seeds on performance of ruminants. *Animal Science Journal* **17**, 869–876.

INSTRUCTIONS TO AUTHORS

Papers must be in English (British spelling). English will be revised by a proofreader, but authors are strongly urged to have their manuscripts reviewed linguistically prior to submission. Contributions should be sent electronically. Papers are considered by referees before acceptance. The manuscript should follow the instructions below.

Structure: Title, Authors (initials & surname; an asterisk indicates the corresponding author), Authors' affiliation with postal address (each on a separate line) and e-mail of the corresponding author, Abstract (up to 250 words), Key words (not repeating words in the title), Introduction, Materials and methods, Results and discussion, Conclusions, Acknowledgements (optional), References.

Layout, page size and font

- Use preferably the latest version of **Microsoft Word**, doc., docx. format.
- Set page size to **B5 Envelope or ISO B5 (17.6 x 25 cm)**, all margins at 2 cm.
- Use single line spacing and justify the text. Do not use page numbering. Use indent 0.8 cm (do not use tab or spaces instead).
- Use font Times New Roman, point size for the title of article **14 (Bold)**, author's names 12, core text 11; Abstract, Key words, Acknowledgements, References, tables and figure captions 10.
- Use *italics* for Latin biological names, mathematical variables and statistical terms.
- Use single ('…') instead of double quotation marks ("…").

Tables

- All tables must be referred to in the text (Table 1; Tables 1, 3; Tables 2–3).
- Use font Times New Roman, regular, 10 pt. Insert tables by Word's 'Insert' menu.
- Do not use vertical lines as dividers; only horizontal lines (1/2 pt) are allowed. Primary column and row headings should start with an initial capital.

Figures

- All figures must be referred to in the text (Fig. 1; Fig. 1 A; Figs 1, 3; Figs 1–3). Use only black and white or greyscale for figures. Avoid 3D charts, background shading, gridlines and excessive symbols. Use font **Arial** within the figures. Make sure that thickness of the lines is greater than 0.3 pt.
- Do not put caption in the frame of the figure.
- The preferred graphic format is EPS; for half-tones please use TIFF. MS Office files are also acceptable. Please include these files in your submission.
- Check and double-check spelling in figures and graphs. Proof-readers may not be able to change mistakes in a different program.

References

- **Within the text**

In case of two authors, use '&', if more than two authors, provide first author 'et al.':

Smith & Jones (1996); (Smith & Jones, 1996);
Brown et al. (1997); (Brown et al., 1997)

When referring to more than one publication, arrange them by following keys: 1. year of publication (ascending), 2. alphabetical order for the same year of publication:

(Smith & Jones, 1996; Brown et al., 1997; Adams, 1998; Smith, 1998)

- **For whole books**

Name(s) and initials of the author(s). Year of publication. *Title of the book* (*in italics*). Publisher, place of publication, number of pages.

Shiyatov, S.G. 1986. *Dendrochronology of the upper timberline in the Urals*. Nauka, Moscow, 350 pp. (in Russian).

- **For articles in a journal**

Name(s) and initials of the author(s). Year of publication. Title of the article. *Abbreviated journal title* (*in italic*) volume (in bold), page numbers.

Titles of papers published in languages other than English, German, French, Italian, Spanish, and Portuguese should be replaced by an English translation, with an explanatory note at the end, e.g., (in Russian, English abstr.).

Karube, I. & Tamiyra, M.Y. 1987. Biosensors for environmental control. *Pure Appl. Chem.* **59**, 545–554.

Frey, R. 1958. Zur Kenntnis der Diptera brachycera p.p. der Kapverdischen Inseln. *Commentat.Biol.* **18**(4), 1–61.

Danielyan, S.G. & Nabaldiyan, K.M. 1971. The causal agents of meloids in bees. *Veterinariya* **8**, 64–65 (in Russian).

- **For articles in collections:**

Name(s) and initials of the author(s). Year of publication. Title of the article. Name(s) and initials of the editor(s) (preceded by In:) *Title of the collection (in italics)*, publisher, place of publication, page numbers.

Yurtsev, B.A., Tolmachev, A.I. & Rebristaya, O.V. 1978. The floristic delimitation and subdivisions of the Arctic. In: Yurtsev, B. A. (ed.) *The Arctic Floristic Region*. Nauka, Leningrad, pp. 9–104 (in Russian).

- **For conference proceedings:**

Name(s) and initials of the author(s). Year of publication. Name(s) and initials of the editor(s) (preceded by In:) *Proceedings name (in italics)*, publisher, place of publishing, page numbers.

Ritchie, M.E. & Olff, H. 1999. Herbivore diversity and plant dynamics: compensatory and additive effects. In: Olff, H., Brown, V.K. & Drent R.H. (eds) *Herbivores between plants and predators. Proc. Int. Conf. The 38th Symposium of the British Ecological Society*, Blackwell Science, Oxford, UK, pp. 175–204.

Please note

- Use '.' (not ',') for decimal point: 0.6 ± 0.2; Use ',' for thousands – 1,230.4;
- Use '–' (not '-') and without space: pp. 27–36, 1998–2000, 4–6 min, 3–5 kg
- With spaces: 5 h, 5 kg, 5 m, 5°C, C : D = 0.6 ± 0.2; $p < 0.001$
- Without space: 55°, 5% (not 55 °, 5 %)
- Use 'kg ha^{-1}' (not 'kg/ha');
- Use degree sign ' ° ' : 5 °C (not 5 ^{O} C).